GEOCHEMISTRY AND MINERALOGY OF NAMURIAN SEDIMENTS IN THE PENNINE BASIN, ENGLAND.

by

MUMTAZ AHMED AMIN

Thesis submitted in fulfilment of the
requirements for the
Degree of Doctor of Philosophy

Department of Geology,
University of Sheffield.

July, 1979

SUMMARY

This study deals with the mineralogy and geochemistry of some Namurian sediments from the Central Pennine Basin, England. The rocks were collected from the Mam Tor area and a borehole at Tansley near Matlock.

The Mam Tor rocks (R_{1c} zone) consist of closely associated turbidite sandstones and shales. In the Tansley Borehole (R-E zones) the Ashover Sandstone overlies a condensed sequence of marine and non-marine shales with a volcanic clay at the base.

Petrographic and X-ray diffraction studies, together with major and trace element analyses, have been carried out on whole rock samples and separated size fractions.

The Mam Tor sandstones are greywackes, whereas the Ashover sandstones are arkoses. In the sandstones, kaolinite, chlorite and iron oxides are partly of diagenetic origin. The mineralogy of the rocks is comparatively simple; quartz, kaolinite and illite are the principal minerals, with lesser amounts of feldspar, siderite, pyrite, dolomite, calcite and organic matter. Chemical and mineralogical variations in the Mam Tor rocks are due to textural differences, particularly grain size fractionation. Further information on the association of elements with minerals is provided by correlation analysis and t-tests. Chlorite is shown to be rich in iron and illite is the 1Md polytype. It is concluded that these rocks have not reached the stage of deep burial diagenesis. Replacement reactions are important in the sandstones, but not in the shales.

The volcanic clay is identified as a K-bentonite and originated by reaction between basalt and seawater.

The transition from non-marine to marine shales is accompanied by increases in the contentsof illite, pyrite, calcite and organic matter and a decrease in the kaolinite content. Siderite is confined to the non-marine shales in which phosphate and TiO_2 are relatively concentrated.

The marine shales are enriched in Ni, V, Zn, Cu, Sr and Pb, whereas the non-marine shales are higher in Zr. The concentration of Cu, Sr and Pb are the most effective discriminators, using discriminant function analysis, between the two groups of shales. The trace element enrichment is attributed mainly to organic matter and pyrite.

The variation in SiO_2/Al_2O_3, quartz/combined silica, TiO_2/Al_2O_3 and Na_2O/K_2O ratio are related to grain size, the rate of sedimentation and distance from source. The distribution of diagenetic minerals is attributed to changing physico-chemical conditions including salinity. The change from the pyrite to the siderite stability field is considered to reflect decreasing pH and rising Eh.

The lateral variation in facies deposited contemporaneously in different sectors reveals the influence of the Derbyshire Block acting as a submarine ridge. It is shown that the textural and geochemical characteristics of the Mam Tor rocks are similar to those of turbidites. The data of the Tansley Borehole sediments indicate their similarity to those from a shallow water, semi-restricted, basin environment onto which a deltaic sedimentation was encroaching.

ACKNOWLEDGEMENTS

The writer would like to express his sincere thanks and gratitude to Dr. D.A. Spears for supervision, advice and much valuable discussion throughout this work, and also to Professor C. Downie for his permission to use the facilities in the Department of Geology, University of Sheffield.

I also wish to thank Dr. R. Kanaris-Sotiriou and Mr. V.A. Somogyi for their technical advice during the time spent on chemical analysis.

Thanks are also due to Mr. G.S. Bryant, the clerical and technical staff of the Department for their help during this work.

My thanks are extended to Miss P. Mellor and Miss J. Lewis for typing the thesis.

Finally, I wish to express my gratitude to the Ministry of Higher Education and Scientific Research of Iraq for providing the grant which made this work possible.

CONTENTS

LIST OF TABLES

LIST OF FIGURES

LIST OF PLATES

CHAPTER 1

Introduction

The aim of this introductory chapter is to provide a geological background to the present work. A brief account of the previous geochemical investigations is presented. It is also relevant to describe the palaeogeography and history of sedimentation in the Central Pennine Basin, in order to ascertain the likely geochemical variation to be encountered in the rocks of the present study. Finally the lithology and stratigraphy of the studied rocks are described.

1.1 Previous Investigations

As this study is really an extension of work undertaken by several investigators on the geochemical and mineralogical characteristics of the British Carboniferous sediments, a review of previous work is significant in this respect. In this review particular emphasis is placed upon the clay rich sediments and it will also make unnecessary a discussion of geochemical principles as such because they will be conveyed in the context of the British Carboniferous.

Nicholls and Loring (1960, 1962) studied shales, mudstones and associated rock samples from the Coal Measures, Bersham Colliery Borehole, North Wales. Their data are listed in Table 1.

In their first investigation (1960), they emphasised the relationship between variations in Na^+/K^+ ratio and rate of sedimentation. After excluding the possibility of albite being present, they suggested that the variation in the Na^+/K^+ ratio might be explained by one of the following possibilities:

TABLE 1: Major and Trace Element Analyses of the Bersham Rocks (Nicholls and Loring, 1962)

Major Elements %			Trace Elements (ppm)		
Element	Mean	s.d.	Element	Mean	s.d.
SiO_2	63.37	4.14	B	61*	8
Al_2O_3	20.46	2.22	Ba	492	69
Fe_2O_3	0.89	0.61	Co	33	22
FeO	2.18	0.86	Cr	130	30
MnO	0.03	0.02	Cu	33	9
MgO	0.94	0.25	Ga	24	6
CaO	0.25	6.71	Li	104	64
Na_2O	0.49	0.13	Ni	64	32
K_2O	3.03	0.48	Pb	6	2
H_2O^+	4.82	0.63	Rb	143	17
H_2O^-	0.99	0.29	Sr	74	23
P_2O_5	0.12	5.36	V	162	48
CO_2	0.66	0.48	Zr	258	81
C	0.78	0.77	Mo	Below Detection Limit 2 ppm	

*All these figures are 'rounded off'

A. Na^+ adsorption on a degraded illite

B. K^+ adsorption on a degraded illite

C. Cation exchange of K^+ for Na^+ in the degraded illite

They concluded that cation exchange was most likely as it agrees with the accepted rate of sedimentation. Thus they suggested that the degraded illite supplied to the basin of deposition had a higher Na^+/K^+ ratio than the illite now present.

In a more detailed investigation (Nicholls and Loring, 1962) major, minor and trace elements analyses were presented for mudstones, seatearths and coals. The mineralogy of the sediment was comparatively simple, with quartz, illite and kaolinite being the principal components, with lesser amounts of chlorite, sulphide, siderite and organic matter.

Changing physico-chemical conditions within the sediments were deduced from the presence of iron sulphides (FeS and FeS_2) and siderite. Precipitation or formation of these minerals did not appear to have had a great influence on the trace element distribution. Sorption was claimed to be the most significant process controlling the content of the trace elements. Organic matter, colloidal iron monosulphide and clay minerals, especially illite, were the principal absorbents.

Spears (1963, 1964) investigated the major element geochemistry of a sequence including the Mansfield Marine Band from a borehole penetrating Westphalian Coal Measures at Little Smeaton, Yorkshire. Quartz and clay minerals (illite with subsidiary kaolinite and chlorite) were shown to be the chief minerals of detrital origin in all samples. Major elements of non-detrital origin were considered to be mostly combined in the diagenetic minerals. Physico-chemical conditions (pH-Eh trend) were deduced from the diagenetic minerals, (pyrite, siderite and phosphate) and was referred only to the conditions present within the sediment and not to those

prevailing at the water-sediment interface. Also, Spears considered that the time factor was important in the production of conditions suitable for the development of diagenetic minerals, particularly pyrite.

Free silica or quartz values were found to be dependent upon grain size which in the sequence examined was related to the rate of sedimentation.

Titanium, like quartz, was thought to be detrital in origin, and to vary with the grain size. Free silica/combined silica and total silica/alumina ratios were thought to vary with the rate of sedimentation and grain size, whereas alumina/combined silica ratio was found to be independent of grain size and used to express the composition of the clay minerals for which a detrital origin is suggested.

The distribution of sodium and potassium were similar and illite was thought to be responsible.

The variation in the Na^+/K^+ ratio was found to be comparable with the distribution of quartz and titanium, and thus related to the rate of sedimentation. A decrease in the Na^+/K^+ ratio was attributed to cation exchange which could be more complete during slowly accumulating finer-grained sediments. Spears, however, would now suspect that changes in whole rock Na^+/K^+ ratio is related to grain size and the increased importance of albite in the coarser grained sediments (personal communication). Table 2 shows the data of Spears (1964).

Bloxam and Thomas (1969) studied the shales belonging to, and associated with, the Gastrioceras subcrenatum Marine Band, from the North Crop of the South Wales Coalfield. The purpose of their study was to compare the palaeontological and geochemical characteristics of the succession. They divided the sections, on the basis of Lingula and other fossils into four environmental phases, as follows:

TABLE 2: Major Element Analysis of the Mansfield Marine Band (Spears, 1964)

	Mean	S.D.
SiO_2	48.36	11.37
TiO_2	0.79	0.20
Al_2O_3	20.57	4.73
FeO	2.92	1.51
Fe_2O_3	3.74	2.01
MnO	0.17	0.17
MgO	2.48	2.20
CaO	3.14	7.73
Na_2O	0.70	0.16
K_2O	3.66	1.00
H_2O^+	5.07	1.39
P_2O_5	0.21	0.22
CO_2	0.04	10.45
C	2.86	2.88
S	2.51	2.39

a. Fresh Water

b. Brackish Water

c. Inshore Marine

d. Offshore Marine

The elements analysed were those considered to have the greatest potential value in differentiating the different environments. Detrital quartz, organic carbon, quartz/organic carbon, Na^{+}/K^{+} and Th/U ratio were used as parameters of the relative sedimentation rates, which was in agreement with the distribution pattern based on palaeontological criteria. In addition the Fe^{3+}/Fe^{2+} ratio was used as an indicator of pH conditions. Their chemical data are summarised in Table 3.

Curtis (1967, 1969) studied the geochemistry of the Mansfield Marine Band in the Westphalian Coal Measures, with special emphasis on the trace elements distribution. On the basis of goniatites and Lingula, the succession was divided into a lower marine part passing upwards into non-marine strata through a brackish water phase. In the first paper (1967), pyrite was shown to be dominant in the marine shales, whereas siderite was associated with the non-marine shales. In the later paper (1969) consideration was given to the oxides representative of sedimentary components, namely:

a. Al_2O_3 indicative of total clay fraction

b. acid soluble sulphur indicative of pyrite

c. total alkalis as illite content

d. total diagenetic iron as a measure of the non-detrital component of the sediments

When these major sediment components were correlated with the trace element data (marine and non-marine shales) it was found that Ga, B, Cr,

TABLE 3: Major and Trace Element Analyses from the Rocks of the South Wales Coalfield (Bloxam and Thomas, 1969)

	Mean	s.d.
Fe^{3+}	1.62	0.70
Fe^{2+}	4.26	1.29
Mg	1.50	0.32
Ca	1.05	1.18
Na	0.68	0.36
K	4.39	0.45
P	0.11	0.11
CO_2	1.04	1.99
C*	1.79	2.08
S	1.00	0.76
Quartz	26.77	7.86
U ppm	7.6	4.6
Th ppm	13.3	2.3
Th/U	2.3	1.7
Qtz/C	41.7	34.5
Na/K	0.16	0.09
Fe^3/Fe^2	0.50	0.48

*All elements except C (organic) are corrected for quartz

(total 63 samples)

V, Sr, Ba, Co and Ni correlate with the clay content, whereas Pb, Cu, also V and Ni correlated with acid soluble sulphur. On the other hand, correlation of the major/trace data, only in the marine shales, revealed the following:

a. Ba, Co, Ni, Cu and Pb, correlate with organic matter/carbon and pyrite, and also to a lesser extent with the clay

b. Mn associated with the total diagenetic iron

c. Ga, B, Cr, V and Sr associated with the clay

Analytical data for the Mansfield Marine Band are shown in Table 4.

Nichol et al (1970, 1971) carried out a regional geochemical reconnaissance in South Derbyshire and Devon. Their work was primarily concerned with the minor element content of stream sediment samples and in addition a variety of rocks and soil samples were analysed, enabling geochemical maps of the areas concerned to be compiled. Geometric mean values are given in Tables 5 and 6.

Hirst and Kaye (1971) presented a series of mineralogical and chemical analyses for a sequence of Upper Visean Carboniferous sediments from Rookhope,Durham. After a factor analysis test, it was found that the variance of the data could be attributed to six main factors. Four of these factors were related to depositional processes and variation in the environment of sedimentation and these included sorting, rate of deposition, calcite precipitation and the detrital supply. The other two factors were interpreted as diagenetic and concerned siderite and pyrite formation. Their data are shown in Table 7.

Sulaiman (1972) studied the geochemistry of Namurian argillites (siltstones and shales) from Ireland, which was originally sampled for a study of the clay mineralogy by Cockett (1966, from Sulaiman). Cockett found that:

TABLE 4: Major and Trace Element Data of the Mansfield Marine Band (Curtis, 1967, 1969)

Major Elements in %			Trace Elements in ppm		
Element	Mean	S.D.	Element	Mean	S.D.
SiO_2	47.49	11.04 (5.13)	Ga	32	7
Al_2O_3	20.28	4.77 (2.47)	B	80	21
MgO	2.66	4.58 (4.61)	Cr	110	24
CaO	1.87	4.58 (1.40)	V	258	46
Fe_2O_3	8.76	4.36 (2.33)	Co	23	5
FeO	4.80	4.58 (2.57)	Ni	66	16
CO_2	2.88	4.00 (2.25)	Cu	69	38
S	1.52	1.69	Pb	42	35
			Sr	123	63
			Ba	794	1427
			Mn	929	561

Figures in parenthesis are the S.D., excluding two samples of low SiO_2 and Al_2O_3 values.

TABLE 5: Geometric Means for Facies of the Different Formations, South Derbyshire and Adjoining Counties (Nichol et al., 1970)

Element ppm	Namurian-Visean		Namurian		Westphalian	
	Argillaceous	Arenaceous	Argillaceous	Arenaceous	Argillaceous	Arenaceous
Mo	11	<2	2	<2	<2	<2
As	17	*	<5	*	<5	*
Sc	4.4	*	<0.5	*	<0.5	*
Ni	100	35	110	45	170	60
V	270	60	155	85	145	30
Cu	110	15	45	20	25	20
Cr	100	65	100	60	95	20
Pb	25	15	30	25	50	30
Co	30	20	45	20	100	30
Mn	900	420	620	600	2900	50
Ti	4500	3000	4400	3600	5000	1000
Fe_2O_3%	2.2	1.2	4.5	2.8	8.5	2.2

*Not analysed

TABLE 6: Geometric Means of the Dartmoor and Torrington Namurian and Westphalian Shales (Nichol et al., 1971)

Element ppm	North of Dartmoor		Black Torrington	
	Namurian	Westphalian	Namurian	Westphalian
As	<5	<5	5	<5
Cr	110	65	120	110
Co	19	17	18	30
Cu	40	20	35	35
Pb	22	10	16	24
Mn	275	300	335	650
Mo	<2	<2	n.a.	n.a.
Ni	60	40	60	70
Sn	<5	<5	n.a.	n.a.
V	110	45	140	120
Zn	65	55	55	60
Ti	3300	2600	3500	3500
Fe_2O_3 %	2.1	2.2	3.7	3.9

n.a. = not analysed

TABLE 7: Major and Trace Element Data of the Argillaceous and Arenaceous Sediments (Hirst and Kaye, 1971)

Major Element %		Trace Element in ppm	
Element	Mean	Element	Mean
SiO_2	65.35	B	111
TiO_2	0.69	F	919
Al_2O_3	14.32	V	47
Fe_2O_3	5.11	Cr	80
MnO	0.19	Ni	40
MgO	0.90	Cr	18
CaO	1.94	Rb	158
Na_2O	0.31	Sr	162
K_2O	2.92	Zr	261
H_2O^+	2.39	Ba	303
H_2O^-	0.67	Pb	15
CO_2	2.73		
C	2.09		
S	0.51		

1. The kaolinite content decreases from north to south
2. The illite and chlorite increased in the same direction.
3. Mixed layers illite/montmorillonite in the central region of Ireland.

Using semi-quantitative data he determined seven clay mineral provinces, whereas Sulaiman, for the sake of simplicity, reduced them to three provinces as follows:

1. Kaolinite province in the north (near-shore area of the Namurian Sea, delta topset)
2. Kaolinite, illite, chlorite and mixed layer province in the centre (near-shore, delta slope or foreset).
3. Illite and chlorite province in the south and south-west (offshore, basin or bottomset).

In the first province the concentration of kaolinite was attributed to leaching. Geochemical evidence of leaching is suggested by the reduced values of Mn, Fe, Zn, P, Na, etc. as compared with the average shale, and enriched values of Zr, Nb, Ti,Tn typically associated with resistate phases. He, however, draws a general conclusion concerning the location of trace elements, these are:

a. Ga, P, Zr, Ti,Nb, Th, Sn and Y are included and dispersed within the clay fraction.
b. Rb, Ba, Sr and Pb are associated with illite.
c. Ni, Sn and Zn (substituting for Fe and Mg) occur in the chlorite.
d. Cu, Mo, V, As, Cl, Br and U also with Ni, Zn and Pb associated with organic/or sulphide.
e. Sr, Ce, Y, Sn, Mo and P incorporated in carbonate-phosphate phase

TABLE 8: Mean of Major and Trace Elements in the Different Provinces (Sulaiman, 1972)

Oxide %	Province						
	1	11	111	1V	V	V1	V11
SiO_2	49.98	64.64	66.91	62.76	52.04	59.44	56.81
TiO_2	1.77	0.85	0.57	0.67	0.89	0.76	0.93
Al_2O_3	27.61	17.60	15.90	17.90	21.80	18.50	24.20
Fe_2O_3	4.35	4.30	4.90	4.30	6.56	6.90	7.10
MgO	0.98	1.00	1.00	1.30	1.60	1.90	1.03
Na_2O	0.15	0.40	0.50	0.77	0.82	0.83	0.26
K_2O	1.05	2.20	2.30	2.10	3.70	3.10	4.10
C	9.76	7.30	5.60	4.20	7.00	3.56	1.70
S	0.50	0.40	0.49	0.78	1.05	0.99	0.00
Element ppm							
P	336	727	510	354	561	538	374
Cl	632	111	128	195	214	305	86
Br	12	3	3	4	8	6	3
Ga	27	18	21	17	24	21	30
Ba	376	452	441	448	690	653	747
Rb	46	87	95	92	165	142	186

Oxide	Province 1 Near Shore Top Set	Province 2 Delta Slope Foresets	Province 3 Bottom Set Basin
CaO	0.75	1.49	1.62
CO_2	0.66	2.67	2.16
Element ppm			
V	220	213	234
Mn	404	364	840
Ni	59	68	59
Zn	10	66	91
Cu	43	82	66
As	8	19	25
Y	34	34	42
La	64	33	41
Co	81	46	59
Nd	52	26	31
Zr	375	138	155
Mo	n.d.	31	29
Sn	4.5	4.3	5.4
Pb	26	31	30
U	5.6	11	10
Th	2.5	1.0	1.1

TABLE 9: Mean of Major and Trace Element of the Namurian Argillites (Sulaiman, 1972)

Element	%	Element	ppm	Element	ppm
SiO_2	58.91%	P	525	Sr	112
TiO_2	0.89%	Cl	296	Y	40
Al_2O_3	19.66%	Br	6	La	42
Fe_2O_3	6.13%	V	227	Co	58
CaO	1.52%	Mn	713	Nd	32
CO_2	1.83%	Ni	60	Zr	173
MgO	1.57%	Zn	77	Nb	14.5
Na_2O	0.69%	Cu	67	Mo	25
K_2O	2.82%	Ga	22	Sn	5
C	5.12%	As	24	Pb	30
S	0.60%	Ba	581	U	9.6
		Rb	125	Th	10.7

Chemical data of the different provinces are shown in Table 8, whereas Table 9 shows the overall major and trace element averages of the Namurian argillites of Ireland.

Thomson (1971) in a regional geochemical reconnaissance study of the stream-sediments in England and Wales, presented some relevant chemical data on the Bowland Shales, and also quoted data from Atkinson (1967) and Fletcher (1968) on the Visean/Namurian marine Black Shales in County Limerick, south-west Ireland, and the southern Pennines (Table 10).

Spears and Sotiriou (1976) studied the titanium distribution in some Carboniferous sediments. They concluded that:

a. the change in the TiO_2/Al_2O_3 ratio was related to depositional sorting and maturity of the sediments.

b. the maximum TiO_2/Al_2O_3 ratio in the silicate lattice is about 0.025

c. high and low values of the TiO_2/Al_2O_3 ratio, indicate the presence of basic and acidic volcanic components, respectively

Trewin (1968) reported the occurrence of several K-bentonite beds in the Pendleian-Arnsbergian (E_1-E_2) succession of the Millstone Grit in Staffordshire, Derbyshire and Cheshire, and correlations were made between these areas. X-ray study of these clay rich beds, revealed the presence of mixed-layer, randomly interstratified mica-montmorillonite with variable amounts of kaolinite and were thus identified as K-bentonites. This mineralogy contrasts markedly with the shales above and below them, which were found to contain detrital quartz, chlorite and mica. The K-bentonite beds were thought to have originated by the alteration of wind-blown volcanic ash. Chemical analyses of the K-bentonite beds for their alkali content are shown in Table 11.

TABLE 10: Geometric Mean of the Visean/Lower Namurian Black Shales (Thomson, 1971)

Element ppm	Bowland Shale Group E1	Edale Shales South Pennines Fletcher (1968)	Clare Shale, Ireland Atkinson (1967)
Mo	17	11	27
Cu	89	110	70
Se	7.6	4.4	2.9
V	344	265	365
Pb	69	25	22
Ga	15	19	15
Ti	1700	4500	24200
Ni	122	100	54
Co	21	30	13-20
Mn	206	905	340
Cr	118	100	87
As	17	17	4-11
Fe_2O_3%	4.7	2.9	4.5

TABLE 11

Alkali Content of Selected K-Bentonites

K-Bentonite	K_2O%	Na_2O%
B_1	2.30	0.87
B_2	4.10	0.68
B_5	4.17	0.42
B_6	3.66	0.71

From the foregoing account, the general distribution of major and trace elements in the Carboniferous sediments of Britain might have been controlled by one or more of the following variables:

1. the nature of detrital or source rock
2. the rate of sedimentation
3. precipitation
4. sorption
5. redox potential
6. palaeosalinities (palaeontological evidence)

Grain size which is mostly related to the rate of sedimentation may be assessed, as has been suggested, by the following parameters:

1. quartz or free silica content
2. free silica/combined silica ratio
3. the Na^+/K^+ ratio
4. organic carbon content

5. quartz/organic carbon

6. titanium/Al_2O_3 ratio

Most of these have been shown to agree with the rate of sedimentation as derived from palaeontological studies.

In argillaceous sediments surface phenomena or sorption plays an important role in affecting the distribution of metal cations. It seems feasible that the availability of these metal cations at the site of deposition and increasing distance from shore lines would tend to give more opportunity for trace element incorporation, while a slow rate of sedimentation would also favour sorption since it allows more time for sorption to occur.

Colloidal iron monosulphides and hydroxides, organic matter, aluminium and manganese hydroxides, as well as clay minerals have a great adsorptive power, hence they form highly active sites for immobilising many dissolved ionic species. During exposure of these materials, to the depositional environment, sorption and to a lesser extent lattice substitution are recognised widely as important mechanisms, although certain geochemical differences in the trace element distribution pattern are expected to occur.

Precipitation of certain ionic species from sea water and removal or alteration of minerals under natural conditions depends upon several factors. The most important of which are:

1. the pH of the solution

2. the redox potential of the solution

3. the temperature and pressure of the solution

4. the ionic strength of the solution

5. the ionic potential of the ions in solution

Thus from the bulk chemistry of a consolidated rock, it may be difficult to decide which factors have contributed to its present state. However, the development of iron carbonates and sulphides in certain argillaceous sediments indicates a range of physico-chemical conditions under which they have formed. In this case, experimental studies on the stability of iron minerals point to the great importance of Eh-pH conditions and thermodynamic concentrations or activities of ionic species (Huber, 1958; Garrels and Christ, 1965; Berner, 1964a,1964b, 1964c; Curtis and Spears, 1968).

Many elements can exist in more than one oxidation state, like iron, manganese, sulphur, vanadium, copper and cobalt. Therefore, the association of these elements is useful in interpreting the physico-chemical conditions.

The status of a number of geochemical measurements of palaeosalinity are in doubt, for example boron, however the palaeontological evidence is most important in this connection. Thus palaeosalinities may be assessed from the macro- and micro-faunal distribution. It must be appreciated that the representation of palaeosalinity changes is relative rather than absolute, but marine, brackish and fresh water sediment can be differentiated and geochemical differences sought between the groups.

1.1.1 General Considerations

The Carboniferous clay-rich sediments may be regarded as consisting of two types of components, the detrital fraction which was derived from the source rock in particulate form, and carried in suspension; and the non-detrital fraction which was present in solution and has been formed within the sediments by some chemical means. However, this is not always the case, for there are some non-detrital phases which may be derived from detrital unstable mineral due to weathering during transportation.

The detrital fraction consists of those minerals stable during weathering, mainly quartz, rutile, zircon and to a lesser degree feldspar. The insoluble hydroxides of iron and manganese might have been transported as colloids, thus they are included with the detritals. Also, the clay minerals are regarded largely as detrital which have been derived from unstable minerals during weathering, particularly from feldspars. Organic material whether derived from land or sea are also regarded as detrital.

The non-detrital fraction includes those minerals which have been formed in the sedimentary environment by precipitation and from reaction of detrital components with solutions; pyrite and carbonates are most important in this respect.

The most important information concerning a rock is revealed from a study of the chemical processes by which the rock is formed. Classification of these events on time basis, is therefore of value in this respect. Spears (1963) described changes during weathering, transport and when the sediment is in direct contact with the depositional water, asyngenetic. Diagenetic changes involve modification beneath the sediment/water interface while the sediment is unconsolidated. Subsequent changes are termed epigenetic. It is more likely, that the first two stages are most important during the formation of a sedimentary rock.

In the course of syngenesis and diagenesis, both detrital and non-detrital minerals incorporate elements from solution by sorption (in its widest sense). The principal types of sorption are isomorphous substitution, ion exchange, absorption and adsorption. With regard to the first mechanism, the substitution may take place in the octahedral or tetrahedral sites. The governing factors are charge, ionic radius of the participating ions. Ion exchange concerns reactions taking place at the solid-liquid interface between anions and cations held at, or near, the

surface of solid materials, with ions present in the surrounding mobile phase. Absorption phenomena caused by unsatisfied valences form an essential part of ion exchange processes. In adsorption, elements are held at the phase boundary by purely physical forces. These mechanisms are discussed more fully by Degens (1965). Some principles governing sorption (Mason, 1966) are as follows:

1. The amount of sorption increases as the grain size of the adsorbent decreases, and hence its surface area increases. Thus, clay sized particles, colloids and finely disseminated organic matter are very important in this respect.
2. Sorption is favoured if the sorbate forms a compound of low solubility with the sorbent.
3. The amount of a substance sorbed from solution increases with its concentration in that solution.
4. Highly charged ions are sorbed more readily than lower charged ions.

During the accumulation of the Carboniferous clay rich sediments, sorption of one variety or another might have been an important factor in the incorporation of elements. Rubidium can substitute for potassium, particularly in the interlayer site in illite. However, some of the detrital components, especially organic matter and iron hydroxides, are rendered unstable in the depositional environment and consequently the elements enriched by them will be redistributed among the sediment compounds.

The relative importance of the original detrital contribution varies from element to element. For most of the major elements, it is probably significant with regard to Si, Al, Ti and Zr. For other elements such

as K, Na, Mg, Ca and Fe, this contribution varies, for they occupy the structural sites in the clay minerals, particularly illite and chlorite, and thus may be regarded partly as detrital.

The diagenetic minerals are responsible for the enrichment of certain major elements in the sediments. Thus, carbonate increases the contents of calcium, magnesium, manganese and iron, while pyrite undoubtedly influences the abundance of iron. Therefore some of the calcium, magnesium, manganese and iron must have been present in solution, within the sediment.

In the Carboniferous sediments, the contribution of detrital minerals is dependant on distance from shoreline and sorting during transportation. Increasing distance from shoreline is reflected in the rocks by a decrease in detrital quartz and feldspar contents and increase in clay and organic carbon contents. This varied contribution seems to have influenced parameters such a depth, sedimentation rate, fauna and may be salinity as well. The reflection of these processes is exhibited by the Carboniferous cyclothemic sequences or units, i.e. marine bands, in that the lower part of it consists of mudstone with typically marine goniatites, which is replaced in the overlying beds by Lingula indicating brackish water. The top of the marine band is marked by the presence of non-marine lamellibranchs. The marine sequence, thus passes from fully marine at the base, through progressively more brackish water until the marine element is fully lost. This trend is commonly accompanied by steadily increasing sedimentation rate, i.e. increase in grain size and quartz. Through this sequence, diagenetic minerals such as pyrite are abundant in the lower part associated with typical marine fauna, while carbonates, mostly siderite with a lesser extent of dolomite, ankerite, are associated with the brackish and non-marine parts (Spears, 1964; Curtis, 1969;

Hirst and Kaye, 1971). This full gradation in the sequence, however, is not always present and some of the faunal phases are absent in the Carboniferous sediments studied by Nicholls and Loring (1962), and Bloxam and Thomas (1969), but the relationship between iron diagenetic minerals was still similar to those mentioned above.

From the distribution of pyrite and iron carbonate and phosphate, Spears (1964) attributed this change to a trend of increasing Eh and decreasing pH from the stability field of pyrite (lower part of the sequence) into that of siderite (upper part of the sequence). While Nicholls and Loring (1962) more or less interpreted their results in a similar way to that mentioned above. Thus the change in the nature of the non-detrital iron minerals from pyrite to siderite as the succession is ascended, almost certainly reflects a change in the physico-chemical conditions within the sediment

Finally, from the preceeding discussion and inspection of the analytical data of the Carboniferous sediments, it appears that the distribution of major and trace elements have been influenced by various processes by which the elements are incorporated into the sediments. These fall under the following headings:

1. The detrital contribution is dominant for Al, Si, Ti and possibly so for certain trace elements such as Zr, Cr and B, and to a lesser extent with regard to elements occupying the structural sites in the clay minerals, such as potassium, sodium, iron and calcium in illite. Magnesium and iron are partly involved in the octahedral layer of chlorite. Rubidium, strontium and barium substitute for potassium in illite, while gallium proxying for aluminium, regardless of the type of clay mineral. Also associated with the clay minerals and possibly sorbed on them are Co, Cr, Li, Zn, Cu, Ni, Pb, V and Zr, especially by illite and chlorite.

2. Trace elements likely to be incorporated in the iron-diagenetic minerals, either through precipitation or sorption, include largely Cu, Zn, Ni, Pb, Ba, Co, As, Sn, Mo, Sr and to a lesser extent V.

3. Elements associated or sorbed by organic matter are Co, V, Ni, Zn, Cu and Mo, but on redistribution after diagenetic trans-formation releasing some of these elements to be incorporated in pyrite and siderite.

These considerations suggest that variation in the distribution of major and trace elements is to simplify interpretation of physico-chemical conditions. For most of the Carboniferous sediments, the relation between major and trace and change in palaeoenvironments, may be reflected by the following:

1. Marine or basin sediments contain less quartz and probably feldspar and more clay, particularly illite, than the brackish and non-marine sediments. This is reflected in a lower SiO_2 and Na_2O and a higher Al_2O_3 content in the former than in the latter.

2. In more general terms, marine sediments show a slightly lower Na/K ratio than the non-marine ones. This depends on the relative abundance and type of clay mineral in the clay rich sediment, while in a coarser-grained sediment, it indicates the importance of albite and illite.

3. Marine sediments generally contain higher amounts of organic matter than the non-marine sediments. However, this is not always true, for some Carboniferous sediments, which are interpreted as non-marine, have been shown to have higher organic matter than the marine ones (Sulaiman, 1972). In this case however, the organic matter

consists of detrital plant fragments which are more inert towards trace elements.

4. Marine sediments are characterised by the abundance of pyrite, while the less marine sediments show development of siderite.

The inference drawn from the above generalisation is that trace elements associated with organic matter and pyrite (Co,Ni,Cu,Pb,An,Cu) tend to be more concentrated in the marine sediment than in the brackish and non-marine sediments.

1.2 Geology of the Central Pennines

The Pennines may be divided on a structural basis into the Northern Pennines - fault blocks of slightly tilted strata; the Mid-Pennines - an area of steep north-east/south-west folds; and the Southern Pennines - an asymmetrical anticline pitching northwards (Hudson and Cotton, 1943).

The area defined as the 'Central Pennines' extends from the Craven Highlands in the north, to the Derbyshire Uplands in the south, with the Yorkshire Coalfield and the Lancashire Coalfield delineating the eastern and western limits respectively (Figure 1).

The greater part of the Pennines is occupied by Carboniferous rocks at outcrop. The Northern Pennines is occupied by Carboniferous Limestone and Yoredale beds; the Central Pennines by the Millstone Grit and some Coal Measures; and the Southern Pennines by Carboniferous Limestone of the Derbyshire Dome, flanked on the west and east by Millstone Grit and Coal Measures. The major divisions of these rocks and their approximate European equivalents are shown overleaf.

1.2.1 Palaeogeography and Sedimentation

The variation in the lithology and distribution of the Carboniferous sediment is a reflection of the prior existence of two different units. These are the massifs or 'rigid blocks' which were relatively stable regions of delayed subsidence, and the basins or 'troughs' which appear to have subsided more readily and thus received substantially greater quantitites of sediment (Figure 2)

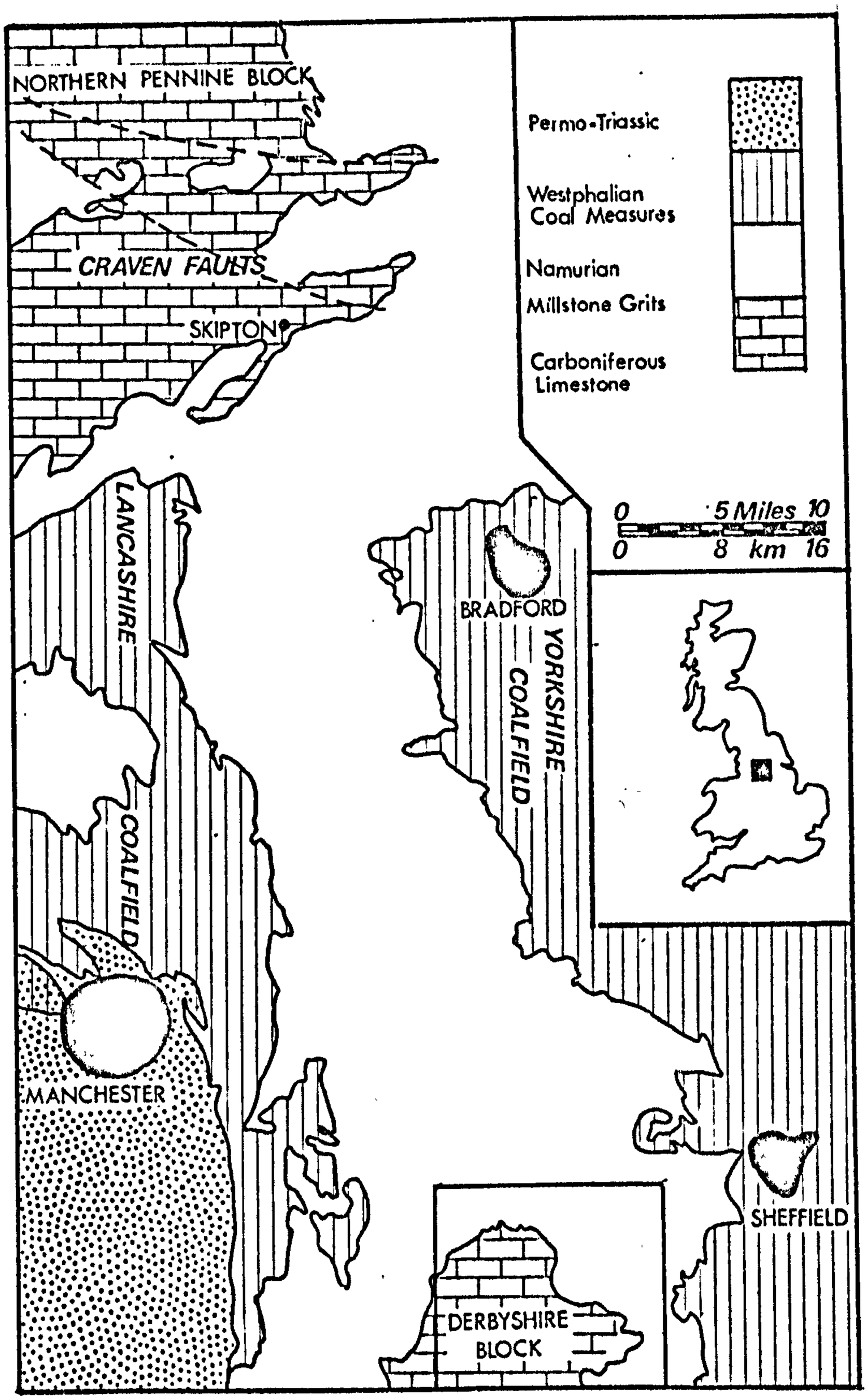

Fig.1 Map of the Central Pennine Basin, showing the general geology of the region. The study area is outlined and the overall location is shown in the inset map.

Division of the Carboniferous System

UPPER CARBONIFEROUS

Coal Measures	(Westphalian)
Millstone Grit Series	(Namurian)

LOWER CARBONIFEROUS

Carboniferous Limestone Series	(Visean and Tournaisian)

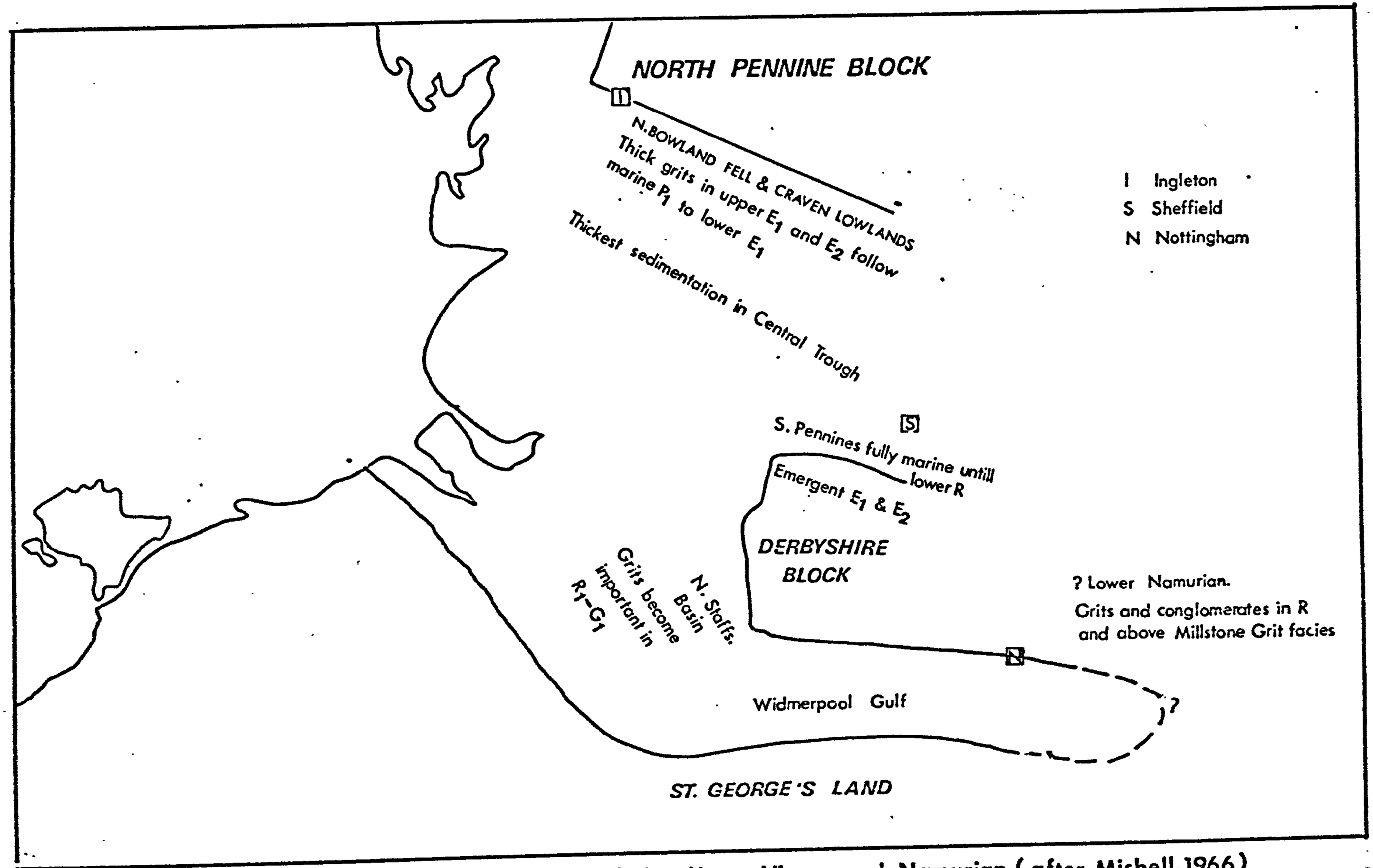

Fig.2 Palaeogeography of the Central Province during Upper Visean and Namurian (after Mishell, 1966)

The Central Pennine Basin probably developed in Lower Carboniferous times (Walker, 1966). It was bounded to the north by the line of the Craven Fault and to the south partly by the Derbyshire Massif and further south by the St. Georges Land and the Mercian Highlands (Hudson and Cotton, 1945). Subsurface and seismic data (Kent, 1966) show that on the eastern side of the Derbyshire Massif the basin extends to beyond Nottingham. The eastern and western margins of the basin are not well known. The separation of these structural areas is not always indicated by the presence of faults, however, the development of marginal limestone reefs is regarded as a transitional phase from block to basin.

During the Lower Carboniferous times, goniatite and thin shelled lamelli-branch -bearing black shales and thin argillaceous limestone were deposited in deeper water within the basin forming the basin facies. Meanwhile in the clear water over the massif, limestones were deposited forming the shelf facies. This type of sedimentation shows no obvious pattern of repetition in the sediments deposited; it was followed by a rhythmic type of sedimentation of limestone, mudstone and sandstone (Yoredale type). The last appears to have been mostly deltaic. By the end of the Lower Carboniferous times, the rhythmic Yoredale sedimentation had advanced to just north of the Craven Faults, and did not spread south where the black shale deposition continued (Bowland Shales). But in the most southern part of the basin (nearer to St. Georges Land) quartzitic sandstone cemented in places by secondary silica and carbonate, were laid down and are referred to locally as 'crowstones' (Edwards and Trotter, 1954).

In the early part of the Upper Carboniferous the deltas advanced further south into the slowly subsiding area depositing sandstones (Skipton Moor Grit) in the northern part of the basin. In the extreme south of the marine basin, beyond the influence of the dominant detrital supply, the quite deep sedimentation of the clays proceeded, depositing the Edale shales.

On the submarine surface which fronted the shallow delta southerly flowing turbidity currents were common at intervals during the sedimentation of clays (Allen, 1960). Much of the material carried by these currents was transported through major channels with widths up to 750 m and depths of

45 m(Walker, 1966). These channels are thought to cut the delta slope by the turbidity currents upslope of the submarine fans. The channels were very persistent features and extended southwards for considerable distances from the delta top and down the delta front. Towards their head, in the very shallow part of the delta, the infill is predominantly extremely coarse grained arkosic sandstones and pebbly sandstones with variable amounts of locally eroded mudflakes and siltstone blocks. The infill occurs as massive beds up to 3 m thick at the base of the channels with thin, roughly horizontal bedding, lenticular in the middle, and medium cross bedding at the top. This implies deposition from a waning current (Collinson, 1968). In the deeper water at the foot of the delta slope (submarine fans) and into the basin, two types of sediments were laid down. The first type is generally thin, parallel sided, fine grained, graded sandstones interbedded with mudstones. The sandstone have abundant sole structures and the maximum grain size is 2 mm. These represent deposition away from the delta front and are referred to as distal turbidites. The Mam Tor sandstones and the lower part of the Shale Grit in the southern part of the basin are included in this category. The second type is thick and poorly graded sandstone, interbedded with much thinner mudstone. Directional sole marks are uncommon in the sandstones which have a maximum grain size of 1 cm. These indicate deposition nearer to source and are proximal turbidites.

This type of sedimentation manifests itself in the upper part of the Shale Grit and the lowest part of the Grindslow Shales.

After the deposition of the Shale Grit, the basin was entirely filled by the submarine fans (Shale Grit phase) and there was no space at the southern end for the formation of an apron of distal turbidites (Figure 3). Gradual shallowing of the water, coupled with further southward advance

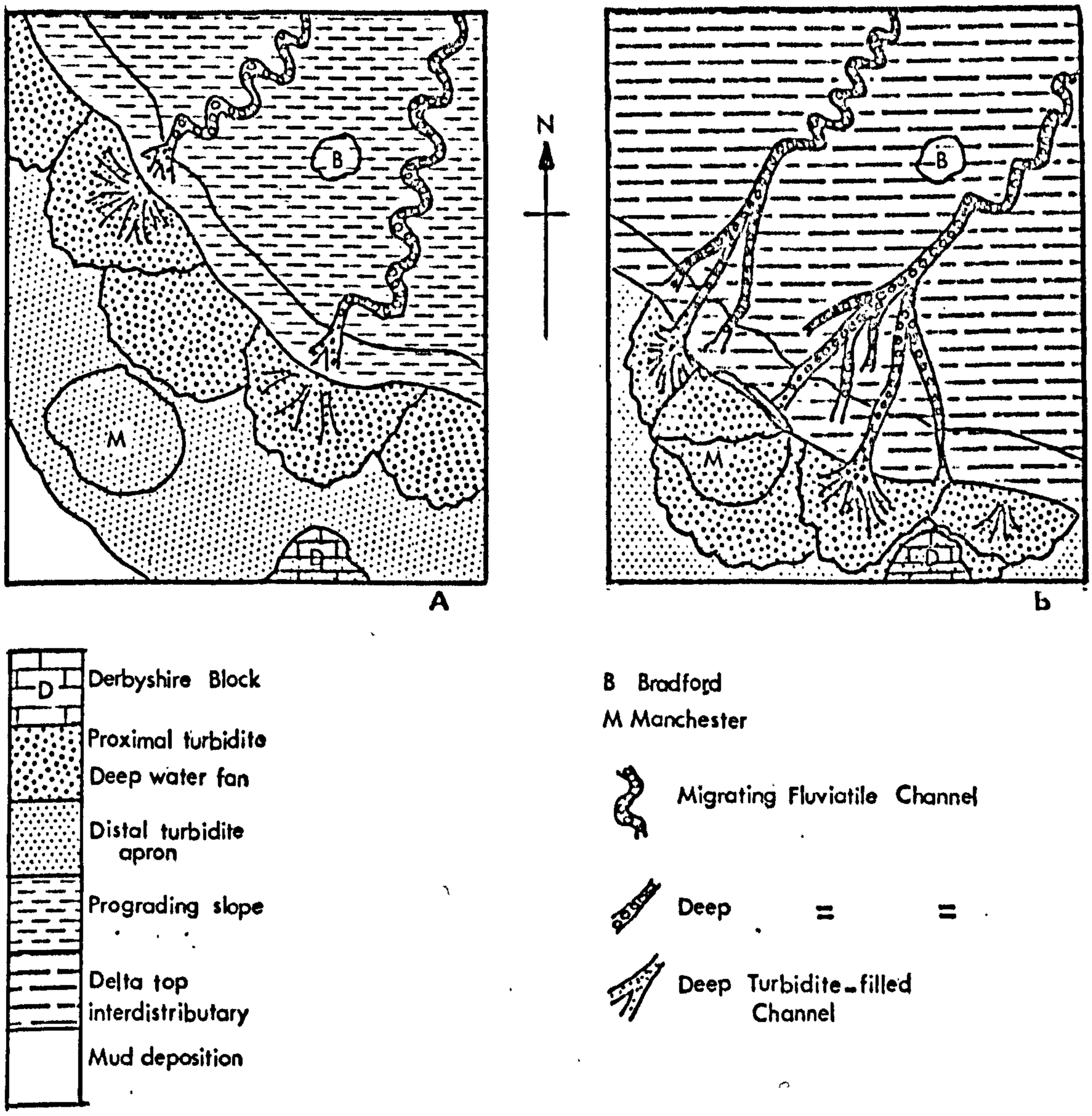

Fig.3

Maps of suggested palaeogeographies of part of the Central Pennine Basin, during earlier Namurian.

Map A shows the suggested situation at the time immediately before the deposition of Mam Tor Beds and the Shale Grit.

Map B shows the situation during the deposition of the Grindslow Shales and the Kinderscout Grit.

(After Collinson, 1968).

of the delta led to turbidity currents ceasing or certainly decreasing in importance. Thus the sediments deposited on the slope (above the submarine fans) of the delta became much sandier and coarser grained (upper part of the Grindslow Shales). At this time in the Upper Carbonifeorus, aggradation due to sedimentation, swelled up bottom topography of the basin. Thereafter sedimentation took on a deltaic character and can be grouped into delta top, front and slope deposits. Inter-distributary environments are represented by a complex association of thinly bedded, rippled, cross bedded and parallel laminated, medium coarse siltstones and sandstones with extensive burrowing activity. Migrating fluviatile channels are characterised by massive, cross-bedded, horizontal bedded and lenticular shaped coarse sandstone. This type of sedimentation is represented by the Kinderscout Grit, Middle Grit and the Rough rock. By this time the basin was covered by paralic sediments (Reading, 1964).

On the subaerial part of the delta swampy conditions were occasionally favourable for soil development and growth of vegetation, which manifest themselves in seatearth and the occasional coals.

These sediments of the late Namurian show the characteristic Millstone cyclic sedimentation (Stevenson and Gaunt, 1971). The sedimentary cycles or cyclothems consist of:

Coal
Seatearth
Siltstone or Sandstone
Grey Mudstone becoming silty upwards
Dark Mudstone frequently marine at or near the base

The cycles are often incomplete with one or more elements missing and others expanded.

One distinctive feature of these cycles is the widespread occurrence of their thin marine mudstone. This implies a sudden increase in the rate of regional subsidence over a very wide area or possibly could be due to eustatic rises of sea level (Reading, 1964; Collinson, 1968). Commonly, the end of this marine period is marked by increase in the supply of detrital material into the basin, thus making conditions unfavourable for biological activity. This silting-up continued with the rate of deposition exceeding that of subsidence, leading to the deposition of coarse sediment. Continuation of this process builds up the sediment near to, or at, water level, thus favouring plant growth and the initiation of another cycle.

Most of the features of the Upper Carboniferous are shown in the hypothetical palaeogeographic reconstruction of Figure 4 (after Walker, 1966). It shows the facies of North Derbyshire arranged laterally rather than vertically and gives the interpretation of the facies in terms of their environment. The observed vertical facies sequence can be visualised in terms of a southward advance of the facies belts - with successive facies lapping onto the Derbyshire Massif.

Finally, to sum up these events, the sequence ranges from the Edale Shales (marine basin shale), through the Mam Tor sandstones (distal turbidites) and the Shale Grit (distal with subordinate proximal turbidites) into the Grindslow Shales (slope environment) which is covered in turn by the near shore or coastal plain Kinderscout Grit, Middle Grit and the Rough Rock, indicating a southward advance of the deltas into the North Derbyshire area. The eustatic rise in sea level during sedimentation manifests itself as a thin marine mudstone which is then overlain by a coarsening upward sequence.

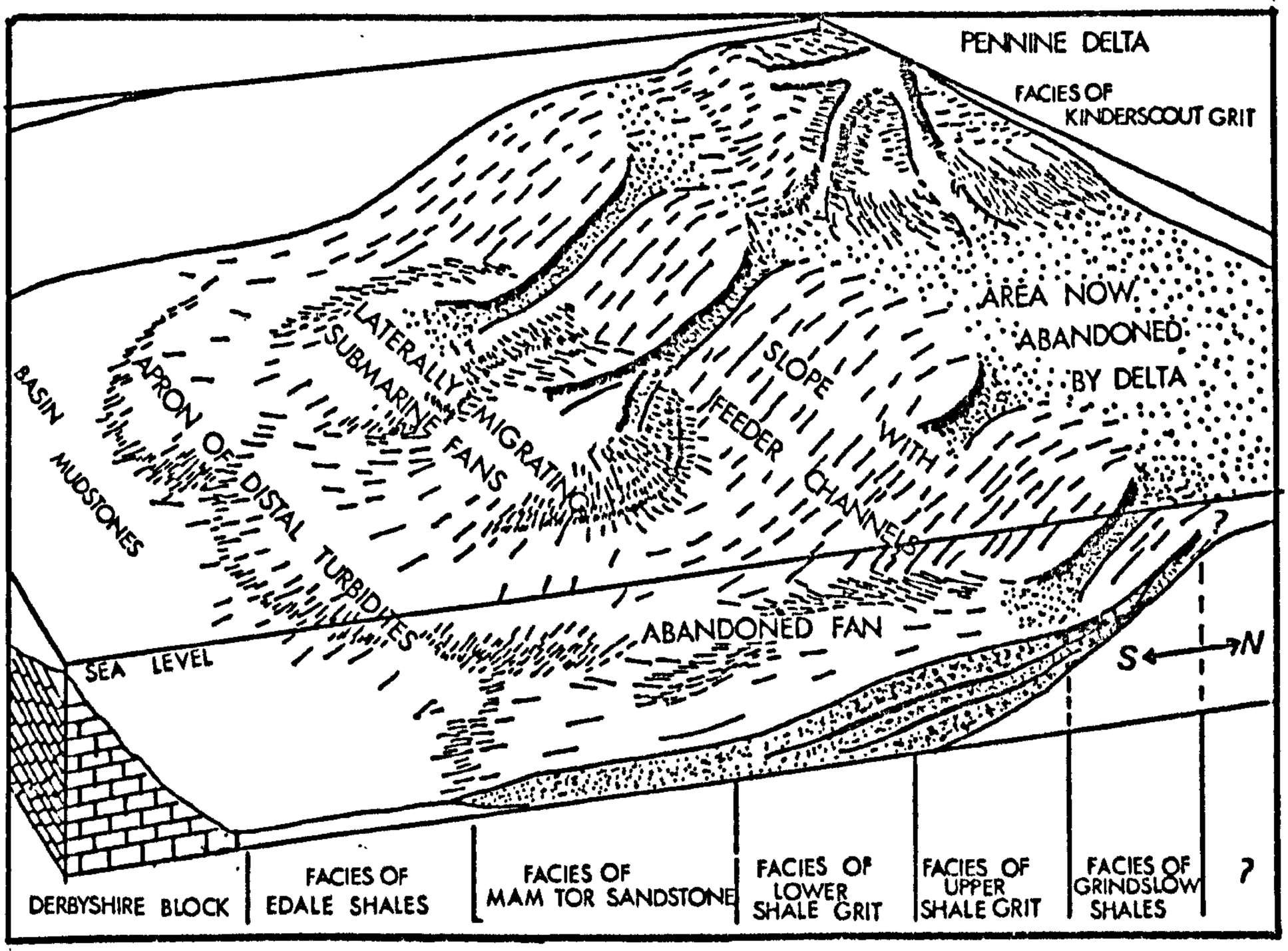

Fig.4

Hypothetical reconstruction of the Namurian R_{1c} zone facies of North Derbyshire, arranging the formations laterally rather than vertically and giving interpretations of their environments of deposition. The observed vertical sequence can thus be visualised in terms of a southward advance of facies belts. (After Walker, 1966)..

1.2.2 Classification of the Namurian (Millstone Grit Series)

The Millstone Grit facies is characterised by the occurrences of thin, goniatite-bearing mudstones and these are used to recognise the stages and zones into which the Namurian has been divided. The base of the Namurian is defined at the entry of Cravenoceras leion; the top is defined as the base of the Gastrioceras subcrenatum Marine Band. Stages and zones of the Namurian are listed in Table 12 (after Stevenson and Gaunt, 1971).

The chief lithostratigraphic division of the Millstone Grit, in the Chapel-en-le-Frith district are as follows:

Rough Rock Group: Yeadonian Lower Gastrioceras Age (G_1)

Six-Inch Minor or Pot Clay Coal
Rough Rock and Rough Rock Flags } G_{1b}

Shales with Gastrioceras cancellatum Marine Band at Base (G_{1a}-G_{1b})

Middle Grit Group: Marsdenian (Upper Reticuloceras Age, R_2)

Shales with Redmires Flags, Simmondley Coal and Ringinglow Coal
Chatsworth Grit } R_{2c}

Shales with Roaches Grit and Corbar Grit (Ashover Grit) and Heyden Rock; Reticuloceras gracile Band at base (R_{2a}-R_{2c})

Kinderscout Grit Group: Kinderscoutian (Lower Reticuloceras Age, R_1)

Kinderscout Grit
Shales
Shale Grit
Mam Tor Beds } R_{1c}

Upper part of Edale Shales with Homoceras magistrorum Band at the base (R_{1a}-R_{1c})

TABLE 12: Stages and Zones of the Namurian

Stage	
Yeadonian (G_1)	Gastrioceras cumbriense (G_{1b})
	G. cancellatum (G_{1a})
Marsdenian (R_2)	Reticuloceras superbilingue (R_{2c})
	R. bilingue (R_{2b})
	R. gracile (R_{2a})
Kinderscoutian (R_1)	R. reticulatum (R_{1c})
	R. nodosum (R_{1b})
	R. circumplicatile (R_{1a})
Alportian (H_2)	Homoceratoides prereticulatus (H_{2c})
	Homoceras undulatum (H_{2b})
	Hudsonceras proteus (H_{2a})
Chokierian (H_1)	Homoceras beyrichianum (H_{1b})
	H. subglobosum (H_{1a})
Arnsbergian (E_2)	Nuculoceras nuculum (E_{2c})
	Cravenoceratoides nitidus (E_{2b})
	Eumorphoceras bisulcatum (E_{2a})
Pendleian (E_1)	Cravenoceras malhamense (E_{1c})
	E. pseudobilingue (E_{1b})
	C. leion (E_{1a})

Beds below Kinderscout Grit Group: Alportian, Chokierian, Arnsbergian and Pendleian (Homoceras H_2, and H_1, and Eumorphoceras E_2 and E_1)

Lower part of Edale Shales: bed with Cravenoceras leion at base

1.2.3 Thickness and Lithological Variation of the Namurian (Millstone Grit)

In the Central Pennine Basin, the Namurian shows its maximum thickness in the northern part, around Skipton, where it reaches 1350 metres (Stephen et al. 1953). It suffers irregular attenuation in a south-easterly direction; the sequence is 405 metres thick around Ashover, and about 165 metres east of Matlock (Smith et al, 1967). However, the Namurian sequence in north-east Staffordshire (west of the Derbyshire Massif) reaches a thickness of 1290 metres (Evans et al, 1968). The thickness of the different ages of the Namurian in the aforementioned areas are as follows:

Age	North Metres	South-East Metres	South-West Metres
G_1	68.18	36.36	71.21
R_2	159.00	288.00	356.36
R_1	242.42	39.39	178.18
H	68.18		128.18
E_2	60.16	45.45	292.12
E_1	697.00		242.42

The variation in thickness seems to be not only the result of variation in subsidence in the area of deposition, but it is further complicated by the relative amount of detrital contribution either from the north or south.

The main rock types of the Namurian are sandstones, often coarse (known as grits) and the interbedded siltstones and mudstones in which

marine fossils are confined to thin bands of dark grey mudstone. There is generally great lateral and vertical variation in the arenaceous beds and their associated silty mudstones, but in contrast the marine mudstone bands with goniatites show a widespread geographical persistence. Figure 5 shows the north-south thickness variation and sedimentation facies of the Namurian of the Central Pennine Basin.

Near the source of the detrital sediment coarse sand is dominant and it decreases in abundance away from the source towards the deep basin where fine sand, silt and clay are dominant. For example the Mam Tor sandstones and Shale Grit (fine grained distal turbidites) thin to the south and south-west of the Peak District, and would appear to be replaced by shales (Green et al. 1887; in: Allen, 1960). Towards the north they maintain their individuality as far as the Holmfirth and Rochdale districts (Mid-Pennine) where they pass into thick coarse sandstones (Stephen et al. 1953), which are distinct from those of the flysch-like Mam Tor sandstones and Shale Grit. Generally this southward thinning is exhibited by most of the Namurian sandstones. In contrast, the Ashover Grit, which in the south-eastern part of the basin ranges from 60-90 metres in thickness, and consists of medium coarse grained sandstone with bands of pebbles thins northwards and passes into a fine grained sandstone interbedded with siltstone and mudstone (Smith et al. 1968).

1.2.4 Source and Derivation of the Upper Darboniferous Sediments

The first sedimentological study of the Namurian (or Millstone Grit Series) in the Central Pennine Basin was carried out by Sorby (1859) who concluded that the sediments had been derived from a crystalline terrain lying to the north-east. This conclusion was later substantiated by Gilligan (1920) who showed that the only possible source area lay in the

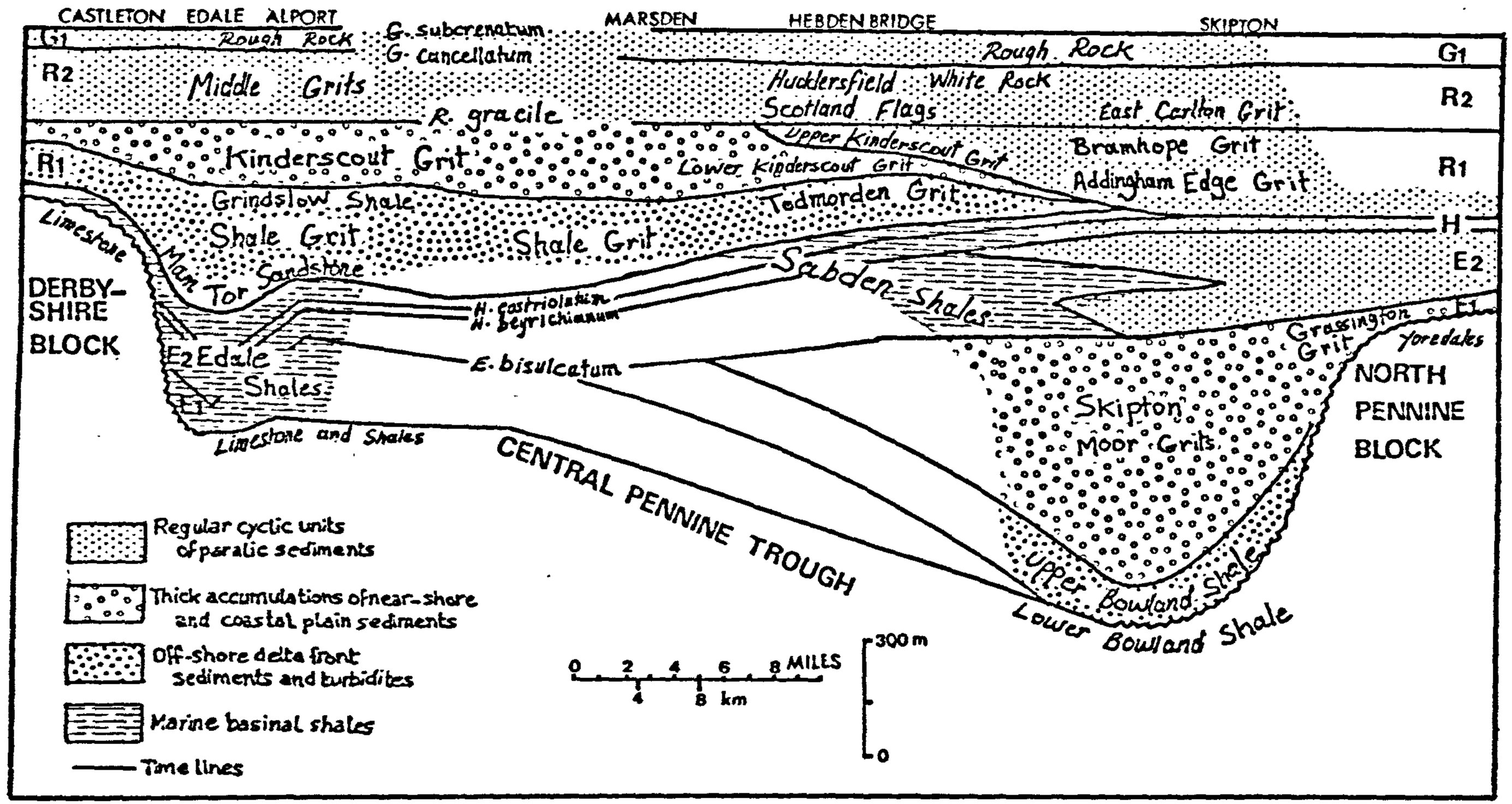

Fig.5 Diagrammatic cross section of the Namurian of the Central Pennine Trough. (Reading, 1964)

north of Scotland and its continuation north-eastwards towards Scandinavia. The mineralogical constitution of the sediments strongly suggested that the northerly land mass consisted of gneisses, schists and granites. The presence of fresh feldspar in some sediments and absence in others was attributed to variation in weathering.

This broad palaeogeographical picture was confirmed by cross bedding and sole mark measurements (Allen, 1960; Mason, 1961; Walker, 1966; Collinson, 1968).

In contrast to this dominant northerly derivation, some of the Namurian sediments in the south and south-western parts of the basin are thought to have a southerly source. In the Alport valley and the type area of Edale, siliceous mudstones and siltstones, known as Alport Crowstones (E_1) are believed to be derived from the south (Reading, 1964), and in north-east Staffordshire crowstones up to (H_2) were also derived from the south (Holdsworth, 1964b; in Evans et al. 1968) based on direction of sole structures. These crowstones were considered by Holdsworth (1963; in Stevenson and Gaunt, 1971) to have been deposited by northward flowing turbidity currents bringing material from the south Midland Landmass. Mayhew (1966) concluded that the Ashover Grit was deposited from a river system flowing from the south-east and St. Georges Land and its extension eastwards was believed to be the source.

From this brief resume, sedimentation in the Central Pennine Basin is apparently governed by a variety of factors, including proximity to, and episodic uplift of the source area, differential subsidence in the area of deposition, variation in provinance and widespread changes of sea level.

1.3 Lithology and Stratigraphy of the Studied Rocks

The Namurian rocks studied in this investigation come from the Mam Tor Beds at the type locality of Mam Tor and from a borehole at Tansley,

Derbyshire (Figure 6). For detailed information the reader is referred to Stevenson and Gaunt (1971) and Smith et al. (1967).

1.3.1 Mam Tor Beds

The type locality (Sheet No. 399, 1 inch,SK128835,Grid Reference) lies to the north of the main Carboniferous Limestone outcrop of the Derbyshire Dome. The Mam Tor Beds consist of alternating sequences of sandstones, siltstones and shales originally described by Jackson (1927), as the Mam Tor Sandstones. This name was found inappropriate when these beds were examined over a large area, as the sandstone was often not well developed. For this reason the term 'Mam Tor Beds' has been introduced (Gaunt; in Stevenson and Gaunt, 1971) although synonymous with the older term.

The following description is largely based on the detailed study carried out by Allen (1960) and Mason (1961):

At this locality the highest Edale Shales and some 120 metres of the Mam Tor Beds are exposed in the landslip-scar on the eastern side of the hill. The passage from the Edale Shale to the Mam Tor Beds is marked by increase in the silt content of the shales and the development of some thin sandstones, which form a transition to the overlying beds.

The succession of the Mam Tor Beds is made up of large numbers of cyclic units, the whole showing certain similarities to flysch deposits. The cyclic unit which usually varies from 0.90 to 2.42 m in thickness, consists of massive sandstones at the base grading upwards through laminated sandstones and laminated siltstones into shales and mudstones. The overall sedimentary pattern has affinities with the Edale Shales at the base, there being a marked shale component, towards the top the sandstone component increased in abundance, indicating an approach to shale

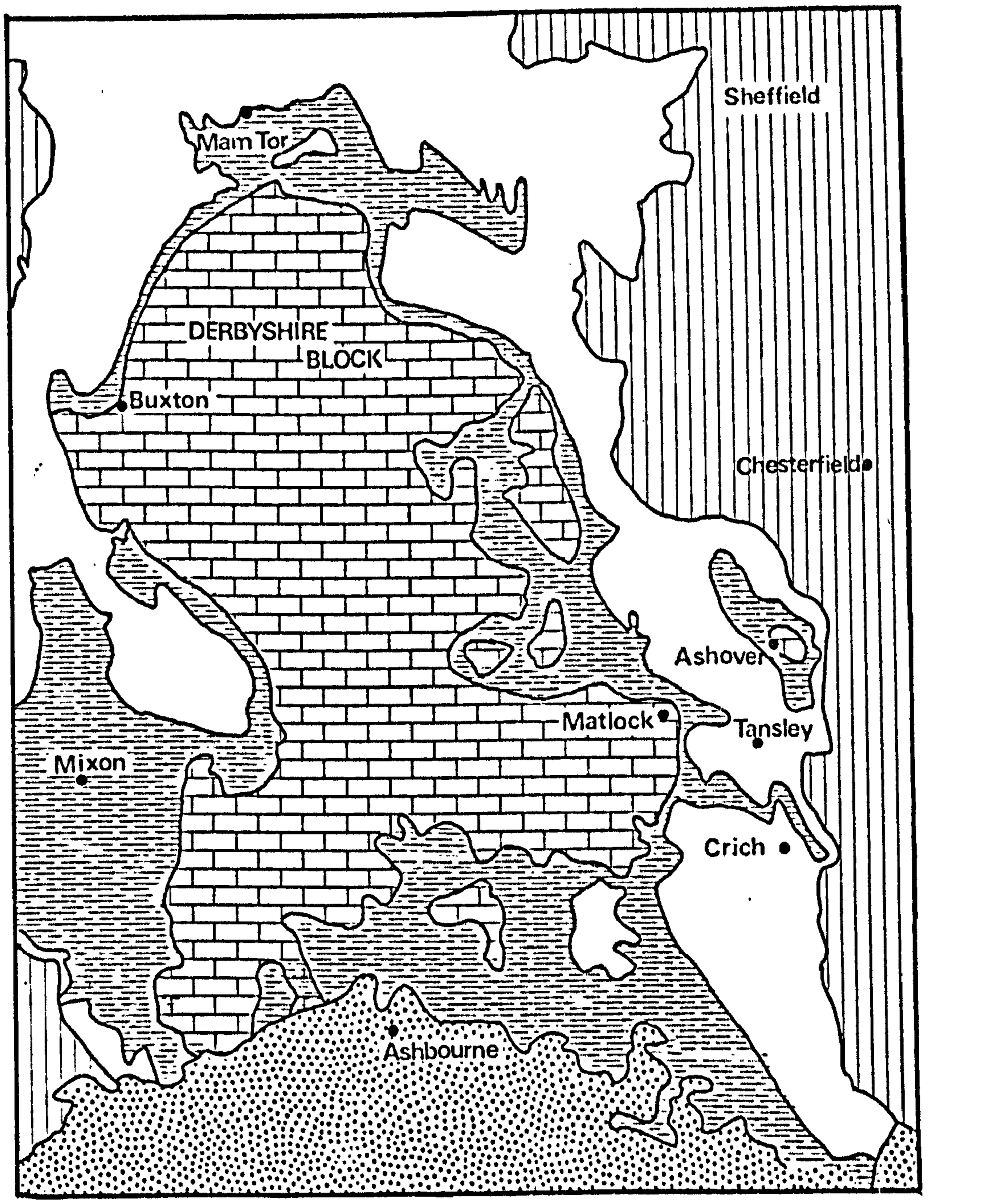

Fig.6 Geological map showing the location of Mam Tor and Tansley.

grit conditions. Likewise, the shales become sandier in the higher parts of the succession. The shales yield, in places and specially towards the base, Reticuloceras reticulatum, indicative of the R_{1c} zone. The underside of the sandstones bear a variety of sole markings, those of most importance are: grove casts, flute casts, trail casts and burrows, and load casts. In addition grading (upward decrease in grain size) is exhibited by the sandstones. Penecontemporaneous deformational structures include, convolute bedding, crumpled bedding, slump ball structures and corrugated bedding.

The Mam Tor Beds are interpreted (Allen, 1960) as a sequence of turbidites originating at intervals on the delta slope to the north. The sandstones represent rapid deposition interupting the slow accumulation of clays in the marine environment.

The Samples (Mam Tor Beds)

Three small sections were sampled at the type locality (SK128835 Grid reference), along the face of the Mam Tor Beds. The vertical gap between section A and B is about 3 metres, and that between B and C is 5½ metres. Specimens were taken from the middle part of the thin individual beds of either sandstone or shale. Whereas, in the case of thick beds, specimens were collected from the lower, middle and upper parts.

The succession largely consists of alternating fine-medium grained sandstones and shale. Nevertheless, sometimes transition from shale to sandstone is through silty shales or shaly sandstone.

White mica flakes are common in both sandstone and shale, but are more conspicuous and coarser grained in the former. Generally both sandstone and shale develop a brown rusty colour on the weathered surface.

The position of each sample is depicted in Figure 7 which is a composite section and their description is given in the following Table (13).

1.3.2 Tansley Borehole (NGR. SK 33045958)

Tansley lies in the Ashover area of Derbyshire sited to the east of the Carboniferous Limestone outcrop of the Derbyshire Dome. Almost all the Namurian succession is present, together with the P and D_2 zones of the Carboniferous (Visean) and the associated Upper Lava of Matlock. The following information is taken from Ramsbottom et al. 1962:

The Namurian: There is no break between the Visean and Namurian, the limestone of the Carboniferous Limestone Series passes upwards into transitional beds of shale with bands of limestone, near the top of which a band with Cravenoceras leion Bisat is taken as marking the base of the Namurian.

The highest beds encountered in the borehole where the main part of the Ashover Grit occurs between 20.38 m and 81.73 m although thin bands of sandstone continue to 166.58 m. A thin seatearth rests on the Grit and in turn is overlain by 45 cm. of black shale with fish debris. Apart from the rare plant fragments these were the only fossils found above the Ashover Grit.

The Ashover Grit, apart from a 2.40 m band of mudstone and seatearth near the top, consist of sandstone in which coarse crystalline dolomite is present as a cement. Below is a group of argillaceous, micaceous siltstones with sporadic bands of sandstones in which the cement consists of ankerite, siderite and calcite. The only fossils found inthese beds are scattered plant fragments Belorhaphe kochi from 126 m to 129 m and fish scales at 130.88 m.

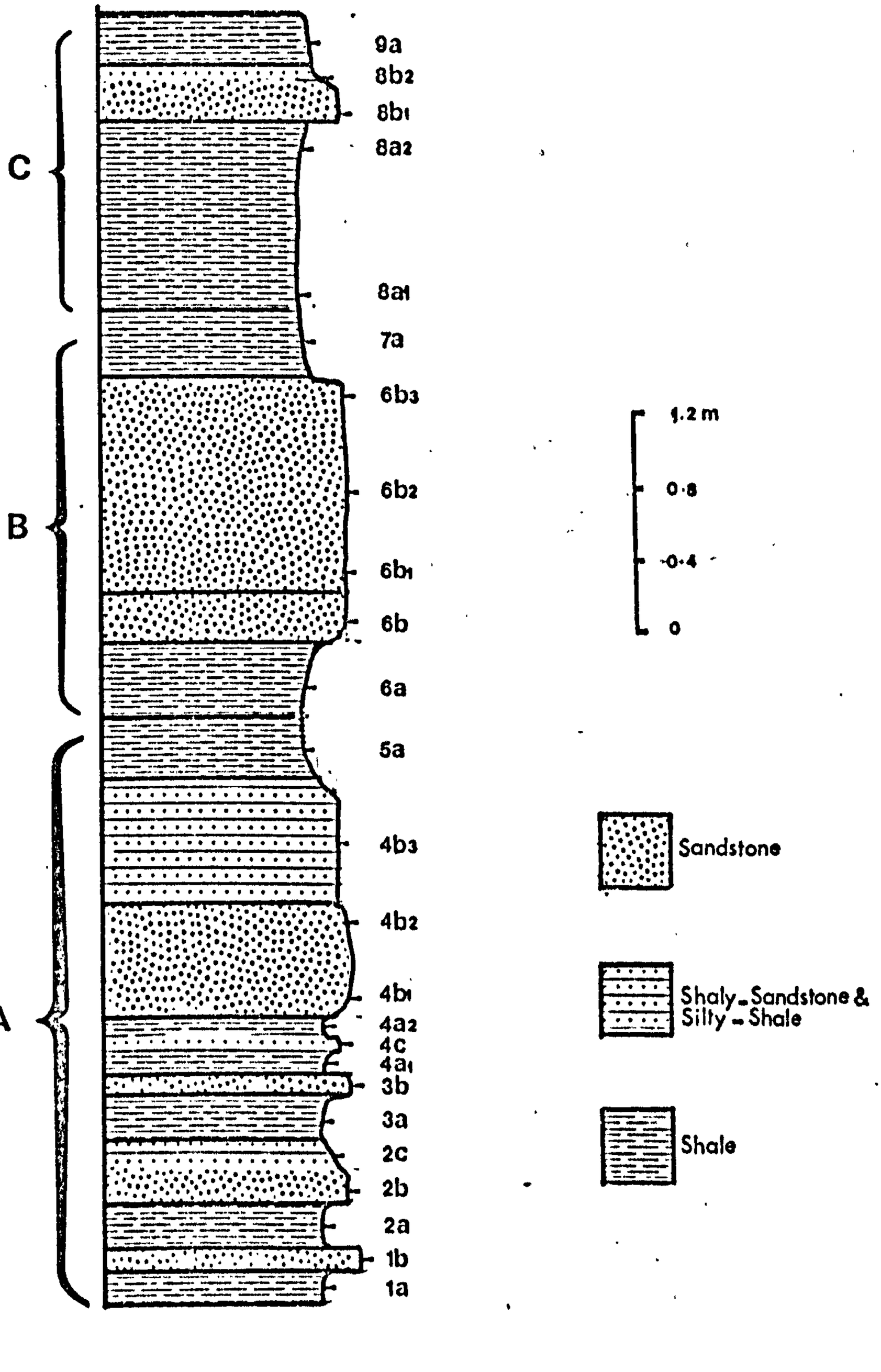

Fig. 7 Composite section of the Mam Tor Beds.

TABLE 13: Lithological Description of the Mam Tor Rocks

Sample Number	Description
Top	
9a	Black, fissile shale, with minute mica flakes.
$8b_2$	Grey sandstone with shale partings and mica flakes.
$8b_1$	Grey sandstone with fine mica flakes.
$8a_2$	Black, slightly fissile fine grained shale with mica.
$8a_1$	Black, slightly fissile, fine grained shale with minute mica.
7a	Black, fine grained, fissile shale.
$6b_3$	Brownish-grey sandstone with large mica flakes.
$6b_2$	Brownish-grey sandstone with mica flakes.
$6b_1$	Grey sandstone with mica flakes.
6b	Brownish-grey sandstone with mica flakes.
6a	Black, slightly fissile shale with mica flakes.
5a	Black, slightly fissile shale with minute mica flakes.
$4b_3$	Brownish-grey shaly sandstone with mica flakes.
$4b_2$	Grey sandstone with fine lamination and mica flakes.
$4b_1$	Laminated dark-grey with few mica flakes on outside part and light grey inside.
$4a_2$	Black, fissile shale with minute mica flakes.
$4a_1$	Grey, finely laminated siltstone with small mica flakes.
4a	Black, fissile shale with mica flakes.
3b	Grey sandstone with minute mica flakes.
3a	Greyish-black, finely laminated silty shale with mica flakes.
2c	Grey, silty sandstones with abundant mica flakes.
2b	Grey sandstone, with mica flakes and shows slight laminations.
2a	Black, fine grained, fissile shale.
1b	Grey sandstone with finely disseminated white mica flakes.
1a	Black, fine grained shale which show slight fissility

The strata below the siltstones are largely dark grey mudstones often silty above the R. reticulatum horizon. The marine fossils above this horizon occur in beds which are not silty and which form a small proportion of the succession. The goniatites are found in distinct thin bands within these fossiliferous beds.

Ironstone bands occur sporadically in the mudstones, and bands of cank (ankerite-dolomite) are found usually in those mudstones containing marine fossils. Pyrite occurs as granules, nodules, crystals and rods, although these forms are usually confined to well defined bands which rarely contain marine fossils.

Below the R. reticulatum horizon there is a closely packed sequence of goniatites and other phases with some occasional apparently barren bands. Ironstone is rare, but cank is more frequently found. Pyrite occurs in the same form as above, but is even more abundant and usually associated with the less marine and apparently non-marine phases, although in certain instances marine shells are preserved in pyrite. Table 14 summarises the proved faunal succession.

Throughout the largely marine sequence (Lower Reticuloceras, Homoceras, and Upper Eumorphoceras) several distinct faunal phases have been recognised (Ramsbottom et al. 1962). These tend to occur in definite order which reflects the cyclic nature of the sedimentation. The major faunal phases are: (1) Fish phase: (2) Planolites phase: (3) Lingula phase: (4) Mollusc spat phase: (5) Anthracoceras or Dimorphoceras phase: and (6) Thick shelled goniatite phase.

The order in which these phases are listed is that in which they occur in the cyclic succession, although seldom is any cycle found which is complete. The sequence of these faunal phases is thought to represent the incursive stage of increasing salinity associated perhaps with increasing depth. A phase marking the end of a faunal sequence may

TABLE 14: The Zones and More Important Horizons Proved in the Tansley Borehole

Stage	Zone	Thickness in Metres	More Important Marine Horizons Proved
R_2	Reticuloceras bilingue	193.01	R. bilingue (Salter), R. bilingue early mut. Bisat
	R. gracile	6.95	R. gracile Bisat, R. gracile early mut.
R_1	R. reticulatum	17.85	R. reticulatum
	R. eoreticulatum	10.43	R. of the moorei/stubblefieldi group Homoceras cf. striolatum R. eoreticulatum and R.nodosum
	R. circumplicatile	7.43	cf. R. dubium R. adpressum and R.todmordenense Homoceras henkei and Homoceratoides varicatus
H	Homoceras eostriolatum	4.15	Homoceratoides prereticulatus Homoceras eostriolatum Homoceras undulatum Homoceras smithi Hudsonoceras proteus
	Homoceras beyrichianum	7.26	Homoceras beyrichianum
	Homoceras subglobosum	4.34	Homoceras sp. nov. H. subglobosum
E_2	Nuculoceras nuculum	4.24	N. nuculum with Eumorphoceras bisulcatum and E.bisulcatum mut.β N. nuculum N. nuculum with Cravenoceratoides fragilis
	Cravenoceratoides nitidus	10.71	Cravenoceratoides cf. nititoides brachiopods and trilobites Cravenocreas holmesi Cravenoceratoides edalensis
	Eumorphoceras bisulcatum and Cravenoceras cowlingense	2.30	Cravenoceras sp. and E. cf. bisulcatum
E_1	Cravenoceras malhamense and Eumorphoceras pseudobilingue	5.63	No goniatites, abundant fish debris, a few lingula and conodonts
	Cravenoceras leion	3.93	Eumorphoceras sp. with brachiopods, crinoid debris and a trilobite Cravenoceras leion

be followed by apparently barren beds which may indicate the establishment of non-marine conditions.

Carboniferous Limestone Series (Visean)

Cawdor Group (P_2): The uppermost rocks of the Visean consist of mudstones with bands of dark limestone about 13.70 m thick from 288.82 m to 302.5 m. These are underlain by 5.38 m of dark limestone with sporadic mudstone parting, down to 307.86 m. These rocks are considered to be of Posidonia age. The lower goniatite is Neoglyphioceras at 300.70 m and beds above this are of P_2 age, while those below are of P_1 age.

Matlock Group (D_2): This group consists generally of grey to light grey limestone, just over 30 m. thick, and contains a porcellaneous bed near the middle. Fossils are scattered through the limestone, and the most notable of these is Lithostrotion. The upper beds commonly contain a flat Gigantoproductid. At 338.03 m, there is a molluscan fauna consisting of gastropods including Euphemites sp. a Nuculid lamellibranch and Pseudamussium.

Volcanic Rocks: This is followed by basaltic lava, 4.5 m of which were penetrated at Tansley (the Upper Lava of Matlock). The top of the lava flow consists of toadstone clay which is probably detritus, largely of basaltic origin. This clay is about 82.50 cm thick, the top 3.8 cm contains brachiopod fragments, Grains of pyrite are fairly common in the clay.

The Samples

The samples were collected from the core store of the Institute of Geological Sciences, Leeds. The following Table (15) lists the sample number, the depth at which they were encountered, lithology, and its

representative faunal phase. The position of each sample, through the section, is illustrated in Figure 8.

1.4 Associated Igneous Rocks

Basaltic igneous rocks occur in the Lower Carboniferous rocks of Derbyshire, Staffordshire and Nottinghamshire (Edwards and Trotter, 1954). In Derbyshire they are locally called 'toadstones', and constitute a basic series of both contemporaneous and intrusive rocks, comprising lava flows, tuffs, agglomerates, sills and dykes, which are generally confined to the upper half of the known thickness of the Carboniferous Limestone. A full description appears in Arnold-Bemrose (1907), Sargent (1918) and Tomkeieff (1926).

The lavas range from olivine basalt to olivine dolerite in mean grain size and are amygdaloidal because of their extrusive nature. The rock itself consists of ferromagnesian minerals which are commonly altered to chlorite and iron oxides. Pseudomorphs of olivine phenocrysts are sometimes infilled by calcite and rimmed by ilmenite and hematite. Plagioclase laths range in composition from albite to oligoclase and are generally altered. The groundmass consists of a mesh of feldspar laths and fine grained alteration products in which pyrite is sometimes found. In the least altered specimens the essential ferromagnesian minerals are olivine and augite. However, specimens from outcrop as well as boreholes are invariably altered through chloritisation, carbonation and haematisation which is attributed to late stage hydrothermal alteration, rather than subaerial weathering (Smith et al. 1967).

The basaltic lava flows are usually overlain by green clay (or brown if oxidised) which is generally called 'toadstone clay' in which fragments of fine grained basalt occur. In addition pyrite is a conspicuous mineral

TABLE 15: Sample Number, Depth*, Lithology and Faunal Phase of the Tansley Borehole Rocks

Sample Number	Depth in Metres	Lithology	Faunal Phase
1	19.60	Shale, slightly silty	Fish debris and plant fragments from 19.60 m to 178.5 m. Fish scales and scattered plant debris Belorhaphe kochi at 127.73 m and 128.53 m.
2	23.48	Sandstone, grey, fine grained, with many micaceous parting	
3	28.80	Seatearth, dark grey to grey, sandy	
4	60.48	Sandstone, grey purple, brown and pink; coarse to medium grained, locally very micaceous; graded bedding common throughout; false bedded in parts; rusty joints	
5	65.40		
6	66.30		
7	67.35		
8	87.06		
9	95.95		
10	100.90		
11	104.13	Siltstone, dark grey argillaceous with bands of light grey to brownish-grey sandstone up to 3.9 m; burrow in top 33.6 m.	
12	110.15		
13	115.23		
14	127.73		
15	128.53		
16	129.55		
17	130.88		
18	135.08		
19	140.40		
20	141.00	Mudstone grey to dark grey, silty except 140.03 m to 141.2 m, sporadic thin ironstone bands	
21	141.03		
22	141.83		
23	150.60		
24	151.78		
25	166.75	Siltstone, dark grey argillaceous	
26	170.43	Mudstone, dark grey, silty in parts above 172.9 m, with sporadic thin ironstone bands, numerous pyrite granules from 173.48 m to 173.55 m.	
27	170.65		
28	173.50		
29	178.50		Lingula Barren changes to Goniatite
30	178.85		
31	178.98		
32	179.08		
33	179.10	Mudstone, dark grey	
34	179.35		
35	179.48		
36	179.61		
37	181.03	Mudstone, dark grey with 0.08m 'cank' at base	Spat

* Converted from ft to m.
1 ft = 30 Cm

TABLE 15 (continued):

Sample Number	Depth in Metres	Lithology	Faunal Phase
38	185.40	Mudstone, dark grey laminated, silty; with sporadic thin ironstone bands and pyrite nodules	Goniatite Fish Fragments
39	186.90		
40	188.40		
41	191.93		
42	192.66		
43	193.80		
44	195.04		
45	198.30		
46	201.49	Mudstone, dark grey silty, slightly canky at about 201.9 m.	
47	201.68		
48	201.86		
49	202.04		
50	202.63		
51	205.80	Mudstone, dark grey, laminated near the top, with pyrite	Fish scales
52	207.98		Spat
53	209.18	Mudstone, dark grey, with 0.11 m cank at at 210.11 m.	Goniatite
54	210.11		
55	227.43	Mudstone, dark grey, ankeritic in bottom 0.15 m.	Goniatite, A/D
56	228.28		Goniatite, Spat
57	228.96	Mudstone, dark grey, canky from 229.33 m to 229.42 m	Goniatite, A/D
58	229.35		
59	238.45	Mudstone, dark grey with pyrite nodules	Goniatite
60	240.38	Mudstone, dark grey	Spat
61	241.24	Mudstone, dark grey	Goniatite
62	255.43	Mudstone, dark grey	Spat
63	256.33	Mudstone, dark grey, slightly calcareous	Spat
64	262.64	Mudstone, dark grey with pyrite nodules	Spat
65	271.40	Mudstone,dark grey, canky	Spat-fish
66	279.03	Dolomite, dark grey carbonaceous, with few patches of collophane	Leiopteria longirostrio
67	285.25	Mudstone, dark grey, canky	Posidonia,A/D Goniatite
68	288.03	Mudstone, dark grey, calcareous, with pyrite nodules	Barren

TABLE 15 (Continued):

Sample Number	Depth in Metres	Lithology	Faunal Phase
69	289.18	Mudstone, dark grey, calcareous, with pyrite nodules	Carboniferous Limestone Series
70	298.53	Mudstone, dark grey, calcareous	
71 72 73	338.25 338.30 338.40	Clay, grey at top, green below, with rounded inclusions of amygdaloidal basalt, abundant pyrite in top 0.43 m; and it forms the toadstone clay which is 0.83 m thick. Contains brachiopod fragments	

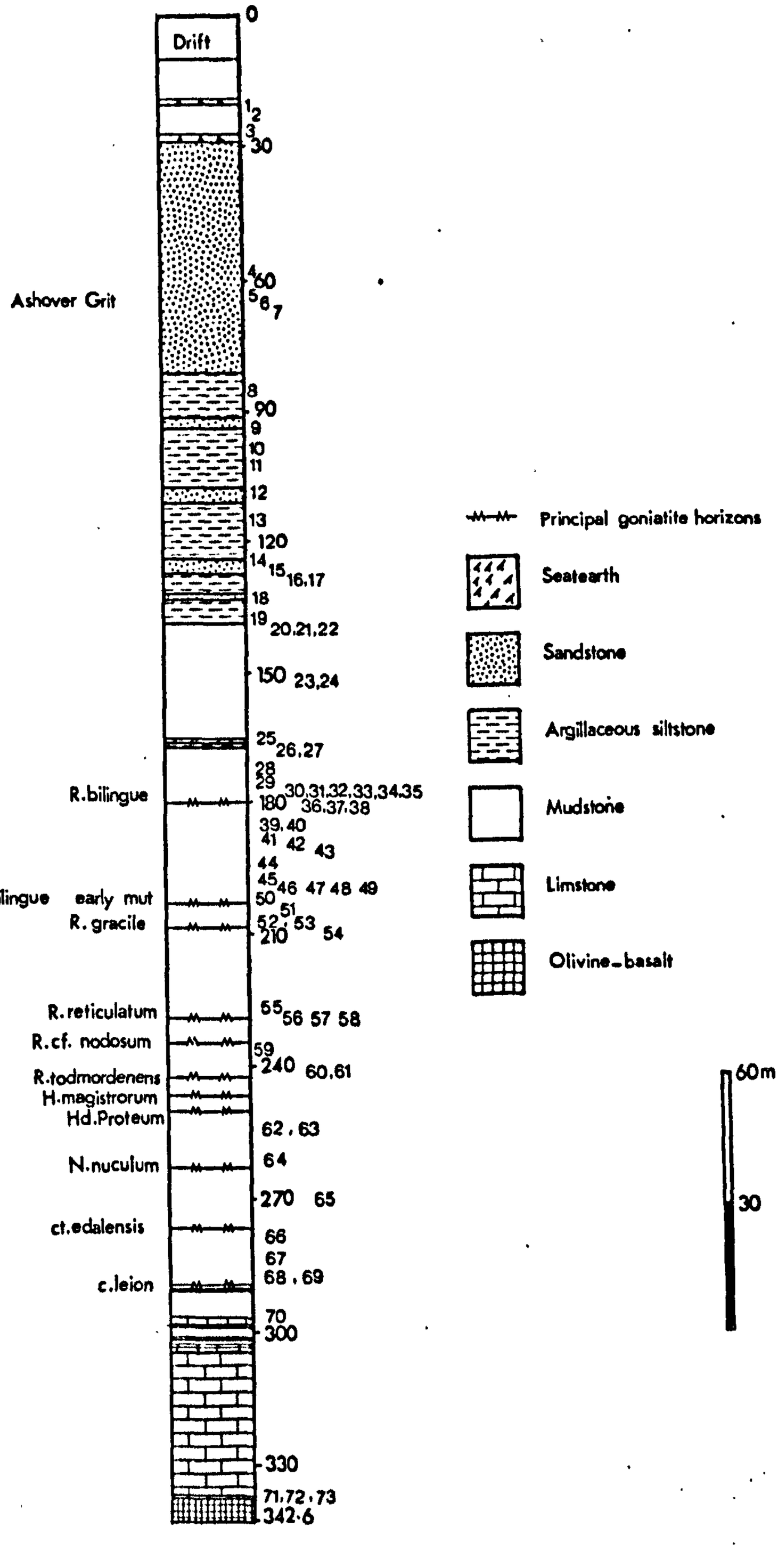

Fig.8 Section of the Tansley Borehole(after Ramsbottom et al. 1962)

1-73 are the numbers of samples.

in these clays. The toadstone clay generally represents alteration products of the lava flow itself. However, the same type of alterations, from the Upper Lava of Matlock, have been reported to occur under sub-aerial weathering (Garnett, 1923).

CHAPTER 2

Experimental Techniques

In this Chapter the techniques used to prepare the samples for mineralogical and geochemical studies are described.

2.1 Sample Disaggregation

The samples were broken into pea-size fragments and the associated fine grained material discarded. Then about 50 grams of the sample were placed in a 1000 ml. polythene bottle containing 800 ml. distilled water, and mechanically shaken for a period of two to four days. It was hoped to disaggregate the samples without altering the grains.

2.2 Size Separation

The sediment obtained by the previous procedure was wet sieved to separate the grains greater than 53 microns (270 mesh). The finer fraction was collected in a beaker and after allowing to settle, and if flocculation occurred, the excess water was decanted. This was repeated until the sediment remained in suspension. An average of ten washings were usually required.

Even after ten or more washes not all samples remained in suspension. These samples were transferred to a polythene centrifuge tube, and the washing continued. At this stage there were a few samples which were still not in suspension, and these were finally dispersed in hot 2% sodium carbonate solution (Jackson, 1956). Although the samples were carefully washed the composition of these samples will be modified, particularly the sodium content. The dispersed samples were size fractioned in measuring cylinders using the following settling times (after Jackson, 1956).

Microns	Millimetres	Time	Remarks
53	0.053		Fraction wet sieved and washed
31	0.031	1 minute 56 seconds	Fractions sedimented
22.1	0.022	3 minutes 49 seconds	
15.6	0.0156	7 minutes 40 seconds	
7.8	0.0078	31 minutes	
3.9		2 hours 3 minutes	
2	0.002	7 hours 47 minutes	

After the required settling time for any particular size fraction had elapsed, the top 10 mls of suspension were syphoned off and collected in 1000 ml beakers. This supernatent liquid contained the finer fractions ready for the next stage. The sediment which had settled in the cylinders contained not only the required size fraction, but also some finer sizes. The cylinders were therefore refilled, shaken and 10 mls syphoned off, again after the required time interval. This was repeated until the supernatant was clear (five to ten times).

This procedure was followed for each particular size fraction until all of the silt fraction (> 2 microns) were removed.

The decanted water and sediment collected previously, contained the clay fraction. Because the time required to sediment progressively smaller particles increases very rapidly, the centrifuge technique was used. The technique employed for the separation of less than 2 micron fraction has already been established by previous workers in the Department of Geology.

The following times for centrifuging were calculated from the equation of Hathaway (1955) using the experimentally determined acceleration and deceleration times for the particular centrifuge.

Size in Micron	Speed	Time until switch-off	Total time
2	900 r.p.m.	2 mins. 22 secs.	2 mins. 45 secs.
1	1200 r.p.m.	4 mins. 59 secs.	5 mins. 29 secs.
0.5	2400 r.p.m.	5 mins. 4 secs.	5 mins. 54 secs.
0.1	2400 r.p.m.	2 hrs. 2 mins. 13 secs.	2 hrs. 3 mins. 3 secs.

As mentioned previously, the size fraction sedimented by centrifuging was washed free of the finer particles by repeated electric shaking with distilled water and centrifuging. This procedure was followed until the required size fractions were obtained. These size fractions were then cleared of any excess water and evaporated to dryness in an over at 50°C.

The objective of this laborious and time consuming exercise was to obtain size fractions for mineralogical and geochemical analyses. In geochemical studies of major and minor elements in sedimentary rocks, it is often more important to know in which mineral an element is contained, rather than the total abundance in the rock. Furthermore, different minerals are enriched in different size fractions and a study of the distribution of an element in size fraction may indicate the mineral with which the element is associated.

2.3 Thin Sections

Thin sections of sandstone were prepared and examined microscopically as an essential part of the petrographic study. Grain size measurements and mineral identification as well as quantification of major components were carried out, in order to facilitate and aid interpretation of parameters related to depositional and diagenetic environments. Although the mineral percentages obtained by this method do not have the accuracy of other methods

employed in the present study, they give an indication of whether or not a variation exists between samples.

2.4 Heavy Mineral Study

Procedure of Heavy Minerals Investigation: After disaggregating and separating the samples, into the different size fractions, the heavy minerals were extracted from the sand (> 53 μm) and silt (< 53-22.1 μm) fractions of four samples.

Each fraction (3-5 grams) was treated with hot 30% HCl, washed with distilled water and further treated with hot 30% H_2O_2 to remove carbonates, iron oxide coatings and organic matter. Phosphate minerals would be lost in this process. Bromoform (Sp. gr., 2.89) was used for the heavy minerals separation.

Once separated the heavy minerals were first examined with a binocular microscope and split into different groups, based on colour of the mineral. The basic procedure for their identification was the immersion method (Kerr, 1959). Liquids of various indices were used, and with the use of a petrographic microscope, the approximate limits of the refractive indices of a mineral were determined.

Other optical properties were then determined, such as pleochroism, extinction, isotropy, cleavage, interference colour and optical figures usually completed the identification.

After a mineral had been identified,it was possible to recognise it again under reflected light using a binocular microscope. Then a mount of several grains of a particular mineral was prepared. A quantitative determination of abundance was not attempted during this study.

2.5 X-ray Diffraction

The X-ray diffraction method is the principal method of determining the mineralogical composition of shales and sediments containing clay size material. For shales and sandstones prepared by a controlled repetitive technique, areas or heights of diffraction peaks can be interpreted in terms of quantities or ratios of mineral species. However, research workers on clay mineralogy have reported that the results are 'semi-quantitative' and values obtained must be considered to be plus or minus 2, 5, 10% or still more (John, Grim and Bradley, 1954; Brindley, 1961; Gibbs, 1965; Pierce and Siegul, 1969; Carroll, 1970).

X-ray diffraction was used in the present study to determine the overall mineralogical composition, quartz and feldspar contents as well as clay mineral quantification.

2.5.1 Whole Sample Mineralogy

This was investigated initially using standard back-filled aluminium holders.

2.5.2 The Clay Minerals

These minerals were mainlystudied using orientated smear mounts. Both whole sample and separated size fraction were treated in the same manner.

The smear technique of Gibbs (1965) was employed. About 50 mg of previously prepared powdered sample was placed in a small agate mortar are further ground for three minutes. It was then made into a paste with water, ground again and transferred to a glass mount. Care was taken to ensure a uniform smear, which was then dried. Essentially this same procedure with minor modification, is used widely to prepare oriented specimens (Kinter and Diamond, 1956; Weir et al, 1975; Wakatsuki et al, 1977).

Each sample prepared was X-rayed as follows:

(1) Air dried.

(2) Treated with ethylene glycol by placing the smear mount for one hour in a dessicator filled with ethylene glycol at 70°C.

(3) Heated for 375°C for two hours.

(4) Heated for 550°C for two hours.

These treatments are necessary to identify the clay mineral groups present. The behaviour of the lattice spacing under different conditions is a diagnostic feature of the mineral groups. The optimum temperature of collapse of illite-mixed layer clay minerals to 10Å is about 375°C, for 30-minutes (Austin and Leninger, 1976). Whereas the heating to 550°C was used to differentiate chlorite from kaolinite (Brown, 1961).

X-ray Routine: A Phillips X-ray diffractometer with nickel filtered CuKα radiation at 36 kV and 26 mA was used throughout. The specimens were scanned at 1°2θ per minute from 4°2θ to 35°2θ. The chart speed was 5 x 240 mm/hour; pulse height analyser was at lower level -2.5, with the 1.0 window. Rate meter range was 1 x 10^2 with time constant 1.

The peaks position were measured in terms of 2θ and then converted to their corresponding d- spacings. Minerals were then identified using the ASTM X-ray diffraction data files.

2.5.3 Semiquantitative Estimation of Clay Minerals

Peak areas were determined by weighing. A constant base line was drawn on the XRD-trace, using a set of French curves. A high quality draughting film was used in tracing the areas, the peaks were then cut out and weighed.

Cubitt (1975) demonstrated statistically that peak area measurements are superior and more effective than peak height measurements for

distinguishing between samples. Furthermore, it was stated that the most effective preparation technique, judged by the peak area criterion, is the smear method.

The recalculation of the peak areas to percentages for each specimen was attempted. The proportion of illite present was measured from the area of the 10Å on the glycolated trace, the proportion of kaolinite was indicated by the area of 7.1Å and that of chlorite by the 14.2Å peak, both on the air dried trace. The difference between the measurements of the 10Å peak on the glycolated trace and the 375°C heated trace, was considered as the mixed layer proportion.

However, XRD study of clay minerals gives only the relative abundance of these minerals. To get the absolute percent of each clay mineral, the quantity of toal clay which equals the weight percentage of the clay in the sample was deduced from the norm calculation following the method of Nicholls (1962).

The clay minerals were then proportioned to this total clay figure according to the individual calculated percentages. It was found that the recalculated XRD and norm values closely agree to within $\pm$ 5%, especially for kaolinite and illite. To minimise this error, due to employing two different methods, the average value from the norm and the recalculated XRD values was taken as the representative figure for each individual clay mineral.

Finally, it must be remembered that the XRD clay mineral percentages were obtained using the whole sample smears, because these were found to give more approximate value to the norm calculation than employing the <2 μm clay smear.

2.5.4 Identification of Clay Minerals

The clay minerals were mainly identified on the separated clay fraction. The criteria for their identification were mostly obtained from Brown (1961) and Carroll (1970). Figure 9 shows the behaviour of chlorite, illite + mixed layer and kaolinite with various treatments.

Chlorite: was identified on the well defined reflections at 14.01Å (001), 4.72Å (003) and 3.52Å(004). The 7.05Å (002) reflection was observed only in a few samples of the whole rock. The first three reflections were seen in nearly all the sandstone and shale samples. There were no significant changes in the intensity or position of the basal reflections after glycolation. Heating to 375°C, removed the first basal reflection, but generally there was no change. On the other hand heating to 550°C, generally produced a decrease in the intensity of (003) and (004) reflections and increased the intensity of the (001) reflection which showed a slight decrease in the (001) spacing to 13.85Å-13.71Å. Treatment with 10% HCl removed the basal reflections.

This behaviour of chlorite on heating suggests that it is an iron rich variety (Triplehorn, 1970; Henson, 1973). This is because Fe chlorite shows a greater shrinkage parallel to C-axis than do Mg-chlorite. However the removal of chlorite after treatment with 10% HCl is a further indication that chlorite is Fe-rich rather than Mg-chlorite as the latter is less readily dissolved by acid treatment (Shaw, 1973).

Illite: is defined as a mineral group including fine mica which was identified on the characteristic basal reflections at 9.92-9.98Å (001), 4.95Å-5Å (002) and 3.33Å (003). The peaks showed no significant changes in the location of their basal reflections after glycolation, moderate heating or treatment with 10% HCl. Glycolation induced the development

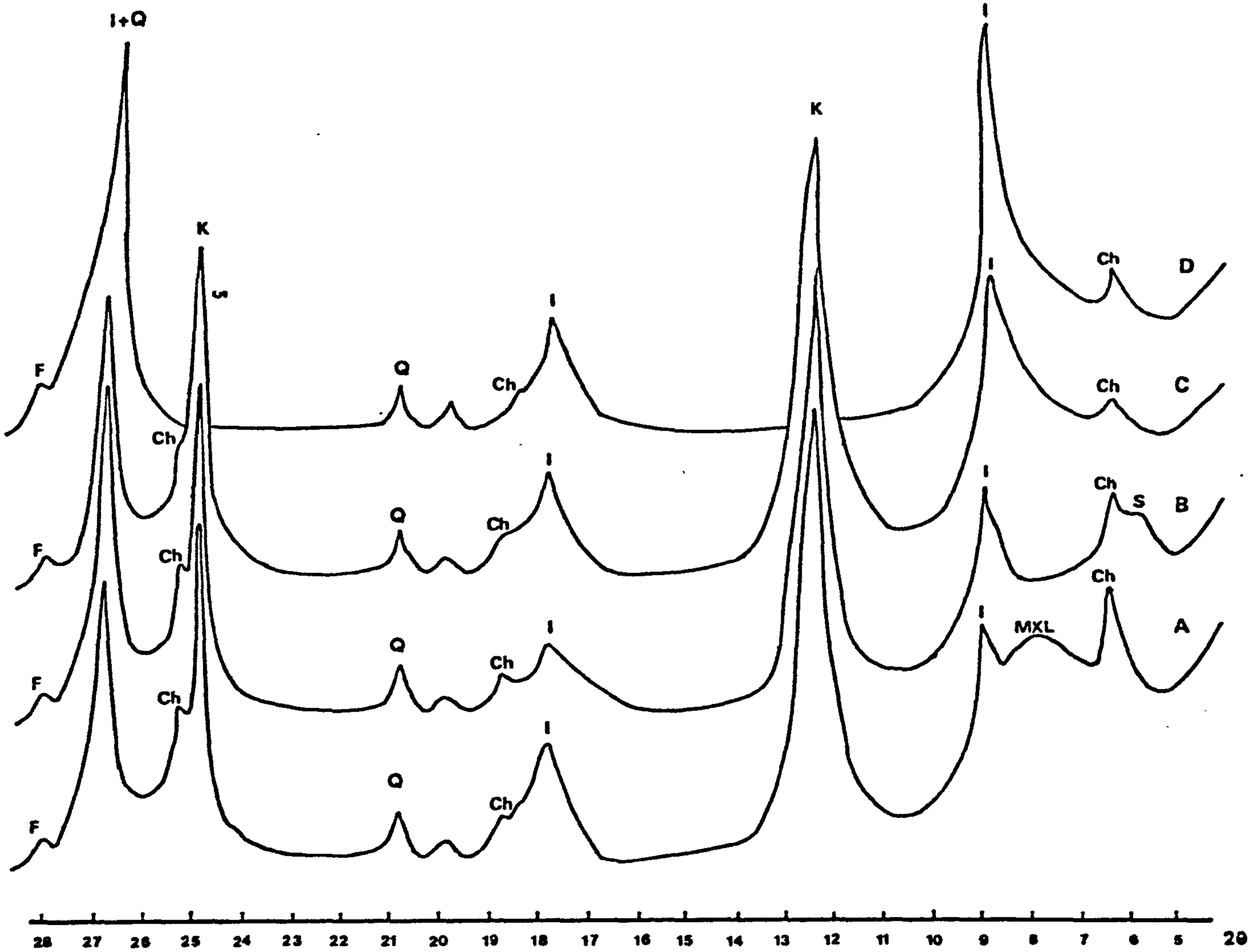

Fig.9 X-ray diffraction pattern of minerals. Ch-chlorite, I-illite, K-kaolinite, Q-quartz, F-feldspar (plagioclase), MXL-mixed layer, S-smectite. Traces are, A-untreated, B-glycolated, C-heated to 350°C, D-heated to 550°C. CuK_{α} radiation.

of a slight symmetry and increase in the intensity of the first and thrid basal reflections, while the second reflection sometimes showed a slight decrease in its intensity. Heating to 375°C and 550°C resulted in progressive sharpening of the diffraction reflections.

The tailing-off in the illite peak has been interpreted by Velde and Hower (1963) and Gaudette (1965), to indicate a mixed layering, while Maxwell and Hower (1967) stated that this phenomenon is an intrinsic feature of illite which, in addition to being disordered, is potassium deficient and has a high H_2O content. However, inthe present study, the mixed layer mineral was indicated either by a hump between 12.61-10.04Å or by the asymmetry of the illite peak. In the first case the position of the peak apex varied along the specified range of d-spacing. On glycolation it either disappeared or was reduced significantly and only in a few samples was the 15.49Å observed. This most probably indicates an illite/smectite layering. The appearance of smectite peaks at 15.49Å was believed to be related to its proportion in the mixed-layer mineral. On the other hand heating to 375°C and beyond resulted in incomplete collapse of the mixed-layer mineral to 10Å.

Kaolinite: was identified by its characteristic, well defined basal reflections at 7.16Å (001) and 3.57Å (002). It was not affected by glycolation, moderate heating and acid treatment, while heating to 550°C removed the basal reflections.

Distinction between Kaolinite and Chlorite

In most samples the resolution of the kaolinite and chlorite doublets at 3.57Å and 3.52Å was very clear, while that around 7.16Å-7.05Å was not observed. Nevertheless, a slight asymmetry, occasionally towards lower d-spacing was shown by the 7.16Å peak. Acid treatment removed the basal reflections of chlorite and no significant changes were recorded in the

intensity of kaolinite peaks at 7.16Å and 3.57Å. In fact they showed a slight increase in their intensity, which indicated negligible interference by the chlorite peaks. Therefore, it was assumed that by drawing a perfect image of the part of kaolinite peak (7.16Å) towards high spacing would remove the interference of any chlorite present. The resulting basal reflection was then attributed to kaolinite only.

2.5.5 Quartz Determination

Quartz is an important constituent in sedimentary rocks and a number of methods are in use for its determination. One widely used method involves a potassium pyrosulphate fusion (Trostel and Wynne, 1940). Quartz is isolated by this method and is quantitatively retained for gravimetric determination. A disadvantage of this method is that feldspar is partially unaffected and any feldspar present is,therefore, included in the quartz figure. Therefore this method would tend to give quartz values higher than the true one in sandstone whereas in the shales with small amounts of feldspar it should not appreciably alter the quartz data. However, the method takes a long time and requires a monopoly of laboratory space and equipment. The analysis does require care, so it is advisable to run duplicates.

An alternative to the above method is the X-ray diffraction technique described by Till and Spears (1969), which is both rapid and precise. This method is based on the use of an internal standard, boehmite (54 Cera hydrate) which is added to the ignited sample in fixed proportions. Ignition of the sample destroys the clay minerals and removed their interfering peaks from the XRD traces. The relative intensity of the quartz peaks is also increased. A standard working curve was produced using samples of known quartz content, which was determined using the method of Trostel and Wynne (1940).

Procedure

All samples were treated uniformly in the following manner. About 2 gm of powder sample was dried in an oven at 110°C. Then the sample was ignited in a silica dish at 950°C for three hours. Ignition loss was accurately determined. The sample was then further ground to a talc-like consistency in an agate mortar. Next. 0.9 gm of sample was mixed with 0.1 gm of boehmite and the mixture was homogenised mechanically. After this, the sample was packed into an aluminium holder using a back-filling technique and scanned in a Phillips 2kW X-ray diffraction unit under the following conditions:

CuKα-Ni filtered radiation
1, 0.1, 1 degree slits
36 kV, 26 mA
Scan range ½° 2θ/minute
Chart speed 120 cm/hour

The sample was scanned from 13.0-15.5°2θ and 20°-30°2θ. A constant base line was drawn on the diffractograms using a set of French curves. The areas under the boehmite 6.18Å peak and the quartz 4.26Å were measured. A polar planimeter was not used, instead it was found more accurate to weigh peaks prepared from an overlay of high quality draughting film. To avoid any operator inconsistency in obtaining the quartz content of unknown sample from the curve, the following original formula was used:

$$Y = 0.0317 + 0.0201X + 0.000305X^2$$

where X = quartz content in ignited sample

Y = quartz (4.26Å)/boehmite (6.18Å) peak area

Finally, these quartz values must be corrected for the ignition loss.

The present writer determined the quartz content of some samples following

Trostell and Wynne's method; a comparison of the results of XRD and gravimetric determinations is shown in Table 16. It can be seen that the quartz contents obtained by the gravimetric method are generally higher than those found by the XRD method.

2.5.6 Feldspar Determination

The same method of quartz determination was extended to include feldspar (albite and microcline) by Fellows and Spears (1978). The method involves spiking of a mudrock base with standard feldspars. X-ray diffraction areas were used to construct standard working curves. The only difficulty encountered in this method is that albite was found to undergo partial conversion to K-feldspar. Fortunately this conversion was not total and the albite content could be determined using the standard working curves shown in Figures 10, 11 and 12.

The operating conditions of the X-ray diffraction unit and measurements of peak areas procedure were the same as those employed for quartz determination. The only modification was that the total area of boehmite peaks, 14.5^{o} and 28.3^{o} were measured. This was found to give more reliable results than using only one. The areas of albite peak, 27.95^{o}-$28.02^{o}2\theta$ and that of microcline, 27.52^{o}-$27.67^{o}2\theta$ were also measured.

To obtain the albite and the microcline contents, the following steps were followed:

1. Find the ratio of albite peak/boehmite peaks area, and the albite is obtained from Figure 11.
2. The total microcline content is obtained from Figure 12 again expressing the microcline peak area as a ratio of the total boehmite area.

TABLE 16: Comparison of XRD and Gravimetric Determinations

Till and Spears	Quartz after Correction for IG.L.	Trostel and Wynne
20.19	17.92	19.05
50.96	46.17	44.63
65.95	63.19	67.54
21.21	18.88	20.24
71.76	68.66	69.47
34.32	31.31	34.75
24.45	21.65	22.38
72.66	68.01	71.43
24.98	22.24	22.88
70.42	68.33	71.23
75.23	73.08	78.16
59.27	55.93	57.55

Fig.10

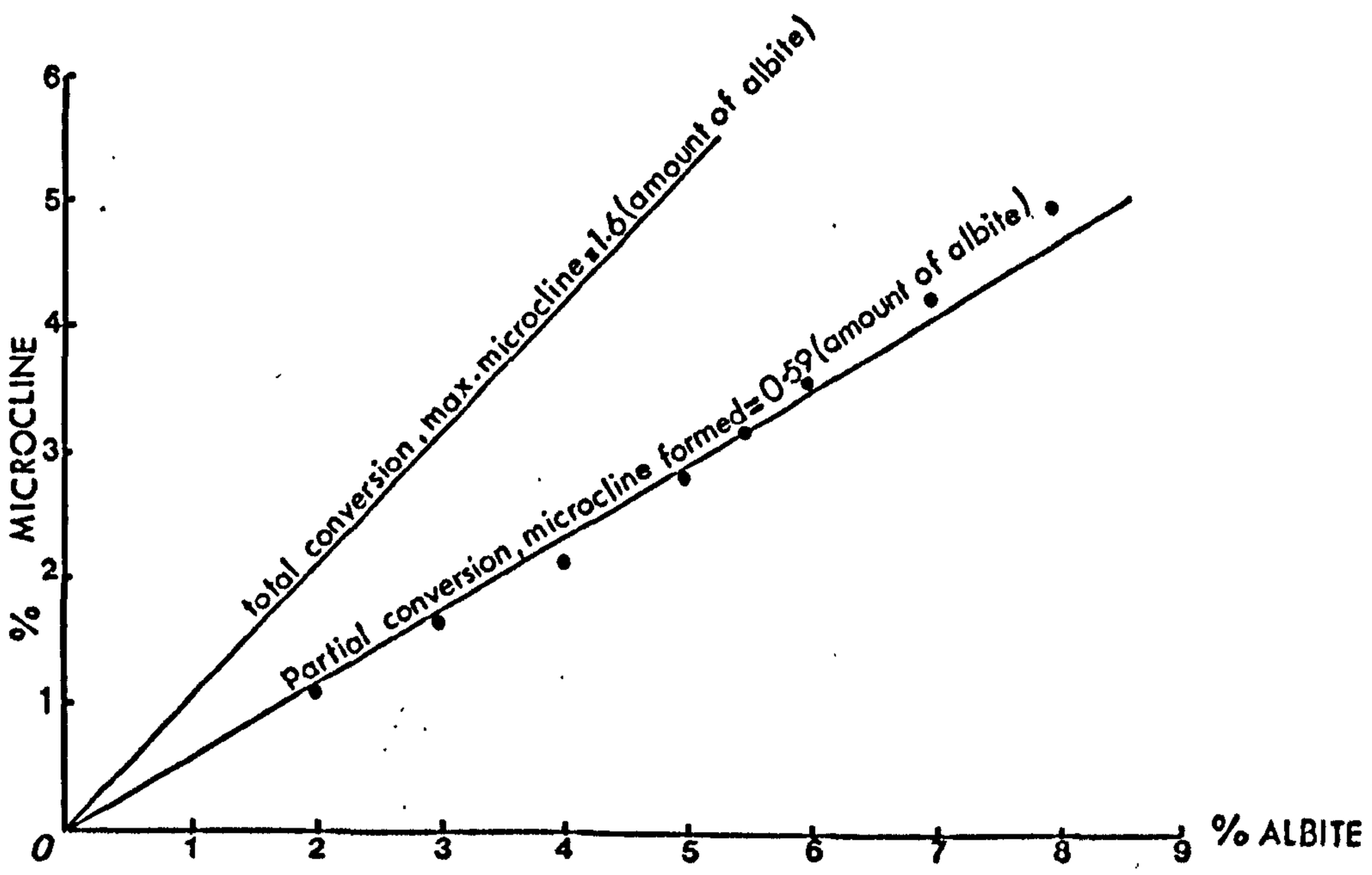

Fig.11

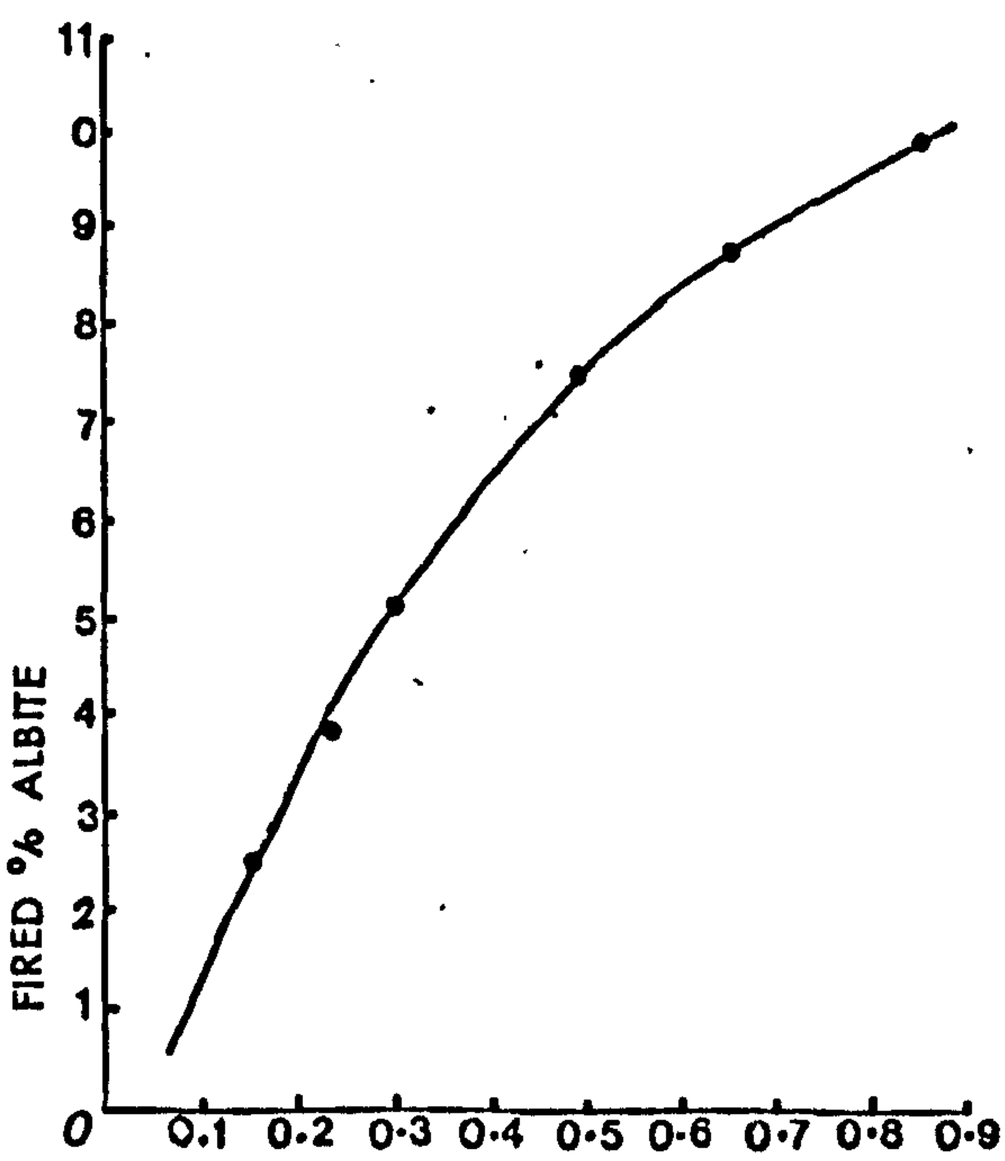

Fig. 12

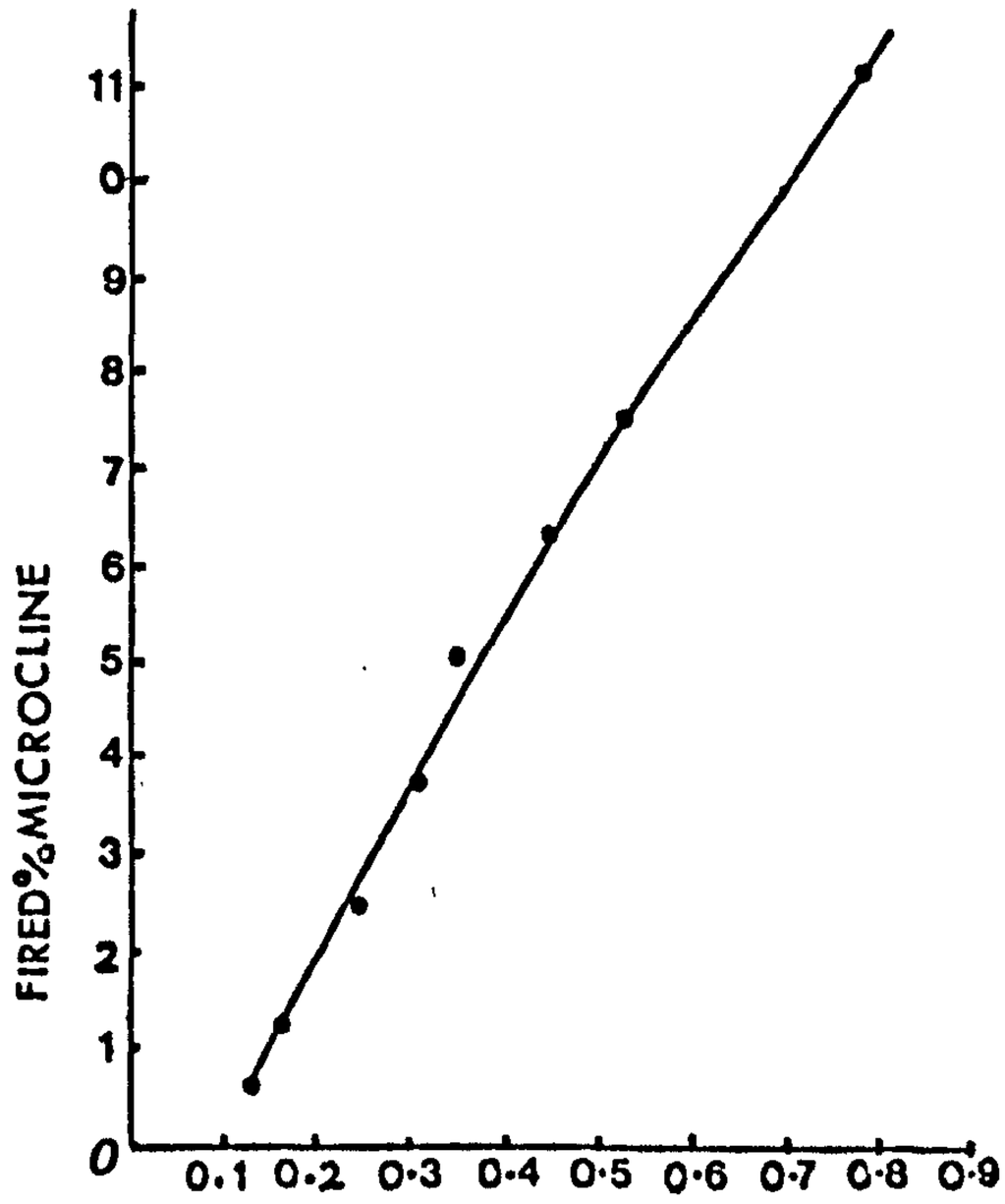

Fig.10 : The partial conversion of albite to microcline at the ignition temperature at 950°C microcline formed = 0.59 (amount of albite). Also shown is the line denoting total conversion maximum microcline = 1.06 (amount of albite).

Fig.11 : The relationship between the percentage albite, in ignited samples, and the ratio of area albite diffraction peak to area combined boemite diffraction peaks.

Fig.12 : The relationship between the percentage microcline, in ignited samples, and the ratio of the area microcline diffraction peak to area combined boemite diffraction peaks.

3. Use Figure 10 to get the microcline percent produced from the albite during ignition and this value is deducted from the total microcline.

2.6 X-ray Fluorescence Spectrometry

This technique is designed for a large number of samples as well as being sufficiently accurate and precise for a maximum number of elements when calibrated with adequate standard (Fairbairn, 1953).

Preparation of Samples

Samples collected from the field were cleaned of any superficial materials, washed and dried. About 50 gm. in weight was hammered off the samples and were then reduced to small chips using a jaw crusher. The fine powder resulting from this process was discarded, in order to avoid any contamination. The small chips were then placed in a Tema Mill and ground for two minutes. The sample was further ground in an electric agate mortar until no gritty feel could be detected. The powder samples were stored in clean, dry and airtight glass jars, ready for major and trace element analyses.

2.6.1 Major Element Analyses

The elements Si, Al, Ti, Fe (total), Ca, Mg, Mn, K, P and S were determined using the fusion technique outlined by Norrish and Chapell (1967) and described by Norrish and Hutton (1969). The technique was adopted with only minor modification and with direct computer processing of X-ray intensity data out from the spectrometer on punched paper tape. The main advantages of using glass discs were the elimination of mineral grains and the diminution of matrix absorption effects. As rocks vary appreciably in chemical composition, they also differ in overall mass

absorption coefficient. This results in a varying X-ray response for a particular element in different rock matrices. By using the fusion method, it enables calibration to be more applicable to a very wide range of rock types.

Preparation of Glass Discs

Powder samples were fused with flux (La_2O_3, Li_2O_w and $Li_2B_4O_4$) and sodium citrate in the following proportions - 0.373 gm, 2.00 gm. and 0.027 gm respectively. The fusion was carried out in a Pt-Rh-An allow crucible which was heated on a Meker burner for about 15-minutes. Heat, slowsly at first, and finally with the full heat of the burner until the decomposed sample and the flux appear as a homogeneous molten glass. Next the molten glass was poured onto a graphite dish, kept at 230°C on a hot plate. Immediately an aluminium plunger (also kept at 230°C) was brought down quickly and gently pressed onto the molten glass which quenches to form the disc. The graphite dish with the glass disc was then placed on an asbestos mat, on another hot plate kept at a lower temperature. Later, when the glass disc had cooled, it was cleaned and ahy projections from its edge removed. Finally the discs were stored in self-sealing polythene envelopes, ready for analysis.

The blank specimen was prepared by adding pure SiO_2 instead of sample and follows the procedure already described. It was usually required to determine the actual weight loss of the sample on fusion. This was done by cooling the melt in the crucible which was then weighed, before making the disc. The loss percent is given by:

$$\text{Loss} = \frac{\text{Measured loss in g. of sample - Measured loss in g. of blank}}{\text{Sample weight in g.}} \times 100$$

Because sodium citrate was added to the fusion mixture as an oxidising agent, sodium was not determined using the glass disc. In addition, the XRF method gives total iron and therefore ferrous must be determined separately by wet chemical method and then its ferric equivalent subtracted from the total iron. Table 17 lists replicate analysis of one sample for major elements and their coefficients of variation.

Instrumental Conditions

The general instrumental conditions are given in Table 18. A Phillips X-ray fluorescence spectrometer (p.w. 1220) was employed, and an FS48 instrument standard (supplied by Norrish, Soil D, Australia) was run with each set of samples.

Ferrous Iron

The commonly used method for this determination involved titration with potassium dichromate and was not reliable for rocks containing organic matter, because the ferric iron and dichromate present can easily be reduced by organic matter. As an alternative, the method devised by Shapiro (1960) was used and this was found by Spears (1963) to be the best for shales containing organic matter.

In this method orthophenanthroline was added to 10 mg of powder sample in a plastic bottle, followed by H_2SO_4 and HF; the bottle was placed in a steam bath. The orthophenanthroline complexed with the ferrous iron as it went into solution. The red colour of the complex was developed by adding a buffer of diluted sodium citrate. After this, the solution was centrifuged to remove any particular matter.

Spears (1963) emphasised the need for rigid control on experimental conditions, due to the fact that the colour development of the complex changes with time. For this reason, after centrifuging, the solution was

TABLE 17: ReplicateAnalyses of One Sample for Major Elements and the Coefficients of Variation

	1	2	3	Coefficient of Variation
SiO_2	75.27	75.91	75.37	0.45
Al_2O_3	9.49	9.511	9.64	0.83
TiO_2	0.50	0.48	0.50	2.02
Fe_2O_3	5.79	5.84	5.80	0.39
MgO	0.80	0.83	0.87	4.30
CaO	0.32	0.35	0.33	5.05
Na_2O	1.06	1.04	1.08	1.88
K_2O	0.80	0.82	0.80	1.73
MnO	0.24	0.17	0.16	22.51
P_2O_5	0.11	0.12	0.10	9.17
SO_3	0.09	0.13	0.09	27.18
IG.L.	4.64	4.91	4.96	3.51
Total	99.11	100.16	99.70	

TABLE 18: Instrumental Conditions used for XRF Major Element Determinations

Element	2θ	Diffracting Crystal	Counter	Collimator	kV	mA	PHA	t(secs)
K	50.60	pE(1-1)	Flow	Fine	60	24	Ext	10
Fe	57.46	LiF(3-1)	Flow	Fine	60	24	Ext	10
Mn	62.95	LiF(3-1)	Scint.	Fine	60	32	Ext	100
S	75.80	pE(2-1)	Flow	Coarse	60	32	4-2	100
Ti	86.13	LiF(3-1)	Flow	Fine	40	24	Ext	10
P	89.51	pE(2-1)	Flow	Coarse	60	32	4-2	100
Si	109.17	pE(2-1)	Flow	Coarse	60	32	Ext	40
Ca	113.13	LiF(3-1)	Flow	Fine	40	16	Ext	10
Mg	136.60	ADP(1-1)	Flow	Coarse	60	32	4-2	100
Al	145.20	pE(2-1)	Flow	Coarse	60	32	Ext	40

immediately transferred into a small polythene bottle and kept in total darkness for three hours before commencing reading on the spectrophotometer. Furthermore, the samples (nine in one run) and the standard Tl were steamed absolutely uniformly and the time lapse between development of colour complex and measurement on the spectrophotometer was kept as constant as possible.

Duplicate analysis of some samples with low ferrous iron were carried out and the results were found to be in good agreement. However, for those samples with high ferrous iron, the average of two or three measurements were always undertaken. Replicate analysis of the standard Tl gave a coefficient of variation 2.65.

Carbon Dioxide

This was determined by the method of Groves (1951). About ½ gm. of powder sample was transferred to a round bottom flask which was connected to a series of U-tubes, two containing sofnolite and the last one $CaCl_2$. The apparatus was connected to a suction pump. Air free of CO_2 and H_2O was then drawn through the apparatus for 20-minutes, after which the U-tubes were weighed. Again air was drawn for a further 5-minutes and the U-tubes were weighed to ensure stabilisation of the apparatus. The CO_2 evolved by adding phosphoric acid to the powder sample, followed by careful heating. The gas was absorbed by the sofnolite, and water released by sofnolite was absorbed by $CaCl_2$. When no further gas was evolved, air was drawn through the apparatus for five minutes, after which the U-tubes were again weighed to find the amount of CO_2 evolved. Six replicate analysis of one sample with a mean of 5.52%, the coefficient of variation was 5.65.

Na Determination

Sodium was determined by atomic absorption spectrometer. An accurately weighed 0.1 gm of rock powder was placed in a platinum crucible. This was treated with a 2 ml. of $HClO_4$, followed by a 5 ml. of HF. The crucible and its contents were then heated gently at first, on a radiator. When the greater part of the HF has been removed and the $HClO_4$ started to fume, the heat was increased, until the residue was completely dry. Next, the crucible was cooled and 1 ml. of $HClO_4$ was added, followed by filling the crucible to about three-quarters of its volume with distilled water. This was followed by a gentle warming until most of the residue had gone into solution. The content of the crucible was then transferred into 250 ml. flask, and topped up to the mark with distilled water. At this stage, the solution was ready for measurement by the atomic absorption spectrometer. A set of standards were run with each batch of five samples. The readings were converted to ppm of Na_2O by means of calibration graphs. To obtain the $Na_2O\%$ the following formula was used:

$$\% Na_2O = \text{ppm } Na_2O \times 10^{-6} \times \text{volume} \times \frac{100}{\text{wt. of sample in gm.}}$$

Duplicate analysis of four samples (1.01, 0.91), (1.27, 1.23), (1.45, 1.52), (2.07, 2.02) indicate a fair precision.

Water Determination

Water determination was carried out in two stages. First hygroscopic water (H_2O^-) was determined by recording the weight loss when the samples were dried at 105°C overnight. The second, which involves the determination of combined water (H_2O^+) in the clay mineral lattice, was determined using the Penfield tube method.

Into a weighed Penfield tube, about 0.6-1.0 gm of powder sample was transferred and the tube was re-weighed to obtain the accurate weight of

sample. The tube was then clamped at a slight angle and wrapped by a moistened filter paper round the tube near the open end. The sample was heated gently, and when the water began to collect, the heat was gradually increased to the full heat of the bunsen burner, until the sample became a bright red. Next, the part of the tube between the powder sample and water was heated to softness, and the end containing the powder was drawn off. The tube containing the water was then cooled, wiped clean, air dried and weighed. This was followed by drying the tube at 110^{o}C in an oven for at least one hour, after which it was cooled and re-weighed. The weight of water given off was then deduced, the percent of water calculated using the following formula:

$$\% H_2O^+ = \frac{\text{wt. of water given off}}{\text{wt. of sample}} \times 100$$

The method was fairly precise as indicated by the values of duplicate analysis for three samples, as follows: (7.84, 7.87), (4.45, 4.40), (2.92, 2.86).

Determination of Iron in Pyrite

Acid soluble iron was determined by the method of Wilson (1955) with some modification.

When 2.2' dipyridyl was added to the sample a liquate, the red ferrous dipyridyl complex formed, the optical density of which was measured at 522 μm. All the iron was reduced by the use of hydroxylamine hydrochloride.

As the acid soluble iron of interest was in pyrite, the samples were first treated with 3N HCl, in a water bath kept constantly at 70^{o}C. After reaction ceased, the samples were centrifuged and supernatent acid was discarded, and then repeatedly washed (five times). Next, they were

treated with 25% HNO_3 kept at 70°C, to decompose the pyrite for an exact time of 30-minutes. For all the samples the experiments were rigorously controlled and all received identical treatment. Only the samples with a high pyrite content were analysed in this manner.

Organic Matter

At first, it was decided to use a simple ignition loss method to determine the organic content of the samples. This method had been used in this Department by Knowles (1961) and later by Spears (1963) with some modification. This, of course, gives an estimate of the total organic matter present. It was justifiable, since Greensmith (1955) demonstrated that the organic content so derived was proportional to the organic content chemically determined. The method was the elimination of hygroscopic water by heating in air at 250°C, and burning off the organic material at a constant temperature of 395°C. The loss in weight between 250°C and 395°C was taken as an estimate of the organic content. Through this process, careful heating is required, otherwise the temperature could rise to about 420°C by burning organic matter, at which temperature pyrite starts to decompose.

According to Marston (1967), the weight loss from clays on heating over the temperature range 110°-375°C can be attributed almost entirely to loss of organic material due to oxidation. However, this method could be applied satisfactorily to samples containing small amounts of pyrite, although in the latter case some adjustments were made.

Moreover, Marston (1967) demonstrated that using a wet chemical method (chromic acid) did not overcome the difficulty of obtaining accurate organic percentages. This is because the method was employed for pure organic carbon determination. However, in the majority of

shales, the organic matter present is not pure carbon, but a complex of organic molecules. Therefore this method could not be used, since it would tend to give a much lower value of the organic matter, than the heating method.

During the present study, the heating of samples in the temperature range 110^{o}-$395^{o}C$ was tried, but it was found to be unreliable when the chemistry of the rocks was recalculated to normative minerals. This is because a large number of the samples are rich in pyrite. Consequently the following procedure was used:

1. The equivalent SO_2 of HNO_3 soluble iron (Pyrite iron) was calculated.
2. The CO_2 was determined as described previously.
3. The H_2O^+ was obtained by the Penfield method.
4. The fusion loss when making the glass disc for major element analysis, was recorded. However, this loss does not include the hygroscopic water, because all analyses were carried out on an oven dry basis.
5. The organic matter content was obtained by subtracting the sum of SO_2, H_2O^+ and CO_2 from the value of the fusion loss.

It was found that the organic matter data were more reliable than those derived by the former heating method. However, since the relative variation of organic matter content was more important to the study than the absolute amount present, it was assumed that at least the interference by siderite and pyrite would be sufficiently small and not mask any such variations.

2.6.2 Trace Element Analyses

The elements Ni, Co, Mn, V, Cr, Zn, Cu, Rb, Sr, Y, Zr, Pb and Ba were determined in a similar way to that described by Norrish and Hutton (1964).

Pellet Making

A boric acid backing disc was prepared, about 3 gm of powder sample was placed onto the disc and subjected to 12,000 p.s.i. pressure for 3-minutes.

The instrumental conditions used for each element are given in Table 19. Calibration was undertaken by using a U.S. Geological Survey international standard.

The element concentration in the sample was obtained by using the corrected count rates (C.R.) and mass absorption coefficient (M.A.C.) as follows:

$$\text{Element (ppm)} = \text{Corrected C.R.} \times \text{M.A.C.}_{\text{sample}} \times \frac{K}{\text{M.A.C.}_{\text{standard}}}$$

The mass absorption coefficient were determined according to Heinrich (1966) using the major element analysis. Duplicate analysis of two samples for trace elements (Table 20) indicates a fair precision of the technique.

2.7 Norm Calculation

The calculation of mineral composition from chemical analyses of sedimentary rocks is important in studying argillaceous rocks, because they are not amenable to microscopic examination. Calculating gross mineral composition of a rock from its chemical composition can be justified where:

TABLE 19: Instrumental Conditions used for XRF Trace Element Determinations

Element	Diffracting Crystal	Collimator	Counter	Kv	mA	$^{o}2\theta$	t(secs)	Line	$^{o}2\theta$	t(secs)	$^{o}2\theta$	t(secs)	X-ray Tube
Ni	Li (220)(1-1)	Fine	Flow	60	32	70.00	20	Kα	71.20	100	75.18	20	W
Co	Li (220)(1-1)	Fine	Flow	60	32	75.18	20	Kα	77.85	100	93.00	20	W
Mn	Li (220)(1-1)	Fine	Flow	60	32	93.00	20	Kα	95.19	20	105.00	20	W
Cr	Li (220)(1-1)	Fine	Flow	60	32	105.50	40	Kα	107.10	100	120.50	20	W
V	Li (220)(1-1)	Fine	Flow	60	32	120.50	40	Kα	123.23	100	124.00	20	W
Zr	Li (220)(1-1)	Fine	Scint.	60	32	31.00	20	Kα	32.10	100	33.20	20	W
Y	Li (220)(1-1)	Fine	Scint.	60	32	33.20	20	Kα	33.91	100	34.62	20	W
Sr	Li (220)(1-1)	Fine	Scint.	60	32	34.62	20	Kα	35.85	100	36.80	20	W
Rb	Li (220)(1-1)	Fine	Flow	60	32	36.80	20	Kα	37.97	100	39.14	20	W
Zn	Li (220)(1-1)	Fine	Flow	60	32	59.20	20	Kα	60.53	100	65.50	20	W
Cu	Li (220)(1-1)	Fine	Flow	60	32	65.50	100	Kα	68.75	20	-	100	W
Pb	LiF(200)(3-1)	Fine	Flow+Scint.	60	32	33.00	20	Kα	33.92	100	34.50	20	W
Ba	LiF(220)(1-1)	Fine	Flow	60	32	126.82	20	Kα	128.82	100	130.82	20	W

TABLE 20: Duplicate Analysis of Two Samples for Trace Elements (ppm)

	Sample 1		Sample 2	
	1	2	1	2
Ni	34	36	88	87
Co	11	13	10	13
Mn	742	726	397	386
V	46	43	134	136
Cr	116	122	165	163
Zn	68	67	103	102
Cu	12	14	45	44
Rb	26	23	115	115
Sr	71	68	100	98
Y	27	26	43	47
Zr	259	261	167	167
Pb	15	14	36	35
Ba	249	259	433	458

1. the qualitative gross mineral composition is known
2. the chemical analysis of the rock is accurate
3. the exact composition of each mineral in the rocks is known

In many studies, the first proposition is known and the second is assumed to be accurate; but the third is very difficult to fulfil. Several schemes have been described, dealing with such calculation (Imbrie and Poldervaat, 1959; Miesh, 1962; Nicholls, 1962).

In the present study, the scheme of Nicholls was followed because it was originally employed to argillaceous rocks of similar composition to those concerned in this present work. Depending on the evidence obtained from XRD study of the rock concerned in the present study, some minor modifications were introduced. Since montmorillonite was not detected as an individual peak (on both air dried and glycolated smear) its calculation was excluded. In addition, by employing the method of XRD feldspar determination, it was possible to allocate some of the alkalies to the feldspars, and not entirely to the illite.

In following this scheme, however, the normative minerals, especially the clay minerals, are not expected to represent the actual mineral composition. This is because the individual clay mineral composition is variable and very difficult to determine. However, by comparing XRD traces of individual samples and their normative minerals, it was generally found that the scheme was justified in illustrating the picture of relative variation in rock compositions. From the norm calculation the presence of illite, kaolinite and chlorite was indicated and this was substantiated from XRD work. Either illite or kaolinite was the most abundant, depending on rock type and minor amounts of chlorite also occur. In addition the presence of diagenetic minerals such as pyrite, siderite, dolomite-ankerite and calcite were detected by XRD.

CHAPTER 3

Petrography of the Millstone Grit Series

In this Chapter, a brief account of the previous petrographic work carried out on the Millstone Grit Series is presented. This is followed by more specific petrographic work undertaken by the present writer on the sandstones studied. The use of the optical microscope was intended to confirm and possibly extend the chemical approach to mineralogical data.

3.1 Previous Work

Petrographic studies of the arenaceous members of the Millstone Grit Series were undertaken by, among others, Gilligan (1920), Greensmith (1955), Smith et al. (1967) and Stevenson and Gaunt (1971).

The sandstones have been described as arkosic and subarkosic and these immature feldspathic sandstones range in age from R_1-G. With few exceptions they are poorly sorted and of medium sand grade (BSI). They consist of patchily interlocking quartz of dominantly igneous origin with a subordinate metamophic variety; primary micas (muscovite and hydrobiotite), feldspars include ubiquitous orthoclase and microcline and minor plagioclase. The feldspars are usually heavily altered to kaolinite which forms the matrix together with other clay minerals. Chlorite is present as an alteration product of hydrobiotite. Ferric oxides and hydroxides, described as geothite, are commonly disseminated throughout the matrix as a result of siderite and hydrobiotite oxidation. Secondary cement is sporadic and present usually as quartz overgrowths and carbonates. Heavy minerals include zircon, tourmaline, rutile, anatase, ilmenite, leucoxene, garnet, apatite with traces of staurolite and monazite.

The finer grained argillaceous and micaceous sandstones within the subarkosic units have been interpreted as part of a turbidite sequence. Allen (1960) described the Mam Tor sandstones at the type locality. The range in modal composition of the sandstones is as follows:

Component and Size		Laminated Sandstone	Non-Laminated Sandstone
Unstable Components	Quartz	13.1 -74.3 %	55.6 -81.2 %
	Feldspar	0.3 - 2.0	1.0 -11.90
	Siderite Aggregates	2.10-85.2	tr. -10.0
	Rock Fragments	tr. - 4.4	1.20- 6.50
	Mica		
	Wood Fragments	0 - 2.90	0 - 1.30
	Matrix	tr. -20.90	tr.
	Size	fine-medium sand	medium sand granule

Quartz appears as angular grains chiefly of simple type. The detrital matrix consists of sericitic clay minerals. The feldspars are chiefly orthoclase, albite and microcline, and locally these are replaced by kaolinite or calcite. The sandstones containing clay are usually poorly sorted with little or no calcite and quartz cement, and are classified as the greywackes of Pettijohn (1957). A few of the non-laminated sandstones are rich in calcite (up to 42.6%) and these are well sorted and classified as orthoquartzite.

3.2 Present Work

The following account deals with the thin section study of the Mam Tor Sandstones and the Ashover Grit. Some twelve specimens were studied from the Mam Tor sandstones and heavy minerals were separated from those samples.

In view of the small amount of sample available from the Ashover Grit, only three samples were subjected to such study and additional information will be presented from other worker's contributions.

Modal analysis is based on measurements made by point-count method, although sampling and other errors inherent in modal analysis of a limited number of samples are likely to be serious; the results obtained give an idea of the compositional range.

3.2.1 Mam Tor Sandstones

Considered as a whole, the sandstones investigated have a relatively narrow range in mineralogical compositions. This is illustrated in Figure 13, where the three major end components, quartz, matrix and unstable components (feldspar rock fragments, mica and carbonate) have been re-calculated to 100 percent. In the most part, the sandstones resemble in texture the greywackes of Pettijohn (1957), although few of them are characterised by the absence of significant quantity of matrix, and therefore similar to Pettijohn's orthoquartzite and subarkoses. In these sandstones, the detrital quartz grains range from fine silt to coarse sand in size. However, the dominant fraction of the grains falls in the fine and medium sand size grades, according to Wentworth's (1922) grade scale. The modal sizes range from 0.09-0.4 mm (Table 21). More specifically, the frequency distribution of the various size grades is shown in histograms (Figure 14). The variation of size distribution is linked with the mineralogy and texture. Generally, the argillaceous sandstones are finer grained and more poorly sorted than the relatively clean and better sorted sandstone, i.e. quartz cemented sandstone (Plate 1). This variation is also exhibited by different parts of a single sandstone bed. For example, specimens $^{6}b_1$, $6b_2$ and $6b_3$ represent the basal, middle and top parts of a sandstone bed, respectively. It can be seen from Table 21,

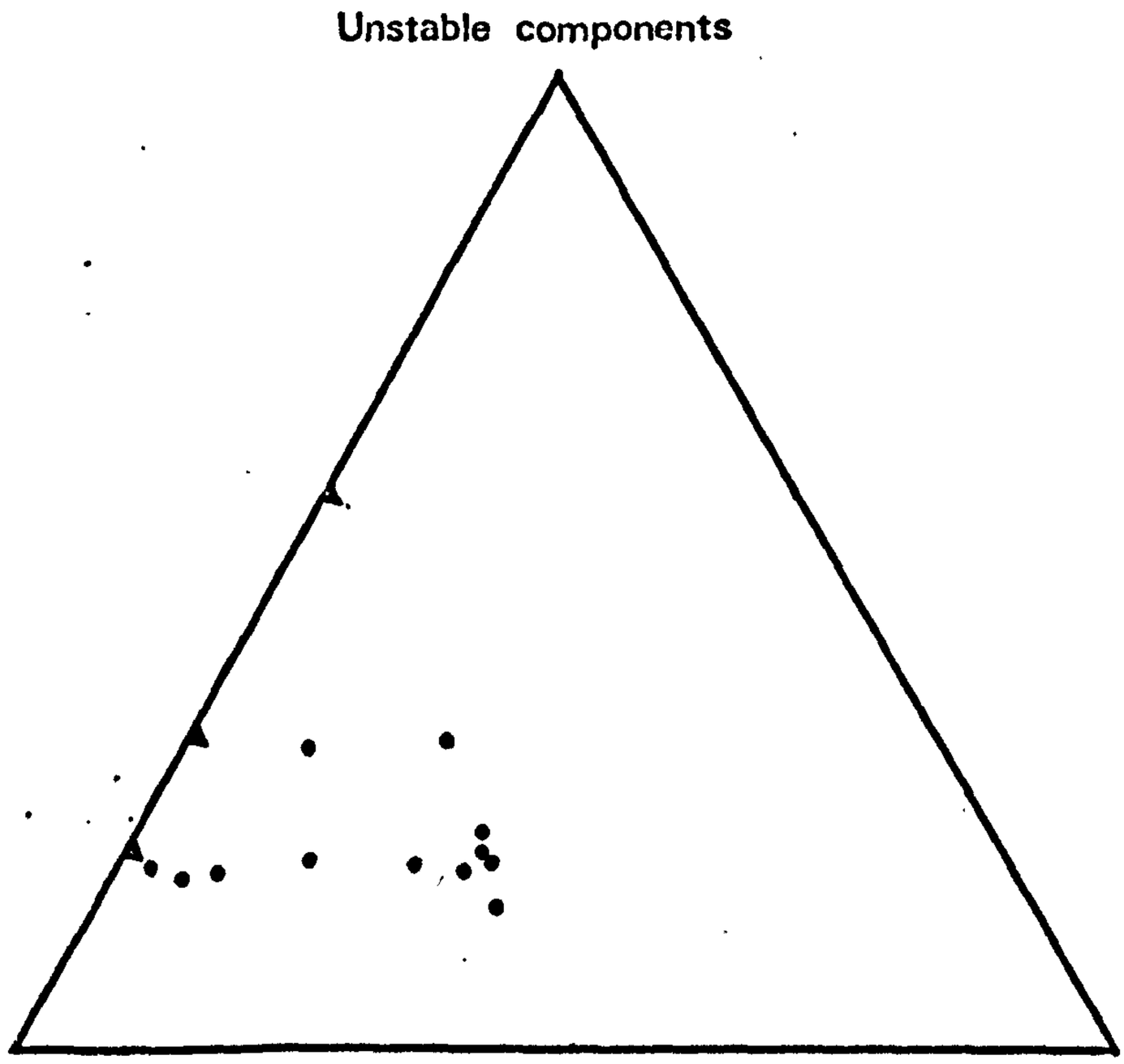

Fig.13 Diagram showing the percentages of quartz, matrix and unstable components (feldspar, rock fragments, sericite and mica).

• Mam Tor

▲ Tansley Borehole

TABLE 21: Showing Quartz and Matrix Percentages, with Range and Mode of Sizes

Mam Tor Sandstones				
Sample Number	Quartz	Matrix	Range of Size in mm	Mode
1b	47.06	31.91	0.03-1	0.09-0.2
2b	46.10	34.29	0.03-1	0.09-0.4
3b	50.68	33.11	0.03-0.6	0.09-0.4
$4b_1$	75.81	7.22	0.03-0.6	0.09-0.2
$4b_2$	43.31	24.41	0.03-0.8	0.09-0.2
$4b_3$	44.89	33.33	0.03-0.8	0.09-0.2
6b	47.80	36.66	0.03-0.8	0.2 -0.4
$6b_1$	63.85	18.48	0.07-1	0.2 -0.4
$6b_2$	71.32	9.31	0.03-1	0.2 -0.4
$6b_3$	76.57	4.60	0.07-0.8	0.2 -0.4
$8b_1$	53.54	28.67	0.05-1	0.2 -0.4
$8b_2$	56.98	12.56	0.05-1	0.2 -0.4
Tansley Borehole - Ashover Sandstones				
Sample Number	Quartz	Matrix	Range of Size in mm	Mode
5	42.88	0.00	0.09-1	0.2 -0.4
6	73.00	0.96	0.09-1.6	0.2 -0.6
12	68.00	0.00	0.07-0.6	0.09-0.2

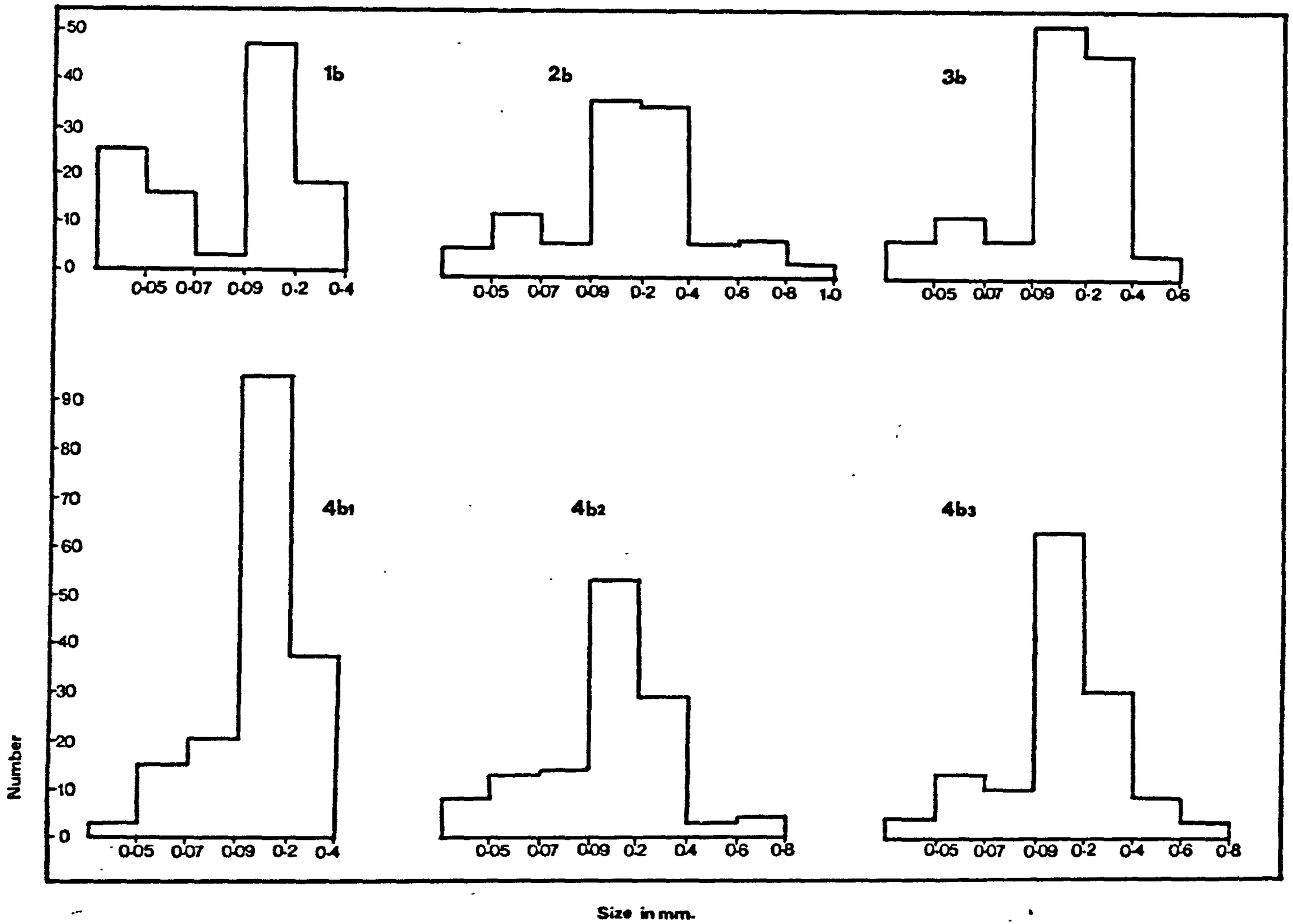

Fig.14 Histograms showing the distribution of grain size in the Mam Tor sandstones.

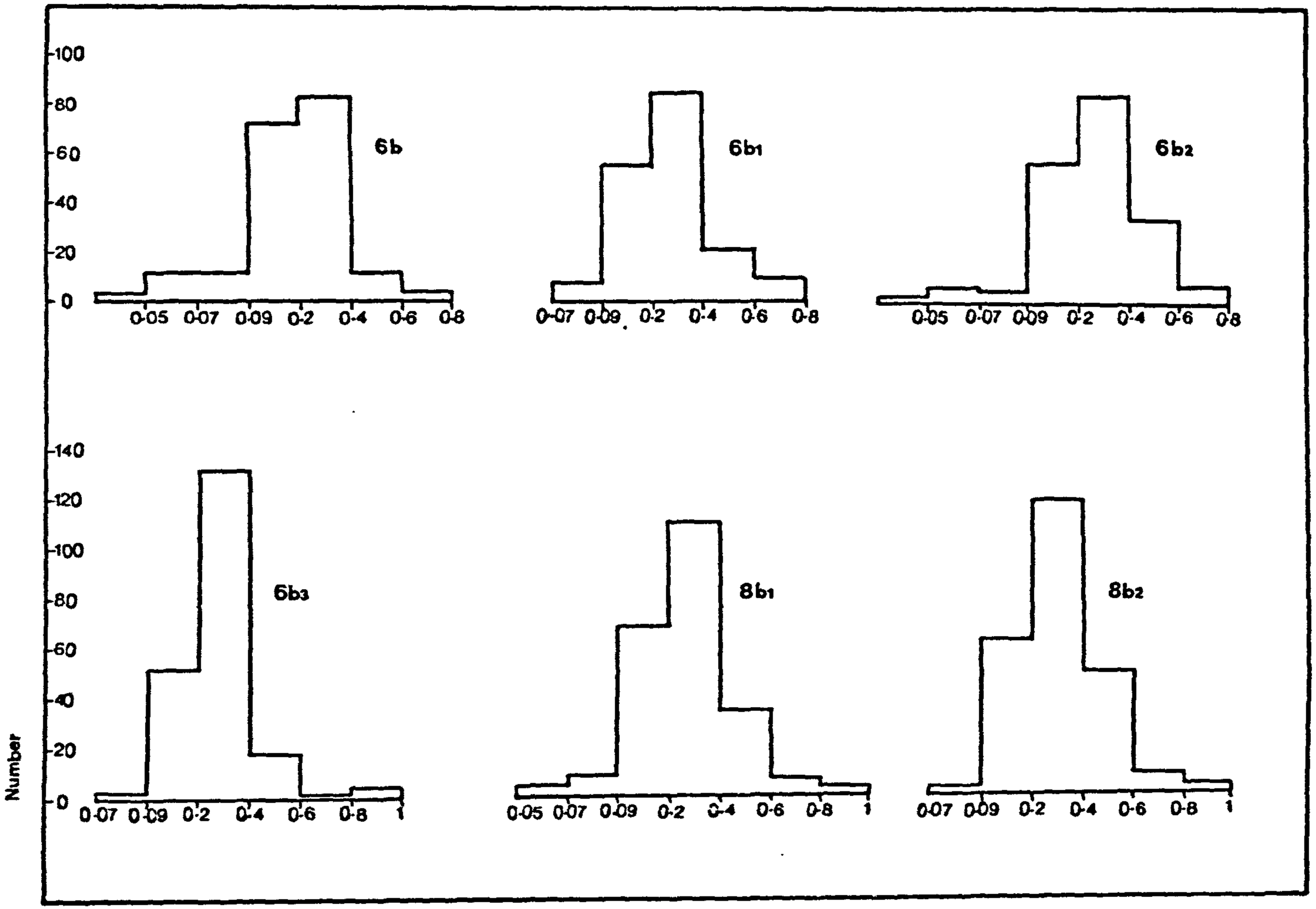
100
80
60
40
20
0
6b
0·05 0·07 0·09 0·2 0·4 0·6 0·8
6b1
0·07 0·09 0·2 0·4 0·6 0·8
6b2
0·05 0·07 0·09 0·2 0·4 0·6 0·8
140
120
100
80
60
40
20
0
Number
6b3
0·07 0·09 0·2 0·4 0·6 0·8 1
8b1
0·05 0·07 0·09 0·2 0·4 0·6 0·8 1
8b2
0·07 0·09 0·2 0·4 0·6 0·8 1

Size in mm.

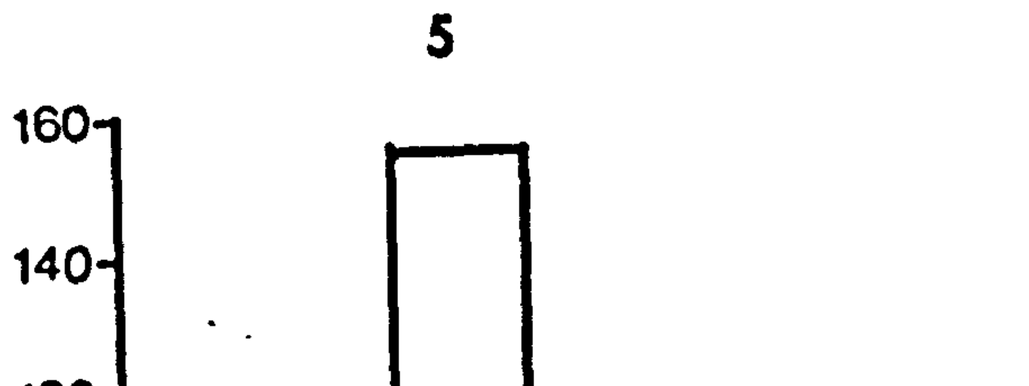

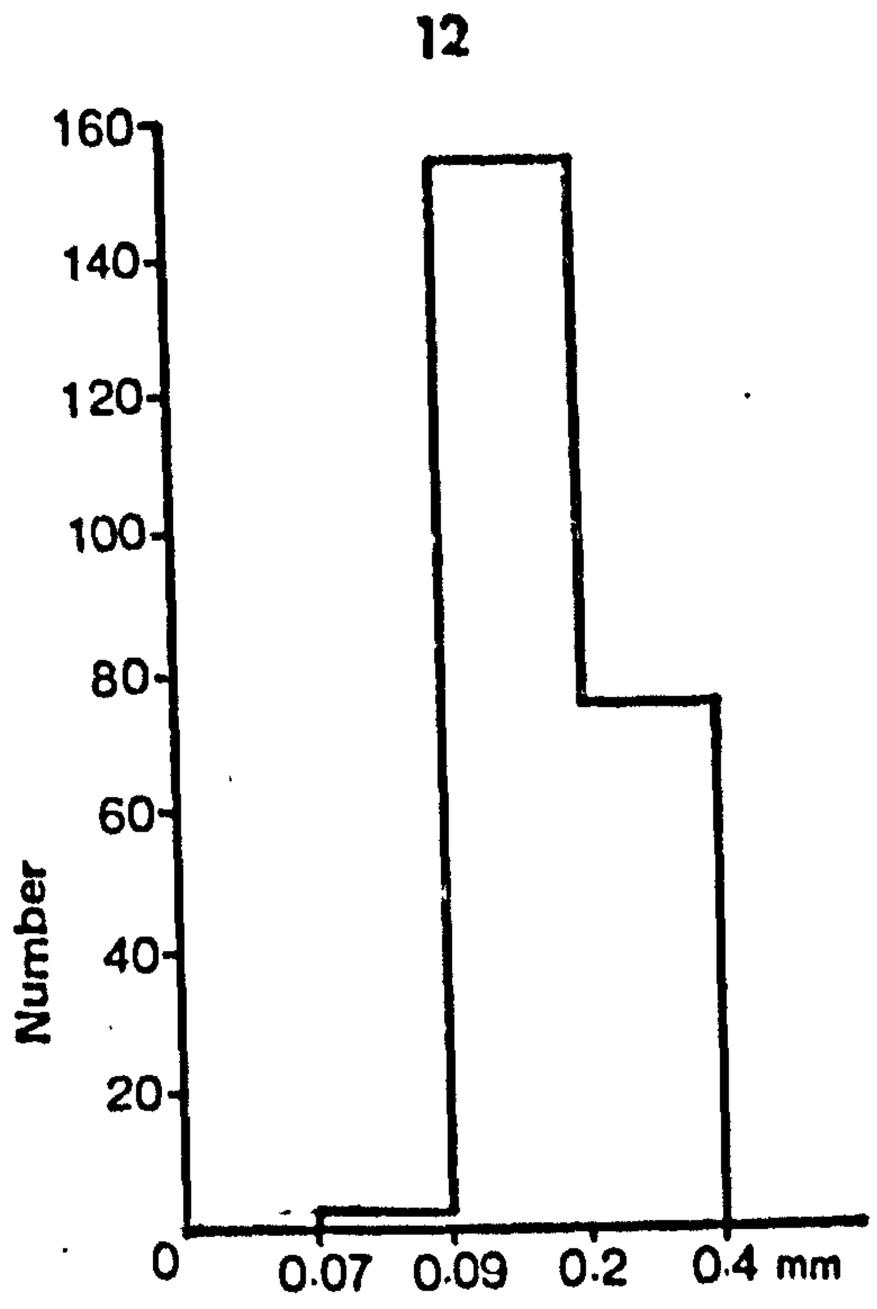

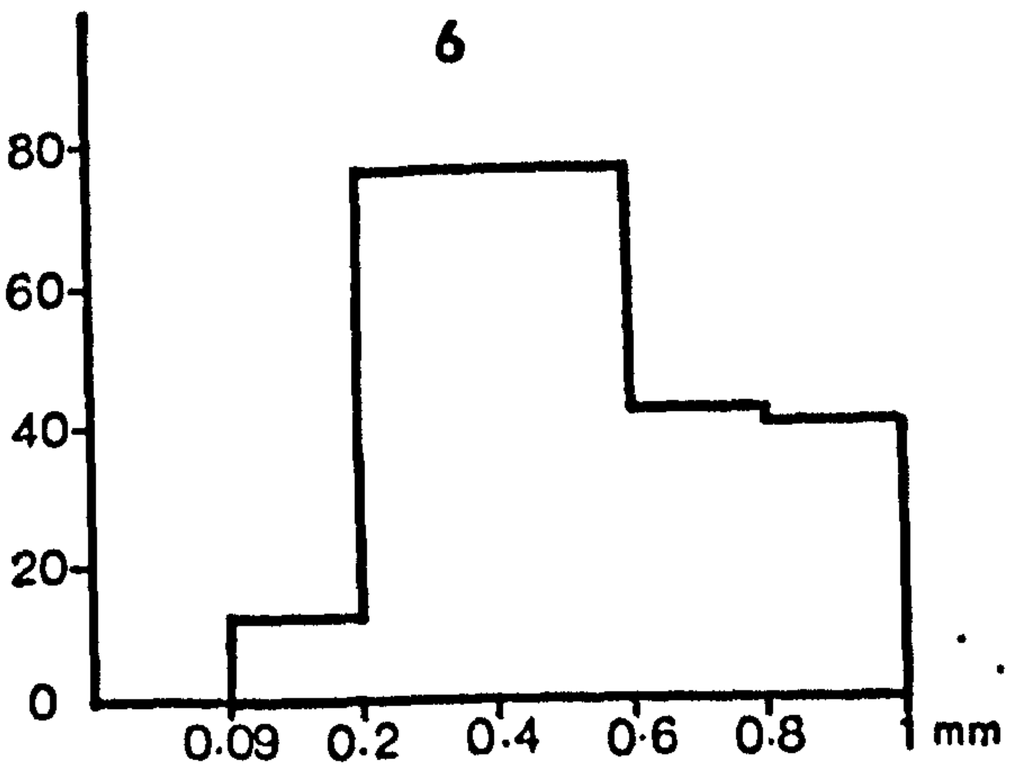

Histograms showing the distribution of grain size in the Ashover sandstones.

that the amount of quartz increases upwards, and the matrix content decreases. As demonstrated by the frequency size distribution, the percent of coarse fraction becomes dominant in upwards direction. Likewise, this is also exhibited by different beds in the succession, the higher beds are relatively more coarse grained than the lower beds.

In the argillaceous sandstones the very fine matrix constituents called clay, fill the spaces between the dominantly angular-subangular sand grains and by compaction has become coherent, binding and hard clastic grains. Its specific composition is not determinable in thin section. In those sandstones which bear little matrix, the sand grains are subangular-subrounded and generally exhibit close fitting with welding and pressure solution. Original clastic boundaries are barely distinguishable in welded groups. However, some of the sandstones contain a small amount of calcite as cement (Plate 2) but the quartz grains are bounded by the clay and the secondary enlargements of the quartz.

Mineralogy

Quartz: The content ranges from 43-77 percent by volume and appears as angular to subangular grains in the matrix rich sandstones, the main variety being of the non-strained type, although several grains with shadow or undulose extinctions are present. Commonly, quartz grains show trails of liquid inclusions while tourmaline, zircon and apatite are frequently encountered as inclusions inside quartz grains (Plate 2).

In those sandstones where the clay matrix is dominant, secondary quartz overgrowths are either small or lacking altogether. However, these sandstones may develop patchy quartzitic texture in parts where the clay is absent. Secondary quartz in the form of cryptocrystallographically continuous overgrowths on detrital grains is observed where the clay matrix is lacking.

In addition some quartz grains are observed with secondary overgrowths developed on the clean surface, but inhibited on the side heavily coated with clay.

However, some overgrowths can be distinguished from the detrital grain by the presence of a dusty line or a zone of inclusions representing the original surface of the detrital grains (Plate 3). Nevertheless, sometimes clear idiomorphic quartz grains are observed. In such cases, it seems the original grains were bounded by clean surfaces or that the secondary quartz overgrowths have replaced the clay on the detrital grain, so that the contact with the original surfaces may be obscured or invisible.

Feldspar: (2.22-9.30) This consists of plagioclase and probably orthoclase. Plagioclase being relatively albite rich (demonstrated by 3.18Å diffraction peak) and showing multiple or polysynthetic twinning (Plate 3), together with combined carlsbad twinning. Most of the untwinned feldspar, presumed to be orthoclase, is heavily altered, and microcline is the least abundant, compared to albite or the untwinned feldspar. Most of the untwinned feldspar and to a lesser extent albite, have been altered or replaced by calcite in which remnant feldspar can be observed, or by microcrystalline aggregates of clay minerals of low birefringence (Plate 4). Nevertheless, others show a combined replacement by calcite and microcrystalline clay aggregates. On the other hand, some have been replaced by sericite or fine mica.

It is believed that the microcrystalline aggregates of clay are kaolinite as indicated by optical and X-ray studies (very sharp peak of kaolinite). Nevertheless, in the aforementioned description of the arenaceous members of the Millstone Grit Series, authigenic kaolinite after feldspar is well documented. However, comparison of optical properties and form of the microcrystalline aggregates in the Mam Tor rocks with photographs of authigenic kaolinite (Kulbicki and Millot, 1963; Wilson and Pittman, 1977) showed their very close similarities.

Secondary overgrowths have not been observed on the feldspar grains. Minerals, like rutile, apatite and quartz are present as inclusions within the feldspars. In some sandstones, feldspar grains have intimately interlocked contacts or in other instances, they have been distorted by fracturing, between the contiguous grains, as a result of compaction.

Matrix: The matrix comprises the very fine groundmass of clay minerals, together with the fine grains of quartz, feldspar and other detrital components. In addition brown iron oxides are common, with black carbonaceous material are disseminated throughout the matrix, which constitutes up to 37% by volume, of the whole rock. Particularly, it forms a dominant component in the lower Mam Tor sandstone beds.

Rock Fragments: (0.7-2.77%) The rock fragments consist chiefly of the igneous variety, which is encountered as composite grain embodying several quartz grains, or quartz and feldspar moulded together (Plate 5). Rock fragments of metamorphic origin, are less abundant and consist of many elongated quartz grains, showing extreme strain shadows (Plate 6). Nevertheless, very few shale fragments are observed as well (Plate 6). The igneous and metamorphic rock fragments are relatively more abundant in the sandstones having coarser maximum grain size than in the finer ones, in which shale fragments are observed.

Carbonates: Carbonates range between 1.4-14.15 in volume, and are present as two different varieties. The first is as microcrystalline, brown sideritic mudstone grains (Plate 7). This variety is abundant in the lower and upper Mam Tor sandstones and appears as detrital grains. The second variety which consists of calcite occurs in some of the Mam Tor sandstone. It must be remembered that calcite is present essentially as replacement of the feldspars and in extreme cases it may appear as original cement.

Mica: The chief components of mica are oxidised biotite and muscovite of detrital origin (Plate 7), but subordinate amounts of authigenic chlorite and sericite (Plate 8) are also present (up to 13%). Sometimes, hydro-biotite alteration to chlorite and the development of iron oxide, is clearly seen in thin section. The micas are often bent between the rigid clastic grains as a result of compaction (Plate 8).

3.2.2. The Ashover Grit

The same constituent grains are present in the Ashover sandstones as the Mam Tor sandstones (Figure 13), but the Ashover sandstones are almost matrix-free. They are well sorted and are mainly of arkosic-subarkosic composition. Two of the sandstone specimens (at depths of 66.30 and 110.15 metres) consists of tightly packed angular-subangular clastic grains which exhibit penetrating and interlocking contacts as a result of pressure solution (Plate 9), and quartz overgrowth is observed in these sandstones. The other specimen (at depth of 65.40 metres) is a carbonate cemented sandstone (Plate 9). The clastic grains seem to be floating inside the cement.

The grain size varies from fine to very coarse sand, but the majority are of medium to coarse in size (see Table 21). The quartz content in these sandstones ranges between 42-73%, the feldspar content is about 15%, carbonate reaches a maximum of 40%, mica is up to 3.5%, rock fragment have a highest value of 2.90%, and the maximum matrix content is about 1%. Feldspar comprises microcline and orthoclase, perthitic in part (Plate 10). Quartz and feldspars have both been replaced to varying degrees by carbonate. In extreme cases only feldspar relics are left inside the carbonate. In addition to calcite, replacement of feldspar by sericite and microcrystalline-clay is also common. Only a limited number of samples were studied in the present work. Additional samples were studied by Elliot

(in Ramsbottom et al. 1962) who described the whole succession in the Tansley Borehole on which the present studies were carried out. He stated that the sandstones constituting the Ashover Grit consist of subangular, angular and less frequently, round grains of quartz, feldspar, with flakes of muscovite and biotite. The grain size varies from 0.06-2.5 mm. The matrix consists largely of a clay mineral belonging to the kaolinite group. Below a depth of 65.40 m dolomite,generally coarse crystalline is present as cement. The heavy mineral suite includes apatite, garnet, leucoxene, rutile, tourmaline, zircon and iron ore.

The subsidiary bands of sandstone below the Ashover Grit which are interbedded with siltstones are rather fine grained, but of similar composition to the sandstones described above. The cement however, consists of ankerite, siderite and calcite. The siltstones consist of an argillaceous matrix containing subangular and angular grains (usually 0.03 to 0.6 mm diameter) of quartz, albite and orthoclase, with flakes of biotite (commonly altered) and muscovite.

Additional information on the Ashover Grit is provided by Smith et al (1967), who examined eleven specimens from five localities along the outcrop of the Ashover Grit, in the area in which the Tansley Borehole is located. Their results are shown in Table 22. Almost all the sandstones are subarkosic in composition. The major components and heavy minerals of these sandstones are similar to those described above.

Texture of the Sandstones: Classified according to textures, the sandstones fall into the following categories:

1. Sandstones that are loosely packed, i.e. cemented by calcite
2. Sandstones that are moderately packed, but without abundant interlocking or penetration contacts, i.e. cemented by clay and subordinate carbonates.

TABLE · 22: Modal Analysis of the Ashover Grit. Percentages of Minerals by Volume (Smith et al. 1967)

Mineral	Range	Mean
Quartz	64-79	73
Orthoclase	4-11	7
Plagioclase	< 1- 1	-
Microcline	1- 5	2
Muscovite	< 1- 3	1
Biotite and Hydrobiotite	< 1- 7	1
Kaolinite and other Clay Minerals	2-21	12
Chlorite	< 1- 2	1
Rock Fragments	< 1- 3	1
Geothite and Fe_2O_3	< 1- 6	2

3. Tightly packed or interlocked sandstones, i.e. cemented by quartz with little clay.

The textural classification is based on the degree of packing and interlocking of the detrital grains and on the nature of cementing materials. There is no clear cut boundary between these three groups in the sandstones studied, and indeed gradations are to be expected between the various textures. In the same thin section for example, it is observed, that a part in which moderately packed sand grains are present passes upwards into tightly interlocked, quartz cemented portions.

The close packing in these sandstones is believed to be chiefly the result of compaction due to deep burial. This is indicated in some sandstones by the distorted form of muscovite and biotite lathes, feldspar and quartz grains. Whereas others yielded to this overburden by the development of sutured or interlocking contacts, especially the quartz grains, as the result of solution precipitation along the surfaces of adjacent grains.

3.2.3. Composition of Heavy Minerals

The heavy minerals make up less than 1 percent of any sample. The heavy minerals present in the sand fraction are closely comparable with those of the silt fraction. The only observed difference is that the garnet and epidote are more abundant in the >124 μm sand fraction than in the finer sand and silt fractions.

Zircon is the most common heavy mineral. Tourmaline, rutile (anatase) and muscovite are always the next most abundant minerals, in that order. Opaque iron oxides, chlorite, biotite are common, but never abundant. The remaining minerals which include garnet, epidote and sphene are rather scarce (1 percent) especially in the silt fraction.

Zircon: Minute long and short prismatic euhedral crystals of zircon are found as well as very well rounded grains (Plate 11). Most are clear or pink coloured varieties, but yellow, brownish, smoky and purple varieties are always present. Some of the zircon grains are highly fractured.

Rutile (Anatase): Rutile is present as long prismatic crystals, and angular grains. They are brown, yellowish brown, reddish brown and deep red in colour (Plate 12). Knee shaped twins were observed.

Tourmaline: Several colour varieties of tourmaline are present, namely green, bluish green, brown and dark green. The green and brown varieties are usually euhedral with some black inclusions, while the other varieties are very well rounded (Plates 13, 14). These varieties are mostly iron tourmaline.

Garnet: Pale pink, orange or colourless varieties of garnet are found, the first variety being the most dominant (Plate 14). The grains are fresh, transparent and are strongly etched giving a rhombic pattern. The presence of etched garnets demands plenty of time after deposition for intrastratal solution to etch the grains (Hemingway and Tamar-Agha, 1975).

Epidote: The epidote is green and yellowish green in colour. It occurs in granular aggregates (under reflected light). The zoned interference colours are distinctive of epidote. The green variety resembles broken glass fragments. A few composite grains of epidote and garnet were observed (Plate 15).

Muscovite: Colourless transparent flakes of muscovite are chiefly present.

Biotite: This is present as brown and reddish brown flakes. Most of the flakes show variable kinds of alterations, loss of pleochroism, partial

decolourisation and alteration to chlorite (Plate 16). In extreme cases of alteration it forms brown granular aggregates.

Chlorite: Chlorite occurs in pale green flakes which contain relics of altered biotite. However, few composite flakes of chlorite and biotite were also observed.

Sphene: The colour of sphene is yellowish brown. It shows a rhombic form and lack of complete extinction is very characteristic.

Opaque Minerals: These mostly include the iron oxide minerals.

Leucoxene: Occurs as white or orange grains in reflectedlight. They are rounded and have a porcellaineous surface texture.

3.3 Discussion

The petrography and heavy minerals of the sandstones, suggest an input from acid igneous and metamorphic rocks, into the depositional area. The apparent dominance of monocrystalline detrital quartz grains over 'strained' and polycrystalline grains together with fresh sodic and potassic feldspars not only indicate an acid igneous source, but also great rapidity in transport, deposition and burial. In general the evidence supports Sorby (1859) and Gilligan's (1920) views on the derivation of the Millstone Grit from a northerly landmass, composed largely of granites, grantoid gneisses and schists. This view is supported by other workers who studied the Millstone Grit (Greensmith, 1957; Allen, 1960; Smith et al. 1967; Walker, 1966; Collinson, 1968).

The association of fresh and altered feldspars may be due to their relative stabilities with decomposition taking place prior to/or after deposition. Butler (1953), Blaxland (1974) and Bjorlykke (1975) reported the alteration of feldspars to kaolinite and sericite as a result of granite

weathering. The altered feldspar grains would probably break up during transportation and thus the resultant clay minerals would be regarded as primary after deposition.

On the other hand, post-depositional changes could have brought about these changes. Wilson and Pitman (1977) carried out a detailed thin section/scanning electron microscope study of thousands of sandstones representing many ages, compositions and depositional environments. Their results indicated that authigenic clays are far more common than previously recognised and they drew attention to the importance of authigenic clay in sandstones.

In the present study, the alteration of feldspars and other minerals due to weathering of the source rock, has no doubt contributed to the clay content of the sediments but to what degree is conjectural.

The fact that feldspars alter in the sandstones examined in the present study to a microcrystalline clay mineral, probably kaolinite, suggests that kaolinite in the sandstones may be in part a breakdown product of the feldspars. In addition, feldspars altering to sericite was also observed. Therefore, some of the kaolinite and sericite was probably formed during diagenesis and is thus secondary.

The general decrease in feldspar content (Table 21) with decrease in grain size of the sandstones, depends on the abrasion and sorting of the sediments. However, as most of the grains, in the clay rich sandstones are angular to subangular it implies that sorting was the dominant factor. In addition size, shape and density also play important roles in the sorting process (Allen, 1970). This would imply that smaller, angular and low density grains tend to be transported further than larger, rounded and high density grains.

Since quartz and feldspars have approximately the same density (2.65 and 2.56-2.78 respectively) the decrease in feldspar content can be attributed to sorting, although their inherent chemical instability and lesser mechanical strength may have also contributed to their impoverishment in the finer grained sandstones. Likewise, a prolonged time of transportation over great distance or a decrease in the impetus of transporting medium may tolerate longer time for the chemical and mechanical breakdown to take place. The statistical results of Ethridge (1977) demonstrated that grain size and feldspar content decrease linearly with distance transported which is significant in that it represents the division between front delta platform sediments and prodelta sediments on the marine shelf (turbidites).

On the other hand a decrease or increase in the content of a particular feldspar may indicate a change in the source area and climate which influence the types of derivatives to be transported. Bailey and Irwin (1959) found that the average K-feldspar content of some greywackes increased markedly with decreasing age of deposition. They attributed this increase to changes in composition of the source area with time, namely a progressive increase in the area of granite exposed. In contrast, Middleton (1972) concluded that most of the untwinned feldspar grains in the Charny Sandstones (turbidites) of Quebec, were originally potash feldspar or perthite which has been altered to albite during diagenesis by the action of sodium rich pore waters (connate sea water). In the rocks of the present study, the feldspar is believed to be of detrital origin. The depletion of the Mam Tor sandstones in K-feldspar is due to diagenetic alteration to kaolinite. The abundance of K-feldspar in the Ashover sandstones can be attributed to deposition in fluvial environment as compared to the deep marine environment of the Mam Tor sandstone (see Chapter 1). Thus, the

distance of transport and the inherent instability of feldspar might have played an important role in its distribution. However, the Ashover sandstones were considered to have a southerly source, while the Mam Tor sandstones of a northerly source (see Chapter 1).

With respect to the authigenic quartz cement, it is the most common type of cement in sandstones and has therefore been extensively studied. Generally there are two possible origins for the secondary silica: (1) precipitation from connate solution; and (2) pressure solution of quartz and silicates (Selly, 1976).

The latter is believed to be the case in the sandstones in the present study, as indicated by the compacted, dislocated, and bent clastic grains. These observations have suggested to many workers that as sand is compacted, silica is dissolved at the point of grain contact and reprecipitated instantaneously (Taylor, 1950; Heald and Baker, 1977).

The decomposition of biotite is usually accompanied by loss of Mg, K, Na and the oxidation of ferrous iron to ferric iron. The end product appears to be chlorite, illite, kaolinite and hydrobiotite (Kappor, 1972; Barracan and Iniguez, 1976; Exley, 1976). The alteration of biotite may take place during weathering, transportation or during early diagenesis. Biotite alteration is common in the Millstone Grit sediments and geothite is usually disseminated throughout the matrix of the sandstone.

Carbonate cement is widely distributed in various sedimentary rocks. It consists of calcite, dolomite, ankerite and siderite. These carbonates are commonly formed in the early stages of diagenesis, but on the other hand they could be formed under deep burial (Muravyov, 1970; Selly, 1976; Heald and Baker, 1977).

A discussion of the occurrence of carbonates and associated pyrite, in the sediments in the present study, will be reserved until the sediments in question have been examined more fully from the chemical approach.

In conclusion, the present study substantiates previous petrological studies of the Namurian sandstones. However, the petrographic comparison of the Mam Tor sandstones (turbidites) and Ashover sandstones (fluvial) reveal that the silt and sand size grains are mineralogically similar, except that the Ashover sandstones contain more feldspar of the potash variety. In addition the Mam Tor sandstones have a higher matrix content as would be anticipated. This variation could have resulted from one or more of the following factors:

(1) selective sorting of the sand, silt and clay fractions; depending on the distance of transport.
(2) physical abrasion of detrital constituents during transportation.
(3) chemical weathering during transportation.
(4) diagenesis.

Evidence has however, been previously presented (see Chapter 1, page 24) for a southerly derivation of the Ashover Grit. It seems therefore that a relative decrease in the amount of northerly derived sediments occurred in favour of the southerly derivation. Presumably, the detrital supply from the south increased in post-R_1 times, and it may also imply that feldspathic rocks could have been exposed and subjected to denudation.

The heavy mineral study showed that the crystalline and well rounded zircon and tourmaline, together with rutile, garnet and epidote were the most important minerals. The presence of two varieties of zircon and tourmaline can be related to a varied source rock (Pettijohn, 1957). The crystalline forms of zircon and tourmaline indicate a source of igneous and metamorphic rocks, while the rounded forms suggest a recycling from earlier sedimentary rocks. Likewise, the distance of sediment transport is important

in this respect. Prolonged transport may result in a highly rounded grain, whereas a little worn grain reflects a shorter distance of transport.

On the basis of this petrographic information, however, it can be suggested that the Mam Tor rocks have been derived from igneous, metamorphic and reworked sedimentary rocks.

CHAPTER 4

Mam Tor Rocks

The object of this Chapter is to establish or identify geochemical variation between groups of elements and minerals in closely associated greywackes and shales. The existence of such relationships facilitates geochemical interpretation.

4.1 Major Elements and Mineralogy of Whole Rock Samples

The major element analyses and mineralogical data of the shales and greywackes are listed in Appendix 1. The ranges, means, and standard deviations of elements and minerals in each lithology are shown in Table 23. Mineralogical data was obtained by a method combining both normative and X-ray diffraction results. However, recourse was always made to whole rock X-ray diffraction traces to substantiate these mineralogical compositions, which were found in good agreement. The graphical representation of major elements, quartz and clay minerals trends is depicted as section profile in Figure 15. Expected differences between the two lithologies are evident. In general, total SiO_2, quartz and also their average contents are higher in the greywackes than that of the shales, while the converse is clear for the Al_2O_3 content. This is reflected by the increase in clay minerals content as the quartz content decreases; indicating a mutual dilution between them. The variation in Na_2O content shows a good resemblance to that of SiO_2, suggesting that most of the Na_2O is contained in the plagioclase. Also, its variation is sympathetic with that of the quartz which indicates that both are of detrital origin.

Combined silica, Al_2O_3, K_2O, FeO, MgO, H_2O^+ profile show a close similarity, although their average contents apart from FeO are higher in the shales. It implies, therefore, that the greater part of these elements

TABLE 23: Major Elements and Mineralogy of the Mam Tor Rocks

	Shales			Greywackes (Sandstones)		
Oxides/Minerals	Range	Mean	S.D.	Range	Mean	S.D.
Quartz	11.74-31.31	18.84	5.55	46.17-73.08	60.06	8.28
Combined Silica	28.42-37.85	32.84	3.44	9.71-19.80	14.03	2.76
Al_2O_3	20.07-27.23	23.87	1.68	7.57-15.90	10.84	2.63
TiO_2	0.88- 1.09	1.00	0.08	0.35- 0.83	0.53	0.15
Fe_2O_3	1.69- 5.19	3.67	1.06	0.85- 4.15	2.47	1.04
FeO	1.22- 3.7	1.92	0.72	0.59- 8.55	2.52	2.02
MgO	1.62- 2.30	1.83	0.18	0.48- 2.32	1.00	0.49
CaO	0.09- 0.39	0.23	0.11	0.12- 3.77	0.63	0.95
Na_2O	0.37- 0.82	0.52	0.13	0.90- 1.20	1.08	0.09
K_2O	2.08- 3.11	2.70	0.29	0.50- 1.47	0.86	0.32
MnO	0.02- 0.18	0.08	0.05	0.04- 0.29	0.13	0.07
P_2O_5	0.11- 0.20	0.15	0.03	0.08- 0.32	0.13	0.07
SO_3	0.00- 0.30	0.06	0.12	0.00- 0.32	0.09	0.10
CO_2	0.00- 3.12	0.39	0.92	0.00- 5.52	1.15	1.59
Chlorite	5.13- 8.15	6.89	0.87	1.59- 6.48	3.39	1.66
Illite + MXL	17.37-26.19	22.62	2.90	3.83-10.89	6.14	2.38
Kaolinite	30.16-43.39	36.54	4.31	10.67-25.37	17.91	5.21
Na-Feldspar	3.21- 6.94	4.40	1.12	7.61-10.15	9.09	0.79
Siderite*	0.00- 2.57	1.04	1.04	0.00-13.62	5.89	4.49
Dolomite*	0.00- 0.96	0.90	0.08	0.00- 1.84	1.40	0.62
Calcite*	0.00- 0.26	0.26		0.00- 6.04	1.87	2.79
Pyrite*	0.00- 0.22	0.22	0.01	0.00- 0.23	0.14	0.08
Apatite	0.26- 0.47	0.36	0.07	0.19- 0.45	0.29	0.10
Org. C.	1.08- 3.94	2.18	0.80	0.00- 0.99	0.43	0.33
Excess Fe_2O_3	1.63- 5.20	3.26	1.07	0.72- 3.84	2.33	1.07

*Calculated for the samples containing these minerals only

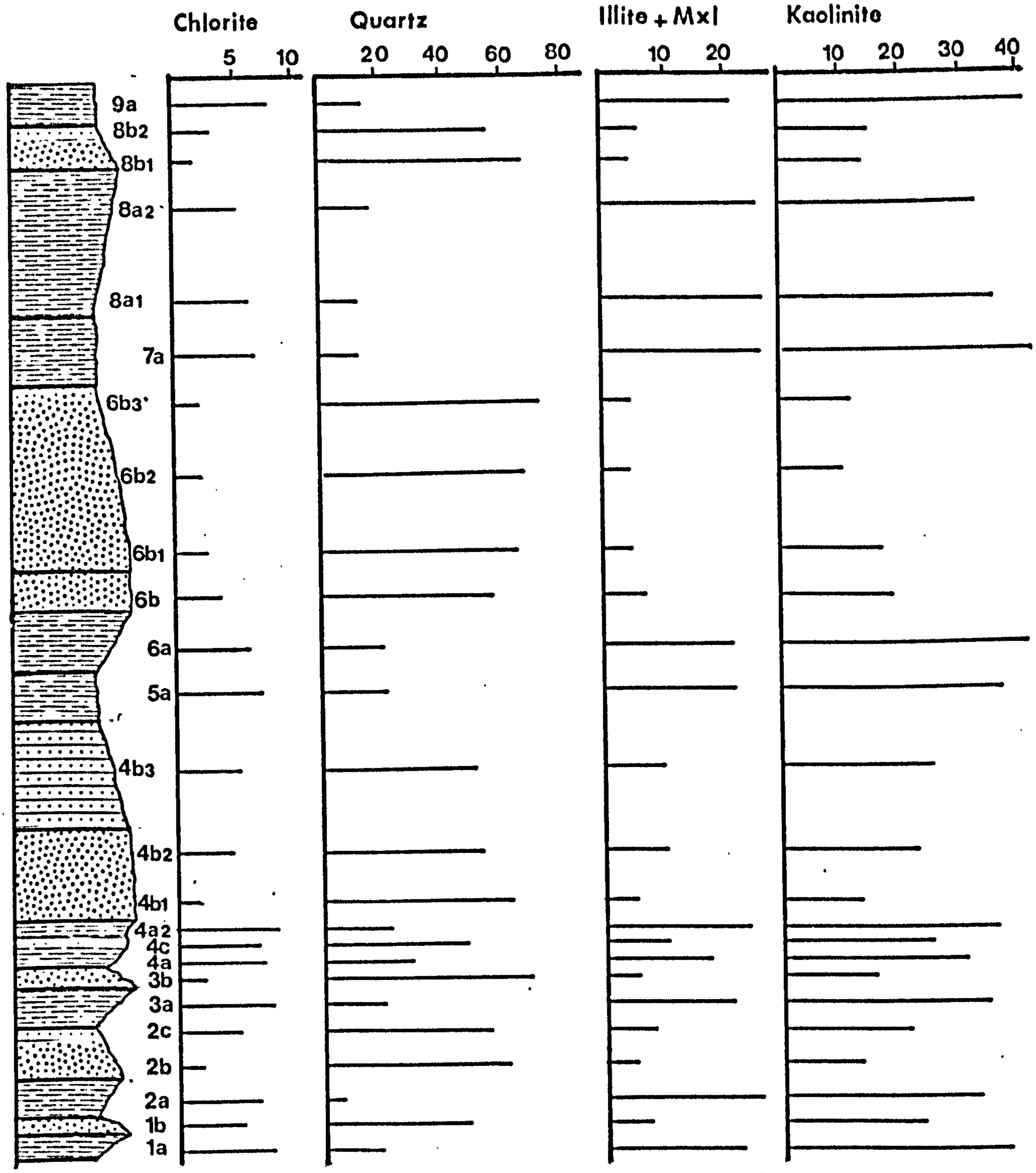

Fig.15 Section profiles showing the variations of mineral and major element contents through the Mam Tor Beds.

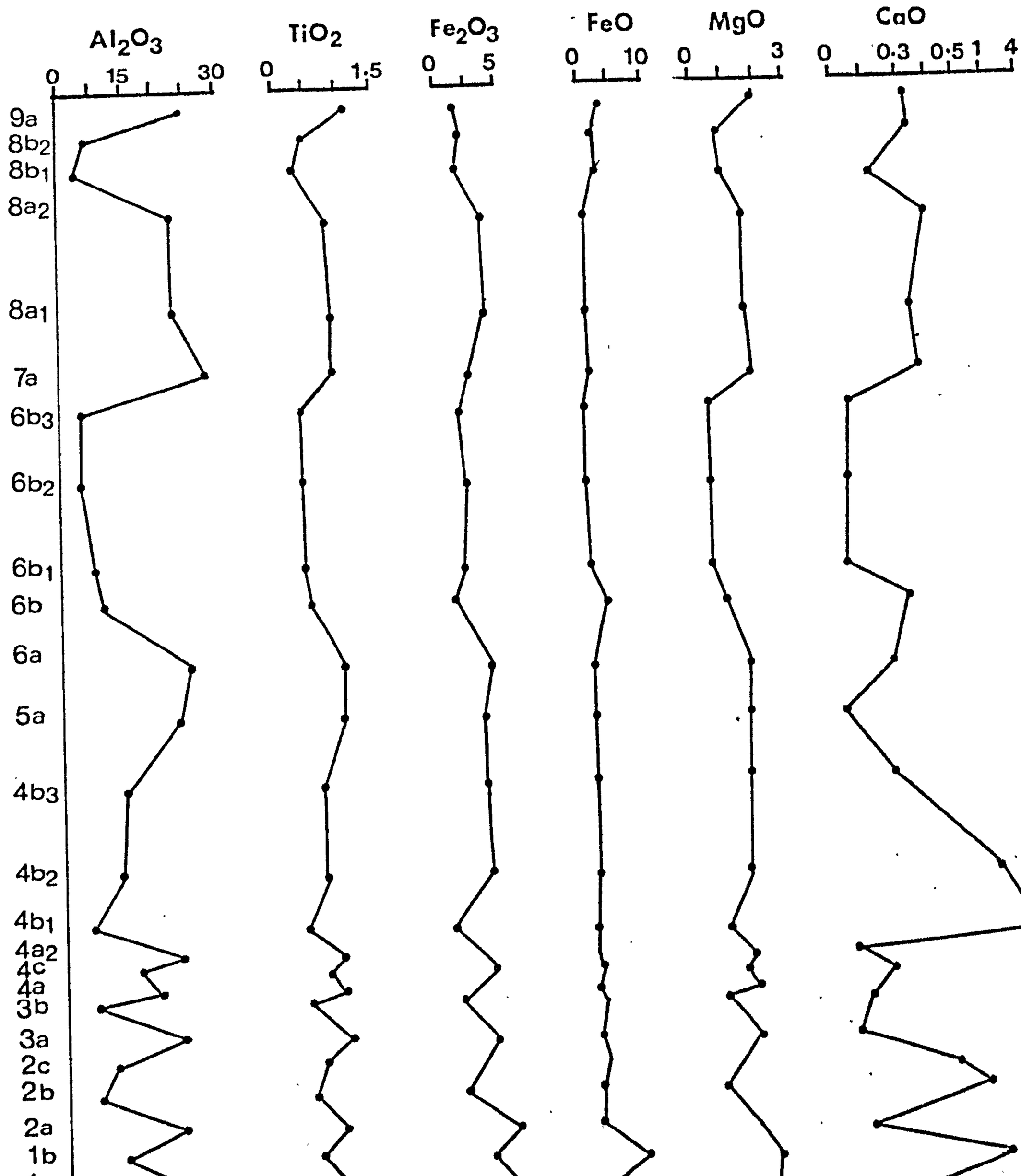
Al_2O_3
0 15 30
TiO_2
0 1·5
Fe_2O_3
0 5
FeO
0 10
MgO
0 3
CaO
0 0·3 0·5 1 4
9a
8b2
8b1
8a2
8a1
7a
6b3
6b2
6b1
6b
6a
5a
4b3
4b2
4b1
4a2
4c
4a
3b
3a
2c
2b
2a
1b
1a

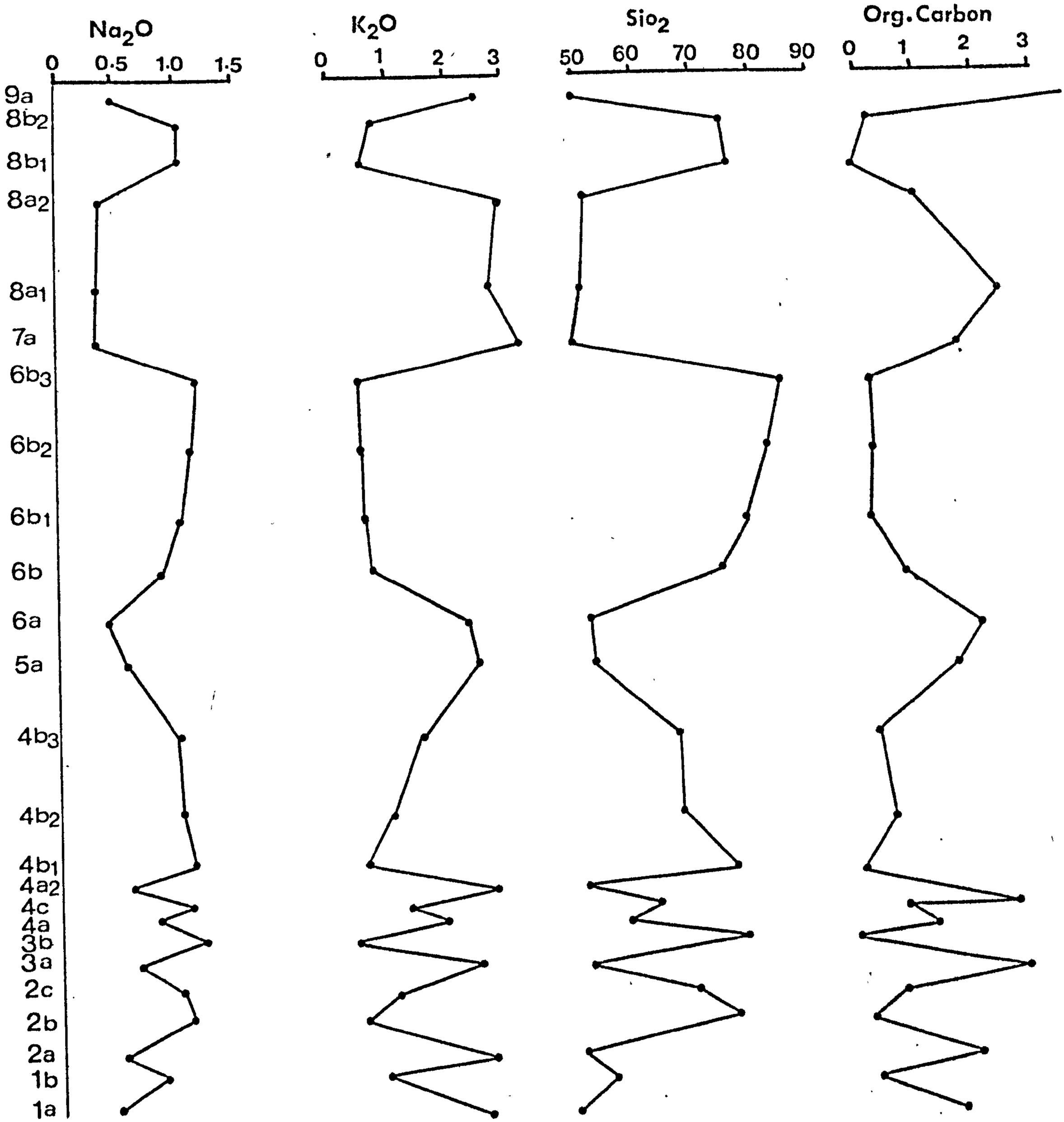
Na_2O
0 0·5 1·0 1·5
K_2O
0 1 2 3
Sio_2
50 60 70 80 90
Org. Carbon
0 1 2 3
9a
8b2
8b1
8a2
8a1
7a
6b3
6b2
6b1
6b
6a
5a
4b3
4b2
4b1
4a2
4c
4a
3b
3a
2c
2b
2a
1b
1a

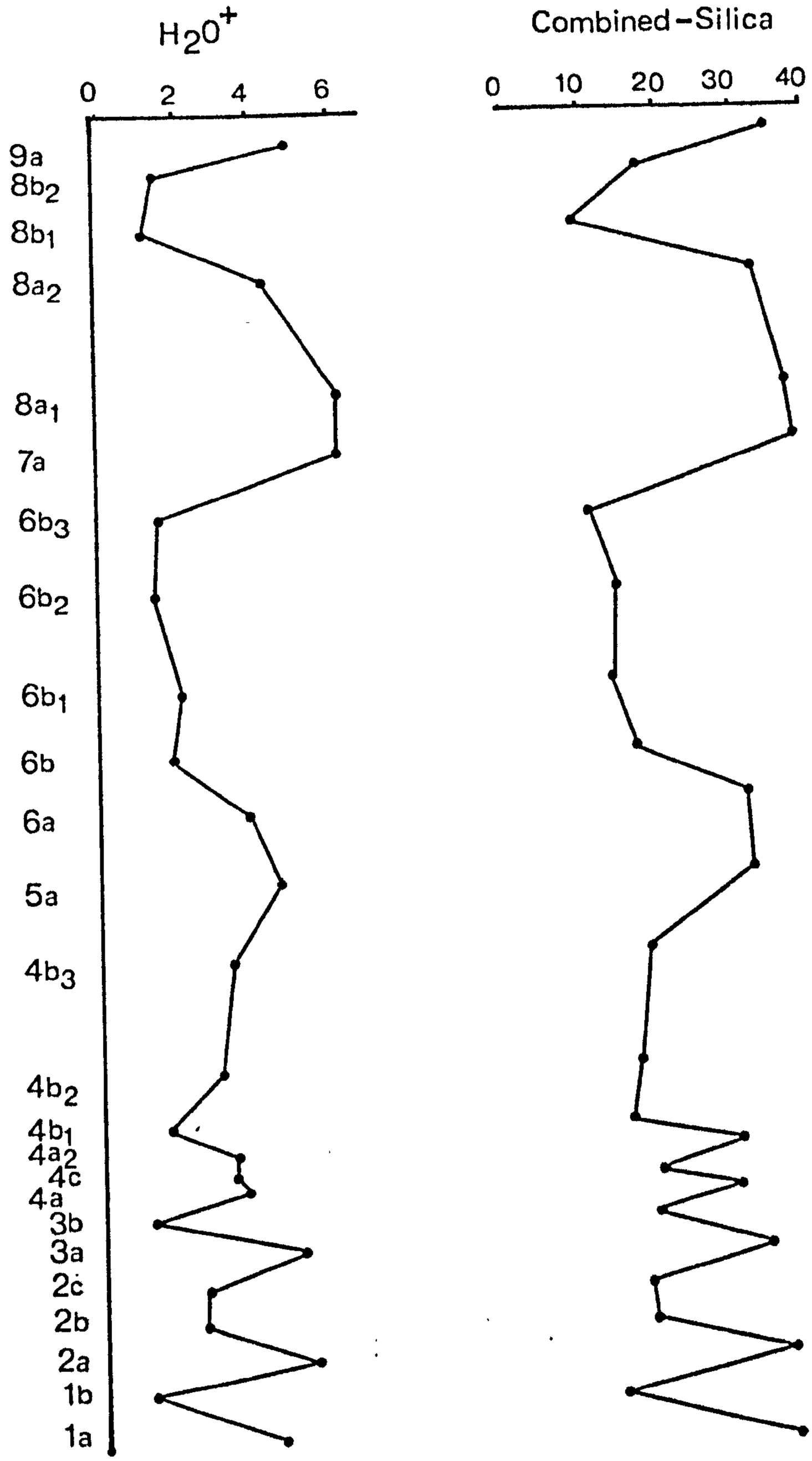
H_2O^+
0
2
4
6
9a
$8b_2$
$8b_1$
$8a_2$
$8a_1$
7a
$6b_3$
$6b_2$
$6b_1$
6b
6a
5a
$4b_3$
$4b_2$
$4b_1$
$4a_2$
4c
$4a$
3b
3a
2c
2b
2a
1b
1a
Combined-Silica
0
10
20
30
40

are contained in the clay minerals, except FeO which is shared between clay minerals and siderite. This is demonstrated by the similarities between kaolinite, illite and chlorite distribution patterns and those of the above mentioned elements. It can be inferred then that K_2O, MgO and some FeO are present mostly in the illite and chlorite. Also TiO_2 trend is similar, suggesting that some TiO_2 could be present in the clay minerals. This is in addition to the detrital rutile as revealed by the heavy mineral study (Chapter 3). The higher TiO_2 content of the shales reflects the fine-grained nature of rutile. The sympathetic variation between organic matter content and the above mentioned elements suggests that organic material is present as very fine particle associated with the clay minerals. The CaO, MgO, and FeO show some resemblance in their variations which imply their association with carbonates, especially siderite and calcite. The relatively higher average of CaO content of the greywackes is a reflection of the more abundant calcite in them. The Fe_2O_3 trend exhibits no systematic variation and it is likely to be associated with clay minerals, pyrite, and its presence as disseminated ferric oxide or hydroxide.

For both greywackes and shales, kaolinite and illite plus mixed layer dominate the clay mineral assemblage, but they show clear difference in their distributions. Greywackes always have a higher relative kaolinite content than the associated shale, while the latter contain a higher amount of illite plus mixed layer. Invariably chlorite dominates the shales and shows wider variation in its amount within the greywackes. Similar results were reported from closely associated sandstones and shales (Glass et al., 1956; Bucke and Mankin, 1971; Gill et al., 1977) or from sandstones only (Kulbicki and Millot, 1963; Triplehorn, 1970; see also Wilson and Pittman

1977). All of these workers have attrtibuted this contrast in kaolinite-illite relative abundance between shales and sandstones or the dominance of kaolinite in sandstones to post-depositional alterations. The latter were ascribed to the higher permeabilities of the sandstones, thus promoted authigenic kaolinite formation. On the other hand, clay minerals in the shales were regarded as detrital with only minor reconstruction by absorption or ion exchange (Bucke and Mankin, 1971).

In the present study, similar conclusions were reached regarding the origin of kaolinite, at least in part, in the greywackes, likewise chlorite was regarded partly as authigenic in origin (see Chapter 3). However, the contrast in the distribution of clay minerals does not exclude factors operated during weathering, transportation and those related to the depositional environment. The similarity in clay mineral composition makes variation due to source area less likely. The higher relative contents of illite and chlorite in the shales suggest that smaller grain size controls their distribution.

4.2 Statistical Correlation

In the previous section a relationship was indicated bwtween the minerals and major elements. These relationships are expressed statistically by means of correlation analysis. The correlation coefficients (r) between pairs of variables were calculated and the results expressed as a correlation matrix. This same statistical method has been widely used to discover and interpret co-varying groups of variables (Till, 1969; Bjorlykke, 1971; Hirst and Kaye, 1971; Stephens et al., 1975).

However, it must be noted that the significance of the correlation coefficients is affected by the phenomenon called close number system, which arises when chemical analysis are referred to a constant sum as in

the case of major elements (Till, 1974). Caution must accordingly be exercised in the interpretation of correlation matrix (Chayes, 1971). This means that if significance is to be attached to a negative value of r, then it must be a great deal more significant than the tables would suggest. Similarly, positive values of r could be smaller than the test would suggest.

4.2.1 Correlation of the Shales and Sandstones

The correlation matrix is based on the maximum possible number of comparisons within the data set. For 25 samples the number of degrees of freedom is 23. This corresponds to a correlation coefficient (r) of 0.399 at the 95% significance level.

The relationships whose correlation coefficients are included within the accpeted minimum significance level of 95% are underlined in the correlation matrix (Table 24). The strongly correlated pairs can be assigned to three groups. In the first group quartz correlates positively with Na_2O and both correlate negatively with many other components. This shows that quartz and Na_2O are directly related. These minerals are the main dilutant in the sediments. The positive correlation of quartz with Na_2O confirms the previous observation that quartz and plagioclase are associated and also that most of the Na_2O is in the plagioclase. The second group consists of combined silica, Al_2O_3, TiO_2, K_2O, MgO and Fe_2O_3. The first four variables give high values for the correlation coefficients, whereas the MgO and Fe_2O_3 although significant are quite lower. It has been noted earlier in this chapter that the vertical profiles of this group are similar and they are interpreted as the elements associated with the clay minerals. The lower correlations for MgO and Fe_2O_3 indicate that these elements are also associated with other minerals in addition

TABLE 24: Correlation Matrix of the Mam Tor Sandstones and Shales

	Quartz	Combsi	Al_2O_3	TiO_2	Fe_2O_3	FeO	MgO	CaO	Na_2O	K_2O
Quartz	1.0000									
Combsi	-0.9541	1.0000								
Al_2O_3	-0.9832	0.9334	1.0000							
TiO_2	-0.9377	0.8507	0.9543	1.0000						
Fe_2O_3	-0.6131	0.4717	0.6182	0.6834	1.0000					
FeO	0.0129	-0.2099	-0.0974	-0.0338	-0.0263	1.0000				
MgO	-0.8582	0.6812	0.8321	0.8626	0.6733	0.3754	1.0000			
CaO	0.2431	-0.2594	-0.2990	-0.3266	-0.3651	0.0670	-0.1458	1.0000		
NaO_2	0.9587	-0.9369	-0.9449	-0.8498	-0.5189	0.0179	-0.7798	0.2747	1.0000	
K_2O	-0.9818	0.9456	0.9907	0.9337	0.6410	-0.1430	0.8078	-0.3002	-0.9461	1.0000
MnO	0.2223	-0.3320	-0.2988	-0.3531	-0.2042	0.7002	0.0692	0.3197	0.1667	-0.3160
P_2O_5	-0.3609	0.1181	0.3222	0.3857	0.5429	0.6616	0.6840	-0.0227	-0.2975	0.2893
SO_3	0.0202	-0.1903	-0.0295	0.0649	0.1960	0.3790	0.2437	0.1693	0.1361	-0.0389
CO_2	0.2029	-0.3356	-0.2888	-0.3303	-0.1932	0.6529	0.0773	0.5295	0.1498	-0.2861

	MnO	P_2P_5	SO_3	CO_2
MnO	1.0000			
P_2O_5	0.4179	1.0000		
SO_3	0.2537	0.3491	1.0000	
CO_2	0.7067	0.4535	0.2471	1.0000

TABLE 24 (cont.): Correlation Groups

Group 1

	Quartz	Na_2O
Quartz	1.0000	
Na_2O	0.9587	1.0000

Group 2

	Combsi	Al_2O_3	TiO_2	Fe_2O_3	MgO	K_2O
Combsi	1.0000					
Al_2O_3	0.9334	1.0000				
TiO_2	0.8507	0.9543	1.0000			
Fe_2O_3	0.4717	0.6182	0.6834	1.0000		
MgO	0.6812	0.8321	0.8629	0.6733	1.0000	
K_2O	0.9456	0.9907	0.9337	0.6410	0.8078	1.0000

Group 3

	FeO	MgO	CaO	MnO	P_2O_5	CO_2
FeO	1.0000					
MgO		1.0000				
CaO			1.0000			
MnO	0.7002			1.0000		
P_2O_5	0.6616	0.6840		0.4179	1.0000	
CO_2	0.6529		0.5295	0.7067	0.4536	1.0000

to the clay minerals. In the third group FeO, CaO and MnO have all correlation with CO_2, while MgO does not show any significant relation with these elements. This may be due to the fact that a very few samples have a high content of carbonates. On the other hand MgO is related to elements in the clay minerals.

K_2O shows better correlation with MgO than Fe_2O_3 which may indicate that most of the MgO is contained in the illite, while the iron is mostly in iron hydroxides and possibly in chlorite.

Therefore, in the sediments studied, FeO, CaO, MnO, CaO and to a lesser extent MgO can safely be assumed to be present in the carbonates, especially siderite and calcite, with insignificant amounts of dolomite (Table 23). In addition, FeO, Fe_2O_3 and MgO are strongly correlated with P_2O_5. This may be the result of closure, i.e. closed number system, or it may indicate the presence of some P in the clay minerals and siderite. P_2O_5, however, has a significant correlation with CO_2.

Petrographic work showed that apatite was present in the sediments studied (see Chapter 3). This mineral probably provides the major source of phosphorous and some CO_2. In addition apatite may contain some FeO and MgO (Deer et al., 1966). Another possibility is that cryptocrystalline collophane is present in the fossil fragments of these sediments, but if so it was not identified.

Fe_2O_3 does not correlate with SO_3, this is the result of presence of insignificant amounts of pyrite in the sediments studied (Table 23). Scatter plots of some significant, bivariant relationships, are shown in Figure 16.

4.2.2. Correlation Matrix of the Sandstones (Greywackes)

Table 25 lists the correlation matrix of the sandstones with the significantly correlated variables underlined.

FIGURE 16 Scatter Plots of Positive and Significant Bivariant Relationships between Major Elements, Mam Tor Rocks.

1. Sandstone

2. Shales

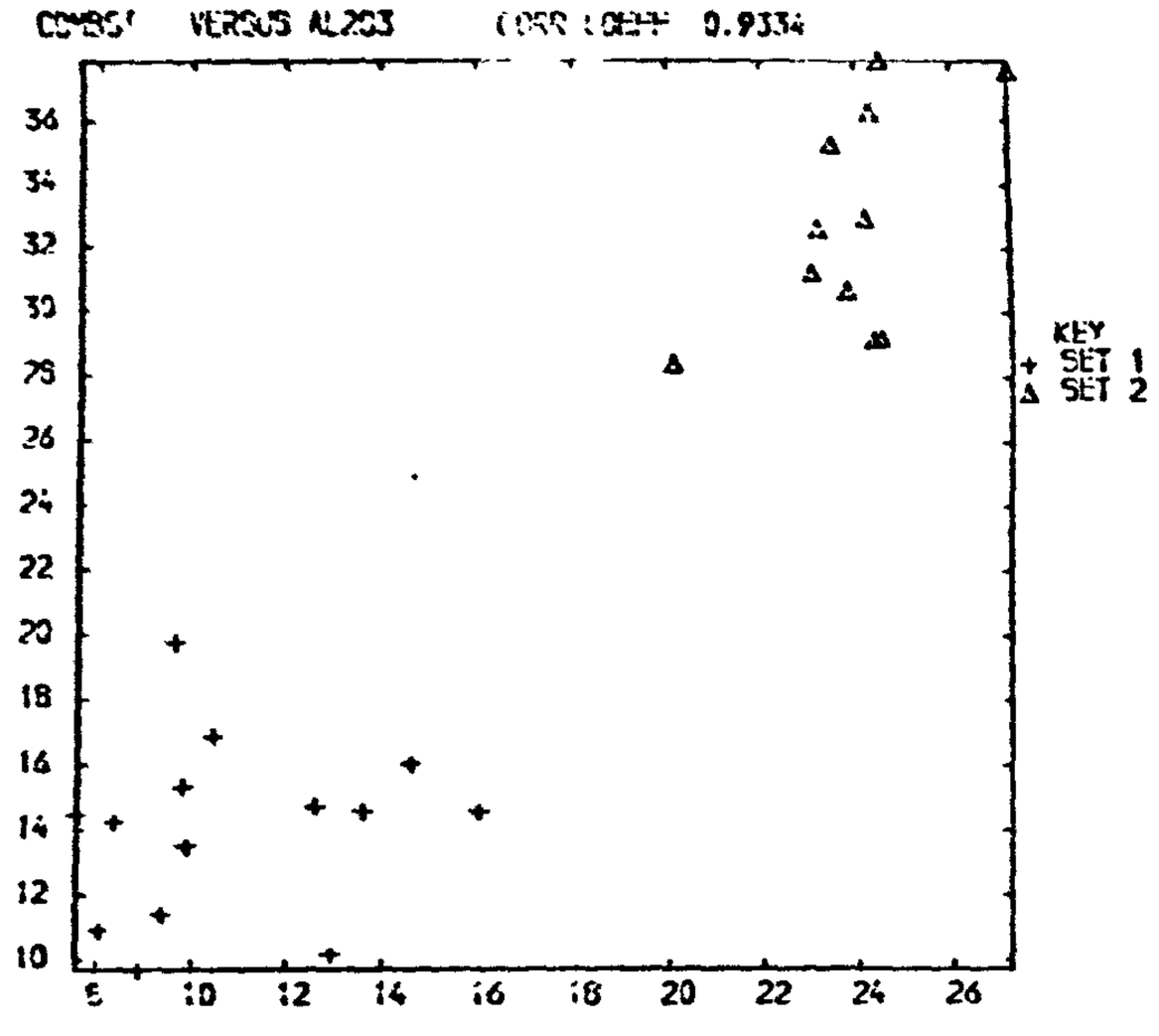
VERSUS AL203
KEY
SET 1
SET 2

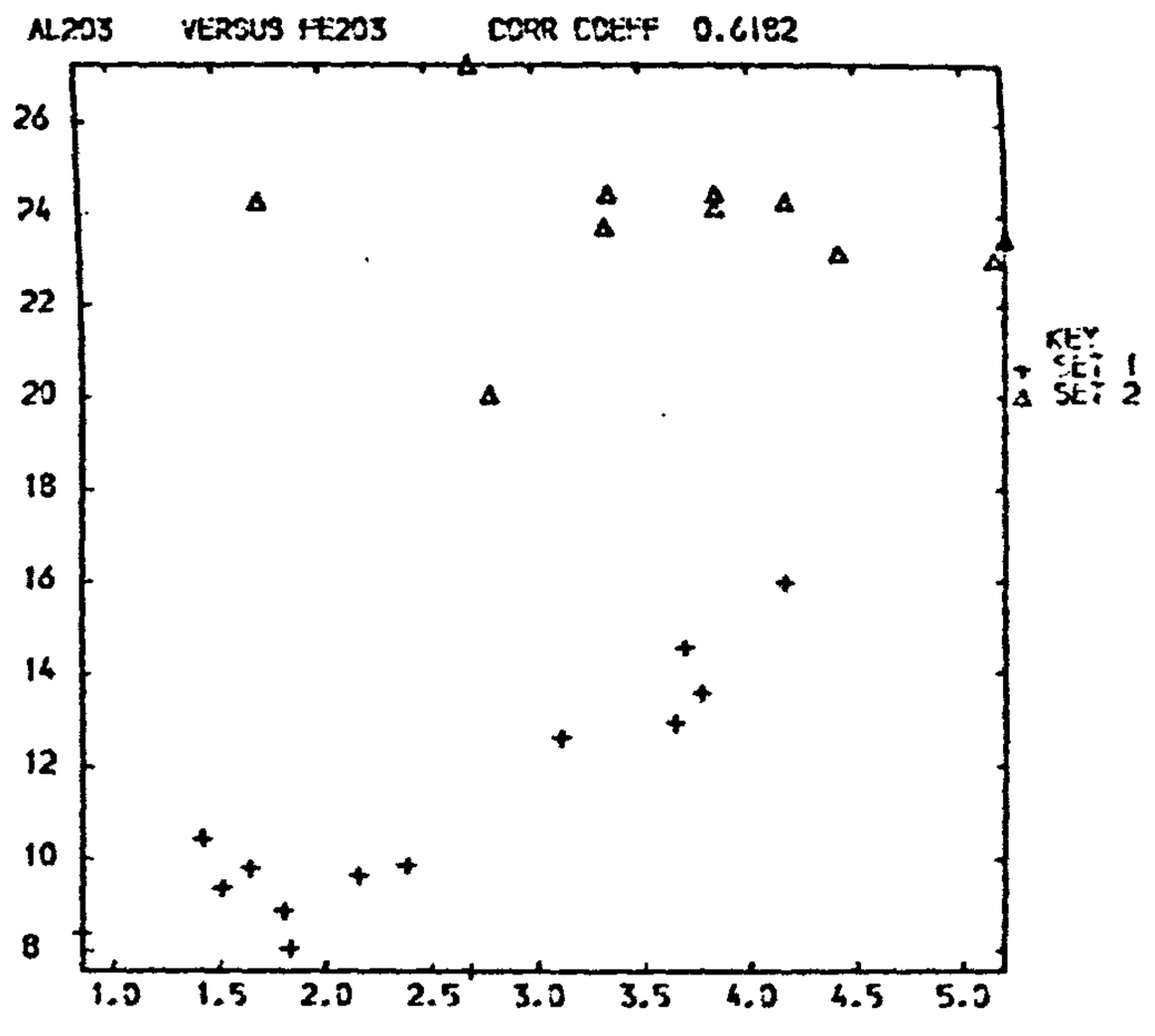
AL203 VERSUS FE203 CORR COEFF 0.6182
KEY
SET 1
SET 2

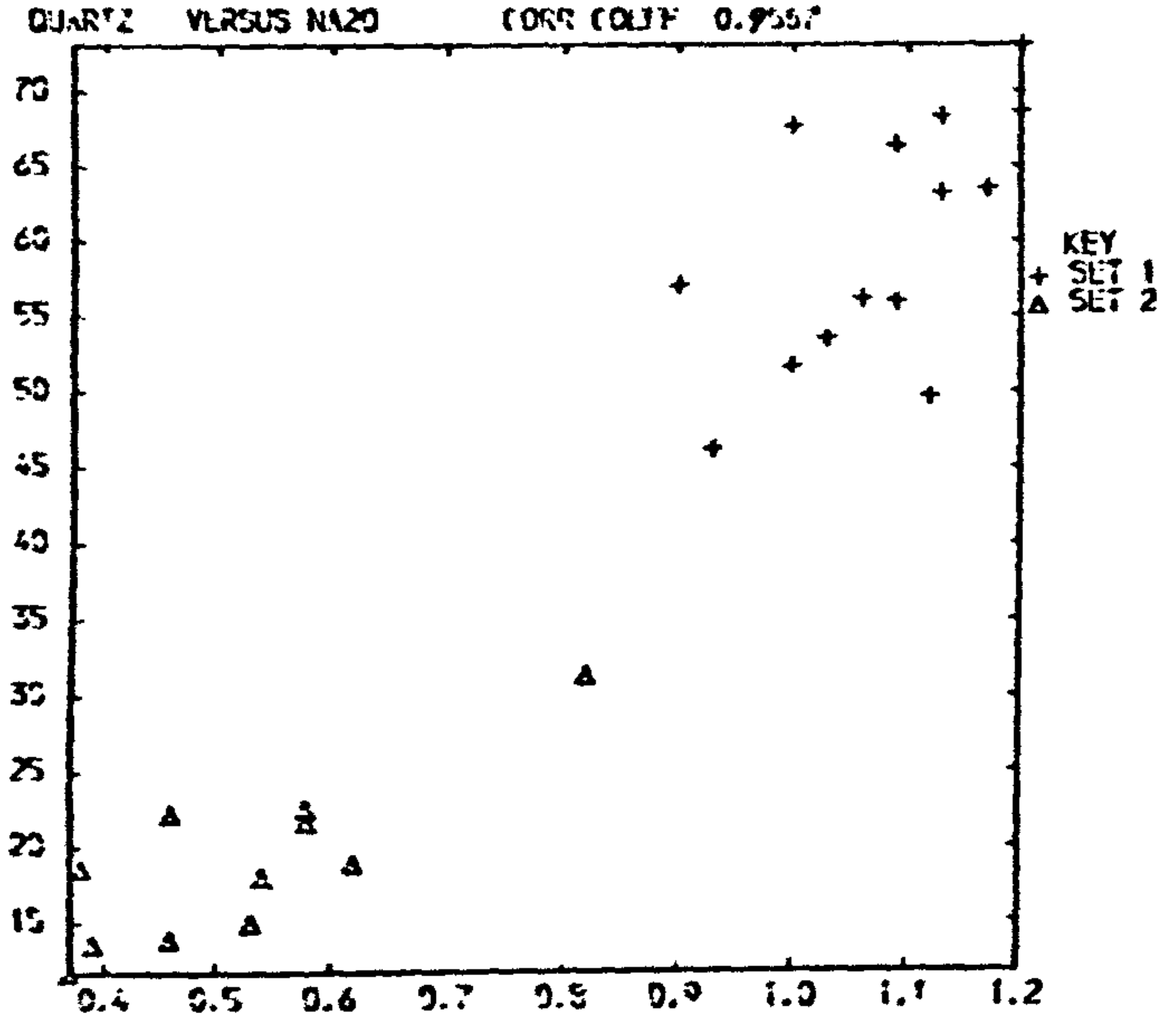
VERSUS NA2O
KEY
SET 1
SET 2

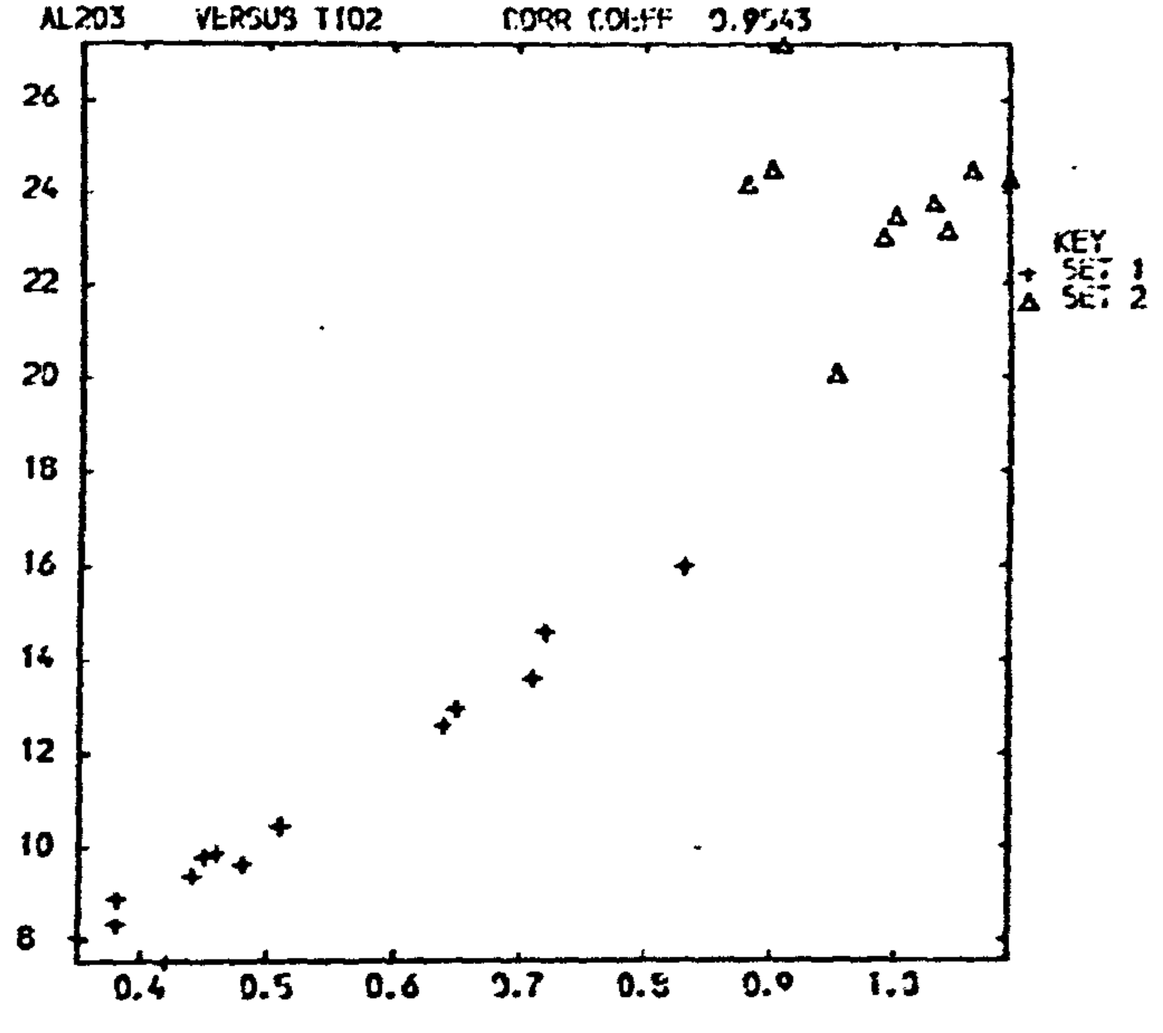
AL203 VERSUS TI02 CORR COEFF 0.9543
KEY
SET 1
SET 2

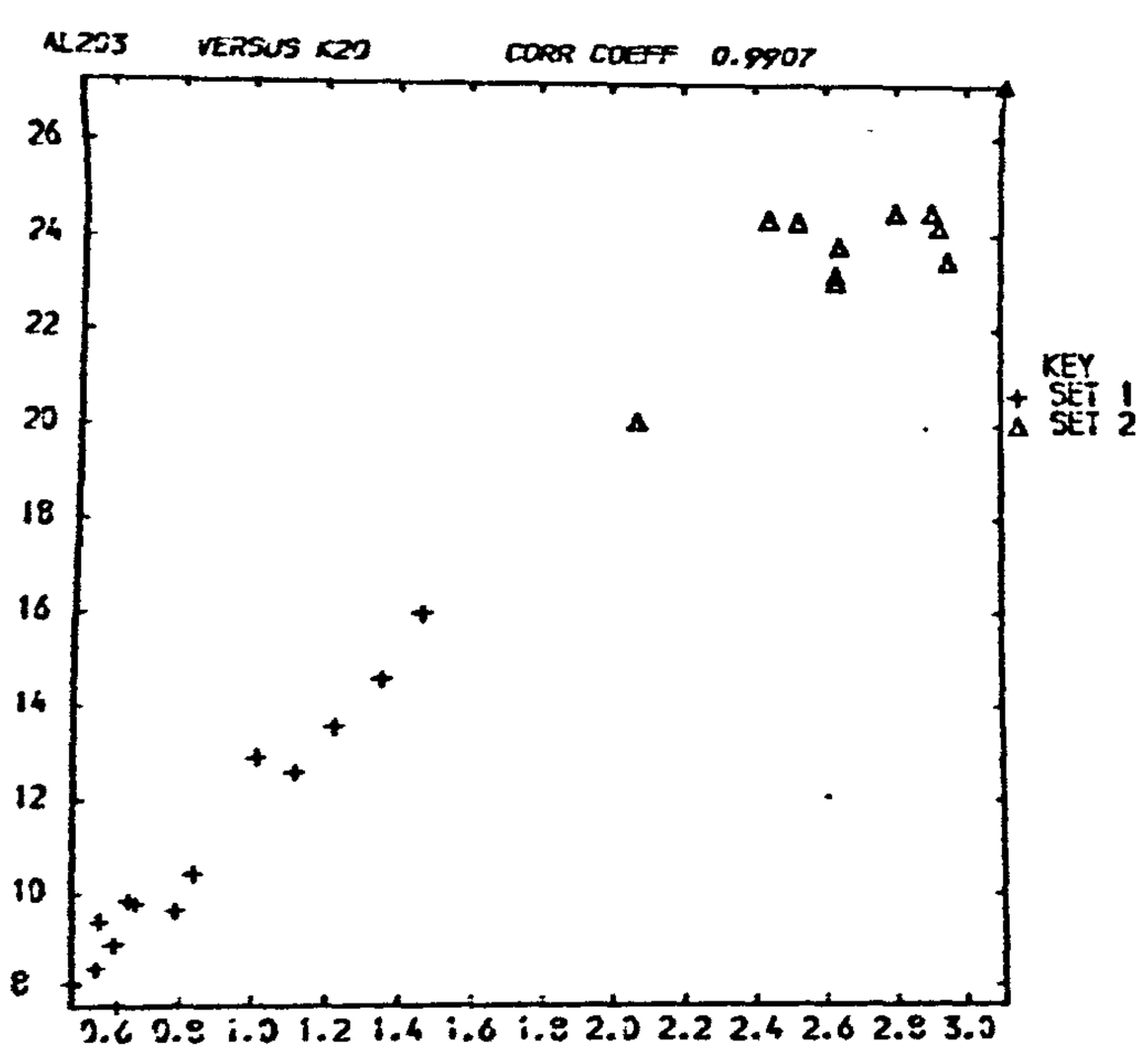
AL203 VERSUS K20 CORR COEFF 0.9907
KEY
SET 1
SET 2

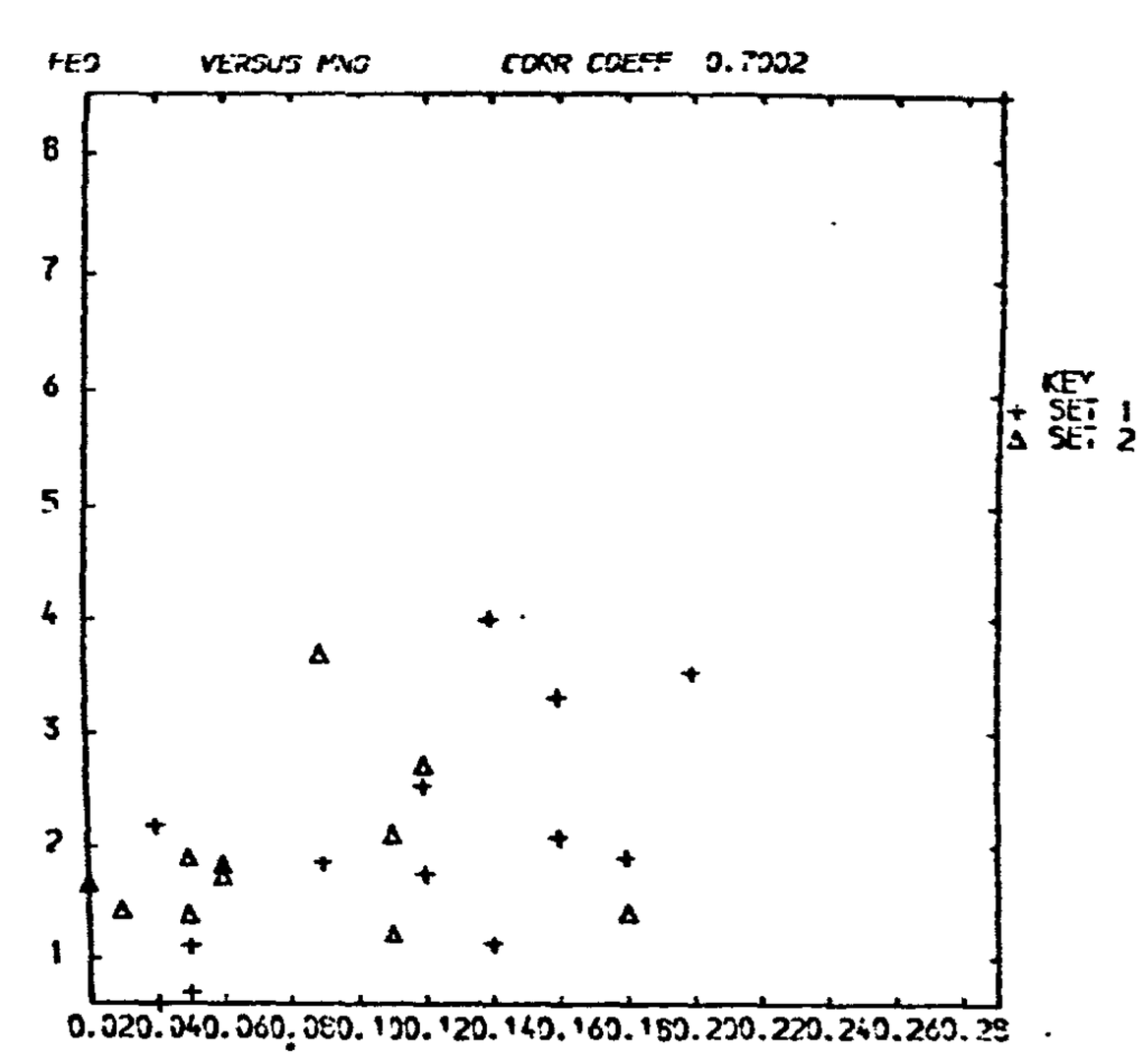
FE3 VERSUS MNO CORR COEFF 0.7002
KEY
SET 1
SET 2

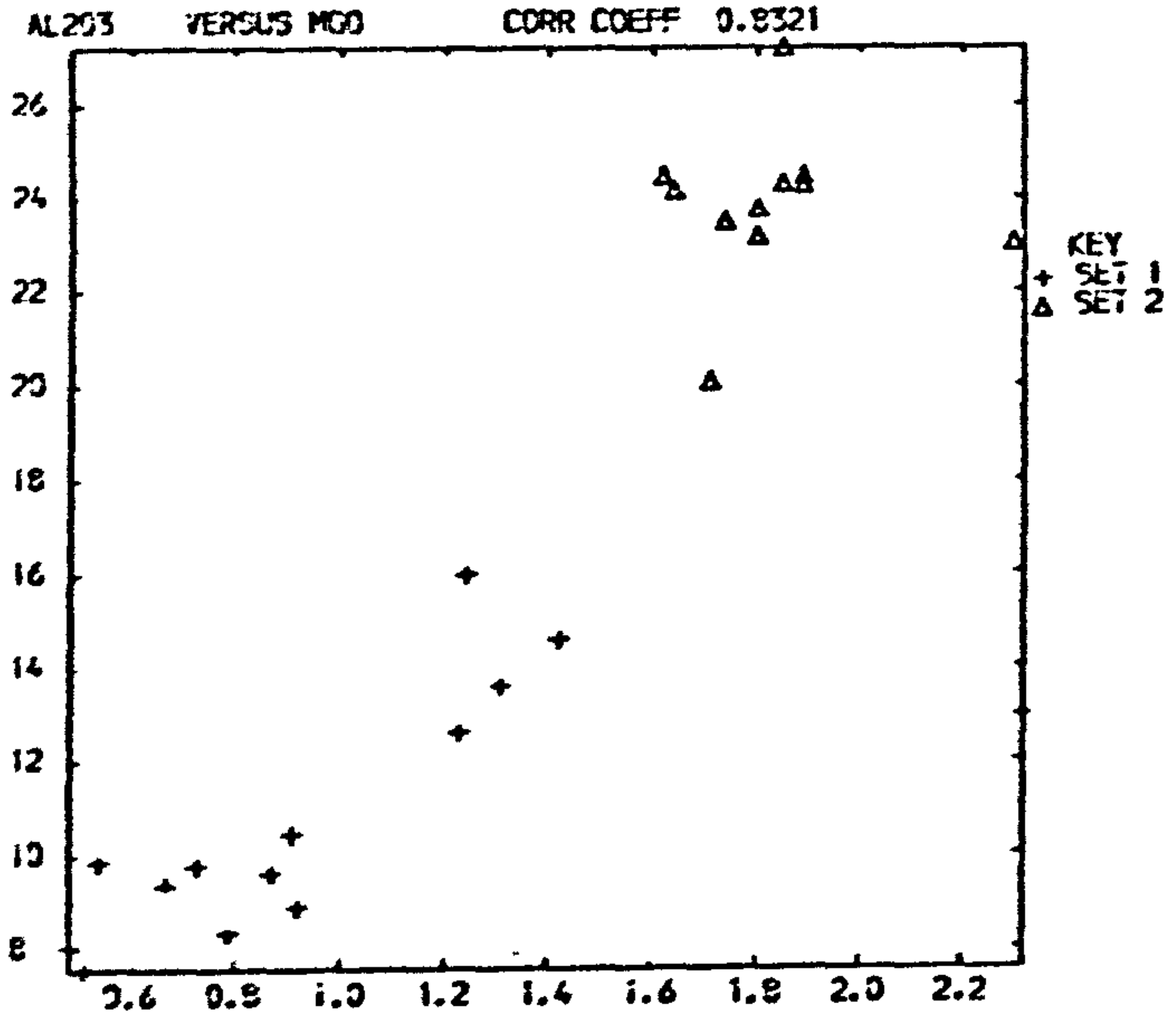
AL203 VERSUS MGO CORR COEFF 0.8321
KEY
SET 1
SET 2

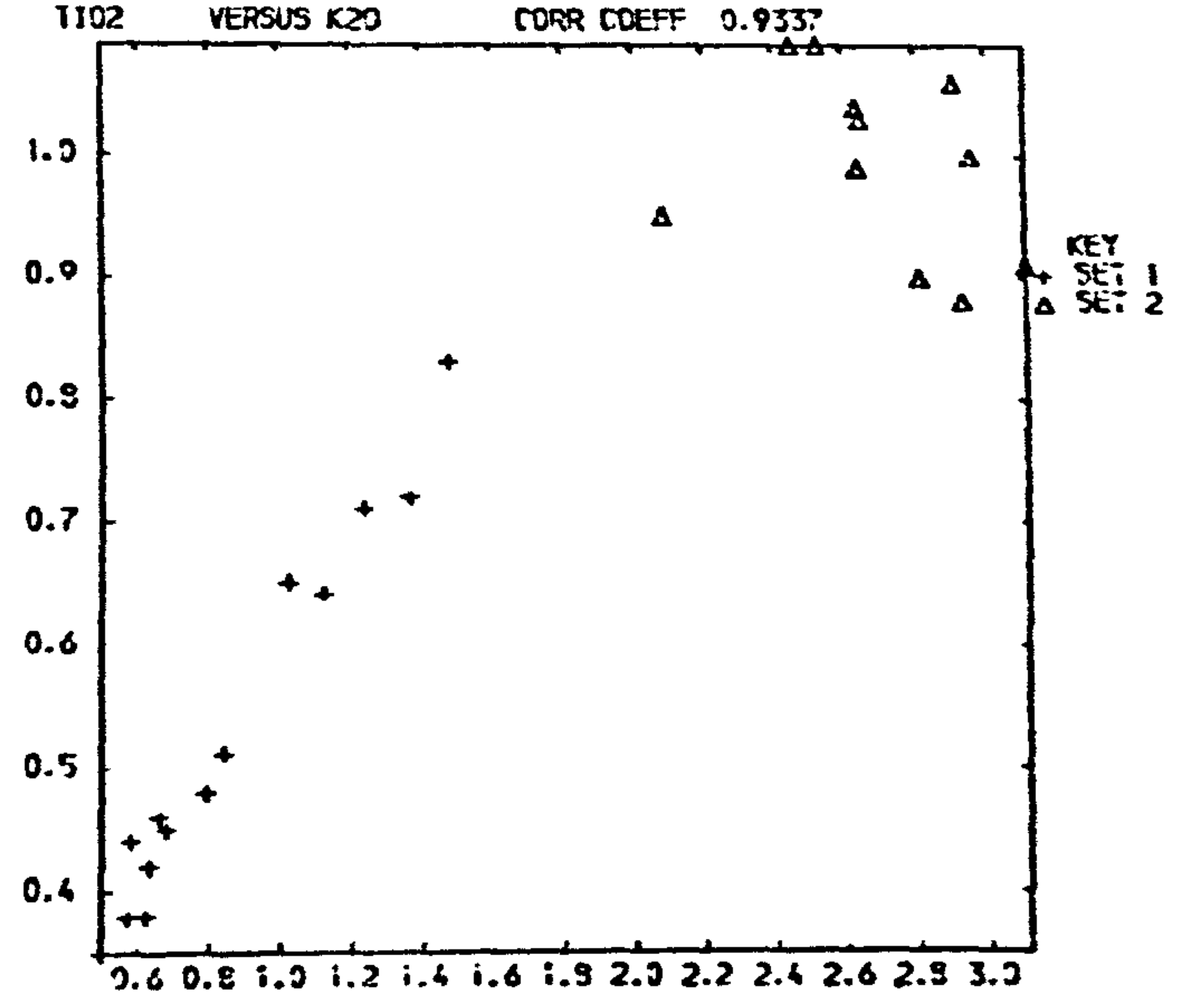
TI02 VERSUS K20 CORR COEFF 0.9337
KEY
SET 1
SET 2

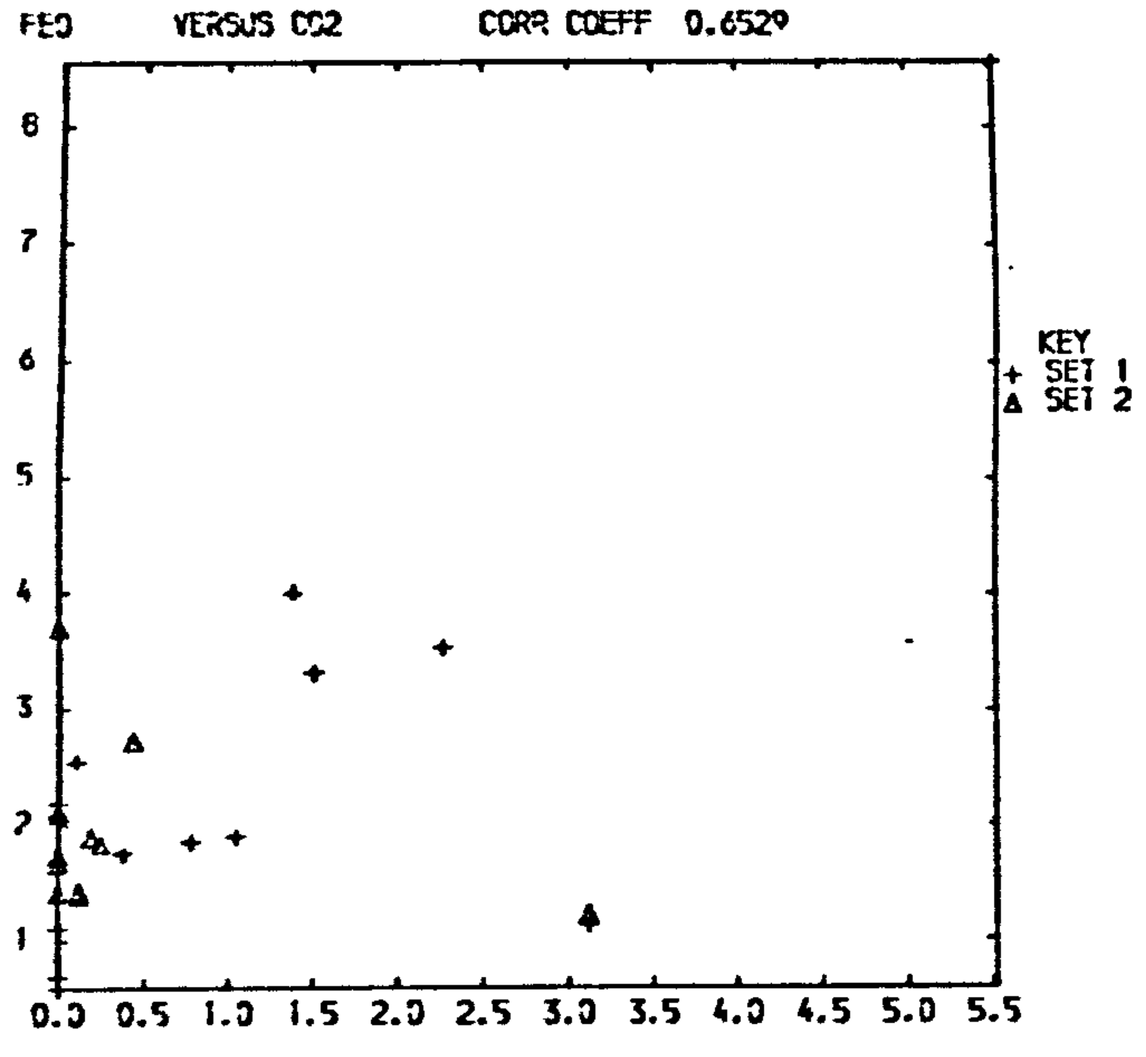
FEO VERSUS CO2 CORR COEFF 0.6529
KEY
+ SET 1
Δ SET 2
8
7
6
5
4
3
2
1
0.0 0.5 1.0 1.5 2.0 2.5 3.0 3.5 4.0 4.5 5.0 5.5

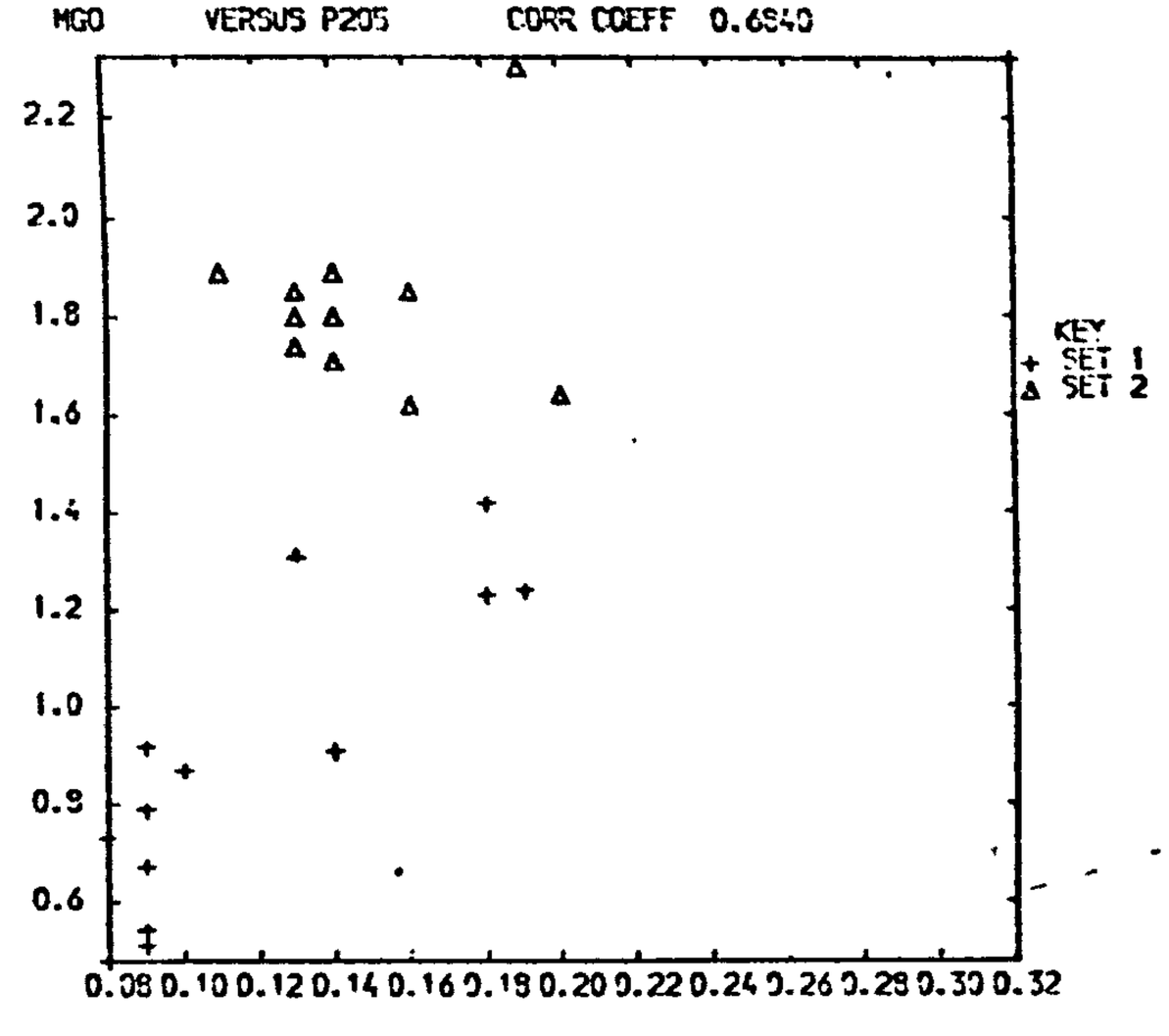
MGO VERSUS P2O5 CORR COEFF 0.6840
KEY
+ SET 1
Δ SET 2
2.2
2.0
1.8
1.6
1.4
1.2
1.0
0.8
0.6
0.08 0.10 0.12 0.14 0.16 0.18 0.20 0.22 0.24 0.26 0.28 0.30 0.32

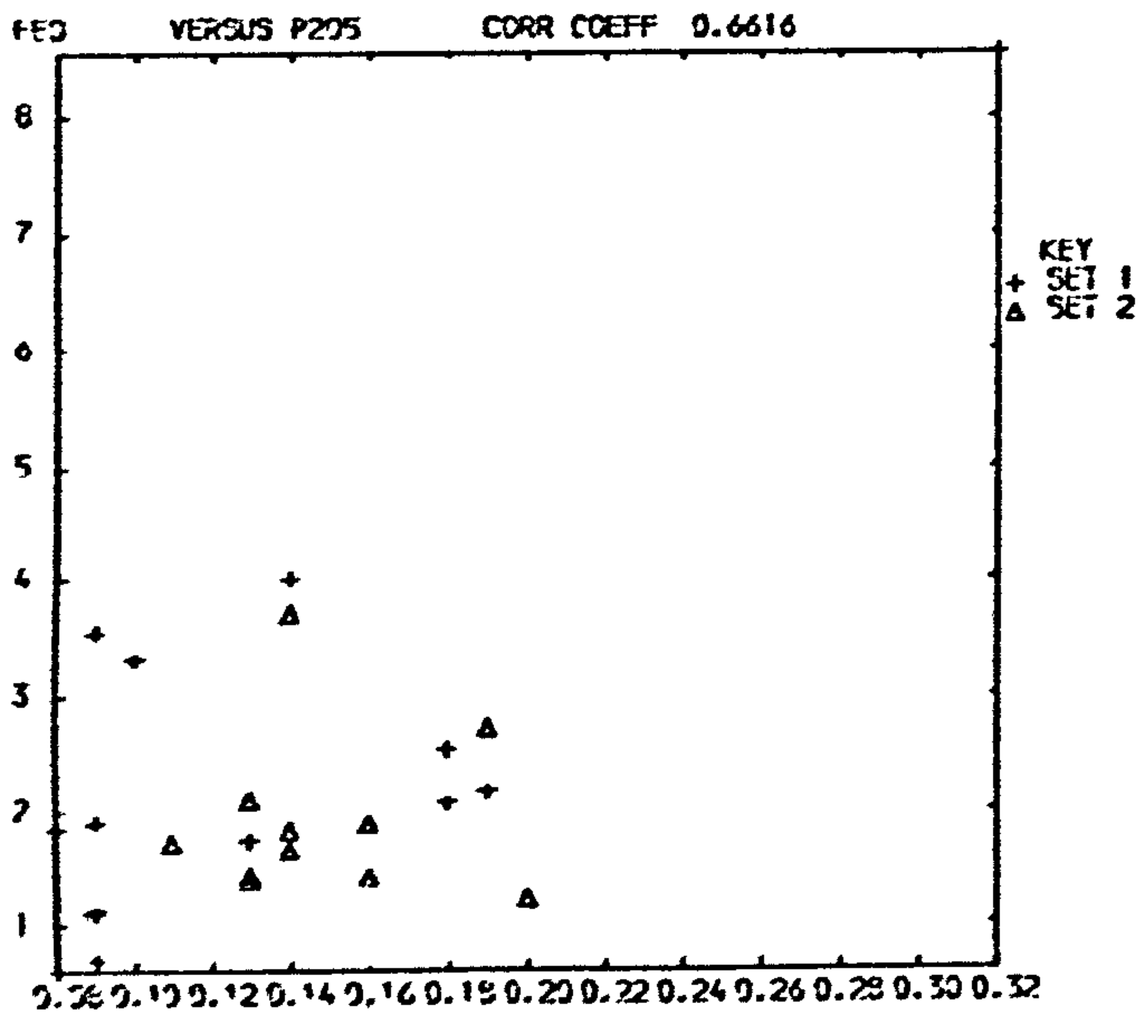
FEO VERSUS P2O5 CORR COEFF 0.6616
KEY
+ SET 1
Δ SET 2
8
7
6
5
4
3
2
1
0.08 0.10 0.12 0.14 0.16 0.18 0.20 0.22 0.24 0.26 0.28 0.30 0.32

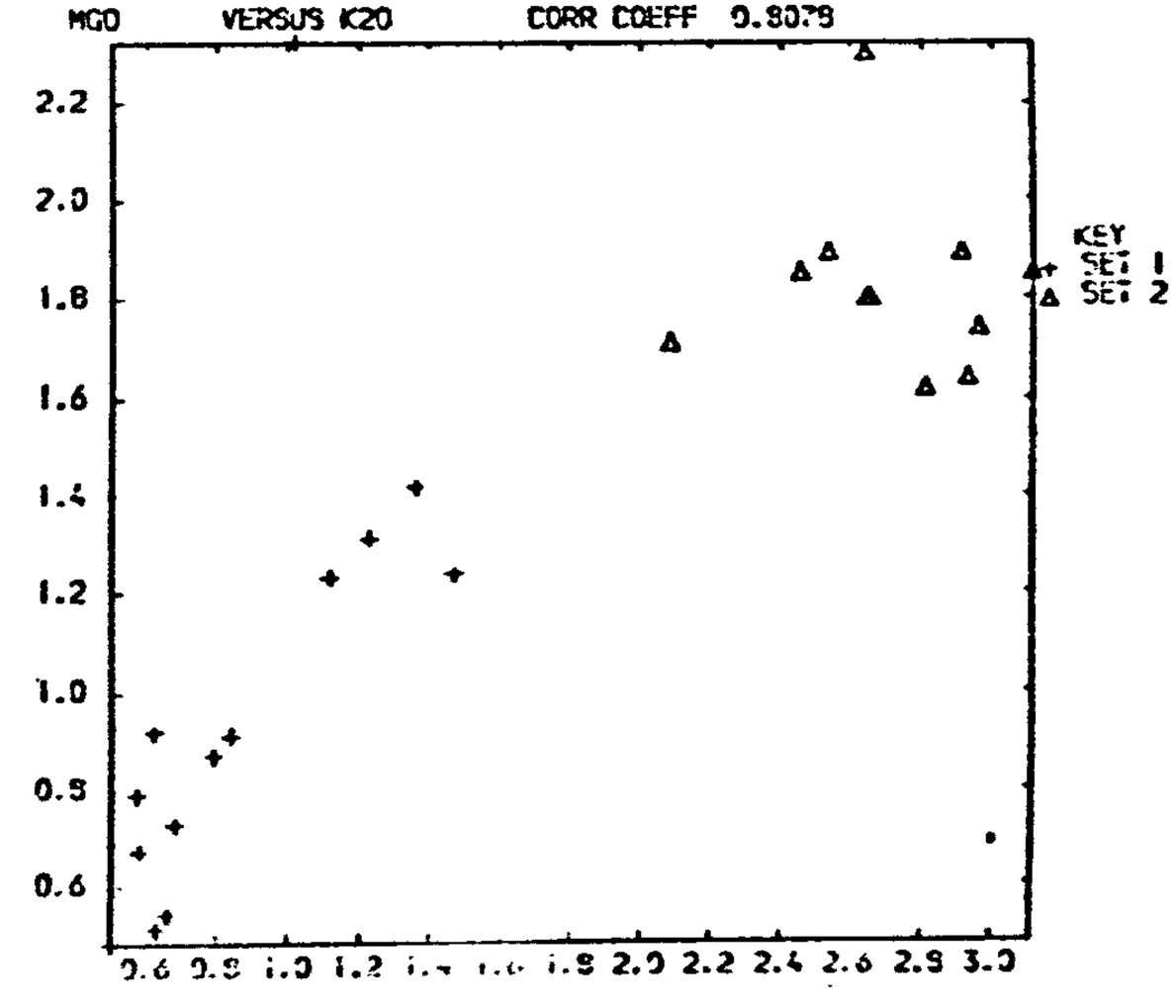
MGO VERSUS K2O CORR COEFF 0.8078
KEY
+ SET 1
Δ SET 2
2.2
2.0
1.8
1.6
1.4
1.2
1.0
0.8
0.6
0.6 0.8 1.0 1.2 1.4 1.6 1.8 2.0 2.2 2.4 2.6 2.8 3.0

TABLE 25: Correlation Matrix of the Mam Tor Sandstones

	Quartz	Combsi	Al_2O_3	TiO_2	Fe_2O_3	FeO	MgO	CaO	Na_2O	K_2O
Quartz	1.0000									
Combsi	-0.3290	1.0000								
Al_2O_3	-0.8587	0.1602	1.0000							
TiO_2	-0.8718	0.2235	0.9827	1.0000						
Fe_2O_3	-0.7097	0.0340	0.8405	0.8846	1.0000					
FeO	-0.6115	-0.1950	0.3105	0.2886	0.2513	1.0000				
MgO	-0.8625	-0.1349	0.7169	0.7023	0.6572	0.8084	1.0000			
CaO	-0.0462	-0.0288	-0.1592	-0.1745	-0.3481	0.0061	0.0992	1.0000		
Na_2O	0.6139	-0.1320	-0.3859	-0.3730	-0.3033	-0.7240	-0.6285	0.1642	1.0000	
K_2O	-0.8609	0.2829	0.9738	0.9851	0.8663	0.2407	0.6717	-0.1743	-0.4018	1.0000
MnO	-0.3981	-0.2428	0.1219	0.0759	0.0033	0.8120	0.6671	0.2355	-0.5606	0.0591
P_2O_5	-0.8285	-0.1454	0.7028	0.7042	0.6748	0.7913	0.9449	-0.0017	-0.5719	0.6563
SO_3	-0.6090	-0.0522	0.5444	0.5631	0.4005	0.4600	0.5549	0.2044	-0.1023	0.4646
CO_2	-0.2927	-0.3375	-0.0742	-0.1052	-0.1484	0.7942	0.5717	0.5266	-0.4050	-0.1519

	MnO	P_2O_5	SO_3	CO_2
MnO	1.0000			
P_2O_5	0.5315	1.0000		
SO_3	0.2547	0.5604	1.0000	
CO_2	0.8136	0.4971	0.4068	1.0000

Quartz shows a negative correlation with all elements, except Na_2O which is significant. This substantiates previous observations that quartz and plagioclase are directly related. The poor correlation of combined silica with all the aforementioned clay related elements is due to the presence of high plagioclase content in the sandstones, i.e. combined silica/alumina is 6/1. On the other hand, the strong and significant correlation between Al_2O_3, TiO_2, Fe_2O_3, MgO, K_2O and P_2O_5 tend to imply that these elements are mostly contained or associated with the clay minerals. FeO, MgO, CaO and MnO are significantly correlated with CO_2, indicating their presence in siderite and calcite, since these sandstones contain more carbonates than the shales. $MgO-SO_3$ and $P_2O_5-SO_3$ relationships are believed to be false as a result of closure phenomenon or may indicate that they co-vary together but without genetic relation.

4.2.3. Correlation Matrix of the Shales

Table 26 shows the correlation matrix with the significant relationships underlined.

The quartz and Na_2O significant correlation confirms the previously held view that plagioclase and quartz have sympathetic relation. The weak correlation between combined silica, Al_2O_3, TiO_2 and MgO could be due to the lack of systematic and marked variations of their content in the shales. Similar observation was noted by Vistellius (1970), with regard to Fe_2O_3 and FeO in standard silicate rocks. The Al_2O_3 and K_2O are more sympathetic than the above mentioned elements, thus they have a significant correlation. This also means that illite is abundant in these shales which is in agreement with the results of norm calculation (see Table 23). FeO, MgO, CaO and MnO have insignificant correlation with CO_2, which is due to the low

TABLE 26: Correlation Matrix of the Mam Tor Shales

	Quartz	Combsi	Al_2O_3	TiO_2	Fe_2O_3	FeO	MgO	CaO	Na_2O	K_2O
Quartz	1.0000									
Combsi	-0.8949	1.0000								
Al_2O_3	-0.7674	0.5887	1.0000							
TiO_2	0.1742	-0.3887	-0.0938	1.0000						
Fe_2O_3	-0.0588	-0.1397	-0.1538	-0.0660	1.0000					
FeO	-0.2180	0.1515	0.0778	0.4252	-0.4734	1.0000				
MgO	-0.0718	-0.2265	0.0236	0.3755	0.2268	0.6010	1.0000			
CaO	-0.4969	0.5131	0.4375	-0.5258	-0.1801	0.2854	0.0302	1.0000		
Na_2O	0.8152	-0.6747	-0.8473	0.2686	-0.0033	-0.0667	0.0724	-0.7193	1.0000	
K_2O	-0.7418	0.5707	0.7872	-0.3351	0.2108	-0.2655	-0.0667	0.2346	-0.6943	1.0000
MnO	-0.4868	0.5565	0.3018	-0.6096	-0.0713	0.1342	0.0128	0.7940	-0.5472	0.2475
P_2O_5	-0.0499	-0.0065	-0.0930	-0.4248	0.3252	0.0063	0.1580	0.6537	-0.3544	-0.0573
SO_3	0.0334	-0.3091	-0.0094	0.1968	0.2195	0.2487	0.7025	-0.0897	0.1058	0.1313
CO_2	0.0398	-0.0608	-0.0246	-0.4995	0.1326	-0.2966	-0.2454	0.4693	-0.2934	0.1924

	MnO	P_2O_5	SO_3	CO_2
MnO	1.0000			
P_2O_5	0.4927	1.0000		
SO_3	0.1795	0.0283	1.0000	
CO_2	0.2102	0.7064	-0.1181	1.0000

content of carbonates in these shales. The poor correlation of Fe_2O_3 with all other elements is due to its erratic variation, which is not in sympathy with others. This also may indicate its presence in the clays, goethite, and some in pyrite, although the latter mineral is present in insignificant amounts. CaO-MnO-P_2O_5-CO_2 significant correlations indicate their presence in carbonate-apatite.

4.3 Compositional Variation of the Greywackes

Chemical data of the Namurian greywackes are given in Table 23 including the means and standard deviations. In those greywacke samples which represent individual beds (Figure 15) it is clear that a significant compositional variation exists between them. Likewise, samples from different parts of the bed (2b, 2c); ($4b_1$, $4b_2$); ($6b_1$, $6b_2$, $6b_3$) and ($8b_1$, $8b_2$) reveal, more or less, gradual variation. Figure 17 shows the distribution of major elements within a bed. Quartz and Na_2O are similar in their distribution pattern. The rest of the elements generally show a similar trend to that of Al_2O_3, which indicates their association in the clay minerals. However, the presence of variable amounts of Na-feldspar and siderite in different parts of the bed, result in slight dissimilarities between Al_2O_3, combined silica and FeO.

The contents of quartz and Na-feldspar generally decrease towards the top of the bed, except in one in which the inverse relation is shown.

In as much as these greywackes were produced from turbidity currents (Allen, 1960) graded bedding (i.e. coarse to fine upwards) would be anticipated. Thus they show an upward grading of grain size. Reverse graded bedding, i.e. from fine to coarse has been recorded from some turbidites (Pettijohn, 1957; Selly, 1976). The variation between beds has been recorded in other turbidite sequences by Webber and Middleton

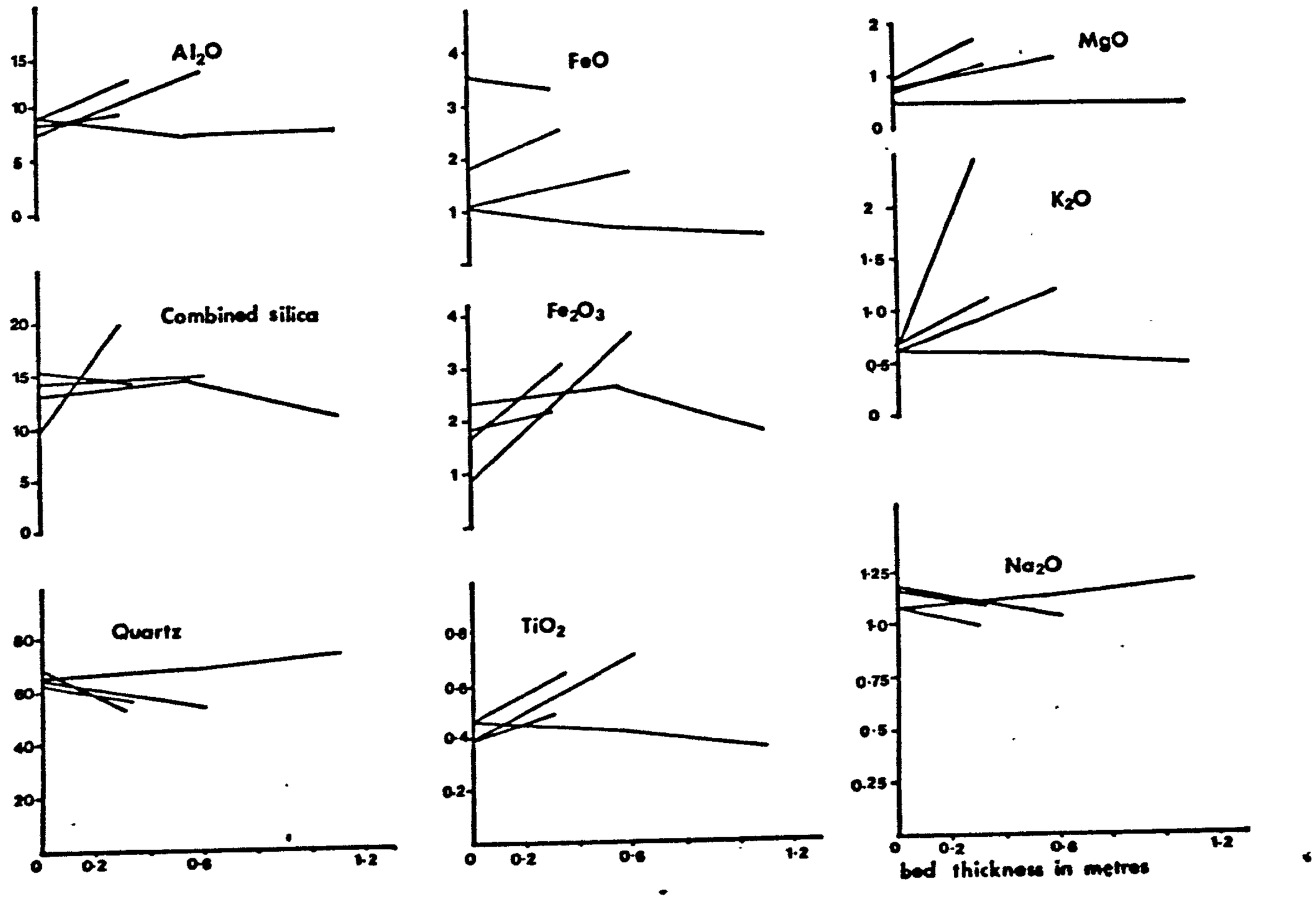

Fig.17 Distribution of major elements within abed

(1961) and Condie (1967). Such variations are explained by one or a combination of the following:

1. The site on the submarine slope from which the turbidity currents originate could influence the mineralogical composition. These variations could result from the segregation of minerals as a function of transport distance from the shoreline due to mechanical abrasion and grain size sorting.

2. The composition of sediments ariving at the basin edge would vary from one point to another along the shoreline depending on the composition of the intermediate source land. Such is the case in the outer margin of the Mid-Atlantic States (Kelling et al., 1975).

However, since the greywackes investigated in the present study showed similar mineralogy, but with variation in mineral proportions, it is believed that flocculation in the amount of material transported by turbidity currents and sorting were the most important factors.

4.4 Provenance

The presence of clastic mineral grains and rock fragments (especially shale clasts) in the Namurian greywackes (see Chapter 3) suggest a source composition unlike that inferred from their chemical compositions. Most of the minerals seem to be of detrital origin and the partial alteration of feldspar and biotite with the formation of kaolinite and chlorite may have had little effect on the chemical composition of the greywackes. If isochemical diagenesis is assumed, source rocks may be inferred from the greywacke compositions.

Table 27 lists the average chemical composition of the Namurian greywackes and other greywackes of different ages and geographic locations.

TABLE 27: Comparison of Major Elements in the Mam Tor (Namurian) Greywackes and other Greywackes

Oxides	1	2	3	4	5	6
SiO_2	74.84	64.70	70.00	69.73	64.43	54.89
Al_2O_3	10.84	14.80	13.20	13.88	15.48	15.62
TiO_2	0.53	0.50	0.60	0.45	0.62	1.15
Fe_2O_3*	2.47	1.50	1.00	1.48	6.54	10.05
FeO	2.52	3.90	3.90	2.88		
MgO	1.00	2.20	2.09	1.78	3.12	3.82
CaO	0.63	3.10	0.70	1.08	2.22	5.29
Na_2O	1.08	3.10	4.00	2.90	3.74	4.90
K_2O	0.86	1.90	1.20	1.47	2.44	0.71
MnO	0.13	0.10	0.10	0.12		0.17
P_2O_5	0.13	0.20		0.13		0.22
SO_3	0.09	0.40				
Ig. Loss	5.24	4.60	2.10	3.99		3.72

*Total Fe as Fe_2O_3

1 - Average Mam Tor Greywackes

2 - Composite Greywacke (Pettijohn, 1957)

3 - Timiskaming Greywackes, Ontario (Macpherson, 1958)

4 - Composite Harz Mountain Greywacke (Huckenholz, 1963)

5 - Average Wyoming Greywacke (Condie, 1967)

6 - Average Volcanic Greywacke (Chappell, in: Nance and Taylor, 1977)

It is apparent that the Namurian greywackes contain more silica and less Al_2O_3 than other greywackes which may be attributed to the distance of transport and sorting.

When the composition of the greywackes is expressed in terms of Na_2O, CaO and K_2O, following Condie (1967), it overlaps that of granodiorite and granite (Figure 18). One feature common to all greywackes is their enrichment in Na_2O and depletion in CaO when compared to these intermediate granite rock types (Table 28). Comparison with metamorphic rocks indicates a distinct depletion in K_2O content. Likewise, when the Namurian greywackes are expressed in terms of TiO_2, MgO and total Fe_2O_3, they overlap that of granite, granodiorite and quartz diorite (Figure 18). Comparison with granite reveals that the Namurian greywackes are relatively enriched in MgO and Fe_2O_3, which may indicate contribution from a more mafic rock in the source area. It is clear however, from the data in Tables 27 and 28 and Figure 18, that contribution from a volcanic source is at a minimum, as indicated by the marked enrichment of volcanic greywackes in Fe_2O_3, MgO, CaO and Na_2O. Moreover, the absence of volcanic minerals and rock fragments in the Namurian greywackes is compatible with these assumptions. There is also the stratigraphic evidence (page 7) which demonstrated the presence of volcanic mudstones (K-bentonites) in the lowest Namurian shales (E_1-E_2) as compared to the Mam Tor rocks (R_{1c}).

On the other hand, this inference about source rock is not entirely satisfactory in that it does not take into account the geological factors responsible for change in grain size and the change in mineralogy, due to the effect of different factors of transport and environment.

Ethridge (1977) reported that the Upper Devonian standstones are lithic arenites, lithic wackes near the primary metamorphic terrain and grade into quartz wackes at greater distance into the basin. The marked

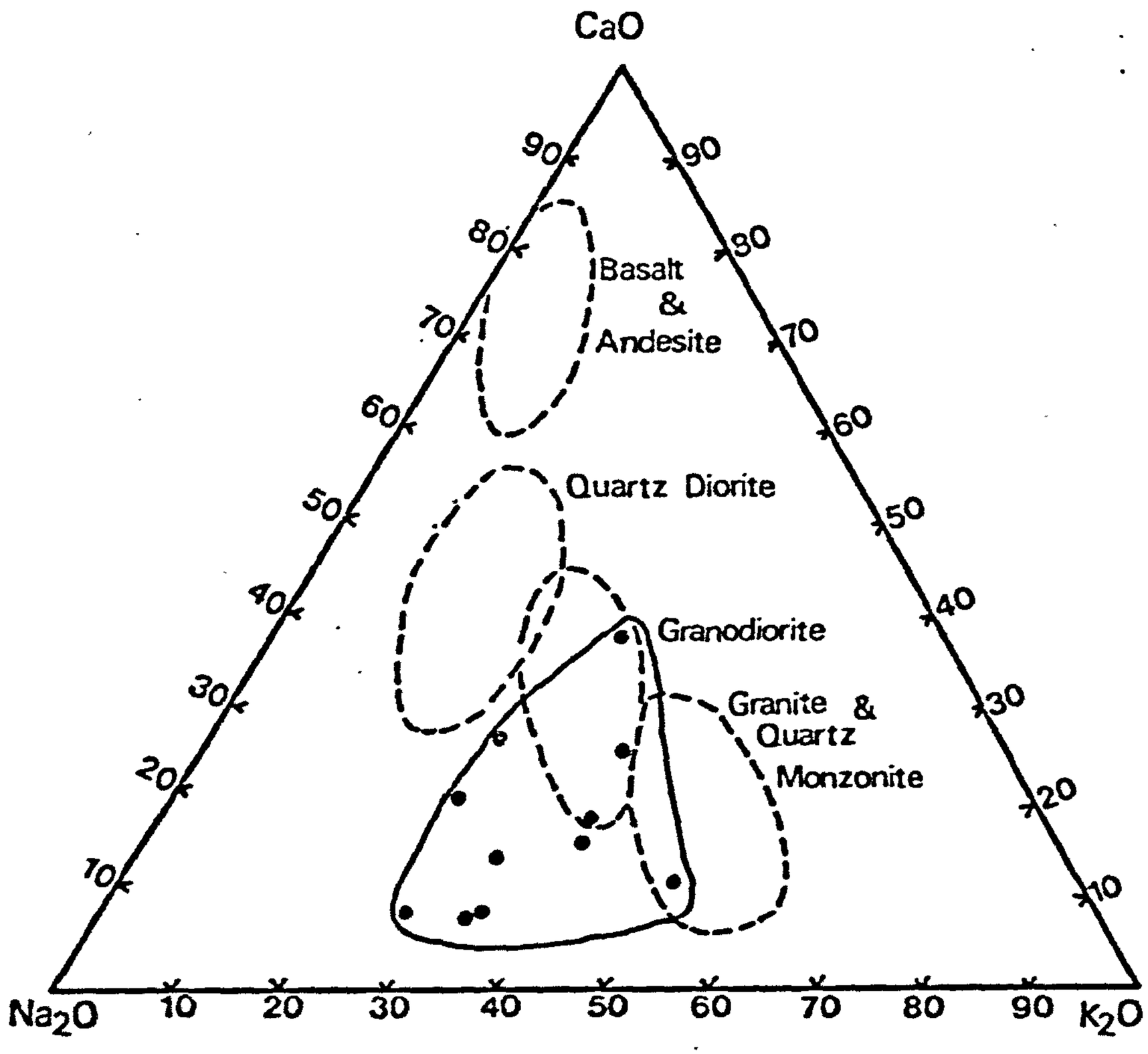

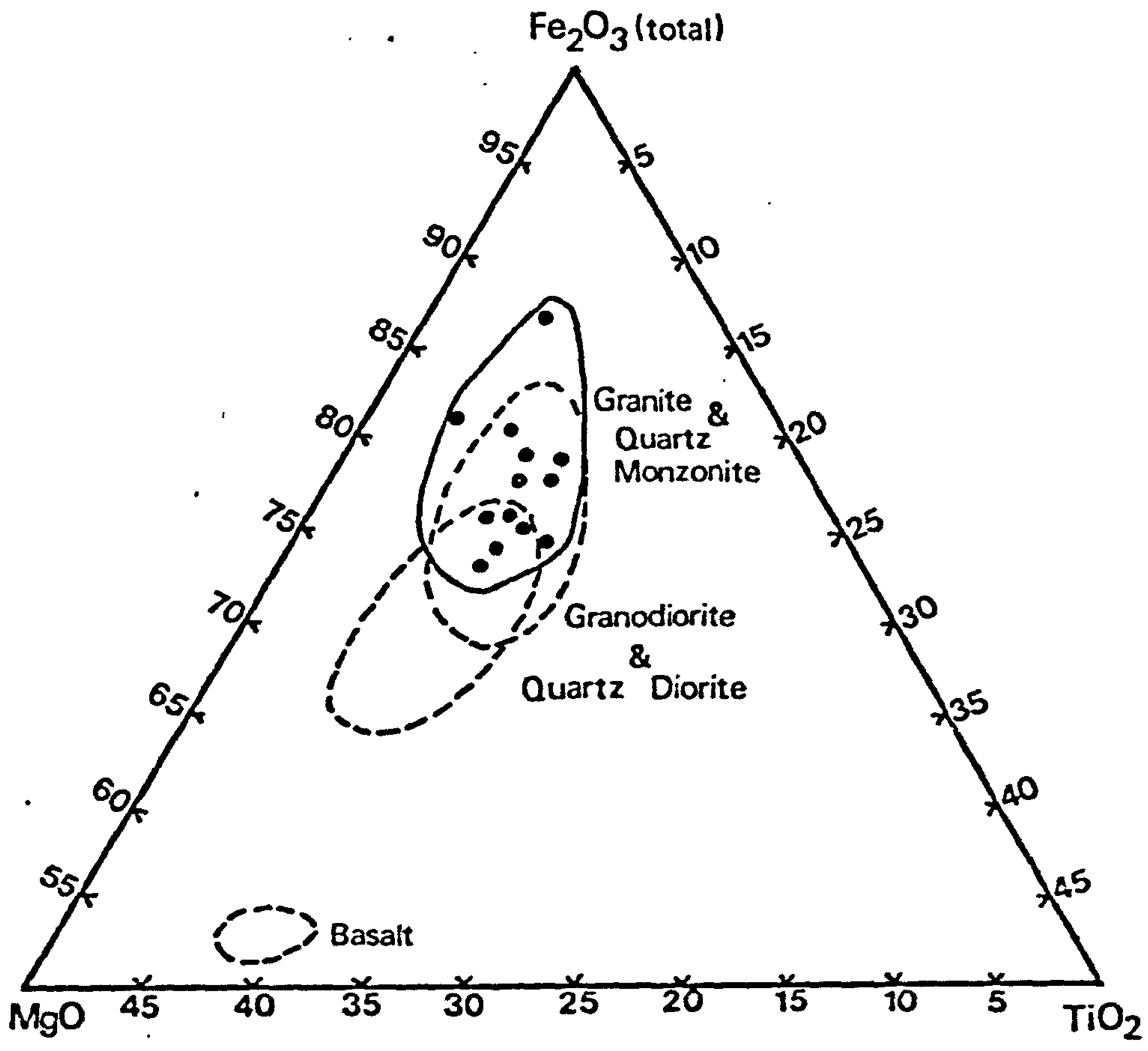

Fig.18 Diagrams showing the compositional range of the Mam Tor greywackes (solid line) and the common igneous rocks (dashed lines).

TABLE 28: Comparison of Major Elements in the Mam Tor (Namurian) Greywackes and Common Igneous and Metamorphic Rocks

Oxides	1	2	3	4	5	6
SiO_2	74.84	72.08	66.88	66.15	51.33	70.70
Al_2O_3	10.84	13.86	15.66	15.56	18.04	14.50
TiO_2	0.53	0.37	0.57	0.62	1.10	0.50
Fe_2O_3	2.47	2.72	4.21	5.16	9.73	1.60
FeO	2.52					2.00
MgO	1.00	0.52	1.57	1.94	6.01	1.20
CaO	0.63	1.33	3.56	4.65	10.07	2.20
Na_2O	1.08	3.08	3.84	3.90	2.76	3.20
K_2O	0.86	5.46	3.07	1.42	0.82	3.80
MnO	0.13					0.1
P_2O_5	0.13					0.1

1 - Average Mam Tor Greywackes (2-5 from Condie, 1967)

2 - Average Calc-Alkali Granite

3 - Average Granodiorite

4 - Average Quartz Diorite

5 - Basalt

6 - Average Quartzofeldspathic Gneisses (Poldervaart, 1955)

decrease of polycrystalline quartz, rock fragments and feldspar contents at greater distance from the source was also noted. This decrease was significant between delta front-delta platform sediments and prodelta sediments in the marine shelf (turbidites). Data on Holocene sediments suggest that fine-grained metamorphic rock fragments and to a lesser extent polycrystalline-quartz are mechanically unstable and are destroyed by physical abrasion within a few miles of transport (various workers in Ethridge, 1977). Thus it was suggested that physical abrasion is one of the important factors affecting sediment maturity, with selective sorting and chemical weathering being of secondary importance.

Kelling et al. (1975) concluded that most of the pronounced mineralogical changes of sediments in some areas off the Mid-Atlantic States occur between the shelf edge and slope areas. They found that quartz tends to increase in abundance with increasing grain size, being highest in the shelf edge samples and lowest in the slope sector. The igneous/metamorphic quartz ratio increases from the shelf edge towards the slope. The proportion of potash feldspar decreases with increase in depth and decrease in grain size of the sediment, whereas plagioclase is opposite in behaviour to K-feldspar.

These variations were attributed to size sorting and the relative resistance to the weathering and abrasion associated with the transportation processes.

In summary, the effect of transport and environment are variable and depend upon relief, climate and source rock type and diagenesis within the basin. Any one variable under a given set of conditions may be very important while the same variable under different conditions may be insignificant in affecting textural and compositional maturity of the sediment.

Therefore, it is difficult if not impossible to deduce the source rock type from the sediment chemistry. However, based on the information obtained

from petrographic study of the Namurian greywackes (see Chapter 3) it can be assumed that acid plutonic and to a lesser extent metamorphic source rock types might have been major contributors. In addition, derivation from pre-existing sedimentary rocks is also indicated.

4.5 Grain Size, Mineralogy and Chemistry

The purpose of this study was to obtain mineralogical and chemical data from different size fractions of the samples studied.

4.5.1. Mineralogical and Chemical Analysis of the Samples with most Size Fractions

Sandstones and Siltstones: Each size fraction separated (see Chapter 2) was subjected to X-ray diffraction study, using the smear method.

The principal minerals identified were quartz, kaolinite, illite, chlorite and Na-feldspar. Figure 19 shows the diffraction patterns for eight different size fractions of a sandstone sample (2c). It can be seen that the quartz peak intensity decreases with decreasing grain size. The second strongest diffraction peak for quartz at 4.26Å (marked Q) was used, because of the interference from illite on the first strongest peak. In a similar way Na-feldspar peak intensity decreases with decreasing grain size (marked F) whereas K-feldspar was not detected. In contrast kaolinite and chlorite peak intensities show continuous increase with decrease in grain size down to 2 μ fraction below which it decreases slightly.

The peak intensity of illite, however, increases with decreasing grain size down to 7.8 μm fraction, below which is decreases. This decrease in illite intensity is accompanied by the appearance of mixed-layer on the lower angle side which increase gradually in the finest fractions.

To express these changes in relative abundance, the X-ray peak height intensities of quartz, feldspar, chlorite, illite (muscovite) and kaolinite

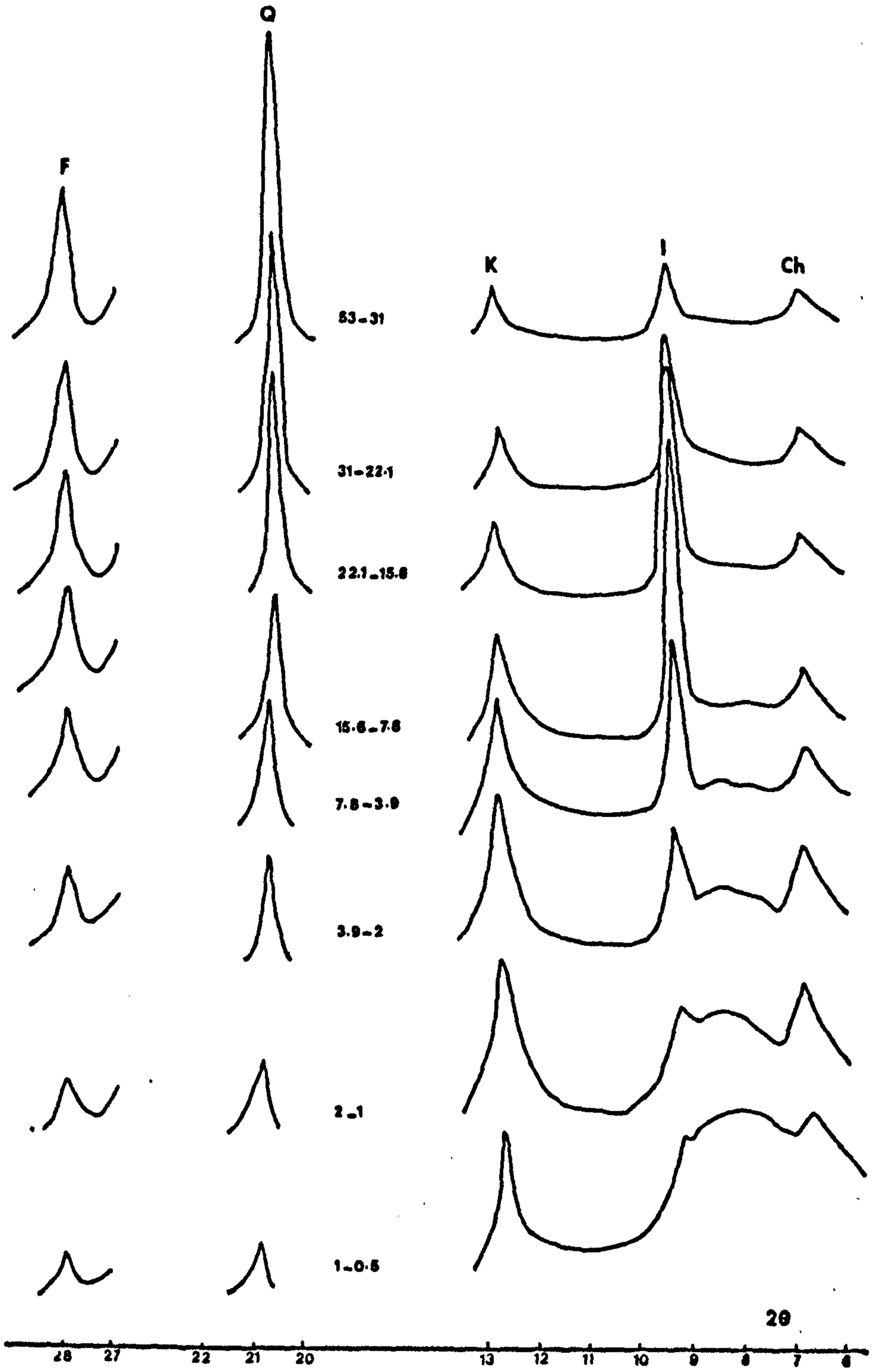

Fig.19 X-ray diffraction patterns of different size fractions,

(sample 2c)

in each size fraction were divided by their respective peak heights in the coarsest fraction (53.31 μm). Since identical conditions and measurements were maintained during the X-ray diffraction study, the resulting ratios when plotted against size fractions would yield a semiquantitative estimation of changes in the minerals abundance. These ratios are shown in Figure 20. It is apparent that quartz and Na-feldspar contents decrease gradually with concomitant increase in the kaolinite and chlorite contents, with respect to decreasing grain size from 53- < 2 μm. The muscovite content is at maximum in the 15.6-7.8 μm fraction.

On the basis of this information, it seems that the mineralogy is not uniform throughout its size range, nor does the mineralogy vary consistently with changing grain size. The low intensity of chlorite in the plus 2 μm, illite in the plus 15.6 μm and kaolinite in the plus 2 μm fraction can be attributed to simple dilution by quartz and Na-feldspar. In contrast, the decrease in chlorite, illite and kaolinite peak intensities below the above mentioned size fractions cannot be explained entirely by changes in the proportions of these minerals with respect to decreasing grain size. Consequently other possible explanations must be sought.

Berry and Jorgensen (1971) studied the mineralogical and chemical characteristics of various size fractions from Quaternary glacial clay, redeposited in marine environments. They found that with decreasing particle size, there was a gradual decrease in the content of Na-feldspar and quartz, with contemporaneous increase in the amount of chlorite and illite from 64.0-0.2 μm fractions, while in 0.2-0.1 μm fraction, chlorite and illite showed far greater intensities. In contrast the clay minerals in the minus one micron were found to be amorphous to X-ray and showed very broad peaks. They attributed the low intensities of chlorite and

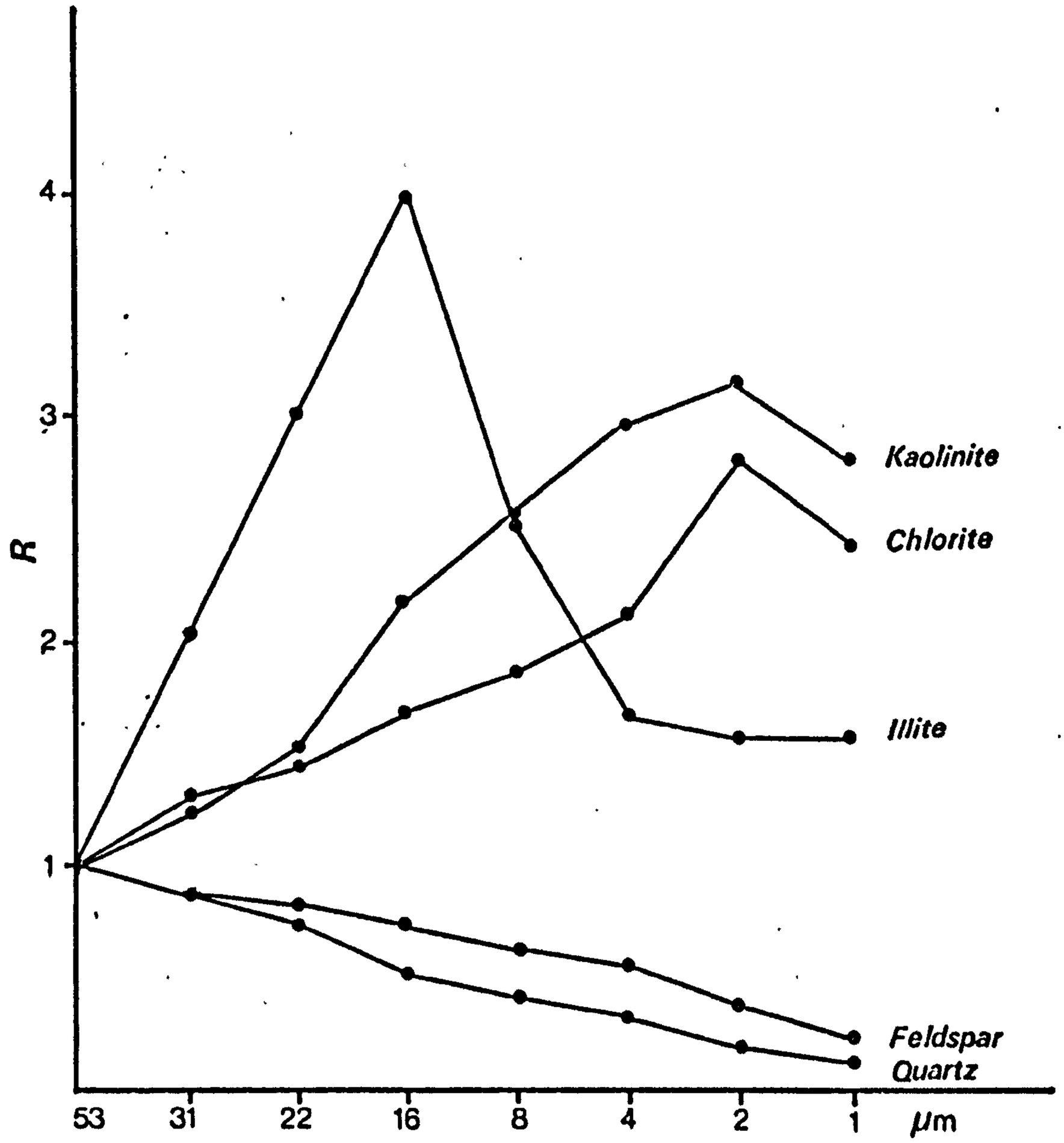

Fig.20 Plot of X-ray intensity ratio(R) of minerals in each size fraction relative to their abundance in the coarsest fraction.

illite in the plus 4 μm fraction to simple dilution, whereas their increase in the 0.2-0.1 μm could be due to the size sorting of minerals, with different types of chlorite and illite being abraded more easily and completely to a smaller size. It may also represent authigenic growth of illite and chlorite in the weathering and transport environment rather than the diagenetic environment.

Townsend and Reed (1971) investigated some mineralogical and chemical properties of Panamanian latosol. A comparison of the X-ray patterns of the coarse and fine clay fractions revealed somewhat greater peak intensities for the clay minerals in the coarse clay fraction. Their data was interpreted as to indicate a more well crystallised kaolinite in the coarse clay and silt fraction.

The present writer separated, by hand picking under a binocular microscope, muscovite flakes from the sandstones. A smear was then prepared and subjected to X-ray diffraction study. It was found that the basal reflections were very strong, symmetrical and narrow. This is considered to indicate a very good crystallinity, possibly as a result of more K^+ and less H_2O^+ in the structure (Carroll, 1970). In addition the response of extremely fine clays to X-ray is believed to be partly responsible for producing lower intensity, since amorphous material and organic matter are more abundant in the fine clay. However, the more persisting increase in the kaolinite and chlorite peak intensities with decreasing grain size could be due partly to their authigenic growth as revealed by the petrographic study (see Chapter 3).

In summary, the increase in illite and kaolinite intensities in the coarse silt fraction is attributed to the decreased dilution by quartz and Na-feldspar. In contrast, their lower intensities in the fine silt and clay fractions is the result of poor crystallinity, and possibly other structural factors.

The chemical analyses of the different size fractions of samples 2c and 4c are listed in Appendix 1. A comparison between the grain size and major element distributions is illustrated in Figure 21. A gradual decrease in the contents of SiO_2 and Na_2O with a concomitant increase in the content of Al_2O_3, Fe_2O_3, MgO and K_2O and to a less extent FeO is apparent as the grain size decreases. The antipathetic variation of SiO_2 and Al_2O_3 is reflected by the decrease in SiO_2/Al_2O_3 ratio with decreasing grain size (Table 29). This is in accord with the X-ray results which revealed a continuous decrease in the peak intensities of quartz and Na-feldspar and increase in those of mica, kaolinite and chlorite, down to the fine silt fraction. However, no marked chemical changes accompany the lowering of X-ray diffraction intensities of the 10Å and 14Å peaks with further decrease in grain size. Consequently, the lowering of illite and chlorite peak intensities in the fine silt and clay fractions must be influenced by atomic structural factors and possibly by the grain size or still other factors.

The maximum TiO_2 content is in the 15.6-7.8 μm fraction, the minimum content is in the 31-53 μm fraction. On the other hand, the TiO_2/Al_2O_3 ratio, generally increases as the grain size increases, indicating the enrichment in TiO_2 relative to the clay minerals in the coarser fractions. Moreover, the SiO_2/Al_2O_3 and TiO_3/Al_2O_3 ratios, show similar trend of variation, generally increase with increasing grain size (Table 29). The most likely explanation for this is that rutile and anatase (see Chapter 3, heavy mineral study) are present as fine grained detrital grains in the silt-fraction,in addition to its presence as fine needles of rutile adhering to clay minerals or quartz. Nevertheless, the incorporation of some titanium in the clay mineral structures is possible. Very slight variation in the content of CaO is noticeable in the different size fractions. This

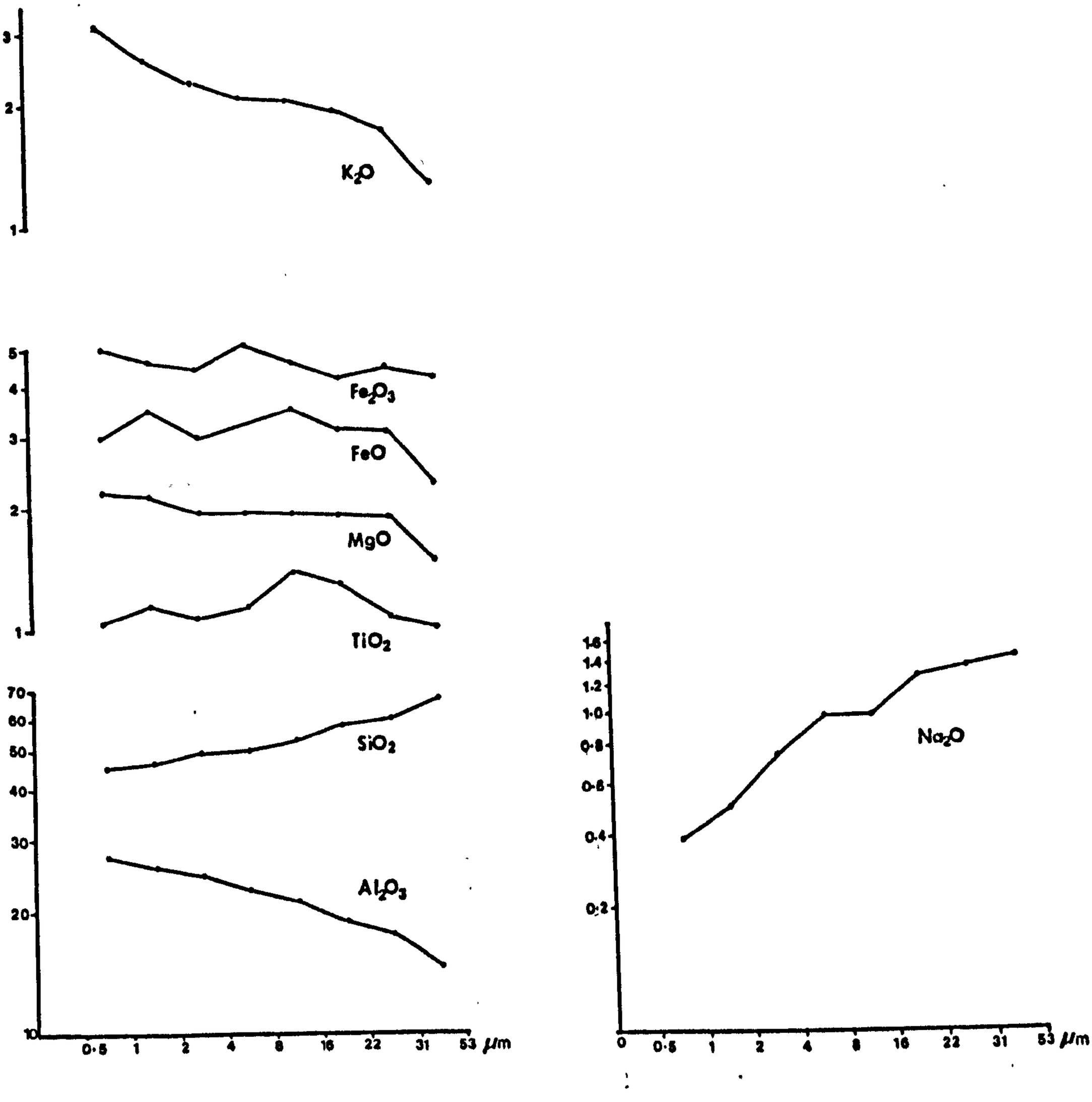

Fig.21 Major elements of different size fractions (sample 2c). *Log distribution.*

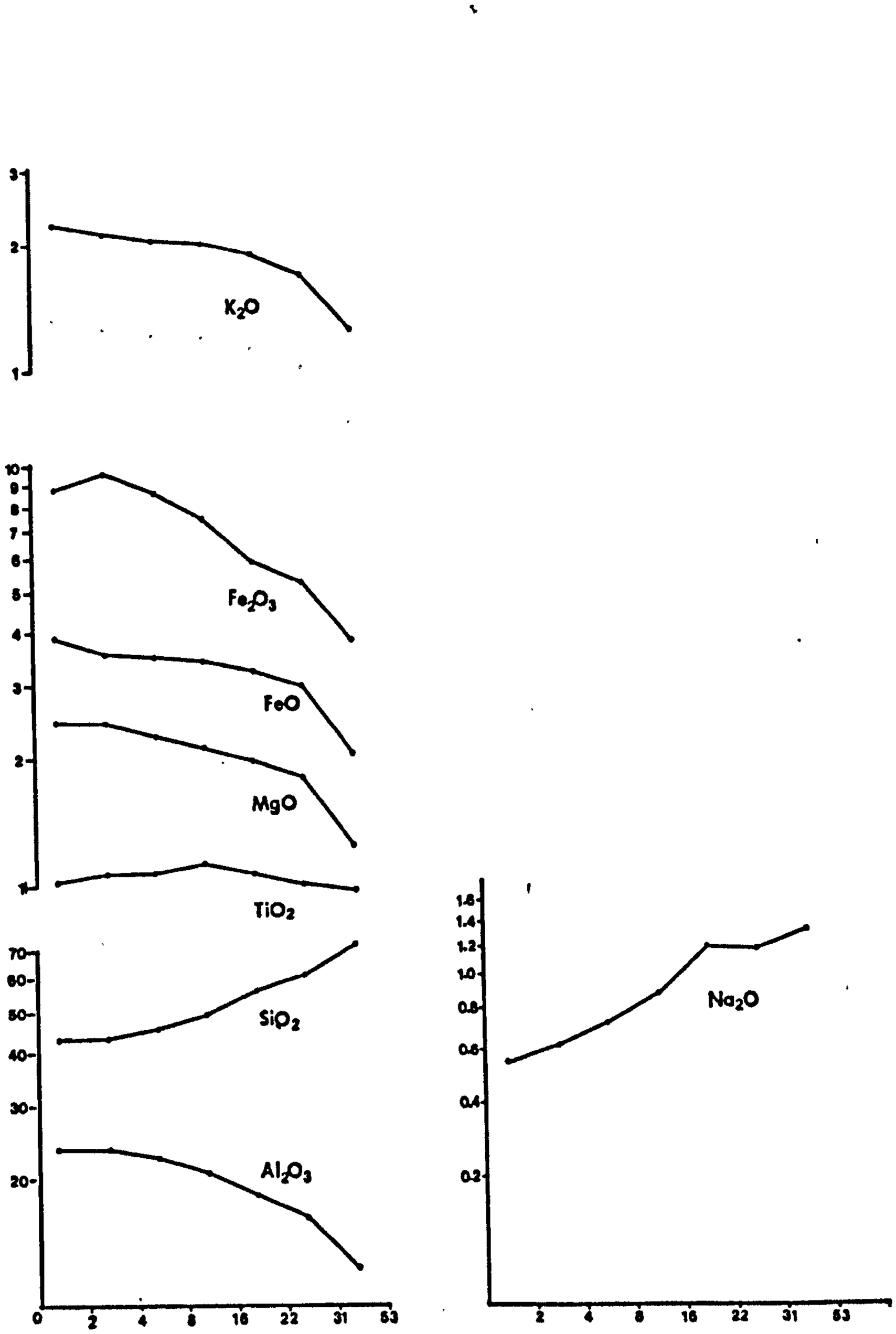

Fig.21 Major elements of different size fractions(sample 4c), *Log distribution*.

TABLE 29: SiO_2 and TiO_2/Al_2O_3 Ratios of Different Size Fractions

		Size in μm							
Sample Number	Element/Al_2O_3	0.5-1	1-2	2-3.9	3.9-7.8	7.8-15.6	15.6-22.1	22.1-31	31-53
2c	SiO_2/Al_2O_3	1.67	1.80	2.00	2.22	2.50	3.13	3.3	4.53
	TiO_2/Al_2O_3	0.037	0.046	0.043	0.049	0.066	0.069	0.060	0.065
4c			1.84	1.90	2.03	2.36	3.08	3.69	5.88
			0.043	0.047	0.048	0.053	0.059	0.061	0.065

		Size in μm			
2a		0.5	0.5-1	1-2	2-3.9
	SiO_2/Al_2O_3	1.6	1.66	1.67	1.78
	TiO_2/Al_2O_3	0.021	0.026	0.028	0.032

could be due to the insignificant amount of carbonates present in these samples, which was not detected on X-ray diffraction traces or it may represent calcium held in the clay mineral structures. A similar trend is exhibited by MnO. The ignition loss increases markedly with decreasing grain size, which is attributed to the higher content of structural water in the fine fractions, due to the higher clay mineral content. However, the residue, after ignition of the finer fraction, is black in colour in contrast to the light grey residues of the coarser fractions. This implies that organic materials are more abundant in the finer fractions than in the coarser fractions.

P_2O_5 shows slight variation through the different size fractions, but it is relatively more abundant in the clay fractions than in the silt fraction. This could be ascribed partly to the presence of phosphorous in clay mineral structures or could be due to the association of very fine needles of apatite with the clay fraction.

Comparison with whole rock analysis indicates a continuous decrease in SiO_2, while TiO_2 and Na_2O each show an increase in a particular silt fraction and then decrease. Also, it is clear that there is a gain in Al_2O_3, Fe_2O_3. MgO, P_2O_5 and K_2O. The increase in K_2O is accompanied on the X-ray diffraction trace, by a decrease in the intensity of discrete mica and the appearance of hydrated illite and/or illite + smectite mixed layer. In the same way, FeO and MgO increase could be related to increase in chlorite.

Shales: A shale sample (2a) was found to consist almost entirely of a very fine silt and clay, thus it was suitable to study the mineralogy and chemistry of its different size fractions.

Glass smear mounts of each size fraction were X-rayed in the untreated state, then after treatment with ethylene glycol, after heating 375°C

and finally heating to 550°C. The results of these procedures are shown in Figure 22. It is clear that the mineralogy of all size fractions is similar and consisting of chlorite, illite/mixed layer, kaolinite and quartz. However, traces of plagioclase peak were observed only in the 3.9-2 μm and 1-2 μm fractions at 3.18Å. The mixed layer mineral forms a broad peak between 12.61-9.92Å (7-8.9 2θ) with maximum intensity at 11.15Å (8.2θ). After glycolation this broad peak disappears without the development of a new peak at lower angles, except in the 1-2 μm and 3.9-2 μm fractions, where small peaks at 15.49-15.1Å were observed. This is interpreted as due to smectite in the mixed layer. It is also apparent that the content of illite/smectite mixed layer increases with decreasing grain size, whereas the illite peak progressively becomes less sharp in the untreated sample, and discrete illite is not observed in the less than 1 μm fraction. Heating to 350°C and 550°C gives a marked increase in the peak intensity of illite, with increase of d-spacing from 9.98Å to 10.04Å. This is due to collapse of mixed layer, dehydration of illite which is attaining a much more ordered structure, similar to that of muscovite (Carroll, 1970).

The chlorite peak remains, more or less, in the same position (14.1-14.01Å) in the untreated and glycolated states. Heating to 350°C either removes or reduces it markedly in intensity, but on heating to 550°C it increases in intensity with slight decrease in d-spacings at about 13.67-13.79Å. This behaviour is characteristic of Fe-rich sedimentary chlorites (Brown, 1961; Carroll, 1970). The chlorite peak intensity, however, decreases slightly with decreasing grain size. The kaolinite peak intensity remains relatively the same in the untreated, glycolated and 350°C heated states, but heating to 550°C destroys it. Its intensity increases with decreasing grain size down to 0.5 μm below which it decreases slightly.

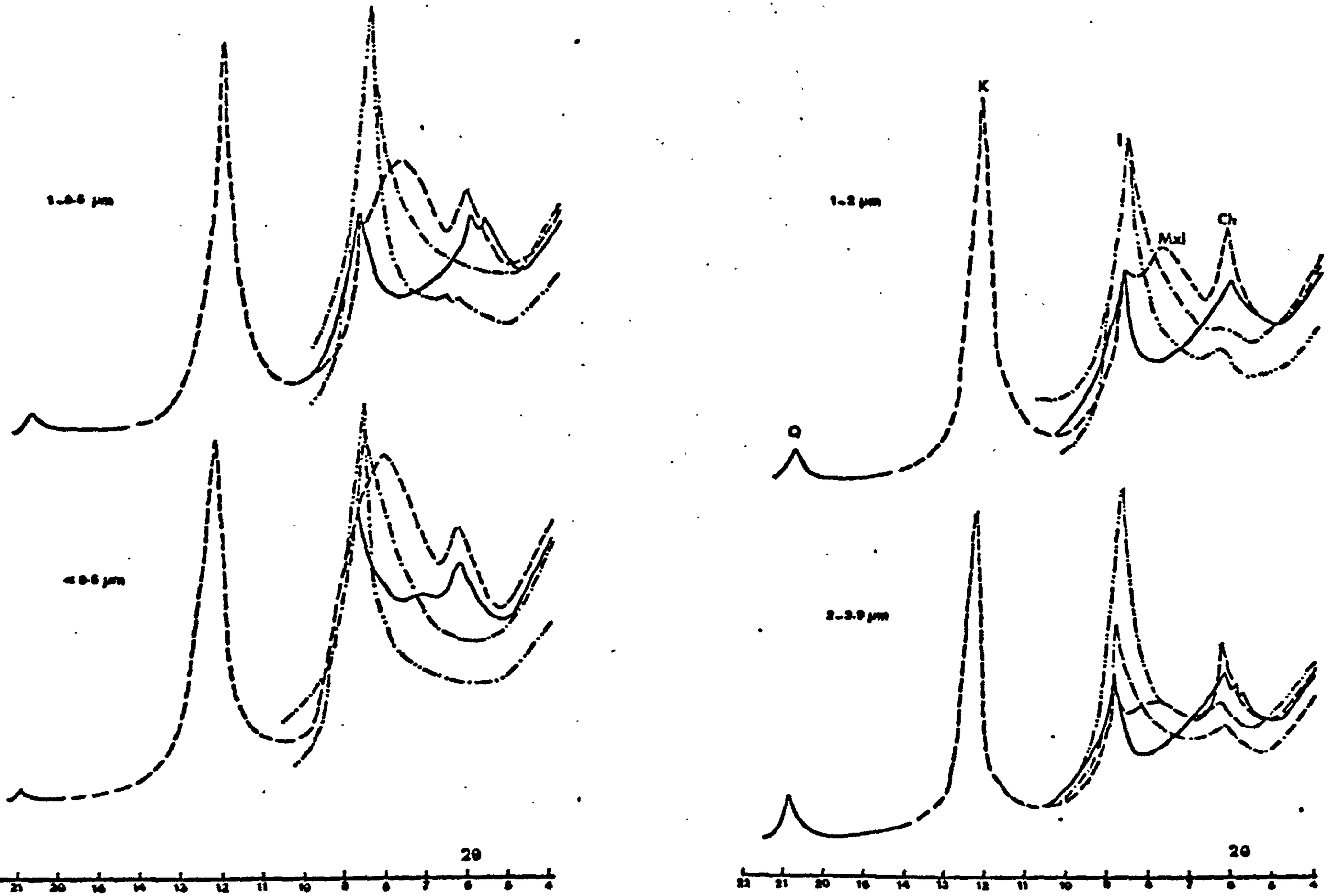

Fig.22 X-ray diffraction patterns of different size fractions(sample 2a),Ch-chlorite,I-illite,K-kaolinite,MxI-mixed layer, Q-Quartz.In each case the traces are, _ _ untreated, _____ glycolated, ____ heated to 350°C, ____ heated to 550°C CuK_{α} radiation.

The quartz peak (4.24Å) intensity decreases with decreasing grain size, but it persists even the finest fraction. Whereas Na-feldspar peak was observed only the coarsest fractions.

The chemical data of the different size fractions are included in Appendix 1. The major element distribution through these size fractions is graphically shown in Figure 23. The SiO_2 and Na_2O contents decrease with decreasing grain size and are antipathetic with those of Al_2O_3, Fe_2O_3 and K_2O. This is in agreement with the mineralogical results. The TiO_2 trend is similar to that of quartz and Na_2O, and its highest content is in the very fine silt. This substantiates the results from the previous samples, indicating that TiO_2 is mostly detrital. Again the SiO_2/Al_2O_3 and TiO_2/Al_2O_3 ratios show a gradual increase as the grain size increases (Table 29). Likewise the FeO and MgO contents are in sympathy and decrease with decreasing grain size. This may be attributed to the slight decrease of chlorite content with respect to decreasing grain size as revealed by X-ray study and it is likely that chlorite is most abundant in the coarse clay fraction.

On the basis of this mineralogical and chemical data the most noticeable change is the progressive increase of illite/smectite mixed layer and a concomitant increase in K_2O with respect to decreasing grain size. This would be expected if the increased proportion of non-expandable 10Å layers are of illite composition, or in other words, decrease in the proportion of expandable smectite. This is indicated by the appearance of 15+Å peak in the glycolated specimens in the 1-2 and 2.3-9 μm fractions, while it is not observed in the finer fractions.

Further evidence is obtained from the measurements of d-spacings of illite/smectite peak in the coarse and fine fractions. Using the d-spacing migration curves of Weaver (1956), the 11.15Å peak in the >0.5 μm

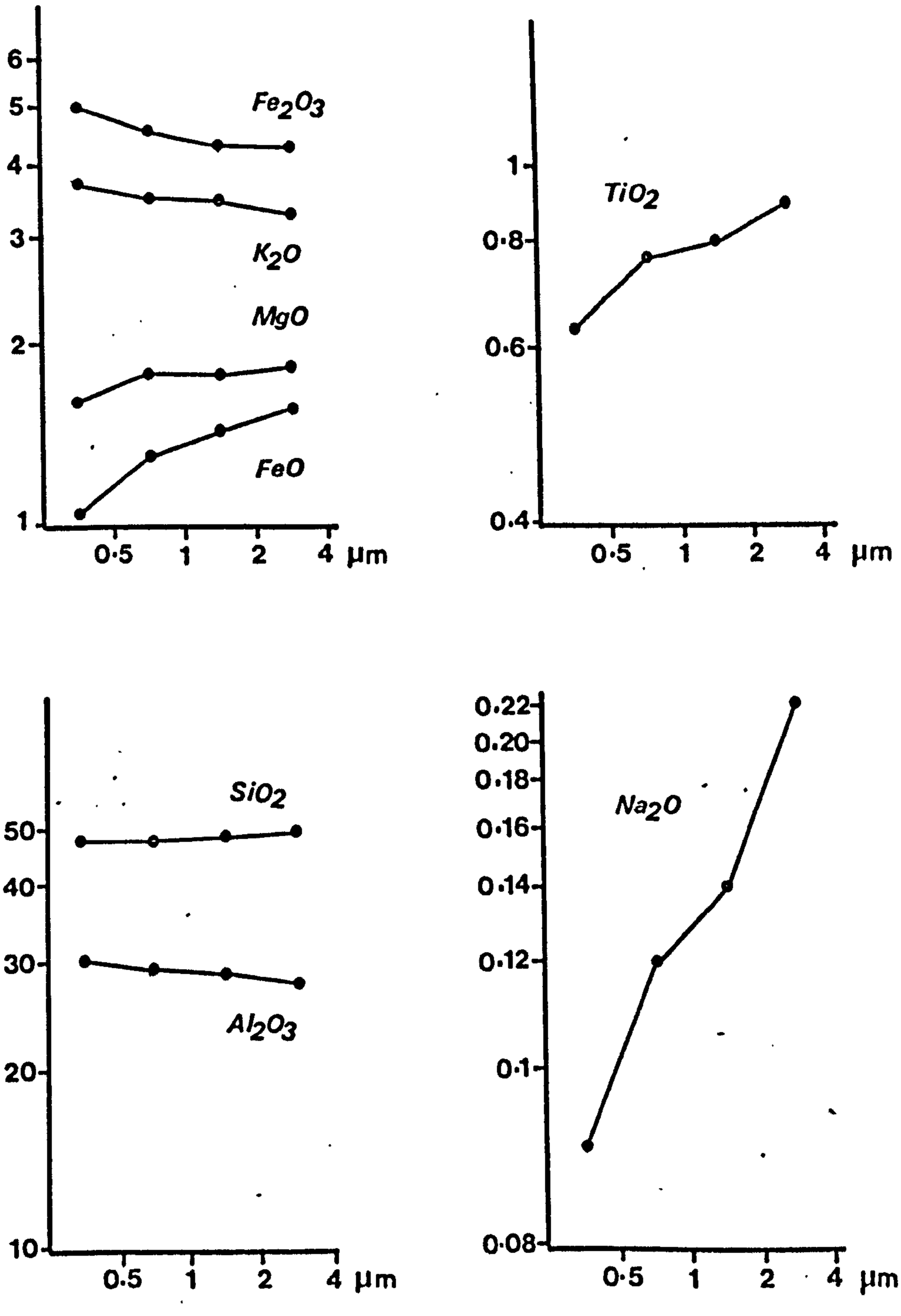

Fig.23 Major elements of different size fractions(sample 2a), *Log distribution.*

fraction corresponds to 20% expandable smectite, whereas the 10.8Å peak in the <0.5 μm corresponds to 15% expandable smectite. Thus the increase in K_2O with decrease in size fraction can be correlated with an increase in the 10Å proportion of the mixed layer of illite/smectite.

In this respect the work of Perry and Hower (1970, 1972) on the Gulf Coast pelitic sediments may be relevant. They studied the mineralogy and chemistry of the Gulf Coast sediments including data on the different size fractions. They noted the increase of quartz and feldspar abundance with increasing grain size, with these minerals dominating the 5-20 μm and >20μ m fractions. The <1 μm fraction however, was dominated by an illite/smectite mixed layer mineral. Discrete illite (mica) in the <1 μm fraction decreased in abundance with increasing sample depth. They also noted that the K_2O content increased with decreasing grain size. As indicated on the diffraction patterns there was a concomitant increase in the potassium content of clay size fractions with decreasing expandability. They concluded that illite/smectite mixed layers undergo a decrease in expandability from 80 to 20% smectite layers with increasing depth. This was attributed to the breakdown of detrital illite (mica) which serves as the major source of potassium, due to deep burial diagenesis.

Hower et al. (1976) carried out a similar study on the Gulf Coast sediments. Their findings were like those of Perry and Hower. They concluded that potassium released by K-feldspar and mica during deep burial (metamorphism) from the coarsest fraction was incorporated in the illite/smectite, thus increasing the illite content. The mineralogical and chemical changes suggested that the reaction in shale is smectite + K - feldspar + mica = illite + chlorite + quartz.

However, according to Smith and Yoder (1956), Velde and Hower (1963), Velde (1965), Maxwell and Hower (1967), the mica or illite polymorph accompanying

deep burial metamorphism should be of 2M form. The present writer attempted to determine the polymorphic forms of illite from the <2 μm fractions which were treated for 30-minutes with hot 10% HCl and consequently heated to 600°C to remove any interference from chlorite and kaolinite. The criteria of distinguishing illite polymorphs, obtained fromthe aforementioned workers, were used. No characteristic peaks of 2M and 1M polymorphs were observed in the clay fractions, and it is assumed that the polymorphic form of illite is 1Md, indicating that the Namurian sediments have not been subjected to deep burial metamorphism.

4.5.2 Mineralogy and Chemistry of Samples with Less Size Fractions

The samples belong to two groups, the first sandstones and the second shales.

Their mineralogical characteristics are exemplified by the sandstone sample $6b_3$ and the shale sample 6a. The peak height intensities of the clay minerals, Na-feldspar and quartz are shown in Table 30.

It is apparent that Na-feldspar quartz peak intensity increases with increasing grain size while the chlorite and kaolinite peak intensities increase with decreasing grain size. High illite peak intensity is believed to reflect its good crystallinity in the coarse fraction rather than its abundance. This is due to the fact that muscovite is present in the coarse fraction, while its fine grained counterpart in the finer fraction is represented by degraded illite.

Appendix 1 lists the chemical data obtained from the different size fractions of the sandstones and shales. The distribution of major elements among these size fractions in each group is shown in Figure 24. In both sandstones and shales the SiO_2 and Na_2O contents show a gradual increase with respect to an increase in grain size. The Na_2O is mostly concentrated

TABLE 30: Intensities of X-Ray Peak of Clay Minerals, Na-Feldspar and Quartz in Different Size Fractions (μm)

	Sandstones				Shales		
Intensity in cm	<2	2-7.8	7.8-53	>53	<2	2-7.8	7.8-53
Chlorite	4.5	3.7	2.5	0.8	6.4	5	3.9
Illite	3	4	3.5	8.5	7.5	7.5	10.5
Kaolinite	35	27	22	4	38	30	24
Na-Feldspar	3.3	7.5	10.5	10	0.8	2.1	3.0
Quartz	4.1	9.5	13	30	0.8	3.2	7

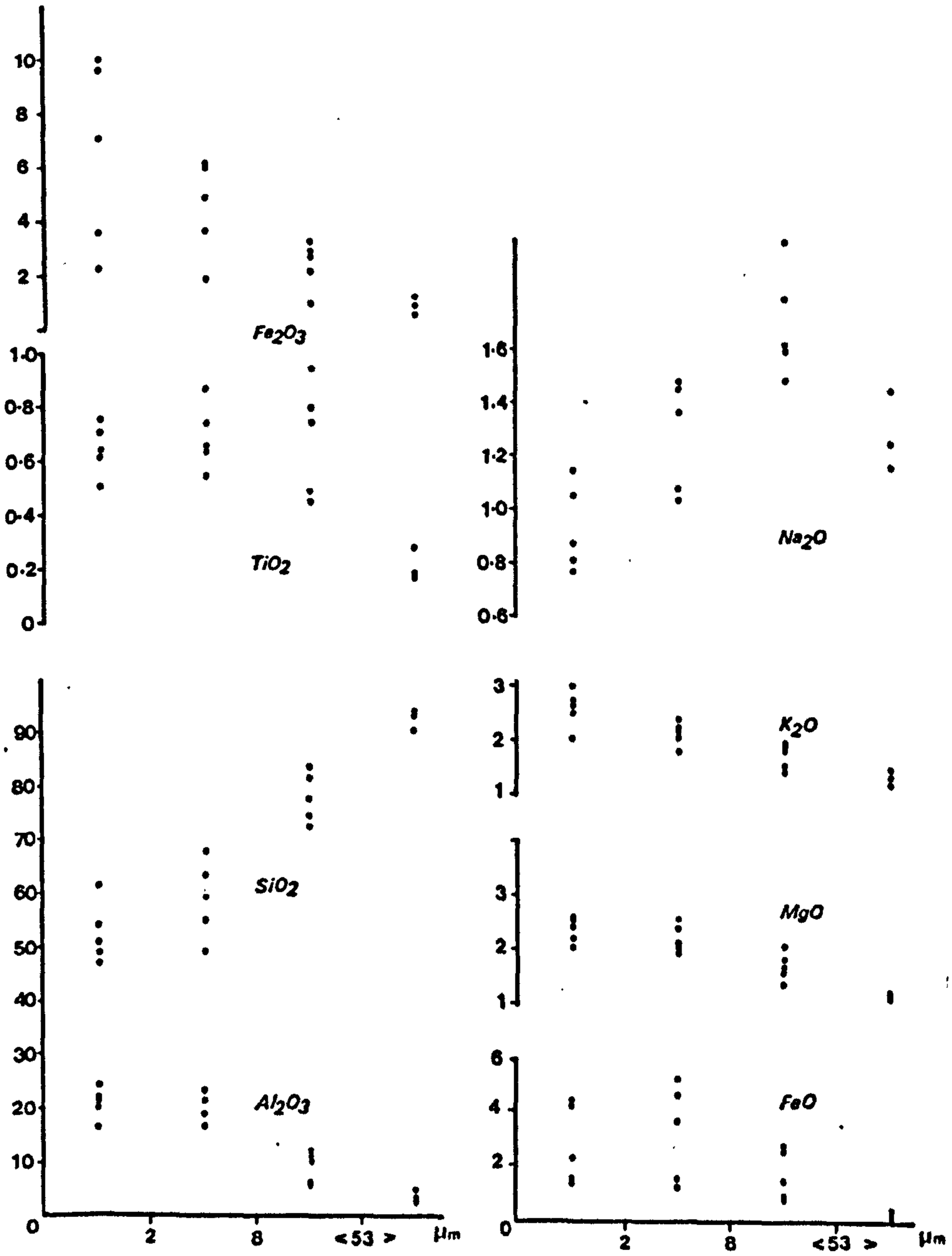

Fig·24 Major elements of different size fractions of sandstones.

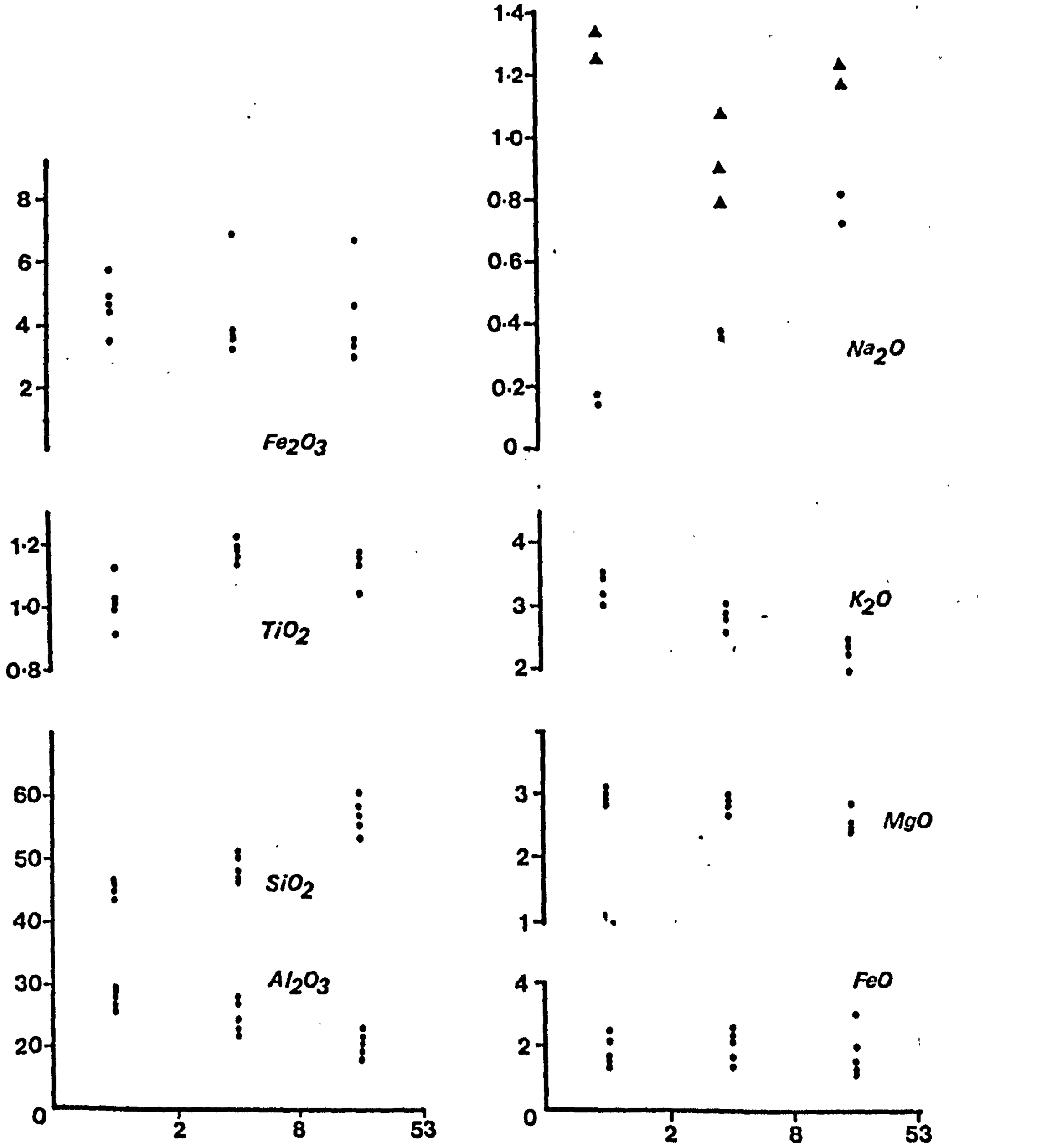

Fig.24 Major elements of different size fractions of shales.

▲ Na_2CO_3 treated

in the 53.8μm fraction in the sandstones. However, those shales showing very high Na_2O content in the clay fraction are unusual due to treatment with Na_2CO_3 (see Chapter 2). The TiO_2 content for the most part is similar to SiO_2 in the <53 μm fraction but it decreases markedly in the >52 μm fraction. The SiO_2/Al_2O_3 and TiO_2/Al_2O_3 ratios vary in a similar way up to the 53 μm fraction and then depart, showing antipathetic relationships (Table 31). In contrast the Al_2O_3, K_2O and MgO contents are in sympathy and increase with decrease in grain size. An almost similar pattern to that of the Al_2O_3 is exhibited by Fe_2O_3 in the sandstones, but a somewhat less pronounced trend is shown by FeO due to the presence of siderite in some sandstones. The Fe_2O_3 and FeO content in the shales show less variation but generally they are more abundant in the less than 7.8μ fraction, which may be due to the presence of some siderite and hydroxide, together with variable amounts of chlorite and illite in these shales. However, pyrite was not detected in any of the X-ray traces. The CaO content is more or less constant except in one sample which contains minor amounts of calcite.

In the previous sections it was noted that the increase of potassium with some of the iron and magnesium with decreasing grain size could have been the result of burial diagenesis.

On the other hand, similar trends of element variations with grain size could take place in the depositional environment. Wright (1974) studied the mineralogy and chemistry of sand, silt, and clay fractions of the surface sediments from the Southern Barents Sea. The terrigenous clay minerals are a variable mixture of micaceous debris and illite with chlorite, minor montmorillonite and occasional kaolinite. The major elements K_2O, Fe_2O_3, TiO_2, MgO, P_2O_5 and Al_2O_3 contents were shown to increase with decreasing grain size and were partitioned between illite and chlorite.

TABLE 31: SiO_2 and TiO_2/Al_2O_3 Ratios of Different Size Fractions Sandstone (b), Shale (a)

		Size in µm			
Sample Number	Element/Al_2O_3	<2	2-7.8	7.8-53	>53
3b	SiO_2/Al_2O3 TiO_2/Al_2O_3	2.63 0.030	3.79 0.039	6.72 0.067	
$4b_1$		3.79 0.030	5.19 0.042	11.61 0.064	
6b		1.86 0.035	2.04 0.037	5.78 0.077	17.03 0.051
$6b_3$		2.29 0.032	2.76 0.034	6.94 0.071	25.91 0.045
$8b_1$		2.25 0.028	2.83 0.033	12.46 0.071	28.07 0.048
1a		1.72 0.039	2.18 0.050	3.03 0.054	
3a		1.79 0.042	2.21 0.048	2.65 0.048	
5a		1.65 0.035	2.07 0.049	3.06 0.057	
6a		1.57 0.032	1.75 0.042	2.42 0.050	
9a		1.55 0.035	1.72 0.043	2.31 0.052	

Thus it seems that the variation in element content with decreasing grain size, does not necessarily suggest occurrence under conditions of deep burial diagenesis. However, other evidence would lend support to one or the other alternatives.

4.6 Mineralogy and Chemistry of Clay Fractions

In the previous sections the variations in mineralogy and chemistry of 25 whole rock samples together with the different size fractions from 14 samples were discussed. The <2 μm size fraction from the 25 samples is considered in this section. The analyses are shown in Appendix 1. The X-ray study revealed that kaolinite, illite and mixed layer illite/smectite, chlorite and quartz are the major minerals with minor plagioclase and occasional carbonates. The relative abundance of each clay mineral is expressed as a percentage of its 001 peak area (Table 32). It is apparent that kaolinite is generally the dominant mineral in the clay fractions from both shales and sandstones, but when illite and mixed-layer illite/smectite are considered together, this is more abundant than kaolinite from the clay fractions of some shales. On the other hand, quartz, plagioclase and to a lesser extent carbonates are more abundant in the sandstone's clay fractions as shown by their X-ray traces and the higher SiO_2 and Na_2O contents.

Relationships examined between the mineralogical and chemical data for the clay fractions are in Table 33 which is a correlation matrix showing underlined the significant positive relations.

The correlation between SiO_2 and Na_2O is due to the higher content of quartz and plagioclase in the sandstone's clay fractions. The latter also contain some carbonate and this is reflected by the significant SiO_2-CaO relationship. Kaolinite is the more abundant clay mineral in the sandstone's clay fractions and this is indicated by the correlation of

TABLE 32: Areas of Clay Mineral Peaks Expressed as Percentages, <2 μm Fraction, Mam Tor Rocks

Sample Number	Chlorite	Kaolinite	Illite	Mixed-Layer	Illite + MXL
1a	14	42	28	16	44
1b	10	68	8	14	22
2a	13	38	33	16	49
2b	12	63	10	15	25
2c	14	52	12	22	34
3a	5	37	46	12	58
3b	7	58	7	28	35
4a	12	33	31	23	55
4c	14	55	15	16	31
$4a_2$	16	29	31	24	55
$4b_1$	5	77	11	7	18
$4b_2$	11	52	23	14	37
$4b_3$	14	47	17	22	39
5a	8	30	34	28	62
6a	12	40	25	23	48
6b	13	60	11	16	27
$6b_1$	16	45	13	26	39
$6b_2$	16	65	13	7	19
$6b_3$	16	55	21	8	29
7a	14	39	26	21	47
$8a_1$	7	42	39	12	51
$8a_2$	15	31	34	20	54
$8b_1$	8	66	9	17	26
$8b_2$	10	49	12	29	41
9a	14	38	26	22	48

TABLE 33: Correlation Matrix of Chemical and Mineralogical Data from the Clay Fractions

	SiO_2	Al_2O_3	TiO_2	Fe_2O_3	FeO	MgO	CaO	Na_2O	K_2O	MnO
SiO_2	1.0000									
Al_2O_3	-0.6752	1.0000								
TiO_2	-0.6752	(0.5468)	1.0000							
Fe_2O_3	-0.2836	-0.2622	0.0588	1.0000						
FeO	-0.2471	-0.3851	-0.0961	0.2365	1.0000					
MgO	-0.8130	(0.4246)	(0.6305)	0.0485	(0.4559)	1.0000				
CaO	(0.7148)	-0.5987	-0.5303	-0.3354	0.0442	-0.2902	1.0000			
Na_2O	(0.5513)	-0.6065	-0.2161	0.0680	-0.0129	-0.5018	0.3084	1.0000		
K_2O	-0.5429	(0.9403)	(0.5458)	-0.3915	-0.5030	(0.4127)	-0.4642	-0.5224	1.0000	
MnO	0.1906	-0.4472	-0.3208	0.0607	(0.5468)	0.0336	0.3356	-0.0197	-0.5043	1.0000
P_2O_5	-0.3546	-0.2825	0.1737	(0.5900)	(0.6820)	(0.4395)	-0.1213	-0.1983	-0.4056	0.2777
SO_3	-0.1331	-0.1269	-0.0530	0.1378	0.4673	0.1565	0.1665	0.1492	-0.3042	0.2127
Iglos	-0.7799	(0.5188)	(0.7031)	0.0333	0.1096	(0.7449)	-0.5524	-0.4846	(0.5342)	-0.3060
Chlor	-0.3805	0.2578	0.3399	(0.4345)	-0.1451	0.0973	-0.4258	-0.3956	0.1173	-0.2245
Illmxl	-0.3658	(0.7972)	(0.4217)	-0.3532	-0.6124	0.2028	-0.4665	-0.3171	(0.9149)	-0.5426)
Kaoln	(0.4547)	-0.8405	-0.4982	0.2295	(0.6311)	-0.2233	(0.5622)	(0.4128)	-0.9173	(0.5833)

	P_2O_5	SO_3	Iglos	Chlor	Illmxl	Kaoln
P_2O_5	1.000					
SO_3	0.3186	1.0000				
Iglos	0.1963	-0.1863	1.0000			
Chlor	0.3192	0.1733	0.3609	1.0000		
Illmxl	-0.5333	-0.4876	(0.4465)	-0.0140	1.0000	
Kaoln	(0.4315)	(0.4256)	-0.5285	-0.2506	-0.9644	1.0000

SiO_2-kaolinite. From this it follows that there is a correlation between kaolinite and Na_2O, but it does not indicate a genetic relationship, merely their covariation. The correlations between K_2O, Al_2O_3 and illite/smectite mixed can be explained by the composition of the clay mineral itself. TiO_2 and MgO correlate with Al_2O_3 and K_2O, but the values of the correlation coefficient of TiO_2 are higher than those of MgO. This suggests that the part of TiO_2 associated with the clay minerals is mainly contained in illite. The FeO correlation with MgO and MnO may be attributed to carbonate and chlorite, the former is contained mostly in the sandstone's clay fractions. It seems therefore, that the covariation of carbonate and kaolinite in the clay fraction of sandstone could explain their significant correlation. The correlation of P_2O_5 with Fe_2O_3, FeO and MgO may either be due to closure or it indicates association with clay minerals and carbonates (siderite). The SO_3-FeO and SO_3-kaolinite correlations are most probably the result of closed systems, since a genetic relationship cannot be envisaged. The ignition loss accounts for structural water in the clays and the associated organic matter; thus its correlation with Al_2O_3, TiO_2, MgO, K_2O and illite/mixed layer is likely.

Fe_2O_3 behaves independently of most elements but its correlation with chlorite may indicate their covariation. On the other hand, it may suggest that some Fe_2O_3 is contained in the chlorite. This is because chlorite and iron hydroxides were shown by optical study to be the alteration products of biotite, especially in the sandstones. A similar relationship between Fe and chlorite in the <2 fractions of sandstones has been described by Triplehorn (1970). The latter considered this relation to indicate the iron rich nature of chlorite which was supported by X-ray diffraction study.

4.6.1 Semiquantitative Estimation of Chlorite Composition

The technique employed includes analysis of chlorites in the isomorphous series $(Mg_{12-x-y}Fe''_yAl_x)(Si_{8-x}Al_x)O_{20}(OH)_{16}$. It has been described by Schoen (1962) and used by Collins (1976) to determine chlorite composition from spoils of British colleries. Schoen showed that using the calculated ratio of structure factors for the basal reflections and comparing them with their theoretical counterparts, allows an approximate determination of chlorite composition. In the present work only the 001, 003 and 004 reflections were used to derive the chlorite composition. The general formula for calculating the structure factors is as follows:

$$I = (CF)^2 \left(\frac{1 + \cos^2 2\theta}{\sin^2 \theta \cos \theta} \right)$$

Where I is the intensity in counts/second, C is a constant, F is the structure factor and θ is the diffraction angle. In the first step F001 and F003 and the F003/F001 were calculated, giving values to compare with figures from Schoen (1962), and Collins (1976). The structure factors for the 004 reflection or F004 is then deduced. Next the number of Fe ions per unit cell (value of Y) was found from the other table (Brown, 1955; Schoen, 1962; Collins, 1976).

The range in (for 11 determinations) number of Fe ions per unit cell was found to be approximately 7-10.5 out of a total of twelve, giving a general formula ranging between:

$$(Mg_{1.5-x}Fe''_{10.5}Al_x)(Si_{8-x}Al_x)O_{20}(OH)_{16}$$

and

$$(Mg_{5-x}Fe''_{7}Al_x)(Si_{8-x}Al_x)O_{20}(OH)_{16}$$

The value of x which is the number of Al atoms per four tetrahedral sites was estimated from formula relating chlorite composition to its first basal reflection. Slightly different formulae were employed as reported by Brindley and Gillery (1956), Brown (1961) and Bailey (1972), but that reported by the first authors was better suited, as follows: $d001 = 14.50 - 0.31x$. The d001 averaged 14.01 Å, giving x a value approximately 1.50. Applying this to the above range of formulae, gives the range in chlorite composition:

$$Mg_{3.5}Fe"_{7}Al_{1.5}(Si_{6.5}Al_{1.5})O_{20}(OH)_{16}$$

$$Fe"_{10.5}Al_{1.5}(Si_{6.5}Al_{1.5})O_{20}(OH)_{16}$$

This range in composition indicates that chlorite is largely of the iron variety. However, it is clear from the chemical analyses of the clay fractions that Fe_2O_3 is generally present in higher amounts than FeO, particularly in those of the sandstone. Thus it seems that Fe_2O_3 is likely to be located in chlorite in small amounts. Nevertheless Fe^{3+} can substitute for other cations in octahedral position in the chlorite structure (Brindley and Gillery, 1956; Albee, 1962).

4.6.2 Relation between Crystallographic Properties of Illite and Diagenesis

The transformation of smectite or smectite/illite mixed layer to illite or muscovite is the most widely recognised indicator of the degree of alteration during deep burial diagenesis and low grade metamorphism. The results derived from the Gulf Coast shales have been discussed in detail by Perry and Hower (1970, 1972), Weaver and Beck (1971) and Hower et al. (1976). Similar studies have been carried out on shales from different basins (Foscolos and Kodama, 1974; Heling, 1978; Sordon, 1978). On burial, increasing temperature causes potassium to be

continuously incorporated, thus increasing the illite content at the expense of the smectite in the mixed-layer clay. This process is commonly accompanied by change in the polymorphic form of illite-muscovite and has been evaluated by means of the 2M/1Md polytype ratio, based on the work of Smith and Yoder (1956), Velde and Hower (1963), Velde (1965), Maxwell and Hower (1967). During deep burial diagenesis and incipient metamorphism the crystal structure of illite becomes progressively more ordered with the polytypes 1Md and 1M transforming to 2M type. A summary of diagenetic change affecting the structure of illite is given by De Segonzac (1970), who also gives an account of the transformation of other clay minerals. With increased crystallinity the 001 illite peaks becomes narrower and more sharply defined. The crystallinity index ('Kubler Index') which is the width at half height of the 001 illite peak, has been used by a number of workers as a quick and simple measure of the degree of crystallinity (Foscolos et al., 1976; Rowsell and Swardt, 1976; Jackson, 1977). Within the zone of anchimetamorphism (the transition zone between diagenesis and metamorphism) the width of the illite 001 peak decreases as the degree of metamorphism increases (cf. De Segonza op. cit.).

Furthermore, the crystallographic properties of illite vary with elemental composition (Esquevin, 1969). The latter points out that the ratio of the intensity of 002 (5Å) peak to that of the 001 (10Å) peak gives a good measure of aluminium content; a 002/001 ratio of 0.3 or more is characteristic of Al-rich illite (De Segonzac, 1970; Gill et al., 1977). However, under conditions of deep burial and anchimetamorphism Al-illite (poor Mg) evolve more readily towards the ordered 2M type. When the Kubler Index is plotted against the 002/001 ratio, the pattern obtained gives an indication of the diagenetic stage, as shown by De Segonzac.

On the basis of this information an attempt was undertaken to evaluate the post-depositional effects on illitein the Mam Tor rocks.

Method

The determination of the illite polytype was carried out on the <2 μm fraction which was treated with hot 10% HCl for half an hour, and consequently heated to 600°C to remove interference by other clay minerals. Then a smear mount was prepared and scanned from 4-40 2θ. The crystallinity index (Kubler Index) which is the width of illite 001 peak at half height expressed in mm was obtained from another smear after glycol treatment.

Results

The clay minerals of the <2 μm fraction consist of illite, kaolinite and chlorite (see Table 32). The illite 10Å peak is asymmetrical and always tailed off towards higher d-spacing, but a separate reflection characteristic of a mixed layer mineral was not observed, even after glycolation. The study of the various size fractions indicated the presence of mixed layersin the 0.5-3 μm fraction (page 87). Consequently the asymmetry of illite 001 peak in the <2 μm fraction is considered to reflect the presence of a very small amount of illite/smectite mixed layering. This is supported by the better defined and narrower peak of illite in the silt fraction (see Figure 19), which is strongly influenced by the presence of detrital muscovite. Srodon (1978) found that the amount of illite/smectite mixed layer decrease in the coarser clay and silt fraction.

The criteria for distinguishing illite polytype, following the aforementioned workers, were used. No characteristic peaks for the 2M and 1M polymorph were observed in the <2 μm fraction, or even in the finer

fractions. Therefore, it is assumed that illite is the 1Md polytype. The latter is the most common polytype in sedimentary clays (De Segonzac, 1970, p.314)and it is suggested, therefore, that the Mam Tor rocks are in the zone of normal diagenesis (early-late diagensis) and had not been subjected to deep burial metamorphism. This 1Md polytype can be considered to be largely inherited from weathering of the source rocks and subsequently subjected to aggradation (up take of K^+) in the marine environment and also during compaction (cf. De Segonzac, op.cit. p.32). This is supported by the pattern obtained by plotting the Kubler Index against the 002/001 intensity ratio (Figure 25). It shows a more or less normal diagenetic stage for the Mam Tor rocks. In addition, the majority of illite appear to be an Al-rich variety. However, the disappearance of kaolinite and its transformation to illite or other minerals is commonly considered as an indication of deep burial diagenesis or incipient metamorphism (De Segonzac 1970; Rowsell and Swardt, 1976; Foscoles et al, 1976). The abundance of kaolinite in the Mam Tor rocks substantiated their location in normal diagenetic stage.

In summary, the distribution of clay minerals in the Mam Tor rocks can be attributed to weathering, environment and diagenetic factors.

4.7 Diagenesis and Secondary Minerals

Authigenic minerals formed during diagenesis of the Mam Tor greywackes were described earlier (see Chapter 3). They include kaolinite at the expense of feldspars, particularly orthoclase; chlorite and iron oxide after biotite, quartz overgrowths, replacement of feldspar by calcite and the formation of siderite and very minor pyrite.

Kubler index is the width in mm. of the 10A· peak at half its height

I002/I001 is the ratio of height of 5A Peak to height of 10A Peak

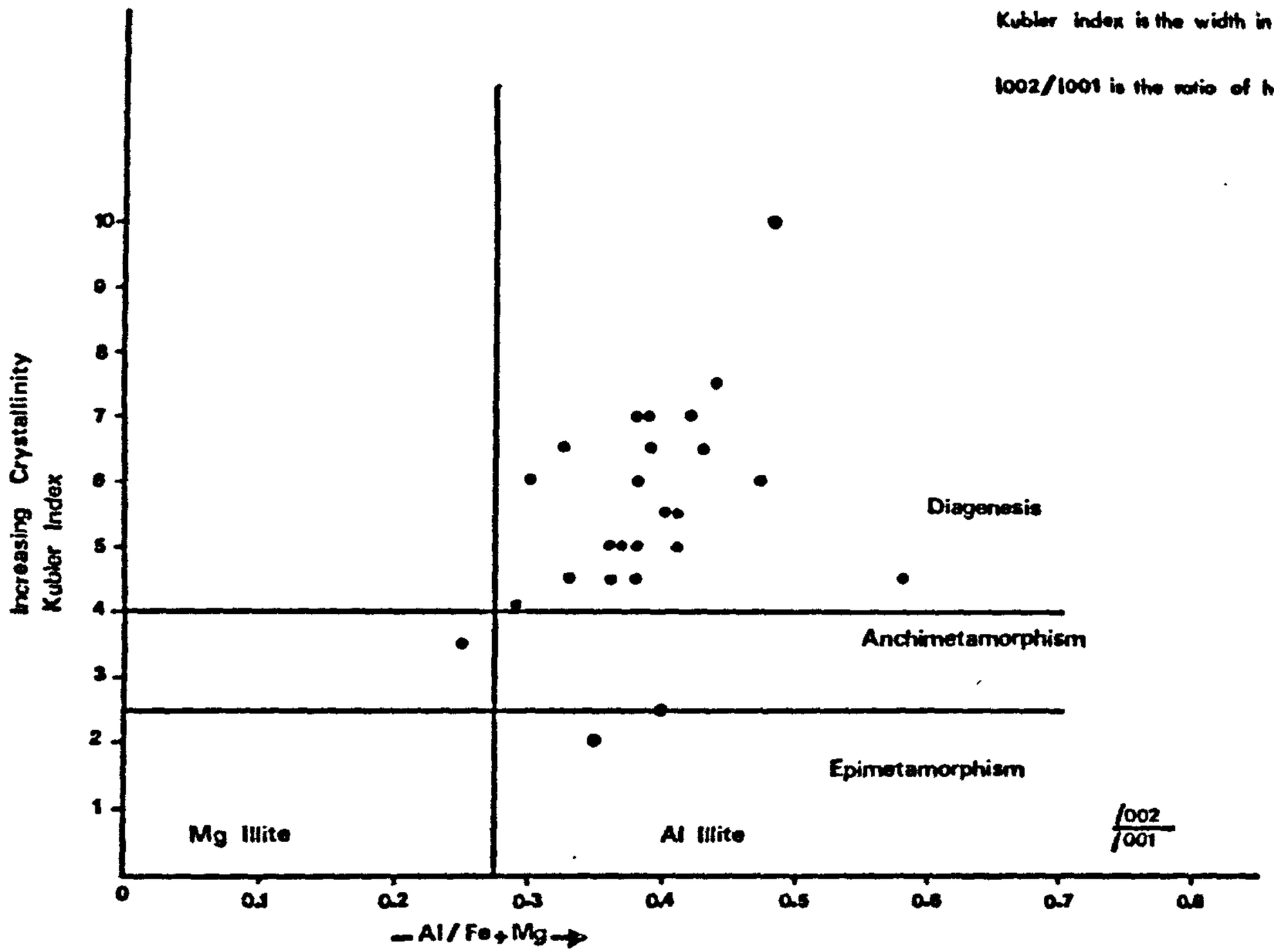

Fig.25 Relationship between illite crystallinity, intensity ratio (I002/I001) and diagenesis in the Mam Tor rocks.

Kaolinite

The mineralogical data shows the enrichment of greywackes in kaolinite and the optical study suggests that at least part of the kaolinite is of diagenetic origin. The formation of authigenic kaolinite in sandstones due to decomposition of feldspar during diagenesis has been widely reported (Greensmith, 1957; Bucke and Mankin, 1971; see also Chapter 3). The genesis and conditions favourable for kaolinite formation during surface weathering are well described by Keller (1970). These are high Al/Si ratios, acid environment and leaching of K, Na, Ca, Mg and Fe. Processes by which clay minerals originate were reviewed by Degens (1965, p.28), and these involve three important mechanisms; the first proposes an interaction of isolated monomeric alumina and silica species with OH^- and H^+ ions forming the basic framework unit; the second includes an intermediate colloidal phase from which crystallisation subsequently proceeds and the third assumes selective leaching of the parent minerals and rearrangement of the remaining silica and alumina.

High temperature alterations of feldspar at 200^{o}C in a dilute acid solution indicate that a poorly crystallised boehmite is formed as an intermediate stage and kaolinite is formed only when silica-monomer can be fixed on active sites of this intermediate product (Oberlin and Couty, 1970). On the other hand, kaolinite formation due to hydrothermal alteration shows that the intermediate stage is mica-montmorillonite (Exley, 1976). The application of these findings to the genesis of kaolinite during weathering and diagenesis encounters the problem of low temperature and very slow reaction, thus the mechanism involved remains obscure. However, the formation of kaolinite during weathering would put dilute surface waters in the kaolinite stability field (Tardy, 1971; Bjorlykke, 1975), with a low K^+/H^+ ratio in order to promote the alteration to kaolinite.

In the Mam Tor greywackes, the required constituents for the newly formed kaolinite may be produced by the breakdown of feldspars, mainly orthoclase. Biotite may also have been asource of silica and alumina. It is necessary of course, that the appropriate concentration of K^+ and H^+ prevailed, otherwise other clay minerals would form. In other words, kaolinite is formed where the ratio of K^+/H^+ (but not necessarily the concentration of K^+ alone) is below a certain value (Keller, 1970, p.798). In the Mam Tor greywackes the low level of K^+/H^+ ratio was probably influenced by other minerals, or an open system. The most likely explanation is the presence of partly degraded illite which acted as a host for the K^+ released from feldspar decomposition. This process is inferred from highly altered orthoclase and the preservation of plagioclase, largely in unaltered state, or alternatively, the plagioclase was metastable. It also follows that pore solutions were rather in equilibrium with plagioclase. To promote this alteration acidic conditions or low pH seems to be another requirement and the decomposition of organic matter attending early diagenesis is the most likely factor. However, the initial porosity and permeability must have influenced the movement of the pore solutions which aided the alteration processes. The importance of these factors in promoting diagenesis in other sandstones has been considered as a basic requirement (Triplehorn, 1970; Rowsell and Swardt, 1976; Heald and Baker, 1977). According to studies of fluid migration in interbedded shale and permeable sand from the Gulf Coast (Magra, 1974), pore solution expelled from the shale during compaction is relatively fresh, due to the effect of ion filtration. In these fresher waters, hydrocarbon solubility is higher than in the more saline water remained in the shale, which would favour hydrocarbon migration from shale to sand. The implication of this factor as applied to the present study is

to help maintain a lower pH in the sand during diagenesis, therefore favouring the alteration of feldspar to kaolinite.

Calcite and Quartz Overgrowths

The presence of calcite, replacing other minerals, and quartz overgrowths were previously described (see Chapter 3). Quartz overgrowths although present in the well sorted sandstones are of minor importance in the argillaceous ones. It was also noted that quartz overgrowth may result from precipitation, due to pressure solution.

According to studies on the silica-carbonate relationship (Walker, 1960, 1962), silica solubility increases with rise in pH, while $CaCO_3$ solubility decreases, thus a decrease in the pH favours solution of $CaCO_3$ and precipitation of SiO_2. However, silica solubility is virtually independent of pH below 9. An exceptional case where inorganic precipitation of silica demonstrated is in the Coorong Lagoon, Australia (Peterson and Borch, 1965). They found that detrital silicates dissolve under high pH (9-10.2) and lowering of pH (7-6.5) causes precipitation of silica. The rise in pH was attributed to plant activity. These conditions, however, are less likely to be encountered in normal sedimentary environments. Temperature has been suggested as an important factor in dissolving silica and precipitating $CaCO_3$ (Siever, 1962; Walker, 1962). The presence of a pressure solution effect in the Mam Tor greywackes would tend to indicate that temperature and pressure could have modified the necessary rise in pH, in order to allow dissolution of silica and precipitation of calcite. The corrosion of feldspar and some quartz is probably an indication of this process. It is also probable that the replacement by calcite is an earlier event preceeding solution-precipitation of silica. The source of $CaCO_3$ could have been provided by the breakdown of calcareous shells and subsequent precipitation of $CaCO_3$ in situ

or calcium and carbon dioxide in solution from a nearby carbonate-bearing bed. As to the source of SiO_2, pressure-solution of quartz grains at their point contacts was probably an important factor in dissolving silica and its precipitation in interstices. Nevertheless, a minor amount of SiO_2 could have been available by alteration of other silicate minerals. Detailed studies on the cementation of the Millstone Grit add still further confirmation to the pressure solution phenomenon as a major factor in silica cementation attending diagenesis, due to compaction (Wright, 1964).

Chlorite and Iron Oxide

In thin section it was seen that chlorite and iron oxide were at least in part, of diagenetic origin, after biotite (Chapter 3). It also appeared that the increase in Fe_2O_3 content of the <2 μm fractions is probably related to the content of chlorite, although this did not account for all the variation in Fe_2O_3. The alteration of biotite possibly was controlled by porosity and permeability of the enclosing greywackes. Alteration of biotite by acid water (Wager, 1944) from the Shap Granite, suggests that hydrobiotite, chlorite were formed as an intermediate stage, but kaolinite seems to be the final product. The importance of ferrous oxidation in the formation of hydrobiotite is demonstrated by experimental data on biotite alteration (Farmer and Wilson, 1970). Similarly the incorporation of Fe^{3+} in chlorite has been shown to occur in oxidised chlorite which contains up to 27% Fe_2O_3 (Chatterjee, 1966). The latter also suggested that an internal oxidation, under weathering conditions, was a possible mechanism. These observations on biotite transformations seem plausible to the present biotite under diagenetic conditions. If so, kaolinite formation could have been aided by biotite alteration and the incorporation of some Fe_2O_3 into the chlorite structure seems likely.

Siderite and Pyrite

The presence of these authigenic minerals in many shales and sandstones has been attributed to reducing and alkaline conditions (Bucke and Mankin, 1971; Reimer, 1972; Triplehorn, 1970). Such conditions are necessary for the development of such minerals and will be discussed in detail later when the Tansley borehole sediments are dealt with. However, in the Mam Tor rocks the aggregates of siderite were considered of detrital origin, at least in the greywackes and siltstones (Allen, 1960, p.196).

In summary, the relatively high permeability compared with shales of the greywackes apparently makes them more susceptible to diagenesis. The formation of calcite and pyrite requires alkaline and reducing conditions. Kaolinite formation is generally compatible with acid conditions which also may have promoted biotite alteration. Silica mobilisation and precipitation of calcite were possibly promoted by high temperature and pressure which have more or less the same effect as rise in pH on the solubilities of quartz and calcite.

These diagenetic events, however, do not imply that neoformation of minerals took place simultaneously. Siderite, pyrite, in the shales, and possibly calcite formation, for example, implies an earlier diagenetic stage, perhaps concurrent with deposition, otherwise iron oxide from biotite alteration would have not been preserved as such. On the other hand, calcite precipitation could have been a later diagenetic event. Silica cementation was perhaps also a later diagenetic event, because the alteration of feldspar and biotite suggests that peremability may have played an important role. However, studies on turbidites under shallow to moderate depth of burial, favour temperature as the primary factor in diagenetic reactions (Galloway, 1974). The latter concluded that

calcite formation was an early diagenetic event, but also continued through later diagenetic stages. On the other hand, clay mineral formation and alteration of quartz and plagioclase were promoted during later diagenetic stages due to burial.

4.8 Trace Elements

Trace elements may be brought to the sedimentation site either associated with the detrital fraction or in solution and precipitated. In addition the release of trace elements (redistribution) and their retention in newly formed minerals occurs during diagenesis, i.e. as in pyrite and siderite. Two processes by which trace element immobilisation takes place are sorption and copreciptiation. Sorption and lattice substitution are recognised widely as important mechanisms (Hem, 1977). Turekian (1977) emphasised the importance of particulate matter in extracting trace elements from the ocean water. However, many elements are influenced by Eh-pH conditions and may show high concentration in specific environments (Wedepohl, 1967).

The substitution of trace for major elements is governed by the charge and ionic radius of the element; in addition the co-ordination of the element plays an important part in this process (Whittaker and Muntus, 1970). The ionic radii of minor and major elements are shown in Table 34 which gives a good guide as to which element may substitute for each other.

Trace element abundance and factors affecting trace element accumu tion in sediments have been the subject of numerous investigations (Krauskoff, 1955). Katchenkov (1967) presented abundance data of minor elements in sedimentary rocks. Wedepohl (1960 - in Chester and Hanna, 1970) investigated the relationship between the trace element content

TABLE 34: Elements and their Ionic Radii* (Mason, 1966)

Minor Elements		Major Elements	
Elements	Ionic Radius (Angstroms Å)	Elements	Ionic Radius (Angstroms Å)
P^{5+}	0.35	Si^{4+}	0.42
Cr^{3+}	0.63	Al^{3+}	0.51
Ni^{2+}	0.69	Ti^{4+}	0.68
Co^{2+}	0.72	Fe^{3+}	0.64
Cu^{2+}	0.72	Mg^{2+}	0.66
Zn^{2+}	0.74	Fe^{2+}	0.74
V^{3+}	0.74	Na^{+}	0.97
Zr^{4+}	0.79	Ca^{2+}	0.99
Mn^{2+}	0.80	K^{+}	1.33
Y^{3+}	0.92		
Sr^{2+}	1.12		
Pb^{2+}	1.20		
Ba^{2+}	1.34		
Rb^{+}	1.47		

of near shore and deep sea pelagic clays. A more comprehensive study of the relationship of a number of trace elements and clay minerals with depositional environments was reported by Degens et al. (1958), Keith and Degens (1959), Lebedv (1967) and Potter et al. (1963). Hence the type of chemical association between trace elements and sediment constituents could be of interest in connection with the depositional environment.

4.8.1 Mam Tor Beds (Whole Rock Samples)

The results of trace element analyses of greywackes (b and c symbols) and shales (a symbol) are given in Appendix 1. Ranges and mean values together with standard devaition for each element are shown in Table 35.

It can be seen that the average contents of Ni, V, Cr, Cu, Rb, Pb, Sr and Ba and to a lesser extent Y and Zn are higher in the shales indicating a dominant association with clay minerals and organic materials. In contrast the Zr content is higher in the greywackes, suggesting the abundance of zircon. It is also apparent that most of these elements, apart from Zr, show less variation among the shales than in greywackes. This is indicated by comapring the standard deviations to the respective average and range values in both shales and greywackes. On the other hand, Co and Mn average content, although higher in the greywackes, show a high degree of variation which could be due to their presence in more than one mineral.

Graphical representation of trace element distribution is illustrated by histograms in Figure 26. The last shows that V, Cr, Ci, Rb, Zr, Pb, Y, and Ba exhibit two maxima. These,somewhat, correspond largely to greywackes and shales, although overlap occurs between them. A less defined pattern is shown by Ni, Zn and Sr indicating higher degrees of overlap in their contents between some of the shales and greywackes.

TABLE 35: Ranges, Means and Standard Deviations of Trace Elements Contents of the Mam Tor Sandstones and Shales

	Sandstones			Shales		
Element ppm	Range	Mean	S.D.	Range	Mean	S.D.
Ni	16-71	37	18	56-113	79	17
Co	4-33	16	9	1-31	12	11
Mn	116-2163	857	565	146-1033	548	371
V	33-95	59	22	113-153	138	10
Cr	49-129	84	24	153-181	167	8
Zn	28-116	67	28	59-132	84	22
Cu	5-30	16	8	28-57	45	8
Rb	22-70	37	16	106-145	130	13
Sr	43-142	75	26	94-127	107	11
Y	12-54	29	12	30-57	39	7
Zr	208-298	253	25	101-254	152	42
Pb	11-28	19	5	36-56	46	6
Ba	139-323	227	62	387-553	459	55

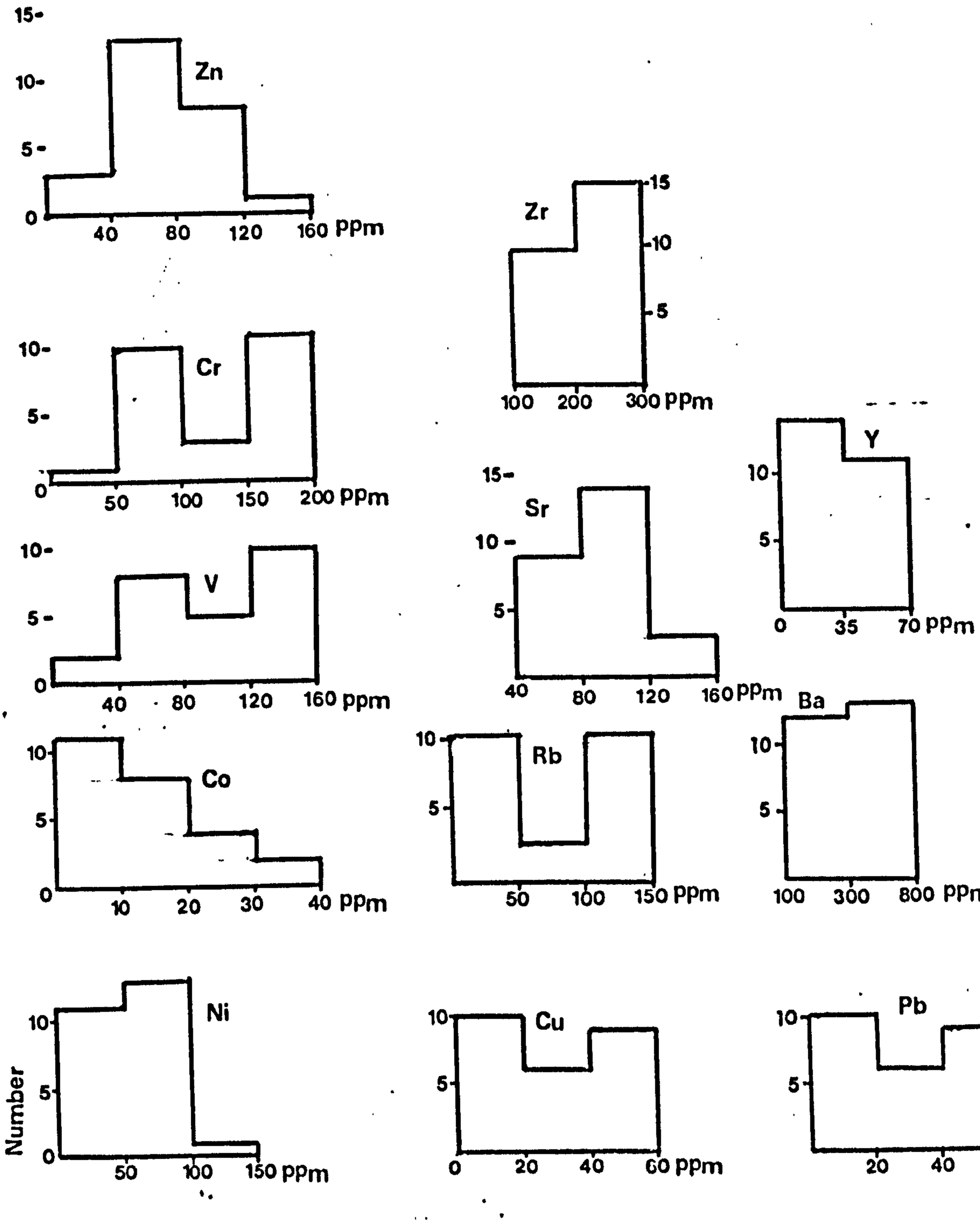

Fig·26 Distribution of trace elements in Mam Tor rocks.

On the other hand, Co shows no specific pattern.

In order to substantiate such bimodal distribution a t-statistic was used to calculate confidence intervals for the difference between the two population means (Koch and Link, 1970, page 89). It was found that Ni, V, Cr, Cu, Rb, Sr, Pb and Ba show a significant difference in the two groups. This difference in trace element contents is chiefly related to the content of clay minerals,organic matter, and probably amorphous materials, since carbonates are present in minor amounts and the pyrite content is insignificant.

This interpretation is substantiated by the analyses of the separated clay fractions of the greywackes and shales (Appendix 1). In the greywacked (marked b) there is a distinctive gain of Ni, V, Zn, Cu, Rb, Sr, Pb and Ba in the clay fraction. In contrast Zr content decreases in the clay fractions suggesting its presence, mostly as zircon. In sample $4b_1$, the Sr content in the clay fraction is lower than that of the whole rock sample. This discrepancy is due to the presence of minor amounts of calcite and the carbonate association of Sr. Similarly, the lower Mn content in the clay fraction of sample $8b_1$ results from the presence of a small amount of siderite in the whole sample. The content of Co fluctuates which could be due to its sharing between more than one mineral. On the other hand, in the shales (marked a) there seems to be a slight gain of Ni, V, Zn, Cu, Rb and Sr in their clay fractions, whereas Co, Y, Mn and Ba contents show unsystematic variations suggesting their presence partly in heavy minerals and feldspar. Therefore it can be stated that the greater part of the trace elements are associated with the clay fractions and elimination of the sand and silt fractions is responsible for the higher abundance of trace elements in the clay fractions which is inagreement with the data obtained by Potter et al. (1963).

To remove the influence of dilution by quartz, the ratios of element/Al_2O_3 is helpful in this respect. The ranges and mean values together with the standard deviations of element/Al_2O_3 ratios, in shales and greywackes, are shown in Table 36.

Nickel

The wide ranges of Ni/Al_2O_3 ratio in both shales and greywackes indicate that Ni is not entirely bound in the structure of clay minerals, which was transported as detrital. The Ni/K_2O ratio of the shales, with one exception,varies between 25.86 and 37.74 x 10^{-4}, suggesting that Ni is not related mainly to illite. The association of Ni with organic matter was shown by Le Riche (1959), but this was considered by Nicholls and Loring (1962) to be of minor importance, with most of the Ni present in the clay mineral structure. Turekian and Carr (1960) ascribed Ni enrichment to organic matter and clay minerals, and postulated that Ni proxies for Fe and Mg in the clay mineral structure. It follows, then, that Ni could be present in chlorite as well as illite. In the present study, organic matter is abundant in the shales, whereas chlorite and iron hydroxide are relatively more abundant in the clay fractions of the greywackes, due to alteration of biotite. Trace element data of biotite indicate that a small amount of Ni (20 ppm) can be accommodated in its structure (Butler, 1953). It is probable therefore, that the association of Ni with chlorite and iron hydroxides could explain the wider variations of Ni/Al_2O_3 ratio in the greywackes. The relatively constant mean value of Ni/Al_2O_3 ratio in both shales and greywackes, suggest that diagenesis had not affected the element content, but greatly modified its distribution and any relationships are unlikely to be clearly defined.

TABLE 36: Elements/Al_2O_3 Ratios in the Mam Tor Shales and Greywackes

Element/Al_2O_3 x 10^{-4}	Shales n = 11			Greywackes n = 14		
	Range	Mean	S.D.	Range	Mean	S.D.
Ni	2.51- 4.34	3.27	0.59	1.62- 5.24	3.31	1.08
Co	0.05- 1.14	0.50	0.43	0.51- 2.40	1.44	0.74
V	5.25- 6.30	5.80	0.28	3.94- 6.72	5.35	0.78
Cr	6.0- 7.38	7.01	0.48	6.00-11.85	7.83	1.52
Zn	2.54- 5.73	3.51	0.92	2.84- 8.65	6.14	2.02
Cu	1.21- 2.35	1.88	0.31	0.62- 2.09	1.48	0.37
Rb	4.73- 5.97	5.46	0.40	2.33- 4.38	3.32	0.68
Sr	3.84- 5.51	4.52	0.58	5.31- 7.03	6.29	0.81
Y	1.10- 2.47	1.64	0.34	1.22- 4.70	2.65	0.91
Zr	3.71-12.66	6.52	2.34	16.00-34.00	24.57	6.05
Pb	1.48- 2.28	1.93	0.24	0.85- 2.65	1.73	0.42
Ba	15.60-23.49	19.33	2.66	16.67-26.88	20.83	2.99

In summary,it may be said that the larger part of Ni is associated with illite and chlorite. Minor amounts of Ni are also presumably contributed by organic matter and iron hydroxide. Nevertheless, very small amounts of Ni may be present in heavy minerals, but this is overshadowed by the above minerals.

Cobalt

The Co/Al_2O_3 ratio in both shales and greywackes is highly variable. The Co/K_2O and Co/Fe_2O_3 ratios were even more variable. This suggests that the greater part of Co is not associated with the illite. Similarly, Co shows no dependance on siderite or organic matter contents. Among the greywackes, the more argillaceous ones seem to contain the highest Co concentration, even higher than the shales. As revealed by optical study, these contain a higher proportion of altered biotite. Furthermore, heavy minerals are also abundant in these greywackes. Trace element data of biotite (Mason, 1966, p.135) indicate that a fair amount of Co (15 ppm) is present in it. Contribution of Co by heavy minerals in greywackes is of considerable importance as demonstrated by Weber and Middleton (1961). The absence of strong relation between Co and illite and/or organic matter makes the contribution by heavy minerals a most likely source in the Mam Tor rocks. Smaller amounts may be in chlorite and possibly iron oxide, due to biotite alteration. Nevertheless, some Co in illite and organic matter is not entirely excluded.

Manganese

The Mn/Al_2O_3 was found to be extremely variable. The highest Mn content (932-2163 ppm) is associated with siderite rich samples, but their variation is not systematic. The association of Fe and Mn in other sediments has been shown by Goldberg and Arrhenius (1958) and Spears (1964). On the

other hand, in the present case, shales and greywackes devoid of siderite still have a moderate concentration of Mn (932-1497 ppm). It seems therefore, that organic matter does not greatly influence the distribution of Mn because the greywackes are generally low in organic matter content. This indicates association with other minerals. The importance of heavy minerals seems unlikely as demonstrated by studies on other greywackes (Weber and Middleton, 1961). Therefore, the most likely hosts seem to be biotite,chlorite and iron hydroxide and possibly illite. Analyses of biotite, hydrobiotite and chlorite show that 0.05-0.76% MnO is present, while in muscovite about 0.05% is incorporated (Wagger, 1944; Butler, 1953; Chatterjee, 1966; Guidotti, et al. 1975).

Thus is it quite clear that in the present case, Mn is largely enriched by siderite. Likewise appreciable amounts may be associated with chlorite, biotite and possibly organic matter and iron hydroxide. A minor contribution by other clay minerals and heavy minerals cannot be discarded.

Vanadium

The V/Al_2O_3 ratio is much less variable inthe shales than in the greywackes. Such moderate variations in the shales suggest association with clay minerals, particularly with illite. This is supported by the variation of V/K_2O ratio which is,with two exceptions, in the range $50.57-56.13 \times 10^{-4}$. This may perhaps indicate minor association with organic matter. The association of V with clay minerals has been widely reported (Goldberg and Arrhenius, 1958; Hirst, 1962; Katchenkov, 1967; Chester and Hanna, 1970). The adsorption on organic matter is reported by Le Riche (1959); while carbonate contribution is of little importance (Nicholls and Loring, 1962).

In the Mam Tor greywackes, the V/K_2O ratio varies between 57.89-85.29 x 10^{-4}, suggesting contribution by minerals other than illite. Again, biotite, chlorite and iron hydroxide seem to influence the V distribution. The V/Fe_2O_3 with few exceptions shows moderate variations, between 20.77-28.82 x 10^{-4}. In addition biotite can incorporate appreciable amounts of V (85 ppm) as shown by analyses presented by Butler (1953). Thus the association of V with chlorite seems also likely. In the Gulf of Paria sediments the higher V/Al ratio in the sands compared to the clays was attributed to adsorption on Fe_2O_3 (Hirst, 1962), following the evidence presented by Krauskopf (1956). Thus the association of V with biotite, chlorite and iron hydroxides is possible in the Mam Tor greywackes. However, small contributions from heavy minerals are also probable, as shown by the data reported by Weber and Middleton (1961). Summarising, V seems to be associated with illite and chlorite in the Mam Tor rocks. Biotite and iron hydroxide appear to be another host for V, particularly in the greywackes. Minor contributions by organic matter and heavy minerals is tentatively suggested.

Chromium

The Cr/Al_2O_3 ratio show moderate variations in the shales compared to that of the greywackes. Similarly the Cr/K_2O ratio in the shales varies between 53.38-73.59 x 10^{-4}, averaging 62.32 x 10^{-4}, with the majority around 60 x 10^{-4}, while that of the greywackes averages 102.58 x 10^{-4}. On the other hand, the Cr/Fe_2O_3 ratio in the greywackes ranges from 25-32 x 10^{-4}. These variations in the ratios show similar patterns to that of Ni and V. A similar association therefore seems to be the most likely explanation. The presence of Cr in the structure of illite and clay mineral in general has been reported by Hirst (1962) and Chester and Hanna (1970). The association of Cr with Fe_2O_3, organic matter and

clay minerals is also shown by Hirst (1962) and Spencer (1966), while strictly detrital contributions are probably another possible source (Nicholls and Loring, 1962). Moreover, Cr substitution in chlorite has been shown from most analyses of natural chlorites (see Albee, 1962). Therefore, a considerable amount of Cr may be considered to be present in the structure of illite and chlorite. Variable contributions are probably related to adsorption on iron hydroxide, especially in the grey-wackes, while some is also likely to be associated with organic matter and heavy minerals.

Zinc

The ratio of Zn/Al_2O_3 in both shales and greywackes shows no consistency. Similarly Zn/K_2O and Zn/Fe_2O_3 were found to be variable. This implies that Zn contribution by constituents other than clay minerals is equally important. In some sediments, Zn immobilisation by carbonate was considered very important (Deurer et al. 1978) while in others it was attributed to detrital minerals (Chester et al. 1976). In the Mam Tor rocks, Zn does not appear to be related to the siderite. Likewise the Zn and organic matter relationship is not clearly defined, so its sorption is of minor importance. Krauskopf (1955, p.453) remarks that, although Zn is commonly associated with carbonaceous sediments, its amount shows no direct relationship with organic matter. The higher Zn/Al_2O_3 ratio in the Mam Tor greywackes points to its assoication with iron hydroxides and heavy minerals. Sorption of Zn by iron hydroxide has been considered an important process in immobilising Zn (Hem, 1977). On chemical grounds (see Table 34) Zn substitution for Mg and Fe seems also possible, thus its association with chlorite is likely. However, Zn association with sulphides is reported widely (Krauskopf, 1955; Stephens et al, 1975) but this is less likely to account for Zn variations

in the Mam Tor rocks because pyrite is either absent or present in very small amounts. The association of Zn with heavy minerals is most probably related to Ti-bearing minerals which are concentrated in the silt fractions.

It appears therefore than Zn is largely related to illite, chlorite and iron hydroxide which are concentrated in the finer fraction of the rocks. An important contribution by heavy minerals is also possible. Minor amounts may be associated with organic and pyrite but evidence is inconclusive.

Copper

The Cu/Al_2O_3 ratio of the shales is variable, but with the majority between 1.8-2.2 x 10^{-4}. Likewise the Cu/K_2O ratio shows some variation, ranging from 10.61-19.45 x 10^{-4} with the majority between 17-19 x 10^{-4}. These variations may indicate that a largeproportion of Cu is associated with clay minerals, particularly illite. In the greywackes the Cu/Al_2O_3 is also variable and the lowest ratio is encountered in the well sorted greywackes and the higher ratio in the poorly sorted ones. Wide variations are also observed in their Cu/K_2O ratios, but the poorly sorted greywackes showed a comparable ratio to those of the shales. Again this supports association with clay minerals. Cu adsorption by ferric hydroxide has been shown to be an important process in its enrichment (Krauskopf, 1956; Steele and Wagner, 1975; Hem, 1977). The Cu/Fe_2O_3 ratios of the Mam Tor greywackes and shales were found to be much more variable, thus association with Fe_2O_3 is probably of minor importance. This is also indicated by the relatively lower Cu/Al_2O_3 average ratio of the greywackes in comparison to the shale. Similarly, contributions by heavy minerals is of little significance. However, very slight enrichment of Cu is encountered in siderite rich samples. The association of

Cu with carbonates has been reported by Turekian and Imbrie (1966), and Deurer et al. (1978). The association of Cu with organic carbon has been reported widely (Krauskopf, 1955; Keith and Degens, 1959; Le Riche, 1959; Blocker et al. 1975). In the present study, comparison of Cu with organic matter content showed no consistent trend, but this does not exclude the presence of small amounts. In the Bersham sediments, it was concluded that most of the Cu was associated with silicates, including quartz (Nicholls and Loring, 1962). The adsorption of Cu by quartz has also been noted by Richardson and Hawkes (1958). The data of the present study do not allow a decision to be drawn regarding such an association.

Finally, it may be stated that Cu is concentrated in the clay minerals. Contributions by Fe_2O_3 and organic matter are less important and least pronounced is the immobilisation by carbonate and incorporation in heavy minerals.

Rubidium

The ratio of Rb/Al_2O_3 in the shales is higher than that of the greywackes. Generally this ratio in the shales varies between 5.28-5.97 x 10^{-4}. It may be considered as moderately variable and most likely to indicate association with clay minerals of the larger part of Rb. Likewise, Rb/K_2O ratio is relatively constant and varies between 46.62-50.96 x 10^{-4}, suggesting association with illite. Nevertheless these variations in the ratios implies that Rb is contained in other minerals and feldspar seems the most likely host. Degens (1965, p.20) states that Rb can substitute for K in illitic minerals, in the interlayer position. It is, however, noteworthy that Rb and K are well known to be correlated in a wide variety of geochemical environments, due to the geochemical coherance of the two elements (Cosgrove, 1973; Stephens, et al. 1975).

The increasing affinity of cation selectively in altered mica towards Rb sorption has been demonstrated by Le Roux et al. (1970), and a review of the subject by Sawhney (1972) indicates that Rb sorption is even greater than that of K.

In the greywackes, the Rb/Al_2O_3 ratio shows wider variation than in the shales. This may be due, partly, to the increased importance of feldspars in the greywackes. The variation in Rb/K_2O ranges from $34.24\text{-}47.95 \times 10^{-4}$ and averaging $46.22 \times 22\ 10^{-4}$, suggests a significant contribution by other minerals. In the Gulf of Paria sediments, the enrichment of Rb relative to K in the clays as compared to the sands was attributed to the increased adsorbance of Rb onto the clay minerals, particularly illite (Hirst, 1962). In the Mam Tor rocks, the significance of such processes is uncertain, but the lower Rb/K_2O ratio in the greywackes in comparison to the shales, may be relevant in this respect.

As to the wide variation of ratios in the greywackes, diagenesis may have modified the distribution of Rb existing in the original minerals. Petrographic study showed that in these greywackes K-feldspar and biotite alteration is widespread; the latter mineral also seems to be another possible host for Rb since trace element data on biotite and its alteration products indicate that Rb is present (Butler, 1953).

It can be suggested, therefore that in the Mam Tor rocks the larger part of Rb is related to illite, while contributions by feldspars, biotite and its alteration products are also important.

Strontium

The Sr/Al_2O_3 ratio in the shales although variable it is generally around 4.5×10^{-4}. It is possible, therefore, that much of the Sr is related to clay minerals. Goldschmidt (1954) remarked that Sr in hydrolysate sediments may be fixed on a moderate scale by sorption, and the

substitution of Sr for K in the interlayer sites in illite was demonstrated in other sediments (Goldberg and Arrhenius, 1958; Mohr, 1959). In the Mam Tor shales the Sr/K_2O ratio varies from 33.11-50 x 10^{-4}, thus Sr is unlikely to be present only in illite. Plagioclase which is present in subordinate amounts may be another Sr bearing mineral. This receives support from trace element data on plagioclase (Mason, 1966, p.134). However, some Sr could be adsorped on clay minerals and organic matter, but the available data does not permit a decision to be made with respect to this contribution. In the greywackes, excluding one sample, the average Sr/Al_2O_3 ratio is higher than that of the shales. The sample excluded has a content of 6.04% calcite and Sr/Al_2O_3 ratio of 16.97 x 10^{-4}. This clearly demonstrates a significant contribution by calcite. The incorporation of Sr in carbonate is widely reported (Bathurst, 1971), due to the greater ease with which Sr enters the lattice structure. However in calcareous argillaceous rocks the situation becomes complicated by the presence of Sr in a variety of minerals, namely clay minerals, calcite, and feldspars. Stephens et al. (1975) found that Sr was mainly associated with carbonates while Hirst (1962) considered Sr to be related to clay minerals in addition to its presence in carbonates. Thus it seems that dominant amounts of either one of these minerals would overshadow the relationship of Sr to the other. Further, the release of Sr from plagioclase and its incorporation in carbonate during diagenesis has been invoked to explain the distribution of Sr between shales and greywackes (Reimer, 1972). In the present study, the enrichment of shales in Sr as compared to greywackes indicate that Sr immobilisation during diagenesis was unimportant. In summary, the data suggests that a large amount of Sr in the Mam Tor rocks is associated with clay minerals but not limited to illite only. High contents of Sr are related to calcite, and some Sr is also located in plagioclase.

Yttrium

The Y/Al_2O_3 ratio in the shales and greywackes is variable, but its mean value is higher in the latter. The Y/K_2O ratio in both shales and greywackes was highly variable, indicating that contributions by illite are not important, but does not exclude the possibility of some present in the clay minerals. The higher average Y/Al_2O_3 ratio of the greywackes suggests association with heavy minerals, iron oxide, and possibly chlorite. There is generally some correspondance between Y/Al_2O_3 and Zr/Al_2O_3 ratios indicating the presence of Y in zircon. Such association is quite common as shown by Deer et al. (1966) while Y may also be present in tourmaline and possibly biotite (Butler, 1953). Therefore, it seems reasonable to suggest that the larger part of Y in the Mam Tor rocks is located in the heavy mineral fraction, while minor amounts are related to clay minerals.

Zirconium

The ratio of Zr/Al_2O_3 in the shales shows wide variation. Lower values of this ratio were found in shales consisting of very fine silt and clay fractions (Sample 2a). The higher ratio is associated with silty sandstones (2c and 4c). The ratio in the greywackes is higher and also variable. In fact, the lowest value (16×10^{-4}) belongs to an argillaceous greywacke overlying the shale with the highest value (12.66×10^{-4}). Thus it seems that a progressive increase in the silt content is matched by an increase in Zr/Al_2O_3 ratio which indicates the presence of Zr, mostly in detrital zircon. This is supported by the heavy minerals study (Chapter 3) and similar conclusions were reached by Hirst (1962) and Stephens et al. (1975). On the other hand, in the Bersham sediments, Zr was attributed to detrital zircon and clay minerals, and

McLaughlin (1958) found that enrichment of Zr in different size fractions of illitic clay was due to the presence of detrital zircon as minute grains.

In the present study, zircon is one of the most abundant heavy minerals and it is concluded that Zr is present mainly as detrital zircon in the Mam Tor rocks.

Lead

The shales show some variation in their Pb/Al_2O_3 ratio, but the majority are around the mean value. Similarly, their Pb/K_2O ratio varies around 17.10^{-4}, suggesting that the larger part of the Pb is contained in the clay minerals, especially illite. Nevertheless, association with organic matter seems of minor importance. The relatively similar Pb/Al_2O_3 mean ratio of the greywackes indicates that contribution by feldspars and carbonates is unimportant. On the other hand, the Pb/K_2O ratio in the greywackes averages 22-64 x 10^{-4}, suggesting minor contribution by other minerals, possibly chlorite, biotite and iron hydroxides. The latter association with Pb has been suggested to account for Pb enrichment in some sediments (Hirst, 1962; Summerhayes, 1972). The first worker also found a great coherance between Pb and illite, while a minor amount was attributed to adsorption onto organic matter. Cosgrove (1973) remarked that Pb is contained in illite and in the present study, Pb-illite relationship although clear, is not very strong and may indicate association with chlorite.

Summarising, the Pb in the Mam Tor rocks seems to be associated largely with clay minerals, and possibly much less so with iron hydroxide and heavy minerals. Nevertheless, a small amount associated with organic matter is not entirely excluded.

Barium

The Ba/Al_2O_3 ratio shows similar ranges in its variation in both shales and greywackes and its mean value is relatively constant which may indicate its association with clay minerals. Sorption of Ba by clay minerals has been regarded as a likely process for its incorporation into argillaceous sediments (Rankama and Sahama, 1950). This view is supported by the association of Ba with illite in some sediments (Hirst, 1962; Nicholls and Loring, 1962). In the Mam Tor shales and greywackes the mean value of Ba/K_2O is 171×10^{-4} and 282×10^{-4} respectively which suggests that illite is not the only major host for Ba and that the most likely Ba-bearing phase seems to be feldspars. The association of Ba with feldspars, in addition to its presence largely in clay minerals, has been reported by some workers (Weber and Middleton, 1961; Summerhayes, 1972). However, the ability of biotite and possibly its alteration products to accommodate Ba may also partly explain the higher ratios in the greywackes according to the data reported by Butler (1953, and references therein). Any association of Ba with carbonates cannot be ascertained because of the swamping effect of clay minerals and feldspars. Hence Ba is concentrated largley by illite and a significant contribution by feldspars is also likely while the association of Ba with biotite, chlorite and iron hydroxide is also tentatively suggested.

4.8.2 Trace Elements of Different Size Fractions of Shales and Greywackes

Trace element data from different size fractions are shown in Appendix 1. The elements which showed a consistent increase in abundance with decreasing grain size are: Ni, V, Cr, Rb, Pb and Ba, and to a lesser extent, Zn and Sr.

The distribution of Zr follows that of the silt and is concentrated in the 7.8-53 micron fraction; confirming its greater abundance in the form of zircon. The lack of relationship of Mn, Co and Y with grain size may be due to control by some heavy minerals and carbonates which are apparently concentrated partly in the silt fractions. Rather similar relationships have been reported by Summerhayes (1972) and Wright (1974).

In order to illustrate the variation of trace element content with grain size the average value of each element from all samples in their respective size fractions are shown in Figure 27 from which it is clear that a linear relationship is displayed by Ni, V, Cr, Rb and Ba, while Zn, Cu and Pb show slight non-linearity. However, all of these elements attain maximum concentration in the less than 2 micron fractions.

Mn and Sr have a broadly similar distribution and are concentrated mostly in the 2-7.8 micron fraction. Co displays the highest discontinuity in its distribution, but still shows higher concentration in the less than 2 micron fraction. Similarly Zr has a discontinuous distribution but of opposite trend to other elements, being abundant in the 7.8-53 micron fraction.

4.8.3 Statistical Correlation of Trace Elements

The correlation matrix of trace elements and some of the major elements in the whole rock samples is shown in Table 37, with the significant correlations underlined. The linked groups formed by related elements are also shown in Table 37. The strongly related elements Pb, Ba, Cu, Rb, Ni, V and Cr correlate with combined silica and H_2O^+ which is explained in terms of the geochemical coherence of these elements with clays and clay minerals. However, these trace elements could either be

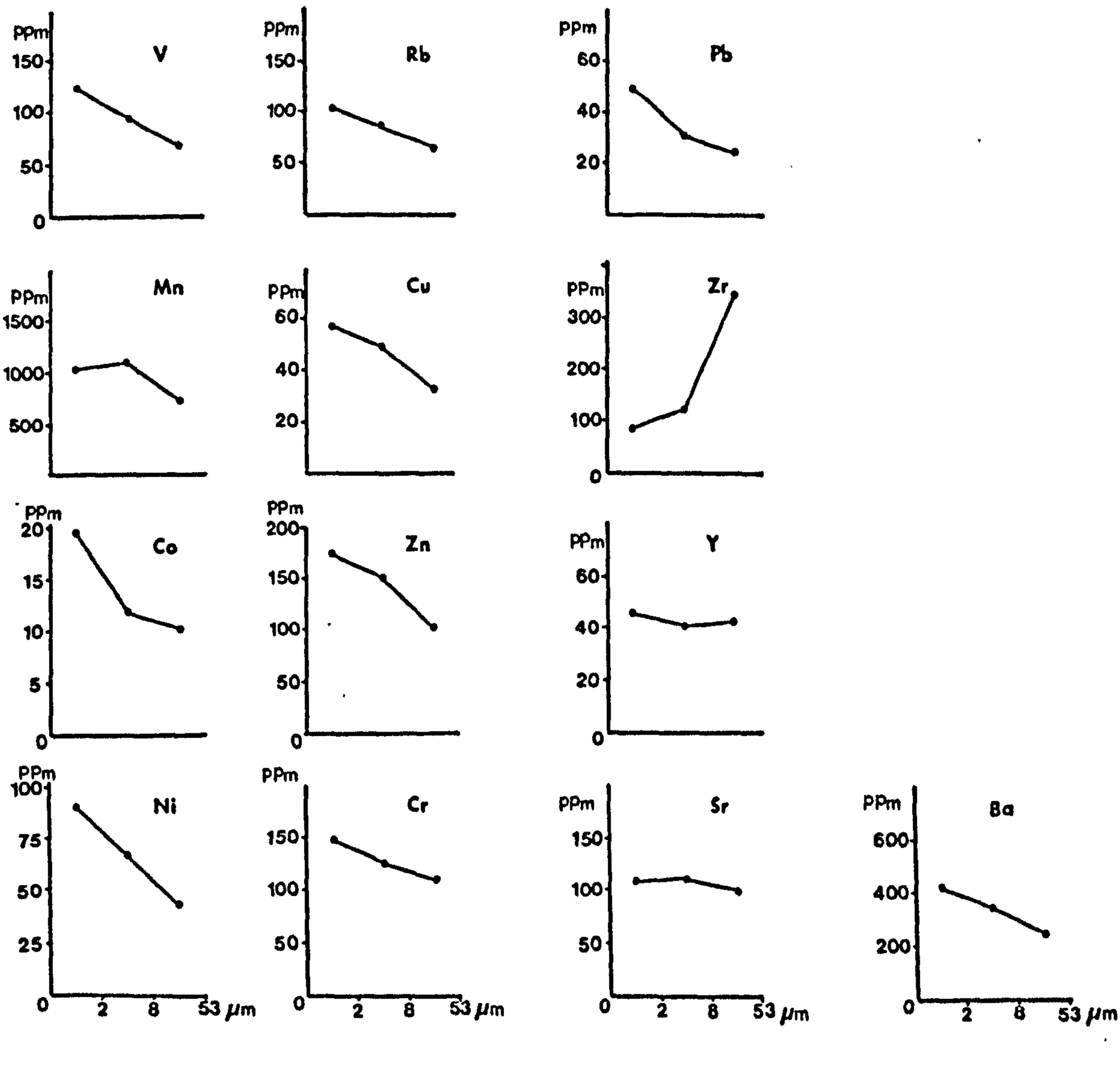

Fig. 27 Relationship between average content of trace elements and grain size.

TABLE 37: Correlation Matrix of Trace and Major Elements in the Mam Tor Rocks

	Pb	Ba	Zn	Cu	Rb	Sr	Y	Zr	Ni	Co
Pb	1.0000									
Ba	(0.9102)	1.0000								
Zn	0.2939	(0.4488)	1.0000							
Cu	(0.8679)	(0.8292)	(0.5729)	1.0000						
Rb	(0.9636)	(0.9261)	(0.4177)	(0.9468)	1.0000					
Sr	(0.6194)	(0.7427)	(0.4969)	(0.6315)	(0.6765)	1.0000				
Y	(0.3996)	(0.5913)	(0.8896)	(0.6032)	(0.5126)	(0.5354)	1.0000			
Zr	-0.8266	-0.7172	-0.3618	-0.8473	-0.8797	-0.4914	-0.3813	1.0000		
Ni	(0.7704)	0.7820)	(0.6675)	(0.8775)	(0.8526)	(0.5994)	(0.6641)	-0.7839	1.0000	
Co	-0.0773	-0.0456	(0.4958)	0.0324	-0.0524	-0.0166	0.3747	-0.0244	0.3753	1.0000
Mn	-0.3542	-0.2722	(0.4300)	-0.0722	-0.2342	-0.0402	0.3200	0.0357	-0.0416	0.3286
V	(0.9326)	(0.9241)	(0.4826)	(0.9582)	(0.9826)	(0.6484)	(0.5710)	-0.8451	(0.8611)	-0.0392
Cr	(0.9211)	(0.9611)	(0.4809)	(0.8935)	(0.9516)	(0.6994)	(0.6777)	-0.7621	(0.8371)	-0.0270
Quartz	-0.9167	-0.9244	-0.4839	-0.9464	-0.9787	-0.6775	-0.5446	(0.8600)	-0.8488	0.0536
Combi	(0.9052)	(0.8456)	0.3214	(0.8812)	(0.9371)	(0.5817)	0.3492	-0.8375	(0.7796)	-0.1267
FeO	-0.2828	-0.0476	(0.4415)	-0.0178	-0.1427	-0.0269	(0.4412)	0.0831	-0.0066	0.2738
CaO	-0.3664	-0.2246	0.0371	-0.2650	-0.2932	(0.3983)	-0.0870	0.2797	-0.2953	-0.1099
Na_2O	-0.7133	-0.6453	-0.2954	-0.7695	-0.7764	-0.4106	-0.3138	(0.7637)	-0.6299	0.1649
H_2O^+	(0.8730)	(0.7991)	0.3204	(0.8437)	(0.8924)	(0.5515)	0.2822	-0.7837	(0.7923)	-0.0741

TABLE 37 (Cont.): Correlation Matrix of Trace and Major Elements in the Mam Tor Rocks

	Mn	V	Cr	Quartz	Combsi	FeO	CaO	Na_2O	H_2O^+
Mn	1.0000								
V	-0.1866	1.0000							
Cr	-0.2907	(0.9483)	1.0000						
Quartz	0.1525	-0.9793	-0.9476	1.0000					
Combsi	-0.2781	(0.9068)	(0.8989)	-0.9544	1.0000				
FeO	(0.7589)	-0.0366	-0.1212	0.0149	-0.2120	1.0000			
CaO	00.2961	-0.3253	-0.2764	0.2425	-0.2567	0.0829	1.0000		
Na_2O	-0.0583	-0.7701	-0.6886	(0.8247)	-0.8441	-0.0667	0.2661	1.0000	
H_2O^+	-0.3384	(0.8831)	(0.8622)	-0.8928	(0.9192)	-0.2889	-0.2862	-0.9601	1.0000

TABLE 37 (Cont.): Correlation Groups of Trace and Major Elements in the Mam Tor Rocks

Group 1

	Pb	Ba	Zn	Cu	Rb	Sr	Y	Ni	V	Cr	Combsi	H_2O^+
Pb	1.0000											
Ba	0.9102	1.0000										
Zn		0.4488	1.0000									
Cu	0.8679	0.8292	0.5729	1.0000								
Rb	0.9639	0.9261	0.4177	0.9468	1.0000							
Sr	0.6194	0.7427	0.4969	0.6315	0.6765	1.0000						
Y	0.3996	0.5913	0.8896	0.6032	0.5126	0.5354	1.0000					
Ni	0.7704	0.7820	0.6675	0.8775	0.8526	0.5994	0.6641	1.0000				
V	0.9326	0.9241	0.4826	0.9582	0.9826	0.6484	0.5710	0.8611	1.0000			
Cr	0.9211	0.9611	0.4809	0.8935	0.9516	0.9664	0.5777	0.8371	0.9483	1.0000		
Combsi	0.9052	0.8456		0.8812	0.9371	0.5817		0.7796	0.9068	0.8989	1.0000	
H_2O^+	0.8730	0.7991		0.8437	0.8924	0.5515		0.7923	0.8831	0.8622	0.9192	1.0000

Group 2

	Zr	Qtz	Na_2O
Zr	1.0000		
Qtz	0.8600	1.0000	
Na_2O	0.7637	0.8247	1.0000

TABLE 37 (Cont): Correlation Groups of Trace and Major Elements in the Mam Tor Rocks

Group 3

	Zn	Co
Zn	1.0000	
Co	0.4955	1.0000

Group 4

	Zn	Mn	FeO
Zn	1.0000		
Mn	0.4300	1.0000	
FeO	0.4415	0.7589	1.0000

Group 5

	Sr	CaO
Sr	1.0000	
CaO	0.3983	1.0000

Group 6

	Y	FeO
Y	1.0000	
FeO	0.4412	1.0000

present partly in the clay mineral structure, adsorbed on them, or associated with iron oxide and organic matter. The weaker relation of Sr and Y with the above elements is indicated by their low values of correlation coefficients, suggesting that they are only partly contained in the clay minerals. Chester and Hanna (1970) demonstrated that in the North Atlantic deep-sea sediments, Cu, Ni, Co, Cr, V, Ba and Sr are partly held in the structure of clay minerals.

Quartz, Na_2O and Zr correlate with each other and all have negative correlation with most of the other elements, reflecting the co-variation of quartz, plagioclase and zircon. Zn correlates with the clay related elements, FeO and Mn, but its highest correlation is with Y which in turn correlates with FeO. In addition Zn correlates significantly with Co which by itself is independent of all other elements. This tends to indicate that these elements have a dual or triple association in clay minerals, carbonates and heavy minerals. Similar associations have been widely reported from other sediments (Le Riche, 1959; Chester et al, 1976; Deurer et al. 1978; Summerhayes, 1971). CaO and Sr correlation suggest contribution by calcite, probably due to the fact that only one sample contains a minor amount of calcite. Scatter plots of some rleationships are shown in Figure 28. Weber and Middleton (1961) studied trace element distribution in the carbonate, quartz-feldspar, clay, and heavy mineral fractions of turbidites. Their data indicated that the greater part of Co and Zr with smaller parts of Cr, Cu, Mn, Ni and Sr are contained in the heavy mineral fraction. To determine the association of an element with a particular clay mineral, a correlation was carried out between trace elements in the <2 μm fraction and the contents of illite and kaolinite as determined by the XRD method. The correlation matrix is shown in Table 38, with those significant relations underlined.

FIGURE 28 Scatter Plots of Positive and Significant Bivariant Relationships between Trace and Major Elements, Mam Tor Rocks.

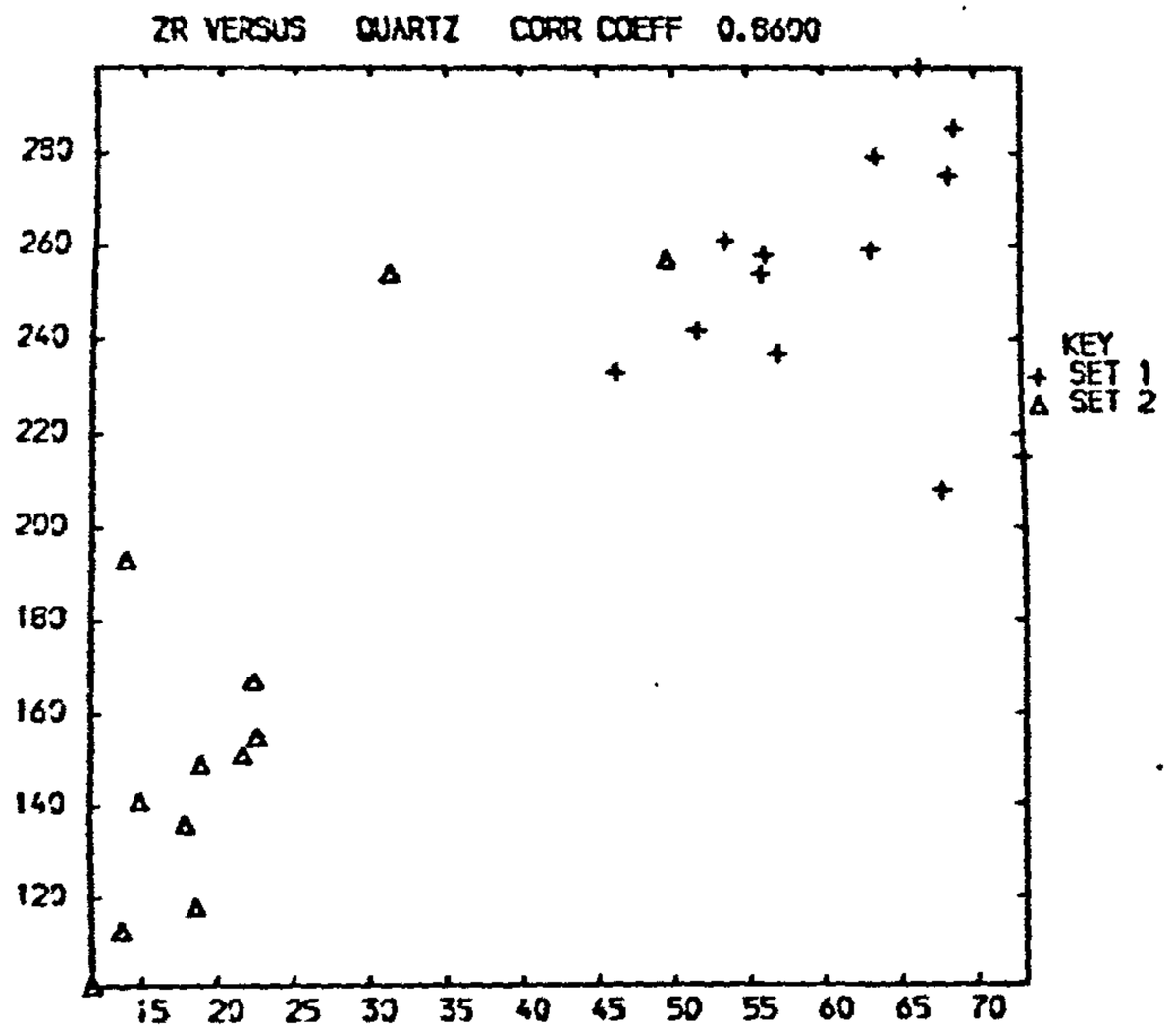
ZR VERSUS QUARTZ CORR COEFF 0.8600
280
260
240
220
200
180
160
140
120
15 20 25 30 35 40 45 50 55 60 65 70
KEY
SET 1
SET 2

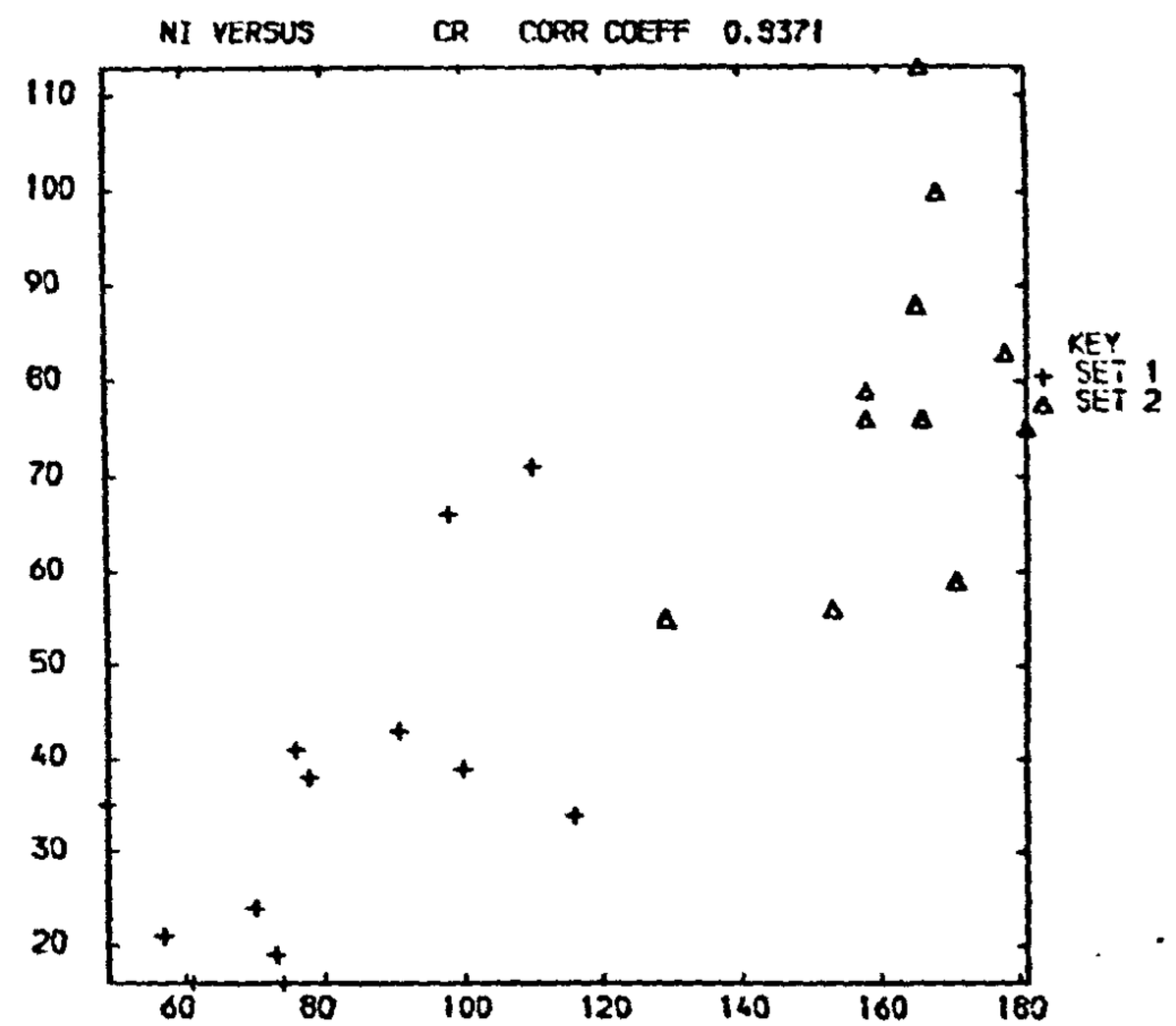
NI VERSUS CR CORR COEFF 0.9371
110
100
90
80
70
60
50
40
30
20
60 80 100 120 140 160 180
KEY
SET 1
SET 2

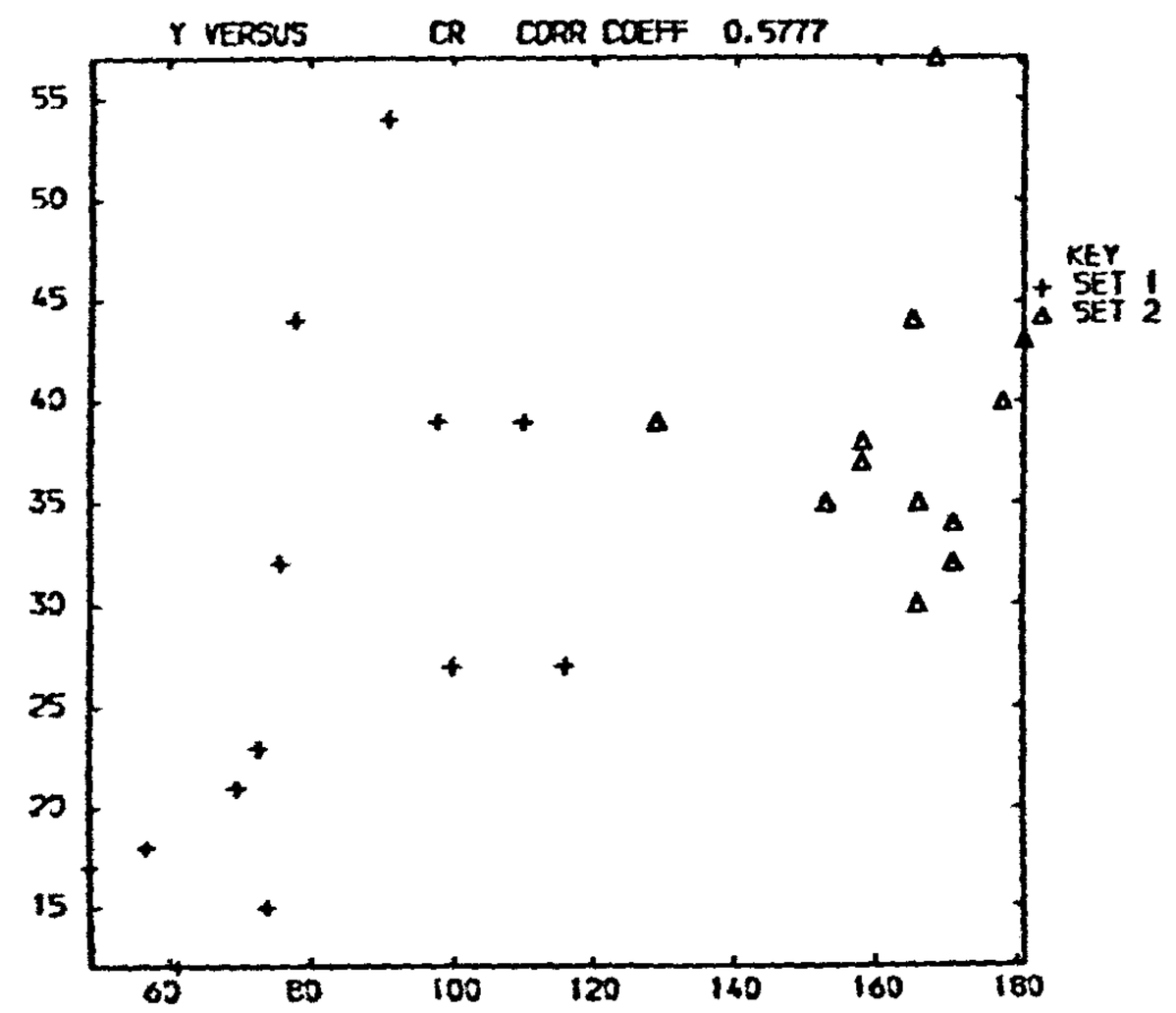
Y VERSUS CR CORR COEFF 0.5777
55
50
45
40
35
30
25
20
15
60 80 100 120 140 160 180
KEY
SET 1
SET 2

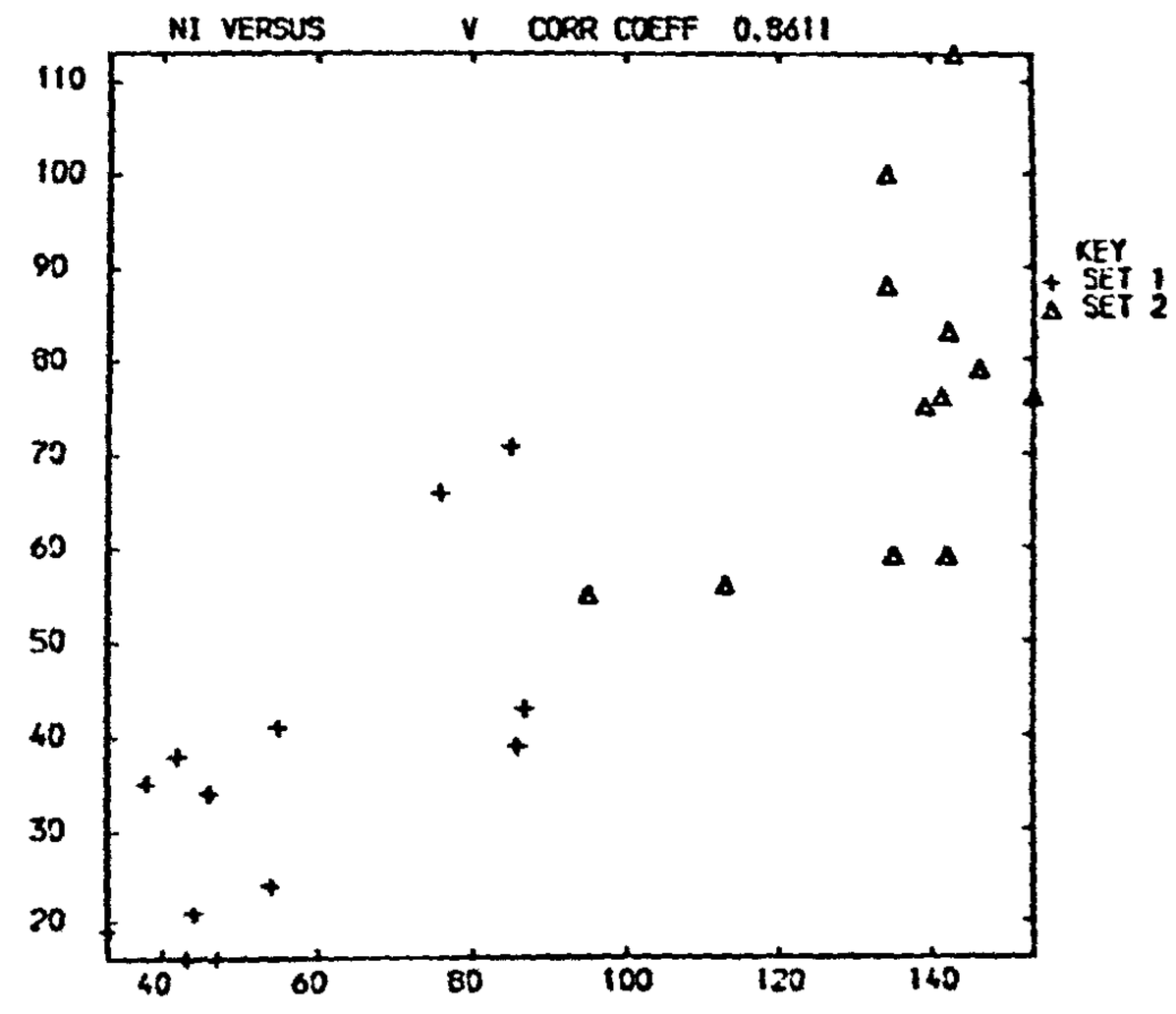
NI VERSUS V CORR COEFF 0.8611
110
100
90
80
70
60
50
40
30
20
40 60 80 100 120 140
KEY
SET 1
SET 2

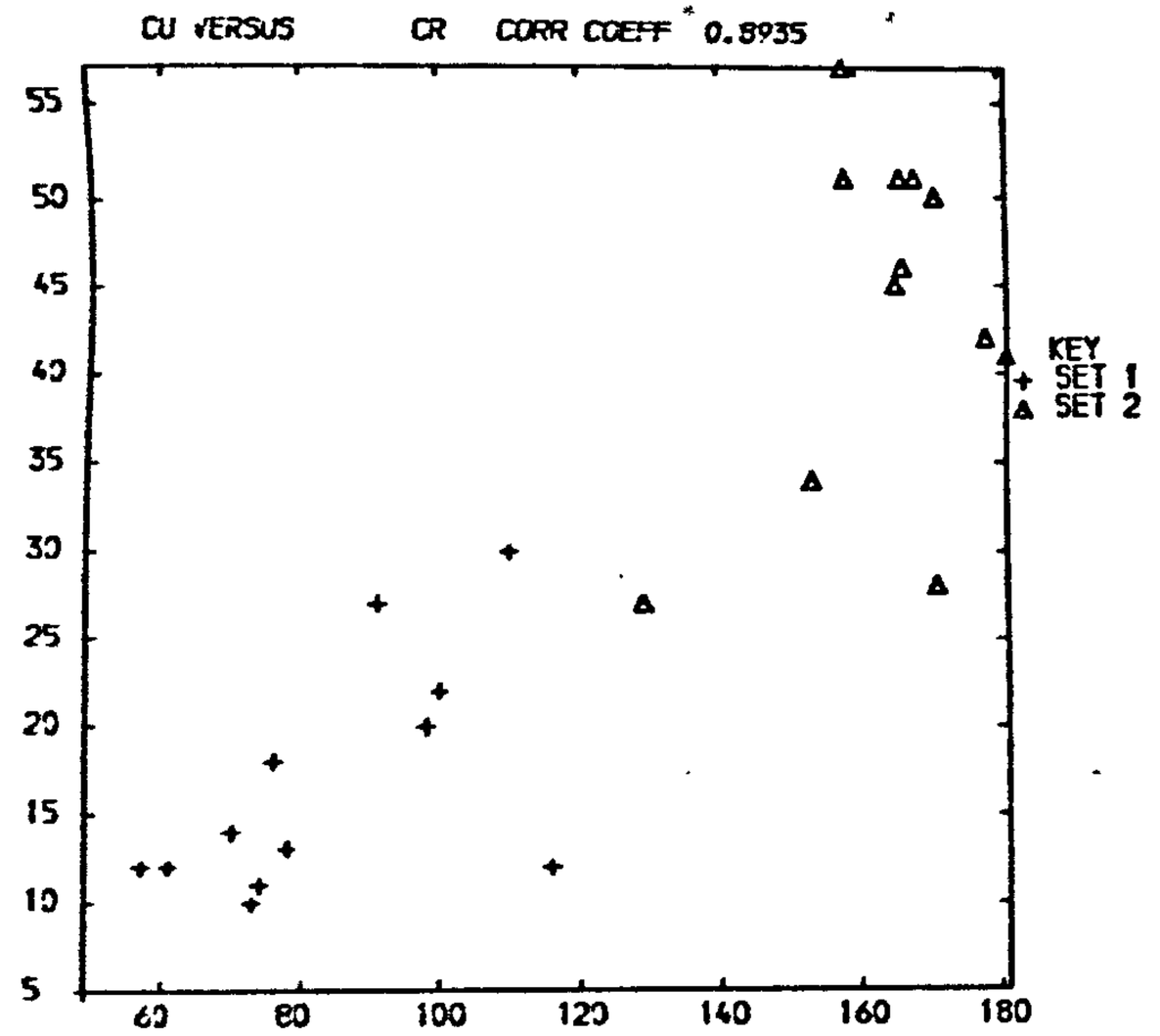
CU VERSUS CR CORR COEFF 0.8935
KEY
SET 1
SET 2

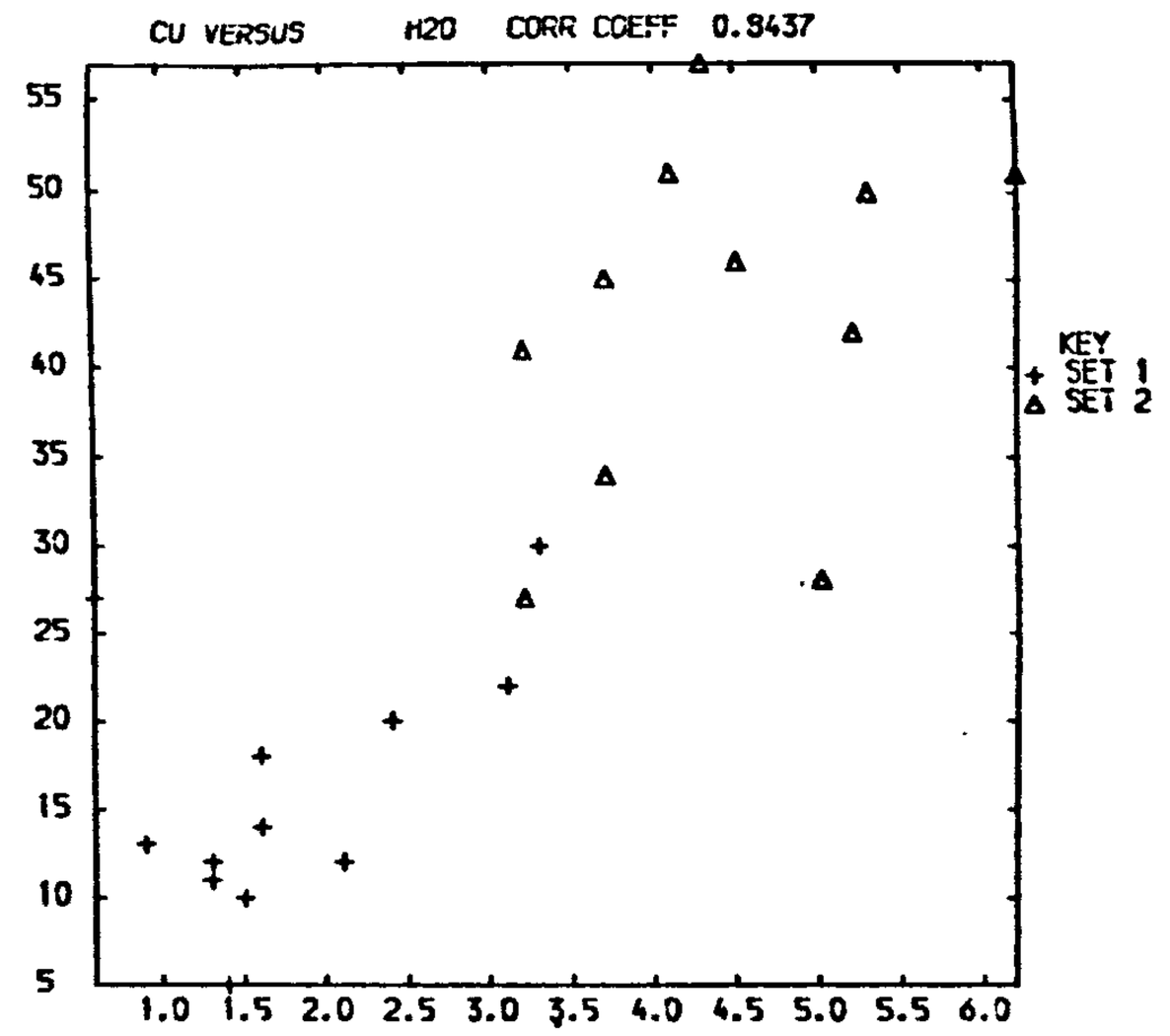
CU VERSUS H2O CORR COEFF 0.8437
KEY
SET 1
SET 2

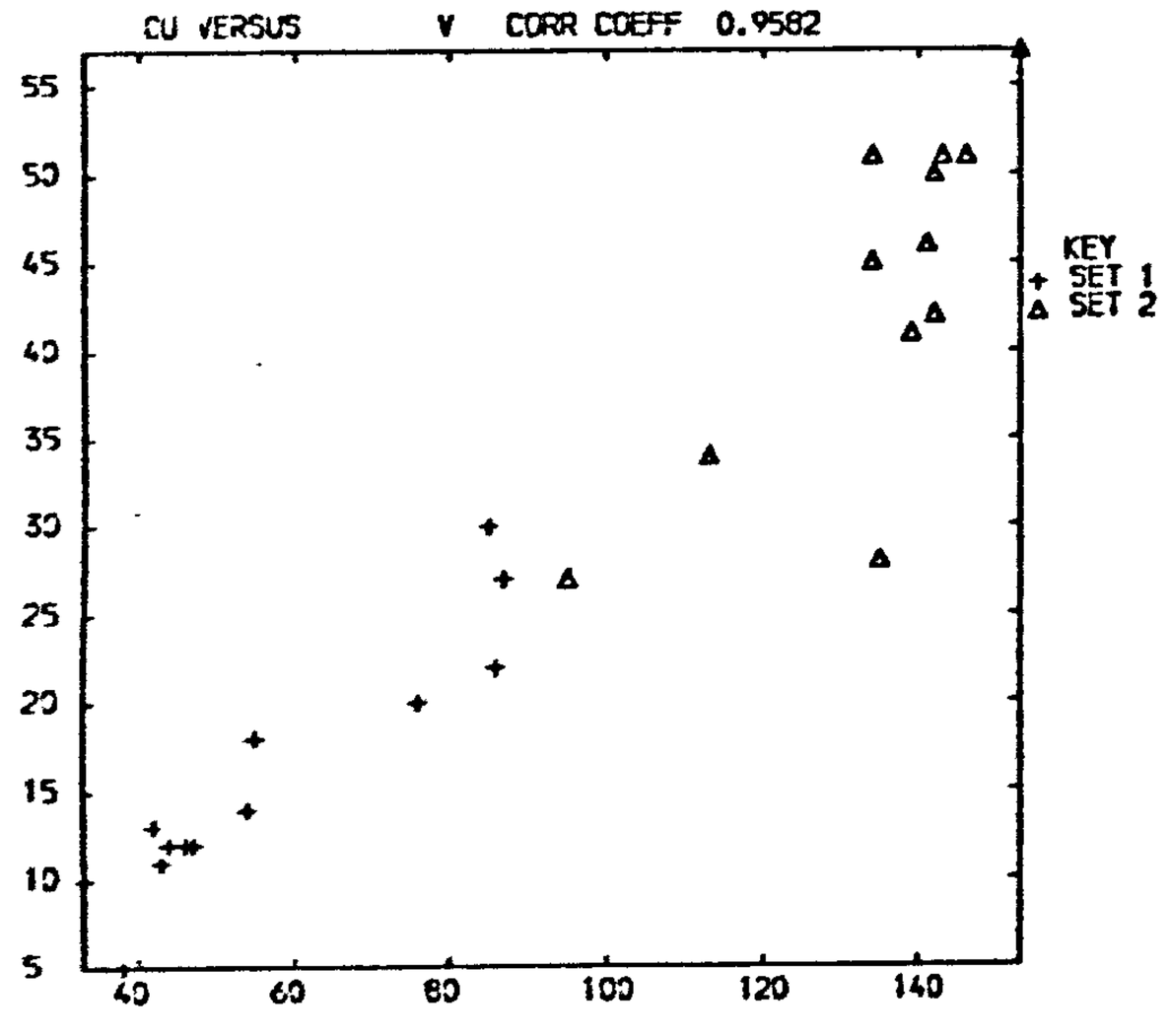
CU VERSUS V CORR COEFF 0.9582
KEY
SET 1
SET 2

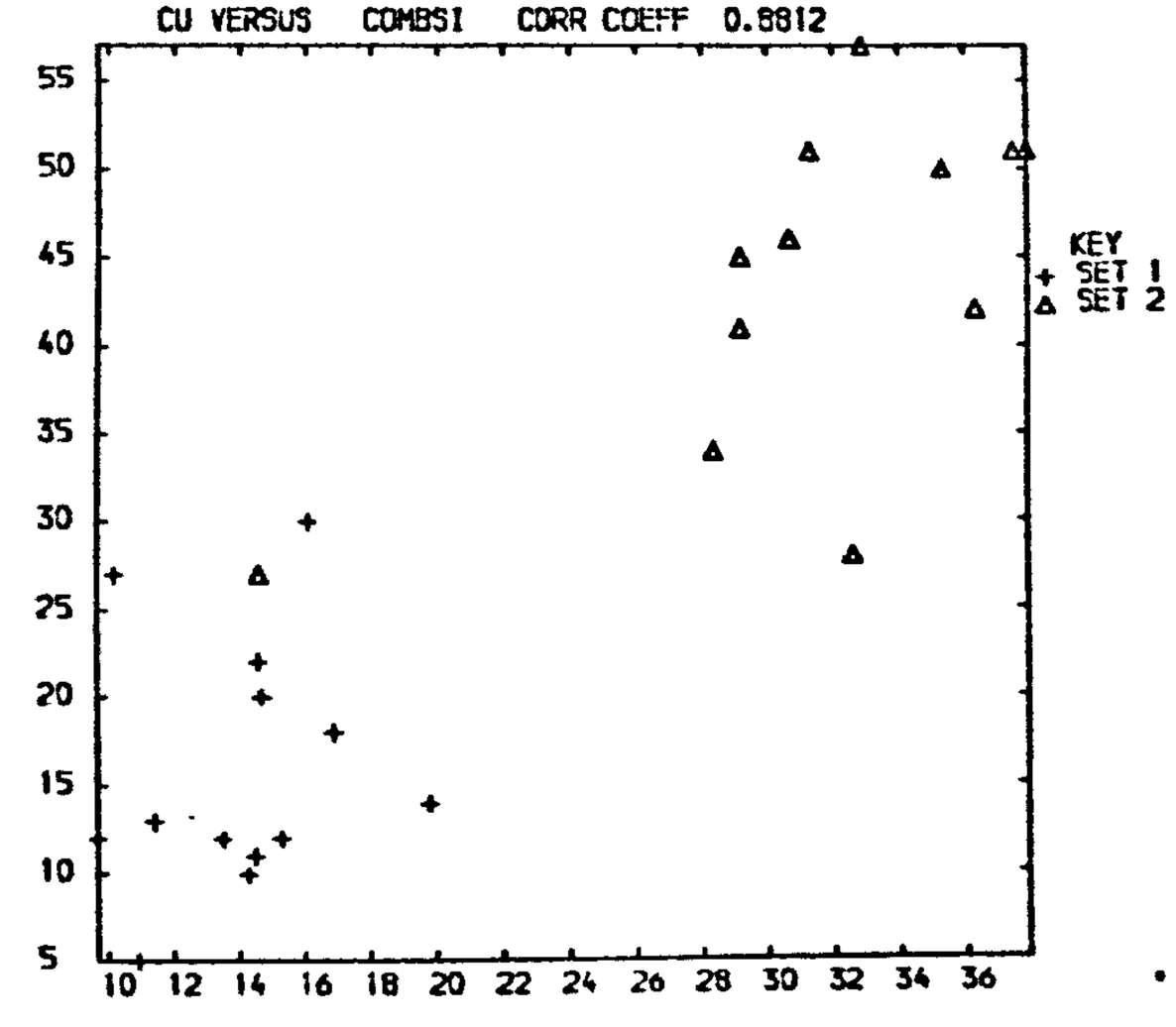
CU VERSUS COMBSI CORR COEFF 0.8812
KEY
SET 1
SET 2

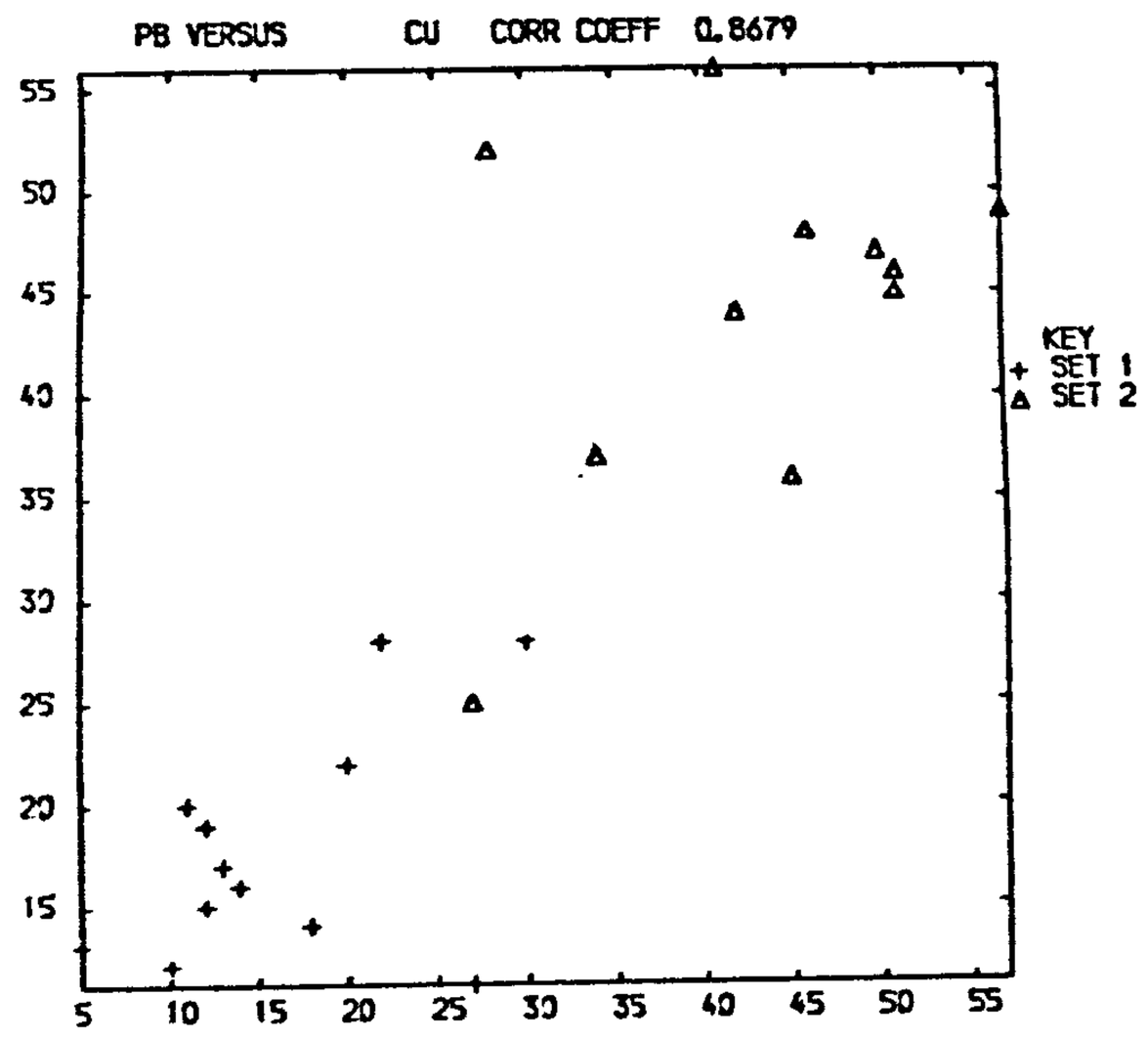
PB VERSUS CU CORR COEFF 0.8679
KEY
SET 1
SET 2
55
50
45
40
35
30
25
20
15
5
10
15
20
25
30
35
40
45
50
55

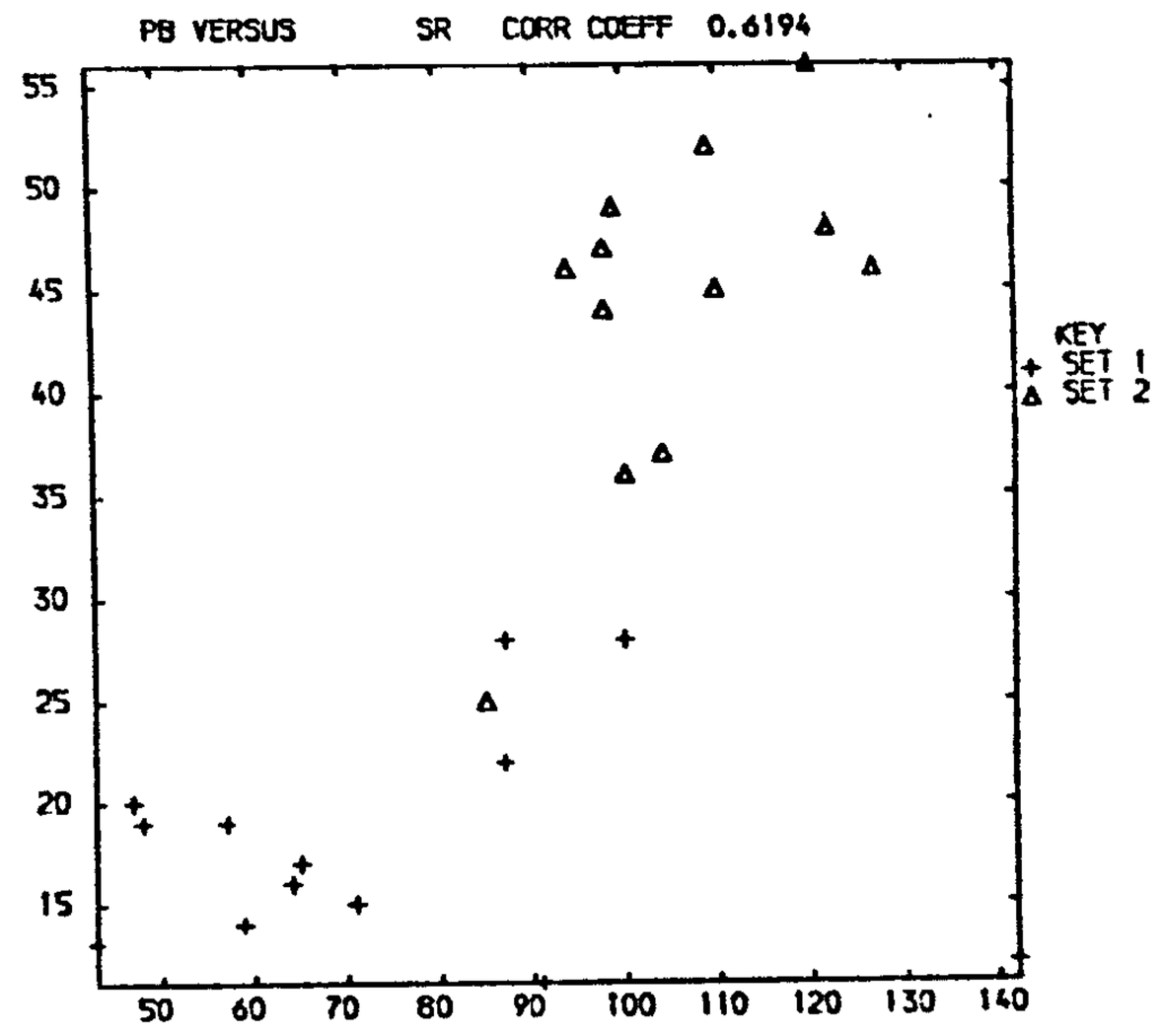
PB VERSUS SR CORR COEFF 0.6194
KEY
SET 1
SET 2
55
50
45
40
35
30
25
20
15
50
60
70
80
90
100
110
120
130
140

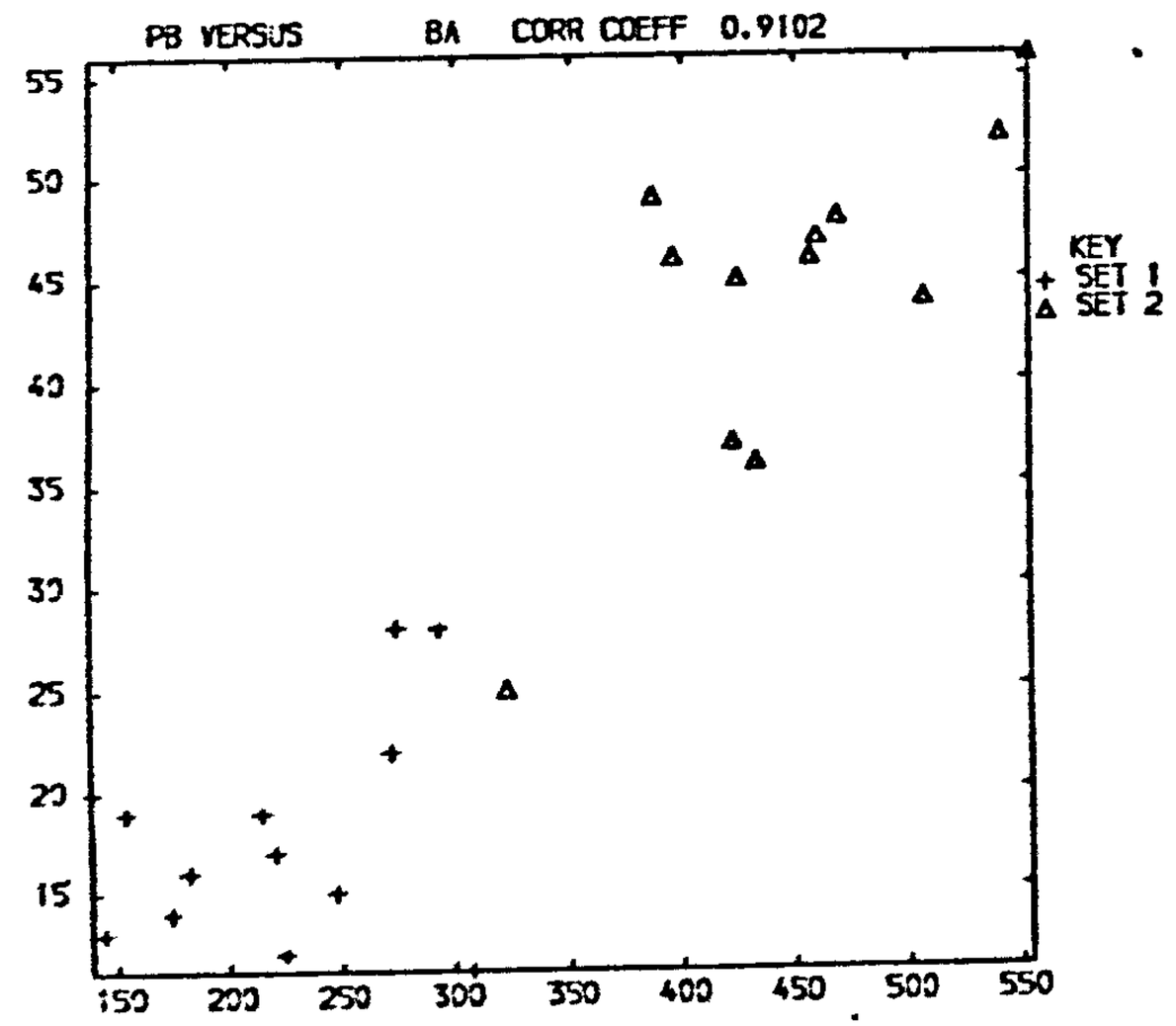
PB VERSUS BA CORR COEFF 0.9102
KEY
SET 1
SET 2
55
50
45
40
35
30
25
20
15
150
200
250
300
350
400
450
500
550

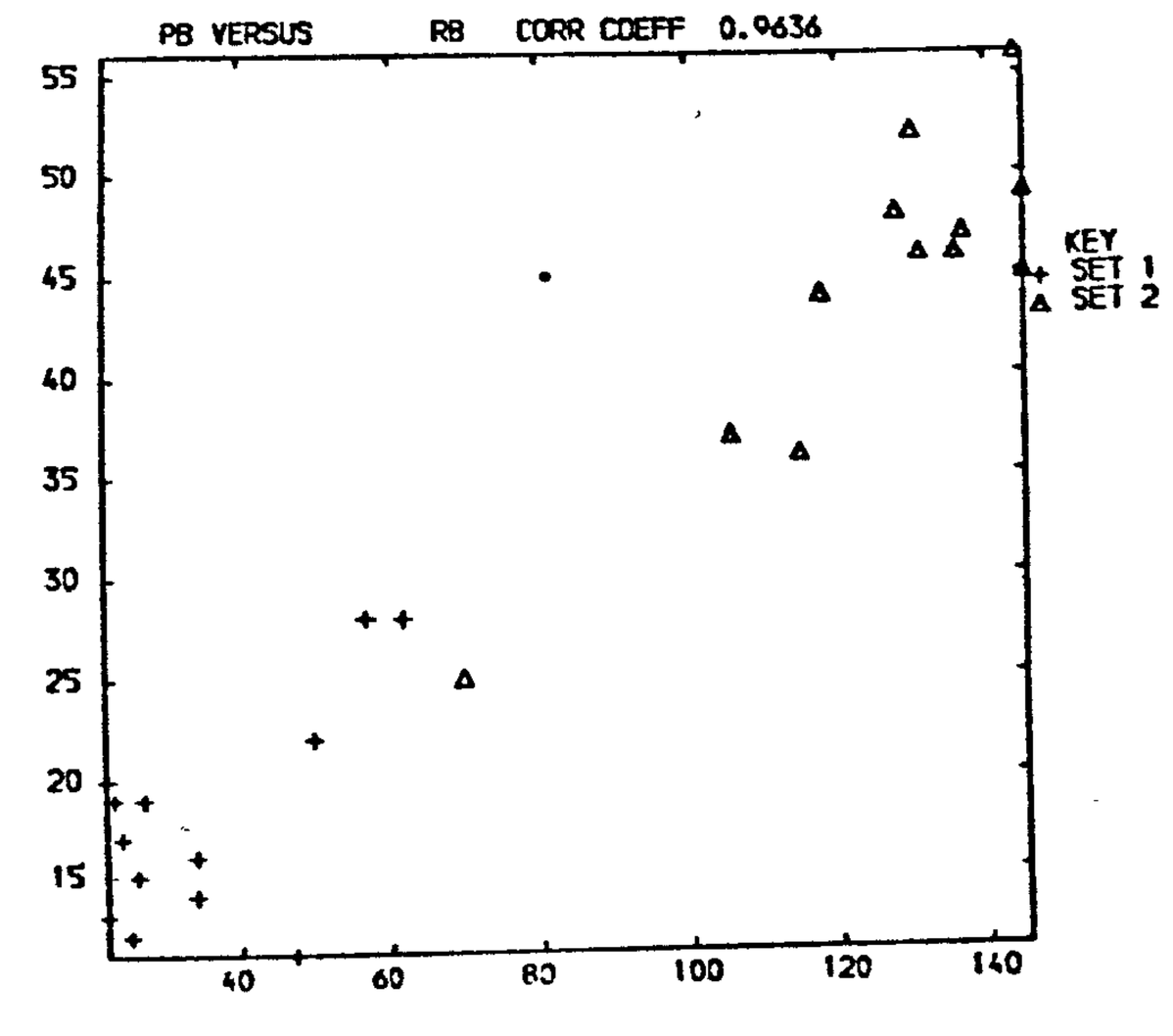
PB VERSUS RB CORR COEFF 0.9636
KEY
SET 1
SET 2
55
50
45
40
35
30
25
20
15
40
60
80
100
120
140

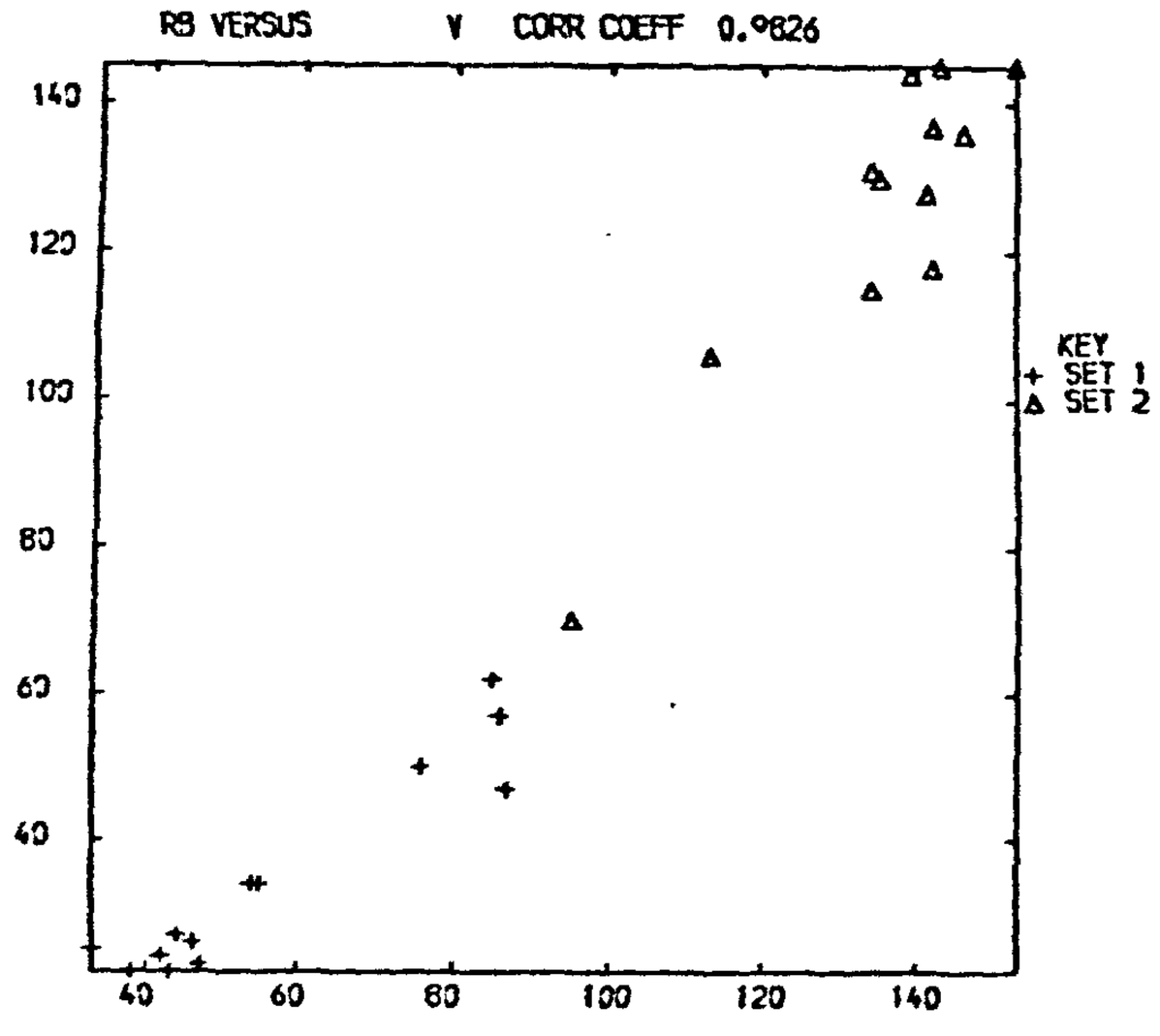
RB VERSUS V CORR COEFF 0.9826
140
120
100
80
60
40
40 60 80 100 120 140
KEY
+ SET 1
△ SET 2

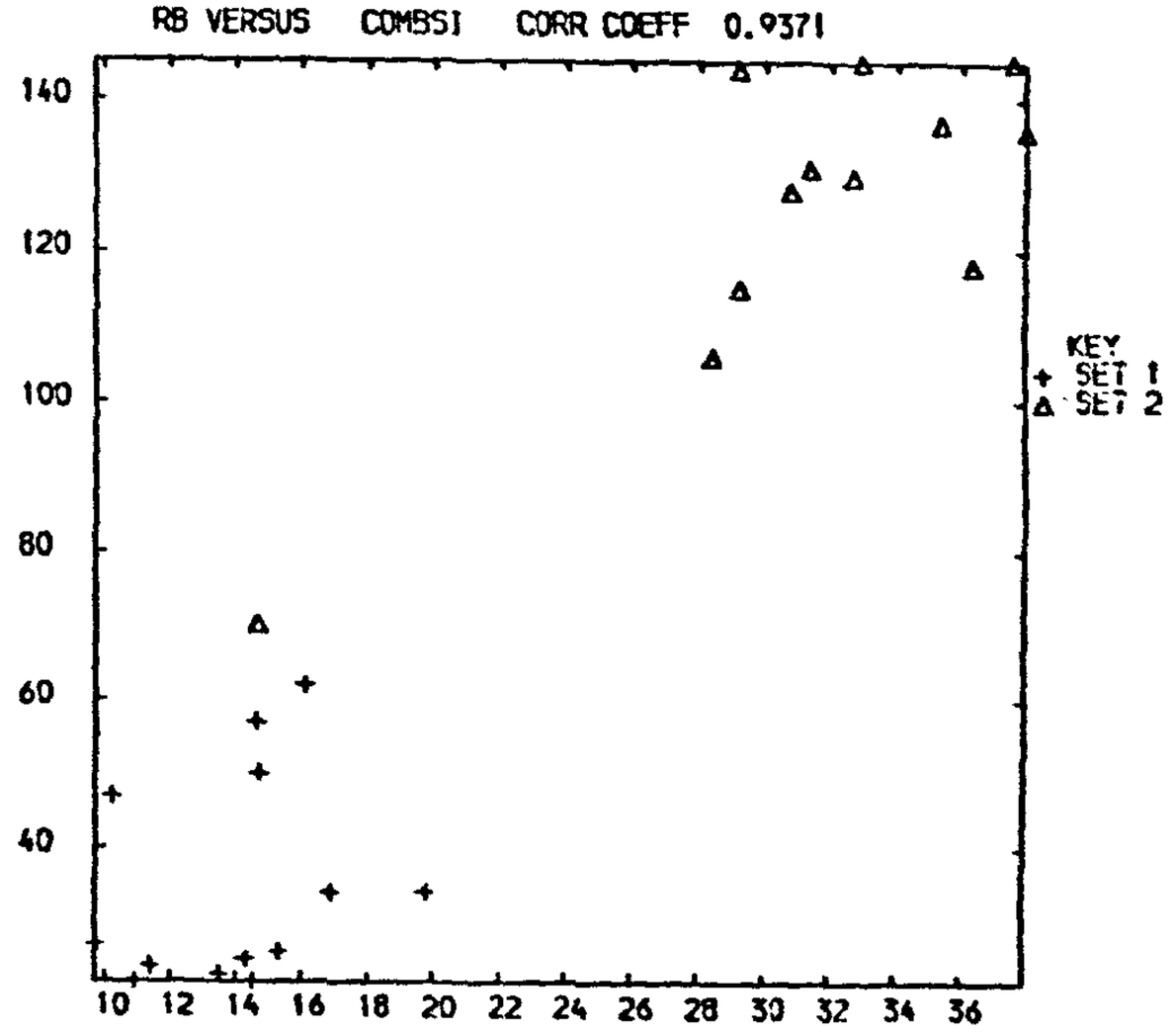
RB VERSUS COMBSI CORR COEFF 0.9371
140
120
100
80
60
40
10 12 14 16 18 20 22 24 26 28 30 32 34 36
KEY
+ SET 1
△ SET 2

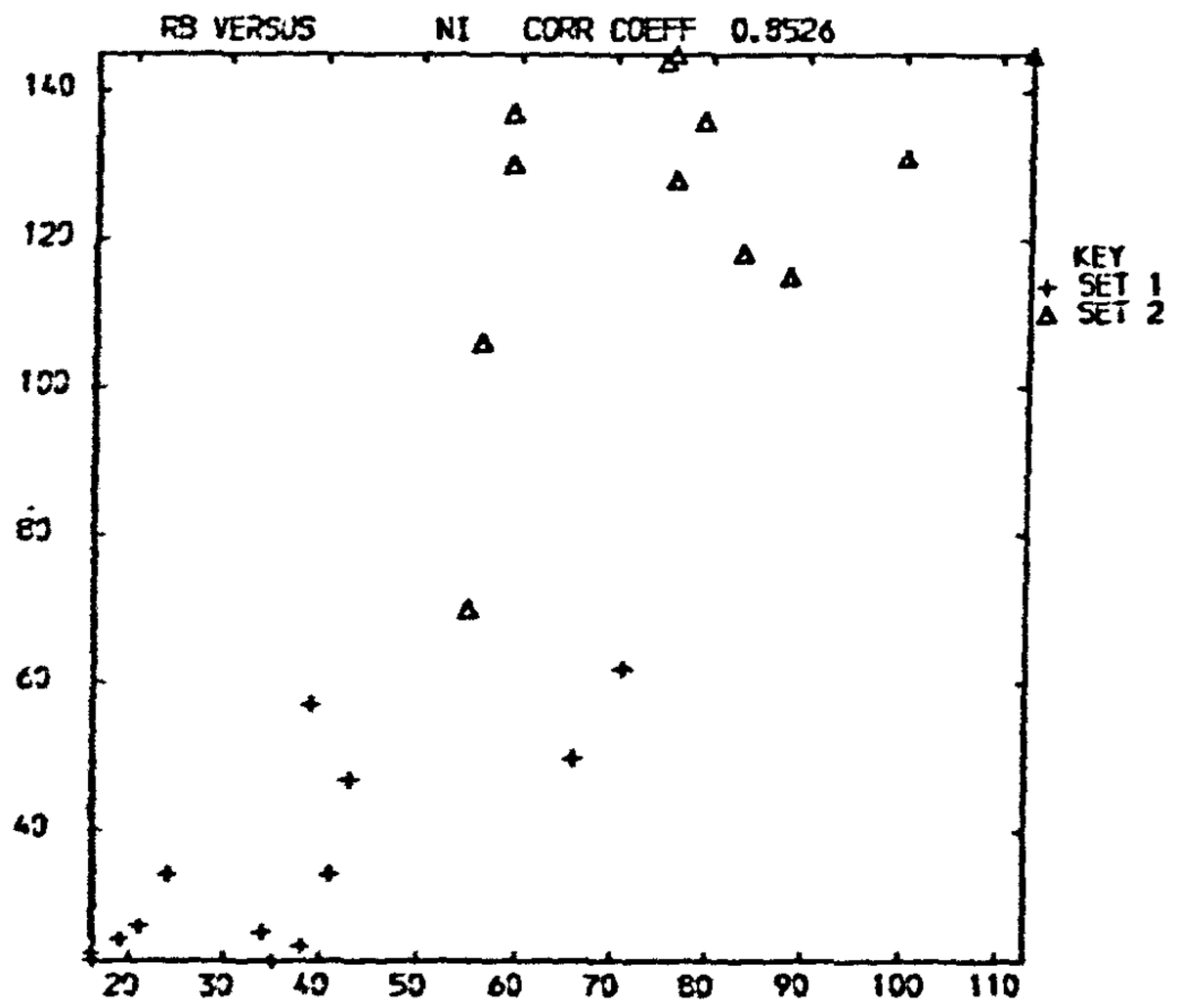
RB VERSUS NI CORR COEFF 0.8526
140
120
100
80
60
40
20 30 40 50 60 70 80 90 100 110
KEY
+ SET 1
△ SET 2

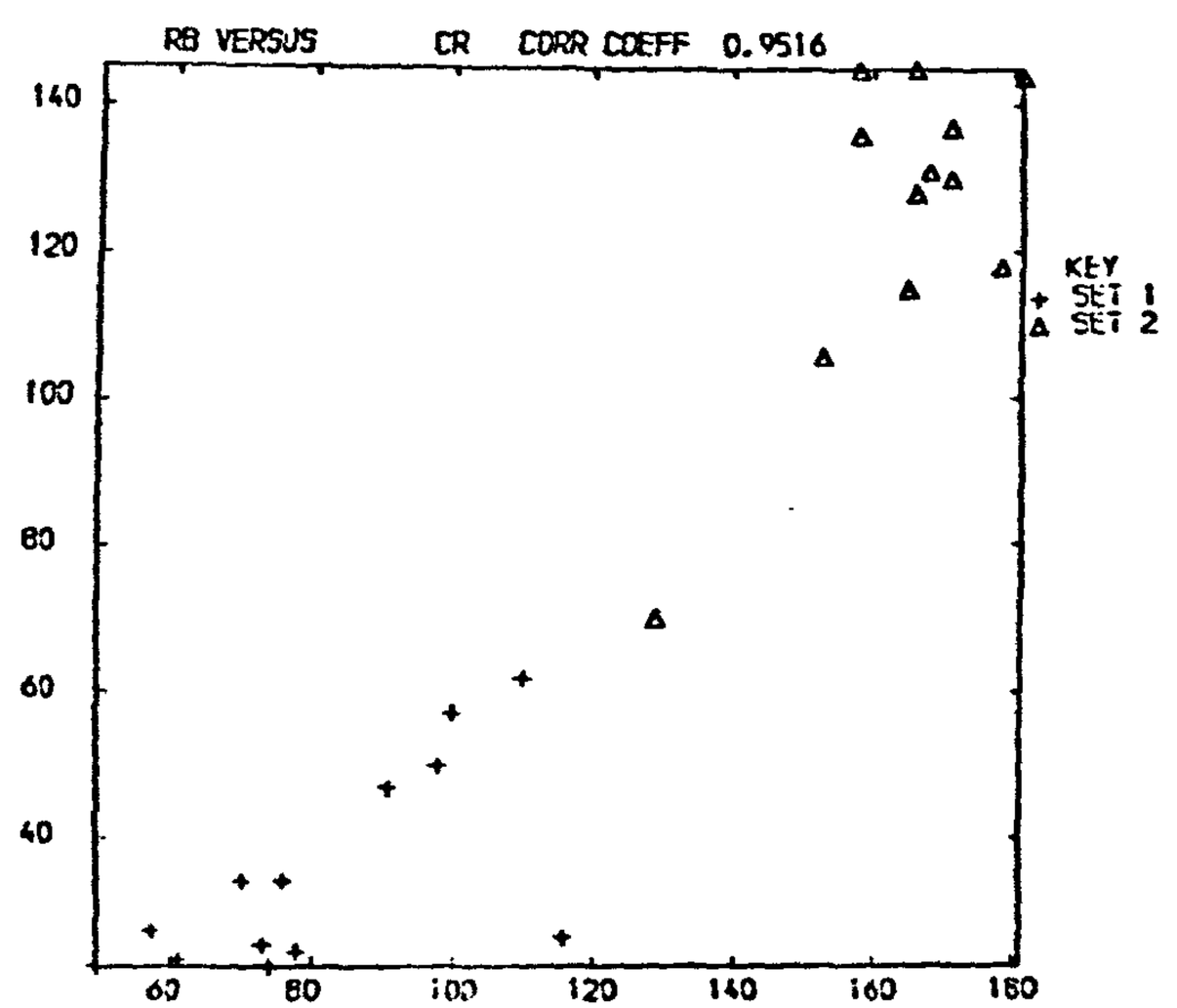
RB VERSUS CR CORR COEFF 0.9516
140
120
100
80
60
40
60 80 100 120 140 160 180
KEY
+ SET 1
△ SET 2

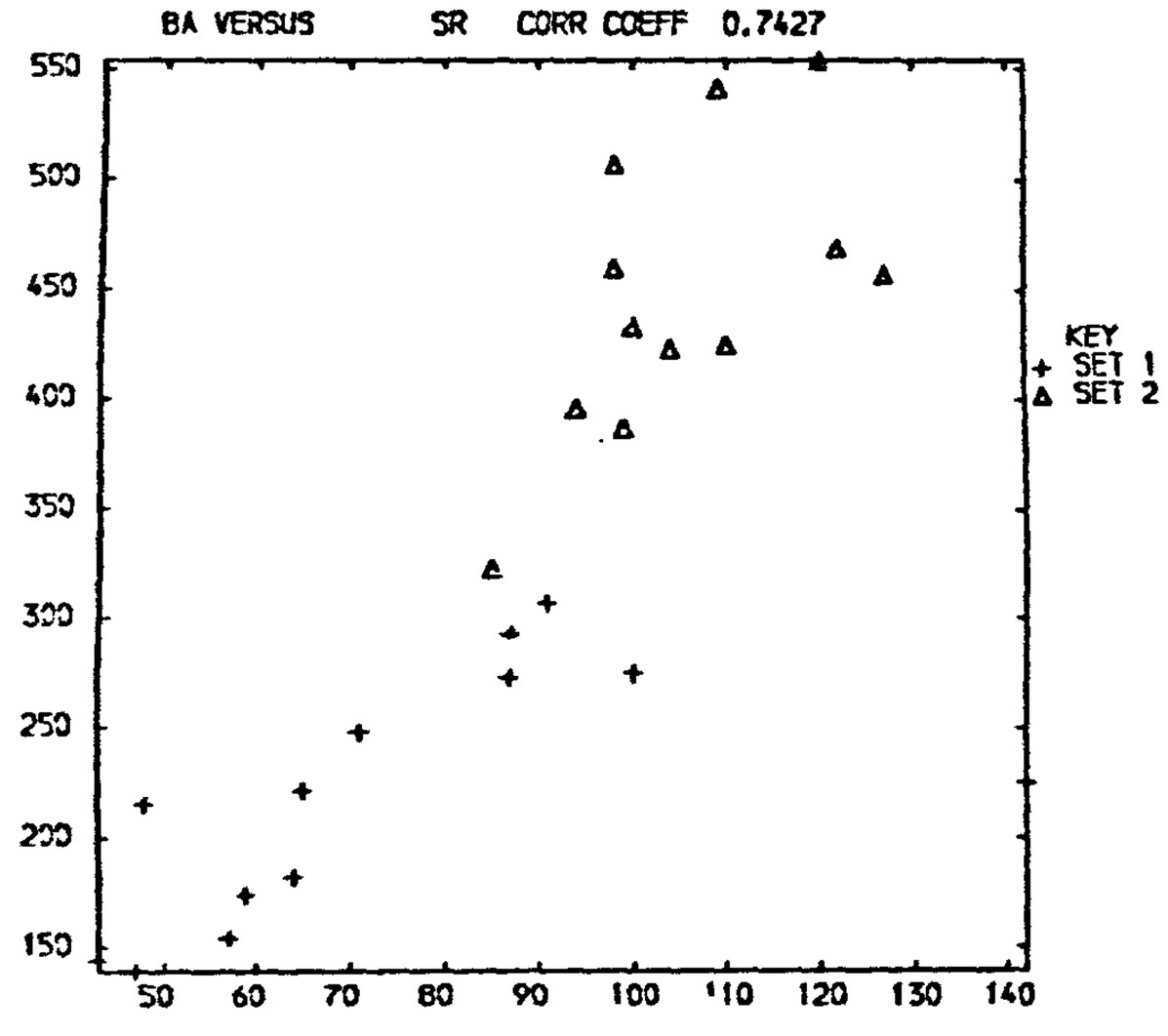
BA VERSUS SR CORR COEFF 0.7427
550
500
450
400
350
300
250
200
150
50 60 70 80 90 100 110 120 130 140
KEY
+ SET 1
Δ SET 2

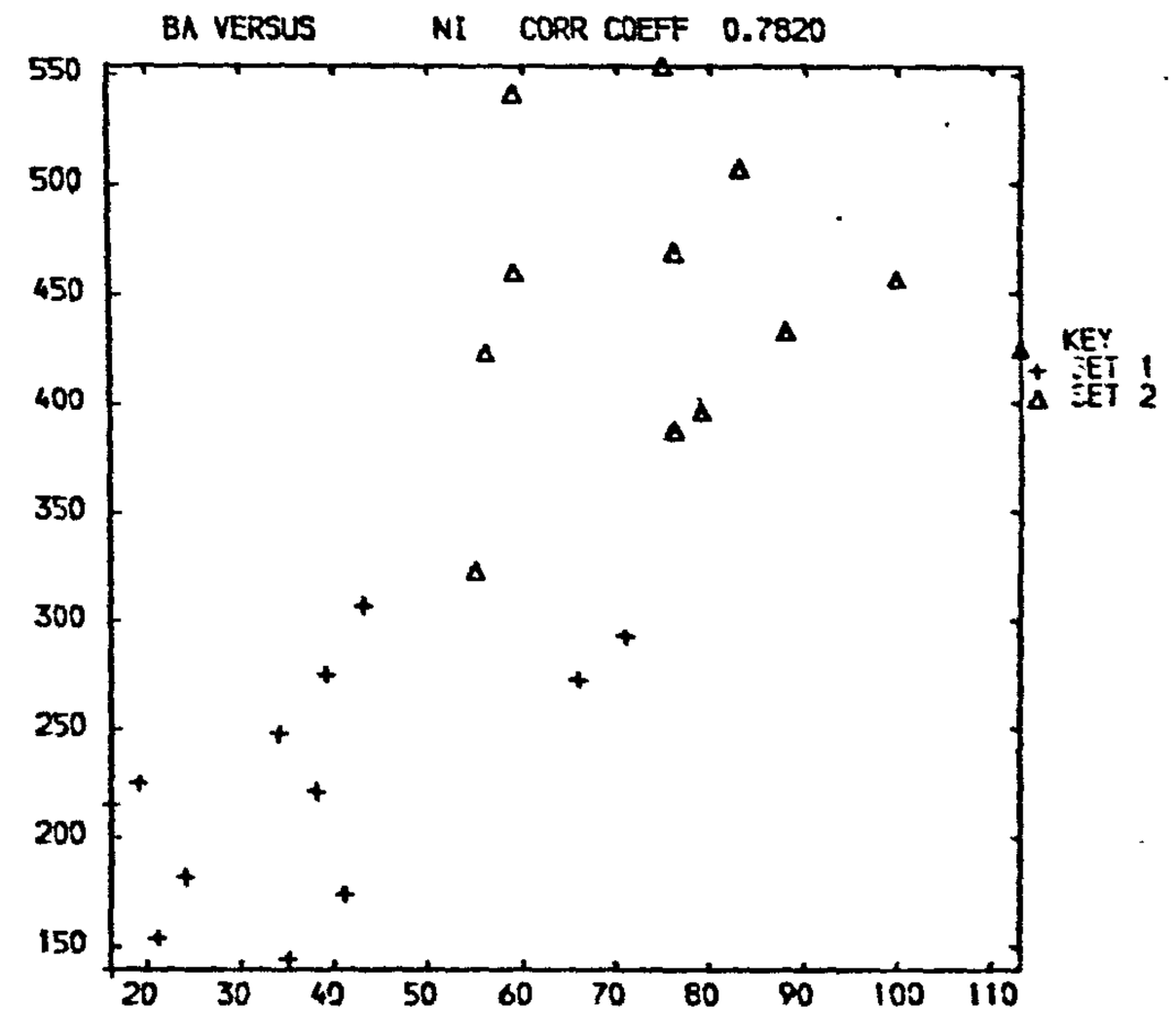
BA VERSUS NI CORR COEFF 0.7820
550
500
450
400
350
300
250
200
150
20 30 40 50 60 70 80 90 100 110
KEY
+ SET 1
Δ SET 2

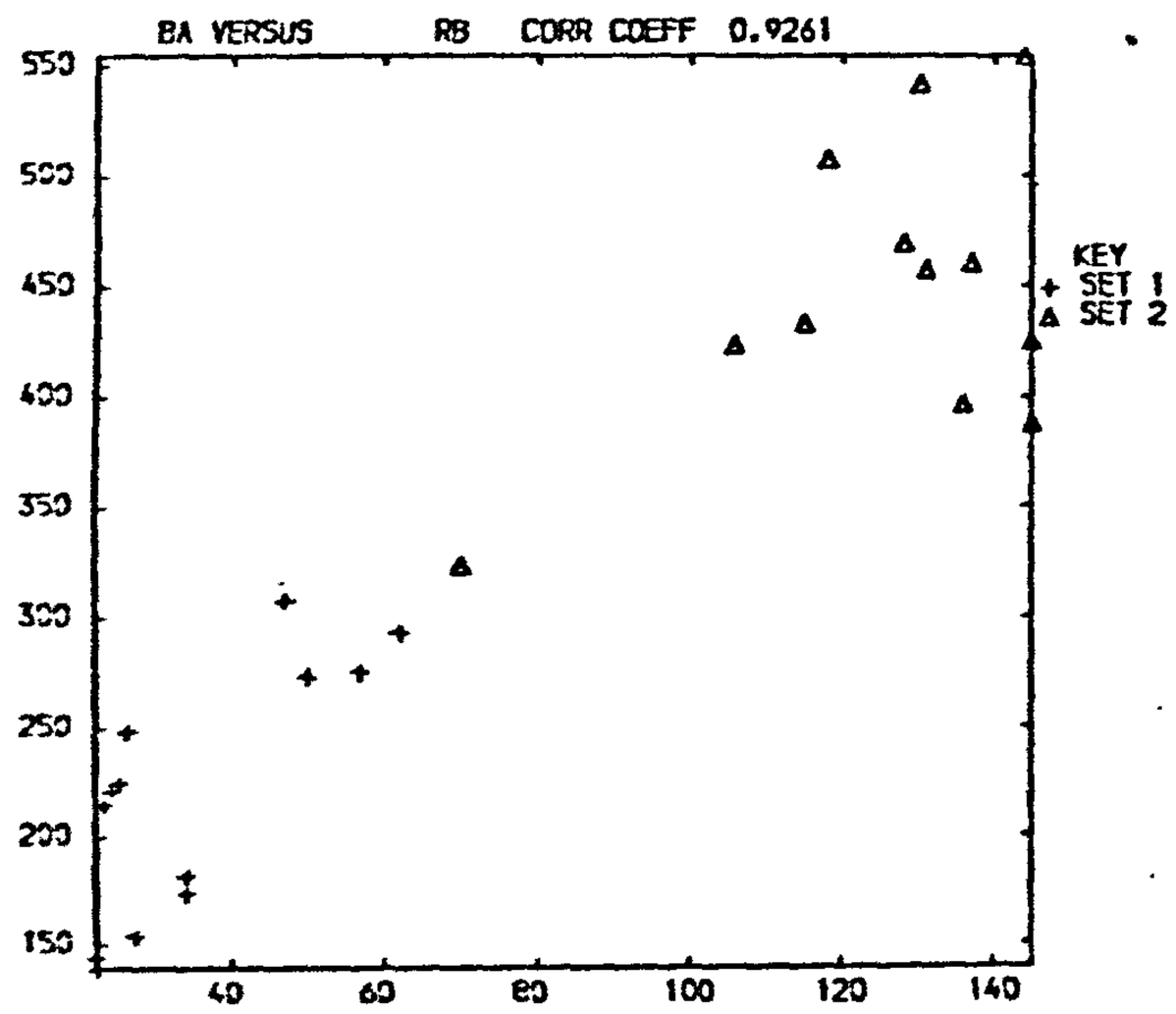
BA VERSUS RB CORR COEFF 0.9261
550
500
450
400
350
300
250
200
150
40 60 80 100 120 140
KEY
+ SET 1
Δ SET 2

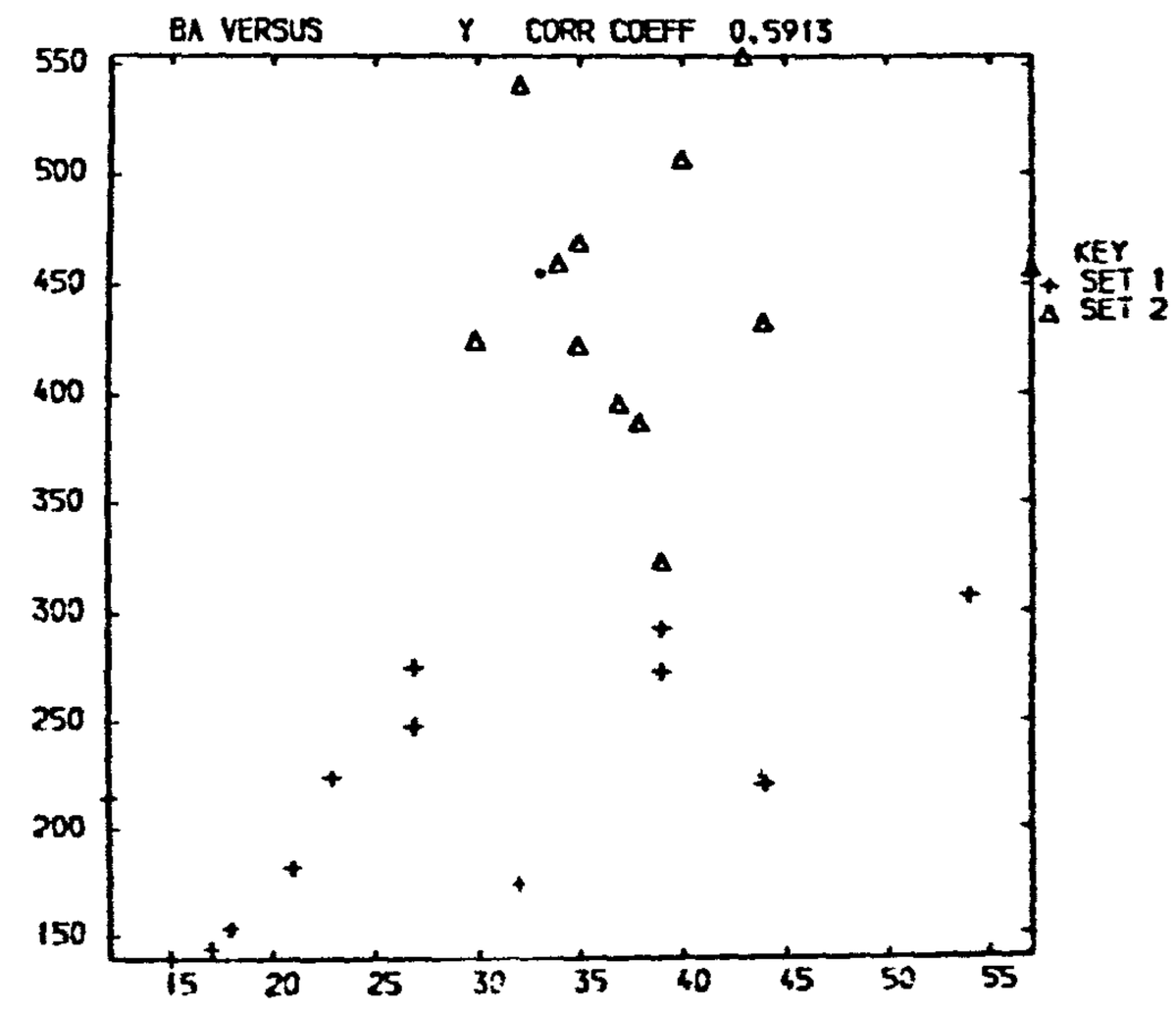
BA VERSUS Y CORR COEFF 0.5913
550
500
450
400
350
300
250
200
150
15 20 25 30 35 40 45 50 55
KEY
+ SET 1
Δ SET 2

TABLE 38: Correlation Matrix of Trace Elements and Clay Minerals of the <2 µm Fraction

	Ni	Co	Mn	V	Cr	Zn	Cu	Rb	Sr	Y
Ni	1.0000									
Co	(0.6915)	1.0000								
Mn	0.3936	(0.5615)	1.0000							
V	0.3398	0.0199	-0.6013	1.0000						
Cr	0.2577	-0.1136	-0.6972	0.9593	1.0000					
Zn	0.2940	0.3815	(0.8100)	-0.6288	-0.6769	1.0000				
Cu	-0.1594	-0.1116	-0.3661	0.1666	0.1119	-0.0284	1.0000			
Rb	0.2847	-0.2544	-0.6327	0.8869	(0.9244)	-0.6648	-0.0654	1.0000		
Sr	-0.0035	-0.3726	-0.4338	0.4064	0.6114	-0.4426	-0.2392	(0.6207)	1.0000	
Y	(0.5888)	0.3137	(0.6227)	-0.1279	-0.1490	(0.7426)	-0.1224	-0.1209	-0.0710	1.0000
Zr	-0.4219	-0.3913	-0.6281	0.1186	0.2288	-0.3420	0.6866	0.0615	0.1033	-0.2996
Pb	-0.1008	-0.2912	10.4653	0.4362	0.5028	-0.2323	0.2870	0.3788	0.2720	0.1418
Ba	012057	-0.2840	-0.6611	0.7874	(0.8991)	-0.5753	-0.0162	(0.8998)	(0.7210)	0.0098
Illite	0.2908	-0.2758	-0.5564	(0.8248)	(0.8786)	-0.5122	-0.1299	(0.9619)	(0.6406)	0.0500
Kaolin	0.2847	0.1682	(0.6149)	-0.8889	-0.9202	(0.5560)	0.0321	-0.9473	-0.5533	0.0258

	Zr	Pb	Ba	Illite	Kaolin
Zr	1.000				
Pb	(0.5782)	1.0000			
Ba	0.2709	(0.5869)	1.0000		
Illite	0.0225	0.5002	(0.9192)	1.0000	
Kaolin	0.0983	-0.4709	-0.9073	-0.9602	1.0000

It can be seen that illite content covaries with V, Cr, Rb, Sr and Ba, which are also correlated with each other. The similarity of Sr, Ba and Rb ionic radii to that of potassium (Table 34) makes their substitution likely in the interlayer position, whereas Cr and V may proxy for Al in the octahedral position. Such an association of trace elements with illite has been invoked to explain their covariation in other sediments (Turekian and Imbrie, 1966; Summerhayes, 1971; Cosgrove, 1973; Stephens et al. 1975). The other correlations are Ni-Co, Ni-Y, Co-Mn, Mn-Zn, Mn-Y, Y-Zn, and Zr-Cu. In the <2 μm fraction Fe_2O_3 is abundant and correlates with chlorite. Hence Fe_2O_3, chlorite and siderite are the most likely host for the above associations of trace elements. The similarity of their ionic radii with those of Fe^{2+}, Fe^{3+} and MgO^{2+} (Table 34) makes their substitution possible. The association of these trace elements with ferric oxide and chlorite has been reported by otherworkers (Bjorlykke, 1974; Kalliokoski, 1975; Steel and Wagner, 1975; Chester et al. 1976). The correlation between kaolinite, Mn and Zn is merely a reflection of the covariation with Fe_2O_3 and chlorite, but without genetic relationships. This is because Fe_2O_3 shows a greater abundance in the <2 μm fraction of the sandstones in which biotite and feldspar alteration result in kaolinite, Fe_2O_3 and chlorite. In addition the possibility of the presence of some of these elements in carbonates is not excluded. The Zr-Pb-Ba association has a negative correlation with kaolinite and a positive relation with illite, although it is insignificant at the 95% level. This may indicate the presence of small amounts of the above elements in the illite.

In order to support such an association of trace elements with clay minerals a test of the confidence intervals for the population means was applied (Koch and Link, 1970, p.89) to see if such partition is real

at the 95% significance level. It must be noted that illite is more abundant in the clay fractions of the shales than in those of the sandstones, whereas chlorite is variable in its content. The results shown below indicate that the mean value for an element is either higher in the clay fractions of the shales or sandstones and the 'No Difference' term indicates no real variations.

TraceElement in the Clay Fractions

Shales	No Difference	Sandstones
V, Cr, Rb, Sr, Ba	Ni, Co, Cu, Y, Zr, Pb	Mn, Zn

It appears that V, Cr, Rb, Sr and Ba are mostly related to illite (because kaolinite has little substitution capacity as compared to illite) while the rest of the elements are, most probably, associated with chlorite, Fe_2O_3, organic matter, carbonates, heavy minerals and feldspars. The enrichment of Mn and Zn in the clay fractions of the sandstones may indicate association with Fe_2O_3 and chlorite, because the latter were found to be the main alteration products of biotite in the sandstone. In addition siderite is relatively more abundant in the sandstones and the association of Mn and Zn with siderite is likely to occur.

Partition of Trace Elements Between Silt and Clay Fractions

The aforementioned statistical test was applied to the trace element data of silt and clay fractions in each of the shales and sandstones and between their silt fractions as well; the results are shown below:

	Silt Fraction	No Difference	Clay Fraction
Shales	Zr	Co, Mn, Sr, Y, Ba	Ni, V, Cr, Zn, Cu, Rb, Pb
Sandstones	Zr	Ni, Co, Mn, Zn, Cu, Sr, Y	V, Cr, Rb, Pb, Ba

	Shales		Sandstones
Silt Fraction	V, Cr, Rb, Pb, Ba	Ni, Co, Cu, Sr, Y, Zr	Mn, Zn

It is evident that in both shales and sandstones Zr is concentrated in the silt fraction, indicating control by heavy minerals. The elements which show no difference between the silt and clay fraction, therefore, would appear to share their distribution among the resistate phase, feldspar, carbonates and clay minerals. The elements V, Cr, Rb, Pb and Ba are highly concentrated in the clay fraction, whereas other trace elements such as Ni, Zn and Cu while showing high concentration in the clay fraction, evidently play a dual or triple role by showing moderate concentration in the silt fraction.

Comparing trace element data in the silt fraction of the shales and sandstones it appears that Mn and Zn are possibly related to carbonates, chlorite, Fe_2O_3, and possibly heavy minerals in the sandstones.

Summary

Except for Co, Y and Zr, most of the other elements are controlled to a varying degree by the content of clay minerals. Cr, Rb, Sr and Ba are associated with illite, whereas the remaining elements are distributed between clay minerals, carbonates, feldspars and heavy minerals. However, the clay related elements could be, at least in part, associated with organic matter and Fe_2O_3.

4.9 Relation between Composition of the Clay Fractions and Lithology

The most important variations in the chemical composition of the <2 μm fractions are shown in Figure 29. The content of quartz in whole rock samples which is proportional to the amount of silt and sand sized material, is compared to variations in SiO_2, Al_2O_3 and Fe_2O_3 contents of the <2 μm fractions. The following variations are the most outstanding in Figure 29.

1. The increase of quartz contents (whole rock samples) is generally accompanied by high amounts of Fe_2O_3 in the <2 μm fractions. This points to the association of chlorite and iron oxide, due to biotite alteration. It also suggests that these constituents are enriched in the clay fractions, and this is supported by the results of the various size fractions. Furthermore, it may indicate that some Fe_2O_3 is incorporated into the chlorite structure; X-ray identification and semi-quantitative estimation of chlorite composition showed its iron-rich nature.

2. The amount of SiO_2 in the <2 μm fraction, in most cases, shows little variation, around 45%. This is significant because the clay fractions consist of different proportions of kaolinite, illite and chlorite (plus small amounts of quartz and traces of plagioclase) each of which contains a different amount of SiO_2. The cause of such constancy is not clear, but it may indicate that diagenesis and the variations in the disaggregation characteristics of the rocks could affect the distribution of different minerals in the clay fractions.

3. The relatively uniform distribution of SiO_2 in the clay fractions is accompanied by somewhat antipathetic relationship between Al_2O_3 and Fe_2O_3. This is quite clear in the upper part of the section, and it is the most pronounced variation in the chemical composition of the clay fraction.

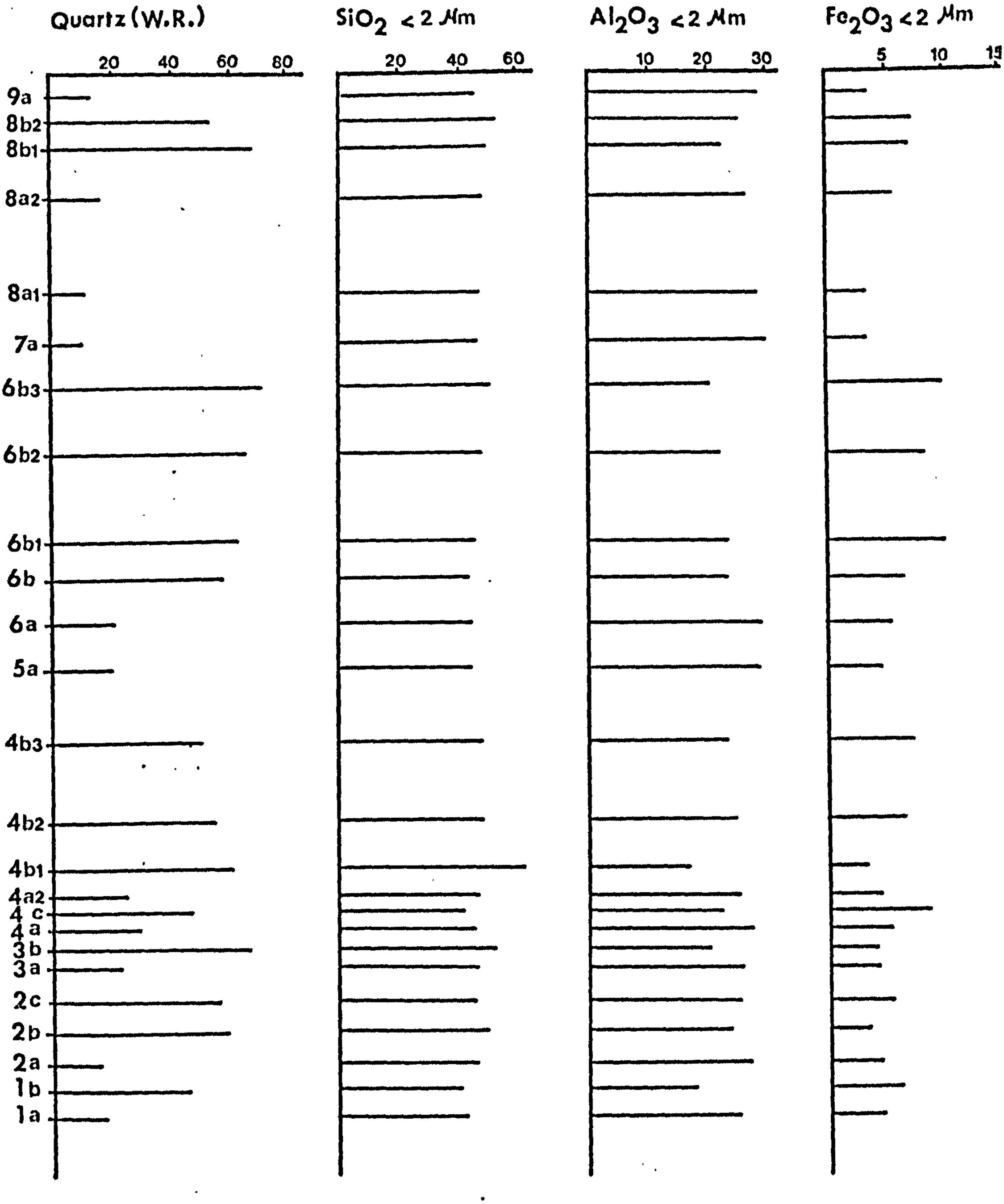

Fig.29 Relationship between quartz(whole rock sample)content and SiO_2, Al_2O_3, Fe_2O_3 contents of the clay fraction.

On the other hand, this reciprocal variation between Al_2O_3 and Fe_2O_3 within the clay fractions of the greywackes only, shows less compatibility and suggests that authigenic Fe_2O_3 and possibly chlorite do not account for all the variation in iron.

4. Analysis of the various size fractions showed that clay minerals and their related major elements increase with decrease in grain size. In a similar way trace elements, except Co, Y and Zr, are enriched to a variable degree in the finer fractions. Statistical correlation supports the relationship between trace element enrichment, clay minerals and Fe_2O_3. This may indicate that diagenesis has not greatly affected the content of trace elements but however, it may have involved a re-arrangement and re-distribution of these elements. The important point is that unexpected major chemical changes other than those related to lithology apparently have not occurred during diagenesis.

4.10 Comparison with other Argillaceous Sediments

Table 39 lists the average contents of trace elements in the Mam Tor greywackes, shales and other argillaceous sediments. The Mam Tor greywacke compares favourably with the Quebec turbidite (anal. 3) except for the latter's enrichment in Zr. Comparison with Normanskill turbidite (anal. 4) shows higher amounts of Cr, Sr, Zr and Ba than in the Mam Tor greywackes, probably indicating the influence of calcite and detrital minerals. It is interesting to note the high enrichment of these elements in the volcanic greywackes (anal. 6) relative to the Mam Tor greywackes and other turbidites. The Mam Tor shale shows similar amounts of Cu and Ba and their lower contents of Ni, V and Cr when compared with the Precambrian argillites (anal. 5), suggesting possible contribution from volcanic sources.

TABLE 39: Average Content of Trace Elements in the Mam Tor Greywackes and Shales and other Argillaceous Sediments

Element ppm	1	2	3	4	5	6	7	8
Ni	37	79	27	43	106	130	42	21
Co	16	12	15	22				
Mn	857	548	540	600	580	870		
V	59	138	43	67	181	210	134	53
Cr	84	167	88	140	200	253	72	31
Zn	67	84						
Cu	17	45	9	33	42	51	33	15
Rb	37	130						
Sr	75	107	110	260				
Y	29	39						
Zr	253	152	810	400				
Pb	19	46					24	12
Ba	227	459	220	380	470	431		

(1-2 from the present study)

1 - Average Mam Tor greywackes

2 - Average Mam Tor shales

3 - Average Quebec turbidites

4 - Average Normanskill turbidite

(3-4 from Weber and Middleton, 1961)

5 - Pre-Cambrian argillites interbedded with greywackes

6 - Volcanic greywackes

(5-6 from Macpherson, 1958)

7 - Marine argillaceous sediments

8 - Freshwater argillaceous sediments

(7-8 from Petter et al., 1963)

When the average composition of the Mam Tor shales is compared with the data for marine and non-marine argillaceous sediments (anal. 7 and 8) it is apparent that, in general, the trace element content in the former is closely similar to, or higher than, in marine argillaceous sediments, which in turn have a higher content than their non-marine counterpart. Hence, it can be tentatively stated that a marine origin for the Mam Tor shales is favoured. However, this interpretation does not justify the validity of trace elements as environmental discriminators because the chemical composition of some non-marine argillaceous sediments (Lebedev, 1967; Cosgrove, 1973) match those of marine seidments. In the present writer's opinion, comparison should be made with sediments laid down in the same basin of deposition. In later chapters the validity of trace elements for discriminating between marine and non-marine environments, will be tested.

4.11 Comparison with Average Shale, Sandstone and Crustal Abundance

Table 40 summarises the average trace element content of the Mam Tor shale and greywacke, together with average shale, sandstone and crustal abundance. Comparison between the trace element abundance shows some remarkable similarities and differences. The Mam Tor shales show good agreement with average shale (anal. 3) except that Cr and Pb, Ba and Sr are at variance. The first two elements show an enrichment while the last two show some dilution in the Mam Tor shales as compared to the average shale. Taking into account the greater clay content of the greywackes, the trace elements show an enrichment compared to the average sandstone (anal. 4). It seems that, in most cases, the concentration of

TABLE 40: Average Content of Trace Elements in the Mam Tor Shales and Greywackes, Compared to those of Shale, Sandstone and Crustal Abundance

Element ppm	1	2	3	4	5	6	7
Ni	79	37	68	2	75	2	78
Co	12	16	19		25	2	50
Mn	548	857	850		950	230	1320
V	138	59	130	20	135	16	240
Cr	167	84	90		100	22	120
Zn	84	67	95	16	70	45	82
Cu	45	17	45		55	13	110
Rb	130	37	140	60	90	220	22
Sr	107	75	300	20	375	250	180
Y	39	29	26	40	33	13	25
Zr	152	253	160	220	165	210	100
Pb	46	19	20	7	13	49	8
Ba	459	227	580		425	1220	180

1 - Average Mam Tor shales

2 - Average Mam Tor greywackes

3 - Average shale

4 - Average sandstone

5 - Average crustal abundance

(3-5 from Turekian and Wedepohl, 1961)

6 - Granite G-1

7 - Diabase W - 1

(6-7 from Mason, 1966)

trace elements in greywackes fall between that of the shale and sandstones. This is anticipated in as much as greywackes are a mixture of shales and sandstones (except volcanic greywackes).

When compared with the estimate of crustal abundance (anal. 5) some elements show either enrichment or impoverishment. If the shales are considered, just for the purpose of comparison, to be the final product of igneous rock weathering, it is apparent that there is an enrichment in Cr, Rb and Pb, and impoverishment in Mn, Sr and Mn. Similarly, comparison of Mam Tor greywackes with the crustal abundance indicates that most of the trace element contents fall between the estimates of acidic and basic igneous rocks (anals. 6,7). It seems, however, that enrichment or dilution of trace elements has taken place during the formation of the Mam Tor sediments and a knowledge of the mechanisms of element enrichment in argillaceous sediments should explain their distribution. The major factors of sorption, precipitation and organic processes have been reviewed by Krauskopf (1955), but unfortunately their relative importance is uncertain.

4.12 Conclusions

The results obtained from the present study are in accord with the proposed origin of the Mam Tor rocks (see Chapter 1). Mineralogical and chemical analyses of whole rock samples (Table 23) represent two lithofacies. These are the argillaceous sandstones (greywackes) which were originally deposited in shallower water on the delta slopes and later transported by turbidity currents and by the shales deposited in deeper parts of the basin ('basin shales'). The former contain a notable concentration of quartz and feldspar, while the latter are relatively enriched in clays and clay minerals. This variation in clay

mineral content is, in the first place, a function of several factors operated during weathering, transportation and those which prevailed in the depositional environments. The similarity of the clay mineral suite in both greywackes and shales suggests that the source area was the same. Therefore sorting, and possibly abrasion, were probably the most important factors influencing the distribution of transported detritus. However, studies on modern basins filled with turbidites in the western North Atlantic (Horn et al. 1971) and in the Redondo submarine canyon, Santa Monica (Beer and Grosline, 1970; see also Chapter 3), demonstrate that sorting is the major factor influencing sediment properties. Increasing distance from shoreline or the main route of flow is matched by increase in clays and fine mica, which are mostly concentrated in the deeper part of the basin.

In the Mam Tor rocks, the effect of sorting is clearly shown not only by difference in clay content between adjacent shales and greywackes, but also within individual beds. This is reflected by either fining upwards (normal graded bedding) with increase in clay content or coarsening upwards (reverse graded bedding) accompanied by decrease in clay content. Samples (2b, 2c) and ($4b_1$, $4b_2$) represent two greywackes beds, each of which were samples from the bottom and top. In the first bed the clay mineral content varies from 19.5% to 35.02% in the second bed from 19.01% to 36.57%. A reverse graded bedding is indicated by samples $6b_1$, $6b_2$ and $6b_3$ which also represent the bottom, middle and top parts of a single greywacke bed, respectively. The contents of clay minerals are 23.8%, 17.02% and 17.86% respectively. Similar variation is present between shales and silty shales (4a, 4c).

The clay mineral suite in both greywackes and shales is the same, consisting of kaolinite, illite + mixed layer, and chlorite. The distribution of these clay minerals in both lithofacies and their finer size fractions

seem to have been influenced by differential sedimentation, due to differences in their grain size and flocculation characteristics. Invariably, kaolinite dominates the clay mineral suite in both lithofacies, followed by illite + mixed layer and chlorite, but in the shales the amount of illite + mixed layer is higher than in the greywackes. On the other hand, study of various size fractions from both lithofacies demonstrated that the relative proportions of illite, and to a lesser extent chlorite, increase with decreasing grain size. Whereas kaolinite seemed to be relatively concentrated in the coarse clay and silt fractions. The higher amounts of illite + mixed layer in the shales and finer size fractions suggest that differences in grain size and possibly differential flocculation have controlled its distribution. Chlorite distribution cannot be related to such effects only because it is partly of authigenic origin in the greywackes.

Kaolinite is more abundant in the greywackes on the basis of whole rock samples and the <2 μm fraction and probably indicates that kaolinite is relatively larger in grain size, being a characteristic of kaolinite originally supplied to the depositional site. Nevertheless, authigenic growth of kaolinite in these greywackes is an important diagenetic process which is likely to enhance its dominance and also its grain size. However, it is difficult, if not impossible, to resolve whether kaolinite enrichment in the greywackes is related to differential sedimentation or diagenesis. Differential sedimentation has been invoked to explain the abundance of kaolinite in near-shore sediments or sandstones (Pryor and Glass, 1961; Praham, 1966; De Segonzac; 1970), while on the other hand, authigenic clays in sandstones are common and kaolinite enrichment is widely reported (see Wilson and Pittman, 1977). The exclusion of one process, therefore, would augment the effect of the other. In the present

study, diagenetic changes are clear in the greywackes, while evidence from the shales is inconclusive.

High permeability of the greywackes was probably an important factor in promoting diagenetic alteration, whereas in the shales a lower permeability inhibited such diagenetic alterations. It may be reasonable therefore to suggest that clay minerals in the shales more nearly represent a detrital suite although this does not exclude minor modification during transport and deposition, or even after burial diagenesis. It involves a simple reconstitution process through sorption, but evidence is lacking. X-ray study of illite crystallographic properties indicated that the Mam Tor rocks have not been subjected to deep burial metamorphism (in the zone of normal diagenesis) and this is supported by the poorly crystalline nature of illite (1 Md polymorph). Hence the proposition that clay minerals in the shales are detrital seems to be reasonably justified. The abundance kaolinite in the Mam Tor shales, and the even more abundant kaolinite in the greywackes supports a primary detrital origin.

Expected differences in chemical composition between shales and sandstones are evident and these are indicated in the shales by increase in the content of clay-related major elements, namely Al_2O_3, Fe_2O_3, FeO, MgO, K_2O and some TiO_2. Further support is obtained from the data of various size fraction from which it can be shown that the above elements are concentrated by clays and clay minerals. Higher CaO content in the greywackes is primarily due to authigenic calcite. In a similar manner, most trace elements,apart from Zr, Y and Co, seem to be invariably enriched in the shale and finer fractions of both shales and greywackes.

The difference in absolute contents of trace elements is essentially dependant on lithology, shales being enriched in trace elements, while

greywackes are relatively depleted. Presumably the original detrital fine clays have these elements accommodated in their structure and possibly adsorped on them and dilution by increase in quartz and feldspar contents decreases the absolute amounts of these elements. However, depositional environment and rate of sedimentation may have played a secondary role in enhancing trace element concentrations in the clays through sorption, but evidence is inconclusive. In addition, diagenesis in the greywackes, has probably modified inter-element relations, indicated by the variation of element-pair ratios. These ratios are usually more variable and/or higher in the greywackes compared to shales, the latter showing better consistency in their element-pair ratios. This may also indicate that these shales have not been diagenetically altered. The correlation between most of these trace elements and clay minerals, or related major elements, may suggest that diagenetic changes occurred without significant loss or gain of these elements. However, in the greywackes it may have involved a redistribution of some elements.

The lack of significant differences in chemical composition except those related to textural variations, may indicate that authigenic mineral formation in the greywackes occurred in a relatively closed system. In other words, the required major elements were supplied by the decomposition of originally detrital minerals. Pyrite, siderite (in the shales) and calcite are quantitatively unimportant in the Mam Tor rocks, although their formation is compatible with alkaline reducing conditions. On the other hand, pyrite and siderite were regarded as detrital in the greywackes (Allen, 1960). The necessary major elements for authigenic kaolinite and chlorite formation in the greywackes were made available by the decomposition of K-feldspar and biotite. Organic

CHAPTER 5

Tansley Borehole

The purpose of this Chapter is to distinguish geochemical characteristics of marine and non-marine sediments of Carboniferous age. Previously established palaeontological evidence is used in interpreting the geochemical data. In addition, this borehole succession extends the age range of the Namurian sediments examined, and also the lateral variation in the facies when compared to the Mam Tor beds.

The major stratigraphical and lithological units of the succession were described in detail in Chapter 1 (see page 27). A total of seventy three samples were studied from the various units (68 Namurian, 2 Visean and 3 volcanic toadstones or mudstones). The sequence is confined to rocks between the Ashover Grit (R_2) and the Carboniferous Limestone Series (D_2) which is underlain by the Upper Lava of Matlock. The upper part of the succesion (173.5 m) consists of non-marine shales or mudtones, siltstones and sandstones which are characterised by plant and fish fragments. Below this Lingula appears at a depth of 178.5 m indicating brackish water conditions. This is followed by goniatite and other fauna bearing shales which consitute the main marine part. Within the latter, samples between 185.4-198.3 m and another sample at 205.8 m are non-marine (following Ramsbottom et al. 1962 description). The Namurian succession extends down to a depth of about 288 m.

5.1 Major Elements and Mineralogy

The major element analyses and mineralogical data are lised in Appendix 2. The range and mean values together with the standard deviations are shown in Table 41.

5.1.1 Shales (Mudstones)

After deducting the quartz values from the total SiO_2 and excluding the sandstones, the volcanic clays and some of the highly calcareous shales, the ranges, means and standard deviations of the major elements in the non-marine and marine shales are listed in Table 42. It can be seen that quartz, combined silica, TiO_2, Al_2O_3, FeO and Na_2O contents are slightly higher in the non-marine shales. In contrast Fe_2O_3, CaO, SO_3, CO_2 and organic matter contents are higher in the marine shales. However, individual non-marine shales, occasionally may show high organic matter content which is most probably related to the type of organic matter in the non-marine and marine shales. Sulaiman (1972) found a high organic carbon content consisting of plant fragments in the Namurian argillites of Ireland, which have been deposited in near shore (fresh-brackish) environments. Nevertheless, the non-marine shales in the present study are characterised by the presence of plant fragments (Ramsbottom et al. 1962). Degens et al. (1957) showed that the organic fraction in marine shales is finely dispersed throughout the clay, whereas in fresh water shales, both finely dispersed and large fragments are found. Therefore it seems likely that organic matter is of different types in the non-marine and marine sediments.

MgO and K_2O show no significant difference between the two groups of shales, whereas MnO and P_2O_5 contents are slightly higher in the non-marine than in the marine shales.

The recasting of chemical analyses in terms of minerals (Appendix 2) helps to explain these variations. Minerals showing variations in their contents are also shown in Table 42. The excess silica may represent the error in the XRD method for quartz determination, even though the non-marine shales generally show higher content of excess silica than

TABLE 41: Ranges, Means and Standard Deviations of Major Elements and Minerals in the Tansley Borehole Rocks (73 samples)

Oxides/Minerals	Range	Mean	S.D.
Quartz	10.20-63.45	23.06	10.24
Combined Silica	10.49-37.69	27.49	5.92
TiO_2	0.12- 2.45	0.77	0.30
Al_2O_3	5.66-25.54	17.40	5.30
Fe_2O_3	0.42-23.41	5.50	4.13
FeO	0.14-21.14	2.21	3.29
MgO	0.40-10.76	1.89	1.35
CaO	0.15-22.70	3.23	4.96
Na_2O	0.03- 1.39	0.60	0.28
K_2O	0.74- 5.13	2.39	0.60
MnO	0.01-0.62	0.12	0.12
P_2O_5	0.01- 0.69	0.15	0.10
SO_3	0.00-13.28	2.54	2.57
CO_2	0.00-27.08	3.75	5.73
H_2O^+	0.88- 8.55	5.54	1.95
Org. C.	0.00-11.90	3.13	2.23
Chlorite	0.00- 8.02	4.12	1.85
Illite + MXL $^+$	3.30-43.36	23.74	6.78
Kaolinite	0.47-40.76	20.77	10.72
Na-feldspar*	0.18- 8.46	3.64	2.39
K-feldspar*	0.88- 9.39	3.28	2.51
Siderite*	0.84-42.72	7.66	11.49
Dolomite*	0.24-43.58	5.70	9.45
Calcite*	0.20-36.31	7.34	8.70
Pyrite*	0.04- 9.91	2.10	2.02
Apatite	0.03- 1.63	0.37	0.24
Excess Fe_2O_3	0.34-10.21	3.09	1.82

*Calculated for samples containing these minerals only

+Mixed Layer

TABLE 42: Ranges, Means and Standard Deviations of Major Elements and some Minerals in the Marine and Non-Marine Shales, Tansley Borehole (Namurian)

Oxides/Minerals	Non-Marine			Marine		
	Range	Mean	S.D.	Range	Mean	S.D.
Quartz	12.42-39.56	23.22	7.36	10.20-25.55	18.78	3.29
Combined Silica	16.32-37.69	30.45	5.03	15.53-32.63	26.41	4.44
TiO_2	0.47- 1.09	0.85	0.14	0.47- 0.94	0.72	0.12
Al_2O_3	11.74-25.54	20.56	3.93	12.35-22.65	17.91	2.85
Fe_2O_3	1.42- 6.65	3.07	1.32	2.21-10.66	7.97	1.78
FeO	0.64-21.14	3.82	4.40	0.24- 7.26	0.96	1.34
MgO	0.92- 3.17	1.69	0.45	1.17- 3.19	1.65	0.45
CaO	0.24- 2.07	0.55	0.42	0.30-14.26	4.19	3.29
Na_2O	0.14- 1.21	0.68	0.24	0.36- 0.84	0.53	0.13
K_2O	1.22- 3.61	2.35	0.51	1.74- 3.02	2.49	0.35
MnO	0.02- 0.62	0.13	0.14	0.02- 0.41	0.10	0.07
P_2O_5	0.03- 0.69	0.19	0.13	0.07- 0.27	0.15	0.05
SO_3	0.00- 3.96	0.91	1.05	0.68- 7.28	4.07	1.65
CO_2	0.00-18.43	2.09	4.24	0.00-12.75	3.56	3.90
H_2O^+	2.56- 8.55	6.14	1.80	4.03- 8.32	6.15	1.17
Org. C.	0.19- 9.05	2.66	1.70	1.45-11.90	4.48	2.27
Chlorite	0.00- 8.02	5.099	1.72	0.00- 5.60	3.36	0.96
Illite + MXL+	16.52-28.96	23.18	4.77	11.14-33.28	26.37	4.72
Kaolinite	12.66-40.76	28.88	8.00	2.56-28.05	17.66	6.35
Pyrite	0.00- 2.39	0.73	0.70	0.60- 4.94	3.09	1.15
Calcite	0.00- 1.59	0.62	0.48	0.00-21.31	8.31	6.42
Total Feldspar	0.00-11.78	4.37	3.46	0.00- 4.83	2.98	1.27
Siderite+	0.84-42.72	7.66	11.49			

+Confined to non-marine samples

the marine ones. In addition some error in employing the XRD method for feldspar determination is likely but nevertheless the variations between the shales is apparent. This random error is indicated by the mean and standard deviation of excess silica in both groups. In the first they are 4.33 and 2.96 while in the second they are 3.35 and 1.71 respectively. It is evident that the non-marine shales (samples 1-28) are enriched in kaolinite and feldspars, whereas the marine shales are characterised by higher contents of illite and calcite. Statistical test of the confidence interval for the population means using a 95% confidence level showed that kaolinite, illite and calcite distributions are significantly different,while that of feldspar is not certain. However, some of the non-marine shales (samples 15,16,17) have a higher illite content, but the difference shows only a very slight shift in clay mineral percentages as compared to the subtle or moderate variation in the marine shales.

Further evidence is provided by the non-marine shales (samples 37-45) which are interbedded within the marine sequence at different levels. The transitional phases (samples 37,38,39) still contain abundant illite while the rest (samples 40-45) show enrichment in kaolinite. This trend of variation is further substantiated by a non-marine shale (sample 51) which occurs lower in the succession in the marine shales because intercalated lower down the sequence, again the kaolinite content is higher than illite. This indicates that the pattern of clay mineral variation is related to depositional environment and is not age controlled. Similar studies on clay mineral variations and depositional environments have been reported from a vertical sequence of deltaic cyclothems, by Brown et al. (1977) who concluded that a change from normal salinities in the marine environments to brackish and fresh water conditions is accompanied by a decrease in illite and an increase in kaolinite. In the present

study however, it is also clear that carbonates (calcite and dolomite) are enriched in the marine shales, particularly those near the base of the Namurian (samples 65,55,67,68) and the top of the Visean (samples 69,70). Carbonate rich shales contain less kaolinite than those with little or no carbonate.

Nevertheless, some of the carbonate rich marine shales (samples 54, 58) show only a slight increase in illite content. The reduction in kaolinite content in most of the carbonate-rich marine shales is in accord with the findings of Grim et al. (1937), Millot (1949, quoted by Grim, 1951), Degens et al (1957) and Amin (1975), who found that illite is the dominant clay mineral in marine sediments but where the sediments are highly calcareous or dolomitic, kaolinite is either absent or present in minor amounts. On the other hand, Brown et al. (1977) found that lateral variations from open-marine to a lacustrine limestone coincide with a decrease in illite and an increase in kaolinite.

It follows that in the sequence of the Namurian sediments, the abundance of specific clay minerals seems to be related to variation in the depositional environments based on fossil evidence. Moreover, pyrite is usually present in higher amounts in the Namurian marine shales than in the non-marine ones. In contrast, siderite is confined to the non-marine shales. A statistical test showed that both of these mineral distributions are significantly different in the two groups. Dolomite is present in both marine and non-marine shales and it is of the ferroan type as revealed by XRD study (30.85 2θ). In a similar manner chlorite shows no preference for either marine or non-marine shales.

Both P_2O_5 and MnO have their highest concentrations in samples 26 and 44, which have the highest siderite content. Therefore the presence of siderite would explain the slightly higher mean values of P_2O_5 and MnO

in the non-marine shales. Tentatively, these relationships may indicate the association of Fe/Mn phosphate mineral (vivianite, $Fe_3(PO_4)_2.8H_2O$) with siderite. On the basis of thermodynamic data it is well documented that in fresh and lacustrine anaerobic environments, vivianite is unlikely to form where large amounts of dissolved sulphides are generated (Nriagu, 1972; Nriagu and Dell, 1974). However because vivianite is unstable, it is unlikely to be preserved in the geological record (Nriagu, 1972) and presumably may well form apatite which might explain its absence or presence in altered form in the non-marine shales of the present study.

The most striking observations about the major elements and mineralogy of the non-marine sediments is that one sample (No. 3) contains the highest proportion of illite and pyrite and can be easily mistaken for a marine. Accordingly, the use of clay mineral relative abundances and iron minerals for environmental interpretation may be of limited application if used alone. The description of the part of the succession in which this sample is located by Ramsbottom et al. (1962) is as follows: it consists of dark grey to grey seatearth, about 1 m thick, sandy in the lower part with cubes of pyrite in the top 72 m. This is overlain by grey mudstones about 1.35 m thick, with nodules of pyrite and pyritous slickensides and there are coal traces at the base and scattered plant fragments. In fact sample No. 3 is situated near the top of the seat earth.

The type of clay mineral in seatearths or underclays may be dominantly illite or kaolinite but the illitic under clays are generally calcareous (Grim, 1951). The depleted character of the seatearth (sample No. 3) in carbonates, therefore, can be attributed to leaching under oxidising

conditions without any appreciable change in the clay mineral compositions, but the presence of minor amounts of pyrite contradicts such an interpretation. Marston (1967) studied the geochemical characteristics of seatearths from the Carboniferous Coal Measures, England, and concluded that the mineralogy of the seatearth was influenced by detrital sedimentation in relatively shallow water (swampy environments) with plant control affecting the degree of sorting, resulting in progressively finer sediments being laid down. Gradual silting up elevated the sediments above the watertable, subjecting them to oxidising conditions which inhibited the formation of diagenetic iron minerals and removed those already present. The principal clay mineral in these seatearths was illite.

Similarly, Nicholls and Loring (1962) analysed seatearths from the Carboniferous Coal Measures, North Wales. They found that illite is the dominant clay mineral in the top part of the seatearth in which significant pyrite was present. In contrast, carbonate decreased progressively from the bottom to the top of the seatearth. This pattern of variation in iron minerals suggested to them that the pH may have been falling slightly and that the Eh was also low. Their interpretation of the genesis of seat earth is that it does not represent a leached horizon, but is the product of slow sedimentation of intensely weathered detrital minerals in waters of progressively increased acidity.

Tentatively, the genesis of seat earth in the present study (sample No. 3) seems to accord better with the hypothesis put forward by Nicholls and Loring (1962).

Several marine shales contain a small amount of gypsum (11.70 2θ). This is certainly the result of pyrite oxidation in the presence of calcite or dolomite under atmospheric conditions. Similar findings have

been reported by Van Tassel (1971), Sulaiman (1972), Quigley et al. (1973), Pedersen et al (1975). The mean value of titanium content of the non-marine shales is slightly higher than that of marine shales. In this respect, Lebedev (1967), and Keith and Degens (1959) data on marine and freshwater clays and shales, indicate that titanium is relatively enriched in the non-marine sediments. Lebedev also stated that one of the most reliable indicators for separating marine from fresh water clays is titanium.

It must be noted that the lowest Namurian (samples 66,67,68) and uppermost Visean (samples 69,70) calcareous shales are marked by high content of excess silica in comparison to the rest of the shales in the succession (Appendix 2). This part of the sequence, the junction of Namurian and Visean, not only in the Tansley Borehole but through Derbyshire, is heavily mineralised and dolomitised with veins of pyrite, chalcopyrite, blende, calcite, fluorite, baryte, smithsonite and various other minerals (Gibson et al. 1913; Ramsbottom et al. 1962; Smith et al. 1967). In addition, chert, silica rocks and various degrees of silicification are commonly associated with these rocks (Orme, 1974). Extensive replacement of silica is commonly recorded in the juxtaposition of toadstones (volcanic lavas and tuffs) and mineral veins with the Visean Limestone. The commonest fabric of silica is microcrystalline quartz which appears sometimes to be cryptocrystalline (isotropic). Nevertheless, transition from chalcedony through lutecite to quartz can often be demonstrated, in a variety of replacement fabrics. Accordingly, it is likely that the high excess silica reported in the present study, represent partly silica of non-detrital origin. It is also interesting to note that Na-feldspar is present in these calcareous shales while the overlying marine shales are nearly devoid of it (Appendix 2).

5.1.2 Sandstones

The sandstones (samples No. 4,5,6,7,12) typically show high SiO_2 and Na_2O contents with low Al_2O_3, TiO_2, Fe_2O_3, SO_3 and organic matter contents (Appendix 2). Their mineralogy (Appendix 2) indicates that they are enriched in quartz and feldspar with small amounts of clay minerals and only traces of pyrite. Some of the sandstones have a relatively high CaO and MgO content, which is reflected by dolomite and a smaller amount of calcite. Apart from sample 12, most of them have a high content of K_2O similar to that of the marine shales and the non-marine silty shales (mudstones), but their mineralogy shows that feldspars are relatively abundant.

The mineralogical data deduced from chemical analysis and XRD study are in agreement with the results of petrographic study (see Chapter 3) which justify their classification as alkosic sandstone.

The relative abundance of specific clay minerals may be affected by errors in the XRD method employed for feldspar determination. Furthermore, the diagenetic alterations of feldspar to clay minerals in these sandstones make their use as environmental indicators unreliable. However, except for sample 4, it seems that kaolinite is either dominant or present in equal proportion to illite.

5.1.3 Volcanic Mudstones (K-Bentonites)

Samples 71, 72 and 73, in descending order are from the locally known 'toadstone clay' overlying the Upper lava of Matlock. These are thought to represent basaltic tuffs (Ramsbottom et al. 1962) containing highly altered fragments up to about 3 mm diameter (Williams et al. 1954).

The chemical nature of the toadstone clay precursor is not known in detail and the chemical data on the Derbyshire volcanic rocks (Table 43) are from altered basalt. The presence of high K_2O and Na_2O in these altered basaltic lava has been described by Sargent (1918) and Tomkeieff (1941). Sargent proposed that the term potash-spilite be given to these rocks attributing the association in Derbyshire of 'spilitic rocks' and basalts to the partial concentration prior to eruption of alkaline constituents in the upper part of the magma which were carried in a volatile state by upward movement of gases. In addition, the intense alteration of the spilitic rocks was ascribed to the action, shortly after extrusion, of hot residual solutions belonging to the lava itself. However, much controversy has raged concerning the origin of spilites (Williams et al. 1954; Oftedahl, 1958). In some instances they were regarded as primary types, in others they were attributed to reaction between the lava and sea water, and/or emanations given off by the lava itself.

In the present study, mineralogical calculations supported by X-ray analysis (Appendix 2) indicate that quartz and pyrite are present in larger amounts in samples 71 and 72, than in sample 73. Illite-smectite mixed layer mineral is the major clay mineral and characterised by broad symmetrical peak with average spacing of the basal 001/001 reflection ranging from 11.2-12.4Å. Glycolation produced no significant change in the peak position or shape, and a discrete illite peak was not observed, contrasting with the overlying shales in which the 10Å peak was usually present. Chlorite is present in minor amounts in the volcanic mudstones. Illite-smectite and chlorite are more abundant in sample 73, the former collapsed, although not completely, to illite on heating to 600°C. In addition, the peak intensity of anatase (25.32 2θ) which

TABLE 43: Chemical Analyses of K-Bentonites (Present Study), Derbyshire Lava and its Weathered Products

Oxide	1	2	3	4	5	6
SiO_2	43.33	43.96	52.85	43.13	45.50	51.00
Al_2O_3	9.65	9.20	18.16	23.25	22.90	23.56
TiO_2	1.29	1.30	2.45	-	4.40	2.94
Fe_2O_3	22.88	23.41	6.11	1.87	-	5.86
FeO	0.20	0.38	0.50	4.81	-	-
MgO	1.79	1.89	3.02	6.50	1.60	3.37
CaO	0.57	0.66	0.68	5.58	9.20	0.51
Na_2O	0.15	0.14	0.11	3.60	-	-
K_2O	2.61	2.70	5.13	3.04	-	-
MnO	0.06	0.02	0.01	trace	-	-
P_2O_5	0.02	0.01	0.01	-	-	-
SO_3	10.75	13.28	4.88	-	-	0.83
Ig. Loss	6.19	3.73	5.65	8.86	14.90	10.10
Total	99.49	100.84	99.56	100.10	98.40	98.11

1,2,3 - K-bentonites from the present study

4 - Spilitic lava, Tideswell Dale (Sargent, 1918)

5 - Greyish white clay (Garnet, 1923)

6 - Yellow tinted clay (Garnet, 1923)

is the principal TiO_2 bearing mineral, is more pronounded in the last sample that in the upper two. Kaolinite, however, was not detected on the XRD traces, although mineralogical calculations indicate its presence in small amounts. This may suggest that some SiO_2 and Al_2O_3 are present in amorphous phases of unidentifiable minerals, or could be too small in amount to be detected by XRD. Similarly, the excess Fe_2O_3 may be present in an amorphous form, since no other crystalline iron mineral, apart from pyrite and chlorite, were revealed by X-ray study. Alternatively it may partly be located in the illite-smectite.

In this respect, the petrographic description of a specimen from 338.58 m deep, at Tansley, by Elliot (in Ramsbottom et al. 1962, p.37) is relevant. "The rock contains fragments of highly altered basalt and fragments of feldspar set in a plentiful turbid brown cryptocrystalline matrix of clay minerals. The feldspars are completely replaced by clay minerals of low birefringence. Chlorite is present in irregular patches and in small vein-like areas. Some patches of chloritic material may be altered fragments of ferro-magnesian mineral, perhaps olivine. Rare small, subangular grains or quartz occur. Grains of pyrite are fairly common in the igneous fragments and in the mudstone." Illitic material was found to be the chief constitutent of the matrix. The underlying lava is also much altered, the commonest alteration products being chlorite, serpentine, calcite and other carbonates, quartz, leucoxene, iddingsite and iron ores. The least altered specimen to be examined was from 342.6 m at Tansley. Elliot reported that this rock contains pseudomorphs of serpentine, rimmed by iddingsite and iron ore after olivine, with lathes of labradorite and grains of augite. Interstitial patches are infilled by chlorite, sometimes by chalcedony while thin needles of apatite are a common contituent.

The subaerial weathering products from the Upper Lava of Matlock of Derbyshire, have been described by Garnet (1923). He found that the weathering of lava resulted in varying degrees of alteration; from the least weathered greenstone, through green earth, to the end product of white clay. The most abundant constituent was found to be ferrous clayey substance of no definite species, with variable amounts of quartz, calcite, pyrite, limonite and anatase, the last mineral formed by alteration of ilmenite. The original ferromagnesian minerals are completely eliminated and in an advanced stage of alteration even the ferrous substance was altered. The abundant white clay had the formula $2Al_2O_3.6SiO_2.3H_2O$ but its identity was not established.

Comparison of the chemical analyses of the altered lava described by Garnet and samples 71 and 72, reveals some differences and similarities in major element removal trends during alteration (analyses 5,6, Table 43). The most pronounced difrerence is that subaerial weathering results in concentration of Al_2O_3 and TiO_2 and to a lesser degree SiO_2, whereas samples 71 and 72 show a pronounced decrease, especially of Al_2O_3 and TiO_2. This difference most likely reflects the influence of environments or conditions under which alteration took place, the lava flows and ashes being regarded as contemporaneous with the limestones and of submarine origin (Arnold-Bemrose, 1907; Sargent, 1918; Francis, 1968).

Important to any interpretation of volcanic rock analysis is the evaluation of the degree and the effects of chemical weathering under sea water. The carboniferous volcanic mudstones may represent either deposition of volcanic ash or alteration of the crust of the lava itself. In both marine and freshwater environments increasing alteration is accompanied by increasing diffusion hydration, but submarine alteration of basaltic lava proceeds faster than that in fresh water and much faster

than in a subaerial environment (Moore, 1966). When the volcanic lavas erupted into the Carboniferous sea, the outer surface was quenched and formed an outer crust of basaltic glass. The latter, with time, in contact with sea water would hydrate to produce palagonite (Moore, 1966, 1970). Such palagonitic glass has been reported from the Matlock lavas (Smith et al. 1967). The alteration, however, may not take place at the time of extrusion of the submarine lava (Moore 1965). In Hawaiian submarine basalts, during replacement of the outer crust of basaltic glass by palagonite, Na, Ca and Mn are lost, and K, Ti and Fe are gained through exchange with sea water (Moore, 1966). Hart (1973) found that during low temperature alteration of basaltic lava by sea water, in oceanic layer 2, K is removed from sea water to form K-rich smectite and Mg to form chlorite while Si, Ca, Fe and Mn were added to sea water. Na, Al, and Ti remained relatively constant during basalt alteration processes. Thompson (1973) showed that K and Fe_2O_3/FeO ratio increases, while Si, Na, Ca, Mg and to a lesser degree Fe are depleted in the altered basalt. Al and Ti, remained more or less unaffected, but in extremely altered lava, Al is lost to sea water.

Chemical data on extraced soluble elements on ash from sub-aerial active volcanoes of central America, demonstrate that Na, Ca, Mn and SO_4 and much less K and Mg, were deposited on the ash surface from volcanic gases during eruption (Taylor and Stoiber, 1973). Presumably in submarine eruption these elements would have been rendered soluble in sea water. Attempts to find evidence for significant amounts of reaction between sea water and basaltic rocks has been extended by Maynard, 1976) who concluded that this interaction is potentially capable of removing K from sea water by low-temperature weathering and Na and Mg by higher temperature hydrothermal reaction with the release of SiO_2 to sea water. This is supported by the findings on chemical changes during alteration under marine and non-marine conditions. Pierce (1970) found that

alteration of basaltic glass under non-marine conditions resulted in a greater depletion of K, Ca and high enrichment of Fe and Ti than it would do under marine conditions. Potassium enrichment appears to be characteristic of submarine alteration, due to adsorption by authigenic clays. He also suggested that alteration took place during extrusion and cooling and that alteration was caused primarily by steam generated by subaqueous flow. Hay and Iijima (1968) found that SiO_2, Al_2O_3, MgO, CaO, Na_2O and K_2O were greatly reduced during alteration of basaltic tuffs caused by ground water circulation, whereas Fe_2O_3 and TiO_2 may show slight enrichment or depletion, suggesting that gradual microsolution precipitation, not hydration, is the mechanism. Moreover, a high pH (9 or more) and salinity were suggested to mark the critical level of rapid alteration. On the other hand, strong depletion, especially of alkalies, may be the result of extreme alteration in saline water (Pederson et al. 1975).

Experimental studies by Furnes (1975) suggest that the alteration process may be relatively rapid, or extremely slow depending mainly upon the following physico-chemical parameters:

(1) The chemical composition of the basaltic glass

(2) The chemistry of the aqueous environment

(3) The temperature during alteration

(4) A time factor

On the basis of this information and from the analysis of the Carboniferous volcanic mudstones, it is clear that the original basaltic lava has been subjected to high degrees of alteration through reaction with sea water. Comparison with the least altered basaltic lava from Derbyshire (Table 43) indicate certain differences or provide a suggestion as to the overall chemical trend of the alteration processes. The volcanic

mudstone, in the present study, show further depletion in CaO and Na_2O which indicates that the feldspars are nearly completely altered. Likewise FeO shows a marked loss and to a lesser extent MgO, suggesting much alteration of the original ferromagnesian minerals or even the secondary chlorite formed as an alteration product of the former minerals. Similarly, Al_2O_3, TiO_2 and K_2O must have been relatively mobile as shown by their substantial loss in samples 71 and 72 in comparison to 73. When the major elements Al_2O_3, TiO_2, MgO and K_2O of 71 and 72 are normalised to the Al_2O_3 of 73, the two-fold increase indicates the quantities of these elements lost during the toadstone clay forming processes. The data also suggest that FeO, CaO and Na_2O must have been the most mobile elements. The increase in Fe_2O_3 in the upper two samples is partly due to the abundance of pyrite.

Although SiO_2 showed some depletion in the upper two samples relative to the third, the amount of quartz is higher in the former. It follows then that the alteration of ferromagnesian minerals or their secondary products has resulted in a major loss of SiO_2 which subsequently formed authigenic quartz. The abundance of authigenic quartz, among other minerals in or associated with tuffs as an alteration product of the original minerals, is well documented (Hay, 1966; see references in Hsu and Jenkyns, 1974; Boles and Coombs, 1975).

The overall pattern of alteration may be summarised as follows. The original composition of the lava is a function of fractional crystallisation of the magma and reaction of the lava with sea water and possibly hot emanations from the lava itself were accompanied by changes of the original mineral assemblage. Subsequently, a wide variety of secondary minerals could have been formed depending on the original minerals, composition of the fluids (ion activities) and pressure-temperature conditions. Continued high temperature reaction of these

secondary minerals with sea water or entrapped pore fluids immediately after eruption resulted in loss of Na_2O, CaO, MgO, K_2O, Al_2O_3, TiO_2 and SiO_2 with the oxidation of Fe to Fe_2O_3. The final alteration products seem to be illite-smectite, chlorite, quartz and pyrite. Similar results from altered submarine lava has been reported by Matthews (1971) who demonstrated the conversion of glass to palagonite and its subsequent alteration to pale coloured clay minerals (montmorillonoids and chlorite). The alteration of basaltic lava was accompanied by a large net loss of MgO and CaO, a marked oxidation of Fe, and gain in K_2O. The conversion also results in some loss of SiO_2 which subsequently formed chalcedony. He envisaged that glass conversion to palagonite took place at high temperatures after eruption, while the alteration of palagonite to montmorillonoids and chlorite occurred within the cold aqueous environment of the sea floor.

5.2 Comparison with other K-Bentonites

The abundance of illite-smectite clay minerals are responsible for the high potassium content of the volcanic mudstones described in the present study. This is typical of K-bentonites which have been described widely from Palaeozoic rocks (Weaver, 1953,1963; Bystrom, 1954; Mossler and Hayes, 1966; Bjorlykke, 1971). More recently, Trewin (1968) described K-bentonites from the Namurian of North Staffordshire and of Edale, Derbyshire. He also showed that these K-bentonites can be correlated with boreholes at Ashover, specifically the Tansley Borehole, from which the K-bentonites in the present case are described. The description given by these authors are similar to those outlined here. They were shown to consist of randomly interstratified mica smectite and formed by alteration of volcanic ash under saline-marine conditions. A slight difference however, was the presence of kaolinite in the K-bentonites described by Trewin (1968). These beds were also shown to be mineralogically

distinct from the associated sediments which contain detrital quartz, organic matter, chlorite and a prominent 10Å clay mineral. These are in accord with the results of the present study.

An important difference between the K-bentonites and the enclosing sediments in the present study, is their higher TiO_2 content and to a lesser extent Zr in the least altered K-bentonite (see trace element data, Appendix 2). These are certainly inherited from the original volcanic materials. Such minerals, or elements, were shown by Weaver (1953) to be restricted to K-bentonites formed entirely from the alteration of volcanic material. Following these descriptions, it seems that some of the alteration products among others, of volcanic material interacting with marine waters, are smectite and illite-smectite clay minerals.

The influence of marine water on the alteration of volcanic tuff is already described and this can be supported indirectly by the clay mineralogy of another suite of altered tuffs, namely tonsteins. These are commonly associated with Coal Measures sediments. A detailed account of the X-ray identification of clay mineralogy and chemistry appears in Spears (1966, 1970, 1977) and Price and Duff (1969). Tonsteins are characterised by abundant kaolinite but a few tonsteins at greater distance from the coal contain illite-smectite mixed layer in addition to a minor kaolinite. The kaolinitisation of the original volcanic tuff was attributed to intense alteration in swampy, peaty, or fresh water environments, providing the system reamins open (Spears, 1971). Spears also suggested that, in addition to acidic water in the peat environment, the concentration of ions must be low to promote the kaolinitisation of the tuff whereas alteration of tuff to illite-smectite was ascribed to less intense action away from the coal environment requiring a closed system of high salinity. These latter tonsteins therefore, may be

regarded as true K-bentonites. Hence it is concluded that volcanic tuff may be alterated to eithertonsteins or K-bentonite depending probably on the salinity of the environment. De Segonzac (1970, p.293) remarks that early diagenetic transformation of volcanic ash in alkaline environments (marine or lacustrine) result in montmorillonite, while similar transformation of tonsteins to kaolinite occur in acidic environments.

Comparison of chemical analyses of the Namurian K-bentonites with other K-bentonites, altered lava and bentonites composed essentially of montmorillonite are shown in Table 44.

The least altered, Namurian K-bentonite (anal. 3) is mineralogically similar to Ordovician K-bentonites from Wales (anal. 4) and Pennsylvania, U.S.A. (anal. 5) but has a lower Al_2O_3 and Na_2O, and higher TiO_2 and Fe_2O_3. The highly altered Namurian K-bentonites (anal. 1, 2) show a marked loss in most elements and a major gain in Fe_2O_3. The high Na_2O content in K-bentonite from Wales was attributed to plagioclase (Bjorlykke, 1971) and both Ordovician K-bentonites were considered to be the result of alteration of tansported volcanic ash in marine environments (Weaver, 1953; Bjorlykke, 1971). Similarities, between the present K-bentonite (anal. 3) and the most altered basaltic lava from the north-east Atlantic (anal. 6) are also apparent. In the latter, however, plagioclase has been replaced by potash feldspar which in turn was altered to sericite with montmorillonoids and chlorite as the predominant minerals (Matthews, 1971).

Bentonite composed of a relatively pure montmorillonite or smectite (anal. 7,8) may either have similar or higher SiO_2 and Al_2O_3, the latter case attributable at least partly to concentration of smectite in the -1μ m fraction.

TABLE 44: Comparison of the Namurian Volcanic Mudstones with other K-Bentonite, Altered Lava and Bentonites

Oxide	1	2	3	4	5*	6	7*	8*
SiO_2	43.33	43.96	52.85	51.30	50.65	47.11	54.24	64.46
Al_2O_3	9.65	9.20	18.16	20.15	27.37	18.37	17.60	21.98
TiO_2	1.29	1.30	2.45	1.65	0.35	1.55	0.50	
Fe_2O_3	22.88	23.41	6.11	2.24	1.15	8.74	4.31	8.03
FeO	0.20	0.30	0.50		0.31	0.16		
MnO	0.06	0.02	0.01		0.002	0.14	0.02	
MgO	1.79	1.89	3.02	0.90	3.75	1.84	3.88	3.38
CaO	0.57	0.66	0.68	0.22	0.73	2.34	1.06	0.02
Na_2O	0.15	0.14	0.11	2.51	0.16	2.41	2.16	0.03
K_2O	2.61	2.70	5.13	5.16	5.89	3.84	0.12	0.79
P_2O_5	0.02	0.01	0.01	0.10	0.03		0.03	
SO_3	10.75	13.28	4.88		0.01			
Ig. Loss	6.19	3.73	5.65		9.26	14.12	15.62	
Total	99.49	100.84	99.56		99.48	100.26	99.55	98.69

*Purified bentonites

1,2,3 - From present study

4 - Ordovician K-Bentonite, Wales (Bjorlykke, 1971)

5 - Ordovician K-Bentonite, Pennsylvania, U.S.A. (Weaver, 1953)

6 - Most altered lava, Swallow Bank, NE Atlantic (Matthews, 1971)

7 - Ordovician bentonites, Utah, U.S.A. (Salughter and Earley, 1965)

8 - Upper Miocene bentonites, Germany (Grim and Guven, 1978)

(5 and 8 from -1 μm fractions)

The msot significant difference is their depletion in K_2O compared to K-bentonites. Surprisingly, these latter bentonites are also interbedded in a marine succession, either as originally transported volcanic ash in the case of the Ordovician bentonites, Utah, U.S.A. (Slaughter and Earley, 1965) or by alteration in situ of volcanic tuff in the Miocene bentonites, Germany (Grim and Guven, 1978).

5.3 Statistical Correlation

In the previous chapter, statistical correlation proved to be a helpful method in revealing inter-element associations and element-mineral relationships. The Tansley Borehole sequence includes different lithologies and statistical correlation might point to the most likely variations in mineralogy and chemistry. The correlation coefficient (r) for seventy-three samples (71 degrees of freedom) at the 95% significance level is 0.230. The correlation matrix is shown in Table 45, with those significant relationships between bivariant elements underlined. The correlation groups or linkage trains formed by covarying variables are also listed in Table 45. It must be noted that this correlation matrix includes major element data from Namurian sandstones, two calcareous mudstones (Visean) and volcanic mudstones, in addition to those of the marine and non-marine mudstones (silty shales) and shales.

The first group includes quartz and Na_2O, suggesting the covariation of plagioclase and quartz. The second group comprises combined SiO_2, TiO_2, Al_2O_3, K_2O and H_2O^+, which largely reflects the association of these oxides with the clay minerals,although small amounts of combined silica, Al_2O_3 and K_2O are also present in feldspars. Nevertheless, the high TiO_2 content of the volcanic mudstones, present in the forms of anatase, is most likely to enhance the correlation coefficient value of TiO_2.

TABLE 45: Correlation Matrix of Major Element of the Tansley Borehole Rocks (73 Samples)

	Qtz	Combsi	TiO_2	Al_2O_3	Fe_2O_3	FeO	MgO	CaO	Na_2O	K_2O
Qtz	1.000									
Combsi	-0.1245	1.0000								
TiO_2	-0.2032	(0.4934)	1.0000							
Al_2O_3	-0.4083	(0.7327)	(0.5147)	1.0000						
Fe_2O_3	-0.3230	-0.3170	0.2052	-0.1553	1.0000					
FeO	-0.0156	-0.2186	-0.1039	-0.0694	-0.2483	1.0000				
MgO	-0.2134	-0.5028	-0.1895	-0.3632	-0.0276	0.1225	1.0000			
CaO	-0.2883	-0.5413	-0.5162	-0.5803	0.0507	-0.1415	(0.5112)	1.0000		
Na_2O	(0.6639)	0.1836	-0.1467	0.0515	-0.4712	0.0902	-0.3047	-0.4295	1.0000	
K_2O	-0.2361	(0.4637)	(0.7431)	(0.4533)	(0.2327)	-0.3745	-0.2067	-0.3179	-0.2109	1.0000
MnO	-0.0543	-0.5103	-0.3045	-0.3278	-0.1333	(0.6050)	(0.5581)	(0.2910)	-0.0516	-0.4048
P_2O_5	-0.4036	-0.1948	-0.2221	0.0425	-0.2027	(0.7007)	0.1879	(0.2387)	-0.1777	-0.3321
SO_3	-0.2919	-0.3188	0.1993	-0.1917	(0.9370)	-0.2862	-0.0160	0.1023	-0.4839	(0.2763)
CO_2	-0.2533	-0.6705	-0.5523	-0.6154	-0.0596	(0.3554)	(0.6762)	(0.8434)	-0.3883	-0.5166
H_2O^+	-0.5459	(0.6032)	(0.4842)	(0.8944)	0.1404	-0.2601	-0.2909	-0.4395	-0.1222	(0.4499)
Org. C.	-0.3893	-0.0015	-0.1823	0.1847	0.1543	-0.2845	-0.0136	0.1278	-0.2317	-0.0663

TABLE 45 (cont.): Correlation Matrix of Major Elements of the Tansley Borehole Rocks (73 Samples)

	MnO	P_2O_5	SO_3	CO_2	H_2O^+	Org. C
MnO	1.0000					
P_2O_5	(0.4920)	1.0000				
SO_3	-0.1594	-0.2048	1.0000			
CO_2	(0.6079)	(0.5260)	-0.0309	1.0000		
H_2O^+	-0.3650	-0.0794	0.0772	-0.5606	1.0000	
Org. C.	-0.1393	-0.0132	0.0600	-0.0139	(0.3376)	1.0000

TABLE 45 (Cont.): Correlation Groups

Group 1

	Qtz.	Na_2O
Qtz	1.0000	
Na_2O	0.6639	1.0000

Group 2

	Combsi	TiO_2	Al_2O_3	K_2O	H_2O^+
Combsi	1.0000				
TiO_2	0.4934	1.0000			
Al_2O_3	0.7327	0.5147	1.0000		
K_2O	0.4637	0.7431	0.4533	1.0000	
H_2O^+	0.6032	0.4842	0.8944	0.4499	1.0000

Group 3

	Fe_2O_3	K_2O	SO_3
Fe_2O_3	1.0000		
K_2O	0.2327	1.0000	
SO_3	0.9370	0.2763	1.0000

Group 4

	FeO	MgO	CaO	MnO	P_2O_5	CO_2
FeO	1.0000					
MgO		1.0000				
CaO		0.5112	1.0000			
MnO	0.6050	0.5581	0.2910	1.0000		
P_2O_5	0.7007		0.2387	0.4920	1.0000	
CO_2	0.3554	0.6762	0.8434	0.6079	0.5260	1.0000

The third group consists of Fe_2O_3, K_2O and SO_3, but Fe_2O_3 correlation with SO_3 is much stronger than that with K_2O or SO_3-K_2O which is attributed to the abundance of pyrite in the marine part of the sequence. In addition, illite is also abundant in the marine shales and it is possible that their covariation is reflected in the correlation of their respective oxides. Such an association of pyrite and illite in marine shales has been reported by Spencer (1966). The fourth group includes FeO, MgO, CaO, MnO, P_2O_5 and CO_2 indicating their occurrence in carbonates. The organic matter seems to be independent of all major elements except H_2O^+. This lack of significant relation is due to the abundance of organic matter in some of the non-marine shales which would mask its covariation, whereas organic matter-H_2O correlation is possibly influenced by some samples in which both of these constituents are abundant. Some of the significant correlations between bivariant elements are shown as scatter plots in Figure 30.

It may be of interest to see the corresponding correlation matrix excluding the sandstones and volcanic mudstones whose high content of some elements may overshadow significant relations within the shales and calcareous shales. The correlation coefficient for sixty-six samples at the 95% significance level is 0.243. The correlation matrix is shown in Table 46, with the significant relation underlined.

Comparison with the first correlation matrix shows that the relation of quartz and Na_2O in the first group is still significant but less strong as evidenced by the lower value of correlation coefficient due to the exclusion of the sandstones. This suggests that plagioclase is present which is in agreement with the mineralogical results. The improved correlations of the combined silica and Al_2O_3 with Na_2O suggests that some Na_2O is also present in the clay minerals. In the second group of combined

FIGURE 30 Scatter Plots of some Positive and Significant Bivariant Relationships between Major Elements, Tansley Borehole.

1. Sandstones
2. Shales
3. Siltstones or Silty Shales
4. Carbonate Rich Shales and Siltstones
5. Volcanic Clays

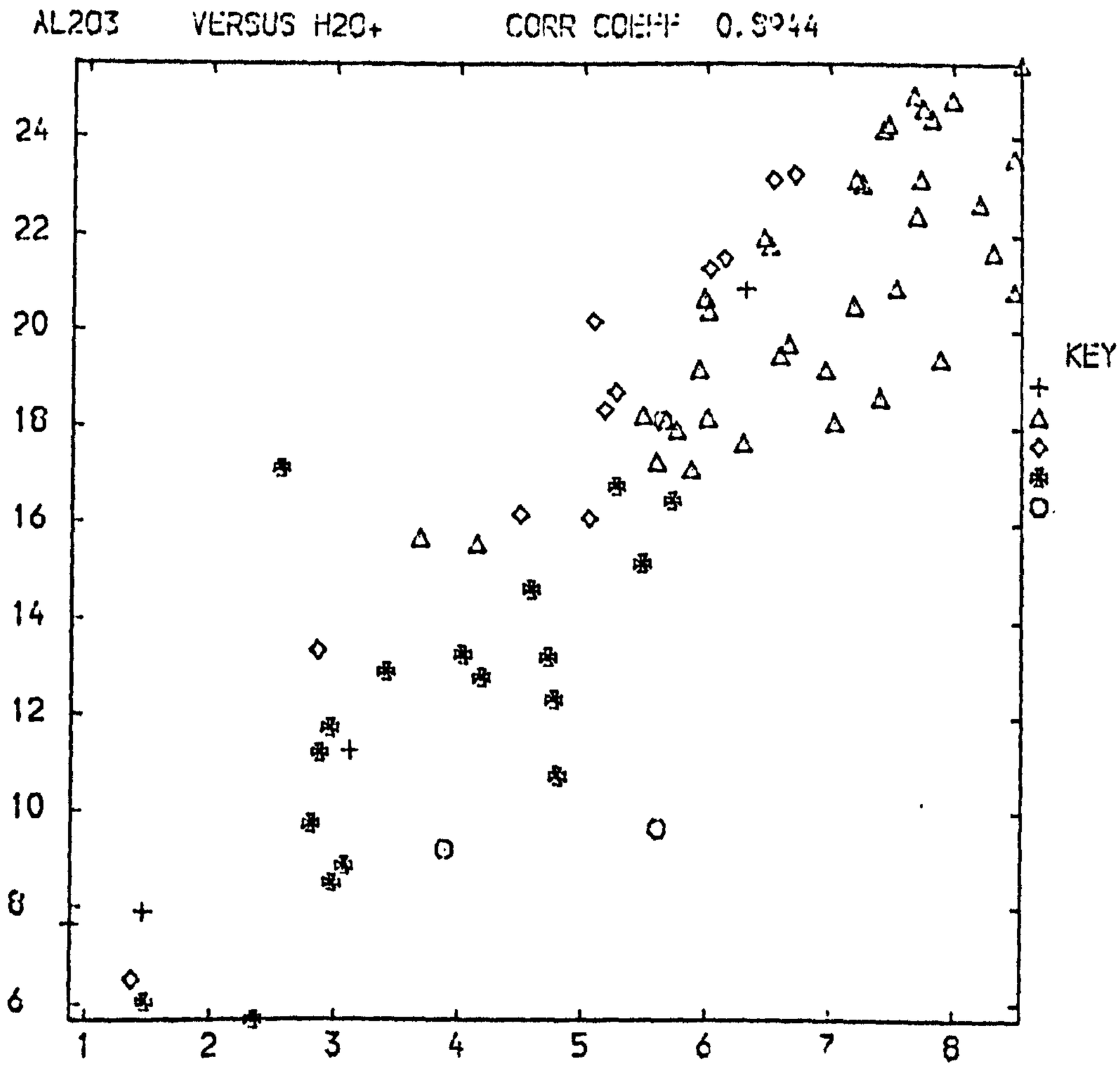
AL203 VERSUS H2O+ CORR COEFF 0.9944
24
22
20
18
16
14
12
10
8
6
1
2
3
4
5
6
7
8
KEY
+
△
◇
O

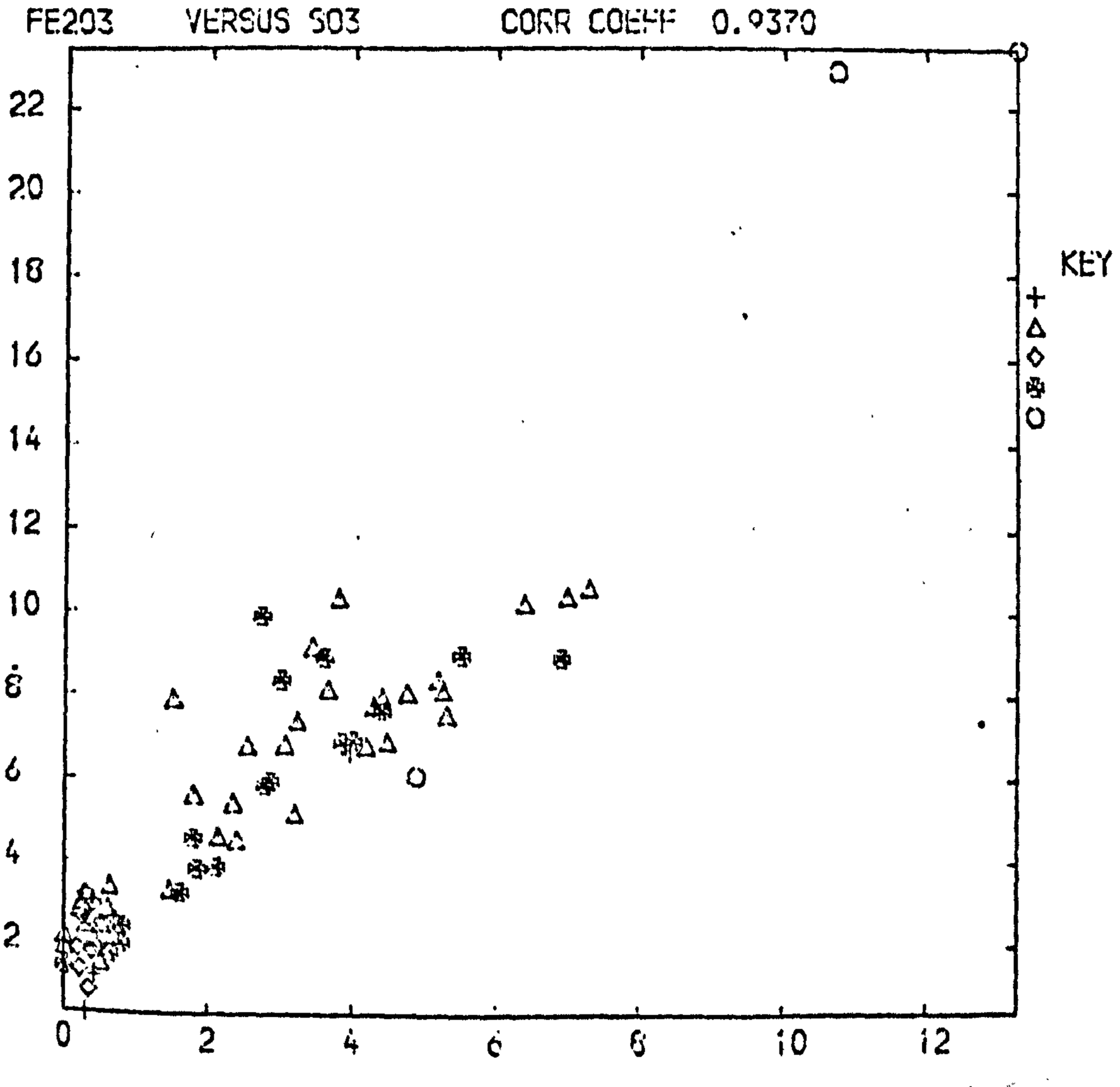
FE203 VERSUS SO3 CORR COEFF 0.9370
22
20
18
16
14
12
10
8
6
4
2
0
2
4
6
8
10
12
KEY
+
△
◇
O

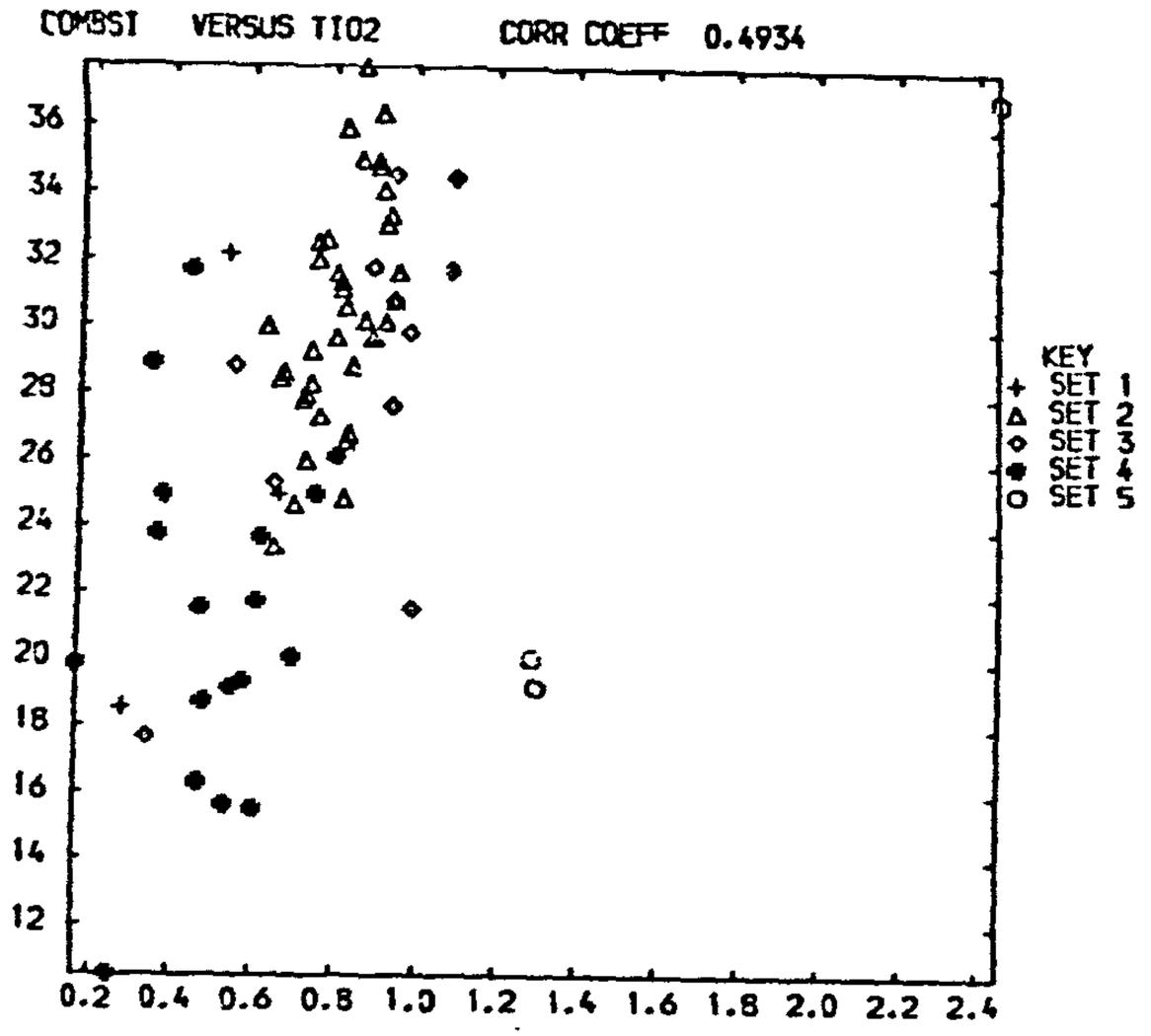
COMBSI VERSUS TIO2 CORR COEFF 0.4934
KEY
SET 1
SET 2
SET 3
SET 4
SET 5

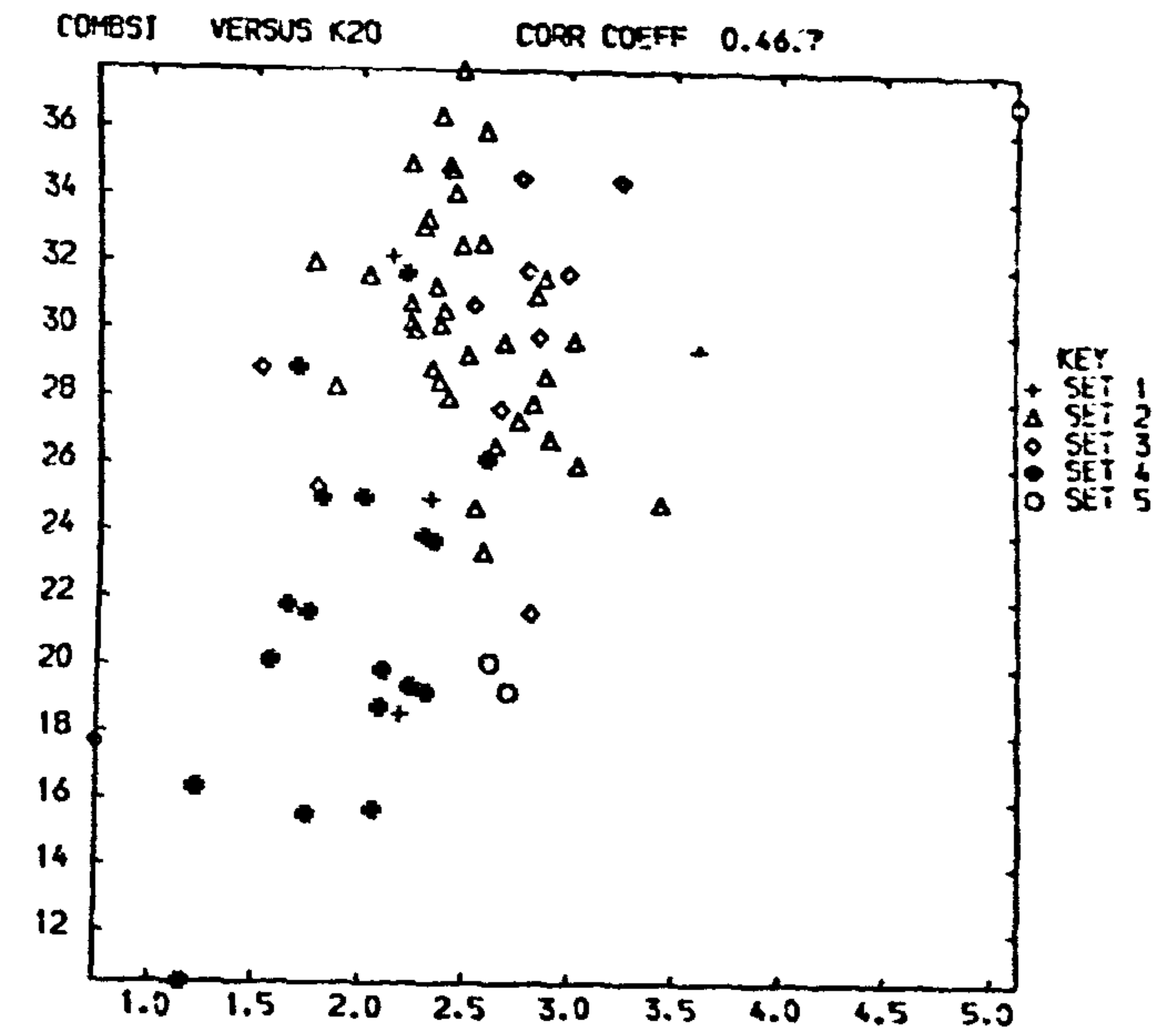
COMBSI VERSUS K2O CORR COEFF 0.46.7
KEY
SET 1
SET 2
SET 3
SET 4
SET 5

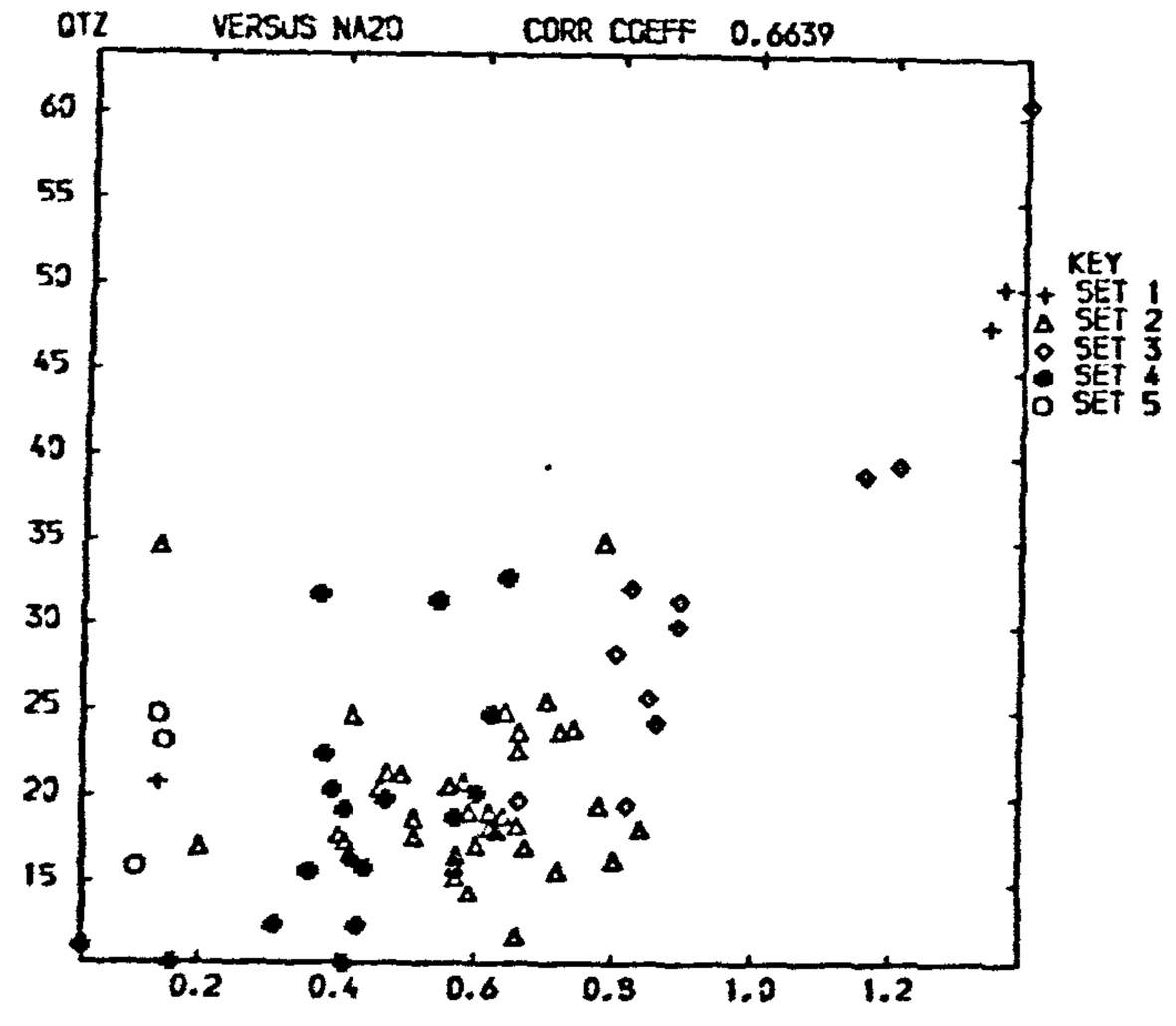
QTZ VERSUS NA2O CORR COEFF 0.6639
KEY
SET 1
SET 2
SET 3
SET 4
SET 5

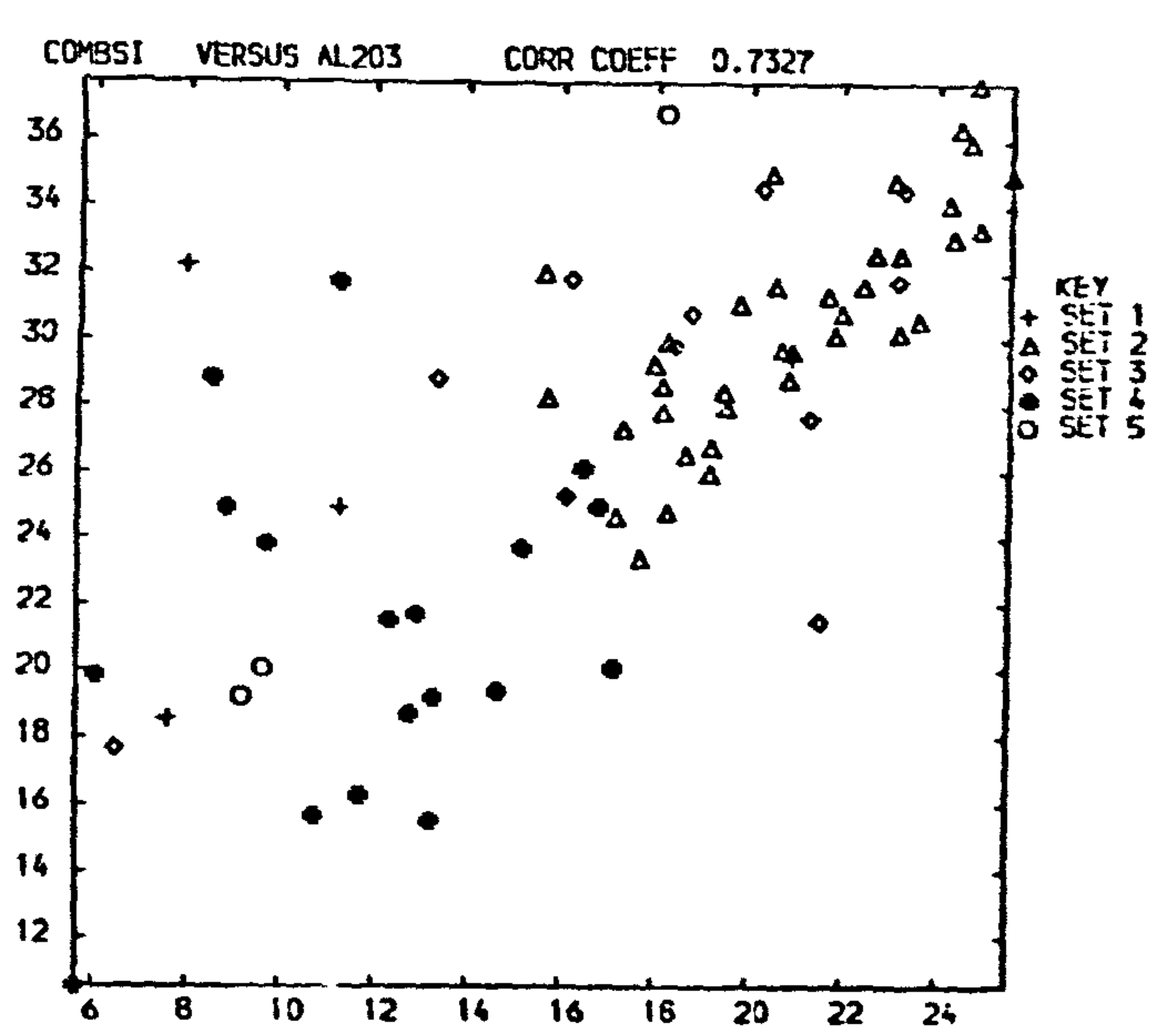
COMBSI VERSUS AL2O3 CORR COEFF 0.7327
KEY
SET 1
SET 2
SET 3
SET 4
SET 5

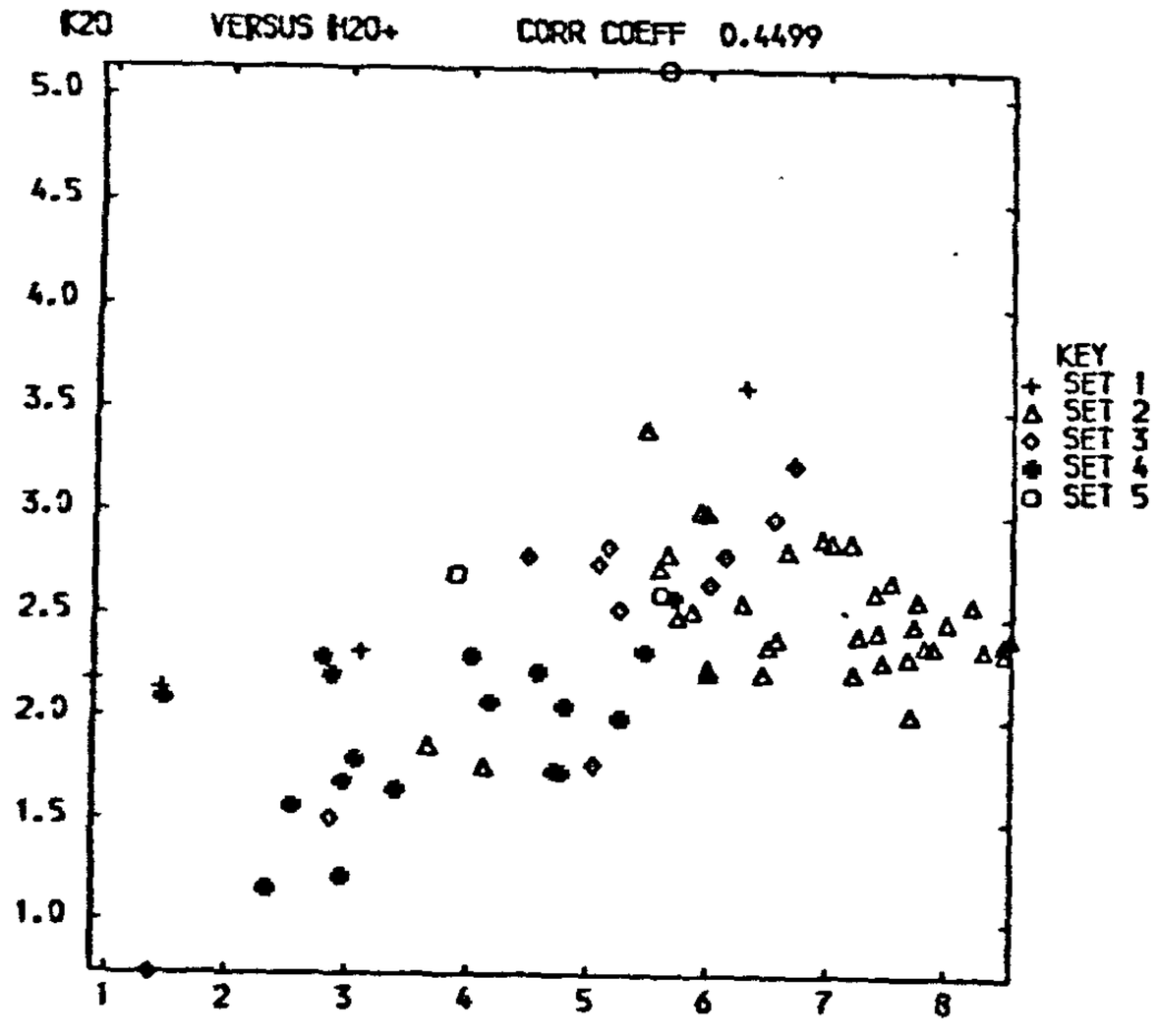
K2O VERSUS H2O+ CORR COEFF 0.4499
KEY
SET 1
SET 2
SET 3
SET 4
SET 5

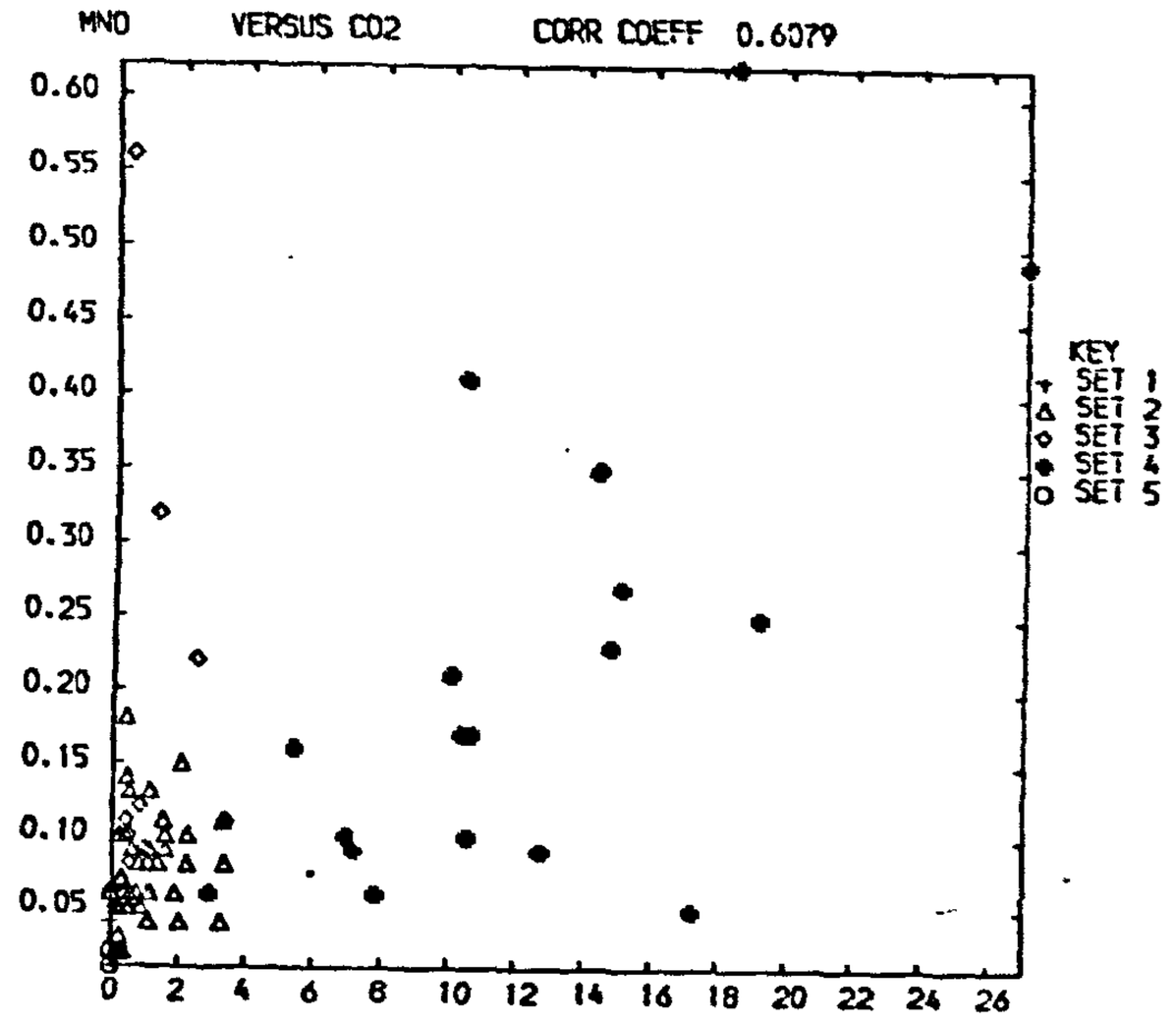
MNO VERSUS CO2 CORR COEFF 0.6079
KEY
SET 1
SET 2
SET 3
SET 4
SET 5

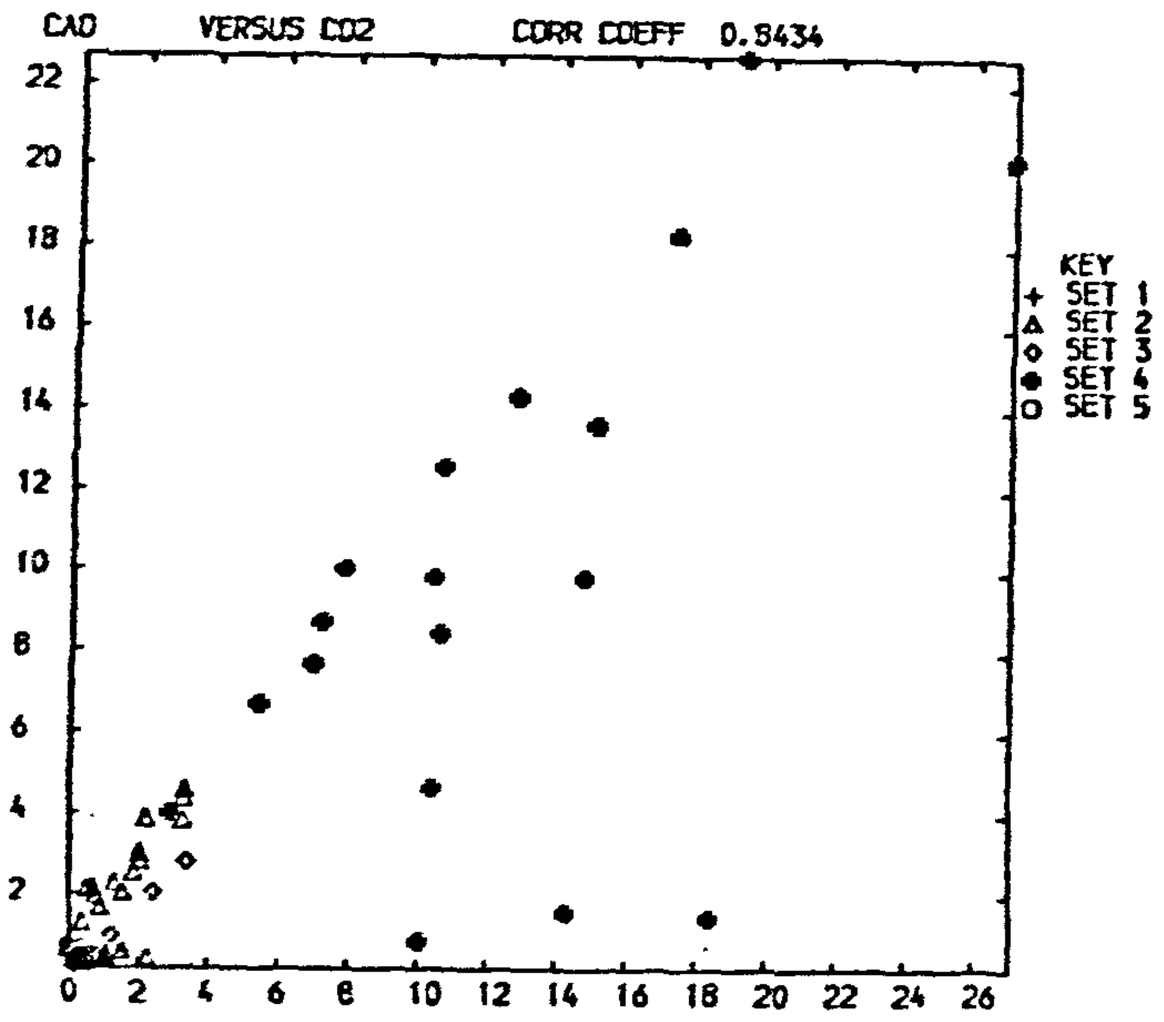
CAO VERSUS CO2 CORR COEFF 0.8434
KEY
SET 1
SET 2
SET 3
SET 4
SET 5

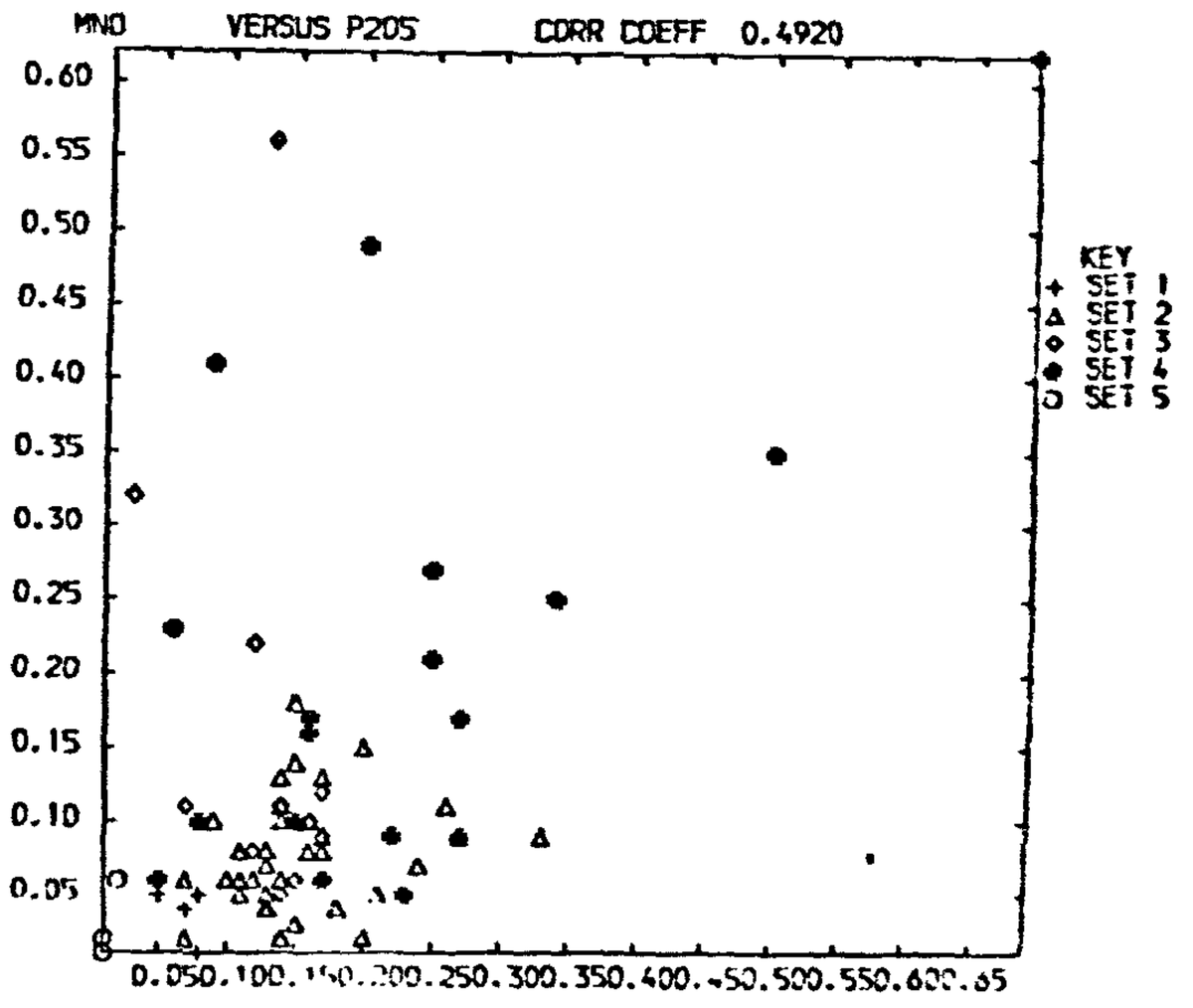
MNO VERSUS P2O5 CORR COEFF 0.4920
KEY
SET 1
SET 2
SET 3
SET 4
SET 5

TABLE 46: Correlation Matrix of Tansley Borehole Shales

	Qtz	Combsi	TiO_2	Al_2O_3	Fe_2O_3	FeO	MgO	CaO	Na_2O	K_2O
Qtz	1.0000									
Combsi	0.1010	1.0000								
TiO_2	0.0927	(0.6649)	1.0000							
Al_2O_3	-0.1266	(0.7520)	(0.8900)	1.0000						
Fe_2O_3	-0.4146	-0.3267	-0.2024	-0.1145	1.0000					
FeO	0.0296	-0.2632	-0.0740	-0.1348	-0.2875	1.0000				
MgO	-0.1456	-0.6037	-0.4766	-0.5108	-0.0960	0.1221	1.0000			
CaO	-0.3406	-0.6249	-0.7628	-0.7517	0.1441	-0.1618	(0.5151)	1.0000		
Na_2O	(0.5069)	(0.3654)	(0.4199)	(0.3488)	-0.3091	0.0966	-0.2839	-0.5527	1.0000	
K_2O	-0.0361	(0.4476)	(0.6070)	(0.5512)	0.2251	-0.4560	-0.3762	-0.3806	0.0944	1.0000
MnO	0.0688	-0.5928	-0.3648	-0.4913	-0.1205	(0.6024)	(0.5693)	(0.2645)	-0.0393	-0.4659
P_2O_5	-0.4169	-0.3058	-0.1453	-0.1393	-0.1203	(0.7137)	0.1867	0.1974	-0.2285	-0.3698
SO_3	-0.3417	-0.3377	-0.2316	-0.1691	(0.9077)	-0.3033	-0.0703	0.1959	-0.3412	0.2203
CO_2	-0.2832	-0.7735	-0.7958	-0.8134	-0.0020	(0.3452)	(0.6898)	(0.8388)	-0.5098	-0.0307
H_2O^+	-0.3046	(0.6279)	(0.7112)	(0.8883)	0.1498	-0.3402	-0.4362	-0.5857	0.1933	(0.5230)
Org. C.	-0.3062	-0.0862	-0.1196	0.0091	(0.4243)	-0.3624	-0.0473	0.0698	-0.2433	-0.0179

TABLE 46 (Cont.): Correlation Matrix of Tansley Borehole Shales

	MnO	P_2O_5	SO_3	CO_2	H_2O^+	Org. C.
MnO	1.0000					
P_2O_5	(0.4575)	1.0000				
SO_3	-0.1338	-0.1078	1.0000			
CO_2	(0.5917)	(0.5038)	0.0361	1.0000		
H_2O^+	-0.5239	-0.2550	0.0626	-0.7337	1.0000	
Org. C.	-0.2532	-0.1896	(0.2410)	-0.0971	0.2281	1.0000

SiO_2, TiO_2, Al_2O_3 and H_2O^+ the relationships are mainly strengthened, except that the correlations of the first two elements with K_2O is reduced, which may be due to the influence of feldspars and detrital titanium minerals, especially in the non-marine part of the sequence. On the other hand the improved relationship between Al_2O_3 and K_2O suggests their association with illite, although the last overshadows the presence of K-feldspars. In the third group which previously included Fe_2O_3, SO_3 and K_2O, the last is no longer correlated significantly at the 95% level, but it still correlated at the 90% significance level. Instead of K_2O the organic matter correlates significantly with Fe_2O_3 and SO_3. These modified relations indicate the covariation of pyrite and organic matter which are abundant in the marine part of the sequence. The decreased degree of K_2O correlation with the above elements could be influenced by the high content of K_2O in the non-marine part which contains, generally, trace amounts of pyrite. In the fourth group which is a carbonate association, most of the element correlations maintain their significance in about the same level, apart from MnO, CaO and CO_2-P_2O_5 correlations which are slightly lowered and that P_2O_5-CaO relation which is not significant.

From this it is clear that MnO is not present in calcite but largely in siderite and dolomite (ankerite). In a similar manner P_2O_5 seems to be either associated with the iron-carbonates or it could be present in a different form in the calcareous shales.

In order to elucidate relationships between elements which are likely to be masked by correlating the major element of all shales in the sequence, the non-marine and marine shales were separated. The correlation matrix for eachwas then obtained. The correlation coefficient for thirty-one non-marine shales at the 95% significance level is 0.355 and that for twenty seven marine shales is 0.381. Comparison between correlation coefficients of the same bivariant elements in both groups is shown in Table 47.

TABLE 47: Correlation of Bivariant Elements in the Non-Marine and Marine Shales of the Tansley Borehole

Related Variables	Non-Marine	Marine	Related Variables	Non-Marine	Marine
quartz-Na_2O	0.5182	-0.0190*	CO_2-FeO	0.9834	0.3943
TiO_2-Combined silica	0.5640	0.7390	CaO-MgO	0.5485	0.5470
Al_2O_3-Combined silica	0.6921	0.9079	MnO-MgO	0.6069	0.8147
K_2O-Combined silica	0.4802	0.5863	P_2O_5-MgO	0.7733	0.2883*
H_2O^+-Combined silica	0.6500	0.7950	CO_2-MgO	0.7292	0.7771
Al_2O_3-TiO_2	0.7147	0.8344	MnO-CaO	0.6197	0.1871*
K_2O-TiO_2	0.8142	0.5881	P_2O_5-CaO	0.5220	0.7396
H_2O^+-TiO_2	0.5795	0.6189	CO_2-CaO	0.6771	0.9327
K_2O-Al_2O_3	0.5770	0.6021	H_2O^+-K_2O	0.4900	0.4621
$C_{org.}$-Al_2O_3	0.3742	-0.2010*	P_2O_5-MnO	0.5539	0.0049*
SO_3-Fe_2O_3	0.9233	0.6678	CO_2-MnO	0.6883	0.4687
MgO-FeO	0.7613	0.7285	CO_2-P_2O_5	0.8568	0.6152
CaO-FeO	0.6485	0.0516*	$C_{org.}$-H_2O^+	0.4830	-0.0323*
MnO-FeO	0.7396	0.7829	Na_2O-Combined silica	-0.0582*	0.6133
P_2O_5-FeO	0.8490	-0.1573*	Na_2O-Al_2O_3	-0.1900*	0.6317
			H_2O^+-Al_2O_3	0.9181	0.8619

*Correlation coefficients below 95% significance level

R(Non-marine) = 0.355 at 95% significance level

R(Marine) = 0.381 at 95% significance level

The main difference is the relationship between quartz and Na_2O which are only significantly correlated in the non-marine part. From this it can be suggested that most of the Na_2O in the non-marine part is located in plagioclase whereas in the marine part it is largely present in illite. Support for such a suggestion is indicated by the significant relation of Na_2O-combined silica and Na_2O-Al_2O_3, only in the marine part. Mineralogical data revealed that, in the marine part, the association of Na_2O, is largely with illite. The relationships among combined silica, TiO_2, Al_2O_3, K_2O and H_2O^+ are largely improved in the marine part as indicated by the higher values of correlation coefficients except K_2O-TiO_2 relationship. In the marine part these elements are located in the clay minerals, apart from TiO_2 which could largely be present as fine particles adhered to clay minerals. In addition, average chemical data (Table 42) indicate that the non-marine part has slightly more TiO_2 compared to the marine part, whereas K_2O content is slightly higher in the marine part. Moreover, K_2O in the non-marine part is incorporated partly in K-feldspar. The relation of organic carbon with Al_2O_3 and H_2O^+ are insignificant and that of SO_3-Fe_2O_3 is lower in the marine part, although it is enriched in pyrite and organic matter. This is certainly the result of lack of strong and sympathetic variations between these constituents in the marine part. On the other hand, the non-marine part contains trace amounts of pyrite with smaller amounts of organic matter with respect to the marine part. But it is noteworthy that one sample (3, seatearth) in enriched pyrite and organic matter. The effect of such an extreme sample can produce a large value of correlation coefficient and this effect has been described by Till (1974, Fig. 5.3). Furthermore, the non-marine part is enriched in kaolinite and subsequently it would contain higher amounts of Al_2O_3 as revealed by average chemical data (Table 42). Therefore, the large values

of correlation coefficients between these elements in the non-marine part can be attributed to the presence of this extreme sample and the higher content of Al_2O_3.

In the marine part the element group associated with carbonates show lower value of CO_2-FeO correlation coefficient and the insignificant CaO-FeO and MnO-CaO indirectly demonstrate the importance of siderite in the non-marine part. MgO-FeO, CaO-MgO and CO_2-MgO correlation coefficient values remain relatively of the same magnitude, suggesting their association with ankerite and siderite which are present in both marine and non-marine parts of the sequence. However, the slight variation in these correlation coefficient values may be due to the presence of high ankerite content in some marine shales. It is also clear that MnO is largely located in the ankerite rather than calcite. On the other hand CO_2-CaO correlation coefficient values in the marine part are higher than its counterpart, indicating the abundance of calcite in the former. This is in accord with the calculated calcite content (Table 42). A striking difference is exhibited by the correlation of P_2O_5. While it shows a high value with FeO in the non-marine part, it is insignificant in the marine part, although ankerite is present in both parts. Moreover, P_2O_5-MgO correlation shows a similar pattern. In contrast, in the marine part, P_2O_5 has a high correlation coefficient with calcite. This variation in the behaviour of P_2O_5 is supported by the results of chemical analyses (Appendix 2), from which it can be seen that P_2O_5 content, generally, is highest in the siderite rich shales. However, it has been tentatively suggested in the previous section (page 135) that P_2O_5 in non-marine shales could be present as hydrous ferrous phosphate (vivianite) but evidence is lacking. On the other hand phosphorous in marine environment is present as carbonate-apatite (Degens, 1965) derived by replacement of carbonate by phosphates or as hydroxy-apatite phase (p.220) produced

initially by organisms. In this respect, it is of interest that in the Tansley Borehole succession the fish beds between 279.28-284.5 m depth contain abundant phosphatic nodules. These were shown to consist either of apatite and a mineral of the kaolinite group or a mixture of apatite and barytes (Ramsbottom et al, 1962). In addition Cosgrove (in: Ramsbottom et al. 1962) showed that the radioactivity in these beds was exceptionally high, due to uranium enrichment in these beds. Furthermore, the marine bands above this horizon (the marine part in the present study) were shown to possess distinctly higher radioactivity than the non-marine part of the sequence. On the basis of this evidence and P_2O_5 correlation through the sequence, it seems that P is present in different forms. The content of P in the marine shales may be due to the preservation of organic compounds, containing P, although much of the originally organic P may now be incorporated in clay minerals and carbonate-apatite. However, some P must be of detrital origin, but this seems not to mask the relative variation of P.

5.4 Trace Elements

The fifty-nine samples for which the data are presented here are shales and silty shales, with few sandstones and volcanic mudstones (Appendix 2), from a total of seventh-three rock samples. Graphical representation of the distribution of trace elements is shown as histograms in Figure 31. From this it is apparent that Ni, Co, V, Cr, Cu, Sr and Pb distribution patterns are more or less similar, so too are Rb and Ba whereas Zn, Y and Zr are independent.

Trace element data (Appendix 2) also indicates that sandstones and canky or calcareous shales contain smaller amounts than non- or less calcareous shales. This is because quartz is not variable in composition and has little or no capacity for incorporating trace elements in its structure or adsorbing them on its surface. Carbonates have a capacity

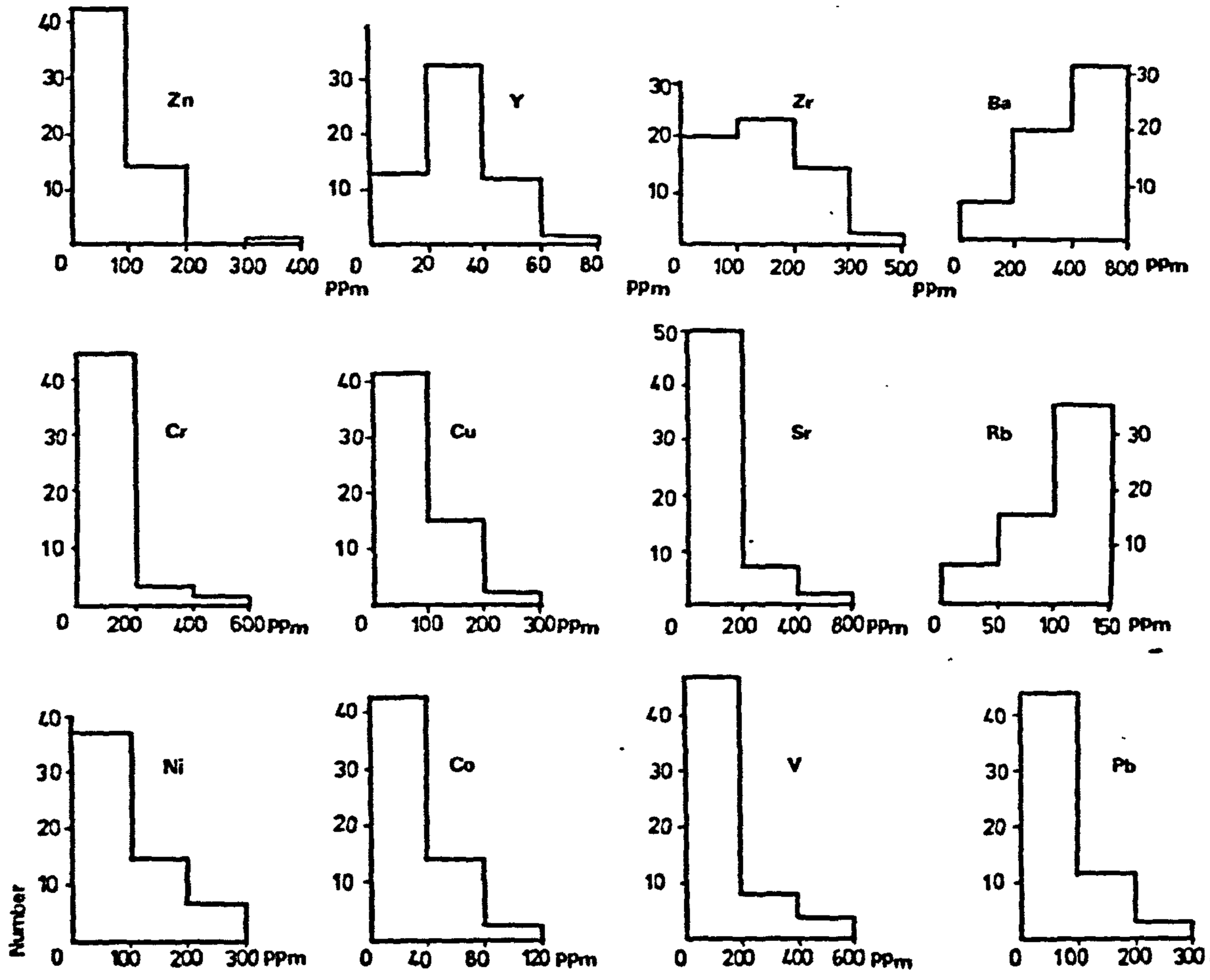

Fig.31 Distribution of trace elements in Tansley Borehole rocks.

for incorporating in their structure few elements, among them manganese and strontium. Consequently, quartz and carbonates can be regarded as the main dilutants.

In order to facilitate the interpretation of trace element distribution the shales are placed in two groups using palaeontological evidence. The first group (twenty five samples) consists of non-marine shales, that contain an average of 2.65% organic matter. The second group (eighteen samples) consists of marine shales with average organic matter content of about 4.50%. Both of these groups have an average content of quartz of about 23%, which proved statistically to be not significant, using the test of confidence interval at the 95% significance level. Accordingly it can be suggested that the effect of quartz dilution on trace element data will be similar in both groups.

In the previous section (Table 42) it was found that the marine shales were enriched in pyrite, illite and calcite compared to the non-marine shales which are enriched in siderite and kaolinite. Also it was inferred that organic matter in the marine shale consists of microscopic, disseminated flakes whereas the non-marine shales are characterised by the occurrence of plant fragments and coaly materials.

The ranges, means and standard deviations of trace element contents in both groups are lised in Table 48. It is clear that Ni,V, Cu, Sr and Pb are greatly enriched in the marine shales, while Mn and Zr in the non-marine shales. Apart from Co and Y, the only other elements showing similarities in their average contents are Cr, Rb and Ba. It follows that these elements are contained in minerals common to both groups. Nevertheless, these mineral contents should not be at great variance. The most likely hosts are, therefore, illite and feldspar. Although illite is relatively abundant and characteristic of the marine shales, the feldspars are generally present in higher amounts in the non-marine shales. There-

TABLE 48: Ranges, Means and Standard Deviations of Trace Element Contents in the Marine and Non-Marine Shales (Namurian) of the Tansley Borehole. (Constration ppm)

		Ni	Co	Mn	V	Cr	Zn	Cu	Rb	Sr	Y	Zr	Pb	Ba
Marine	Range	72-225	15- 71	104-1269	140-628	105-250	68-126	90-248	68-151	112-350	14-57	64-141	82-323	189-777
	Mean	125	35	507	282	153	103	140	113	184	36	101	155	416
	S.D.	42	15	262	140	37	15	41	21	75	10	20	44	113
Non-Marine	Range	32-142	11-107	99-4330	93-168	92-179	30-105	11- 89	35-152	75-216	26-62	75-322	8- 78	287-524
	Mean	76	33	986	125	146	80	47	108	121	37	158	37	413
	S.D.	23	22	1264	19	20	17	17	29	28	8	66	16	83

fore, it seems that the effect of mutual compensation by illite and feldspars would result in lack of differentiation between the two groups using Cr, Rb and Ba. However, the slightly higher averages of Cr and Rb in the marine shales may indicate that these elements have a preference to illite.

The high average content of Zr in the non-marine shales is most likely assignable to the abundance of zircon, since some of these shales are more silty than the marine shales. The distribution of Y is difficult to explain and it is apparent that it is not confined to a particular mineral.

The highest values of Ni and V, in the marine shales are associated with sample 49 which is among the shales highly enriched in pyrite (4.13%). This same sample has the highest Sr content among the Namurian marine shales, and it has also the highest calcite content (20.93%). The only samples (No. 69 and 70) that have a higher Sr content are Visean shales which contain higher amounts of calcite (30.3-36.31%). Samples 29 and 47 are pyrite rich marine shales (3.35 and 4.78% respectively) and these have the highest Cu and Pb contents. Similarly, in these shales, Co, Zn are highly enriched in Sample 64 which contains 3.95% pyrite. In contrast the lowest contents of Ni, Co, V, Zn, Cu and Pb, among the marine shales are associated with sample 66 which has the highest content of ankerite (43.58%). In this same sample the high Mn content is encountered as well. In the non-marine shales, Mn and Co contents reach their maximum values and V at its minimum value in sample 44, which has 42.72% siderite and 2% pyrite. Hirst and Kaye (1971) found that Mn is largely associated with siderite. The Zn content is highest in sample 16 which contains a small amount of siderite (1.48%). Sample 26 has a very high Mn content with high amounts of siderite (28.17%) while the next sample (27) contains

similar amounts of Co, V and Mn, but without siderite. This last sample shows much higher values for organic matter, illite and pyrite, than the other samples. In a similar way, the largest amounts of V, Cu and to a lesser extent Pb are associated with sample 42, which contains more pyrite and organic matter than the overlying samples. Ni concentration is highest in sample 1, which has the highest organic matter content (coaly material) from among the non-marine shales (9.05%).

From this it is apparent that there is no systematic variations between trace element abundance and mineralogical compositions. Nevertheless, it is clear that a distinct separation of the non-marine shales is strongly influenced by Ni, V, Cu, Pb and Sr.

In order to eliminate the effect of dilution by quartz and carbonates, trace elements /Al_2O_3 ratios are used. The ranges, means and standard deviations of trace element/Al_2O_3 ratio in the non-marine and marine parts of the sequence, starting from below the Ashover sandstones, are shown in Table 49. It is clear that the mean values of Ni, V, Cu, Sr and Pb/Al_2O_3 ratios are much higher in the marine part, and also more variable as indicated by their ranges and standard deviations. The mean values of Cr, Zn and Ba/Al_2O_3 ratios are also higher in the marine part, but show moderate differences. Their standard deviations show that Cr and Zn/Al_2O_3 ratios are less variable than the Ba/Al_2O_3 ratio. Only a slight difference in the Co and Y/Al_2O_3 mean values is apparent although they are higher in the marine samples. On the other hand, the Zr/Al_2O_3 mean value is higher in the non-marine shales and also more variable. Because the ratios of Ni, V, Cu, Sr, Pb, Cr, Zn and Ba/Al_2O_3 show wide ranges in both groups and partly because they are higher in the marine part, it is suggested that they are not related to a particular mineral. In the non-marine part, however, the Sr/K_2O mean value was found, with few

TABLE 49: Ranges, Means and Standard Deviations of Trace Elements/Al_2O_3 Ratios in the Non-Marine and Marine Shales of the Tansley Borehole

	Non-Marine			Marine		
$El/Al_2O_3 \times 10^{-4}$	Range	Mean	S.D.	Range	Mean	S.D.
Ni	1.312- 7.41	3.595	1.148	3.48-15.58	7,897	3.997
Co	0.50 - 9.11	1.824	1.910	0.73- 3.98	2.048	0.947
V	4.36- 8.82	6.126	1.20	6.46-51.13	18.054	13.20
Cr	4.82- 8.97	7.011	1.036	6.46-18.83	8.992	2.894
Zn	1.24- 6.22	4.010	1.105	4.05-12.75	6.357	2.367
Cu	0.45- 4.27	2.332	0.905	4.62-15.16	8.550	3.143
Rb	1.44- 6.29	5.131	1.14	5.12- 8.27	6.459	0.766
Sr	3.09- 9.84	5.851	1.306	5.45-49.97	13.808	11.743
Y	1.21- 4.00	1.914	0.733	0.97- 3.31	2.126	0.572
Zr	3.09-17.18	8.110	3.827	4.24- 7.22	5.788	0.797
Pb	0.33- 3.92	1.879	0.915	4.59-13.67	8.755	2.61
Ba	14.25-27.34	19.90	3.544	14.87-60.70	24.35	10.42

exceptions, to be 5.78 x 10^{-4} with a standard deviation of 0.64, which suggests association with illite. Similarly, the mean value of the Rb/K_2O ratio in the non-marine is 48.47 x 10^{-4} (SD = 2.17 x 10^{-4}) and in the marine part is 44.10 x 10^{-4} (SD 1 2.22 x 10^{-4}). Such moderate variations indicate a close association with illite. The rest of the element/K_2O ratios exhibit wide variations, suggesting contributions by other minerals.

The variations in element/Al_2O_3 ratios are shown as section profiles, starting from below the Ashover sandstones (Figure 32). It is evident that most of the elements show much less variations in the non-marine part (samples 14-28) in comparison to the marine part. This may suggest some association with clay minerals. Also, it can be seen that the inflection point in Ni, V, Cu, Sr and Pb/Al_2O_3 profiles is the same and occur at the level of the sample 29 which is the Lingula phase, marking the transition from non-marine to marine shales. In a similar way, but with less striking manner, the Rb, Zn, Cr/Al_2O_3 ratioschange at the same level. The increase in these ratios is maintained in sample 30 and 32 and then decrease at 38 which is a non-marine shale. Values of the ratios remain low through the non-marine shales (38-45). Lower in the sequence are marine shales (46-50) and there is a gradual increase in the element/ Al_2O_3 ratios. A sudden decrease in the ratios occur atthe level of sample 51, which is a non-marine shale. Below the latter, a gradual increase in the ratios marks the return to a marine shale, although there are some fluctuations. In contrast the Zr/Al_2O_3 ratio through the whole sequence shows in general the reverse trend of the above mentioned elements. The Co/Al_2O_3 ratio shows irregular variations in both parts of the sequence. The least variable ratios (with respect to Al_2O_3) appear to be those of Ba and Rb. The highest Ba/Al_2O_3 occurs at the level of samples 49 and 61. These are marine shales enriched in pyrite, calcite and organic matter.

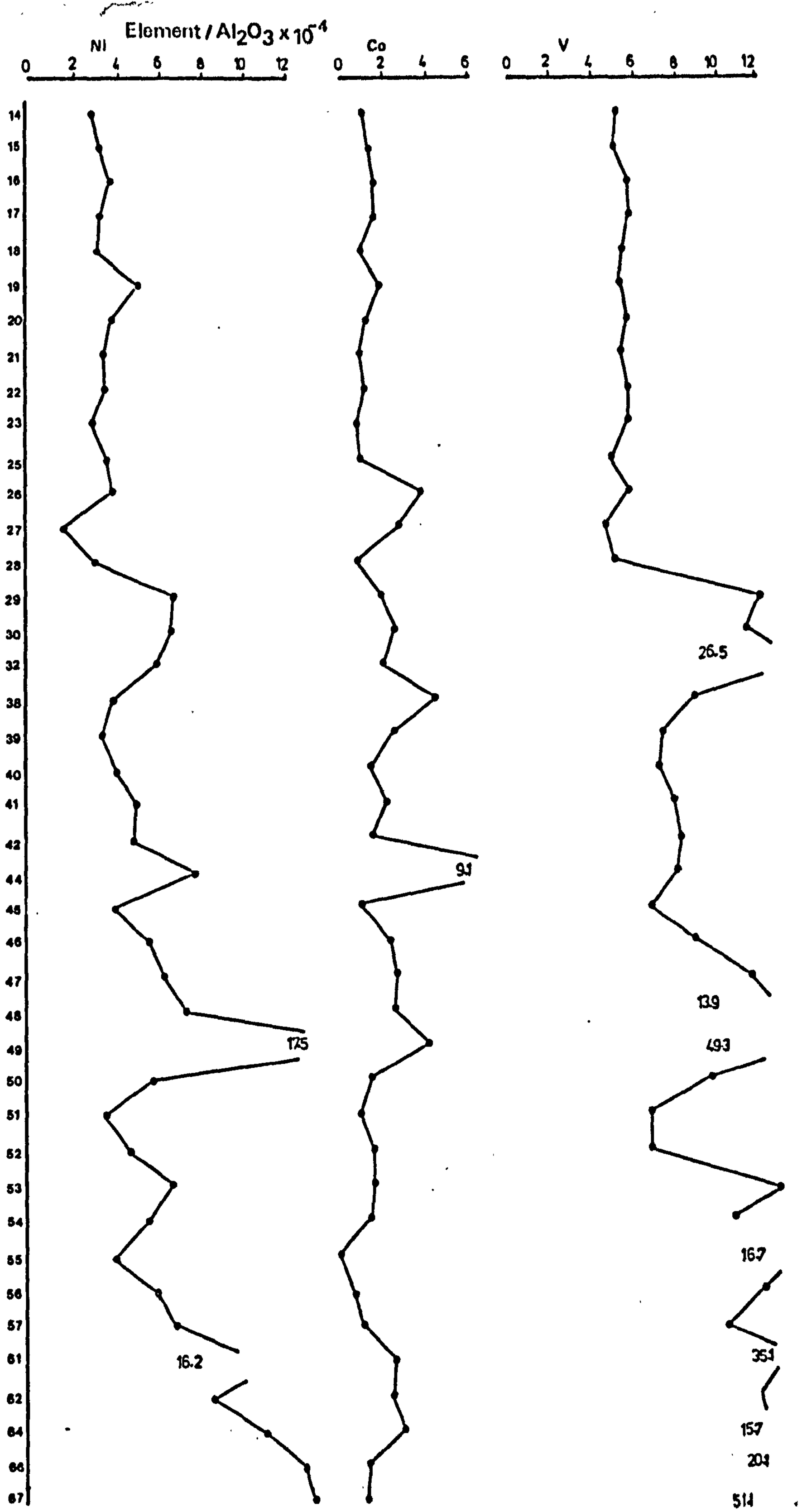

Fig.32 Variation of element/Al_2O_3 ratio through the Tansley Borehole section, the sample no. is shown on the left.

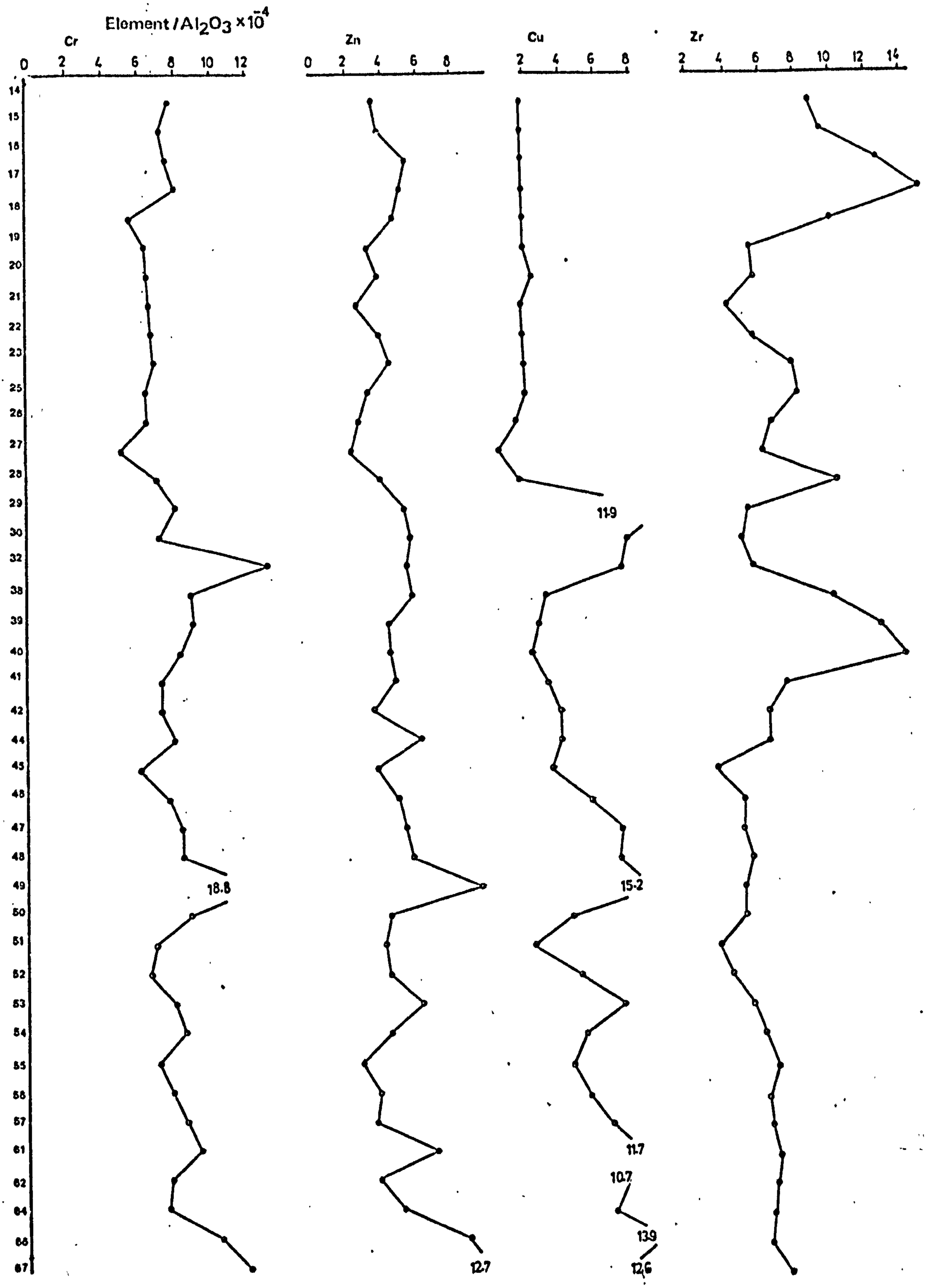
Element / $Al_2O_3 \times 10^{-4}$
Cr
0 2 4 6 8 10 12
Zn
0 2 4 6 8
Cu
2 4 6 8
Zr
2 4 6 8 10 12 14
14 15 16 17 18 19 20 21 22 23 25 26 27 28 29 30 32 38 39 40 41 42 44 45 48 47 48 49 50 51 52 53 54 55 56 57 61 62 64 66 67
11.9
18.8
15.2
11.7
10.7
13.9
12.6
12.7

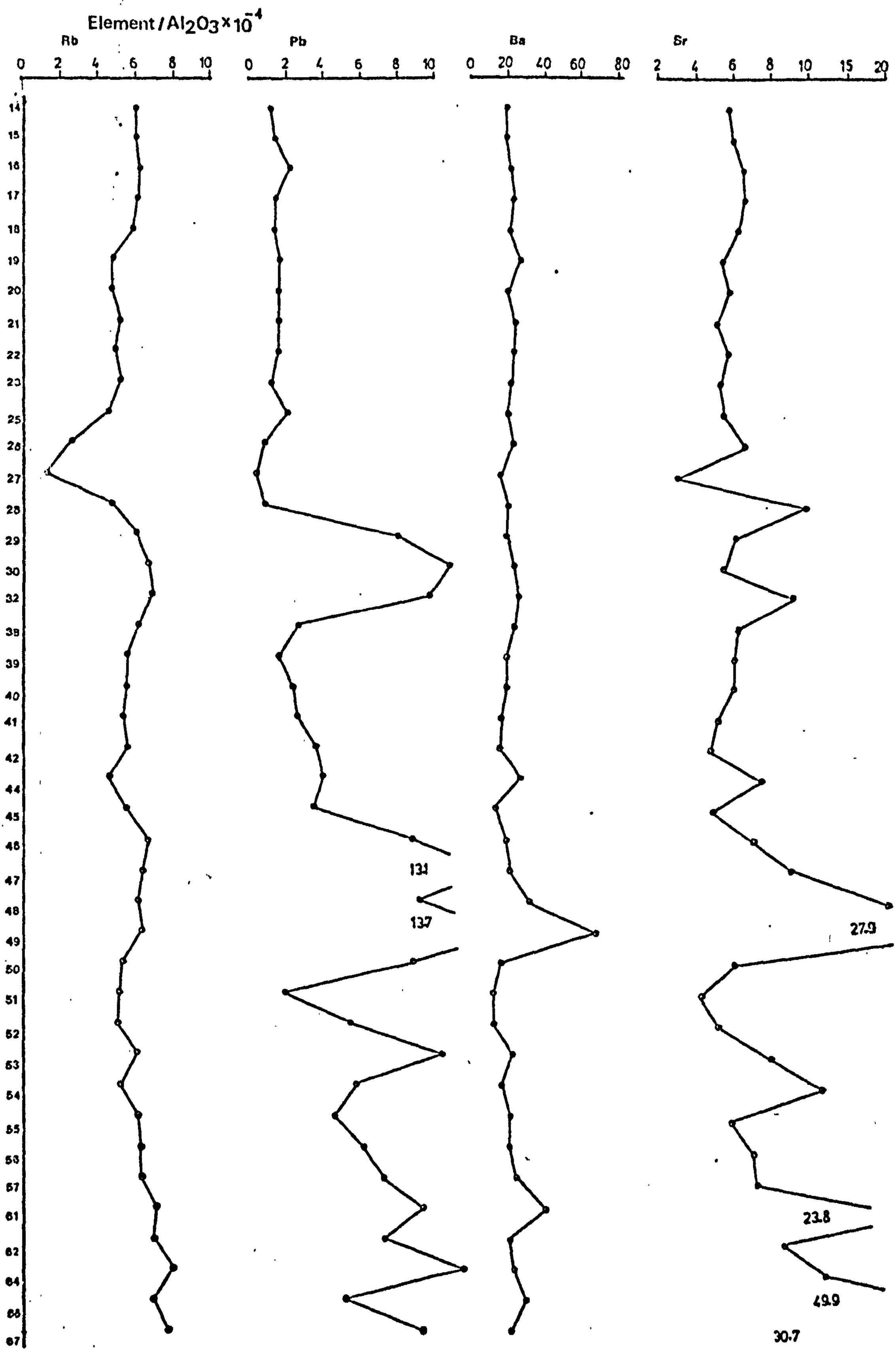
Element / $Al_2O_3 \times 10^{-4}$
Rb
0 2 4 6 8 10
Pb
0 2 4 6 8 10
Ba
0 20 40 60 80
Sr
2 4 6 8 10 15 20
14
15
16
17
18
19
20
21
22
23
25
26
27
28
29
30
32
38
39
40
41
42
44
45
46
47
48
49
50
51
52
53
54
55
56
57
61
62
64
66
67
131
137
27.9
23.8
49.9
30.7

This may indicate the presence of small amounts of baryte, because the latter mineral is present in nodules below the level of sample 61 (Ramsbottom et al., 1962, p.119). It is also clear that the highest ratios of Ni, V, Pb, Cr, Zn, Cu and Sr/Al_2O_3 are associated with the marine shales. In contrast the highest Co/Al_2O_3 ratio is encountered in sample 44, which is a non-marine shale enriched in siderite. On the basis of these data, it is reasonable to suggest that relationships exist between enrichment of some trace elements and abundance of minerals. Ni, Cu, Pb and possibly V are largely enriched in pyrite and organic matter, and Co, Cr and Zn only partially so. The original depositional association might have been with organic matter, but with partial destruction of organic matter during diagenesis the elements would be redistributed. Rb and Ba are concentrated in illite and feldspars although Cr and V may be present in illite, but the relationship is overshadowed by pyrite and organic matter. Sr and Mn are influenced by carbonates, while Zn and Co may be present as well in them. Very little Ba may be attributed to carbonates or baryte. The Zr concentration is mostly related to zircon. On the other hand, Y shows no preference to a particular mineral or trace element. In discussing these relationships, however, the contribution by heavy minerals is discarded, which could be important for some trace elements although definite evidence cannot be obtained.

In these shales, different faunal assemblages are recognised (Chapter 1, page 28) and equated with variations in salinity (Ramsbottom et al. 1962). There are insufficient samples to fully test the palaeontological grouping. Nevertheless, one incomplete, minor cycle was made possible from the available data. Table 50 shows Ni, V, Cu, Pb and Sr concentrations in shales characterised by different faunal phases.

TABLE 50: Relationship between Trace Element Contents and Different Faunal Phases

Sample Number	Ni	V	Cu	Pb	Sr	Faunal Phase
28	59	109	37	17	216	Plant debris and fish scale
29	133	249	248	165	127	Lingula phase
30 32	128 110	228 510	163 143	220 184	112 178	Transitional from Barren beds to goniatite phase
38	46	114	42	32	86	Plant fragment
45	87	153	86	78	105	Fish scale
46 47 48	95 105 103	156 199 204	103 135 108	195 232 134	128 161 304	Transitional from above to goniatite phase (46-50)
49	225	628	194	175	350	Goniatite
50	107	180	90	174	121	Transitional from marine to non-marine
51	81	159	64	51	106	Fish scales and plant fragments
52	96	140	112	122	115	Spat phase
53 54	114 89	233 175	136 94	184 99	147 216	Goniatite
	73	130	57	46	111	Average of nine non-marine shales
	116	227	133	145	142	Average of seven A or D spat phase
	158	457	153	153	246	Average of five goniatite phase

It is clear that sample 29 which represents brackish conditions (Lingula phase) is enriched in Ni, V, Cu and Pb, but with less Sr content than the overlying shale (28) which represents transition to non-marine conditions. Beneath the Lingula bearing shale are barren beds, which mark the transition to a goniatite phase, which was not sampled. In this transitional phase (30, 32, sample 31 not analysed) the contents of Ni and Cu decrease while V and Sr increase, and Pb increases then decreases. This transitional phase is underlain by a non-marine phase (38-45). The last shows a marked decrease in all elements. This non-marine phase passes through transitional beds (46,47,48) to a goniatite phase (49). Trace element concentrations fluctuate through the transitional phase, but culminate at the goniatite phase. The latter overlie a transitional bed (50) containing goniatite and plant fragments, which in turn passes down to a non-marine phase (51). This change is accompanied by a gradual decrease in the trace element contents. A change to a marine condition of intermediate salinity (spat phase 52) is marked by increase in most element contents, except V. Transition to a typical marine condition (goniatite phase 53), is accompanied by further increase in the contents of these trace elements. At the base of this goniatite phase, there is a carbonate band (54) which shows a decrease in trace elements concentration, except Sr. The corresponding variations in the ratios of these elements/Al_2O_3 are shown in Figure 33. The latter shows a similar trend to the change in the absolute amounts of these trace elements. Accordingly, it can be suggested generally, that the change from the least saline, non-marine condition (plant and fish scale phase) through intermediate salinity conditions (spat A or D phase) to a typical marine condition (goniatite phase) is accompanied by increase in trace element contents, although similar phases in differentparts of the succession have variable

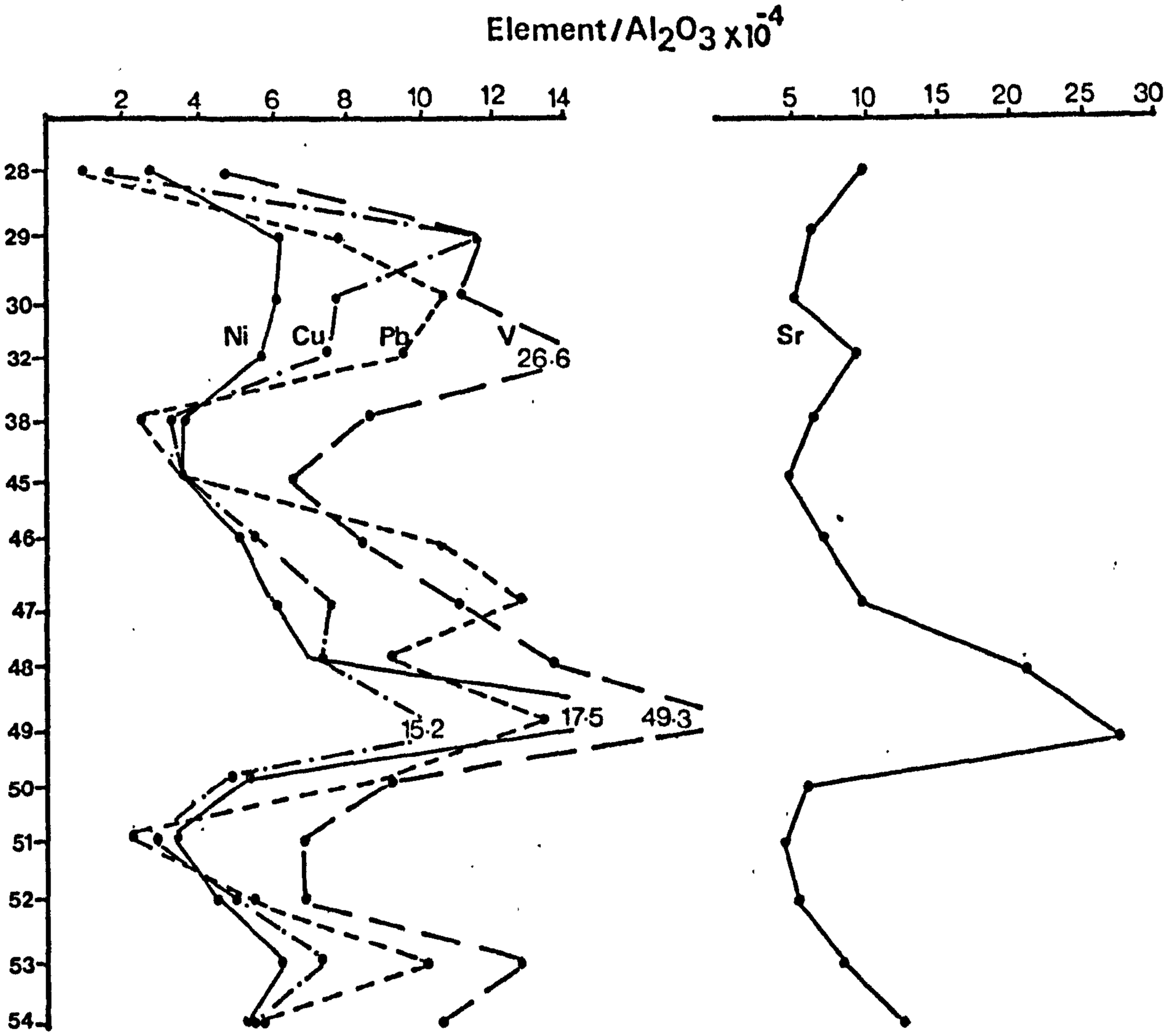

Fig.33 Variation of element/Al_2O_3 ratio through the different faunal phases.

concentrations. This is supported by the average contents of trace elements in these phases (Table 50).

5.5 Comparison with other Shales

Table 51 lists the average trace element contents of the Namurian shales, together with other shales.

Comparison with the average composition of other marine shale (anal. 4 and 7) and average shale (anal.9) shows that the Namurian marine shales contain more Ni, V, Cr, Cu, Pb and Co, but less Zr. On the other hand the average content of trace elements in the Namurian marine shales are within the range of averages of these elements in the black shale (anal. 10) except Zr. The trace element contents of the Namurian non-marine shales as compared with their counterpart (anal.3) reveals similar trends of trace element enrichment as with the marine shales. But comparison with shales in which siderite is abundant (anal. 8) reduces the differences in trace element contents. This is because the Namurian non-marine shales are characterised by the presence of siderite.

The content of Zr mainly results from detrital zircon and generally higher Zr contents are associated with lower concentrations of other trace elements. Accordingly the detrital contribution of silt and sand size minerals is likely to be less important in the Namurian shales than in the other reported shales, apart from the black shales. This may be attributed to slower rate of sedimentation and probably finer grain size of the Namurian shales. Both of these sediment parameters would suggest that the reason for the appearance of high concentration of most trace elements is due to ion exhcange or sorption processes. The latter would be important with respect to enrichment of trace elements in clays and organic matter. Such a process has been invoked to explain the abundance of trace elements in marine shales (Tourtelot, 1964; Spencer, 1966; Gad

TABLE 51: Average Trace Element Contents in the Namurian (Tansley Borehole) Shales and other Shales

	1	2	3	4	5	6	7	8	9	10
Ni	125	76	19	53	43	51	75	71	68	20- 300
Co	35	33	10	15	16	49	31	29	19	5- 50
V	282	125	93	243	268	389	177	160	130	50-2000
Cr	153	146	52	106	134	211	105	130	90	10- 500
Zn	103	80	77	141			97	128	95	100-1000
Cu	140	47	22	48	142	202	73	63	45	20- 300
Rb	113	108			415	283			140	450
Sr	184	121			153	419	550	192	300	25- 400
Y	36	37							26	
Zr	101	158	243	193	153	179	137	207	160	10- 20
Pb	155	37	26	21	97	101	16	50	20	20- 400
Ba	416	413			487	282	350	497	580	450- 700

(1,2 - Present study)

1 - Marine shales

2 - Non-marine shales

(3,4 - Tourtelot, 1964)

3 - Non-marine Carbonaceous shales in which kaolinite is abundant

4 - Marine shales with abundant illite and minor amount of pyrite

(5,6 - Spencer, 1966)

5 - Marine green shales

6 - Marine dark shales

(7,8 - Gad et al. 1969)

7 - Pyritic and calcareous shales (jet rock proper)

8 - Sideritic shales (grey shales)

9 - Average shale (Turkian and Wedepohl, 1961)

10 - Range of average amounts in black shales (Krauskopf, 1955)

et al. 1969). Another consideration is the chemical characteristics of the environment in which the clay minerals and organic matter accumulated and underwent diagenesis. These were probably the most important factors controlling the degree to which sorption processes and the formation of diagenetic minerals affected the final composition of the shales. In this respect, the difference between the trace element contents of the marine and non-marine shales may be attributed to the less saline environment in which the latter were deposited or vice-versa. This is supported by the previously presented average content of trace elements in various faunal phases representing different salinities (Table 50). However, differences in trace element content do not exist only between shales of different geographic locations and depositional environments, but also in marine shales deposited in the same basin. This is indicated by the interbedded green and dark marine shales (anal. 5 and 6, Table 51) of Silurian age (Spencer, 1966). These shales represent the black graptolitic shale band, deposited in a geosyncline that covered much of Wales and Northern England during the early Paleozoic era. The black shales contain relatively higher pyrite and organic matter than the green shales. Spencer concluded that with the relative absence of sulphide and with decreased preservation of organic carbon in the green shales, ion exchange may become important as a determinant of some trace element distribution, particularly Sr, Ba, Cr and V. The higher content of trace elements in the dark shales was attributed to association with organic matter and sulphides. These influences were interpreted for Eh-pH and sulphur diagenesis factors with the lesser involvement of ion-exchange processes.

5.6 Statistical Correlation

For fifty-nine samples (shales, sandstones and volcanic mudstones) the correlation coefficient (r) is 0.257 at the 95% significance level. In order to relate trace elements to mineral phases, some of the major

elements are included in the correlation analysis. The correlation matrix in which significant correlations are underlined is shown in Table 52. Four coherent groups appear to occur, embracing the significantly related variable pairs (Table 52). The first group includes TiO_2, Al_2O_3, Cr, Rb and Ba. Both Cr and Rb have a strong relationship with K_2O indicated by the high value of their correlation coefficients, while Ba correlates only with Al_2O_3. The lack of Ba correlation with K_2O is due to the interference of volcanic mudstones. The latter are unlike the shales and have a high K_2O and low Ba content. This group suggests that Cr, Rb and Ba are concentrated in illite and feldspar. Gad et al (1969) found that Cr and Ba occur mainly in illite or mica. The second group comprises Fe_2O_3, Ni, Pb, V and Cu. The last two elements have a high correlation coefficient value and their correlation with Fe_2O_3 is weaker than that of Ni and Pb. In the previous section (page 150) it was shown that Fe_2O_3 correlates with organic matter. Consequently, Pb, Ni, V and Cu seem to be concentrated in pyrite and organic matter. The third group indicate carbonate association and includes FeO, Co and Mn. This is in agreement with the aforementioned relationships between siderite and ankerite with Co and Mn. The fourth group consists of Na_2O, Zr and Ba, indicating feldspar and zircon association. This is likely to be influenced by the non-marine shales whose average chemical and mineralogical data show high feldspar and Zr contents.

In addition to these groups, some elements have a dual or triple association. CaO-Sr relationship is very strong which indicates that Sr is largely concentrated in calcite. On the other hand CaO correlation with Ni, Mn, V, Zn may suggest a genetic relationship, but it is thought as the result of covariation of calcite and pyrite, particularly in the marine shales. The lack of CaO relationship with Fe_2O_3, Cu and Pb, if CaO-Ni, V, Zn relationships to be correct is attributed to overshadowing by the

TABLE 52: Correlation Matrix of Trace and Major Elements in the Tansley Borehole Rocks (59 Samples)

	TiO_2	Al_2O_3	Fe_2O_3	FeO	CaO	Na_2O	Zr	Pb	Ba	K_2O
TiO_2	1.0000									
Al_2O_3	(0.4963)	1.0000								
Fe_2O_3	(0.2829)	-0.1328	1.0000							
FeO	-0.1350	-0.0749	-0.2461	1.0000						
CaO	-0.5071	-0.5545	-0.0105	-0.1303	1.0000					
Na_2O	-0.1922	-0.0066	-0.4613	0.0970	-0.4060	1.0000				
Zr	0.2296	-0.0066	-0.3918	0.0309	-0.4507	(0.6819)	1.0000			
Pb	-0.0881	0.0693	(0.6238)	-0.3257	0.1264	-0.2644	-0.4349	1.0000		
Ba	-0.1236	(0.3357)	-0.3106	-0.0016	-0.1991	(0.3694)	(0.3010)	0.0596	1.0000	
K_2O	(0.7547)	(0.4578)	(0.2675)	-0.3756	-0.3055	-0.2384	0.0922	0.2346	0.1301	1.0000
Ni	0.2489	-0.2124	(0.6726)	-0.2499	(0.2994)	-0.4835	-0.3794	(0.3758)	-0.3837	0.1718
Co	0.0025	-0.2753	(0.3664)	(0.4667)	-0.1726	0.0412	-0.0608	0.0839	-0.1045	-0.1264
Mn	-0.3023	-0.2051	-0.1919	(0.6007)	(0.3007)	-0.1540	-0.3084	-0.2209	-0.1991	-0.4337
V	0.0175	0.0326	(0.3609)	-0.2680	(0.2640)	-0.3945	-0.3866	(0.6276)	0.1663	0.2302
Cr	(0.8328)	(0.3649)	(0.3137)	-0.1804	-0.2327	-0.3297	0.0249	0.1571	-0.0474	(0.7167)
Zn	-0.2113	0.0034	-0.0690	-0.0763	(0.4854)	-0.1722	-0.2279	(0.2608)	-0.0428	-0.0665
Cu	-0.0352	0.1042	(0.4767)	-0.3090	0.2211	-0.3908	-0.4997	(0.8448)	0.0084	0.2040
Rb	(0.5707)	(0.7445)	0.0777	-0.2729	-0.3704	-0.1413	0.0710	(0.3267)	(0.3146)	(0.7729)
Sr	-0.3513	-0.2938	-0.0689	-0.1453	(0.8510)	-0.3645	-0.3508	0.1657	-0.0462	-0.1374
Y	0.0014	(0.5528)	-0.1345	(0.3122)	-0.0953	-0.1108	-0.1954	0.2210	0.1995	0.0580

TABLE 52 (Cont.): Correlation Matrix of Trace and Major Elements in the Tansley Borehole Rocks(59 Samples)

	Ni	Co	Mn	Y	Cr	Zn	Cu	Rb	Sr	Y
Ni	1.0000									
Co	(0.2994)	1.0000								
Mn	-0.1855	(0.3922)	1.0000							
V	(0.4612)	0.0069	-0.1838	1.0000						
Cr	(0.4066)	-0.0668	-0.3405	(0.3950)	1.0000					
Zn	(0.3025)	-0.2644	-0.0963	(0.2724)	0.0083	1.0000				
Cu	(0.4946)	0.0237	-0.1745	(0.7346)	0.2283	(0.3672)	1.0000			
Rb	0.0330	-0.3287	-0.5217	0.2398	(0.5548)	0.1500	(0.3201)	1.0000		
Sr	(0.3763)	-0.2768	0.0519	(0.3319)	-0.0713	(0.7482)	(0.3103)	-0.1087	1.0000	
Y	-0.1354	-0.0020	(0.2593)	0.1325	-0.0675	0.2083	(0.3162)	(0.3556)	0.0653	1.0000

TABLE 52 (Cont.): Correlation Groups

Group 1

	TiO_2	Al_2O_3	Ba	K_2O	Cr	Rb
TiO_2	1.0000					
Al_2O_3	0.4963	1.0000				
Ba		0.3357	1.0000			
K_2O	0.7457	0.4578		1.0000		
Cr	0.8328	0.3649		0.7167	1.0000	
Rb	0.5707	0.7445	0.3146	0.772	0.5548	1.0000

Group 2

	Fe_2O_3	Pb	Ni	V	Cu
Fe_2O_3	1.0000				
Pb	0.5238	1.0000			
Ni	0.6726	0.3758	1.0000		
V	0.3906	0.6276	0.4612	1.0000	
Cu	0.4767	0.8448	0.4946	0.7346	1.0000

Group 3

	FeO	Co	Mn
FeO	1.0000		
Co	0.4667	1.0000	
Mn	0.6007	0.3922	1.0000

Group 4

	Na_2O	Zr	Ba
Na_2O	1.0000		
Zr	0.6819	1.0000	
Ba	0.3694	0.3010	1.0000

volcanic mudstones. Ni-Co, Co-Fe_2O_3, Ni-Zn, Zn-Pb, Zn-V and Zn-Cu correlations probably suggest that Co and Zn are partly incorporated in pyrite and organic matter. The significant correlation of Cr-Fe_2O_3, Cr-Ni, Cr-V, Rb-Pb and Rb-V, are ascribed to the abundance of pyrite and illite in the marine shales, although it may indicate that a small proportion of Ni, Pb and V are contained in illite. In contrast to these element associations, Y shows no definite relationship and its strongest correlation is with Al_2O_3, in addition to that with FeO, Mn, Cu and Rb. These erratic relationships perhaps indicate contribution by several minerals. Scatter diagrams of some significant correlation are shown in Figure 34.

The volcanic mudstones are excluded from the correlation matrix, and the significant relationships are underlined (Table 53). The depth of the samples is also included. Pyrite, organic matter, calcite and to a lesser extent ankerite are abundant in the lower part of the Namurian succession, especially in the marine shales. This relationship is clearly reflected by the correlation of depth with Fe_2O_3, CaO, Pb, Ni, V, Zn, Cu and Sr. The negative relationship of depth with the rest of the elements is largely due to interference of feldspars, together with higher contents of Zr and TiO_2 of the non-marine shales. This is supported by the correlation of TiO_2 and Al_2O_3 with Ba, K_2O, Cr and Rb, and Na_2O-Zr relationships. Zr correlations with TiO_2 and Na_2O in a similar Carboniferous sediment have been interpreted as indicating detrital association (Hirst and Kaye, 1971). Likewise these correlations may be considered as partly due to illite. In this case, however, K_2O-Ba relationship becomes significant, while previously it was not. The correlation coefficient values of Fe_2O_3 with Pb, V and Cu increase, whereas Ni decrease. Moreover, the Co-Fe_2O_3 relationship is no longer significant. Such behaviour may suggest that Co could be concentrated in carbonates and clay minerals. The FeO-Co

FIGURE 34 Scatter Plots of some Positive and Significant Bivariant Relationships between Trace and Major Elements, Tansley Borehole

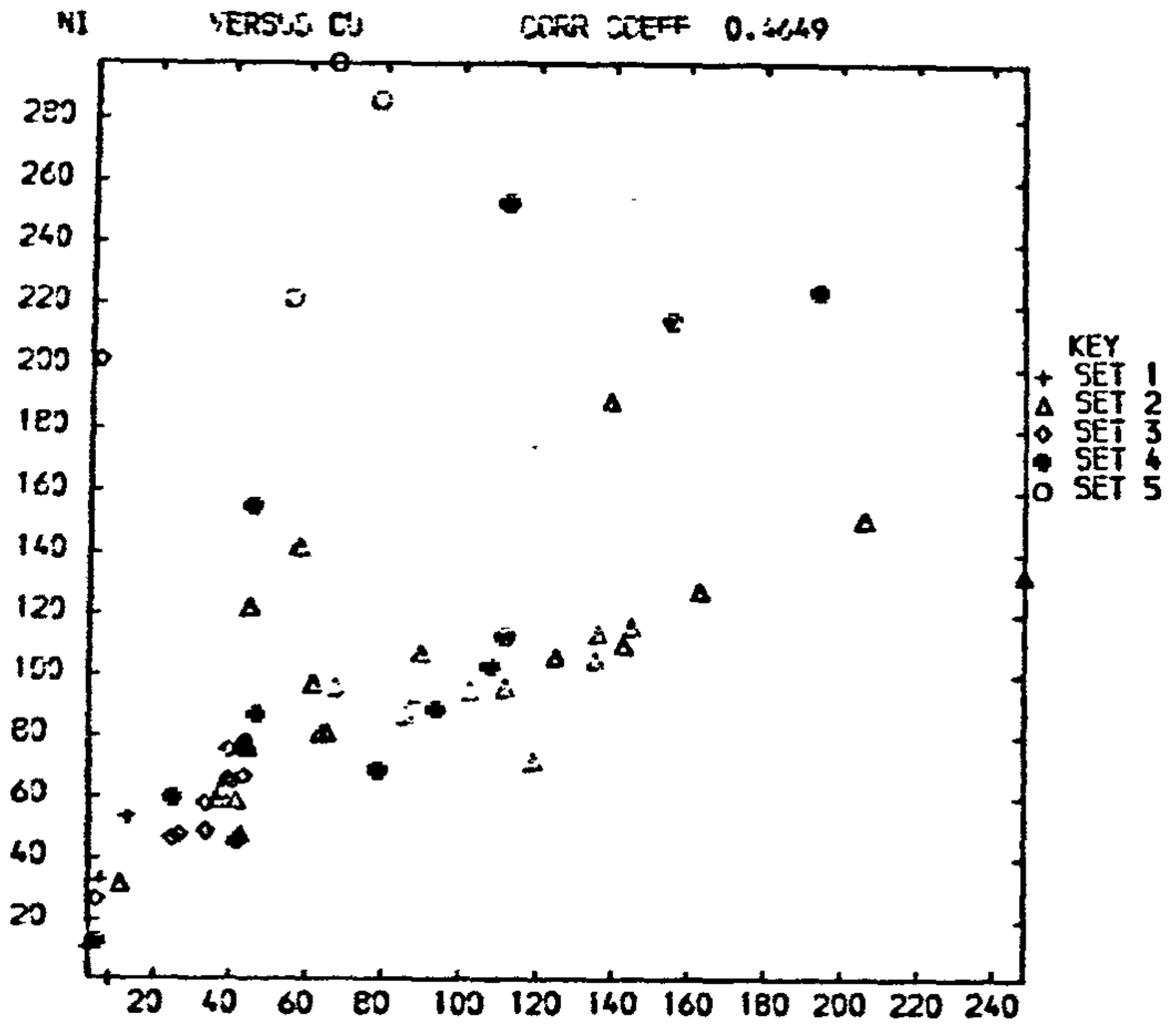
NI VERSUS CU CORR COEFF 0.4649
KEY
SET 1
SET 2
SET 3
SET 4
SET 5

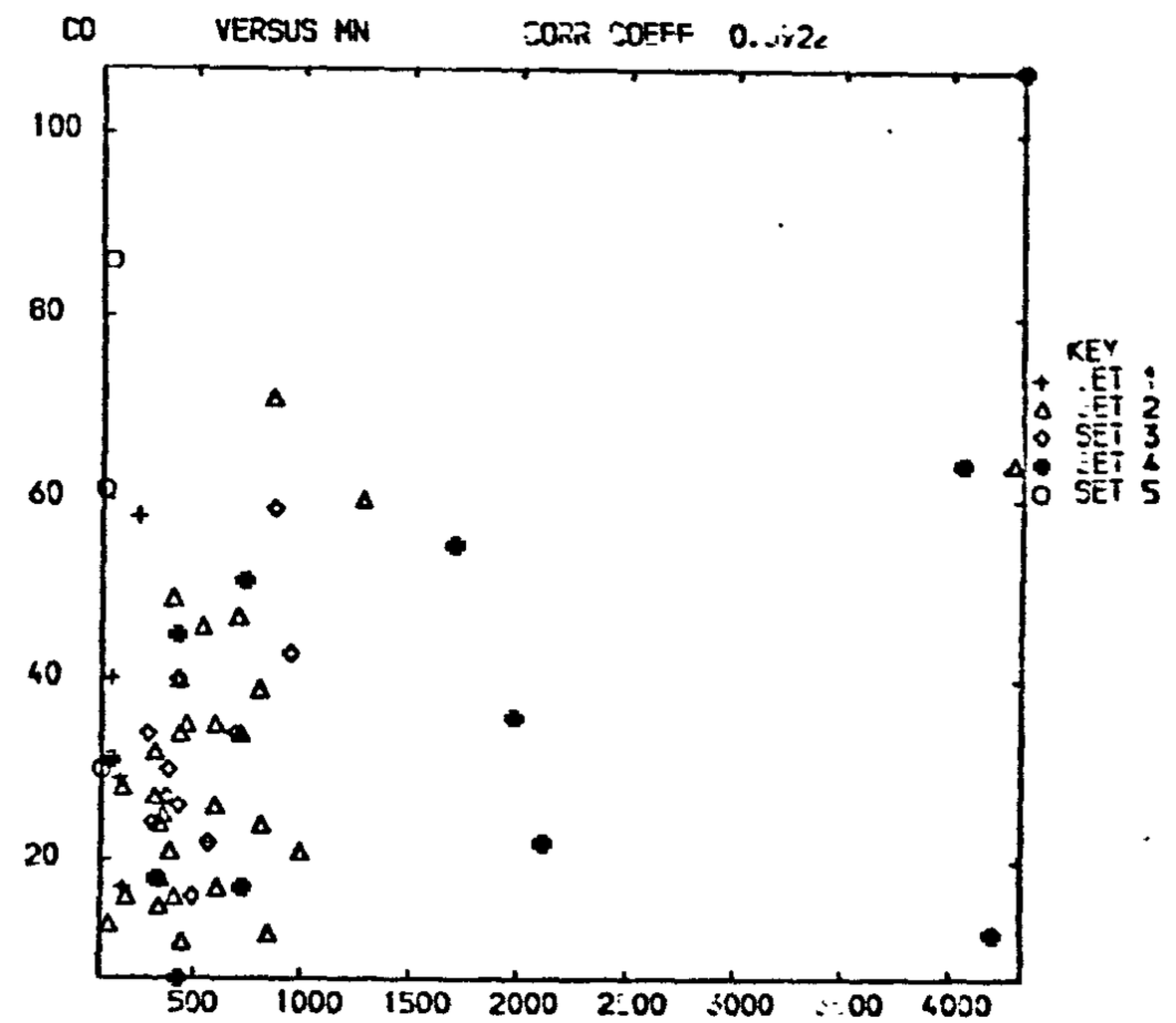
CO VERSUS MN CORR COEFF 0.
KEY
SET 1
SET 2
SET 3
SET 4
SET 5

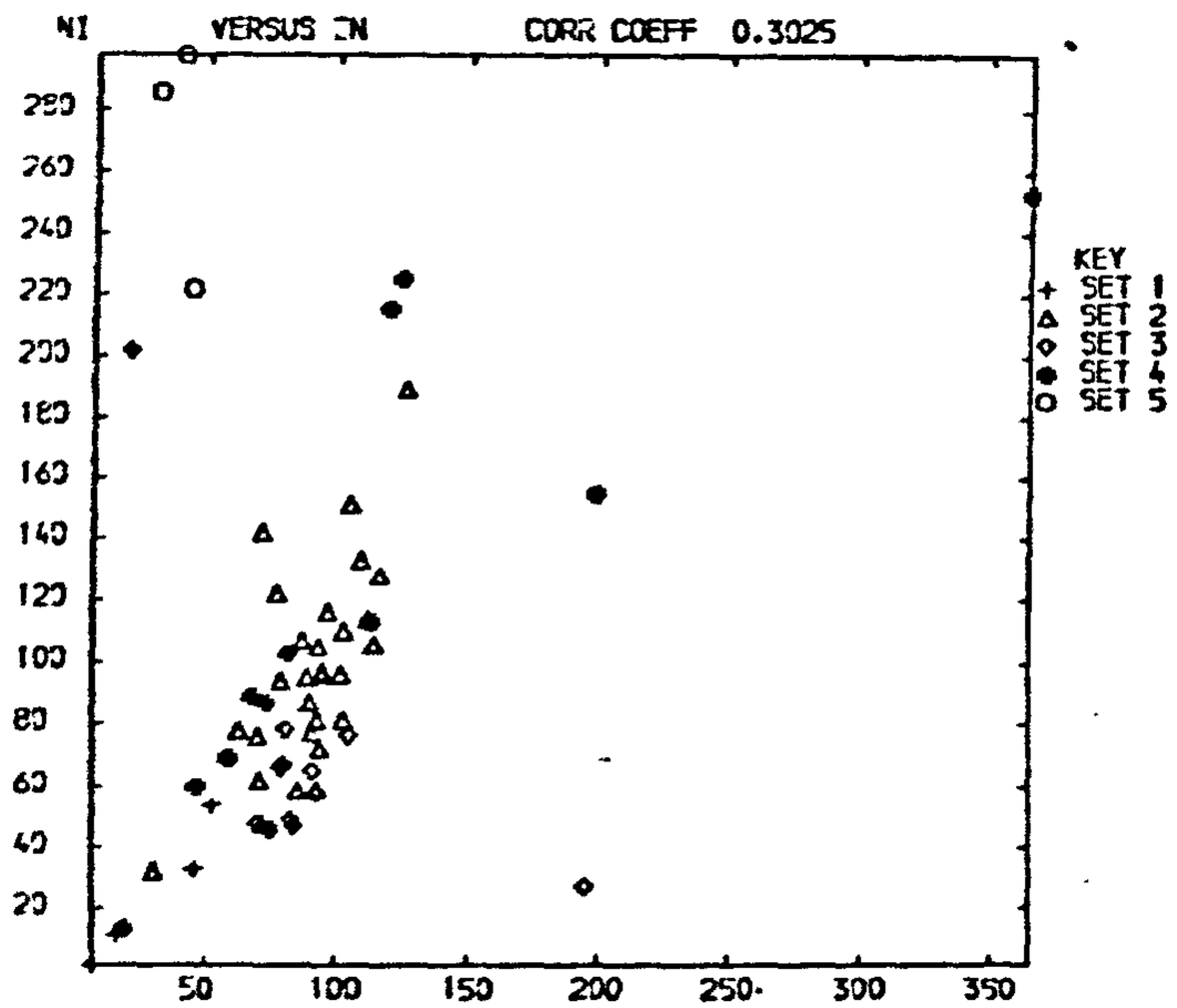
NI VERSUS ZN CORR COEFF 0.3025
KEY
SET 1
SET 2
SET 3
SET 4
SET 5

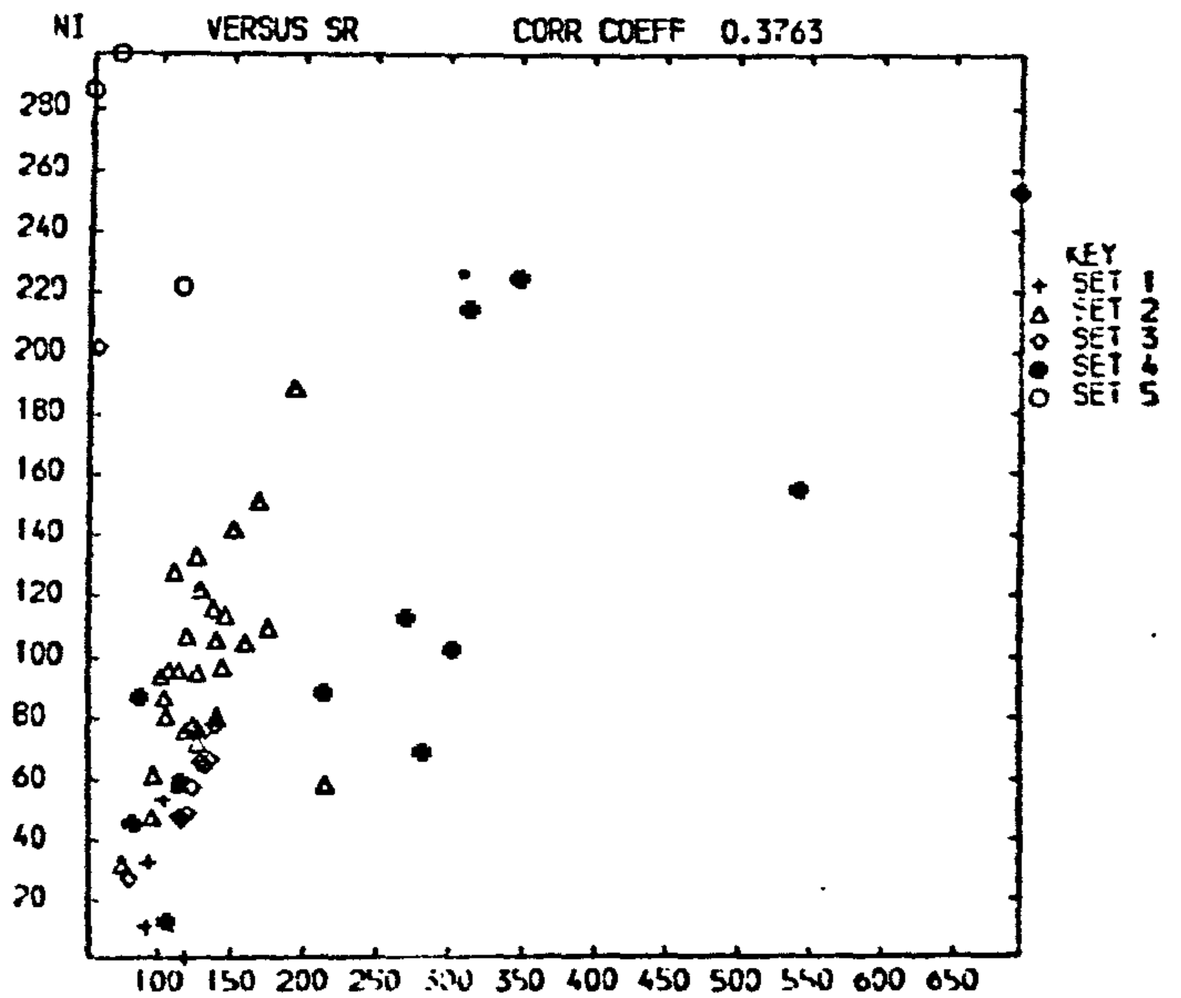
NI VERSUS SR CORR COEFF 0.3763
KEY
SET 1
SET 2
SET 3
SET 4
SET 5

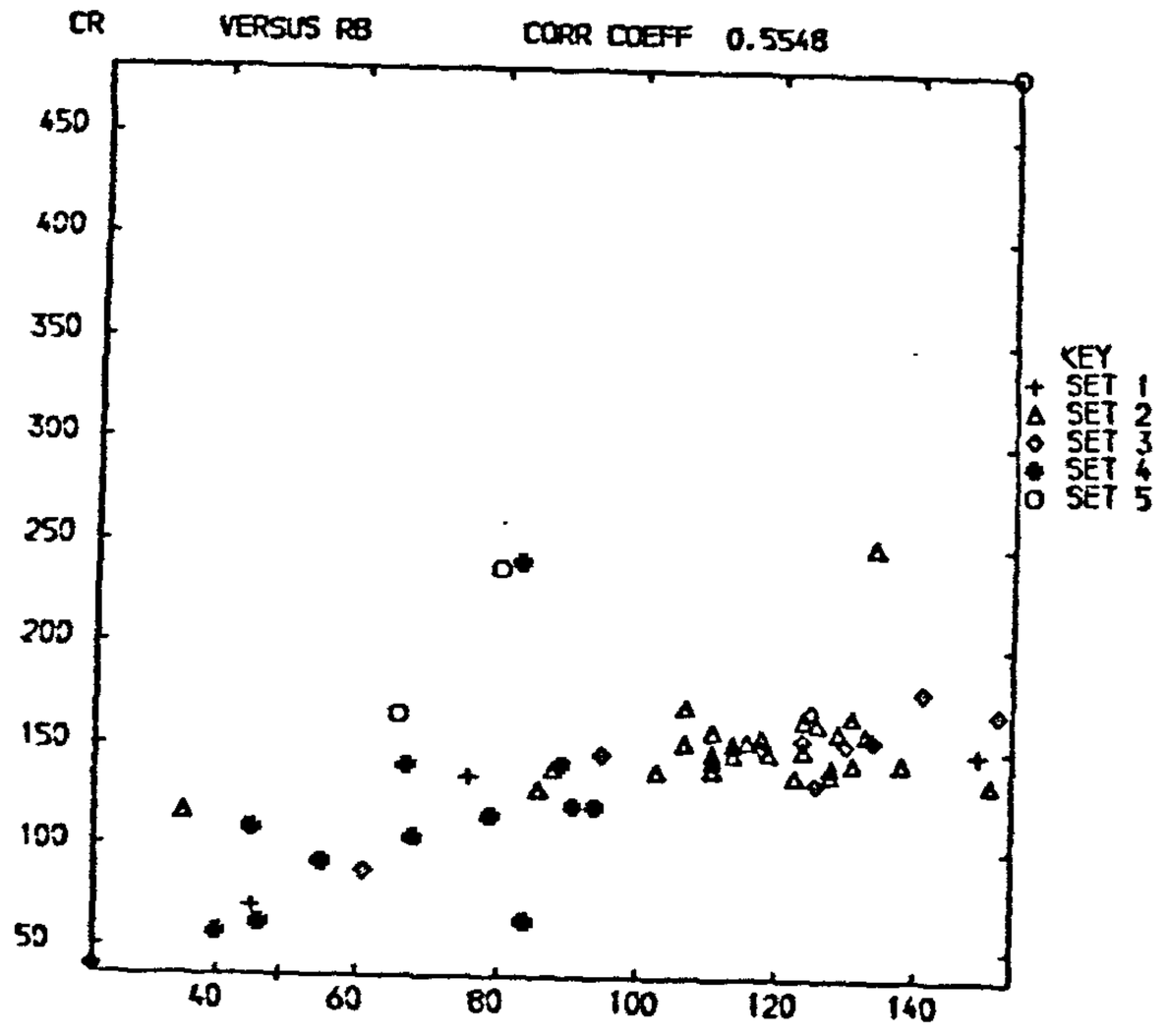
CR VERSUS RB CORR COEFF 0.5548
450
400
350
300
250
200
150
100
50
40 60 80 100 120 140
KEY
SET 1
SET 2
SET 3
SET 4
SET 5

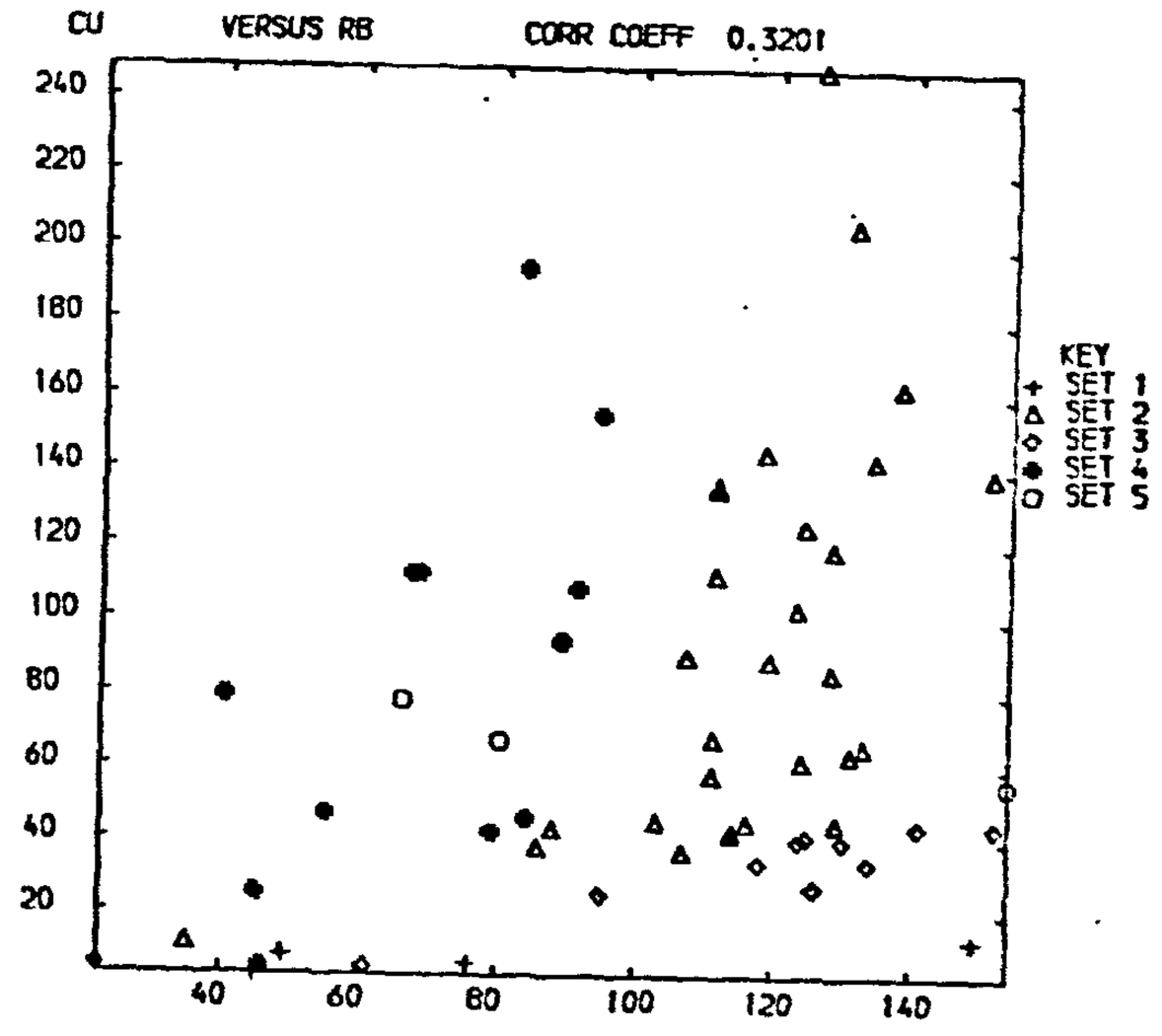
CU VERSUS RB CORR COEFF 0.3201
240
220
200
180
160
140
120
100
80
60
40
20
40 60 80 100 120 140
KEY
SET 1
SET 2
SET 3
SET 4
SET 5

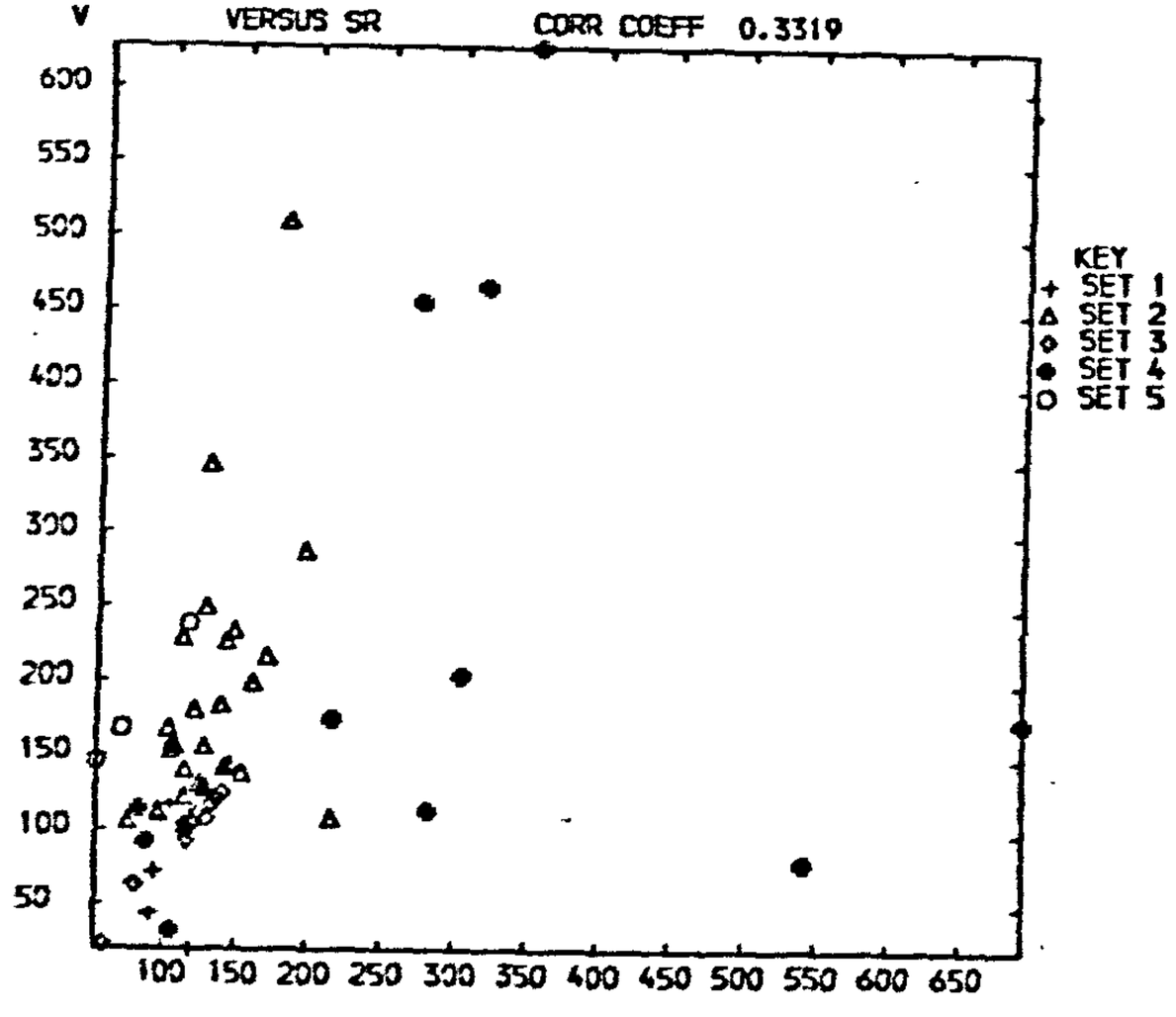
V VERSUS SR CORR COEFF 0.3319
600
550
500
450
400
350
300
250
200
150
100
50
100 150 200 250 300 350 400 450 500 550 600 650
KEY
SET 1
SET 2
SET 3
SET 4
SET 5

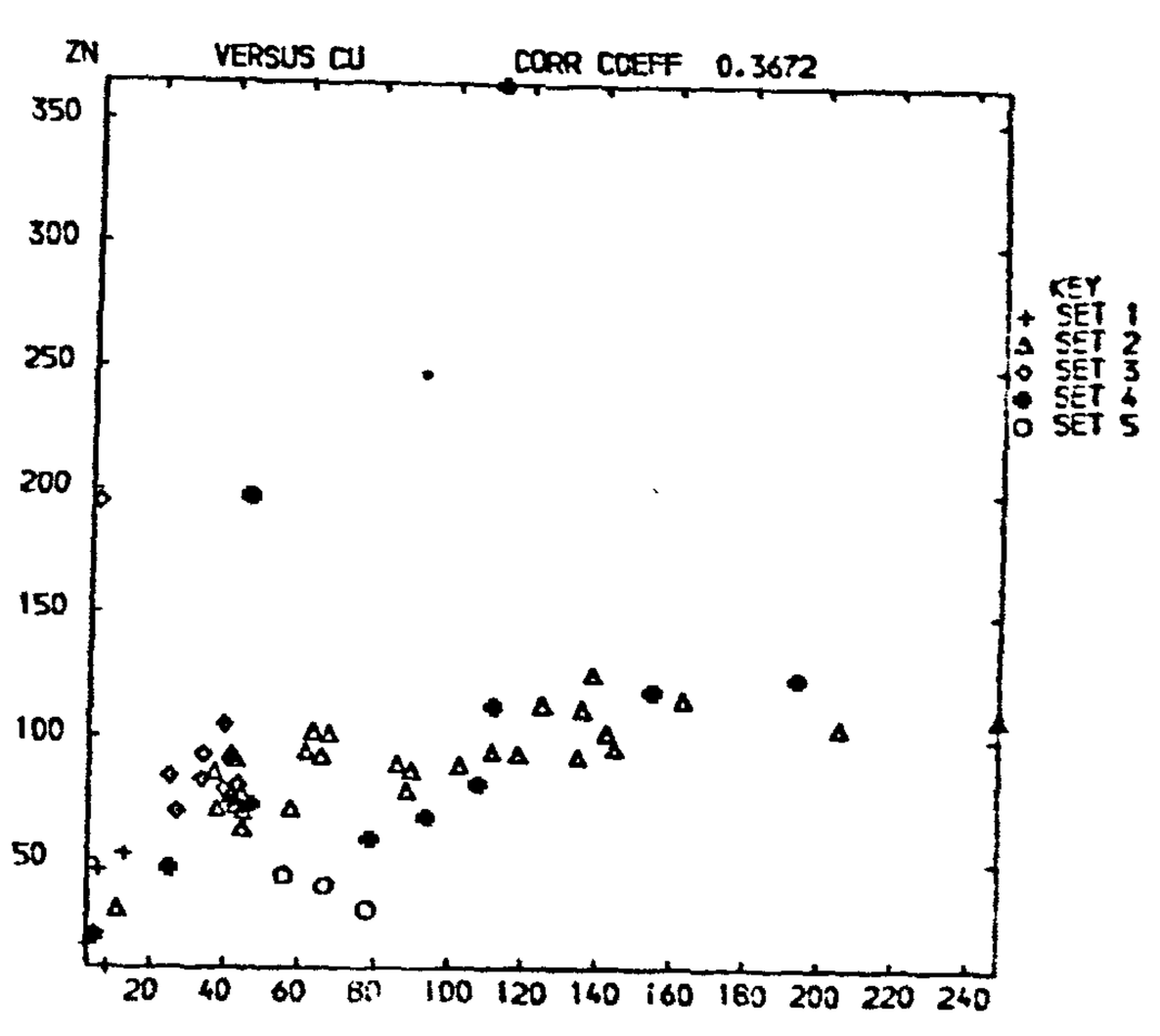
ZN VERSUS CU CORR COEFF 0.3672
350
300
250
200
150
100
50
20 40 60 80 100 120 140 160 180 200 220 240
KEY
SET 1
SET 2
SET 3
SET 4
SET 5

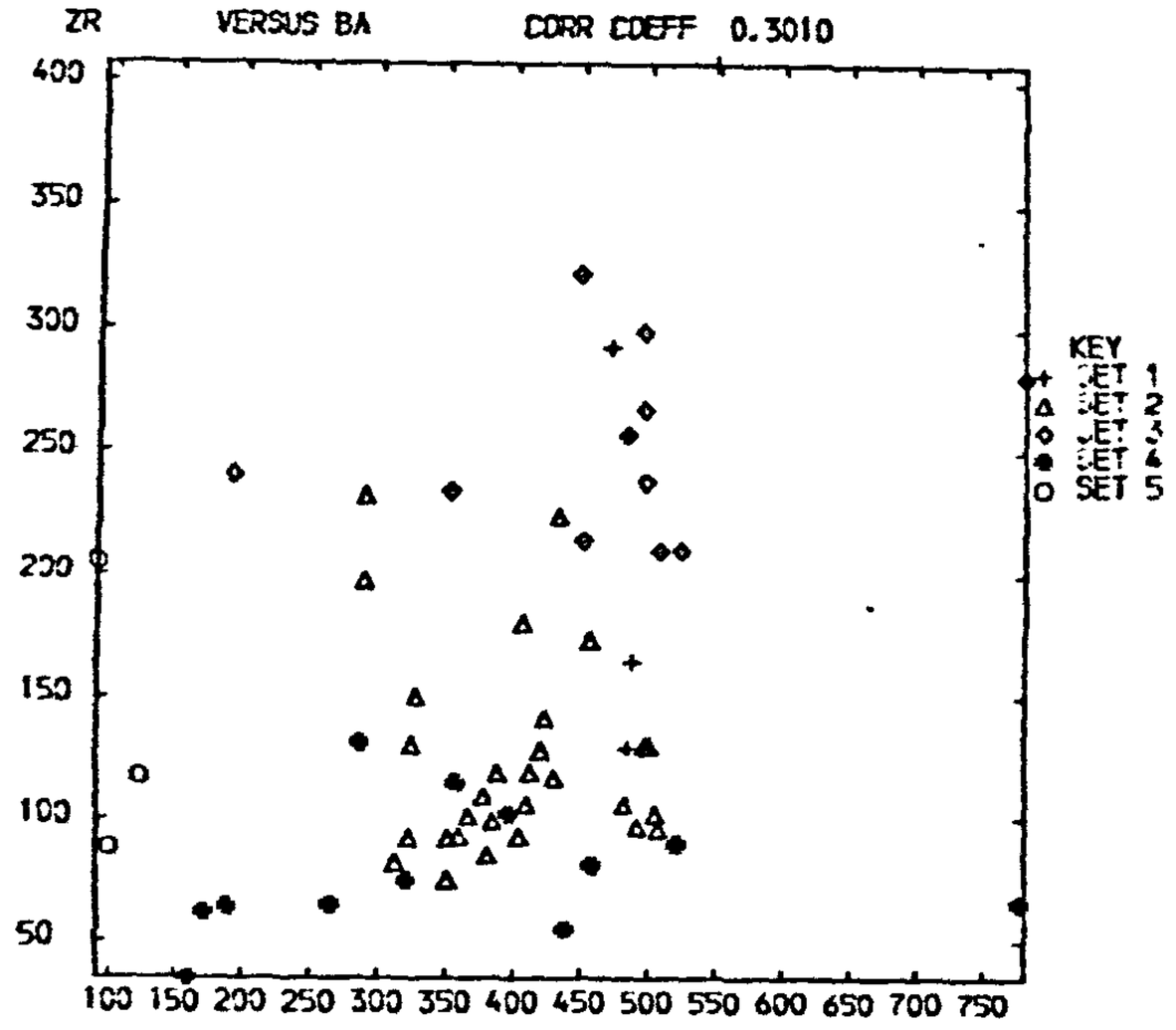
ZR VERSUS BA CORR COEFF 0.3010
400
350
300
250
200
150
100
50
100 150 200 250 300 350 400 450 500 550 600 650 700 750
KEY
SET 1
SET 2
SET 3
SET 4
SET 5

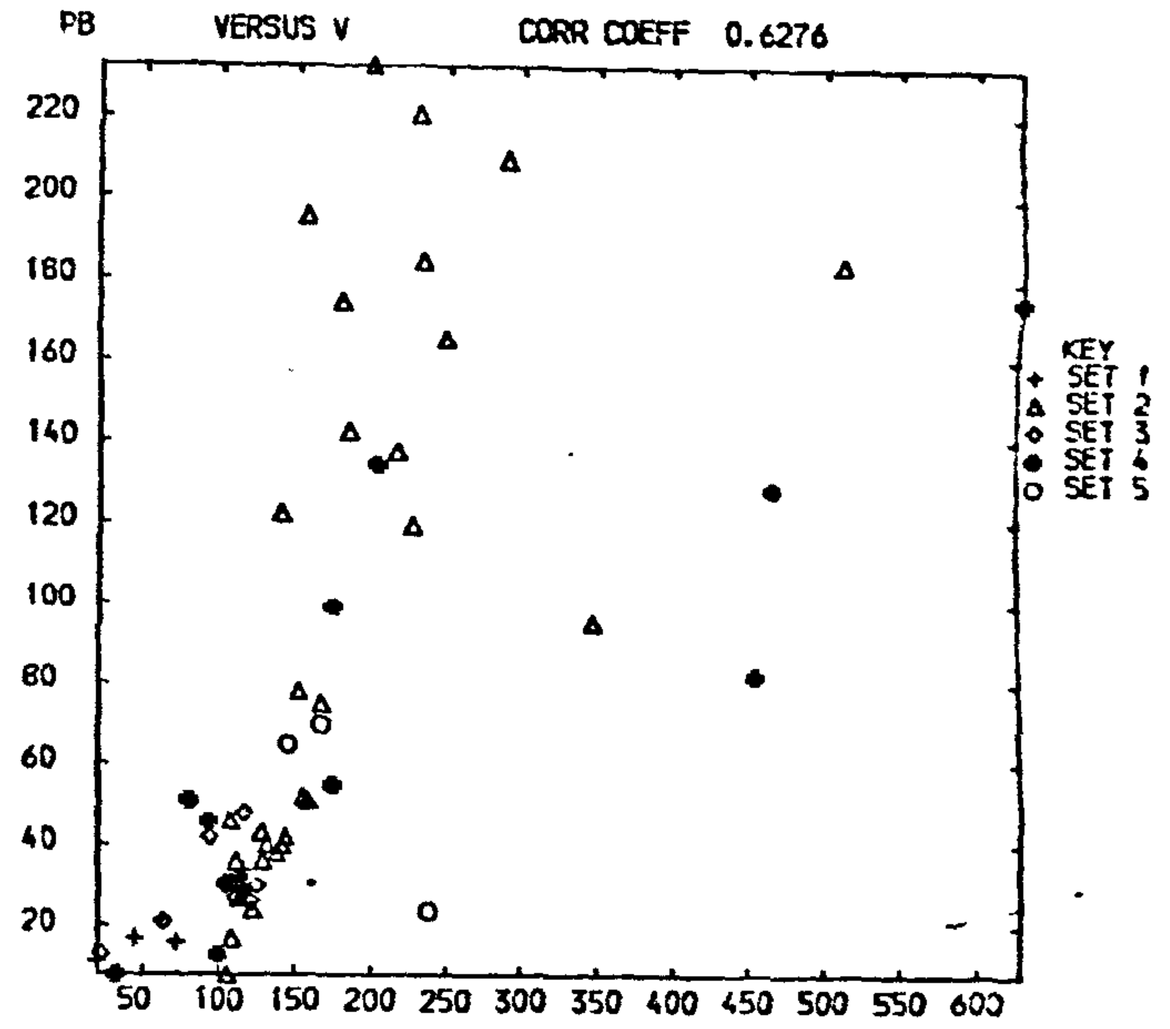
PB VERSUS V CORR COEFF 0.6276
220
200
180
160
140
120
100
80
60
40
20
50 100 150 200 250 300 350 400 450 500 550 600
KEY
SET 1
SET 2
SET 3
SET 4
SET 5

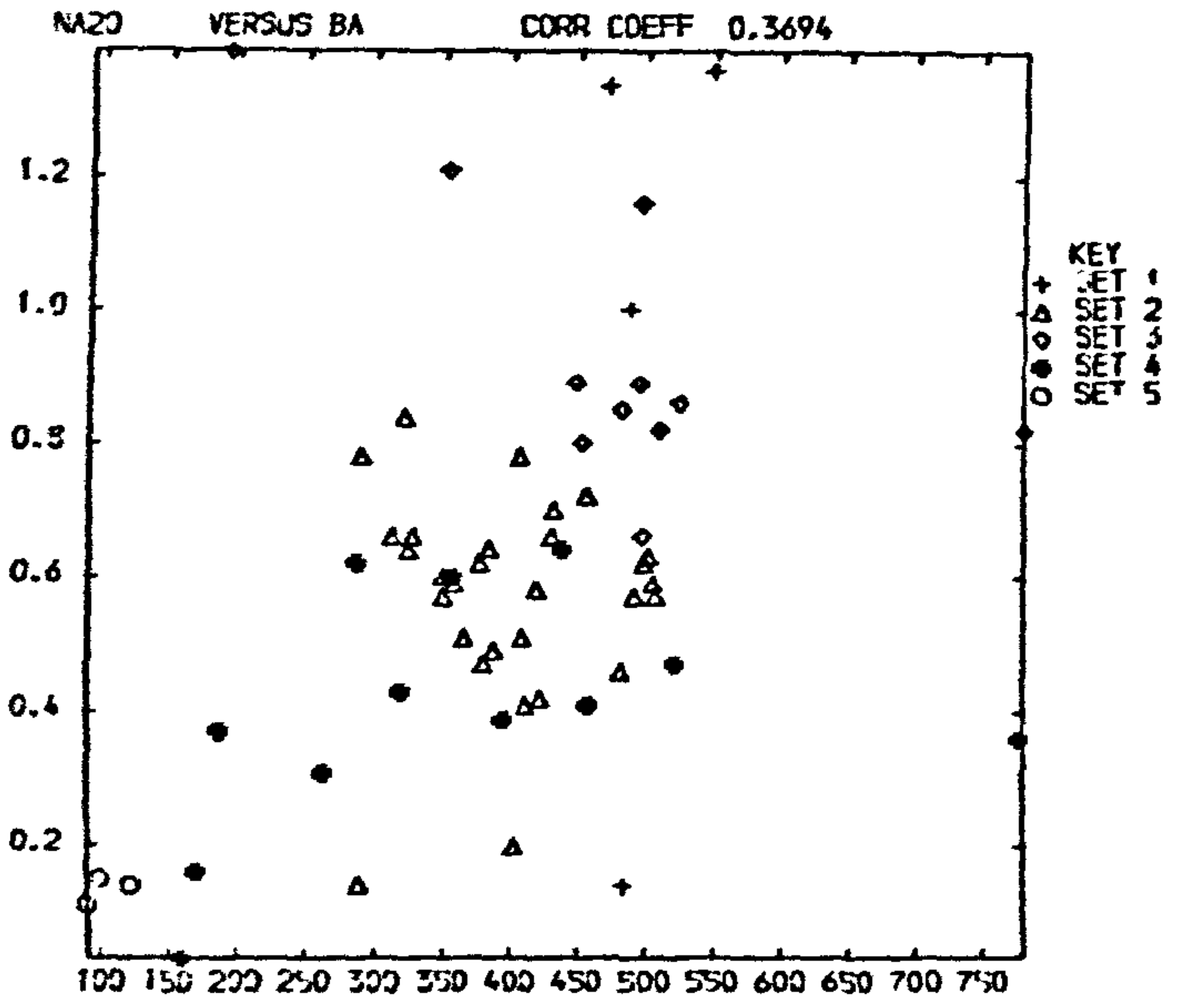
NA2O VERSUS BA CORR COEFF 0.3694
1.2
1.0
0.8
0.6
0.4
0.2
100 150 200 250 300 350 400 450 500 550 600 650 700 750
KEY
SET 1
SET 2
SET 3
SET 4
SET 5

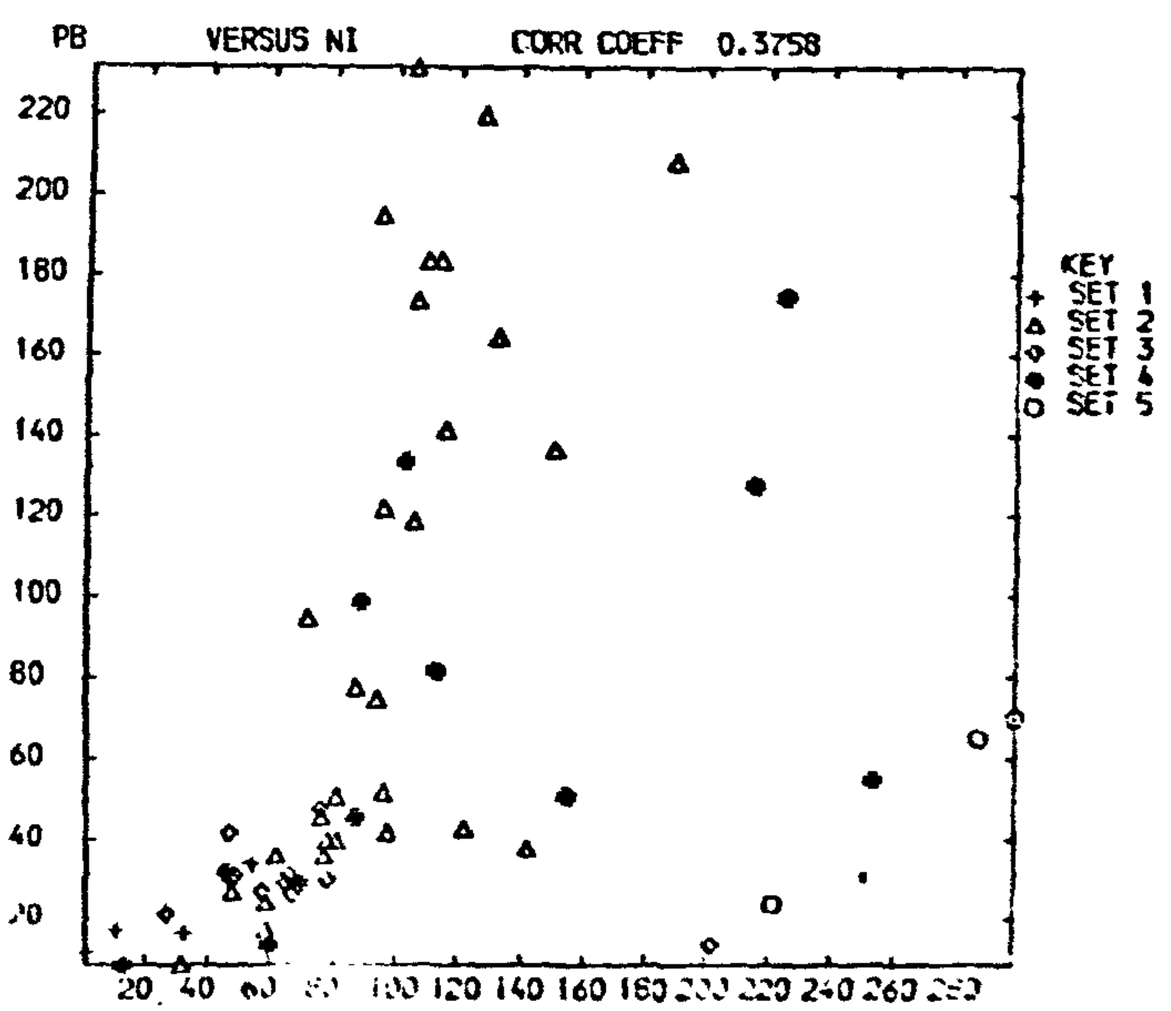
PB VERSUS NI CORR COEFF 0.3758
220
200
180
160
140
120
100
80
60
40
20
20 40 60 100 120 140 160 180 200 220 240 260
KEY
SET 1
SET 2
SET 3
SET 4
SET 5

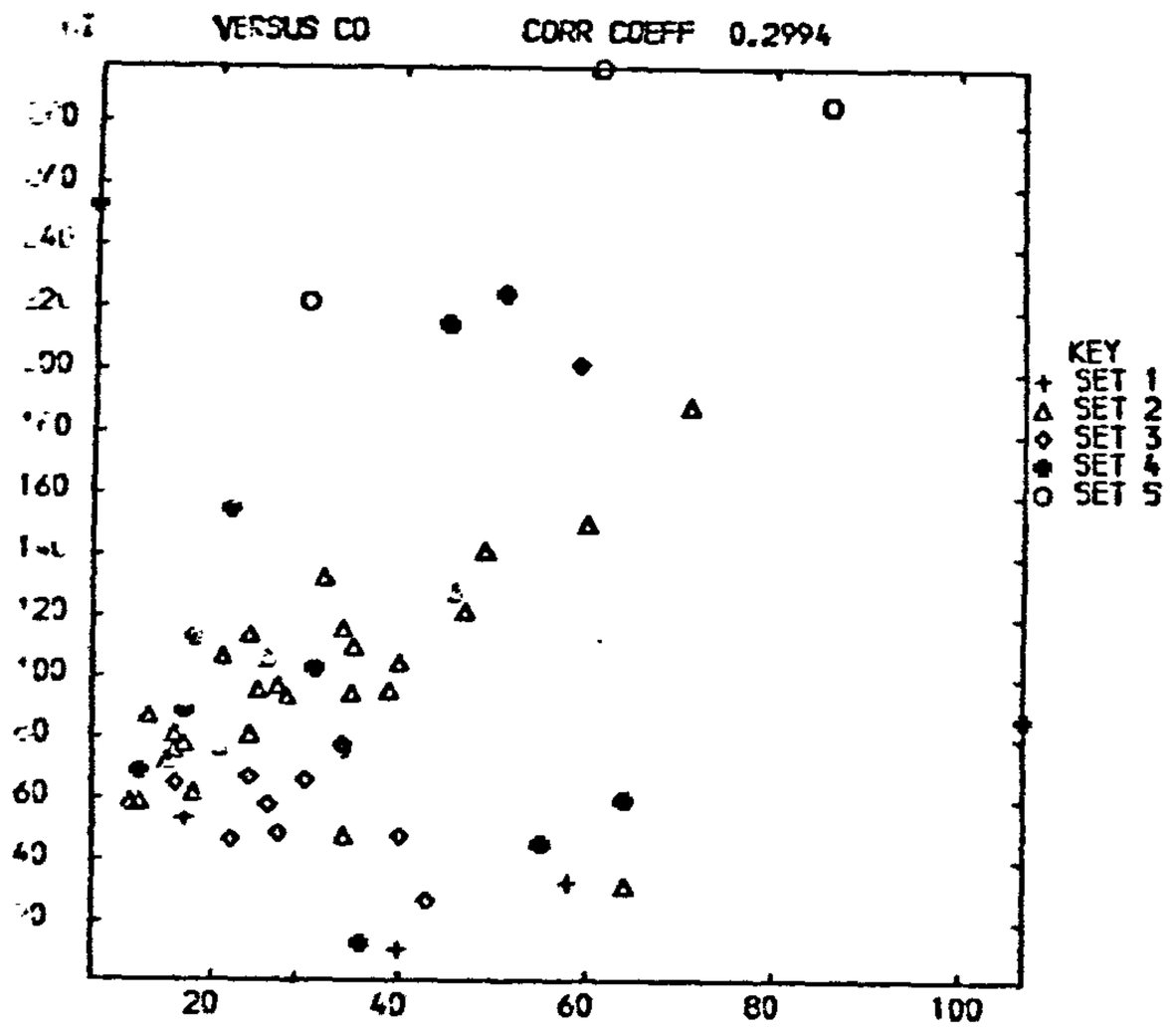
VERSUS CO
CORR COEFF 0.2994
KEY
SET 1
SET 2
SET 3
SET 4
SET 5
20
40
60
80
100

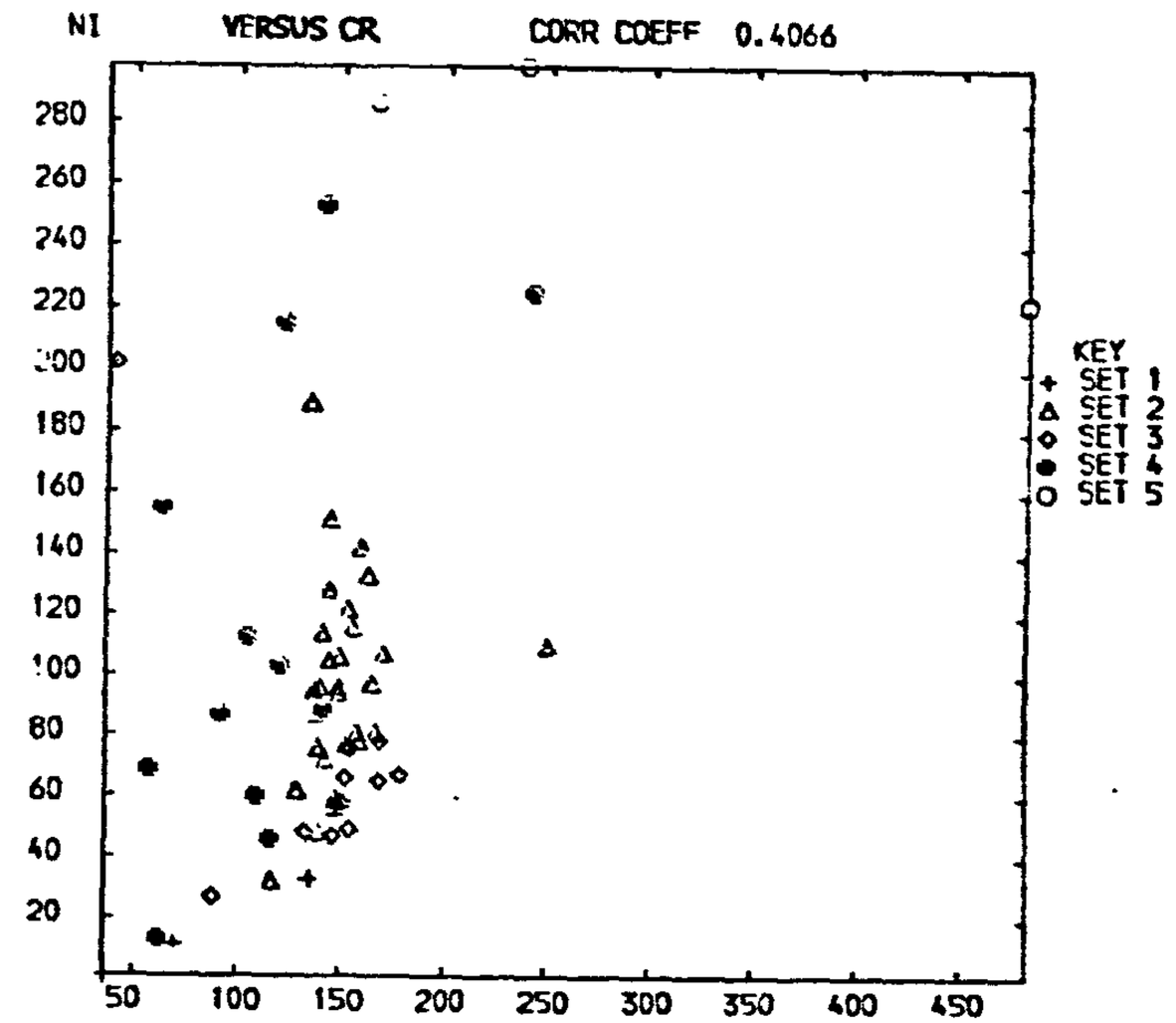
NI
VERSUS CR
CORR COEFF 0.4066
KEY
SET 1
SET 2
SET 3
SET 4
SET 5
280
260
240
220
200
180
160
140
120
100
80
60
40
20
50
100
150
200
250
300
350
400
450

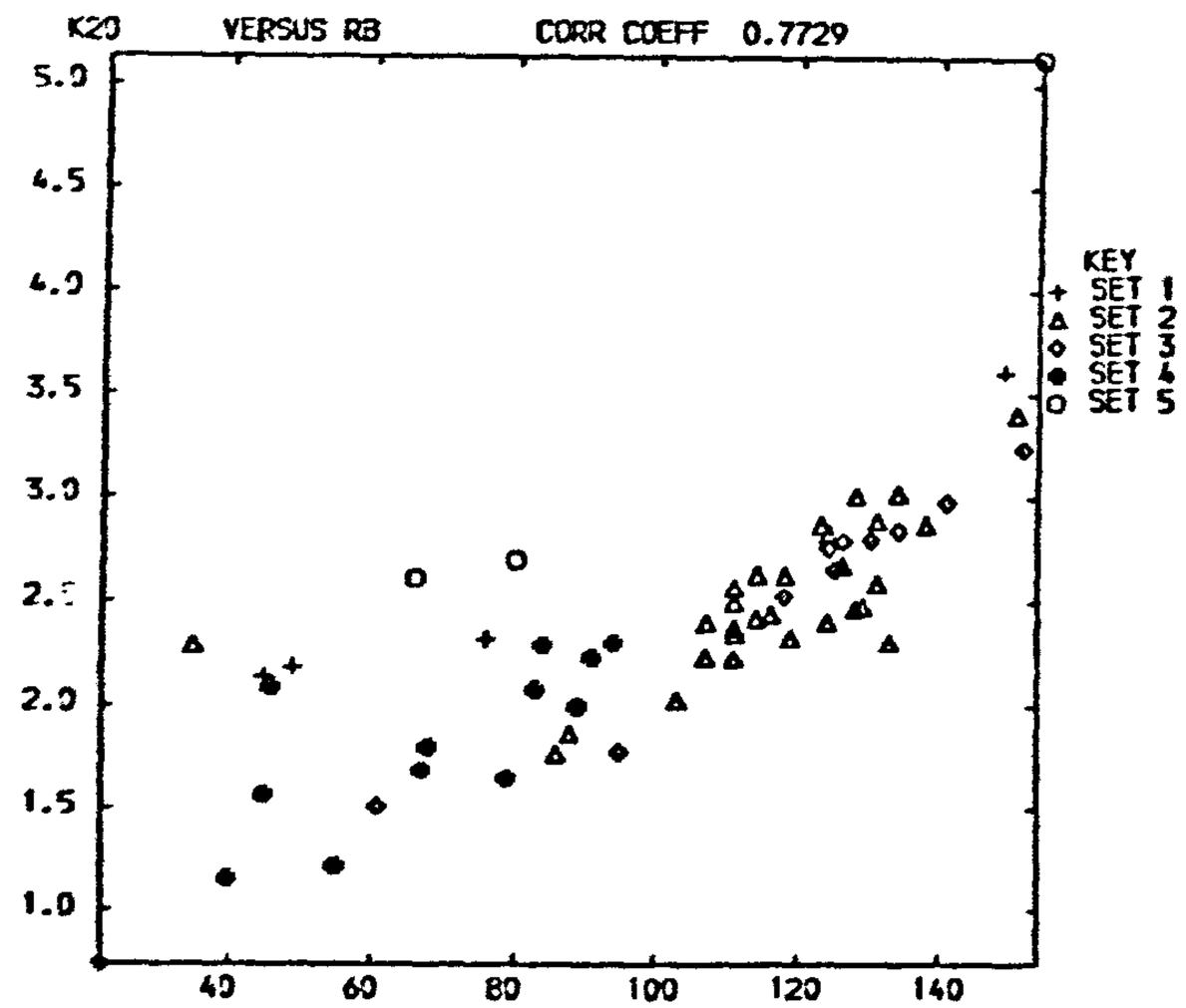
K20
VERSUS RB
CORR COEFF 0.7729
KEY
SET 1
SET 2
SET 3
SET 4
SET 5
5.0
4.5
4.0
3.5
3.0
2.5
2.0
1.5
1.0
40
60
80
100
120
140

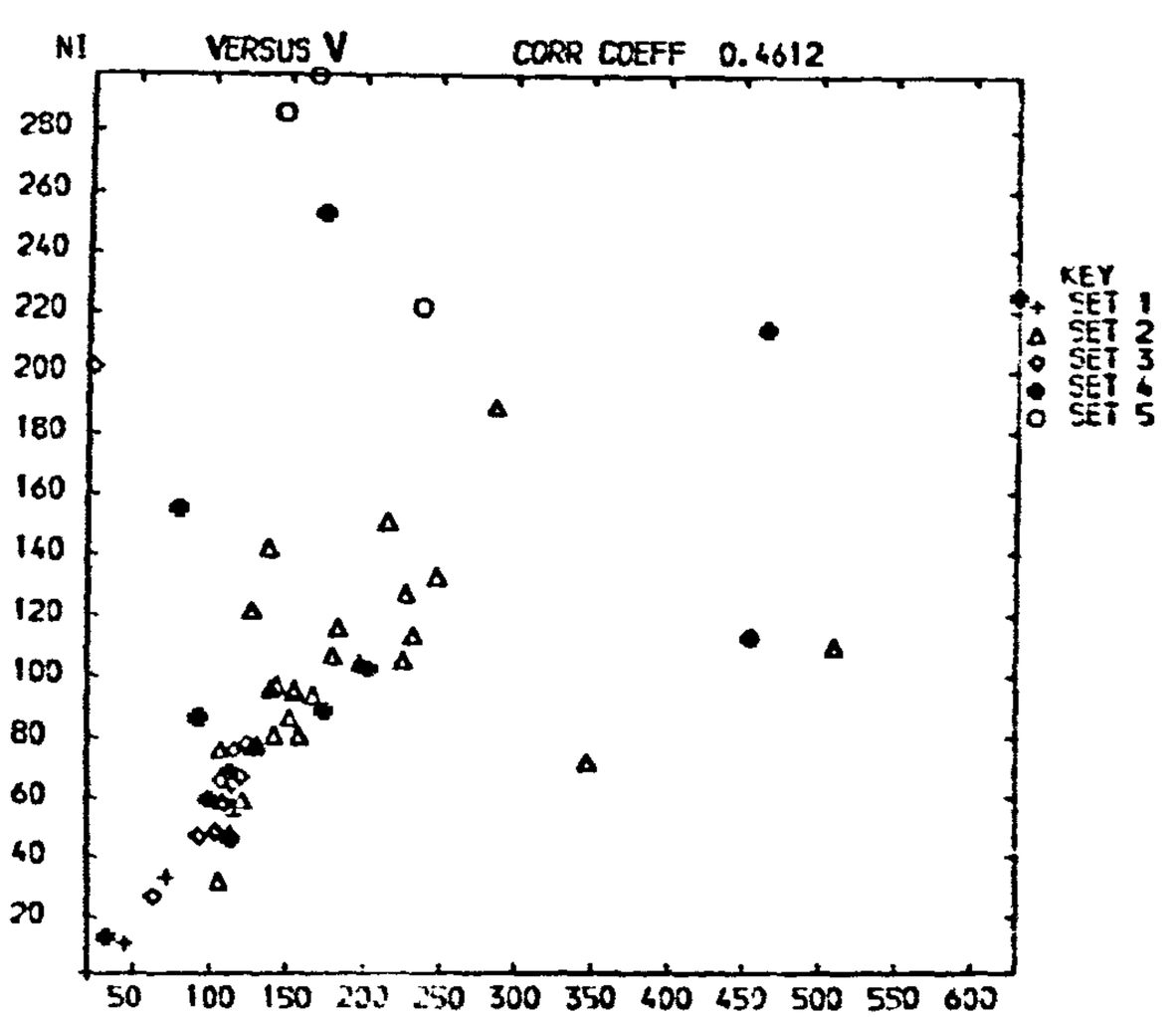
NI
VERSUS V
CORR COEFF 0.4612
KEY
SET 1
SET 2
SET 3
SET 4
SET 5
280
260
240
220
200
180
160
140
120
100
80
60
40
20
50
100
150
200
250
300
350
400
450
500
550
600

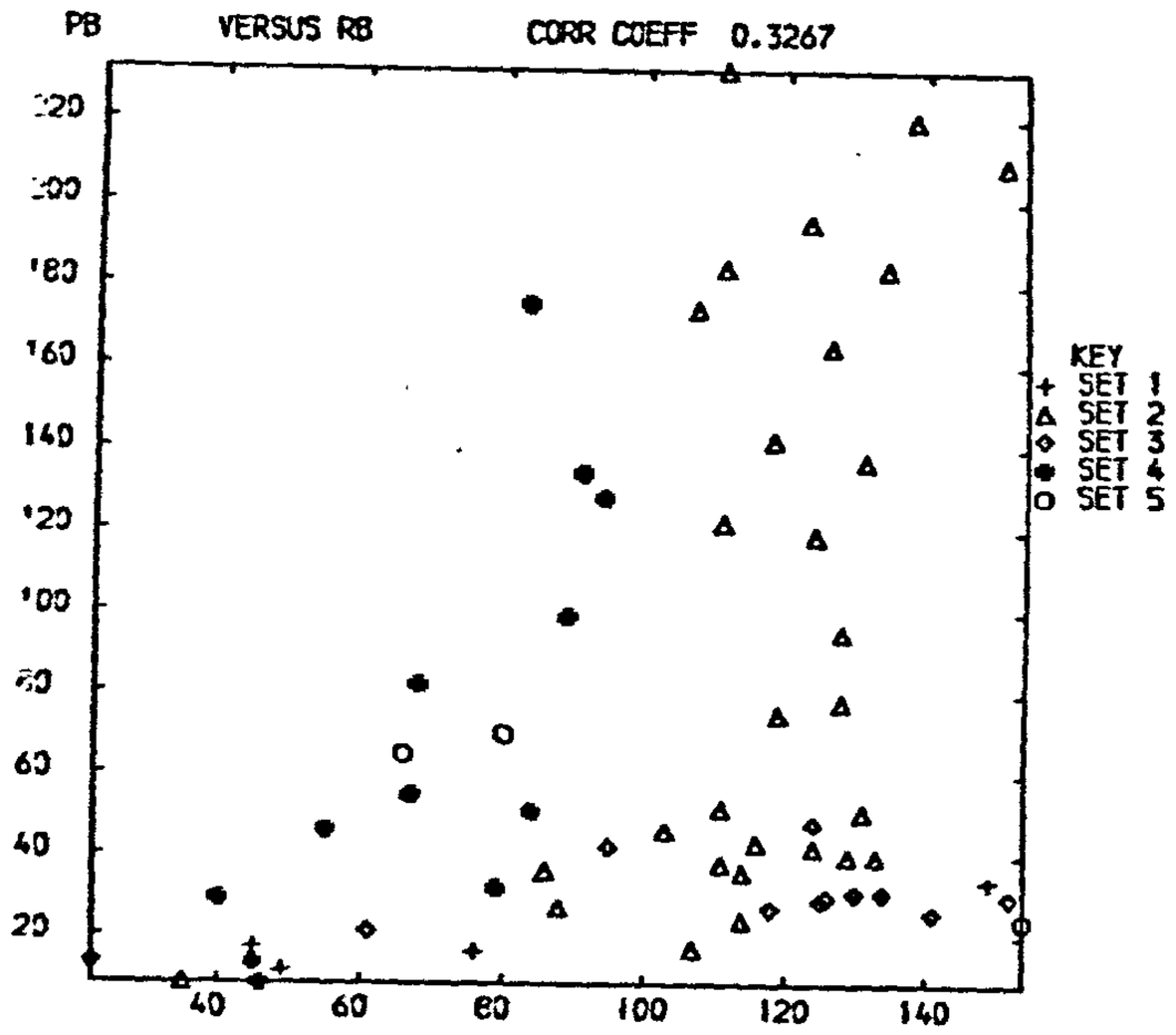
PB VERSUS RB CORR COEFF 0.3267
KEY
SET 1
SET 2
SET 3
SET 4
SET 5
40 60 80 100 120 140

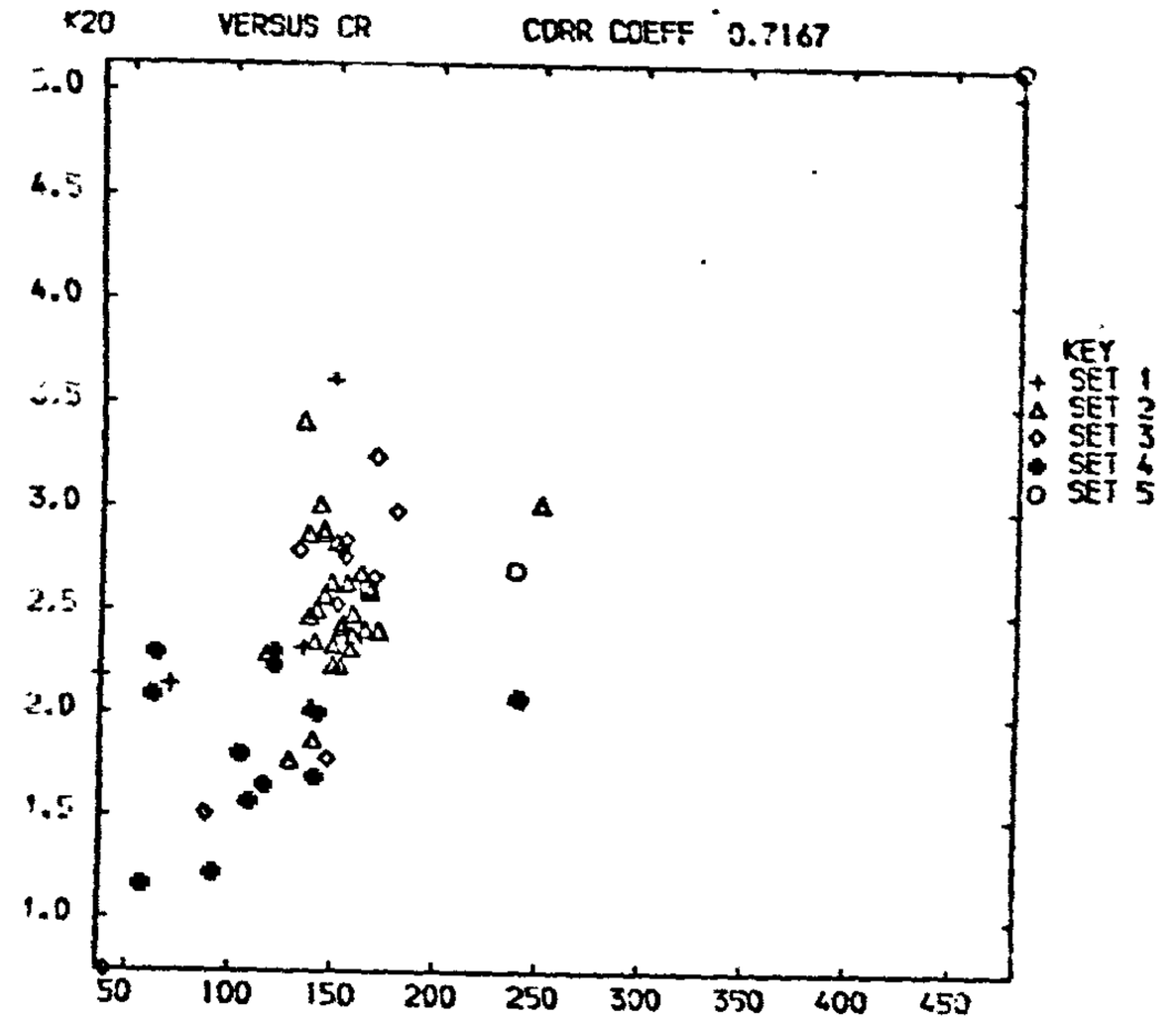
K20 VERSUS CR CORR COEFF 0.7167
KEY
SET 1
SET 2
SET 3
SET 4
SET 5
50 100 150 200 250 300 350 400 450

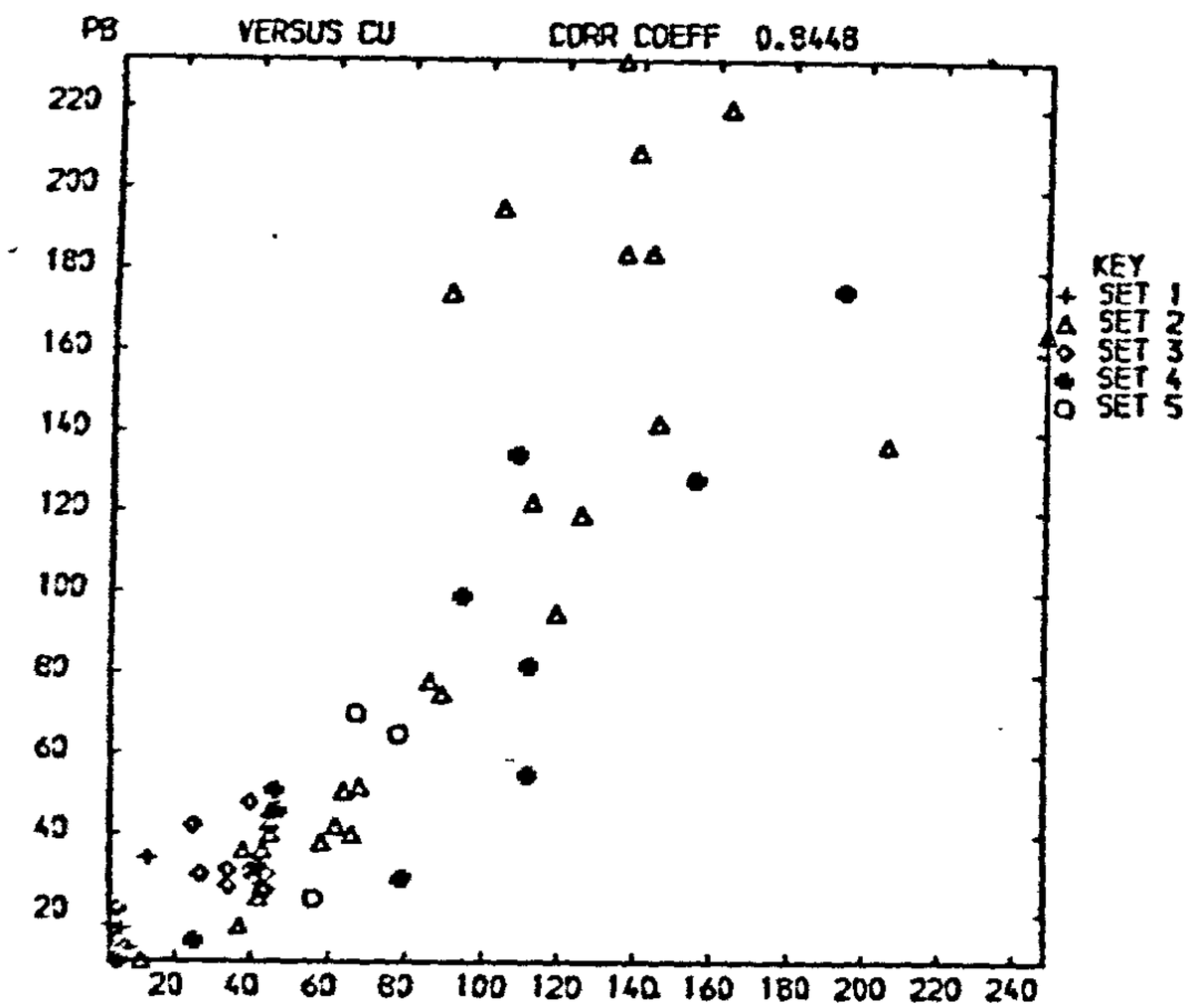
PB VERSUS CU CORR COEFF 0.8448
KEY
SET 1
SET 2
SET 3
SET 4
SET 5
20 40 60 80 100 120 140 160 180 200 220 240

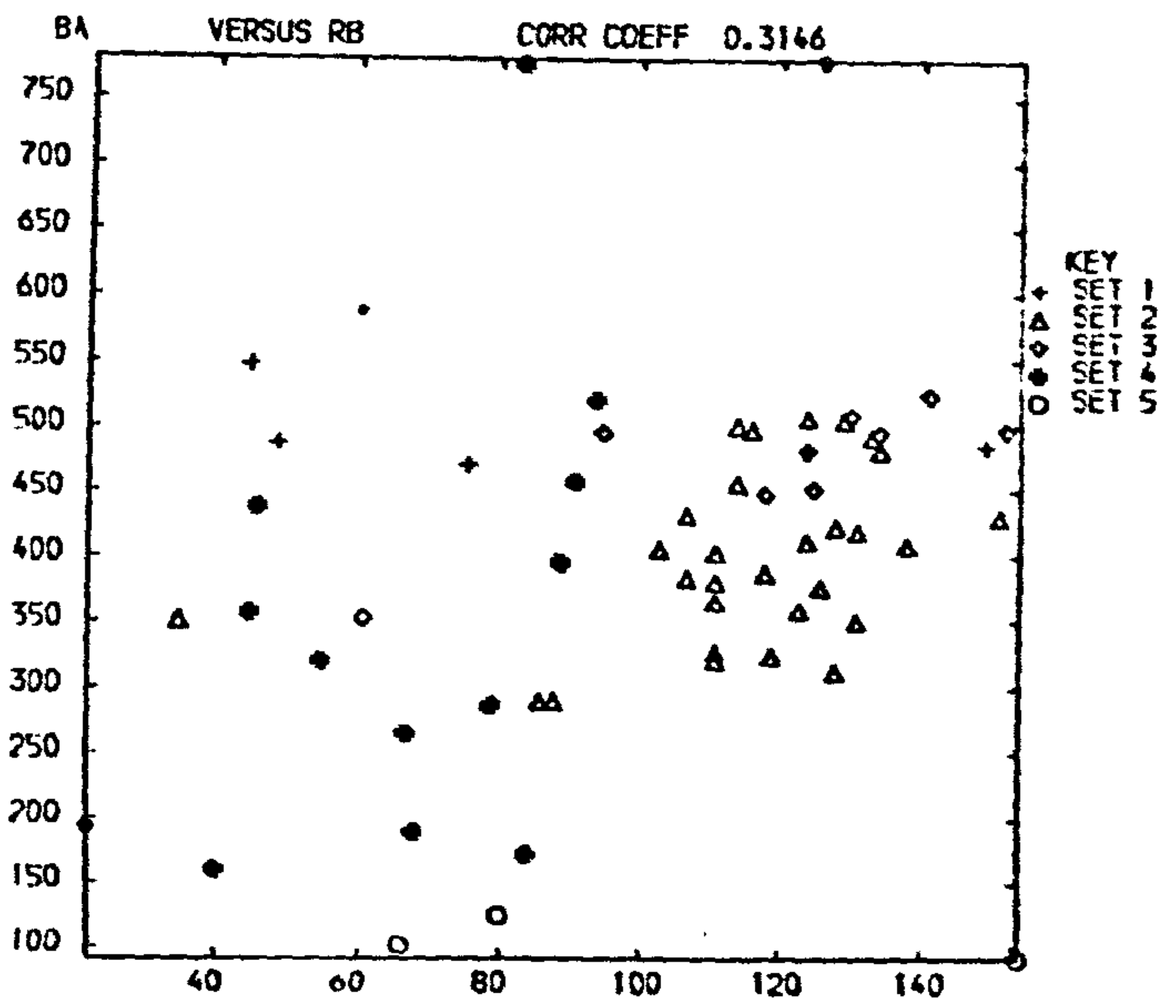
BA VERSUS RB CORR COEFF 0.3146
KEY
SET 1
SET 2
SET 3
SET 4
SET 5
40 60 80 100 120 140

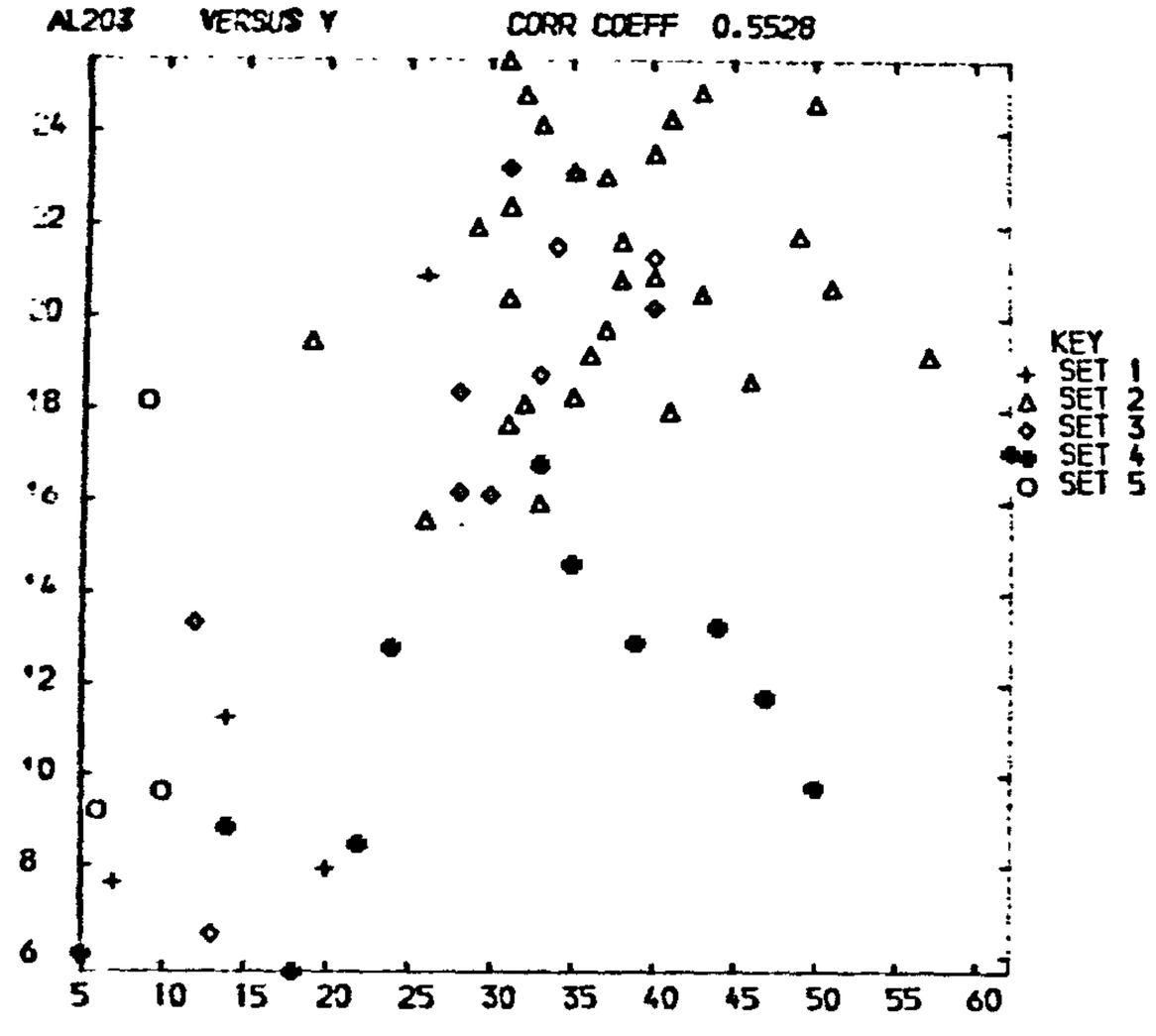
AL203 VERSUS Y
CORR COEFF 0.5528
KEY
SET 1
SET 2
SET 3
SET 4
SET 5

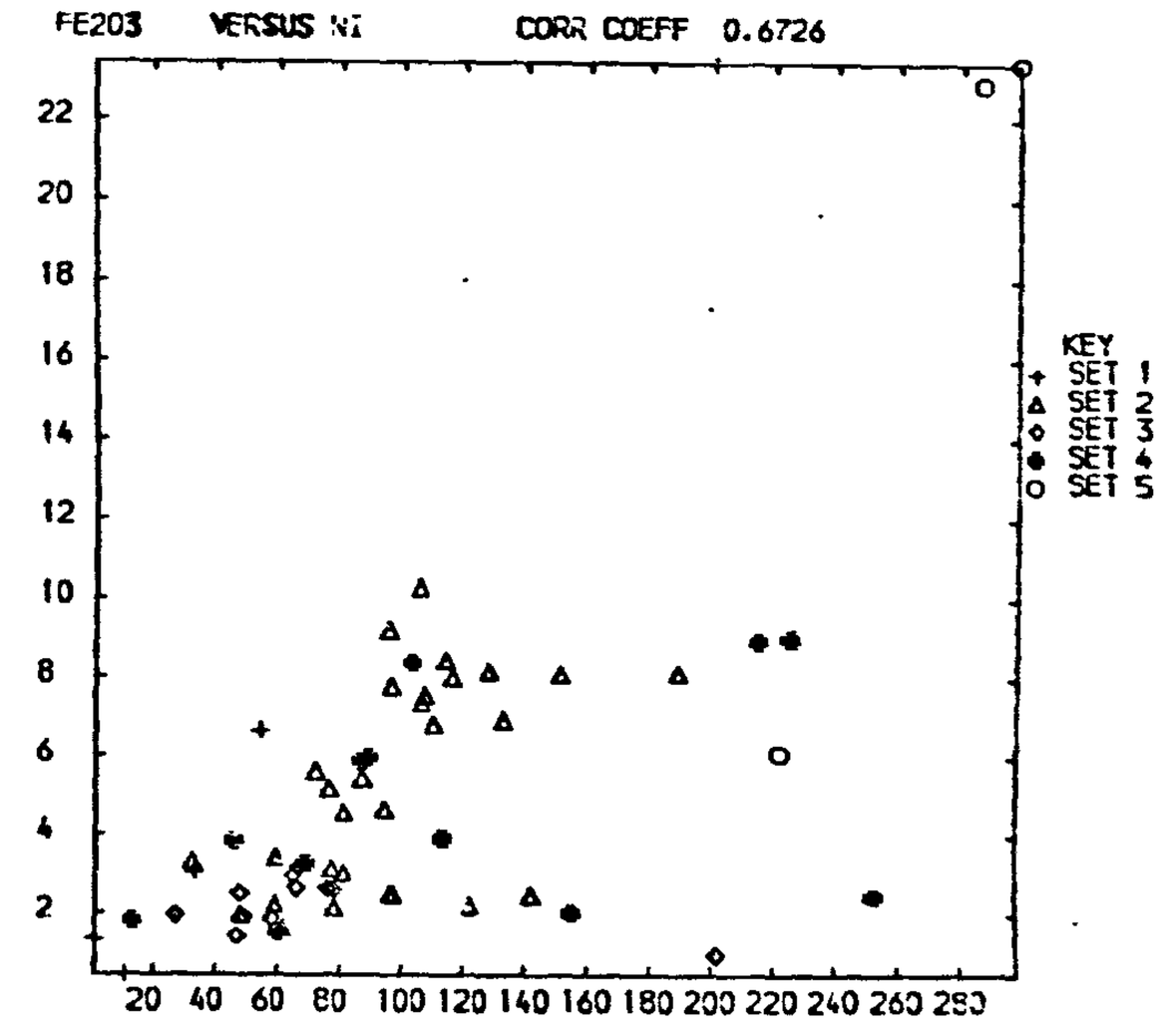
FE203 VERSUS NI
CORR COEFF 0.6726
KEY
SET 1
SET 2
SET 3
SET 4
SET 5

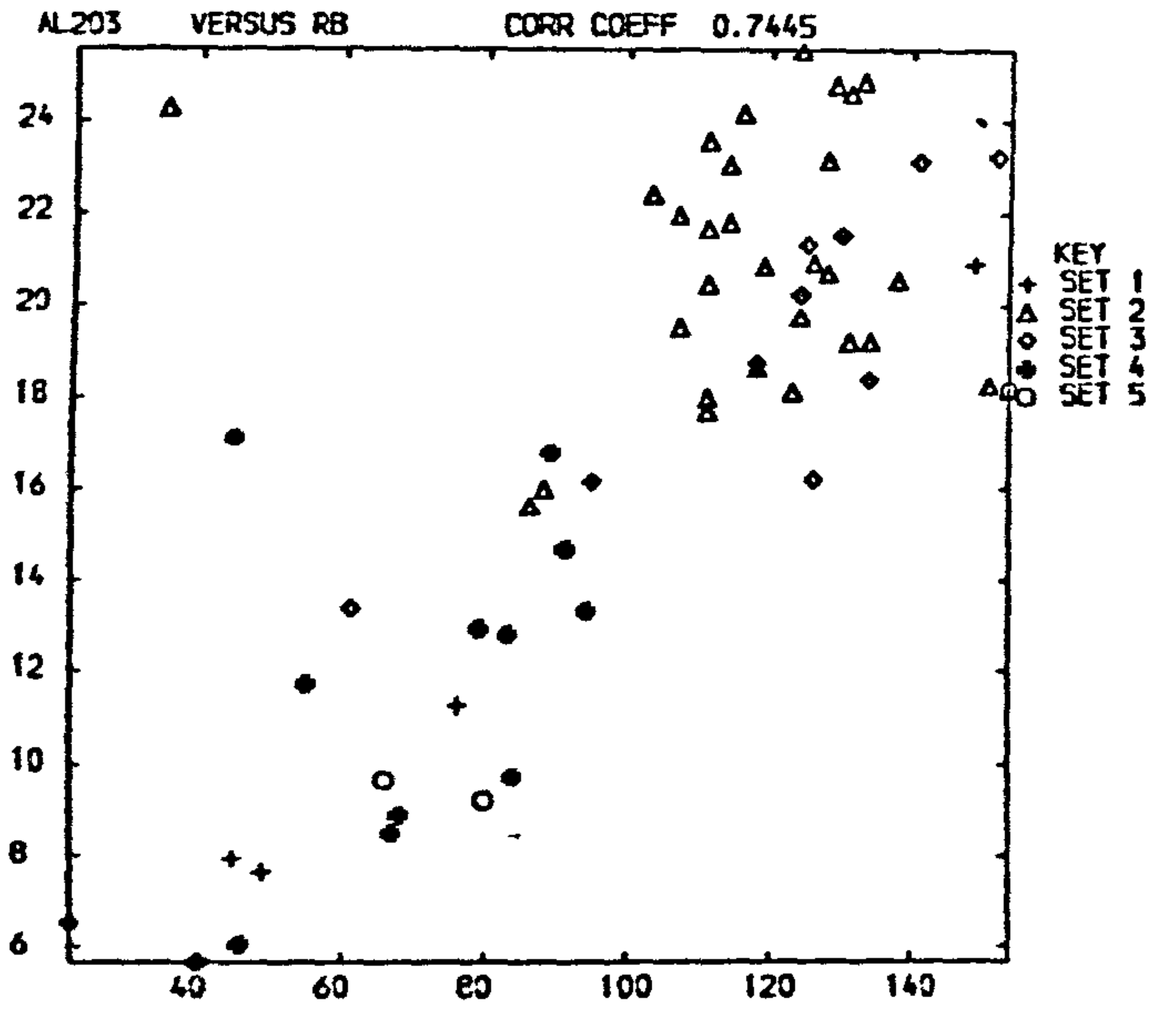
AL203 VERSUS RB
CORR COEFF 0.7445
KEY
SET 1
SET 2
SET 3
SET 4
SET 5

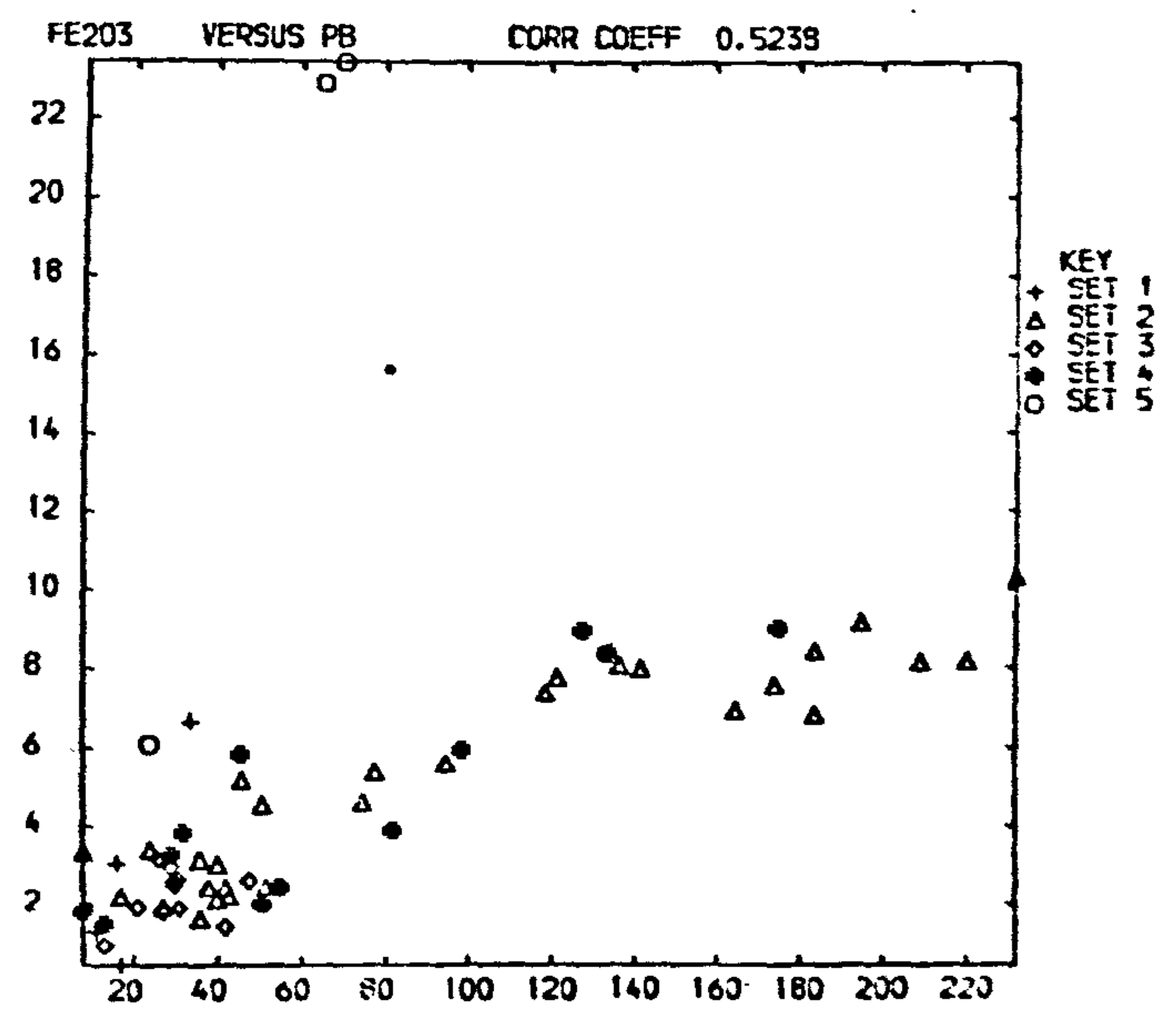
FE203 VERSUS PB
CORR COEFF 0.5238
KEY
SET 1
SET 2
SET 3
SET 4
SET 5

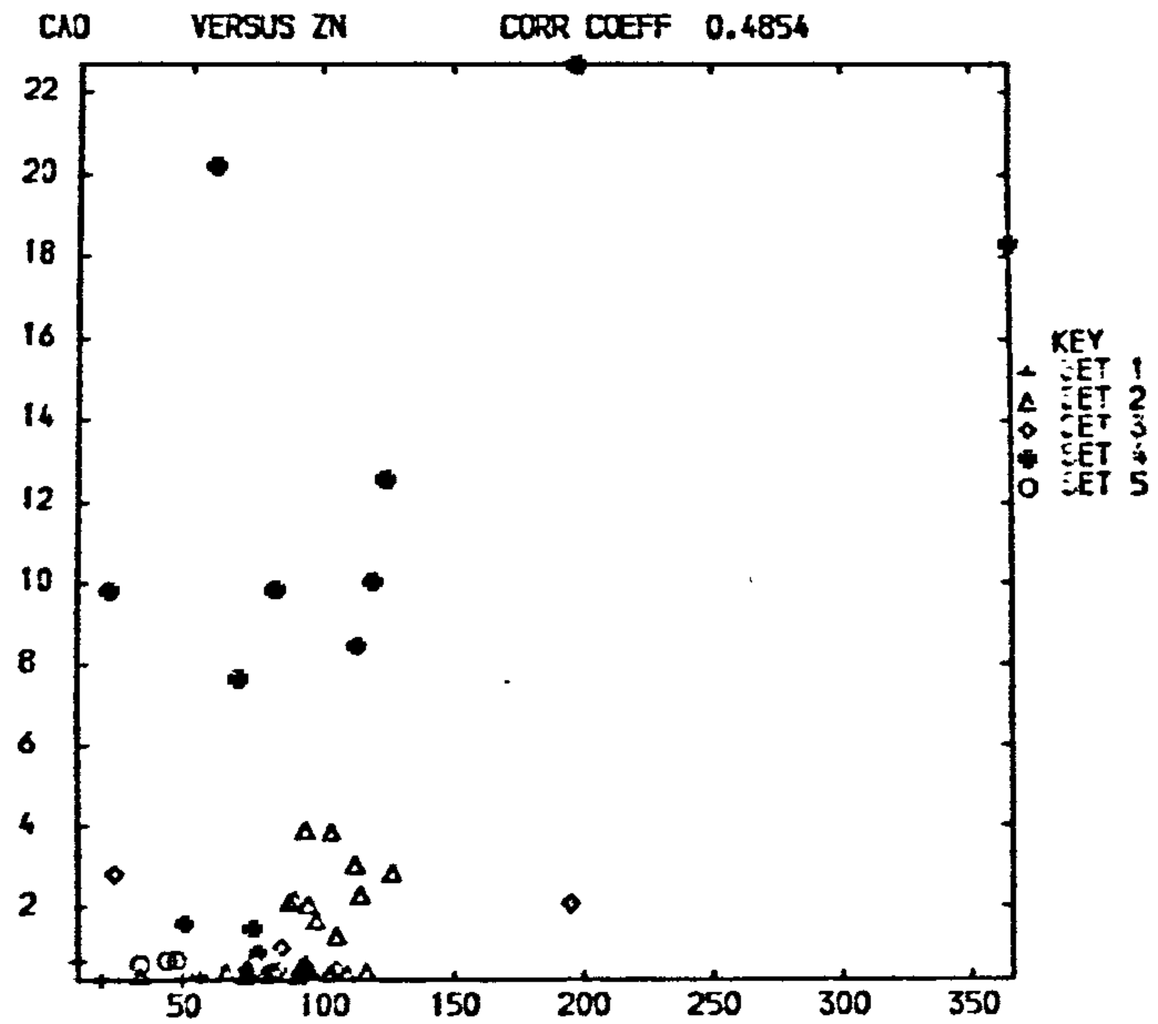
CAO VERSUS ZN CORR COEFF 0.4854
22
20
18
16
14
12
10
8
6
4
2
50
100
150
200
250
300
350
KEY
SET 1
SET 2
SET 3
SET 4
SET 5

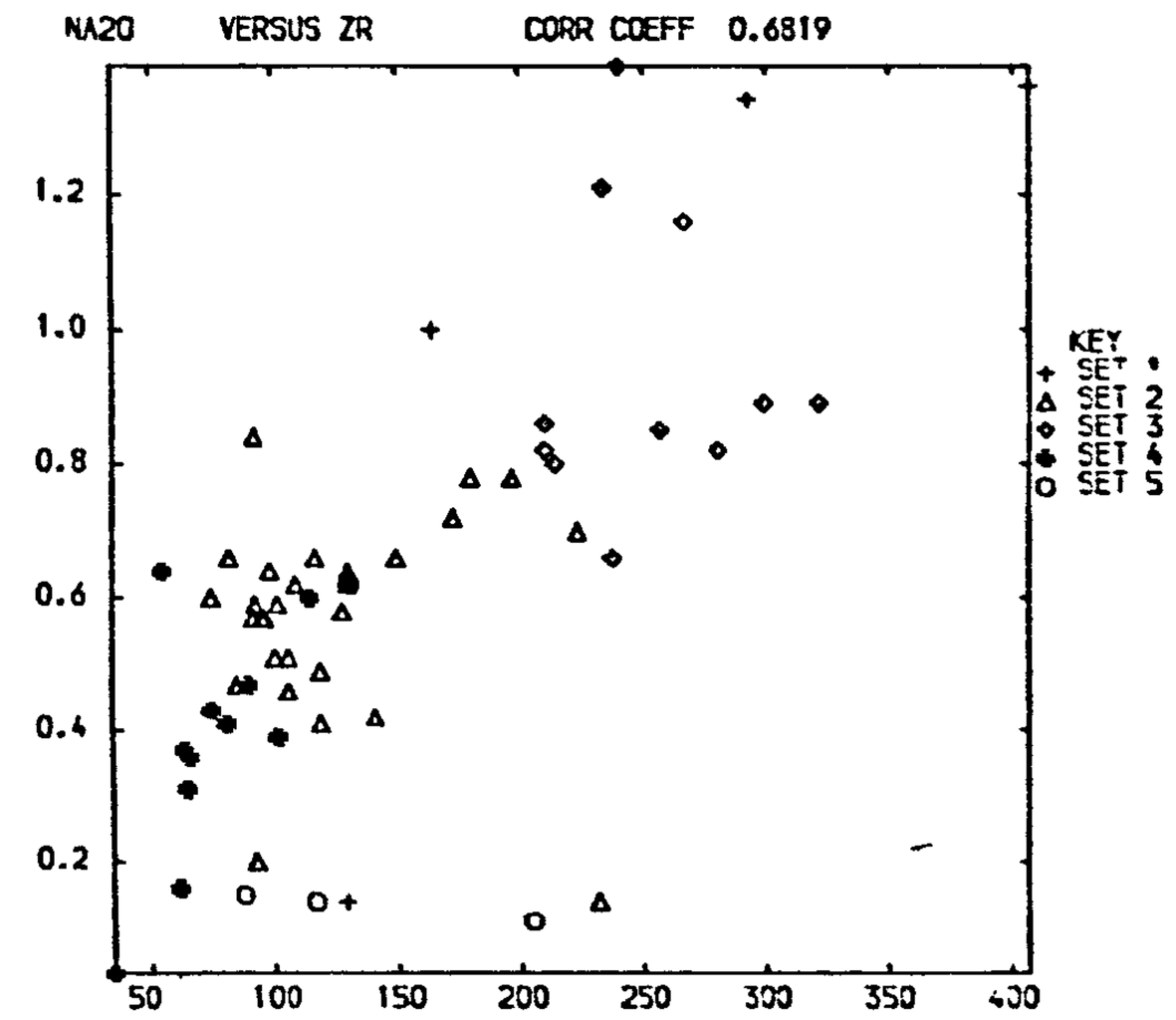
NA2O VERSUS ZR CORR COEFF 0.6819
1.2
1.0
0.8
0.6
0.4
0.2
50
100
150
200
250
300
350
400
KEY
SET 1
SET 2
SET 3
SET 4
SET 5

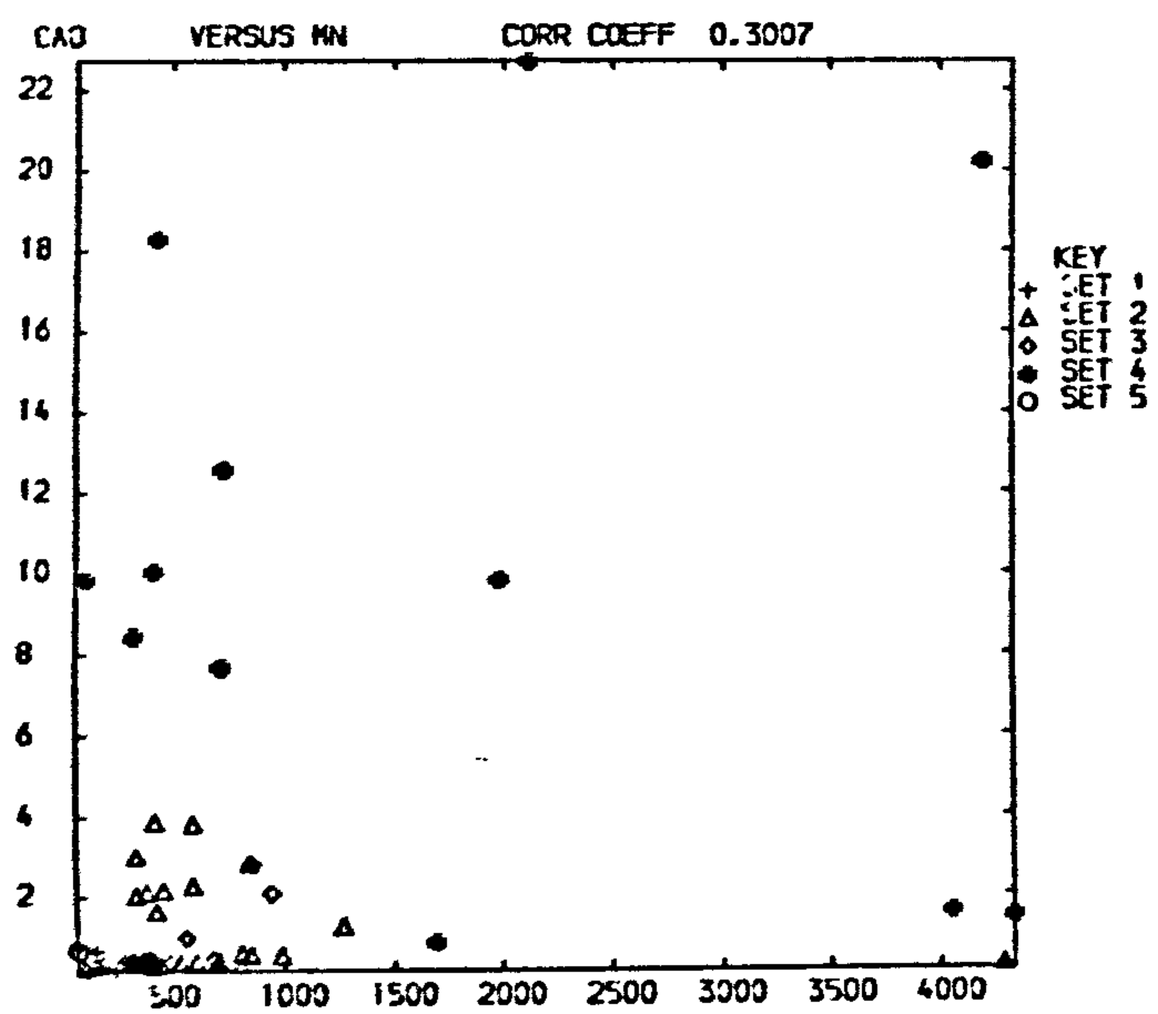
CAO VERSUS MN CORR COEFF 0.3007
22
20
18
16
14
12
10
8
6
4
2
500
1000
1500
2000
2500
3000
3500
4000
KEY
SET 1
SET 2
SET 3
SET 4
SET 5

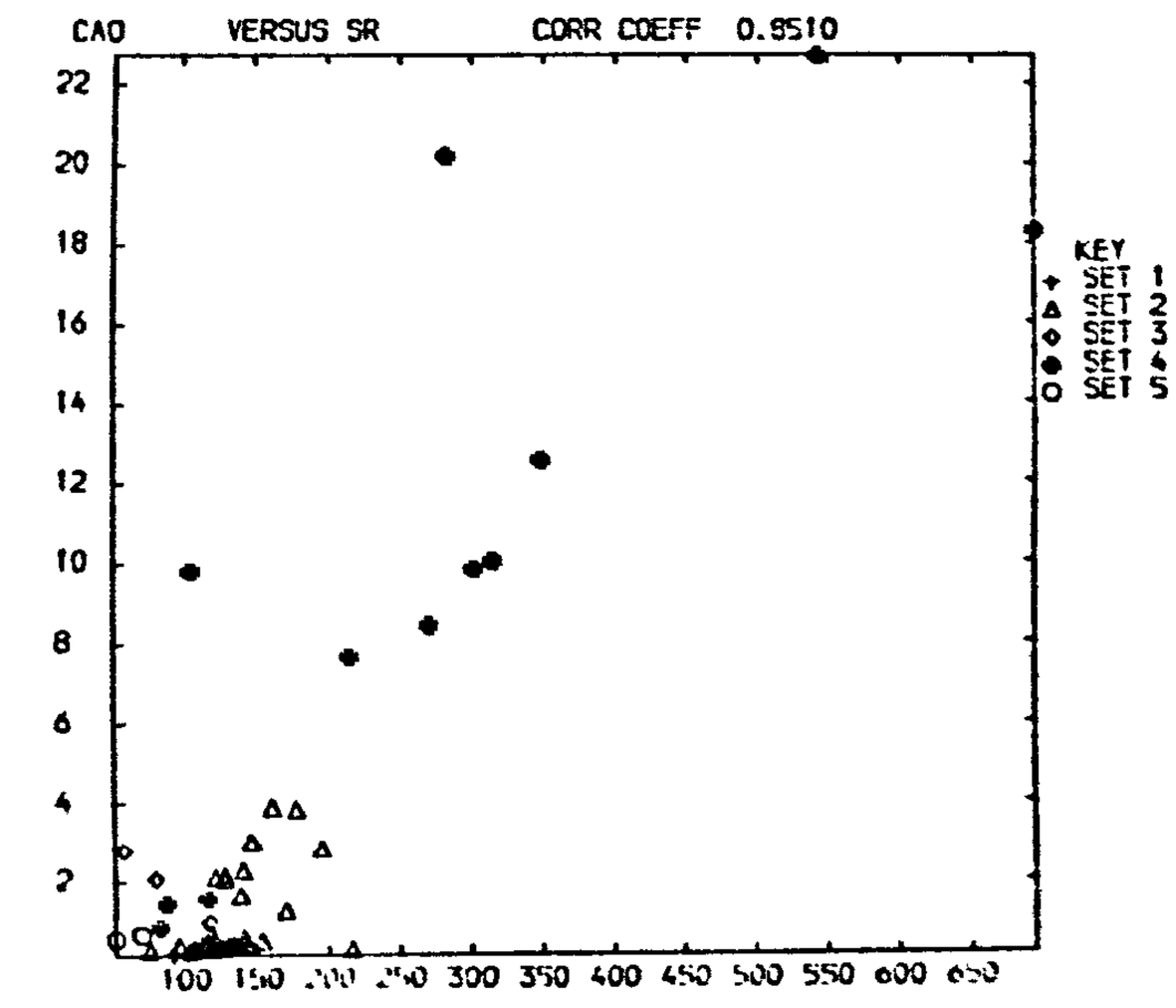
CAO VERSUS SR CORR COEFF 0.8510
22
20
18
16
14
12
10
8
6
4
2
100
150
200
250
300
350
400
450
500
550
600
650
KEY
SET 1
SET 2
SET 3
SET 4
SET 5

TABLE 53: Correlation Matrix of Tansley Borehole Rocks, Excluding Volcanic Mudstones and Including Depth as a Variable

	Depth	TiO_2	Al_2O_3	Fe_2O_3	FeO	CaO	Na_2O	Zr	Pb	Ba
Depth	1.0000									
TiO_2	-0.2367	1.0000								
Al_2O_3	-0.1541	(0.9021)	1.0000							
Fe_2O_3	(0.4754)	0.0265	0.1452	1.0000						
FeO	-0.0960	-0.0742	-0.1111	-0.2511	1.0000					
CaO	(0.5267)	-0.6728	-0.6035	0.0982	-0.1467	1.0000				
Na_2O	-0.4855	0.0791	-0.0934	-0.3916	0.0508	-0.4790	1.0000			
Zr	-0.5222	(0.3024)	-0.0390	-0.5182	0.0250	-0.4618	(0.7296)	1.0000		
Pb	(0.4970)	-0.0205	0.0979	(0.8945)	-0.3402	0.1204	-0.3145	-0.4341	1.0000	
Ba	-0.4881	(0.3776)	(0.2760)	0.0495	-0.0846	-0.2947	0.2284	(0.3368)	0.0255	1.0000
K_2O	-0.1151	(0.6376)	(0.5949)	(0.3632)	-0.3977	-0.3243	-0.1201	0.0575	(0.3566)	(0.4721)
Ni	(0.5248)	-0.1917	-0.0808	(0.4512)	-0.2129	(0.4630)	-0.3600	-0.4424	(0.5246)	-0.1121
Co	-0.0697	-0.1557	-0.1953	0.1262	(0.5594)	-0.1554	0.1688	-0.0153	0.0959	0.0539
Mn	0.1953	-0.3014	-0.2529	-0.1397	(0.5918)	(0.2893)	-0.2323	-0.3210	-0.2370	-0.3331
V	(0.4661)	-0.0539	0.0290	(0.6094)	-0.2671	(0.2701)	-0.4099	-0.4025	(0.6416)	0.2056
Cr	0.0141	(0.6358)	(0.6676)	(0.3460)	-0.1657	-0.2752	-0.1886	-0.0468	(0.3720)	(0.4700)
Zn	(0.4951)	-0.1103	-0.0526	0.1568	-0.1120	(0.4771)	-0.2819	-0.2480	0.2539	-0.1910
Cu	(0.5973)	-0.0102	0.1084	(0.7916)	-0.3154	0.2200	-0.4301	-0.5014	(0.8461)	-0.0052
Rb	-0.0406	(0.7580)	(0.7515)	(0.3430)	-0.2903	-0.3886	-0.1610	0.0340	0.3596	(0.3736)
Sr	(0.5329)	-0.4104	-0.3573	0.1076	-0.1725	(0.8514)	-0.4619	-0.3741	0.1613	-0.1528
Y	(0.3046)	(0.4689)	(0.5280)	(0.2935)	(0.2832)	-0.1560	-0.3203	-0.2354	0.2132	-0.0275

TABLE 53 (Cont.): Correlation Matrix of Tansley Borehole Rocks, Excluding Volcanic Mudstones and Including Depth as Variable

	K_2O	Ni	Co	Mn	V	Cr	Zn	Cu	Rb	Sr
K_2O	1.0000									
Ni	-0.0235	1.0000								
Co	-0.1839	0.1339	1.0000							
Mn	-0.4540	-0.1122	(0.4840)	1.0000						
V	0.2244	(0.5714)	0.0180	-0.1807	1.0000					
Cr	(0.5460)	0.2207	-0.1785	-0.3904	(0.5281)	1.0000				
Zn	0.0172	(0.5794)	-0.2136	-0.1389	(0.2877)	0.2098	1.0000			
Cu	(0.2755)	(0.6445)	0.0228	-0.1813	(0.7419)	(0.4114)	(0.3729)	1.0000		
Rb	(0.8438)	0.0973	-0.2892	-0.5507	0.2289	(0.7031)	0.1494	(0.3415)	1.0000	
Sr	-0.1191	(0.6224)	-0.2366	0.0262	(0.3399)	-0.0083	(0.7402)	(0.3134)	-0.1334	1.0000
Y	(0.2989)	0.1819	0.1485	0.2125	0.1651	(0.3200)	0.1251	(0.3391)	(0.3993)	-0.0064

correlation coefficient value becomes higher and that of FeO-Mn remains of the same magnitude. It is also clear that Pb-Ni-V-Cu relations are improved, while CaO-Sr correlation coefficient value remains approximately the same. The correlations between elements related to pyrite and those associated with illite are again clear. Barber (1974) found that significant amounts of Cu, Ni, Pb and Zn are present in sulfides, while only small amounts of these metals are adsorbed on mineral grains, but Cr and V are largely related to silicates and adsorbed on clay minerals and iron oxides. Zn shows a stronger correlation with Sr than with CaO, probably indicating its incorporation in calcite, because the highest Zn and Sr contents are confined to the highly calcareous shales. On the other hand, its correlations with Ni and V are also improved suggesting its association with pyrite and organic matter.

However, the Zn-Sr relationship is likely to be enhanced in the lowest shales in the succession, due to mineralisation, which was encountered at Tansley as veins of calcite, pyrite, chalcopyrite and blende at the level of samples 68-70 (Ramsbottom et al. 1962, p.141). The association of Y with a particular element is still difficult to explain because it is correlated with several elements.

To clarify some spurious relationships which are masked by the presence of sandstones containing high amounts of feldspar, they are excluded and the correlation matrix reproduced. Most of the relationships between variables described above, remains, except that Fe_2O_3 correlation with Cr and Rb are not significant, Pb-Rb and Pb-Cr correlation coefficient values decreased being 0.2835 and 0.3057 respectively, while those of Ba-Cr (0.5705), Ba-Rb (0.4277) and Rb-Cr (0.6104) are higher than in the previous correlation, due partly to change in the size of groups, hence change in the significance level. This also supports the proposition that Ba, Cr and Rb

are largely related to illite and feldspars. Hirst (1962) and Spencer (1966) have indicated that Cr and Rb are associated with illite.

Following all the lines of evidence obtained in the present study, general conclusions may be drawn. It appears that Ni, Cu and Pb are concentrated in pyrite and organic matter; while the latter and illite, seem to concentrate V. Elements contained in carbonates, organic matter and pyrite are Co, Mn and Zn. Cr, Rb and Ba are related largely to illite and feldspars and Sr is concentrated in calcite. Zr is dominantly present in the form of zircon, whereas Y cannot be assigned to either a particular element group or mineral. In this respect with regard to elements related to diagenetic iron minerals and clay minerals, Curtis (1969) found a similar rleationship (see page 4). In some shales there is evidence of the location of Co in pyrite (Spencer, 1966) but in others only a small fraction of the Co present can be assigned to pyrite (Le Riche, 1959; Nicholls and Loring, 1962; Tourtelot, 1964). The last two authors, also conclude that V is shared between clay minerals and organic matter.

The data of the present study show obvious but not universal relations between some element contents and either the amount of individual minerals or the relative proportions of clay minerals. Nevertheless, some elements may be contained partly in minerals which are not the principal bearing phases, but if such a relationship exists it has been completely masked. Finally, comparing the marine shales with the volcanic mudstones having the highest pyrite and lowest organic matter contents, indicate that the larger amount of Pb and Cu and to a lesser extent V are contained in the organic matter. Therefore these elements were accumulated largely by organic complexing or biological activity. Such a relationship has been indicated in the Whitbian Shales, which are pyrite rich (Gad et al. 1969).

5.7 Visean Shales

Samples 69 and 70 are from the uppermost part of the Visean limestone. Trace element data (Appendix 2) indicate their high content of Sr which is a consequence of abundant calcite. These calcareous shales may be considered to have formed under conditions which were an extension of those prevailing during the deposition of the overlying less calcareous shales, that is a reduction on the rate of supply of detrital constituents and an increase in carbonate precipitation. This is reflected in the lower contents of trace elements associated with clay minerals and zircon. Similarly, the low levels of Cu and Pb can be attributed to the low content of pyrite. In contrast Ni, Zn and to a variable degree Mn, show high concentration. The possibility of these elements being accommodated in dolomite (ankerite) is a very likely explanation since these shales contain minor amounts of dolomite. However, the level of Ni and Zn is much more than can be accounted for by dolomite, because sample 66 (Namurian) has the highest dolomite content, although the Ni and Zn levels are much lower. As noted earlier, mineralisation and dolomitisation are most pronounced at the junction of Namurian and Visean. Accordingly the erratic behaviour of some trace element in this part of the sequence seems to be effected by the presence of some ore minerals. Such a source of trace element has been envisaged to explain the variability of some trace elements in similar Visean sediments (Hirst and Kaye, 1971). It is also interesting that dolomite in the Visean Limestone is epigenetic (Smith et al. 1967, p.264). In the northern Pennines, dolomite (ankerite) and other carbonates are important minerals resulting from mineralisation (Edward and Trotter, 1954) It is worth mentioning that the age of mineralisation is regarded as being Mesozoic but probably not later than Lower Jurassic (Smith et al., 1967, p.42).

5.8 Volcanic Mudstones (K-Bentonites)

In descending order of depth, sample 71, 72 and 73 are volcanic 'toadstone' clays overlying the upper lava of Matlock. Previously, they were regarded as tuff (grain size terminology, page 138) and considered most probably as alteration products of the lava, due to submarine weathering. Also it was found that pyrite, quartz, illite-smectite mixed layer clay minerals, chlorite and anatase were the most important constituents. Pyrite and quartz were present in higher proporitons in the upper two samples, while illite-smectite clay mineral, chlorite and anatase contents were higher in the third sample. Trace element data (Appendix 2) shows that their contents are in sympathy with the variations in mineral proportions. Ni, Co, Mn, Cu and Pb contents are higher in the pyrite rich samples. On the other hand, V, Cr, Rb and Sr levels are higher in illite-smectite rich samples, while Zn is only slightly enriched in it. The Y content is very low in all samples. The Ba content shows a slight decrease in the basal sample, which also has slightly lower amounts of feldspar, while Zr concentration is higher than in the upper two samples.

However, these trace elements are not necessarily present in these minerals, as these rocks may contain ferromagnesian minerals in variable degrees of alteration, which were not amenable to XRD study. Analysis of relatively fresh basaltic glasses from ash-layers in the Mo-clay of northern Denmark, clearly demonstrated the incorporation of most trace elements in the glass itself (Pedersen et al. 1975). Whereas, trace element data on altered sumbarine lavas indicated that Rb, Sr, V, Zr and Ba contents increased and showed good positive correlation with the alteration trends with illite-smectite clay minerals as the alteration products (Hart, 1973). It was also shown that Co, Ni, Cr, Cu and Zn may either have negative, little or no correlation with the alteration trends.

Similar studies on submarine lava flows indicate that Zr, among other elements, may sometimes be depleted to a larger extent in the altered lava crust than in its interior (Thompson, 1973). Such Zr depletion has also been reported to occur in tephra (volcanic ash) deposits from swamps (Khon, 1970).

On the basis of this information, release of trace elements is concomitant with alteration of the lava during reaction with sea water. In the previous section (page 144), the changes in major elements of the Namurian volcanic mudstones were described. The final products were quartz, pyrite, chlorite and illite-smectite. It seems reasonable, therefore to suggest that accompanying these changes, trace elements were partitioned between the principal mineral phases. An interesting point, is that Zr, Quartz and pyrite have an inverse relationship in the Namurian volcanic mudstones, unlike the normal shales. This supports the suggestion that these K-bentonites were formed by processes different from those operating during the deposition of the overlying shales.

5.9 Clay Minerals of the Tansley Borehole Sediments

In this section, the relationship between the crystallographic properties of illite and diagenesis will be described. In addition, the variation of clay mineral contents are discussed; relating them to environmental factors influencing their distribution.

5.9.1 Crystallographic Properties of Illite

In previous section (page 93) it was shown that the crystallinity of illite and its chemical composition are dependant on the degree of diagenesis. This was achieved by calculating the crystallinity index (Kubler index) and the intensity ratio of illite 5Å and 10Å peaks (I002/I001). For the Tansley Borehole sediments, whole rock sample smears were used.

Applying the above mentioned technique, the illite crystallinity index has been plotted against the intensity ratio of illite; this is shown in Figure 35. It can be seen, that illite is poorly crystalline and is slightly aluminous. In other words, the sediments of the present study are in the zone of normal diagenesis and had not been subjected to deep burial metamorphism. It also suggests that illite is of the 1 Md variety and this is confirmed in the present study because characteristic peaks of 2M illite were not observed. Therefore, the only possible modification of illite could have been a simple absorption of K during diagenesis. Accordingly, it can be suggested that illite had not suffered appreciable chemical and structural changes. Thus it represents essentially, the original detrital illite supplied to the basin of deposition. Studies on the weathering of mica reveal similar characteristics of illite peak (Loveland and Bullock, 1975). They showed that the decrease in mica peak intensity, its asymmetry and broadening of its base, are due to considerable loss of K during weathering. Similar results were reported by Rismsaite (1973). The interaction of weathered clay minerals with sea water has been demonstrated to extract an appreciable amount of K by cation exchange (Russel, 1970). Investigations on the selective sorption and fixation of K by weathered mica, support such mechanism (Newman and Brown, 1966; Reichenbach and Rich, 1969; Brown and Newman, 1970; Le Roux et al. 1970; Newman, 1970; Sawhney, 1972). This can be attributed to many factors including electrostatic attraction between the negatively charged 2:1 layers and the positive interlayer cations (Eberl, 1978). For example, a clay with a high negative charge on its 2:1 layers (illite) will remain expanded around cations of high hydration energy (Na, Mg), but will collapse to a mica like structure around a cation of lower hydration energy (K).

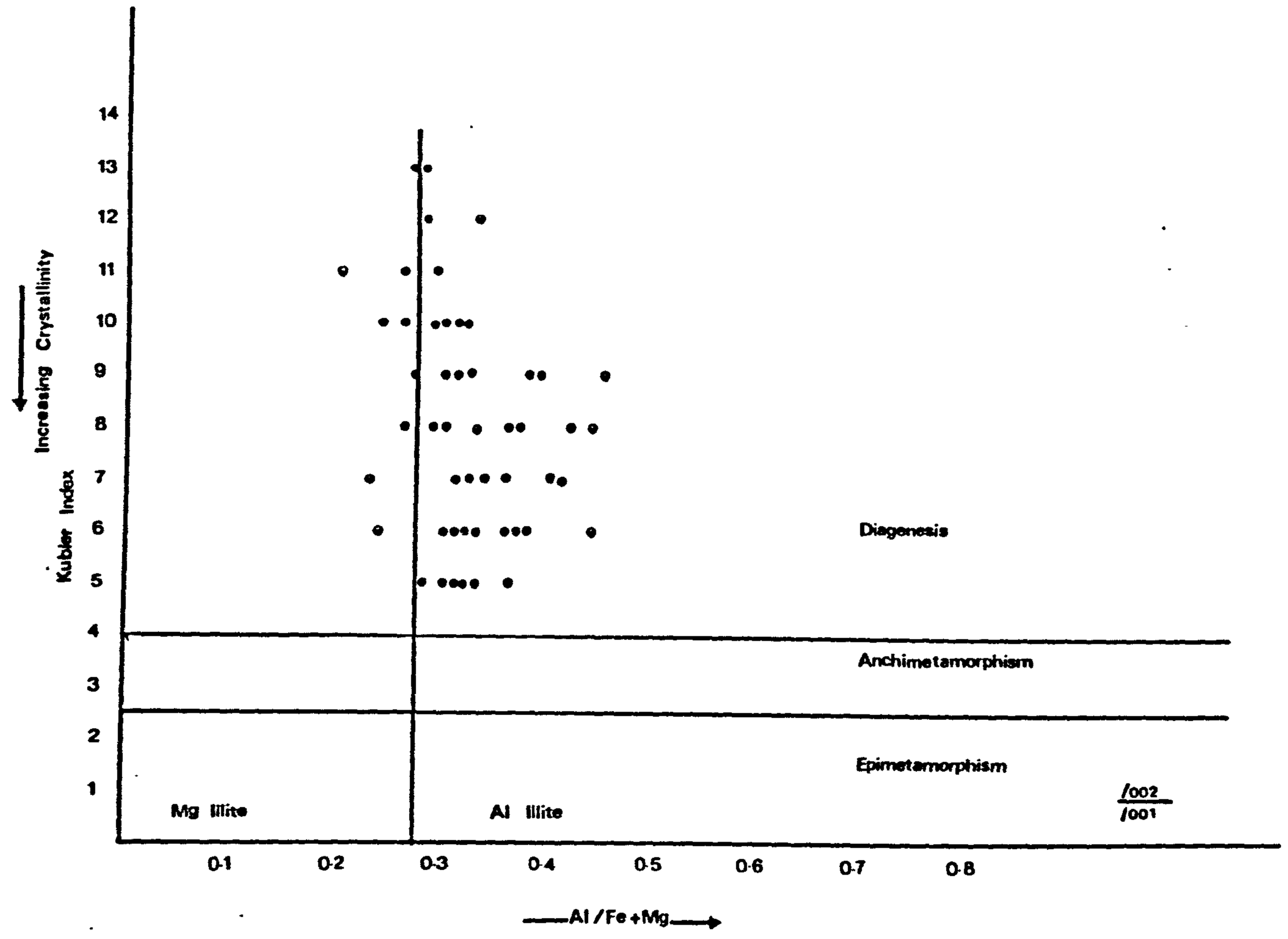

Fig.35 Relationship between illite crystallinity, intensity ratio (I002/I001) and diagenesis in the Tansley Borehole rocks.

5.9.2 Distribution of Clay Minerals

Variations in clay minerals abundance have been widely recognised in ancient and recent sediments. Some workers have considered that seaward change in clay mineralogy as a result of chemical and structural changes in the depositional environments (Grim, 1951; Millot, 1953; Robbins and Keller, 1952; Griffin and Ingram, 1955; Brown et al. 1977). In other studies (Taggart and Kaiser, 1960; Griffin, 1962; Kunze et al., 1968; Morton, 1972; Shaw, 1973; Darby, 1975; Venkatarathnam et al., 1976; Knebel et al., 1977) the variations in clay minerals distribution have been ascribed to change in source, dispersal pattern, size and sorting. Recently, the differential flocculation of clay minerals in the depositional environments, is regarded as a factor enhancing clay minerals segregation (Edzwald and O'Melia, 1975; Birch, 1978). Still other workers envisage more than one process, affecting the distribution of clay minerals (Murray and Harrison, 1956; Parham, 1966; Tank and McNeely, 1970; Weir et al. 1975). Moreover, some investigators have demonstrated the relationship between clay mineral variation and salinity (Brooks and Ferrell, 1970; Edzwald and O'Melia, 1975; Brown et al. 1977). The environmental aspects of clay minerals have been reviewed by Keller (1963) and Mankin (1970).

In the Tansley Borehole shales, illite and kaolinite were shown to exhibit subtle variations in their content between the marine and non-marine shales. Chlorite content was found to be higher in the non-marine shales (see Table 42). The similarity of the clay mineral assemblage in both groups exclude variations in the source area. The absence of montmorillonite may either indicate its absence in the detritus supplied to the basin of deposition, or it could have been converted to illite during diagenesis. Since the shales had not been subjected to deep burial diagenesis, the first alternative seems to be the most likely explanation. The presence of abundant kaolinite

supports this suggestion. The factors which appear to have influenced clay mineral distribution are distance from shoreline, sorting and grain size, dispersal pattern, differential flocculation and salinity. It can be considered that illite was of finer grain size than kaolinite and chlorite. Therefore, it is expected to be carried further off-shore than the coarser clay. Accordingly the non-marine shales deposition seems to be related to near shore areas. Such patterns can be invoked to explain the variation in clay mineral distribution, in the non-marine silty shales and the marine shales. This sorting of sediment by size, has been reported from the Amazon River upon entering the Atlantic Ocean (Gibbs, 1977). On the other hand, many of the non-marine shales, in the present study, which are rich in kaolinite were found to have a similar content of quartz or even less when compared to the marine shales, rich in illite. It implies, then, that differential flocculation, due to variation in salinity, was a significant factor in affecting clay minerals distribution. To illustrate this mechanism, the experimental and field studies of Edzwald and O'Melia are pertinent to this problem. They explained the distribution of clay minerals in Recent sediments as a result of their relative stabilities. The rate of particle flocculation (aggregation) were determined in estuarine solutions, followed by thermodynamic calculations. Their data demonstrated that with increasing water salinity, illite is more stable (less flocculated) than kaolinite which is more stable than montmorillonite. An identical distribution of illite and kaolinite with respect to salinity has been reported from studies on lakes (Brooks and Ferrell, 1970). The basic idea is that kaolinite flocculates upon entering the sea water, followed further seaward by the flocculation of illite. Applying these lines of evidence to the shales of the present study seem to accord with their environment of deposition. Salinity variation between marine and non-marine shale was

established by palaeontological means and this is supported by trace element data. Thus, these factors can account for the variations in clay mineral contents. In addition, finer grain size of illite and distance from shore could have been a contributory factor enhancing this variation. It appears that chlorite behaved in the same way as kaolinite during deposition of the Tansley Borehole sediments. The further increase in illite content accompanied by decrease of both kaolinite and chlorite content in the carbonate rich shales may be attributed to a combination of the above mentioned factors. As their deposition implies very slow rate of sedimentation and minimal detrital contamination, it can be assumed that only the finer particles (illite rich) were delivered to the depositional environment. Moreover, normal salinities were essential for sustaining high productivity of marine organisms; thus differential flocculation was likely to influence the illite content. Similar relationship between clay minerals variation and carbonate contents have been reported from other Carboniferous sediments in England (Amin, 1975).

The Tansley borehole sediments have been described as deltaic sediments (see Chapter 1). A principal environmental variation within a deltaic system is the change from marine conditions in the off-shore area to brackish and fresh water conditions in the subenvironments of the marshy delta plains (see Reineck and Singh, 1975). These correspond to shelf muds in the marine environment and to deposits of variable and complex structural and textural characteristics in interdistributary bays and sediments within the boardering intermediate embayments. A broad relationship may be made possible between these environments and the distribution of clay minerals in the Tansley Borehole sediments. No doubt, the marine shales represent an off-shore mud, deposited in the deeper part of the basin (bottomset). The non-marine shales interbedded with the marine shales and also some

overlying the marine shales can be assigned to subaqueous prodelta environments (forset). This is because illite content was found to be similar or slightly higher than kaolinite, in contrast to the subtle variation in typical marine shales. The overlying non-marine shales and silty shales, may be assigned to delta plain deposits (topset). The Ashover Grit may represent an alluvial deposit or channel filled sands, in the subaerial part of the delta. In summary, it can be stated that distance from shoreline (influencing sorting and grain size) and differential flocculation together with salinity variation were the most important factors controlled the distribution of clay minerals in the Tansley Borehole sediments. The use of clay minerals alone as environmental indicators is unwarranted, but when accompanied with already established depositional and stratigraphic relationships, point to a characteristic relationship between palaeoenvironment and clay minerals assemblage. Moreover, the distribution of clay minerals in the Tansley Borehole sediments supports the deltaic depositional model.

5.10 Comparison with the Mam Tor Rocks

This comparison provides information relating to the lateral variation of facies in adjacent sectors in the southern part of the Central Pennines Basin. The Mam Tor rocks (R_{1c}) belong to the Kinderscoutian stage (R_1). At the type locality, the Mam Tor succession attains a thickness around 120 metres (see Chapter 1). Their lateral equivalent in the Tansley Borehole is represented by about 18 metres (see Ramsbottom et al. 1962). The whole Kinderscoutian stage in the Tansley Borehole succession includes the marine shales represented by samples 55 to 61 (see Table 15). In addition to this considerable thickness reduction of the (R_{1c}) beds in the Tansley Borehole, the sandstones which are important feature in the Mam Tor rocks are absent.

The most important variations in mineral and trace element contents between the Mam Tor shales and their lateral equivalent in the Tansley Borehole are shown in Table 54. There is more kaolinite and less illite in the Mam Tor shales. The contents of Na-feldspar and chlorite show a similar pattern to that of kaolinite, but pyrite, calcite and organic matter are concentrated in the Tansley Borehole shales. On the other hand, quartz content is slightly higher in the Mam Tor rocks.

The concentration of Ni, V, Zn, Cu, Sr and Pb are much lower in the Mam Tor shlaes than in the Tansley shales, whereas Zr, Ba and Cr are higher in the former. This increased concentration of Zr, Ba and Cr suggests a greater contribution by the detrital fraction, particularly the heavy minerals and feldspar. It can be suggested,therefore, that a difference in the depositional environment had existed during the contemporaneous accumulation of these sediments. The most important factors to account for these lateral variations seem to be the change in salinity and/or rate of sedimentation. The abundance of pyrite, calcite and organic matter in the Tansley shales, suggests that they were accumulated in a restricted or partly closed sector, whereas the Mam Tor shales in an open marine environment. Such lateral variation of the facies also demonstrates the influence of the Derbyshire Block which might act as a submarine sill, thus controlling the water circulation between the north western and south eastern part of the Central Pennines Basin (see Chapter 1).

The former is related to the deposition of the Mam Tor shales while the latter to the Tansley shales. The previously established, mineralogical and textural gradation within and between the Mam Tor greywackes and the interbedded shales was considered to indicate deposition of the shales from waning turbidity currents (see page 130). Accordingly, the Mam Tor shales can be regarded as turbiditic muds. On the other hand, the

TABLE 54: Comparison of Mineral and Trace Element Contents, between the Mam Tor Shales and their Lateral Equivalent in the Tansley Borehole

	Mam Tor Shales		Tansley Borehole Shales	
	Mean	S.D.	Mean	S.D.
Quartz	18.84	5.55	18.57	4.6
Chlorite	6.89	0.87	3.16	0.45
Illite + MXL	22.69	2.9	25.28	4.4
Kaolinite	36.34	4.31	18.84	4.9
Na-Feldspar	4.40	1.12	1.77	2.22
Calcite	0.26	-	9.44	8.46
Pyrite	0.22	0.01	2.84	1.17
Apatite	0.36	0.07	0.41	0.12
Org. C.	2.18	0.80	4.60	1.23
Element ppm				
Ni	79	17	131	56
Co	12	11	37	22
Mn	548	370	1154	1380
V	138	10	262	116
Cr	167	8	129	33
Zn	84	21	102	22
Cu	45	8	138	38
Rb	130	13	112	36
Sr	107	11	196	74
Y	39	7	41	13
Zr	153	42	107	35
Pb	46	6	123	54
Ba	459	55	393	111

contemporaneous deposition of their lateral equivalent, further south east was under quieter conditions. This is supported by the abundance of marine fossils, including goniatites, in the Tansley shales. Whereas in the Mam Tor shales, occasionally pelecypods were found but no goniatite (Allen, 1960). It appears, therefore, that the chemical compsoition of the sediments was determined,partly by factors operated in the depositional environment, among which salinity variationplayed an important role. Further elaboration related to these chemical and lithological changes appears in Chapter 7.

5.11 Conclusions

The distribution of some minerals and trace elements in the Tansley Borehole section was shown to be influenced by variations in grain size, and changing physico-chemical conditions including salinity. These parameters seemed to be of greater importance in explaining these changes in chemical composition of the bulk rock samples. Mineralogical changes include the decrease in the contents of quartz and feldspar from the sandstones, through the silty non-marine shales, to the underlying less silty non-marine and marine shales. The last two groups of shales showed somewhat systematic variation in the type of clay minerals which is in accord with the palaeosalinity interpretation. The most significant aspect is the decrease in the content of kaolinite with a concomittent increase in the content of illite in the marine shales or vice-versa. Invariably the TiO_2 content is slightly higher in the non-marine shales and this can be related to distance from shoreline. Evaluation of the degree of diagenesis suggested that the sediments have not been subjected to deep burial diagenesis or metamorphism.

The change from pyrite, organic matter and calcite rich marine shales to siderite rich non-marine shales is, generally, accompanied by a decrease

in illite content and an increase in that of kaolinite. This is believed to reflect salinity variation and changing physico-chemical conditions of the depositional environment, and is not influenced by age of the sediments. Later discussion will focus on this subject (Chapter 7). The contents of some trace element of bulk samples show similarities in their distribution to the above mentioned varaitions in mineral contents and the palaeosalinity, being enriched in the marine shales.

Ni, Cu and Pb are concentrated in pyrite and organic matter; the latter and illite contribute to the V content. The contents of Mn, Co and Zn are shared by carbonate; pyrite and organic matter. Illite contains most of the Cr, Rb and Ba, whereas Sr is related to calcite as well. Zircon is the main host for Zr, while Y is not related to a particular mineral. These changes in the type and proportion of minerals and trace elements can be explained by different depositional subenvironments within the deltaic system. Correlation analysis demonstrated the validity of these changes in mineral, major and trace elements through the succession.

The alteration of volcanic rocks has resulted in the formation of secondary minerals which formed the K-bentonites. The last could have originated by high temperature reaction with seawater, low temperature reaction, or during a later diagenetic stage. Accompanying this alteration some elements were either lost or gained, due to interaction with seawater. The possibility of incorporation of some lost elements in the overlying sediments seems likely.

The lateral variations in lithology, mineralogy and chemistry of sediments, laid down contemporaneously in the southern part of the Central Pennine Basin, can be accounted for by difference in sedimentational regimes and the influence of the depositional environment.

CHAPTER 6

Discriminant Function Analysis

Evaluation in the preceeding Chapter indicated that Ni, V, Cu, Sr and Pb are the most likely elements to dsitinguish between the Namurian marine and non-marine shales of the Tansley Borehole (p.156). Applying each or all of these elements concentrations to distinguish individual samples, however, does not give a satisfactory result. Because of this, the validity of using trace elements as environmental discriminators was tested using discriminant function analysis.

A multivariate discriminant analysis is a method of assigning samples to previously defined populations on the basis of a number of variables considered simulatneously. These populations may be represented by sets or groups of samples. Each group has a number of samples which contain common variables, X_1, X_2 .... X_n. These can be used to establish a discriminant function which permits an unknown individual sample to be classified. Discriminant analysis has been used to distinguish marine from fresh-water shales (Potter et al. 1963) to classify depositional environments of carbonate (Krumbein and Graybill, 1964) or sandstones (Sahu, 1964) to differentiate refractory and non-refractory quartzite (Wood, 1961). For its wider application the reader is referred to Miller and Khan (1962) and Davis (1973).

For two sets of samples, a population described by N variables (X_1, X_2) may be pictured as a cluster of points in N-dimensional space, and the other population, described by the same N variables, as another cluster of points. Discriminant analysis is defined by a N-dimensional plane that most effectively separates the two clusters. The locations of the two populations are described by the N-dimensional co-ordinates of their multivariate means. The degree of distinctness of the two groups

is measured by the distance (D^2) between these means. The significance of this distance is measured by F-values. The discriminant function that provide the maximum difference between the two groups is of the form:

$$R = a_1X_1 + a_2X_2 \ldots + a_nX_n$$

depending on the number of the variables to be used. Where the variables X_1 = Ni, X_2 = Co, ... X_{13} = Ba, as in the case of the Namurian shales. The coefficients a_1, a_2 .... a_n are correspondingly weighting factors or constants, indicating the amount each variable contributes to the discrimination. The discriminant index, RO, is found by substituting the means of the combined populations in the discriminant function. By substituting the means for each set separately, discriminant values for each population are found. An unknown sample is assigned to one of the two populations by substituting the appropriate values for the variables into the discriminant function.

6.1 Program Description

The program used here was written by Davis and Sampson (1966), to compute the discriminant function for two sample sets.

Output from the program consists of the constant terms (a_1,a_2) of the discriminant function, the discriminant index RO, the discriminant values for each of the two groups (R_1 and R_2), the distance (D^2) and the percent contributed by each variable to D^2. An F value for determining the significance of D^2 is produced together with first (N) and second (n_1+n_2-N-1) degrees of freedom.

The program has been tested by Davis and Sampson (1966) using data on carbonate environments published by Krumbein and Graybill (1965, p.363). An additional test was carried out by the present writer on these data and the results were very similar to those published by Davis and Sampson (1966). However, when a large number of variables are used,

those with negative or low positive contributions should be eliminated on successive runs until the F-value for the significance test of D^2 is reduced below the value of the assigned significance level.

6.2 Sample Groups (Tansley Borehole)

In this study, the samples were classified as non-marine or marine, using palaeontological criteria (see Chapter 1). The non-marine group includes sample number 1,2,11,14 ... 23,25,28,38-42 , 44,45 and 51. The marine group is comprised of sample number 29,30,32,46-50,52-57,61-62, 64-67. The total number of samples is forty four, of which twenty five belong to the non-marine group and nineteen to the marine group. It is noteworthy, that the determined average content of quartz for each group is around 23%. Using the test of confidence limits it was found that the difference between these quartz averages, is not significant at the 95% level. Consequently, the effect of quartz dilution would be similar in both groups.

6.3 Results

6.3.1 Tansley Borehole Shales

In the first run all the thirteen trace elements (variables) were included to derive the discriminant index (RO) and the discriminant value for each group (R_1 and R_2). The output is shown in Table 55. It can be seen that only V, Cu, Sr and Pb provide an effective separation between the two groups. This is indicated by the positive and high percent contributed by each element to the discriminant function. The resultant F-values (23.58) exceeds the 99% significance level ($F_{13,30} = 2.79$). This suggests that, jointly the four trace elements decisively discriminated between the marine and non-marine shales. The discriminant index, RO = -18.99, and the discriminant value for the non-marine group $R_1 = -1.82$, while that for the marine group $R_2 = -41.57$. Consequently, any sample

TABLE 55: Results of Discriminant Function Analysis using Thirteen Variables, Non-Marine and Marine Shales of Tansley Borehole

F = 23.5764 with 13 and 30 degrees of freedom

D^2 = 39.74737, R1 = -1.8235, RO = -18.9871, R2 = -41.5708

	Variable	Constant	Percent Added
Ni	1	0.0427	-5.0715
Co	2	0.2347	-0.3182
Mn	3	-0.0042	-2.4946
V	4	-0.0317	11.8498
Cr	5	0.0930	-0.1822
Zn	6	0.1061	-5.3021
Cu	7	-0.1211	27.1410
Rb	8	-0.0507	0.0828
Sr	9	-0.0837	14.2453
Y	10	-0.0778	-0.4165
Zr	11	-0.0249	-3.8057
Pb	12	-0.2258	63.2244
Ba	13	0.0240	1.0476

Non-Marine Shales		Marine Shales	
4.10900	-5.98085	-50.34918	-34.64464
-3.96942	-4.37440	-49.40714	-32.98538
2.50768	1.46859	-45.96118	-28.99888
3.36145	-6.10486	-42.01403	-34.31420
2.54426	0.30381	-54.02592	-44.89394
-0.88921	-0.16491	-46.28638	-41.33585
0.82348	-4.59842	-47.12236	-45.34541
-0.38620	-3.24930	-33.97545	-43.98762
6.02429	-13.88501	-26.69033	-41.38244
1.76102	0.13736	-46.12540	
-2.25180	-16.66022		
-0.00410	-4.62585		
-1.48271			

which has a value more than -18.99 is regarded as non-marine, whereas a value below this would classify the sample as marine. From the listing of sample discriminant values a perfect classification is apparent.

While these variables (V, Cu, Sr, Pb) effectively distinguish between the two grups, they are not necessarily the best. This is indicated by the result of the subsequent run, using only V, Cu, Sr and Pb (Table 56). This shows that only Cu, Sr and Pb yield positive contributions. It is also clear that a perfect classification is retained but the D^2 becomes more effective in differentiating the two groups. This is indicated by the F-value of 44.42 and its corresponding value from the table $F_{4.39} = 3.85$, at the 99% significance level.

The successive elimination of V from the discriminant function also yields an efficient discrimination which is as good as the previous discriminant functions (Table 57). But the effectiveness of the separation (D^2) becomes even higher as indicated by the increase in F = 59.26 compared to its counterpart from the table $F_{3.40} = 4.31$ at the 99% significance level. This successive elimination of less desired variables, demonstrates that the smaller the number of variables needed to classify an unknown sample, the better. Therefore, it seems that the best discriminators are Cu, Sr and Pb. An unknown sample can be assigned to either group by multiplying the constant value of each trace element by its respective concentration and the sum of these products would give the discriminant value.

6.3.2 Mam Tor Shales

The discriminant function analysis was applied to the trace element data of the Mam Tor shales and the non-marine shales from Tansley Bore-hole. The depositional environment of the former was independently established, as marine, by other geological evidence (see Chapter 1).

TABLE 56: Results of Discriminant Function Analysis, using Four Variables, Non-Marine and Marine Shales, Tansley Borehole

F = 44.4158 with 4 and 39 degrees of freedom

D^2 = 17.72316 R1 = -11.4663, RO = -19.1195 R2 = -29.1895

	Variable	Constant	Percent Added
V	1	0.0091	-7.5928
Cu	2	-0.0607	30.5476
Sr	3	-0.0514	19.6220
Pb	4	-0.0915	57.4232

Non-Marine Shales		Marine Shales	
-13.60795	-12.12645	-34.41290	-24.27396
-13.62350	-7.76152	-33.70299	-19.34488
-11.52768	-4.29315	-30.03354	-23.66827
-10.99255	-13.91314	-29.24947	-27.26335
-10.96508	-8.70823	-35.88177	-33.13104
-12.64379	-8.97974	-32.58412	-31.81174
-9.89957	-9.56884	-40.07597	-34.97112
-10.91550	-13.01961	-25.96274	-20.95766
-12.18479	-16.03197	-22.59661	-24.15279
-13.75106	-10.73926	-30.52525	
-11.62630	-16.36292		
-11.31130	-12.55541		
-9.54962			

TABLE 57: Results of Discriminant Function Analysis using Three Variables, Non-Marine and Marine Shales, Tansley Borehole

F = 59.2587 with 3 and 40 degrees of freedom

D^2 = 17.29108 R1 = 11.0001 RO = -18.4667 R2 = -28.2912

	Variable	Constant	Percent Added
Cu	1	-0.0517	26.6457
Sr	2	-0.0429	16.8044
Rb	3	-0.0879	56.5499

Non-Marine Shales		Marine Shales	
-12.90423	-11.51873	-32.76087	-22.82863
-12.97793	-7.41434	-32.55894	-19.98997
-10.96291	-4.49143	-31.19659	-22.96686
-10.43970	-12.67940	-27.95012	-25.93496
-10.37185	-8.54495	-34.27099	-32.82133
-12.03732	-8.71547	-30.40558	-29.97752
-9.45284	-9.29093	-40.42537	-33.91657
-10.37658	-12.71869	-25.13289	-18.78004
-11.68451	-15.60963	-21.44259	-24.66916
-13.11880	-10.24803	-29.50396	
-11.20622	-15.80414		
-10.88026	-12.33834		
-9.21603			

The total number of samples included in the derivation of the discriminant function is thirty six, of which eleven belong to the Mam Tor Shales and twenty five are non-marine shales from Tansley Borehole. The number of variables (trace elements) used was thirteen. The result is shown in Table 58, which lists the discriminant index (RO) of the function (-25.65), the distance of separation between means of the two groups (D^2) and its significance as indicated by F-value. Any sample with a discriminant value lower than -25.65, is classified as marine; if greater than or equal to this it is classified as non-marine. Apart from Mn, V, Zn, Y, Zr and Ba, all the other trace elements contribute positively to the discriminant function. But Co, Cr have the highest contributions as indicated by the percent added. The discrimination between the two groups is significant at the 99% level as shown by the F-value of 4.72, which is higher than $F_{13,22} = 3.08$. Six of the non-marine shales were classified as marine and four of them with the discriminant values -26.56, -26.35, -25.68 and -25.79 are close to that of the discriminant index of -25.65. While the other two have a slightly lower discriminant value of -28.09 and -28.47. These misclassified samples have a relatively lower Co and higher Cr amount than the rest of the non-marine samples. This is similar to the distribution pattern of these elements in the Mam Tor marine shales. As shown by the percent added, these two variables (Co, Cr) have the highest contributions to the discriminant function. However, the Mam Tor Shales are distinctively separated from the non-marine shale, as indicated by their discriminant values which are markedly higher than even the misclassified non-marine shales. If, for example, a discriminant value lower than -28.06 is assigned to the discriminant index, an efficient separation is clear, apart from one non-marine sample having a value of 28.47. This discriminant value (-28.06) is the avarage of the discriminant values of the non-marine

TABLE 58: Results of Discriminant Function Analysis using Thirteen Trace Elements, Tansley Non-Marine Shales in Comparison to Mam Tor Shales

F = 4.7226 with 13 and 22 degrees of freedom

D^2 = 12.4207 R1 = -21.8509 RO = -25.6461 R2 = -34.2716

	Variable	Constant	Percent Added
Ni	1	-0.1361	3.0532
Co	2	0.2892	48.1459
Mn	3	-0.0071	-25.1672
V	4	0.0976	-10.4990
Cr	5	-0.3169	51.0670
Zn	6	0.0010	-0.0269
Cu	7	0.3063	7.2736
Rb	8	-0.0592	10.3575
Sr	9	0.0713	8.3843
Y	10	0.0060	-0.0499
Zr	11	-0.0057	-0.1842
Pb	12	-0.3118	21.5889
Ba	13	0.0376	-13.9424

Non-Marine Shales		Mam Tor Shales
-19.65642	-25.68593*	-34.12920
-18.25275	-20.81456	-32.71702
-21.31729	-25.79438*	-37.32543
-23.65280	-15.49168	-31.13498
-18.50476	-13.51817	-35.01584
-26.56748*	-18.5042	-30.64725
-21.22427	-23.53260	-32.83051
-28.09526*	-21.94939	-35.30767
-23.23130	-20.63562	-35.91578
-17.55813	-16.64544	-36.46954
-26.35112*	-24.05241	-35.49449
-24.59401	-28.47.72*	
-22.17004		

*Misclassified samples

(-21.85) and that of the marine (-34.27). The difference between this value of -28.06 and that established of -25.65, may be influenced by the number of samples present in each group, and the effectiveness of each variable, and may be considered as marginal overlapping.

In order to reduce the number of variables involved, a test of confidence interval for the population mean was applied. It was found that only Co, Cr and Sr have a significant difference. Accordingly, the rest of the variables were eliminated and the result is shown in Table 59.

The latter shows that the F-value is greatly increased (22.41) and it is far past the 99% significance level of $F_{3.25} = 4.68$. This new discriminant function reduced the number of non-marine misclassified samples to four, which were also included in the former discriminant function. Its effectiveness in separating the Mam Tor shales is as good as the other discriminant function. Although separation of the Mam Tor shales from the non-marine shales of Tansley is achieved, their discrimination using the original discriminant function (Table 55) established from the marine and non-marine shales of Tansley reveals a completely different picture. Table 60 shows the results, and it is clear that the Mam Tor shales are classified as non-marine. Comparison of the average concentrations of trace elements in the Mam Tor shales with the Tansley marine shales demonstrates the latter high enrichment in Ni, Co, V, Zn, Cu, Sr and Pb, while Cr, Rb and Ba are slightly lower in concentration than in the former, in which Zr is highly enriched (Tables 48, 54). The variations in trace element contents between the Mam Tor shales and the Tansley non-marine are much less apparent, apart from a slight difference in Co, Cr and Sr, which proved to be the best discriminators separating these shales. This similarity in trace element contents, therefore is the reason for classifying the Mam Tor shales as

TABLE 59: Results of Discriminant Function Analysis using Three Variables

F = 22.4131 with 3 and 25 degrees of freedom

D^2 = 10.63505 R1 = -26.8802 R0 = -30.9146 R2 = -37.5163

	Variable	Constant	Percent Added
Co	1	0.1489	23.6768
Cr	2	-0.3195	54.0332
Sr	3	0.1299	22.2901

Non-Marine Shale		Mam Tor Shales
-23.63412	-26.44391	-33.31243
-28.59580	-10.23070	-41.61212
-30.62196	-18.11395	-40.18296
-35.82598*	-19.18929	-35.22963
-27.53392	-18.09499	-38.67378
-27.05778	-27.20169	-36.00290
-28.26992	-25.93893	-38.39280
-34.34129*	-27.77409	-34.13762
-25.32241	-30.06145	-36.93551
-29.86628	-2.03420	-37.03032
-32.03633*	-28.51988	-41.16900
-29.13374	-37.21015*	
-30.56499		

*Misclassified samples

TABLE 60: Results of Discriminant Analysis of the Mam Tor Shales using Tansley Data (see Table 55)

R1 =	-1.8235	0.7853	-5.7275
RO =	-18.9871	-5.0863	1.2886
R2 =	-41.5708	-3.7808	-0.4149
		-6.4381	-6.0286
		0.3387	-11.7747
		-1.7224	2.99592

non-marine. Thus, it is clear that marine shales from different sections of the same basin have different trace element concentrations. This is due to the presence of subordinate amounts of pyrite and organic matter, together with the abundance of calcite in the Tansley Marine Shales (see Chapter 7).

6.4 Summary

Trace element data of both marine and non-marine shales were used to determine their validity in discriminating between the two groups.

The following was determined:

1. Marine and non-marine shales from the Tansley Borehole can be distinguished on the basis of trace elements abundance. A discriminant function based on V, Cu, Sr and Pb decisively discriminates between the two groups. However, the most effective discrimination was based on Cu, Sr and Pb. These results are in perfect agreement with those determined by either palaeontological criteria or mineralogical data.
2. Applying the discriminant function analysis to the Mam Tor shales in comparison to the non-marine shales of Tansley Borehole shows that Co, Cr and Sr are efficient discriminators. At the most two out of thirty six shales were misclassified. Nevertheless, nearly a complete separation of the Mam Tor shales was achieved.
3. Classification of the Mam Tor shales using the discriminant function derived from the Tansley marine and non-marine shales, revealed the former similarity to the Tansley non-marine shales. Comparison of the average concentration of trace elements in both shales, demonstrates their similar contents of most elements, except a slight variation in Co, Cr and Sr. Consequently, their effectiveness in separating the two groups of shale is an over-emphasised feature.

However, with a larger sample population, a better discriminant function could be obtained. Nevertheless, the efficient separation of the marine shales from the non-marine shales of Tansley Borehole is the most impressive result. This indicates that the use of discriminant function analysis is most promising.

CHAPTER 7

Aspects of Element and Mineral Geochemistry

The use of element pair ratios has often been used to infer the rate of sedimentation and grain size of the sediments. Moreover, the distribution of different diagenetic minerals and enrichment of certain elements have been equated with changing physico-chemical conditions including possible salinity variations (see Chapter 1). This aspect will be considered in this chapter.

7.1 Silicon and Aluminium

7.1.1 Mam Tor

It was shown previously (Figure 15) that SiO_2 and quartz variations were similar and opposite to those of clay minerals and their related elements. Grain size analysis revealed that SiO_2 varies antipathetically with Al_2O_3. Their variation was indicated by the decrease of SiO_2/Al_2O_3 ratio with decreasing grain size (Tables 29 and 31).

Accordingly, this decrease in the ratio can be attributed largely to sorting. As suggested by Pettijohn (1957), this ratio could be considered as a good index of grain size. Table 61 lists the SiO_2/Al_2O_3 ratio of the Mam Tor rocks. Comparison with those of the various size fractions, indicated that the shales fall in the fine silt and clay fraction, whereas the greywackes in the sand fraction. Therefore the change in this ratio can be considered to reflect variation in quartz content,grain size, and sorting all of which are influenced by the rate of sedimentation. Consequently, the higher ratio of the greywackes implies a faster rate of sedimentation and poor sorting compared to the shales. The latter show only a slight variation in the SiO_2/Al_2O_3 which suggest that they

TABLE 61: Variation of SiO_2/Al_2O_3, Quartz and Al_2O_3/Combined Silica Ratios through the Mam Tor Rocks

Sample Number	$\frac{SiO_2}{Al_2O_3}$	$\frac{\text{Quartz}}{\text{Comb-Silica}}$ [1]	$\frac{Al_2O_3}{\text{Comb-Silica}}$ [1]	$\frac{Al_2O_3}{\text{Comb-Silica}}$ [2]	$\frac{\text{Quartz}}{\text{Comb-Silica}}$ [2]
9a	2.07	0.53	0.67	0.92	0.62
$8b_2$	7.82	2.91	0.50	0.72	5.38
$8b_1$	8.71	6.99	0.92	0.78	6.74
$8a_2$	2.12	0.57	0.74	0.80	0.68
$8a_1$	2.10	0.36	0.65	0.77	0.61
7a	1.81	0.31	0.73	0.75	0.33
$6b_3$	10.42	6.70	0.74	0.77	8.65
$6b_2$	10.95	4.71	0.52	0.72	8.60
$6b_1$	8.10	4.91	0.73	0.76	5.87
6b	7.08	3.37	0.62	0.77	4.88
6b	2.11	0.76	0.83	0.77	0.60
5a	2.24	0.74	0.78	0.77	0.67
$4b_3$	4.64	3.22	0.91	0.73	2.47
$4b_2$	5.01	3.67	0.93	0.74	2.84
$4b_1$	9.29	4.45	0.59	0.86	8.47
$4a_2$	2.08	0.74	0.84	0.77	0.55
4c	4.02	3.40	1.10	0.78	2.19
4a	2.98	1.10	0.74	0.76	1.23
3b	8.56	6.03	0.82	0.76	6.50
3a	2.22	0.58	0.71	0.76	0.58
2c	5.60	3.79	0.85	0.68	3.01
2b	8.02	4.13	0.64	0.91	4.13
2a	2.14	0.42	0.67	0.79	0.65
1b	4.35	4.56	1.28	0.70	1.25
1a	2.13	0.49	0.70	0.74	0.55

1 - Ratio without correction

2 - After correction for feldspar and ± silica from norm calculation

a - Shales

b,c - Greywackes and Silty Shales

were deposited under similar conditions. Data on the Gulf of Paria sediments show that where the rate of sedimentation is high, the Si/Al ratio is also high, and decreases from the delta platform sands to the basin clays where the sedimentation rate is low (Hirst, 1962). The SiO_2/Al_2O_3 ratio, however, was considered as an approximate indication of the proportion of quartz to that of the clay minerals, and the use of quartz or free silica/combined silica was preferred (Spears, 1963). The variation of this ratio, in the Mam Tor rocks, is also shown in Table 61, and good resemblance to that of SiO_2/Al_2O_3 ratio is clearly seen. It seems therefore, that there is a general agreement among these ratios, quartz content, and grain size. As quartz is of detrital origin, so the clay minerals with which they are associated. Such an origin has been invoked for clay minerals in many sediments (Hirst, 1962; Nicholls and Loring, 1962; Spears, 1963, 1964). The latter suggested that a moderately variable Al_2O_3/combined silica ratio would indicate a detrital origin. Table 61 lists this ratio for the Mam Tor rocks. In the shales, this ratio varies between 0.65-0.84. As feldspar is present in these shales, together with uncertainties of the combined silica content from norm calculation; it is believed that correcting for Al_2O_3 in feldspar and combined silica would give a more representative ratio. This new ratio, and also the corrected quartz/combined silica ratio, are again shown in Table 61. It is clear that the new Al_2O_3/combined silica ratio is less variable than the previous one, with the majority around 0.75. Therefore, a detrital origin for the clay mineals in the shales seems a reasonable suggestion. In the greywackes, this ratio, in some cases, is slightly high. This may be due to the diagenetic growth of kaolinite, as revealed by petrographic study. Nevertheless, the similarity, in this ratio, between the shales and greywackes, gives further support to the proposed detrital origin for the bulk of clay minerals.

The corrected quartz/combined silica ratios do not change the implications arrived at earlier, but their values are modified. The gradation of this ratio from a better to a less sorted sandstone, through silty shale to shale, suggests that their deposition was linked. Alternatively, the sandstones represent deposition from a high velocity turbidity current and its subsequent waning resulted in the deposition of the shales in the deeper part of the basin. Accordingly, the relationship of the quartz/combined silica or SiO_2/Al_2O_3 with quartz content, grain size, sorting and the rate of sedimentation, is justified.

7.1.2 Tansley Borehole

The SiO_2/Al_2O_3 ratios for these sediments are shown in Table 62. Characteristically the sandstones have a very high ratio, more than 6. The underlying non-marine silty shales show a reduction inthe value of this ratio. These overlie the rest of the non-marine shales (down to sample 28) whose SiO_2/Al_2O_3 ratio is further reduced. These latter shales are underlain by the marine shales (samples 29-36), which show imperceptible changes in their SiO_2/Al_2O_3 ratio, in comparison to the least silty non-marine shales. Below these marine shales there are non-marine shales (37-45) which show a gradual increase in the value of SiO_2/Al_2O_3 ratio and decreases again towards the underlying marine shales. Towards the junction of the lower Namurian and upper Visean, the calcareous shales (sample 66-70) show a high value of the SiO_2/Al_2O_3 ratio. Similarly the K-bentonites (71-73) have a high ratio.

Comparable results are obtained by using the ratio of free silica/combined silica (Table 62).

The decrease in both ratios from the sandstones through the silty into the least silty non-marine shales implies a progressive sorting and consequently decrease in grain size and quartz content. This may be

TABLE 62: Variation of SiO_2/Al_2O_3, Quartz/Combined Silica and Al_2O_3/Combined Silica Ratios through the Tansley Borehole Succession

Sample Number	$\frac{SiO_2}{Al_2O_3}$	$\frac{\text{Quartz}}{\text{Comb-Silica}}^{1}$	$\frac{Al_2O_3}{\text{Comb-Silica}}^{1}$	$\frac{Al_2O_3}{\text{Comb-Silica}}^{2}$	$\frac{\text{Quartz}}{\text{Comb-Silica}}^{2}$
1	2.03	0.59	0.81	0.81	0.59
2	1.98	0.48	0.75	0.78	0.55
3	2.41	0.71	0.71	0.78	0.88
4	10.41	1.56	0.25	0.62	7.16
5	8.71	1.65	0.30	0.57	5.32
6	10.73	3.42	0.92	0.68	10.15
7	6.46	1.92	0.45	0.64	3.73
8	3.95	1.01	0.51	0.70	1.80
9	3.33	1.05	0.62	0.74	1.46
10	5.12	1.37	0.34	0.71	2.83
11	2.34	0.57	0.67	0.75	0.71
12	12.07	3.44	0.37	0.72	9.61
13	3.98	1.41	0.61	0.75	1.97
14	2.41	0.77	0.73	0.73	0.79
15	2.64	0.52	0.58	0.76	0.98
16	2.98	0.75	0.59	0.75	1.21
17	3.24	0.97	0.61	0.74	1.39
18	2.63	1.02	0.77	0.81	1.12
19	2.17	0.54	0.71	0.72	0.55
20	2.02	0.48	0.73	0.79	0.59
21	2.10	0.38	0.66	0.77	0.62
22	2.29	0.52	0.66	0.78	0.79
23	2.48	0.79	0.72	0.72	0.79
24	2.14	0.43	0.67	0.78	0.66
25	2.28	0.62	0.71	0.74	0.70
26	2.35	1.00	0.85	0.85	1.00
27	2.07	0.52	0.73	0.79	0.60
28	2.57	0.83	0.71	0.73	0.86
29	2.33	0.65	0.71	0.78	0.83
30	2.40	0.56	0.65	0.79	0.90
31	2.48	0.72	0.65	0.79	0.92
32	2.42	0.79	0.74	0.79	0.88
33	2.46	0.61	0.65	0.79	0.92
34	2.20	0.53	0.69	0.80	0.74

TABLE 62 (Cont.):

Sample Number	$\frac{SiO_2}{Al_2O_3}$	$\frac{\text{Quartz}}{\text{Comb-Silica}}$ [1]	$\frac{Al_2O_3}{\text{Comb-Silica}}$ [1]	$\frac{Al_2O_3}{\text{Comb-Silica}}$ [2]	$\frac{\text{Quartz}}{\text{Comb-Silica}}$ [2]
35	2.31	0.57	0.68	0.80	0.84
36	2.29	0.39	0.61	0.79	0.81
37	2.95	1.67	0.98	0.94	1.68
38	3.60	1.14	0.59	0.80	1.87
39	4.03	1.23	0.55	0.79	2.20
40	4.28	1.08	0.49	0.79	2.36
41	2.81	0.65	0.58	0.80	1.26
42	2.58	0.86	0.72	1.03	1.36
43	2.34	0.79	0.77	0.79	0.84
44	2.45	0.76	0.72	0.85	1.08
45	2.20	0.56	0.71	0.80	0.77
46	2.64	0.67	0.63	0.77	1.02
47	2.53	0.91	0.76	0.76	0.91
48	2.64	0.94	0.76	0.80	1.02
49	2.69	0.84	0.68	0.76	1.01
50	2.41	0.68	0.70	0.79	0.91
51	2.08	0.43	0.69	0.78	0.62
52	2.29	0.58	0.69	0.76	0.74
53	2.67	0.64	0.61	0.77	1.05
54	2.70	0.82	0.67	0.79	1.10
55	2.63	0.83	0.70	0.79	1.08
56	2.46	0.56	0.64	0.78	0.92
57	2.57	0.80	0.70	0.79	1.01
58	2.57	0.47	0.57	0.79	0.99
59	2.60	0.67	0.64	0.78	0.99
60	2.77	0.76	0.63	0.78	1.13
61	2.94	1.03	0.69	0.76	1.02
62	2.48	0.78	0.72	0.76	0.84
63	2.73	0.72	0.63	0.77	1.05
64	2.67	0.96	0.73	0.76	1.03
65	2.99	1.05	0.69	0.75	1.24
66	3.83	1.06	0.54	0.82	2.21
67	6.41	1.28	0.35	0.85	4.62
68	5.63	0.99	0.35	0.76	3.40

TABLE 62 (Cont.):

Sample Number	$\frac{SiO_2}{Al_2O_3}$	$\frac{\text{Quartz}}{\text{Comb-Silica}}$ [1]	$\frac{Al_2O_3}{\text{Comb-Silica}}$ [1]	$\frac{Al_2O_3}{\text{Comb-Silica}}$ [2]	$\frac{\text{Quartz}}{\text{Comb-Silica}}$ [2]
69	4.86	0.43	0.29	0.86	3.25
70	3.50	0.43	0.41	0.76	1.59
71	4.65				
72	4.78				
73	2.91				

1 - Ratio without correction

2 - After correction for Feldspar and Silica from Norm Calculation

attributed to a decrease in the rate of sedimentation which could have been influenced by velocity of the transporting medium and probably distance from shoreline. On the other hand, the lack of significant difference in these ratios between the lower non-marine and the underlying marine shales indicates similarity in sorting, grain size and quartz content. This is demonstrated by the insignificant difference in the average quartz content of both groups, excluding the silty non-marine shales (page 154). Again the apparent increase in the ratios towards the non-marine shales which are interbedded with the marine shales, suggests an increase in the rate of sedimentation, less sorting, higher quartz content and probably coarser grained sediments. In contrast, the lowest non-marine shale (sample 51) shows no such difference in the ratios which are relatively low. Therefore, it seems that difference in these ratios is likely to exist only when truly non-marine conditions had been established. On the other hand, those non-marine shales which may be regarded as a transitional phase towards the marine conditions would show no difference in these ratios.

In contrast, the high SiO_2/Al_2O_3 of the lower Namurian and upper Visean calcareous shales cannot be accounted for by increase in the rate of sedimentation. This sudden increase in this ratio is attributed to silicification which was previously described (page 137). Similarly, some of these shales show a high free silica/combined silica ratio whereas the lowest shales (sample 69 and 70) have a very low ratio. This irregular variation in this ratio is due to the high amount of silica which was recorded as excess silica in the mineralogical calculation. Consequently the application of these ratios in this case is not suited for comparing rate of deposition and grain size. However, calcareous shales would rather indicate quiet conditions and less detrital supply compared to the non-calcareous marine shales. Likewise, the K-bentonites high ratios

are ascribed to submarine alterations rather than depositional factors (see page 144). The ratio of Al_2O_3/combined silica which expresses the composition of the clay minerals is shown in Table 62 (marked 1). It can be seen that the ratio does not vary systematically through the succession. This is thought to be partly due to the inaccuracy in deducting the amount of combined silica. In order to obtain more accurate variation in the ratios, they are corrected for the content of feldspar and excess silica, and shown in Table 62 (marked 2). It is clear that variation in the Al_2O_3/combined silica ratio is much reduced. It can be postulated then, that this ratio was fixed during weathering and transportation. Thus a detrital origin for the clay minerals can be suggested. The variation of corrected free silica/combined silica ratio, supports the aforementioned interpretation of changing quartz content and grain size with the rate of sedimentation. The deviation of the lower calcareous shales from this general role is still clear. This can be related to silicification, in turn connected to volcanicity (see Ramsbottom et al., 1962; Smith et al., 1967; Orme, 1974). Alternatively it may indicate deposition nearer to shore (see discussion on Na and K). Following this information, it is envisaged that change in the trend of sedimentation may either be gradual or sudden. The first case is shown by the transition from the Ashover sandstone, through the silty shales to the underlying, less silty, non-marine and marine shales. The second case is exemplified by the non-marine shales in the main marine part of the succession.

7.2. Titanium

7.2.1 Mam Tor

The TiO_2 contents and TiO_2/Al_2O_3 ratios for the Namurian sediment are shown in Table 63. For the Mam Tor rocks, TiO_2 content is higher

TABLE 63: Average TiO_2 Content and TiO_2/Al_2O_3 Ratio in the Namurian Sediments

	TiO_2%	$\frac{TiO_2}{Al_2O_3}$
Average 14 Mam Tor Greywackes	0.53	0.049
Average 11 Mam Tor Shales	0.99	0.042
Average 34 Non-Marine Shales (Tansley)	0.85	0.041
Average 30 Marine Shales (Tansley)	0.72	0.040
Average 4 Ashover Sandstones (Tansley)	0.45	0.054
Average 3 K-Bentonites (Tansley)	1.68	0.136

for the shales than the greywackes, while the TiO_2/al_2O_3 shows the inverse relationship.

It was previously shown that TiO_2 and Al_2O_3 profiles were similar and both vary antipathetically with quartz and SiO_2 (Fig. 15). Chemical analysis of different size fractions demonstrated that the highest TiO_2 contents were in the silt and clay fractions, particularly in the 7.8-15.6 micron fraction. The TiO_2/Al_2O_3 ratios of the size fraction (Tables 29 and 31) indicated that this ratio, generally increases as the grain size became coarser. On the other hand, in those rocks which were separated into a few size fractions the TiO_2/Al_2O_3 ratio was highest in the 7.8-53 micron fraction and decreased towards either the coarser or finer fractions. This suggests that TiO_2 follows Al_2O_3 in a general way but the geochemical coherence is not very strong. This relationship between TiO_2 and major elements related to clay minerals was shown to be significant by correlation analysis. Consequently, it can be suggested that sorting was an important factor in concentrating TiO_2 minerals in the clays. The rather lower TiO_2/Al_2O_3 ratio of the shales, compared to the sandstones would favour such a suggestion. Hirst (1962) stated that Ti concentration is related to the sedimentation rate, being higher in the clays than in the sands of the Gulf of Paria. Similarly, the sympathetic relationship between the TiO_2/Al_2O_3 ratio and the grain size in the present study can be related to the energy of the depositional environment. Continuous increase in TiO_2/Al_2O_3 ratio as the quartz content increases, is due to the increased importance of TiO_2 minerals relative to the clay minerals in the coarser grained sediments.

The heavy mineral fractions examined from the Mam Tor rocks revealed the presence of rutile as one of the main minerals (see Chapter 3). Thus the high concentration of TiO_2 in the silt fraction can be attributed to the abundance of rutile.

As to the nature of TiO_2 in the clay fraction of the rocks,no clear cut evidence could be obtained. Rutile, however, was observed in the finest silt fraction. It is possible, therefore, that rutile is probably present as a very fine crystalline TiO_2 deposited along with the small flakes of the clay minerals. Such association has been widely reported (Goldschmidt, 1954; Goldberg and Arrhenius, 1958; Weaver, 1976). This may be attributed to the similarity between Ti-Al geochemical cycles, in many respects.

Accordingly, the rate of sedimentation and sorting can account for the increase in TiO_2/Al_2O_3 ratio and grain size. To a certain extent, the variation of TiO_2/Al_2O_3 ratio seems to be similar to those of SiO_2/Al_2O_3 and free silica/combined silica, in differentiating the sandstones from shales.

7.2.2. Tansley Borehole

The average content of TiO_2 and the mean value of TiO_2/Al_2O_3 ratio of these rocks are shown in Table 63. Again the sandstones show a higher TiO_2/Al_2O_3 ratio than the shales, whereas the TiO_2 content shows the reverse trend. The higher TiO_2 content of the non-marine shales compared to the marine shales can be attributed to the abundance of siltstone in the former (see Chapter 5). This is similar to the findings of Lebedev (1967), who recorded a median TiO_2 content of 0.63% in the marine and brackish water clays and 0.88% in the fresh water clays. Examination of the average TiO_2/Al_2O_3 ratio of the Tansley non-marine and marine shales, indicates their similarity (Table 63). It implies that the clay mineral content is higher in the non-marine shales, and this is supported by the higher average contents of Al_2O_3 and combined silica in these shales (Table 42). Migdisov (1960) showed that the TiO_2/Al_2O_3 ratio of clays remains relatively constant irrespective of facies. The lesser mobility of titanium as compared with aluminium was suggested to result

in TiO_2 enrichment in near shore deposits. These relationships seem to be in accord with those recorded in the present study. Consequently the non-marine shales of the Tansley Borehole can be considered as sediments accumulated nearer to shoreline than the marine shales.

The TiO_2 contents of carbonate rich shales are found to be lower than those free of carbonate. Likewise, the contents of Al_2O_3 and quartz showed a similar variation, excluding the lowest Namurian and upper Visean shales which were thought to have been affected by silicification. The TiO_2/Al_2O_3 ratio for these carbonate rich rocks is similar to the other shales, and remains approximately constant around 0.04. The most likely host of titanium is a fine grained rutile which is largely of detrital origin. Thus, it seems that carbonate rich shales were deposited through very slow sedimentation and under the effect of least detrital supply which was influenced by low velocity current.

The Namurian volcanic mudstones or K-bentonites are characterised by the remarkably higher content of TiO_2 and also TiO_2/Al_2O_3 ratio compared to the overlying shales (Table 63). Migdisov also stated that a high TiO_2/Al_2O_3 could be inherited by clays developed on basic igneous rocks. In modern oceanic sediments the variation of TiO_2/Al_2O_3 ratio has been cited to indicate the influence of volcanic rocks.

In sediments from the Pacific and Indian oceans (Bostrom et al., 1973) the highest Ti/Al ratios were recorded near the oceanic islands and sea-mount chains which are areas of low sedimentation rate, suggesting addition of volcanic materials. On the other hand, high accumulation rate of Al and Ti were found in near shore areas only and these were noted to be of detrital origin. In a previous work (Bostrom, 1970) the Al/Ti ratio has been claimed to indicate the source rock. A high ratio around 20 suggested a terrigeneous source, while weathering products of

oceanic igneous rocks should have low Al/Ti ratio of about 5. This appears to be in accord with the average Al/Ti ratios of the Namurian shales. The Mam Tor shales, the Tansley non-marine and marine shales, give values of this ratio, 21.07, 21.34 and 22.05 respectively. In contrast the ratio for the K-bentonites is 6.49.

In order to elucidate the relationship between TiO_2/Al_2O_3 ratio and lithology, this ratio was plotted against quartz for all the Namurian sediments, except the K-bentonites (Fig. 36). The latter shows that TiO_2/Al_2O_3 ratio increases as the quartz content increases up to or around 50% and then decreases. As would be expected, the quartz content increases as the grain size increases. It seems therefore, that TiO_2 minerals are largely enriched in the mudstones and siltstones (30-50% quartz). Thus it seems that sorting was a most important factor in concentrating TiO_2 minerals relative to quartz in the finer grained sediments. However, if a line is to be drawn through all the analysis on Figure 36, it would most probably intersect the TiO_2/Al_2O_3 ratio axis between 0.02 and 0.03. This gives the TiO_2/Al_2O_3 ratio of the clay fraction. Similar value of TiO_2/Al_2O_3 (0.025) was attributed to the clay minerals in other Carboniferous sediments (Spears and Sotiriou, 1976).

7.3 Sodium and Potassium

7.3.1 Mam Tor

Section profiles for sodium and potassium were shown to be anti-pathetic (Figure 15). The variation of sodium was similar to that of quartz and SiO_2, while K_2O variation resembled those of Al_2O_3 and TiO_2. Petrographic and X-ray studies revealed the presence of albite in both sandstones and shales. Statistical correlation showed that Na_2O and quartz relationship was positive and significant, while both of them have a signficiant but negative correlation with Al_2O_3, combined silica,

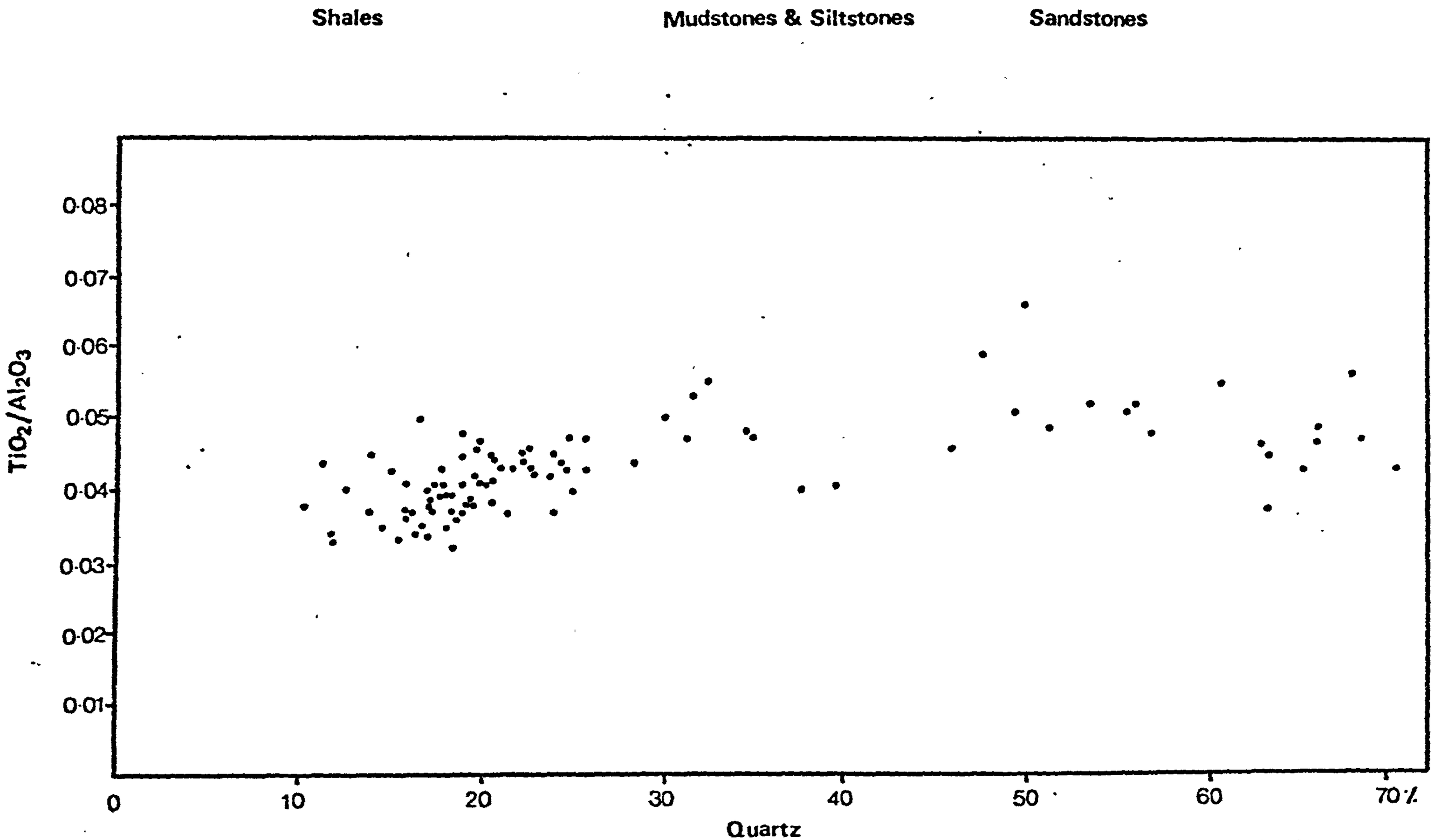

Fig-36 Variation in the TiO_2/Al_2O_3 ratio with quartz content for the Mam Tor & the Tansley Borehole rocks.

SiO_2 and K_2O. It is thus apparent that sodium and potassium are not contained in the same host mineral. Higher content of K_2O in the shales merely reflects the greater abundance of illite in the clay fraction, whereas high Na_2O in the greywackes indicates predominant albite thus the higher Na_2O/K_2O ratio of the greywackes as compared with the shales (Table 64).

Some marine shales have been reported to contain a relatively similar amount of plagioclase in comparison to the Mam Tor shales (Imbrie and Poldervaart, 1955; Weaver and Beck, 1971; Evans and Adams, 1975).

Comparing the variation of Na_2O/K_2O ratio with quartz/Al_2O_3 ratio (Figure 37) indicate that they vary sympathetically in the Mam Tor rocks. This ratio is at maximum in the well sorted greywackes and decrease through less sorted ones into a minimum in the shales. In addition this ratio follows the amount of quartz and grain size in a single bed (samples $6b_1$, $6b_2$ and $6b_3$) of greywacke. Similarly, among the shales the Na_2O/K_2O ratio is lowest in those containing the least amount of quartz.

The variations of Na_2O/K_2O ratio and that of quartz/Al_2O_3 suggest that this ratio is related in some manner to the supply of sediments and is strongly controlled by the fluctuations in the amount of albite. Support for such suggestion is obtained from analysis of different size fractions. The most noticeable change was that albite abundance and Na_2O content decrease while K_2O content and illite abundance increased with decreasing grain size (see Chapter 4). The data also indicated that albite was concentrated in the coarse silt fraction. This tends to imply that albite was originally of finer grain size than the associated quartz. Moreorless similar relationships between chemistry, mineralogy and grain size have been reported from Palaeozoic mudstone (Evans and Adams, 1975).

TABLE 64: Average Contents of Na_2O, K_2O and Na_2O/K_2O Ratio in the Namurian Sediments

	$Na_2O\%$	$K_2O\%$	$\frac{Na_2O}{K_2O}$
Mam Tor Greywackes	1.08	0.86	1.26
Mam Tor Shales	0.52	2.70	0.19
Ashover Sandstones, Tansley	1.27	1.85	0.69
Tansley Non-Marine Shales	0.68	2.35	0.29
Tansley Marine Shales	0.53	2.49	0.21
Tansley K-Bentonites	0.13	3.48	0.04

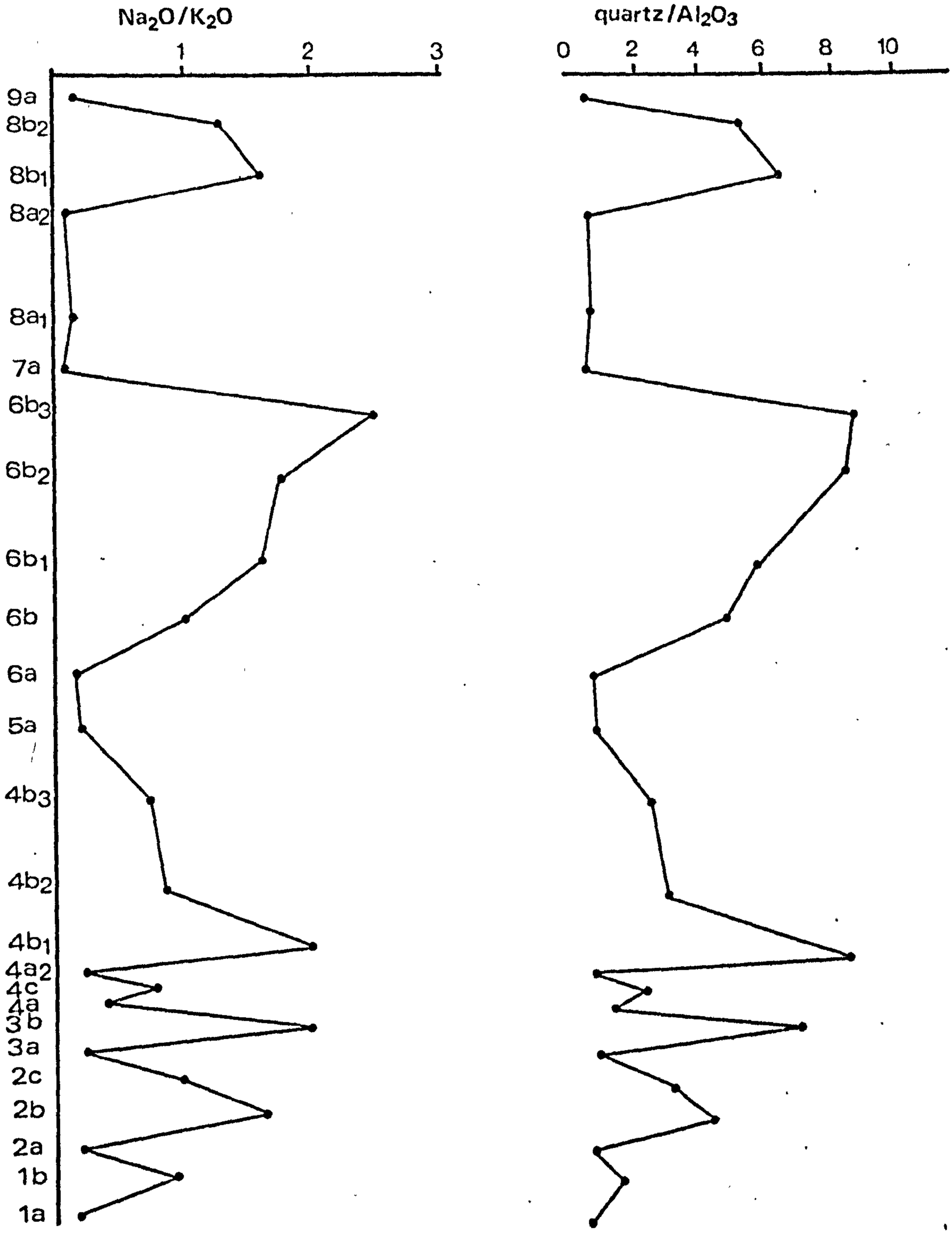

Fig.37 Variation of Na_2O/K_2O and quartz/Al_2O_3 ratios through the Mam Tor section

However, it is unlikely that allthe Na_2O is contained in albite and some of it must be present in illite, but this is overshadowed by the abundance of the former mineral. Nevertheless, data on size fractions from shales (Chapter 4)showed that in the 1-2 micron fraction where albite was not detected, about 0.14% Na_2O could be present in illite. On the other hand it may represent an amount of albite (1.18%) which is undetected by X-ray study. By using chemical data of whole rock sample, the Na_2O unallocated to albite would be somewhat smaller. Even if the explanation of Na_2O is present in plagioclase is not correct, this does not alter the fact that the Na_2O/K_2O ratio does change and apparently influenced by the grain size distribution. This leads to the conclusion that variations in albite and illite contents with the consequent change in Na_2O/K_2O ratio are related to the rate of sedimentation, distance from shoreline, or source and sorting. The further the sediment is away from its source the lesser amount of detrital albite would be incorporated in it and thus the ratio of Na_2O/K_2O would decrease regardless of any cation exchange involvement.

7.3.2. Tansley Borehole

The average contents of Na_2O and K_2O in the Ashover sandstones are higher than those of the Mam Tor greywackes (Table 64); indicating abundant feldspar in the former. The Na_2O/K_2O ratio shows the reverse trend, due to alteration of the K-feldspar by diagenesis in the Mam Tor greywackes. Both plagioclase and K-feldspar are present in the Ashover sandstones, but not all the Na_2O and K_2O however, are incorporated in the feldspars, as they are partly allocated to mica (illite). The relatively lower Na_2O content and Na_2O/K_2O ratio of the marine shales as compared with the non-marine shales reflect the slightly higher illite content in the former and the presence of more detrital feldspar in the latter.

Correlation analysis (Chapter 5) indicated that Na_2O variation was sympathetic with quartz, but this behaviour did not extend to the marine shales when each group was considered separately. In the marine shales, K_2O and Na_2O showed a close coherance with Al_2O_3 and combined silica. On the other hand, Na_2O, in the non-marine shales, was positively correlated with quartz and negatively with Al_2O_3 and combined silica. A possible and most likely explanation is that a relatively large proportion of Na_2O is contained in illite which was slightly more abundant in the marine shales. Likewise in the Pacific pelagic sediments much of the Na was attributed to illite in the presence of Na-feldspar whose contribution to the Na content was also noted (Goldberge and Arrhenius, 1958). In the present study, feldspar was found to be generally more abundant in the non-marine shales, nevertheless the lower marine shales also contain a comparable amount of Na-feldspar. An important departure from this broad trend is that some of the non-marine shales and high proportion of the marine shales are devoid of feldspar. In these shales an Na_2O content up to 0.86% was allocated to illite. It is also important to note that these shales have a comparable amount of quartz. It seems, therefore, that regardless of facies the feldspar content most probably had been influenced by weathering and transportation.

However, the variation of average Na_2O/K_2O from the sandstone, through the non-marine shales into the marine shales is accompanied by decrease in the average quartz content, and probably grain size. This implies, broadly, a gradual decrease in feldspar content and increase in illite content with decreasing quartz content and grain size.

The inverse relationship between the grain size, quartz and feldspar contents and distance of transport has been reported by Kelling et al. (1975) and Ethridge (1977); Gibbs (1977). This is also influenced by

other factors such as abrasion, source, climate, chemical stabilities of minerals, relief and sorting (Todd, 1968; England and Jorgenson, 1973; Ethridge, 1977). The effect of most of these factors largely, tend to increase the chance of feldspar decomposition and sediment maturity.

As the sediments in the present study have a comparable clay mineralogy, the influence of source rock can be discarded. In addition, the presence of Na and K feldspars tends to indicate that palaeoclimatic fluctuations were not great. Probably, it can be suggested that the completeness of weathering, relief of source rock and inherent stabilities of feldspars and sorting were more important factors, in reducing the feldspar content. Sorting and grain size are parameters which are largely controlled by the rate of sedimentation. The similar variation of average quartz content, TiO_2/Al_2O_3 and Na_2O/K_2O ratios, suggests that the decrease in feldspar content from the Ashover sandstone down to the marine shales implies a decrease in the rate of sedimentation. In order to assess the affect of the last factor on the clay minerals (illite), the Na_2O/K_2O ratios for the non-marine and marine shales were corrected for feldspars. With few exceptions, the average ratio for twenty seven non-marine shales is 0.31 and that for nineteen marine shales is 0.18. This difference in Na_2O/K_2O ratio may be ascribed, in part at least, to slight variation in illite proportions in both groups, but it may also largely reflect the lower rate of sedimentation of the marine shales. In a similar manner, the Na/K ratio was shown to be influenced by the rate of sedimentation (Nicholls, 1960; Hirst, 1962; Spears, 1964). The lower this ratio was, the lower rate of sedimentation was inferred due to cation exchange, i.e. Na replaced by K ion in illite (see Chapter 1).

In a previous discussion (page 170) the relationships between clay mineral grain size, settling velocities, and differential flocculation by ions in marine waters, together with the affinity of illite towards

the absorption of K were described. Furthermore, trace elements data (Table 50) indicated that different faunal phases, supposedly representing different salinities, were broadly characterised by variable concentration of these elements. The latter were found to increase in their average abundance from the least marine to a typical marine shale.

It follows that the lower Na_2O/K_2O ratio of illite in the marine shales may then be attributed to a lower sedimentation rate and a contributory salinity factor. A relatively high rate of sedimentation may also permit little time in order that geochemical equilibrium may be attained, hence a high Na_2O/K_2O ratio would be expected.

An important deviation from this somewhat general rule of decreasing Na_2O/K_2O ratio with slower rate of sedimentation is found in the lowest Namurian and upper Visean shales. In these shales Na_2O occurs largely as albite (Appendix 2), although they are mostly rich in carbonates. From a sedimentological point of view, their deposition should require clearer water and slower rate of deposition as compared to the shales without carbonates. This is indicated by the antipathetic relationship between quartz and carbonate and/or clay minerals content. On the other hand, other marine shales with similar quartz content have no feldspars and little or no carbonates. The TiO_2/Al_2O_3 ratio also shows no marked variation but the SiO_2/Al_2O_3 and quartz/combined silica ratios are high in these calcareous shales (Table 62). Thus it seem s that there is a broad relationship between carbonates and feldspar (plagioclase). The incorporation of albite in these shales may be explained by the following possibilities. The first is that albite was detrital and transported as a very fine grains,with the clay minerals, during the slow deposition of these shales. On the other hand, these shales are often interbedded with non-marine shales (see Ramsbottom et al., 1962), and therefore, their deposition might have been near to shore where the detrital influx was

largely composed of very fine material. Following the description by Ramsbottom et al. (1962) the albite was considered as detrital, since volcanic rock fragments were not observed inthese shales. The presence of detrital albite in marine mudstones has been recorded by other studies (Weaver and Beck, 1971). The second possiblity is that albite of authigenic origin. Such an origin has been reported from mudstones and carbonate rocks (Spencer, 1925; Peterson, 1962; Lerbekmo, 1963). They attributed its formation to the salinity of the depositional environments. The third possibility is albite of authigenic origin and related to volcanic activity. Ramsbottom et al. (1962) described such albite and quartz in sediments intercalated or adjacent to basalt, from the Fallgate Borehole near the Tansley Borehole.

Similarly, in Ordovician shales interbedded with K-bentonites, the plagioclase was ascribed to spilitic volcanism (Bjorlykke, 1971). The relationship between sedimentary feldspar and volcanism has been reviewed by Hay (1966). As to the calcareous shales in the present study, it is important to note that they are underlain by the Upper Lava of Matlock. The latter is represented by the K-bentonites whose Na_2O/K_2O ratio is much lower than that of the overlying shales (Table 64). Previously, it was shown that during the K-bentoniteforming process, large amounts of Na_2O, among other elements, was mobilised (see page 144). Consequently, it could have trapped in the connate water of the overlying sediments and under favourable conditions albite, possibly, was formed. However, this is a tentative suggestion and evidence to prove or disprove it is lacking.

In summary, it is concluded that the Na_2O/K_2O ratio is related to the presence, not only of feldspar, but also to illite. The marked increase in feldspar content in the sandstones compared to the underlying non-marine shales, which in turn have a higher feldspar content than the

underlying marine shales, reflects their histories of sedimentation. This is indicated by the Na_2O/K_2O ratio of illite in the marine and non-marine shales. The relatively higher Na_2O/K_2O ratio of the non-marine shales indicates a generally lower maturity and higher sedimentation rate compared to the marine shales.

The origin of albite in the lower Namurian and upper Visean shales is questionable, but Ramsbottom's proposal as detrital could be more conclusive. On the other hand, the depletion of the K-bentonites in Na_2O may suggest that it is likely to be of authigenic origin.

7.4 Magnesium

The content of MgO in the Tansley Borehole sediments is variable (Appendix 2). The correlation analysis showed the significant relationships of MgO with CaO, MnO, FeO, CO_2 and P_2O_5; this was considered as carbonate association (see Chapter 5). It was also substantiated by mineralogical data which demonstrated the presence of siderite, calcite and dolomite (Appendix 2). Accordingly the variation of MgO content can be attributed generally to the presence of one or more than one type of carbonate minerals. In addition other likely hosts for MgO are chlorite and illite which are present in different proportions in the sediments. Rankama and Sahama (1950) suggested that Mg can be transported in solution, present in detrital minerals including clay minerals and can also be sorbed by the sediments. In the Gulf of Paria sediments, the relatively constant Mg/Al ratio was considered to indicate association with detrital clay minerals (Hirst, 1962a). The latter also postulated that sorption had insignificant effect on the Mg content. Illite can accommodate a small amount of MgO compared to chlorite which may contain variable amounts (Deer et al., 1966). In the present study, the relationship of MgO and Al_2O_3 was found not to be significant. This most probably is due to the effect of carbonate minerals which overshadowed this relationship.

To illustrate the association of MgO with clay minerals, the MgO/Al_2O_3 ratios, excluding the samples with high carbonate contents, was calculated for the marine and non-marine shales. The mean value and standard deviation of the ratio in the non-marine shales are 0.072 and 0.01 respectively. The corresponding values in the marine shales are 0.074 and 0.01. Such very moderate difference may as well reflect a relative constancy, thus represent detrital association with illite and chlorite. Consequently, sorption can be considered of little importance which also suggests that the rate of sedimentation had no effect on the distribution of MgO in the clay minerals. The importance of solution rich in Mg is reflected by the ratio in the carbonate rich samples. Those containing siderite have an average ratio of 0.184. It is also found that small amounts of siderite about 5%, does not effect the mean ratio in the clay appreciably. Data on siderite composition (Deer et al., 1966) shows that only a small amount of MgO can be bound in its structure. Dolomite is present in higher amounts in the marine shales than in the non-marine. It is of the ferroan variety as demonstrated by X-ray diffraction and has a d-spacing of 2.895 Å. This is similar to ankerite described from the Green River Formation (Smith and Robb, 1966) which contain between 5.84-8.01% MgO. The average MgO/Al_2O_3 ratio, in the dolomite rich marine shales concerned with in the present case, is 0.433, indicating the highest amount of MgO is located in the dolomite. Likewise dolomite is abundant in few non-marine shales and sandstones and the ratio is found to be equally high. On the other hand, the marine shales enriched in calcite also have an average ratio of 0.113. This calcite has a d-spacing of 3.02Å. According to the information of Chave (1952) this is a low magnesium calcite and may contain up to 6% $MgCO_3$. Thus the high ratio is a reflection of the calcite content. The latter is belived to be of biogenic origin. It is very likely, therefore that the original calcite

shells were high in Mg-calcite which during diagenesis converted to low Mg-calcite. This is supported by many studies on limestones in which calcite has a similar origin (Schlanger, 1957; Fisher, 1968; Winland, 1968; Buchbinder, 1969; Jacka, 1974; Leone and Alaimo, 1974; Selim and Duff, 1974). In addition, these workers have also noted the association of Mg-calcite and dolomite in their studies. The origin of dolomites in British Carboniferous sediments has been investigated by many workers, among them Parsons (1918), Bhatt (1972, 1973), Al-Hashimi (1972), Selim and Duff (1974) and Amin (1975). These dolomites range in composition from low ferroan dolomites to ankerites. Their origins have been ascribed to syngenesis,early and late diagenesis and epigenesis. The last was related to the dolomite of the present study (Smith et al., 1967).

The mean values and standard deviation of the MgO/Al_2O_3 ratio in the Mam Tor shales are 0.077 and 0.01, while the corresponding value in the greywackes are 0.082 and 0.016. This difference can be attributed to diagenetic alteration of biotite to chlorite in the greywackes. The relatively higher ratio of the Mam Tor shales in comparison to the Tansley Borehole shales is probably due to the higher content of chlorite in the former (see Table 54). Accordingly a detrital origin for the bulk of MgO in these shales is a reasonable suggestion.

Finally, it can be suggested that Mg in the Namurian sediments is partly detrital and partly from solution. The processes of sorption are of little importance, if any, but this is not clearly defined.

7.5 Iron, Calcite and Phosphate

In the Namurian sediments iron is present as ferrous and ferric irons. FeO, as determined, is related to siderite and chlorite and the part allocated to chlorite is determined by subtracting the content incorporated in carbonates which are dependant on the CO_2 content. The Fe_2O_3 is shared

among iron hydroxides, illite and pyrite, although iron in pyrite is FeO, it was determined as Fe_2O_3. Generally, illite can accommodate up to 5% Fe_2O_3 and 0.26% FeO in its structure (Deer et al., 1966), while chlorite may contain variable proportions of FeO and possibly some Fe_2O_3. Mineralogical analyses of the shales (Appendix 1 and 2) indicate that the excess Fe_2O_3 is generally below 5% and certainly part of this would be attributed to illite. The FeO content associated with chlorite is variable and this is reflected by its presence in different proportions in the shales.

The most important, diagenetic, iron minerals are siderite and pyrite particularly in the Tansley Borehole sediments, which will be mainly referred to in the following discussion. Siderite is confined to shales, palaeontologically, identified as non-marine while pyrite is present in marine and non-marine shales, but it is dominant in the former. Statistical analyses, indicated that Fe_2O_3 is significantly correlated with SO_3 and less so with organic matter as shown by the value of their correlation coefficient (see Table 46). In the non-marine shales, CO_2, MnO, P_2O_5 and CaO relationships with FeO were much stronger than in the marine shales, indicating association with siderite. On the other hand, CaO correlation with CO_2 and P_2O_5 was stronger in the marine shales. The relationships were considered to reflect the abundance of pyrite, organic matter and calcite in the marine shales. The trend is from pyrite and calcite rich marine shales at the base to siderite rich non-marine shales at the top of the sequence. Such a trend, reflects changing physico-chemical conditions. Similar trends have been noted in several studies on the Carboniferous sediments, England (see Chapter 1). This change from the pyrite stability field to that of siderite was attributed to increased Eh values, probably accompanied by a rise or fall in pH values (Nicholls and Loring, 1962; Spears, 1963, 1964). The latter worker attributed

the abundance of siderite in the non-marine shales to decreasing pH. These interpretations were deduced from two dimensional plots of Eh-pH diagrams. However such calculations invoke the presence of an aqueous solution of relatively constant composition and thermodynamic equlibrium between the solid phases and ions present therein. Therefore, their application is limited, because studies on interstitial water and mineral equilibria in sediments from many basins, strongly suggest that the activities (thermodynamic concentration) of sulfur, carbonate, phosphate and iron species are not constant. The importance of sulfide and carbonate activity variation has been demonstrated in laboratory experiments and in natural environments (Berner, 1963, 1964a,b,c; Hem, 1977) or from theoretical considerations (Huber, 1958; Curtis and Spears, 1968). All of these workers agree that pyrite formation is due to the increase of sulfide activity and it is stable under conditions of low Eh values.

From the stability diagrams presented by the aforementioned workers, it is apparent that progressive decrease in sulfide activity increases the size of the siderite stability field. The limiting factors seem to be sulfide and CO_2 activities. Under reducing conditions the decomposition of organic matter by sulfate reducing bacteria produces CO_2, carbonate and reduced sulfide species. The latter were considered to lower the pH but in the presence of calcium, acting as a buffer would stabilise the pH around 7.5 (Berner, 1963). On the other hand, the reduction of sulfate by bacteria to sulfide and carbonate was shown to have no effect on pH, while in the absence of sulfate this would result mainly in CO_2 production, thus decreasing the pH (Dyrssen and Hallberg, 1979). Another possiblity, is that H_2S could reduce CO_2 to form other organic compounds, such as methane (Zobell, 1964; Ormond and Taylor, 1978) and the reduction of sulfate would result in high pH (Zobell, 1963). These conditions of increasing sulfide activity therefore, result in consumption of CO_2 or it could be

buffered by calcium. Since siderite is dependant on a high activity of CO_2, it would be stable under lower pH conditions. It appears that sulfide is the most important factor in limiting or preventing the formation of siderite.

Another pathway which provides insight into the relative variation in pH, is the involvement of calcite and phosphate under reducing conditions. In the Tansley Borehole sediments, the average P_2O_5 content is 0.19% in the non-marine shales, particularly enriched in siderite rich sample (0.69) while that of the underlying marine shales, rich in calcite, is 0.15%. In few cases, iron rich dolomites(ankerite) are located in the marine part, but their P_2O_5 content is similar to the rest of the shales rich in calcite. From the distribution of calcite it can be inferred that high pH values were necessary to promote calcite precipitation or tolerate its stability if it was of organic origin. This is because it would be rendered soluble if it encounters medium of high CO_2 activity. The elimination of calcite and the formation of siderite in the non-marine shales suggests a lower pH value, but the activities of Ca^{++} and carbonate species are also important. This also implies that phosphate would be relatively metastable with high pH and becomes more stable with decreasing pH. Another possibility for explaining the higher average P_2O_5 content of the non-marine shales is that detrital contribution is more important as implied by their higher quartz and Zr contents. This, however, fails to explain the highest P_2O_5 content found in the highly enriched siderite shale. Information on this subject is provided by studies on the geochemical trend in some sediments of anoxic environments (Rosenqvist, 1970; Troup et al., 1974; Emerson, 1976; Emerson and Widmer, 1978). Their data show that in the presence of high sulfide activity, the pore waters in the sediments are satured with respect to siderite and vivianite (hydrous ferrous phosphate). These latter minerals were not always positively identified, particularly siderite.

Rosenqvist considered that a high activity of Fe, phosphate and CO_2 promote siderite and vivianite formation; high Ca and increasing pH favour Ca-apatite formation, whereas very low sulfide activity results in iron sulfide formation. These results are substantiated by further elaboration on the same subject (Nriagu, 1972; Nriagu and Dell, 1974). The latter stated that vivianite is unlikely to be formed in sulfide generating anoxic environment unless phosphate activity is very high. It may be envisaged therefore, that high activities of sulfide and Ca would promote iron sulfide and Ca-apatite formation, while their depletion results in the formation of siderite and vivianite. The co-existence of siderite and vivianite and/or the presence of vivianite as inclusion in siderite has been shown to occur in peat deposits which are depleted in sulfate and with 5-7 pH values (Kovalev and Generalova, 1969). According to this information, the high content of P_2O_5 in the siderite rich shales of the present study, may be considered to reflect the decrease of sulfide and Ca activities during their deposition. It also implies high CO_2 and phosphate activities and consequently a lowering of pH values. Because numerous variables are involved during diagenesis of anoxic sediments, minerals may, sometimes, show erratic distribution.

It is interesting to note that in the marine shales of the Tansley Borehole, there are beds with abundant fish remains containing phosphatic nodules (Ramsbottom et al., 1967, p.119). The latter noted the occurrence of apatite in these nodules. The association of Ca-apatite, pyrite, carbonate, opal and uranium is characteristic of phosphorite deposits, accumulated in reducing shallow shelf or gulf environments (D'Anglejan, 1967; Turekian, 1968; Price and Calvert, 1978).

Thus, the distribution of phosphate with respect to diagenetic iron minerals reveals a similar Eh-pH condition prevailed during the accumulation of the Tansley Borehole sediments.

After the pathway of changing physico-chemical conditions has been proposed, it is pertinent to discuss the factors and processes involved. The change in the type of iron mineral from the marine to the non-marine shales could have been influenced by different factors. These are the abundance of organic matter and its type, the availability of dissolved sulfate (salinity) and the concentration of iron compounds and their reactivity. Other factors such as the rate of sedimentation and grain size might have played an important role, but their significance is difficult to infer, due to the involvement of many factors. Presumably the quantity and quality of marine organic matter (see section 7.7.4) control the degree of sulfate conversion to sulfide by sulfate reducing bacteria. The processes involved are described by Zobell (1963, 1964) and Boctor et al. (1976). Sulfide species can be generated by reduction of sulfate from the overlying water or from organic sulfur compounds, but the latter is of minor importance (Zobell, 1963, 1964).

Thus sulfate reduction would result in a decrease in sulfate concentration in the sediment and consequently a concentration gradient is set up, this sulfate diffuses downwards from the overlying water. This decrease of sulfate with depth has been demonstrated in several studies (Berner, 1964; Shishkina, 1964; Bischoff and Ku, 1971, Krom and Sholkovitz, 1978). The latter also noted that sulfate reduction occurs either at the sediment interfaces or within few tens of centimetres below the surface. In such environment the most abundant sulfide species are H_2S and HS^- (Garrels and Naeser, 1958; Berner, 1964). During the deposition of Tansley Borehole marine shale, accumulation of organic matter was high, as indicated by their content of marine fossils. Furthermore, the salinity

was also high and probably accompanied by slow rate of sedimentation. These provide favourable conditions for supplying sulfate and increasing the activity of reduced sulfide species in the sediments. Consequently, reaction with reduced iron results in the formation of iron sulfide. This process continues, depending on the amount of reactive organic matter and the availability of sulfate. After iron sulfide formation the activity of CO_2 is expected to increase and this may react with the remainder of iron to form siderite. On the other hand, this trend may change in the presence of high calcium activity, resulting in calcite precipitation. Such processes of calcite and sulfide immobilisation have been shown to occur in reducing environments (Tikhomirova, 1960; Bischoff and Ku, 1971). Accordingly, this can account for the abundance of pyrite and calcite in the Tansley marine shales, while the former would explain the association of siderite and pyrite in the non-marine shales. Alternatively, the depletion in sulfate (low salinity), decrease in the amount of organic matter and change in its type together with a faster rate of sedimentation may account for the decrease or presence of pyrite in little amounts in the non-marine shales.

However, it is commonly observed that the first iron sulfide to form in reducing environments is FeS, and this has been called hydrotroilite and other names (Berner, 1963, 1964; Zobell, 1963, 1964). The first worker showed that the transformation of FeS to FeS_2 will not occur in the absence of elemental sulfur (S^o). Since this reaction involves electron transfer; equally other pathways are possible and that the former reaction is not the most important at low temperature has been demonstrated by other studies (Skripchenko, 1969; Rickard, 1975). In some cases, this transformation was related to excessively high reducing conditions and sulfur concentration (Skripchenko, 1969). On the other hand, a sufficiently slow rate of deposition and extremely slow rate of reduction have been proposed for this transformation (see Berner, 1964).

The availability of iron can be attributed to various sources (Curtis and Spears, 1968; Bischoff and Ku, 1971; Bischoff et al., 1975; Krom and Scholkovitz, 1978). External sources are ferric oxide and hydroxide sorbed on detrital constituents during transportation which during diagnesis would be redistributed to form the iron diagenetic minerals. The extraction of iron from the structure of clay mineral is another possibility. The importance of organic matter in transporting various elements is important in this respect and its role is outlined elsewhere (page 215). Another possible source is volcanic and this is considered in a later section (page 226).

In summary, it appears that the change in the type of diagenetic iron mineral in the Tansley Borehole sediments was influenced by a change in physico-chemical conditions including salinity, and the quantity and quality of organic matter. In addition, the rate of sedimentation might have been a contributory factor. It also seems that pH plays a more important role than Eh as shown earlier. The coexistence of both pyrite and siderite in some non-marine shales, support the above suggestion. Depending on the amounts of utilisable organic matter and the availability of sulfate, the activity of sulfide could be limited. Where sulfide was available pyrite formed, and in its absence organic matter decomposition results in CO_2 generation, thus favouring siderite formation. The distribution of calcite and phosphate is in accord with the proposed changes in pH. Finally, it can be stated that in ascending from the marine to the non-marine shales, the change in physico-chemical condition was a slight increase in Eh and a lowering of pH. This was probably related to the sediment itself and not the overlying water.

Similar trend of variation in physico-chemical conditions can also be applied to the Mam Tor rocks, if the iron minerals were of diagenetic origin. However the siderite aggregates and the pyritised plant debris, at least in the greywackes and siltstones,have been considered as detrital

(Allen, 1960). Such pyrite has been described from Silurian greywackes, north Wales (Love, 1971). Accordingly, some of the pyrite and siderite in the Mam Tor rocks must have been formed in the shallow parts of the delta and later transported into the deeper part of the Central Pennines Basin.

7.6 Manganese

Correlation analyses (Chapter 4 and 5) showed that MnO relationship with FeO, P_2O_5 and MgO is stronger than that with CaO. This was considered to indicate association with siderite and dolomite (ankerite). The data also indicated that an amount in excess of approximately 500 ppm is related to siderite or dolomite. It follows that Mn immobilisation with pyrite was of little importance. Similar findings were reported by Gad et al (1969) from pyrite nodules which have a content of Mn ranging from 21-340 ppm. In contrast other pyrites were shown to contain up to 1000 ppm Mn (Keith and Degens, 1959). It appears, therefore, that pyrites formed in different sediments have variable concentrations of Mn, characterising the specific geochemical conditions prevailed during diagenesis. This is supported by studies of pyrites in sediments of various ages (Tikhomirova, 1960). Further insight into the processes involved in Mn distribution during diagenesis of sediments is provided by recent works. Several studies have demonstrated that upon shallow burial, a layer of sediment may encounter reducing conditions where dissolution of manganese bearing phases can occur, while pyrite is likely to be formed (Li et al., 1969; Bischoff and Ku, 1971; Robins and Callender, 1975). The concentration of Mn in pore water commonly occurs at the boundary between oxidised and reduced mud layers, and this can migrate upwards by diffusion. Subsequently this Mn is precipitated in a relatively oxidising environment at the sediment-water interface, which explains the high enrichment of such sediments in Mn.

This process, would result in some fractionation of iron from manganese in reducing sediments where sulfate is reduced to sulfide, thus favouring pyrite formation. The separation of manganese from iron has been attributed to the difference in their complexing with organic matter (Krom and Sholkovitz, 1978). The latter concluded that iron is organically bound while Mn is present mainly as soluble inorganic complexes which under reducing conditions migrates upwards into the oxidised surface layer. Similar results have been reached from studies on the Dead Sea and other marine sediments (Nissenbaum, 1977). Most of the above mentioned workers calculations showed that excess Mn in pore water is saturated with respect to $MnCO_3$ in the reduced sediments, although it has not been positively observed. These findings imply that under conditions favourable for iron sulfide formation, Mn will maintain a considerably longer time in solution. This process willgive rise to a variable distribution of iron and manganese.

In the present study, the high increase of Mn content in siderite enriched shales can be related to the diagenetic iron mineral growth outlined in the previous section. It is inferred that a change from pyrite to siderite stability field was accompanied by slight rise in Eh and decrease in pH. Accordingly, it may be reasonable to suggest that during pyrite formation, most of the Mn would have migrated upwards by diffusion towards the relatively less reducing environment at the sediment water interface. Likewise, reducing conditions were also essential for siderite formation, thus other factors have to be considered. The effect of CO_2 concentration seems one of the important factors. Bearing in mind the very high CO_2 activity required for siderite, it is likely that under such conditions, Mn could be incorporated into siderite either as $MnCO_3$ solid solution or as Mn substituting for Fe. Stability diagrams for Mn compounds

at fixed activities of sulfur, shows that the above mentioned Eh-pH conditions, coupled with high concentration of Mn and bicarbonates are readily immobilised as $MnCO_3$ (Hem, 1977). Further support is obtained from the spectrochemical classification of the ligands (anion and cation). This shows that Mn forms a more stable complex with carbonate and phosphate than with S, while Fe complex with S is more stable on the other hand (Mackay and Mackey, 1972, Table 12.15). Moreover the difference in Mn behaviourmay be partly attributed to its MnS structure which is different from that of FeS, together with other complex factors related to sulfides (Evans, 1964). All these factors could imply a limited substitution of Fe by Mn in the pyrite structure. Deer et al. (1966) remarks that in pyrite there is only very limited replacement of Fe by Mn. Thus, it is thought, that during pyrite formation, the larger part of Mn will remain in solution until conditions favourable for siderite are established. On the other hand, Mn substitution for Ca in calcite is also limited, due to differences in their ionic radii, being 0.8Å and 0.99Å respectively. Comparison with Fe^{2+} (0.76Å) makes its substitution much easier. The evidence provided by manganese distribution therefore follows the proposed trend for siderite and phosphate. On the same ground, the enrichment of dolomite (ankerite) by Mn seems also likely, based on structural similarities rather than Eh-pH conditions. This would explain the high content of Mn in the dolomite concerned with in the present study, although it is of epigenetic origin (Smith et al. 1967). However, dolomites of different origin have been shown to contain high amounts of Mn (Spears, 1963; Deer et al., 1966; Barber, 1974; Deurer et al. 1978). In this work it seems that Mn follows the general pathway proposed for siderite formation.

The origin of manganese can be ascribed largely to association with Fe-Mn hydroxides and oxides which act as scavenger for Mn in solution (Hem 1977). In addition adsorption on organic matter and clay minerals or

even complexing with organic compounds are also important in this respect (see page 215). This association is modified during diagenesis which results in its redistribution, due to the influence of the above mentioned factors. This process will give rise to fractionation of iron and manganese in the different bearing phases.

7.7 Causes of Trace Element Enrichment

A knowledge of the reasons behind element enrichment is important to studies of sedimentary rocks, because this is related to the depositional environment and the chemical processes involved in transporting and concentrating the various elements. The environment may vary in salinity as well as organic productivity both of which may influence Eh-pH conditions in the water and at or near the sediment-water interface. In the following sections, the role of organic matter of different origins, syngenetic minerals and clay minerals will be considered, and emphasis is placed on organic matter and its relation to trace elements. The above constituents are present in both marine and non-marine shales, but in variable proportions and some of the elements associated with them are characteristically different in their amounts. Accordingly, this brief review of the processes involved is pertinent to the problems of the present study.

7.7.1 Distribution of Organic Matter

The distribution of organic matter and its decomposition products has been described by many workers (quoted in Manskaya and Drozdova, 1968). Some of them considered that most of the dead planktons and benthos are the primary source of organic matter in the marine environments. The subsequent decomposition, due to oxidation and bacterial action, occur in the upper strata of the oceans, and during accumulation on the sea floor. Other workers indicated that decomposition is sometimes

influenced by the size of the plankton. Large size (1 mm diameter) reached maximum depth, while smaller sizes showed variable decomposition. Nazarkin (1960) studied the distribution of organic matter (living organisms and their decomposition products) in the Barents, Caspian and the Black Seas. He demonstrated that accumulation of organic matter in the marine sediments is controlled by the biological productivity, the depth and size of the basin and the rate of sediment accumulation. The first factor played a decisive role in the different basins, followed by the depth factor.

In large basins, however, the concentration of organic matter in marine sediments is high in shallow areas and drops in a seaward direction (Strachov, in Manskaya and Drozdova, 1968). This is supported by other studies (Hallam, 1967). The latter substantiated some of the above mentioned factors in affecting organic matter distribution and attributed the high concentration to upwelling of nutrients in the shallow waters. The organic matter content was found to be highest in fine grained sediments laid down in anaerobic waters, specifically the deeper parts of near shore basins partly isolated from circulation by sills. He noted, however, that only small fractions of the planktonic organic matter is preserved, in the sediments, while a significant proportion is supplied by detritus from land and benthonic algae. Similar studies on lakes or bays, also showed the sympathetic variation of organic matter and clays which are concnetrated in the deeper part (>50 ft.) due to high phytoplankton productivity (Schoettle and Friedman, 1973; Blocker et al., 1975). Following these lines of evidence, it can be suggested that the content of organic matter reaches its highest values in shallow water environments where plankton producvitity is appreciable. Anoxic conditions is an important factor in preserving or causing a slower decomposition of the organic matter.

7.7.2 Interaction of Organic Matter and Trace Elements

The association or enrichment of trace elements in carbonaceous shales has been widely reported (Davidson and Lakin, 1961, 1962; Krauskopf, 1955; Keith and Degens, 1959; Wedepohl, 1967; Blocker et al., 1975). In some of these cases the accumulation of trace elements has resulted in metalliferous carbonaceous shales. Such enrichment of trace elements attracted the attention of many workers who studied the interaction of metal-organic matter complexes (chelation), specifically the humic fraction which forms the major part of organic matter in sediments. The humic acids consist of polymerised carbon connected to which are side chains which carry various functional groups or ligands (Swain, 1970; Jackson et al., 1978). It is these functional groups (hydroxyl, carboxyl, etc.) which determine thereactivity of humic acids towards metals, or other organic compounds and sediments. The ligands make them behave as negatively charged species and subsequent interaction result in neutralisation, of this charge. Initially this leads to dissolution of trace elements from the original bearing phases, and upon saturation of humic substances with metal leads to flocculation and co-precipitation of metals. Mechanism by which metallic ions, in solution, interact with soluble, colloidal or particulate matter may range from physical adsorption to chemisorption and these have been discussed by several workers (Krauskopf, 1955; Degens, 1965; Jackson et al. 1978). The latter also reviewed the most important aspects of organic matter. In the following review the interaction of metals with organic matter will be briefly described. Rashid (1974) studied the absorption of metals on humic acids isolated from marine sediments and peat. At pH 7 and in the presence of equal amounts of Co, Mn, Cu, Ni and Zn, in reacting solution, effective absorption of various metals was achieved

but that of Cu was preferentially higher, due to chelation, cation exchange and surface adsorption. Similar results were obtained in treating the humic acids separated from the peat with metals solution. Treating the humic acids from the peat with sea water, absorption was limited to Zn. This was attributed to undersaturation of sea water for transitional metals and supersaturation with alkali and alkaline earth metals. From this, it would appear that these elements should be relatively concentrated in sea water, in order for effective absorption to take place. Ferguson and Bubela (1974) demonstrated that a significant proportion of Cu, Pb and Zn is removed from solution by absorption onto the particular organic matter. The presence of Na and Mg in solution reduced the absorption of Zn, but that of Pb and Cu was appreciable, even in strong brines. Metal saturation values indicated that particular organic matter could remove sufficient amounts of metals to form an ore deposit if organic matter is abundant. This may be approached only in solutions whose metal concentrations were at least twice that of sea water. This suggests that in sea water selective enrichment of metals could take place. Fraser (1961) concluded that Cu, in swampy environment, is bound to organic matter, forming chelate compound. At high pH Cu salt was precipitated during the summer, while through the autumn and spring seasons, this compound was not observed. Precipitation was attributed to the mobility of carbonate ions in equilibrium with Cu at high pH. It follows then that pH plays an important role in metal redistribution and precipitation. The interaction of iron with marine humic acids which is relevant to other metals has been demonstrated from the Narragansett Bay sediments (Picard and Felbeck, 1976). Their results indicated that the humic fraction strongly influenced or involved in the transportation and accumulation of iron in the Bay sediments.

The humic acid/iron ratio was shown to be the effective parameter in regulating the mobilisation and precipitation. An increase in the ratio is accompanied by increasing solubility of iron, forming metallo-organic complexes. A decrease in the percentage of soluble iron and acid result when increasing amount of iron was added to a constant proportion of humic acid. Eventually, saturation of humic acid with iron caused the precipitation of complexes, due to charge reduction on the humic acid. It seems, therefore, the concentration of different reacting species also plays a significant role in metal enrichment. The role of humic acids as solvents in the weathering of minerals has also been studied. Baker (1973) indicated that metal humates resulting from organic weathering exhibits low solubility in water, thus reducing metal solubility. When humic acids were present, the insoluble humates were rendered soluble. The presence of inorganic species in aqueous solution, however, promoted the coagulation of humic complexes. In a similar study, Singer and Navrot (1976) showed that humic acids extracted metals from basalt in the following sequence: Cu > Zn > Mn > Cr > Co > Ni > Al > Fe > Mg > Ca. They also considered that these complexes may have an important role in providing micro-nutrients. The association of V. Mo and Cr with organic matter has been described by Szalay and Szilagyi (1967) and Szilagyi (1971). The first workers performed experiments under conditions similar to those of natural environments. It was concluded that V was reduced by humic acids, resulting in V concentration with an enrichment factor about 50,000:1. In earlier studies it was demonstrated that U is similar to V and this would explain their enrichment in coals and carbonaceous shales. The enrichment was related to the reducing capacity of organic matter of the soluble anionic metal species to exchangeable cation which

may be absorbed by organic matter. Studies on mobilisation, concentration and accumulation of metals by organic matter, however, has demonstrated that organic compounds characterised by different functional groups may either show high or low reactivity towards metals (Rashid, 1972). The latter also noted that coagulation of humic acid occurs with high concentration of organic matter. Guy et al. (in Jackson et al., 1978) results indicated that at pH 6 Cu was distributed equally as dissolved metal-organic complexes and adsorped on particulate organic matter. Below pH 6-3.8 the organic complexes were largely present as uncomplexed or free species.

From this information, it seems that metallorganic matter interaction is a very complex process. In the first place, organic acids interaction result in metallorganic complexes and upon saturation they may develop colloidal properties. Subsequently it could be adsorbed on inorganic species or other organic species, or particulate matter which, with time, lead to their accumulation. On the other hand, metals may be initially associated with insoluble humates and other compounds but subsequent reduction by humic acids would render them soluble and be incorporated with inorganic compounds. Physico-chemical conditions play an important role in solubilisation of elements together with the relative concentration of the participating reactants. Concentration of elements in the organic fraction is also dependent on the composition of the organic compound involved in the reaction. It also seems that mobilisation of elements by organic acids is sometimes a selective process. All of these processes, from the geochemical point of view, could lead to the enrichment of metals in carbonaceous sediments.

7.7.3 Influence of Inorganic Compounds and Clays

The presence of sulfides, carbonates and clays may affect the absorption behaviour of metals. Rashid and Leonard (1973) investigated the pathway of solution-precipitation of various metal carbonates and sulphides to which a solution of Cu, Ni, Mn and Fe was added gradually. Each system was treated in the presence of humic acid and in its absence. The content of metals was recorded at a point to yield their precipitates as carbonates, sulphides and hydroxides. It was found that the presence of humic acid enhanced the solubilities of both carbonates and sulphide at pH 8.5, in the order Ni > Cu > Mn > Fe. The solubility of metal sulphides was generally lower than that of carbonates, apart from Mn and Cu which were highly solubilized. For the hydroxide, the magnitude of solubility was much lower than that for carbonates and sulphides. It was, however, the pH was not adjusted and varied from 10.7 to 3.0. The implication of these results is that in anoxic basin of reduced sediments favourable for sulphide formation, in the presence of organic matter, the amount of metals must be high to cause precipitation.

Another point is that sulphides and carbonates would compete with the humic acid complexes for metals. Gardner (1974) carried out studies on sea water in which the relative quantities of organic and inorganic ligands are typical of sulphide-rich (anoxic) marine waters. The organic acids used were amino acid and hydrocarboxylic. His analysis indicated that bisulphide and polysulphide complexes strongly influenced trace element solubility, but not the organic acids. He, however, suggested that other organic acids (humic acids) could be important in trace element mobility. The association of metals with inorganic ligands is substantiated by studies on the Dea Sea (Nissenbaum,

1977). The latter observed that solution-precipitation of minor and trace elements is influenced largely by chlorides and sulphides, respectively. Saxby (1973) simulated artificially diagenetic reaction occurring in sediments under reducing conditions. He found that about 90% of the metal-organic complexes are converted to metal sulphide, particularly pyrite.

Bondarenko (in: Jackson et al., 1978) found that at weakly acid pH, Cu fulvates (fulvic acid complexes) were more stable in solution, whereas Cu humates (humic acid complexes) were more stable at neutral and weakly alkaline pH. The presence of divalent cations and H_2S, in artificial sea water, caused precipitation or marked decrease in the stability of Cu complexes. It follows then that there is a competition for metals by organic and inorganic species. The organic complexes may also be adsorbed or co-precipitated with sulphide. The interaction of organic matter with clay minerals may also be important process in metal absorption. Schnitzer and Kodama (1972) studied the reaction of fulvic acid with Cu adsorbed on montmorillonite surface. They observed that fulvic acid can interact with Cu, but this decreased with increasing pH. In their earlier work they showed that these complexes are soluble in water if the molear metal/fulvic acid ratio is 1:1 or less, but if higher, the complexes become insoluble. This might lead to co-precipitation of metals with organic matter and/or clay minerals. It is important to note that organic acids reactivities vary depending on its type, the pH and amount of organic matter (Jackson et al. 1978). This information reveals the great complexity of various interactions. Metals may interact with organic acids forming complexes and upon increasing concentration may coagulate (colloidal) or adsorbed on clay mineral surfaces. On the other hand, sulphides, organic matter and clay minerals may compete for metals.

In applying these ideas to sediments, trace elements may show strong or no correlation with either sulphides or clay minerals and organic matter, depending on the behaviour of various elements and their affinity towards one or the other, and the pH of the medium.

7.7.4 Type and Composition of Organic Matter

The organic matter in sedimentary rocks may consist largely either or biological or vegetal substances. An important variable is the proportion of marine to terrestrial organic matter (Philippi, 1974). It must be noted, however, that organic substances of plant differ from those of plankton organic matter, and also differ in their chemical character and in the content of various organic compounds (Degens, 1965; Manskaya and Drozdova, 1968; Philippi, 1974). Vegetal organic matter forms lignite and carbonaceous plant remains which consist of lignin and cellulose with small amounts of protein, while marine organic matter is rich in protein, amino acid, lipid and fatty constituents with minor amounts of lignin and cellulose. In addition to these inherent differences, the composition of organic matter also depends on its environment of deposition (Philippi, 1974; Powell et al., 1976). It follows, therefore, that organic matter of different origins will vary in composition and the content of the various decomposition products.

Regardless of origin, organic matter in both marine and non-marine sediments, is the result of chemical and biochemical transformation of their decomposition products. The final products show similarities in their types, but may have pronounced difference in their compositions and contents (Manskaya and Drozdova, 1968; Swain, 1970; Jackson et al., 1978). These are: (1) hydrocarbon compounds; (2) amino acids and their derivatives; (3) carbohydrates; (4) heteroaromatic compounds; (5) humic compounds (humic acids, fulvic acids and humates). The last are secondary products

and result from biochemical transformation of a variety of the above mentioned organic compounds, and also constitute the larger part of organic matter in soil, peat and sediments. Reference has already been made to the reactive properties of these humic compounds towards metals, which leads to their enrichment. Such association of organic matter and high metal content can occur in nature as peat, coal, petroleum, non-marine and marine carbonaceous shales (Razdorozhnyy, 1968; Manskaya et al., 1968; Manskaya and Drozdova, 1968; Boychenko et al., 1968; Kovalev and Generalova, 1969). In the non-marine environments, elements may be concentrated by the plants or their decomposition products.

On the basis of these lines of evidence, it is clear that metal enrichment can occur in both marine and non-marine environments, but in the latter case enrichments are commonly associated with brackish environments (Swain, 1970). On the other hand, in many sedimentary sequences containing marine and non-marine shales, metals are always present in higher amounts in the marine part, such as the case of the Tansley Borehole sediments concerned with in the present study, or those reported by other workers (Keith and Degens, 1959; Tourtelot, 1964). The first workers, related these differences to the origin and composition of the organic matter in the marine and fresh water shales. The latter worker also attributed the enrichment of metals to the abundance of marine organic matter and its importance in concentrating trace elements. He then stated that because the organic matter in both non-marine and marine shales are coaly plant remains and humic compound, both terrestrial origin, sorption properties were advocated to be the cause of enrichment of metals in the marine organic matter. Such processes played an important role as these organic compounds moved from the relatively dilute waters of the non-marine enrivonment to the relatively concentrated water of the marine environment, with time as the next important factor.

Although enrichment of metals occurs in coal deposits, the environments in which they accumulated have often been described as brackish lacustrine, swampy or bogs, lakes, lagoons (Razdorozhnyy, 1968; Swain, 1970). In such environments, seasonal variation may result in high salinities, possibly even more than normal sea water salinities (Picard and High, 1972; Heckel, 1972). Thus they are similar to a semi-restricted, reducing environment in this respect. More convincing evidence is indicated by the study of peat bog iron (Kovalev and Generalova, 1969). They investigated the distribution of iron in high moor, intermediate and low moor bogs, with the amount of material introduced from the outside decreasing from the first to the last. Their data indicated that iron is highly abundant in the lower moor bog in which reducing conditions prevailed, due to decomposition of organic matter. In this same bog the content of HCO_3, Mg, Co, K + Na are highly enriched and to a lesser extent Cl. Accordingly it can be assumed that water salinity plays a significant part in element concentration.

Another important variable is the composition of organic matter. Powell et al., (1976) studied the variation in the distribution and type of organic matter in cyclothemic Carboniferous sediments, Northern England, and also in a marine band from the south-east Midland Coalfield. It was found that plant organic matter in the East-Midland Marine band decrease from the low to the high salinity shales. Similarly, the marine shales are characterised by highly soluble or extractable organic matter and lighter hydrocarbon as compared to the non-marine shales. The ratio of saturated/aromatic hydrocarbons showed maximum decrease in the highly saline marine shales. They attributed these differences to the source of organic material, and partly to the depositional environments. Philippi (1974) showed that the molecular weight of organic compounds from plants

is considerably higher than that originated from marine organic matter. Khaylov (1968) stated that humus compounds in sea water are different from that in soil and fresh water humus, in that lighter molecular weight humic acids are more abundant in the marine organic matter.

This is supported by studies on humic compounds relationship with salinity (MacFarlane, 1978). The latter found that, from freshwater of the river to the salt water of the marine environment, the high molecular weight fractions of humic substance, which are low in reactive functional groups, would precipitate faster with increasing salinity than low molecular weight fractions which are rich in reactive functional groups, and thus resist flocculation. The higher proportions of the low molecular weight and high aromatic compounds in the organic fraction of the marine environment (Manskaya et al., 1968) would favour high reactivity with metal (Jackson et al., 1978). The latter also stated that humus from lignite (plant) is highly condensed and has few functional groups, which makes it less reactive towards metals. The influence of salinity on the structure of organic matter has been shown by the study of hydrocarbon (Hunt, in Degens, 1965). With increasing salinity the structure changes to aromatic type. Further elaboration on the same subject indicated that progressively more saline (alkaline) water is accompanied by increase in H_2S content (Swain, 1970, p.160). The occurrence of unsaturated aromatic compounds was found to enhance the reactivity of oil towards metals (Vinogradov, in Manskaya and Drozdova, 1968).

Following these lines of evidence, it may be stated that the type of organic matter and the depositional environment in which it is accumulated and underwent diagenesis are the most important factors in controlling the enrichment of elements. In addition, the amount of organic matter also seems to be of great importance in this respect. Moreover, time may be considered a significant factor in promoting organic matter reaction with metals.

However, this brief review is a very simplified picture of the various paths leading to the formation of organic matter in nature. The transformation of organic matter is very complex, depending on its original composition, the physico-chemical conditions and the biochemical reactions that result in its decomposition to various compounds. Furthermore, the role of these latter components of the organic matter is extremely large. Nevertheless, depending on the particular importance of either plant or animal organic matter, there may be a variation in the organic constituents of sedimentary rocks.

7.7.5 Origin of Metal Enriched Sediments

The origin of increased metal contents in oceanic sediments is controversial, and it has been attributed to various sources which are accompanied, sometimes, by clear evidence whereas in other instances evidence is not clear. Some workers consider the source to be terrigenous and elements are carried in suspension or solution which are later incorporated in the sediments. The processes involved are those mentioned earlier and involve organic matter, clay minerals and Fe-Mn hydroxide interaction with metals in sea water. Such processes have been demonstrated tooccur during mixing of river-sea waters (Sholkovitz, 1976) or under marine conditions (Turekian and Imbrie, 1966; Bischoff et al., 1975). Other studies, however such as that of the modern sediments of the Black Sea, demonstrate that elements distribution is not uniform and depends on the manner of transportation (Glagoleva, 1961). It was shown that when suspension is dominant process, concentration of metals occur in a localised coastal zone, while the role of solution becomes more important in seaward direction resulting in pelagic sediment enrichment. This process, by itself, can explain metals enrichment in marine sediments. While this undoubtedly is a common process, the importance of minor and trace elements

from biological origin has been taken into account to explain the enrichment of marine sediments (Bostrom et al., 1974, 1978; Moor and Bostrom, 1978). The latter stated that metal enrichment can only be explained by admixture of biological and detrital origin. It was also shown that high productivities of marine organisms, which displayed little variation in elemental composition in both the Pacific and Atlantic Oceans, occur close to shallow water areas. Similar studies on water columns in the Atlantic and Pacific Oceans indicated the involvement of metals in the biochemical cycle (Sclater et al., 1976). Thus it appears that at least in part some contribution of metals is provided by biological matter. According to this information the chemistry of marine sediments could show a wide variation in space and time reflecting or recording conditions in the depositional environment.

In recent years, however, the enrichment of deep sea sediments with metals has received considerable attention. These sediments are largely found near active volcanic areas, as metalliferous deposits in the East Pacific (Piper, 1973; Cornan, 1976; Froelich et al., 1977); South Eastern Pacific (Dymond and Corliss, 1977); Equatorial East Pacific (Bostrom, 1970; Sayles and Bischoff, 1973); Equatorial Atlantic (Bonatti et al. 1978); Mid Atlantic Ridge (Humphris and Thomson, 1978); Red Sea (Brockampet al., 1978), or as in the Afar Rift, Ethiopian Plateau (Bonatti, et al., 1972). The association with volcanic rocks led to the suggestion that these deposits formed, primarily, as a result of metal precipitation due to volcanic emanations or hydrothermal solution that formed by sea water reaction with the volcanic rocks. The leaching of metals by hydrothermal sea water reaction with basalt has been experimentally demonstrated to be an effectiveprocess in metalliferous sediment formation (Seyfried and Bischoff, 1977; see also page 167). One aspect common to most of the above mentioned studies, is that hydrothermal Fe-Mn phases are converted

to Fe-Mn hydroxides, due to cooling by sea water, and these act as scavengers for elements released by the volcanic source or those already present in sea waters. Goethite and Fe-rich smectite are commonly found in such deposits. On the other hand, metal enrichment may be associated with the hydrothermally formed amorphous and crystalline sulphide phases, which in turn may be converted to Fe-Mn hydroxides. The formation of sulphides and enrichment in metals has been described from submarine basalt, due to quenching of the hot volcanic rocks on the sea floor (Desborough et al., 1968; Moore and Calk, 1971; Moore and Fabbi, 1971). Despite these Fe-Mn hydroxides or sulphides of hydrothermal origin, the association of pyrite with organic matter has been demonstrated in the Red Sea sediments (Saxby, 1972). The latter found that in some areas pyrite formation is prinicpally a non-biological process, whereas in other areas, in sediments containing up to 1% organic matter, sulphate reducing bacteria plays a dominant role. It can be safely suggested, therefore that under reducing conditions, Fe-Mn oxide of hydrothermal origin may be converted through normal diagenesis to metal sulphides. However, hydrothermal metal enrichment is significant at or near the site of the volcanic rocks and their importance decrease in moving away from these sites, where detrital, biogeneous and hydrogeneous contribution becomes relatively more important (Bostrom et al., 1973; Dymond et al., 1977). Nevertheless, distal migration of hydrothermal elements may also contribute to the content of sediment derived largely from detrital source.

It is apparent from these studies that volcanic exhalation is capable of explaining the high concentration of elements in the pelagic sediments. The application of this view as a general rule has been disputed by Strakhov (1976) who suggested metals of detrital origin are carried far into the pelagic areas of the oceans where it is enriched in muds. In

contrast, the exhalative-sedimentary theory is held by Oftedahl (1958). Such controversy also exists about metal enrichment in ancient deposits, such as the marly shales of North West Germany (see Krauskopf, 1955; Wedepohl, 1967) which contain an abnormal concentration of metals, particularly in the shallower parts of the ancient basin.

From the preceeding discussion, some generalisation may be made about the environment in which metal concentration is most likely. Detrital sedimentation may result in metal enrichment in near shore areas which are rich in organic matter and terrigeneous sediments. The other possibility is that normal sedimentation may lead to concentration of metals in pelagic and partly restricted shallow areas in which biological productivity is very high that their remains are incorporated in the sediments before complete decomposition. The last possibility is the hydrothermal or volcanic exhalation which produce locally high enrichment of metals. However, differentiation of these sources may be possible in studies covering wide areas in which changing physico-chemical, biological, hydrological conditions and physiography of the basin, together with the processes involed are clearly defined. On the other hand, establishing the importance of any one source in localised areas where different processes are involved is very difficult if not impossible.

7.8 The Namurian Sediments

7.8.1 Tansley Borehole Shales

In the Tansley Borehole, the sequence consists of marine and non-marine shales. Trace element data indicated that Ni, V, Cu, Pb, Zn and Sr are enriched in the marine shales. In contrast Zr and Mn are present in higher amounts in the non-marine shales. The rest of the elements showed no significant variations in their contents between the two groups of shales. The content of Sr is influenced by calcite which is abundant in the marine shales.

According to these data and in the light of the aforementioned review of organic matter, it is interesting to see the causes for trace element enrichment in the marine shales. The following lines of evidence are important in this respect:

1. The lateral variation in the thickness of the Namurian sequence in the Central Pennine Basin (see Chapter 1) demonstrates clearly that the condensed sequence of the Tansley Borehole was laid down in shallow water, near the Derbyshire Block. Similarly, the vertical variation in lithology in the Tansley Borehole sediments, proved that the marine shales were deposited in the deeper part of this shallow water area.

2. The marine shales are identified by the abundance of marine fossils in them. This suggests that high productivity existed during their deposition. The effect of this, coupled with the relatively shallow depth of water led to the accumulation of abundant marine organic matter. In contrast, the non-marine shales are characterised by the presence of plant fragments which suggest vegetal origin. It is clear, therefore that there is difference in the type of organic matter in both groups.

3. Paleontological evidence suggested that the transition from marine to non-marine shales is a reflection of decreasing salinity. This is supported by trace element data obtained during the present study. It seems also logical to postulate that elements must have been abundant in the marine evironment to provide nutrients for the marine organisms, whereas their depletion inhibited or did not tolerate life in the non-marine environment.

4. The amount of organic matter in the marine shales was found to be nearly twice that of the non-marine shales. In addition pyrite is relatively

abundant in the marine shales. This demonstrates that the latter were deposited under reducing conditions in a relatively restricted sector or gulf of the Central Pennine Basin.

5. The higherconcentration of Zr in the non-marine shales may be considered to reflect the faster accumulation rate of these shales. It also indicates that these shales are more diluted by detrital influex.

Differences in the composition of marine and non-marine organic matter are to be expected. Similarly, their decomposition products may be alike but wide variations in their composition could have existed. As indicated previously the marine organic compounds may exhibit high reactivity towards metals in solution, adsorbed on suspended materials or even in the sediments. Under reducing conditions, the decomposition of organic matter before its burial would lead to slow diagenetic process affecting both the sediments and pore water (Dryssen and Hallberg, 1979). Likewise bacterial decomposition of organic matter can increase the pH in many ways, including sulphate reduction (Zobell, 1964). Accordingly, the conditions during the deposition of marine shales, in the present study, would be reducing and alkaline. The latter are the most favourable conditions for the formation of metallorganic complexes, on large scale. Taking into account the higher content of organic matter, in the marine shales, its decomposition products would have been more abundant. These include organic acids and insoluble particulate matter. The first interact with metals in solution while the latter adsorb metals. Upon saturation, the soluble metal-organic complexes could have been rendered unstable, causing their precipitation. Another possibility is that these metal-organic complexes could be adsorbed onto the less reactive, insoluble organic substances or clay minerals. On the other hand, iron sulphides under these favourable conditions are also formed.

Because FeS by its own role is a very good sorbent, this would result in a direct competition for metals. Thus, depending on the behaviour of particular metal may be associated with pyrite and/or organic matter. It is also, perhaps, possible that metal-organic complexes are co-precipitated with the iron sulphides. It follows then, that metals are mostly associated with pyrite, organic matter and less so with clay minerals.

It must be noted,however, that under alkaline conditions calcium carbonate is formed (Zobell,1964) and Sr is most likely to be incorporated in it, due to the ease it enters the calcite structure. Moreover $CaCO_3$ may adsorb metals and thus co-precipitate them (see references in Jackson et al., 1978). This results in further complication and variable concentrations of metals in the different sorbent compounds.

It is also important to note, that the proposed high salinity may affect the decomposition products of organic matter; resulting in more reactive compounds, and also provide the required metals. In a similar way, the slower rate of accumulation of the marine shales, coupled with the influence of organic matter decomposition would prolong the time necessary for reactions. Generally, all of these factors favour the enrichment of metals in the marine shales.

Assuming that conditions during the deposition of non-marine shales were the same and also the decomposition products of plant remains were similar, except the depletion of water in sulphate, then it is clear that the amount of organic matter would account for the decreased metal enrichment. On the other hand, the absence or presence in small amounts of pyrite and calcite in the non-marine shales, suggests that conditions were less alkaline and reducing. The abundance of siderite in them indicates that CO_2 production from the decomposition of organic matter, at least partly, would account for the decreased pH.

Under these conditions, leaching of metals, due to inorganic metal complexes formation, may be postulated to take place which results in migration of metals. On the contrary, the conditions are still reducing and most metals are likely to be present as metal-organic complexes, due to their reactivities with organic matter. Also, metals may be adsorbed on particulate matter, or incorporated in carbonates, oxides and hydroxides. The solubility of metal-organic complexes is much higher with increasing pH and only at a very low pH do free ions exist (see Jackson et al., 1978). Thus it can be assumed that metal enrichment by organic matter is higher with increasing pH. The process of leaching, in near shore environment, has been invoked to explain the depletion of metal in organic matter, in the Namurian argillites of Ireland (Sullaiman, 1972; see Chapter 1). In the latter case, however, the organic matter in both the basin and near-shore facies were spores and plant remains, but it was more abundant in the latter. Even in such cases, difference in the composition of organic matter may be slight but still exist, as demonstrated by Powell et al. (1976; see previous section).

Another important aspect in the present study, is that the proposed salinity decrease during the deposition of the non-marine shales, could have played a significant role in metal enrichment. In addition, their faster rate of accumulation might have allowed less time for the interaction of organic matter with sea water. Comparing a non-marine shale which contains 9.05% organic matterwith a marine shale containing 4.33% organic matter, indicated that the marine organic matter is enriched in V, Zn, Cu and Pb. This partly demonstrates the important role of the type of organic matter played in concentrating metals. In summary, it is thought that the amount of organic matter and its type together with the availability of metals and Eh-pH conditions controlled the distribution of trace elements in the marine and non-marine shales of the Tansley Borehole. In the light of

such complexities, it is not surprising that attempts to solve relationships of metals with organic matter, sulphides and clays are usually tentative.

7.8.2 Mam Tor Shales

Trace element analyses revealed that these shales have a content similar to that of the Tansley non-marine shales, except Co, Cr and Sr which proved to be the best discriminators in distinguishing between the two shale groups. On the other hand, comparison with the Tansley marine shales showed that the Mam Tor shales were depleted in the contents of Ni, Co, V, Zn, Cu, Sr and Pb, while Zr showed the reverse trend. Mineralogical composition demonstrated that the contents of organic matter, pyrite and calcite are much higher in the Tansley marine shales. To explain the reasons behind this difference in trace element contents, it is relevant to discuss the factors influencing the deposition of these shales. The Mam Tor shales were deposited in marine environment and in the deeper part of the Mid-Pennine Basin, as shown by the lateral thickness variation of the Namurian sequence (Chapter 1). Lithological description also showed that size gradation from turbiditic sandstones through silty shales to shales were characteristic of the Mam Tor Beds. In addition, mineralogical data obtained from the present study indicated that compositional gradation within the same layer is not restricted to the underlying sandstone but extends to the overlying shales (see Chapter 4). It follows then that these shales were deposited by the same turbidity current and do not represent a pelagic or hemipelagic mud deposit which lack such compositional gradation. Moreover, these shales were found, occasionally, to bear pelecypods but no goniatite, and the silty shales were rich in detrital, small fragments of carbonised and pyritised plant remains which are concentrated on the bedding planes (Allen, 1960). These are characteristics of mud turbidite and were shown to be an important property, in distinguishing them from pelagic or hemipelagic muds, by recent

studies on turbiditic sequence in the western Mediterranean Sea (Rupke and Stanley, 1974). It was demonstrated that mud turbidites were characterised by a compositional gradation which is a continuation of that in sand-silt layers, high content of detrital minerals, abundance of plant fragments and only a small amount of marine organic remains. The hemipelagic mud layer contained higher amounts of clay with dominant shelly marine remains and lack of compositional gradation. They concluded that the sand-silt-mud unit was deposited from a single turbidity current. The mud turbidite was suggested to represent the distal portion of a turbidite, deposited by slowly moving, less dense tail of a normal high density turbidity current. Alternatively, it could be due to low density turbidity current which transported fine grained sediments from the shelf break area. According to this information and the data from the present study, the origin of the Mam Tor shales as mud turbidite seems to be justified. Its implication points to the importance of the Derbyshire Block which acted as a submarine barrier during the deposition of the Namurian sediments in different sectors of the southern part of the Mid-Pennine Basin. The Mam Tor Shales were deposited in the north-western or northern sector while the Tansley marine shales in the partly protected sector to the south-east (see Chapter 1). Therefore it seems most likely that the Mam Tor shales were deposited in an open marine environment, whereas that of the Tansley marine shales was a partly restricted gulf. In the latter, salinity must have been higher to sustain the growth of marine organisms and promote their productivity at high level. After their death, they accumulated on the gulf floor and subjected to the action of bacterial decay. The effect of this combined probably with a slower rate of sedimentation helped to enhance trace element concentration through the aforementioned processes. In contrast, the continuity of disturbance by successive turbidity currents, in the open marine environment,

inhibited the establishment of suitable conditions for the growth and productivity of marine orgnisms at large scale. These might have also prevented a prolonged interaction of particulate inorganic and organic matter with sea water. The absence or presence of little amounts of pyrite and calcite in the Mam Tor shales, suggests that conditions were not favourable for their formation. Thus, trace element concentration by these constituents was insignificant. On the other hand, the smaller amount of organic matter and its nature (plant remains) could have been a contributory factor in their effectiveness towards interaction with metals, i.e. their low ability to extract elements from sea water. Generally, therefore, it can be inferred that conditions prevailed during the deposition of the Mam Tor shales were not favourable for trace element concentration. In this respect, they resemble the Tansley non-marine shales; thus their similarities in trace element contents, and the type of organic matter. An important aspect emerges from this discussion, the significance of trace element concentrations by the autochthonous marine organisms and/or their decomposition products. The higher amount of marine organic matter, in the Tansley marine shales, has undoubtedly increased the contents of some trace elements through various processes. The results also show that the variations in palaeosalinity as determined by palaeontological methods have a direct influence on the chemistry.

The origin of elements enriched in the Tansley marine shales cannot be solely attributed to marine organic matter and pyrite. This is because part of these elements is undoubtedly contributed by other sources. Trace element data indicated only a slight variation in Rb, Cr, Y and Ba contents in the Tansley marine and non-marine shales, and also the Mam Tor shales. These elements therefore, are essentially contained in the structures of clay minerals and feldspars, thus they are largely of detrital origin. Similarly, the Zr content reflects primarily the abundance of detrital

zircon. Most of the remaining trace elements, in the Tansley non-marine and Mam Tor shales, may be conveniently partitioned into two parts. The first is inherited and the second is sorbed during transportation and after arrival to the basin of deposition. It is difficult, however, to assign a more important role to one or the other. If it is assumed that sorption was of minor importance in the non-marine environment, the larger portion of these trace elements may be considered as inherited in the detrital minerals. Accordingly, the increase of trace element contents in the marine shales above the average amounts present in the non-marine shales, can be attributed to organic matter and pyrite. However, this does not exclude that initially these trace elements, not contained in detrital minerals, were the result of weathering products and subsequent transportation in suspension and solution. Therefore it can be suggested that trace elements in the Namurian sediments are of terrigeneous origin. The uptake of elements by marine organisms and sorption processes during transportation and diagenesis, may be regarded as a factor for concentrating these elements. The extent of this uptake is dependent on flocculation of salinity which could influence the above agents in concentrating trace elements.

Earlier in the discussion the importance of volcanic rocks as a major contributor of trace elements to marine sediments was described. In this respect, it is noteworthy that the Tansley marine shales overlying the Carboniferous limestones, are underlain by the Upper Lava of Matlock. The alteration of this lava is manifested by the occurrence of volcanic mudstones (K-bentonites) which were previously dealt with (see Chapter 5). The likelihood of element leaching during the alteration process cannot be excluded, and evidence obtained from the present study supports this. Although it may be a provisional source, but the occurrence of pyrite reveals further supporting evidence. In the marine shales, pyrite is

associated with high amounts of organic matter, whereas the K-bentonites having insignificant amounts of organic matter contain the highest percent of pyrite. Moreover, comparing trace element contents of both the marine shales and K-bentonites indicated that appreciable amounts of Cu, Pb and V are associated with organic matter. This suggests that pyrite in the K-bentonite has formed by hydrothermal reaction with the lava, while in the marine shales it is a result of normal diagenesis. Studies on pyrite distribution in some areas in the Red Sea demonstrate similar patterns (Saxby, 1972). Consequently, the contribution of elements from this source is most likely, as revealed by the recent studies on the pelagic sediments of the Atlantic and Pacific Oceans. Such a source might have been of minor importance compared to sea water. On the other hand, it could have been initially the reason for increasing salinity during the deposition of the marine shales. Although this may be a speculative view and questionable, this source is likely to supply nutrients which attract marine organisms. Thus the problem becomes similar in many aspects to that of silica, whether of organic origin or inorganic versus volcanic origin (see Hsu and Jenkyns, 1974). The data of the present study cannot resolve these aspects of the problem, but it does indicate that a minor amount of elements could have been of volcanic origin.

CHAPTER 8

General Conclusions

The following conclusions are drawn from the present study:

1. The Mam Tor section consists of alternating sandstones, siltstones and shales. They are considered as turbidites transported by intermittent currents originated on the delta slope to the north. The sandstones represent a fast deposition which is interrupted by the slower accumulation of muds in the deep marine environment (Allen, 1960).

The succession of the Tansley Borehole represents deposition in a deltaic system. The latter is characterised by different subenvironments changing from off-shore marine, through brackish to fresh-water. Litho-logical description indicated the coarsening upwards in grain size from the marine shales through a more silty non-marine shale to siltstone and sandstone. Overlying the latter, are seatearth and carbonaceous non-marine shales. The Namurian succession is underlain by the Visean calcareous shales and limestones which in turn overlie the Upper Lava of Matlock. The Namurian marine shales are characterised by the presence of different faunal phases which are equated with changing palaeosalinity.

2. Petrographic and heavy mineral study was undertaken. The X-ray diffraction method used for the quantification of quartz and feldspar abundances. A method combining the results of X-ray diffraction and normative calculation is employed in the estimation of clay mineral content. Most of the major elements and all the trace elements are determined by X-ray fluorescent spectrometer. FeO measurements are carried out using spectrophotometer and those of Na_2O by atomic-absorption spectrometer.

A total of 161 samples are analysed for major elements of which 88 belong to the Mam Tor rocks and these represent 25 whole rock with 63 of different size fractions; the remaining 73 belong to the Tansley Borehole rocks and include 68 Namurian, 2 Visean and 3 volcanic mudstone samples. A total of 108 samples are analysed for trace elements, 59 belong to the Tansley Borehole rocks and the rest represent determination on the whole rock samples and different size fractions from the Mam Tor rocks.

3. Petrographic work revealed that the Mam Tor sandstones are generally of the greywacke type, whereas the Ashover sandstones are arkosic. They consist of quartz, feldspar, rock fragments, mica and carbonates (calcite, siderite, dolomite). In addition the fine matrix of clay minerals is characteristic of the Mam Tor sandstones. The latter fall in the fine and medium sand grades, while the proportion of the coarser size is higher in the Ashover sandstones. The Mam Tor sandstones are typical turbidites, either fining or coarsening upwards. Authigenic minerals include kaolinite after feldspar and chlorite and iron oxide from biotite alteration. Moreover, replacement of feldspar, particularly orthoclase, by calcite and sericite is common. Both, plagioclase and K-feldspar are present in the Ashover sandstones which also have the highest carbonate content. Heavy minerals present in the sandstones as a whole include zircon, tourmaline, rutile, garnet, epidote, muscovite, biotite, opaque mineral and leucoxene. The heavy mineral fraction does not exceed 1% of the whole rock. The first three minerals are the most abundant in all the size fractions studied, while garnet and epidote are more abundant in the coarser fraction. The source area is believed to be dominantly igneous and metamorphic rocks, with a minor contribution by pre-existing sediments.

4. Major elements and minerals distributions through the Mam Tor rocksare similar. Quartz and plagioclase are abundant in the sandstones and both decrease in the shales. In contrast, the content of clay minerals and elements related to them are higher in the shales. Invariably kaolinite is the most abundant clay mineral, but the content of illite and mixed layer mineral is higher in the shales. The chlorite content is variable and both kaolinite and chlorite are partly of diagenetic origin in the sandstones. The TiO_2 mineral (rutile) is more abundant in the shales than in the sandstones. This pattern of variation in minerals and major elements is substantiated by correlation analysis. The content of siderite is high only in a few cases, while pyrite is present in small amounts or absent.

5. Compositional variation between and within individual sandstone beds is present. This is related to the graded textures characteristic of turbidites. Similar variation is noted from the interbedded shales. This can be attributed to flocculation in the velocity of turbidity currents and distance from the source or shoreline which controlled size sorting during transportation.

6. To provide a supporting evidence, for the abovementioned variation the relationship between the mineralogy, chemistry and grain size was studied. It was found that with decrease in grain size, the contents of SiO_2 and Na_2O decrease with concomittant increase in the elements associated with the clay minerals. This decrease in SiO_2 and Na2O contents is reflected by a decrease in quartz and Na-feldspar peak heights on the X-ray traces. Consequently it is considered that quartz and plagioclase contents vary in a similar way. The illite peak showed a reduction in its height in fractions less than 8μm, and ascribed to poor crystallinity and possibly fine grain size. The persistence of higher peak intensities for kaolinite

and chlorite with decreasing grain size is attributed to coarser grain size; partly as a result of their diagenetic growth. The most consistent increase in major element content with decrease in grain size is that of K_2O. The content of TiO_2 is at a maximum in the 8-16 μm fraction and decrease in the coarser and finer fraction. The SiO_2/Al_2O_3 and TiO_2/Al_2O_3 ratios in general, show a similar pattern of variation and increase with increasing grain size, but the second ratio behaves as such up to the 53 μm fraction and then decreases slightly.

7. Semi-quantitative estimation of clay minerals from the less than 2 μm fraction showed that kaolinite is the most abundant clay mineral. When illite and mixed layer are considered together, this becomes more abundant in the clay fraction of the shales. The abundance of kaolinite in the clay fraction of the sandstones is also indicated by the correlation of SiO_2 and kaolinite. On the otherhand, illite is correlated with K_2O and Al_2O_3 which in turn are correlated with TiO_2 and MgO. The relationship of Fe_2O_3 and chlorite is considered to indicate their association as a result of biotite alteration in the sandstones. The chlorite is inferred to be an iron rich, as revealed by its behaviour on the X-ray traces, and also by semiquantitative estimation of its composition.

8. From the evaluation of crystallographic properties of illite, it is demonstrated that illite is of the 1 Md polytype. The latter is characteristic of the diagenetic zone. Accordingly, there can be only a slight modification of illite through absorption of potassium during transportation and diagenesis.

9. The authigenic growth of kaolinite during diagenesis is promoted by the high permeability and porosity of the sandstones. The alteration of K-feldspar supplied most of the necessary constituents for the formation of kaolinite. A low pH is attained through decomposition of organic

matter, and the proper K/H ratio is maintained by the absorption of K on degraded illite supplied to the depositional site. This process is thought to take place in a relatively closed system.

10. The replacement of detrital constituents in the sandstones by calcite and quartz overgrowths can be attributed to several factors. Firstly, the antipathetic relation between silica and calcium with pH. Silica solubility increases with rising in pH, particularly above 9, while calcite is precipitated and vice versa. However, the effect of temperature and pressure can be an important factor in modifying the pH required, for the solution-precipitation of silica and calcium. The source of calcium may be organic or inorganic, while that of silica is the result of pressure-solution of quartz grains at their contacts, due to compaction.

The alteration of biotite can be envisaged as contemporaneous with that of feldspar, thus probably aided kaolinite formation. The main products after biotite are chlorite and iron oxide. The formation of authigenic minerals is considered to span the early and late stages of diagenesis.

11. Trace element data of bulk rock samples showed the enrichment of shale in most elements, except Zr, Co and Mn. The bimodal distribution of Ni, V, Cr, Cu, Rb, Pb and Ba is shown to be significantly different between the shales and sandstone through a t-test. This is attributed to the abundance of clay minerals in the shales and further support is obtained from trace element data of the clay fractions from sandstones and shales. The high Zr and Co contents of the sandstones are ascribed to a greater detrital contribution from heavy minerals, while the high Mn content is related to siderite, biotite and chlorite. In addition Sr is partly contributed by calcite and Y by heavy minerals.

Evaluation of element/Al_2O_3 ratio, indicated that in the shales these ratios are less variable than in the sandstones.

The relationship between grain size and tracœ element content demonstrated that with decrease in grain size, the contents of Ni, V, Cr, V,Cu, Zn, Rb and Pb increase continuously. The discontinuity is shown by Mn, Co, Zr and Y. The association of most of the former trace elements with clay minerals is substantiated by statistical t-test and correlation analysis. The latter test showed the relationship of illite with V, Cr, Rb, Sr and Ba, while the rest of elements are shared among all the minerals.

12. The distribution of major and trace elements in the shales is considered to reflect association, largely, with detrital clay minerals. The better consistency of element pair ratio of the shales supports such interpretation. On the other hand, diagenesis of the sandstones has not greatly modified the content of trace elements, but it may involve a redistribution of elements. The most noticeable variation is the general increase of Fe_2O_3 content in the clay fraction of the sandstones with increase in the quartz content of bulk sample. Apart from this observation, diagenesis has no significant effect on the chemical composition. The difference in chemical composition between the shales and sandstones is attributed to textural variations. The latter are influenced by the depositional environment and factors operated during transportation and deposition. Obviously, the shales represent accumulation in a deeper part of the basin and also further away from the source or shore-line. Consequently, it implies a reduction in the power of the transporting medium which results in a better sorting of the sediments. The sandstones undoubtedly represent deposition in a shallower part of the basin, nearer to source, which subsequently transported by higher energy turbidity currents into the deep basin, thus the poor sorting and coarser grain size of the sandstones.

13. Mineralogical and chemical studies of the Tansley sediments demonstrated the existence of some important variations in ascending the succession. The quartz and feldspar cotnents increase from the marine to the silty non-marine shales and culminate in the Ashover sandstone. However, the less silty non-marine shales, directly on top of the marine shales, showed no such difference. The average contents of quartz, TiO_2, combined silica, Al_2O_3, FeO, MnO, Na_2O and P_2O_5 are higher in the non-marine than in the marine shales. The latter are characterised by the higher average contents of Fe_2O_3, CaO, SO_3, CO_2 and organic matter. The contents of MgO and K_2O shows little variation between the two groups of shales. Mineralogical variations include the abundance of feldspar and kaolinite in the non-marine shales, to which siderite is also confined. On the other hand, the proportions of illite, pyrite and calcite are higher in the non-marine shales. Illite varies with the proposed salinity change, with the abundance increasing in the marine shales.

This distribution of illite also extends to some non-marine shales interbedded with marine shales in the lower part of the succession. The average content of chlorite is higher in the non-marine shales, thus similar to that of kaolinite. Dolomite (ankerite) is present through the whole succession, but it is more abundant in the marine shales. The highest content of P_2O_5 is associated with the siderite rich shales. Statistical t-test, demonstrated that the distribution of kaolinite, illite, siderite, pyrite and calcite is significantly different in the two groups of shales, in the above mentioned manner. The abundance of specific mineral to distinguish marine from non-marine shales cannot be relied on completely, unless being accompanied by palaeontological evidence. Such a case is typified by the occurrence of seatearth at the top of the succession, in which abundant illite and pyrite are recorded. This important deviation, is ascribed to the process leading to the formation of seatearth.

14. The Namurian succession is underlain by the Visean calcareous shale and limestone which overlie the volcanic mudstone; in turn overlying the Upper Lava of Matlock. The volcanic mudstones show characteristics of K-bentonites. The latter are believed to be the result of submarine alteration of the original lava, due to interaction with seawater. Their mineralogy indicates the abundance of illite-smectite mixed layer as a major clay mineral with a small amount of chlorite. The contents of pyrite and quartz are high, particularly at the top of the K-bentonite. In contrast, the contents of illite-smectite mixed layer and anatase (TiO_2) are higher at the base. Evaluation of the degree of alteration shows CaO and Na_2O as the most mobile element lost during this process, which also resulted in some loss of SiO_2, Al_2O_3, TiO_2, K_2O,MgO and FeO.

During this alteration process it is thought that quartz and pyrite are formed, especially at the top of the K-bentonite. Some of the lost silica is possibly incorporated in the overlying Visean and Namurian calcareous shales. This is indirectly supported by the silicification at this boundary, throughout the Derbyshire area. The alteration of the lava may be attributed to low temperature reaction with the saline sea-water or to a high temperature reaction at the time of lava eruption, or to both in a consecutive manner, i.e. high temperature then low temperature reaction. The presence of the highest amount of pyrite with the smallest content of organic matter in the K-bentonite, is related to high temperature reaction (hydrothermal). Supporting evidence is recorded from other studies.

15. The aforementioned variations in mineralogy and major element chemistry are substantiated by correlation analysis, which idnicated several covering groups at the 95% significance level. The first is quartz and Na_2O suggesting their similar patterns of variation. The second includes combined silica, TiO_2, Al_2O_3, K_2O and H_2O^+, indicating association with clay minerals.

The third is related to pyrite and consists of Fe_2O_3, SO_3 and organic matter. The fourth reflects carbonate association and embraces FeO, MgO, CaO, MnO, P_2O_5 and CO_2. When the marine and non-marine shales are considered separately, different relationships are noted. Quartz and Na_2O correlation is significant in the non-marine shales only, while in the marine shales it is related to illite. A similar reasoning is applicable to K_2O, being partly related to k-feldspar in the non-marine shale. The P_2O_5 is associated with FeO, MgO and MnO in the non-marine shales, whereas in the marine shales it is largely related to CaO.

16. Trace element data shows a similar bimodal distribution for Ni, Co, V, Cr, Zn, Cu, Sr, Pb, Rb and Ba, whereas Y and Zr are not so distributed. Most of these trace elements have a low content in the sandstones and calcareous shales. When the marine and non-marine shales are considered separately, their distinction becomes clear on the basis of some trace elements. The average contents of Ni, V, Cu, Sr and Pb,with a lesser extent Zn, are clearly higher in the marine shales, whereas those of Co, Cr, Rb, Y and Ba are approximately equal in both shale groups, although Cr, Rb and Ba are slightly more abundant in the marine shales. In contrast the average contents of Zr, and Mn, are higher in the non-marine shales. Illite is considered the major host for Cr and Rb, while Ba is contributed by illite and feldspar. Similarly, Sr is shared between calcite and illite, whereas the larger amount of Mn is bound in the siderite and dolomite. Different minerals contribute to the content of Co and Y.

The variation of trace element/Al_2O_3 ratio through the non-marine and marine shales provides further information. Apart from Co, Y, Mn and Zr the other trace elements in the non-marine shales, show a good relationship with clay minerals, particularly illite. This element/Al_2O_3 ratio value becomes higher at the level where the shale is designated as brackish phase and continues through the marine shales. The most striking

feature is the similarity in the variation patterns of Ni, V, Pb, Cu and Sr at the above mentioned level, and so are Cr and Zn, but with less produced change. In contrast Zr shows the opposite variations pattern to the above elements. Undoubtedly this variation is related to enrichment by pyrite, organic matter and calcite, possibly illite as well.

Different faunal phases are recognised in the marine shales and these equated with changing palaeosalinity. It is found that the concentration of some elements do not follow the proposed salinity change, while others do so. In addition, similar faunal phases at different levels in the marine part of the succession show variable concentration of some trace elements. More convincingly, the overall average content of Ni, V, Cu, Pb and Sr show a definite increase from the least saline, through intermediate salinity to a typical saline marine phase.

17. The above mentioned relationships between trace elements and minerals are also indicated by the correlation analysis. The most important associations are Cr, Rb and Ba with K_2O and Al_2O_3; Ni, V, Cu and Pb with Fe_2O_3 and organic matter; Mn and Co with FeO; Sr and CaO; Zr with Na_2O and TiO_2, while Zn and Y are shared with more than one mineral.

More or less a similar relationship between trace elements and mineral are recorded from the K-bentonites. However, an important deviation is observed; the inverse relationship between the content of Zr and the amounts of quartz and pyrite in the K-bentonites. This is different from the same, but sympathetic relationship of Zr with quartz in the over-lying shales. Moreover, comparing the K-bentonites, which have the highest pyrite and lowest organic matter contents, with the marine shales show the enrichment of Pb and Cu and less so Vin the organic matter. This clearly supports the idea of different origins of pyrite, mentioned earlier.

18. Evaluation of the crystallographic properties of illite place the shales in the zone of normal diagenesis. The abundance of illite in the marine shales and kaolinite in the non-marine shales is ascribed to differences of grain size and changing salinity. The first parameter is also considered to be responsible for the higher average content of chlorite in the non-marine shales. The function of high salinity is thought to enhance differential flocculation.

19. The lateral variations in clay mineralogy between the marine shales from Mam Tor and their equivalent in the Tansley Borehole are similar to those encountered between the non-marine and marine shales of the latter locality. Consequently, difference in grain size and salinity change are regarded as the responsible factors.

20. Discriminant function analysis is applied to test the validity of trace elements as environmental discriminators. The most effective and complete separation, between the marine and non-marine shales of the Tansley Borehole, is accomplished using Cu, Sr and Pb. The same statistical test shows that Co, Cr and Sr are good discriminators in differentiating the Mam Tor marine shales from the Tansley non-marine shales. This separation is over-emphasised because the contents of other trace elements are nearly equal in the two groups of shale. This is supported by the classification of the Mam Tor shales as non-marine when tested against the Tansley marine shales.

21. The ratio of a pair of major elements is used to provide a guide to variation in grain size and sorting which are influenced by the rate of sedimentation and distance from source of shoreline. In this respect, the results from petrographic study and chemical data of the various size fractions must be taken into account. The variation of SiO_2/Al_2O_3 and

quartz/combined silica ratios through the Mam Tor section is similar, and both are higher in the sandstones than in the shales. Obviously, it implied a coarser grain size, faster rate of sedimentation and poorer sorting of the sandstones in comparison to the shales. Some silty shales are found to have a higher ratio than the less silty shale. Bearing in mind, the gradation of grain size within a single sandstone or a shale bed or from the sandstone to silty shale; their deposition seems to be connected. It also suggests that the shales are deposited by the tail of turbidity current which deposited the sandstones in the first stage. Evidently, this indicates a reduction in the power of turbidity current in moving away from its source. Accordingly the shales are regarded as turbiditic muds.

The nature of clay minerals is indicated by the variation of Al_2O_3/ combined silica. The latter is shown to be slight, thus a detrital origin for the bulk of clay minerals, particularly in the shales, is suggested. However, diagenesis in the sandstones has imparted some modification and some of them show a higher ratio.

A comparable result is obtained from the SiO_2/Al_2O_3 and quartz/ combined silica ratio variation through the Tansley Borehole succession. The values of these ratios are shown to decrease from the Ashover sandstone, through the silty to the less silty non-marine shales. On the other hand, no such difference is observed between the less silty non-marine and the underlying marine shales. Within the latter, some non-marine shales are interbedded and these show a clear increase in the ratios. Such variation implies a progressive sorting, a decrease in grain size and slowerrate of sedimentation from the sandstones to the least silty non-marine shales. The latter and the marine shales are considered to have a similar history of transportation, but their accumulation in different depositional environments.

An increase in the grain size and rate of sedimentation is responsible for the higher ratios of the non-marine shales interbedded with the marine shales. In contrast, the higher ratios of the calcareous shales at the base of the succession, as it is believed, are ascribed to silicification and so too are the K-bentonites. The Al_2O_3/combined silica ratio, expresses the composition of clay minerals, and show little variation through the two groups of shale. Consequently a detrital origin for the clay minerals is postulated.

Other possible indicators of grain size, sorting and the rate of sedimentation, are titanium, sodium and potassium. Previously, the variation of TiO_2/Al_2O_3 with grain size is shown to be sympathetic with grain size. Rutile is considered to be the TiO_2 bearing phase, and its content is highest in the silt fraction. The TiO_2/Al_2O_3 ratio is found to increase from the shales to the sandstones in both the Mam Tor and the Tansley Borehole rocks. This can be attributed to sorting of the clay minerals and silt size minerals from quartz and also to distance from shoreline. The last factor has imparted a higher TiO_2 content to the Tansley non-marine shales which are deposited nearer to shore.

The ratio of TiO_2/Al_2O_3 is relatively constant in both the non-marine and marine shales of the Tansley Borehole. The higher content of clay minerals in the former can account for such consistency.

The TiO_2 content and TiO_2/Al_2O_3 ratio is much higher in the K-bentonites and this is certainly due to volcanic contribution. Similar conclusions are reached using the Na_2O/K_2O ratio variation. In the Mam Tor rocks, variation in Na_2O content and Na_2O/K_2O ratio is similar to that of quartz and this is indicated by the correlation of Na_2O with quartz and Zr. The Na_2O is assigned to plagioclase whose presence is confirmed by thin section and X-ray diffraction studies. On the other hand, K_2O

is allocated to illite because no other bearing mineral is indicated on the X-ray traces. It follows then that the Na_2O content and Na_2O/K_2O ratio are higher in the sandstone than in the shales.

In the Tansley Borehole rocks, the association of K_2O and Na_2O is rather complicated, due to the presence of plagioclase, K-feldspar and illite. The larger part of Na_2O is associated with albite in the non-marine shales and the sandstones, whereas in the marine shales it is associated with illite. Similarly, K_2O association with K-feldspar is particularly important in the sandstones and it decreases through the silty non-marine shales to the less silty non-marine and marine shales. In the latter an increase in the illite content is a characteristic feature. The Na_2O content and Na_2O/K_2O ratio are found to decrease in a similar manner. These inter-element relationships are supported by correlation analysis. The abovementioned associations of elements and minerals are attributed to decrease in grain sizes, slower rate of sedimentation and a contributory salinity factor. Such an interpretation is not applicable to the lowest Namurian and upper Visean marine, calcareous shales, which contain plagioclase. In these shales the SiO_2/Al_2O_3 ratio is also high while the TiO_2/Al_2O_3 ratio is similar to that of the overlying shales, and secondary silicification is believed to be the cause due to a volcanic contribution. A similar origin is possible for the plagioclase. Alternatively, it is authigenic and resulted from crystallisation of sodium rich connate water. These origins are considered likely, because Na_2O is shown as one of the most depleted elements in the underlying K-bentonites. The latter are characterised by a very low Na_2O/K_2O ratio when compared to the overlying shales. The other possibility, is that these shales are deposited in near shore environments, which received a very fine-grained detritus.

22. The Mg/Al_2O_3 ratio, excluding Mg allocated to carbonates, show a relatively slight variation in the rocks studied, apart from the Mam Tor sandstones. Accordingly, it is postulated that the ratio is fixed during weathering and transportation and sorption is of little importance. The role of Mg-rich solution is indicated by the high Mg/Al_2O_3 ratio in carbonate rich shales.

23. From the aforementioned distribution of diagenetic minerals, the physico-chemical conditions are deduced. The relative trend of variation is a fall in pH and a slight rise in Eh, in ascending the Tansley Borehole succession, excluding the seatearth at the top. The distribution of these diagenetic minerals is controlled not only by changing Eh-pH conditions, but also by the activities (concentration)of the various interacting chemical species. The high activity of sulphate is regarded as a main factor, together with the abundance of marine organic matter, in curtailing the chance of other iron minerals to be formed other than pyrite. The availability of sulfate is probably regulated by changing salinity of the deposition environment. The abundance of pyrite with organic matter in the marine shales to which the marine fauna are confined supports such a relationship. Other factors such as slow rate of sedimentation, finer grain size and a long time, can be important in this respect, but their significance is difficult to infer, due to the involvement of many variables. Depending on the concentration of reducable sulfate and the amount of organic matter, pyrite formation may consume the available sulfate, after which CO_2 concentration increases (rise in pH) and thus allowing siderite to form. The association of a small amount of pyrite with siderite rich shales, makes this a likely possibility. Further supporting evidence, is provided by the distribution of Mn which shows a high enrichment in siderite, and its incorporation is in accord with

the proposed variation in Eh-pH conditions. The latter is related to the sediment-water interface and within a few tens of centimetres below the surface.

The iron required for diagenetic iron minerals can be accounted for by several sources. These include iron oxide films on clay minerals, metallorganic complexes and extraction from within the sediments. In addition the possibility of volcanic contribution is not completely excluded. This is because as mentioned previously, the pyrite in the K-bentonite is most probably of volcanic origin while in the marine shales it is formed through normal diagenetic reactions.

The phosphate and calcite are believed to be largely of organic origin. However, this does not preclude their dissolution and the consequent re-distribution during diagenesis.

Similar variation in physico-chemical condition can be assigned to the Mam Tor rocks which demonstrate that siderite can occur in marine environments. However, these iron minerals were considered of detrital origin, at least in the sandstones and silty shales (Allen, 1960). The origin of dolomite (ankerite) in the Namurian shales is tentatively regarded as epigenetic (Smith et al., 1967), but other modes of genesis are equally possible to explain its formation.

24. The cause of trace elements enrichment in the Tansley marine shales can be attributed to several factors. These are the quantity and quality of organic matter, the physico-chemical conditions, salinity, rate of sedimentation, depth of the depositional basin and time. Organic matter in the marine shales is of organic origin while in the non-marine shales or in the Mam Tor marine shales, it is of terrestrial plant origin. In addition the quantity of organic matter in the former shales is nearly twice that of the latter shales. Decomposition of organic matter produces

an enormous variety of organic compounds, among which, soluble organic acids (humic and fulvic) and insoluble humates are the most important. These would form metal-organic complexes or absorb trace elements. This eventually leads to their saturation and their consequent incorporation in the sediments. It is also inferred that the decomposition products of marine organic matter contain more reactive groups towards trace elements than their equivalent from the plant remains. The role of low Eh-high pH are to allow reduced metals and organic acids to remain a longer time in soluble form, thus enhancing their interaction and lead to the formation of more metallorganic complexes. Increase in salinity is thought to be an important factor in trace elements enrichment and this is previously substantiated by the average content of some trace elements in the different faunal phases. The slower rate of sedimentation and shallower depth of the basin may be considered as a contributory factor; allowing moremarine organic matter to accumulate in the sediment and prolong the time of interaction with metals, thus allowing equilibrium to be achieved. The abovementioned conditions are also favourable for sulfide formation (FeS) which later transforms to pyrite. These are also very good sorbents for trace elemtns. This would result in competition between organic matter and pyrite for trace element sorption.

The decrease in trace element contents, not related to clay minerals, can largely be accounted for by the different type and lower amount of organic matter, lower salinity and faster rate of sedimentation and much less so to the Eh-pH condition. Similar reasoning is applicable to the decrease of trace element contents in theMam Tor marine shales. The latter are described earlier as a turbidite mud, rather than a pelagic mud.

25. Finally, the sympathy in the variation trends of illite, some trace elements, pyrite, organic matter and calcite as opposed to those by

quartz, Na_2O, TiO_2, Zr, kaolinite and siderite, cannot be regarded as a coincidence or fortuitous, in the Tansley Borehole sediments. The distribution patterns of most of the abovementioned, suggest a control of sedimentary environment and not age control. Moreover, they are in accord with the proposed deltaic sedimentation system. A shallow water, off-shore and semi-restricted basin or gulf onto which a delta front is encroaching seems ideal to account for the observed variation in mineralogy and chemistry.

By comparing the Mam Tor and the Tansley marine shales, an important point emerges, namely the role of the Derbyshire Block which acted as a submarine ridge, thus effected the circulation of sea water in the different and adjacent sectors of the southern part of the Central Pennines Basin. The cosanguinity of these depositional environments can be imagined as a deep marine environment to the north-northwest of the Derbyshire Block while to its south-east was a shallow gulf. In the former turbidity currents deposited the Mam Tor sediments, whereas in the latter a slowly deposited mud accumulated.

REFERENCES

ALBEE, A.L. (1962). Relationships between the mineralogical association, chemical composition and physical properties of the chlorite series. Am. Min. 47, 851-870.

AL-HASHIMI, W.S. (1972). Sedimentological studies of the limestone members of the Middle Limestone Group in Northumberland. Ph.D. Thesis, University of Newcastle-upon-Tyne.

ALLEN, J.R.L. (1960). The Mam Tor Sandstones: A turbidite facies of the Namurian deltas of Derbyshire, England. Jour. Sed. Pet. 30, 193-208.

ALLEN, J.R.L. (1970). Physical process of sedimentation. Unwin Ltd.

AMIN, M.A. (1975). Sedimentological studies of the Five Yard, the Three Yard and the Four Fathom Limestones from south-west Northumberland to Cross Fell. M.Sc. Thesis, University of Newcastle-upon-Tyne.

ARNOLD-BEMROSE, H.H. (1907). The toadstones of Derbyshire. Their field relations and petrography. Quart. Jour. Geol. Soc., lxii, 241-281.

ATKINSON, W.J. (1967). Regional geochemical studies in County Limerick, Ireland, with particular reference to selerium and molybdinum. Ph.D. Thesis, University of London.

AUSTIN, G.S. and LEININGER, R.K. (1976). The effect of heat treating-sedimented mixed layer illite-smectite as related to quantitative clay mineral determinations. Jour. Sed. Pet. 46, 206-215.

BAILEY, E.H. and IRWIN, W.P. (1959). K-feldspar content of Jurassic and Cretaceous greywackes of Northern Coast Ranges and Sacramento Valley, California. Bull. Am. Assoc. Petrol. Geol. 43, 2797-2809.

BAILEY, S.W. (1972). Determination of chlorite compositions by X-ray spacings and intensities. Clays and Clay Minerals 20, 381-388.

BAKER, W.E. (1973). The role of humic acids from Tasmanian podzolic soils in mineral degradation and metal mobilisation. Geochim. Cosmochim. Acta 37, 269-281.

BARBER, C. (1974). Major and trace element associations in limestones and dolomites. Chem. Geol. 14, 273-280.

BARRAGAN, E. and INGUEZ, J. (1976). Weathering of clay minerals in a Navarre Andosol (Spain). Clay Minerals 11, 269-272.

BATHURST, R.G.C. (1971). Carbonate sediments and their diagenesis. Elsevier Pub. Co.

BEER, R.N. and GROSLINE, D.S. (1971). Distribution, composition and transport of suspended sediment in Redondo Submarine Canyon and vicinity (California). Mar. Geol. 10, 153-175.

BERNER, R.A. (1963). Electrode studies of hydrogen sulfide in marine sediments. Geochim. Cosmochim. Acta 27, 563-575.

BERNER, R.A. (1964a). Iron sulphides formed from aqueous solution at low temperatures and atmospheric pressue. J. Geol. 72, 293-306.

BERNER, R.A. (1964b). Distribution and diagenesis of sulphur in some sediments from the Gulf of California. Mar. Geol. 1, 117-140.

BERNER, R.A. (1964c). Stability fields of iron minerals in anaerobic sediments. J. Geol. 72, 826-834.

BERRY, R.W. and JORGENSEN, P. (1971). Grain size, mineralogy and chemistry of a quick-clay sample from the Ullensaker Slide, Norway. Eng. Geol. 5, 73-84.

BHATT, J.J. (1972). Dolomitisation of Carboniferous Main Limestone Series in South Wales, U.K. Ph.D. Thesis, University of Wales, Cardiff.

BHATT, J.J. (1973). Ca/Mg ratio classification of Main Limestones (Mississippian) in South Wales, U.K. Sed. Geol. 10, 225-231.

BIRCH, G.F. (1978). The distribution of clay minerals on the continental margin of the west coast of South Africa. Trans. Geol. Soc. S. Afr. 81, 23-34.

BISCHOFF, J.L., CLANCY, J.J. and BOOTH, J.S. (1975). Magnesium removal in reducing marine sediments by cation exchange. Geochim. Cosmochim. Acta 39, 559-568.

BISCHOFF, J.L. and KU, T.L.C. (1971). Pore fluids of recent marine sediments: 11, Anoxic sediments of 35° to 45°N Gibraltar to Mid-Atlantic Ridge. Jour. Sed. Pet. 41, 1008-1017.

BJORLYKKE, K. (1971). Petrology of Ordovician sediments from Wales. Norsk. Geologisk Tidsskrift 51, 123-139.

BJORLYKKE, K. (1974). Geochemical and mineralogical influence of Ordovician Island Arcs on epicontinental clastic sedimentation. A study of Lower Palaeozoic sedimentation in the Oslo Region, Norway. Sedimentology 27, 251-272.

BJORLYKKE, K. (1975). Mineralogical and chemical changes during weathering of acid and basic rocks in Uganda. Norsk. Geologisk Tidsskrift 55, 81-89.

BLAXLAND, A.B. (1974). Geochemistry and geochronology of chemical weathering, Butler Hill Granite, Missouri. Geochim. Cosmochim. Acta 38, 843-852.

BLOCKER, A.B., CALLENDER, E. and JOSEPHSON, P.D. (1975). Trace element and organic carbon content of surface sediment from Grand Traverse Bay, Lake Michigan. Geol. Soc. Am. Bull. 86, 1358-1362.

BLOXAM, T.W. and THOMAS, R.L. (1969). Palaeontological and geochemical facies in the Gastrioceras subcrenatum Marine Band and associated rocks from the North Crop of the South Wales Coalfield. Q. Jl. geol. Soc. Lond. 124, 239-281.

BOCTOR, Z.N., KULLERUD, G. and SWEANY, J.L. (1976). Sulfide minerals in Seelyville Coal III, Chinook Mine, Indiana. Mineral. Deposita 11, 249-266.

BOLES, J.R. and COOMBS, D.S. (1975). Mineral reactions in zeolitic Triassic tuff, Hokonui Hills, New Zealand. Geol. Soc. Am. Bull. 86, 163-173.

BONATTI, E., FISHER, D.E., JOENSUU, O., RYDELL, H.S. and BEYTH, M. (1972). Iron-manganese-barium deposit from the Northern Afar Rift (Ethiopia). Econ. Geol. 67, 717-730.

BONATTI, E., GUERSTEIN, M.B.H., HONNOREZ, J. and STERN, C. (1976). Hydrothermal pyrite concretions from the Romanche Trench (equatorial Atlantic): Metallogenesis in oceanic fracture zones. Earth Planet. Sci. Lett. 32, 1-10.

BOSTROM, K. (1970). Submarine volcanism as a source of iron. Earth Planet. Sci. Lett. 9, 348-354.

BOSTROM, K., JOENSUU, O. and BROM, I. (1974). Plankton - its chemical composition and its significance as a source of pelagic sediments. Chem. Geol. 14, 255-271.

BOSTROM, K., KRAEMER, T. and GARTNER, S. (1973). Provenance and accumulation rates of opaline silica, Al, Ti, Fe, Mn, Cu, Ni and Co in Pacific pelagic sediments. Chem. Geol. 11, 123-148.

BOSTROM, K., LYSEN, L. and MOORE, C. (1978). Biological matter as a source of authigenic matter in pelagic sediments. Chem. Geol. 23, 11-20.

BOYCHENKO, Y.A., SAYENKO, G.N. and UDEL'NOVA, T.M. (1968). Behaviour of the concentrating action of plants in the biosphere. Geochem. Int. 5, 1036.

BRINDLEY, G.W. (1961). Quantitative analysis of clay mixtures: In: Brown, G. (Ed.), The X-ray identification and crystal structures of clay minerals. Min. Soc. London, 489-516.

BRINDLEY, G.W. and GILLERY, F.H. (1956). X-ray identification of chlorite species. Am. Min. 41, 169-186.

BROCKAMP, O., GOULART, E., HARDER, H. and HEYDEMANN, A. (1978). Amorphous copper and zinc sulfides in the metalliferous sediments of the Red Sea. Contrib. Mineral. Petrol. 68, 85-88.

BROOKS, R.A. and FERRELL, R.E. (1970). The lateral distribution of clay minerals in lakes Pontchartrain and Maurepas, Louisianna. Jour. Sed. Pet. 40, 835-863.

BROWN, G. (1961). The X-ray identification and crystal structure of clay minerals. Min. Soc. London.

BROWN, G., (1955). The effect of isomorphous substitutions on the intensities of (001) reflections of mica and chlorite-type structures. Min. Mag. 30, 657-665.

BROWN, G. and NEWMAN, A.C.D. (1970). Cation exchange properties of micas. III. Release of potassium sorbed by potassium depleted micas. Clay Minerals 8, 273-277.

BROWN, L.F., BAILEY, S.W., CLINE, L.M. and LISTER, J.S. (1977). Clay mineralogy in relation to deltaic sedimentation patterns of Desmoinesian cyclothems in Iowa-Missouri. Clays and Clay Minerals 25, 171-186.

BUCHBINDER, B. (1969). Selective dolomitisation of micrite envelopes: A possible clue to original mineralogy. Jour. Sed. Pet. 39, 514-517.

BUKE, D.P. and MANKIN, C.J. (1971). Clay mineral diagenesis within inter-laminated shales and sandstones. Jour. Sed. Pet. 41, 971-981.

BUTTLER, J.R. (1953). The geochemistry and mineralogy of rock weathering: (1) The Lizard Area, Cornwall. Geochim. Cosmochim. Acta 4, 157-178.

BYSTROM, A.M. (1954). 'Mixed-layer' minerals from the Ordovician bentonite beds at Kinnekulle, Sweden. Nature 173, 783-784.

CARROLL, D. (1970). Clay minerals: A guide to their X-ray identification. Geol. Soc. Am. Spc. Paper 126.

CHATTERJEE, N. (1966). On the widespread occurrence ofoxidised chlorites in the Pennine Zone of the western Italian Alps. Contr. Mineral. and Petrol. 12, 335-339.

CHAVE, K.E. (1952). A solid solution between calcite and dolomite. Jour. Geol. 60, 190-192.

CHAYES, F. (1971). Ratio correlation: A manual for students of petrology and geochemistry. University of Chicago Press, Chicago.

CHESTER, R., ASTON, S.R. and BRUTY, D. (1976). The trace element partition geochemistry in an ancient deep sea sediment core from the Bermuda Rise. Mar. Geol. 21, 271-288.

CHESTER, R. and HANNA, G.M. (1970). Trace element partition patterns in North Atlantic deep sea sediments. Geochim. Cosmochim. Acta 34, 1121-1128.

COCKETT, A.S. (1966). The clay mineralogy of Irish Namurian sediments. Ph.D. Thesis, University of Southampton.

COLLINS, R.J. (1976). A method for measuring the mineralogical variation of spoils from British collieries. Clay Minerals 11, 31-49.

COLLINSON, J.D. (1968). The sedimentology of the Grindslow Shales and the Kinderscout Grit: A deltaic complex in the Namurian of Northern England. Jour. Sed. Pet. 39, 194-221.

CONDIE, K.C. (1967). Geochemistry of early Pre-Cambrian greywackes from Wyoming. Geochim et Cosmochim. Acta 31, 2135-2149.

CORNAN, D.S. (1976). Basal metalliferous sediments from the Eastern Pacific. Geol. Soc. Am. Bull. 87, 928-934.

COSGROVE, M.E. (1973). The geochemistry and mineralogy of the Permian red beds of south-east England. Chem. Geol. 11, 31-47.

CUBITT, J.M. (1975). A regression technique for the analysis of shales by X-ray diffraction. Jour. Sed. Pet. 45, 546-553.

CURTIS, C.D. (1967). Diagenetic iron minerals in some British Carboniferous sediments. Geochim. Cosmochim. Acta 31, 2109-2123.

CURTIS, C.D. (1969). Trace element distribution in some British Carboniferous sediments. Geochim. Cosmochim. Acta 33, 519-523.

CURTIS, C.D. and SPEARS, D.A. (1968). The formation of sedimentary iron minerals. Econ. Geol. 63, 257-270.

D'ANGELJAN, B.F. (1967). Origin of marine phosphorites off Baja California, Mexico. Mar. Geol. 5, 15-44.

DARBY, D.A. (1975). Kaolinite and other clay minerals in Arctic Ocean Sediments. Jour. Sed. Pet. 45, 272-279.

DAVIDSON, D.F. and LANKIN, H.W. (1961). Metal content of some black shales of the Western United States. U.S. Geol. Surv. Prof. Papers, 424-C-329.

DAVIDSON, D.F. and LANKIN, H.W. (1962). Metal content of some black shales of the western conterminous United States. U.S. Geol. Surv. Prof. Papers 450-C-74.

DAVIS, J.C. (1973). Statistics and Data Analysis in Geology. Wiley, New York.

DAVIS, J.C. and SAMPSON, R.J. (1966). Fortran II program for multivariate discriminant analysis, computer contribution 4. State Geological Survey, University of Kansas.

DEER, W.A., HOWIE, R.A. and ZUSSMAN, J. (1966). An introduction to the rock forming minerals. Longmans.

DEGENS, E.T. (1965). Geochemistry of sediments. Prentice Hall.

DEGENS, E.T., WILLIAMS, E.G. and KEITH, M.L. (1957). Environmental studies of Carboniferous sediments. Part I: Geochemical criteria for differentiating marine and fresh water shales. Amer. Ass. Petrol. Geol. Bull. 41, 2427-2455.

DEGENS, E.T., WILLIAMS, E.G. and KEITH, M.L. (1958). Environmental studies of Carboniferous sediments. Part II: Application of geochemical criteria. Amer. Ass. Petrol. Geol. Bull. 42, 981-997.

DESBOROUGH, G.A., ANDERSON, A.T. and WRIGHT, T.L. (1968). Mineralogy of sulfides from certain Hawaiian basalts. Econ. Geol. 63, 636-644.

DE SEGONZAC, D. (1970). The transforamtion of clay minerals during diagenesis and lower grade metamorphism: A review. Sedimentology 15, 281-396.

DEURER, R., FORSTNER, U. and SCHMOLL, G. (1978). Selective chemical extraction of carbonate-associated metals from Recent lacustrine sediments. Geochim. Cosmochim. Acta 42, 425-427.

DYMOND, J. and CORLISS, J.B. (1977). History of metalliferous sedimentation at deep sea site 319, in the South Eastern Pacific. Geochim. Cosmochim. Acta 41, 741-753.

DYRSSEN, D. and HALLBERG, R. (1979). Anoxic sediment reactions - a comparison between box experiment and fjord investigation. Chem. Geol. 24, 151-159.

EBERL, D. (1978). The reaction of montmorillonite to mixed-layer clay: The effect of interlayer alkali and alkaline earth cations. Geochim. Cosmochim. Acta 42, 1-7.

EDWARD, M.A. and TROTTER, F.M. (1954). The Pennines and adjacent areas. British Regional Geology, Inst. Geol. Sci.

EDZWALD, J.K. and O'MELIA, C.R. (1975). Clay distribution in Recent estuarine sediments. Clays and Clay Minerals 20, 93-100.

EMERSON, S. (1976). Early diagenesis in anaerobic lake sediments: Chemical equilibrium in interstitial waters. Geochim. Cosmochim. Acta 40, 925-934.

EMERSON, S. and WIDMER, G. (1978). Early diagenesis in anaerobic lake sediments - II. Thermodyanmic and kinetic factors controlling the formation of iron phosphate. Geochim. Cosmochim. Acta 42, 1307-1316.

ENGLUND, J.O. and JORGENSEN, P. (1973). A chemical classification system for argillaceous sediments and factors affecting their composition. Geol. For. Stockh. Forh. 95, 87-97.

ESQUEVIN, J. (1969). Influence de la composition chimique des illites sur leur cristallinite. Bull. Centre-Rech. Pau - SNPA, 147-153.

ETHRIDGE, F.G. (1977). Petrology, transport and environment in isochronous Upper Devonian sandstone and siltstone units, New York. Jour. Sed. Pet. 47, 31-52.

EVANS, L.J. and ADAMS, W.A. (1975). Chlorite and illite in some Lower Palaeozoic mudstones of Mid-Wales. Clay Minerals 10, 387-397.

EVANS, R.C. (1964). An introduction to crystal chemistry. Cambridge University Press.

EVANS, W.B. et al. (1968). Geology of the country around Macclesfield, Congleton, Crewe and Middlewich. Mem. Geol. Surv.

EXLEY, C.S. (1976). Observations on the formation of kaolinite in the St. Austell Granite, Cornwall. Clay Minerals 11, 51-63.

FAIRBAIRN, H.W. (1953). Precision and accuracy of chemical analysis of silicate rocks. Geochim. Cosmochim. Acta 4, 143-156.

FARMER, .V.C. and WILSON, M.J. (1970). Experimental conversion of biotite to hydrobiotite. Nature 226, 84-842.

FELLOWS, P.M. and SPEARS, D.A. (1978). The determination of feldspars in mudrocks using an X-ray powder diffraction method. Clays and Clay Minerals 26, 231-236.

FERGUSON, J. and BUBELA, B. (1974). The concentration of Cu(II), Pb(II) and Zn(II) from aqueous solutions by particulate algal matter. Chem. Geol. 13, 163-186.

FISHER, I.S. (1968). Inter-relation of mineralogy and texture within an Ordovician Lexington limestone section in Central Kentucky. Jour. Sed. Pet. 38, 775-784.

FLETCHER, W.K. (1968). Geochemical reconnaissance in relation to copper deficiency in livestock in the Pennines and Devon. Ph.D. Thesis, University of London.

FOSCOLOS, A.E. and KODAMA, H. (1974). Diagenesis of clay minerals from Lower Cretaceous shales of North-Eastern British Columbia. Clays and Clay Minerals 22, 319-335.

FOSCOLOS, A.E., POWELL, T.G. and GUNTHER, P.R. (1976). The use of clay minerals and inorganic and organic geochemical indicators for evaluating the degree of diagenesis and oil generating potential of shales. Geochim. Cosmochim. Acta 40, 953-966.

FRANCIS, E.G. (1968). Effect of sedimentation on volcanic processes, including neck-sill reationships, in the British Carboniferous. XXIII Int. Geological Congress 2, 163-174.

FRASER, D.C. (1961). Organic sequestration of copper. Econ. Geol. 56, 1063-1078.

FROELICH, P.N. BENDER, M.L. and HEATH, G.R. (1977). Phosphorous accumulation rates in metalliferous sediments on the East Pacific Rise. Earth Planet. Sci. Lett. 34, 351-359.

FURNESS, H. (1975). Experimental palagonitisation of basaltic glasses of varied composition. Contrib. Mineral. and Petrol. 50, 105-113.

GAD, M.A., CATT, H.A. and LE RICHE, H.H. (1969). Geochemistry of the Whitbian (Upper Lias) sediments of the Yorkshire Coast. Proc. Yorks. Geol. Soc. 37, 105-139.

GALLOWAY, H.E. (1974). Deposition and diagenetic alteration of sandstone in the Northeast Pacific Arc-related basins: Implications for greywacke genesis. Geol. Soc. Am. Bull. 85, 379-390.

GARDNER, L.R. (1974). Organic versus inorganic metal complexes in sulfidic marine waters - some speculative calculations based on available stability constants. Geochim. Cosmochim. Acta 38, 1292-1302.

GARNETT, C.S. (1923). The 'toadstone clays' of Derbyshire. Min. Mag., II, 151-157.

GARRELS, R.M. and CHRIST, C.L. (1965). Solutions, minerals and equilibria. Harper and Row.

GARRELS, R.M. and NAESER, C.R. (1958). Equilibrium distribution of dissolved sulfur species in water at 25^{o}C and 1 atm. total pressure. Geochim. Cosmochim. Acta 15, 113-130.

GAUDETTE, H.E. (1965). Illite from Fond de Lac County, Wisconsin. Am. Min. 50, 411-417.

GIBBS, R.J. (1965). Error due to segregation in quantitative clay mineral X-ray diffraction mounting techniques. Am. Min. 50, 741-751.

GIBBS, R.J. (1977). Clay mineral segregation in the marine environment. Jour. Sed. Pet. 47, 237-243.

GIBSON, W. and WEDD, C.B. (1913). The geology of the northern part of the Derbyshire Coalfield and bordering tracts. Mem. Geol. Surv.

GILL, W.D., KHALAF, F.I. and MASSOUD, M.S. (1977). Clay minerals as an index of the degree of metamorphism of the carbonate and terrigenous rocks in the South Wales coalfield. Sedimentology 24, 675-691.

GILLIGAN, A. (1920). The petrography of the Millstone Grit of Yorkshire. Q. Jl. geol. Soc. London 75, 251-294.

GLAGOLEVA, H.A. (1961). Regularities in the distribution of chemical elements in modern sediments of the Black Sea. Dokl. Acad. Sci. USSR Earth Sci. 136, 1-4 (Transl.).

GLASS, H.D., POTTER, P.E. and SIEVER, R. (1956). Clay mineralogy of some basal Pennsylvanian sandstones, clays and shales. Am. Ass. Petrol. Geol. Bull. 40, 750-754.

GOLDBERGE, E.D. and ARRHENIUS, G.O.S. (1958). Chemistry of Pacific pelagic sediments. Geochem. Cosmochim. Acta 13, 153-212.

GOLDSCHMIDT, V.M. (1954). Geochemistry. Oxford. Univ. Press, London.

GREENSMITH, J.T. (1955). A study of some Upper Carboniferous sediments with particular reference to the mode and environment of sedimentation. Ph.D. Thesis, University of Sheffield.

GREENSMITH, J.T. (1957). Lithology with particular reference to cementation of Upper Carboniferous sandstones in Northern Derbyshire. Jour. Sed. Pet. 27, 405-416.

GRIFFIN, G.M. (1962). Regional clay mineral facies - products of weathering intensity and current distribution in the Northern Gulf of Mexico. Am. Geol. Soc. Bull. 73, 737-768.

GRIFFIN, G.M. and INGRAM, R.L. (1955). Clay minerals of the Neuse estuary. Jour. Sed. Pet. 25, 194-200.

GRIM, R.E. (1951). The depositional environment of red and green shales. Jour. Sed. Pet. 21, 226-232.

GRIM, R.E., BRAY, R.H. and BRADLEY, W.F. (1937). The mica in argillaceous sediments. Am. Min. 22, 813-829.

GRIM, R.E. and GUVEN, N. (1978). Bentonites. Developments in sedimentology, 24. Elsevier Publ. Co.

GROVES, A.W. (1951). Silicate Analysis. George Allen and Unwin, London.

GUIDOTTI, C.V. and CHENEY, J.T. (1975). Inter-relationship between Mg/Fe ratio and octahedral Al content in biotite. Am. Min. 60, 849-853.

HALLAM, A. (1967). The depth significance of shales with bituminous laminae. Mar. Geol. 5, 481-493.

HART, R.A. (1973). A model for chemical exchange in the basalt-seawater system of ocean layer II. Can. Jour. Earth Sci. 10, 799-816.

HATHAWAY, J.C. (1955). Procedure for clay mineral analyses used in the sedimentary petrology laboratory of the U.S. Geological Survey. Clay Mineral. Bull., 3 (15), 8-13 (1956).

HAY, R.L. (1966). Zeolites and zeolitic reactions in sedimentary rocks. Geol. Soc. Am. Spec. Paper 85, 130 p.

HAY, R.L. and IIJIMA, A. (1968). Petrology of palagonite tuffs of Koko Craters, Oahu, Hawaii. Contr. Mineral and Petrol. 17, 141-154.

HEALD, M.T. and BAKER, G.F. (1977). Diagenesis of the Mt. Simon and Rose Run sandstones in western West Virginia and Southern Ohio. Jour. Sed. Pet. 47, 53-66.

HECKEL, P.H. (1972). Recognition of ancient-shallow marine environments. In: Recognition of Ancient Sedimentary Environments. SEPM Special Publ. 16, 226-286.

HEINRICH, K.F.J., 1966. The Electron Microprobe. Ed. T.D. McKinley, K.F.J. Heinrich and D.B. Wittry, Wiley, New York, 296-377.

HELING, D. (1978). Diagenesis of illite in argillaceous sediments of the Rhinegraben. Clay Minerals 13, 211-219.

HEM, J.D. (1977). Reaction of metal ions at surfaces of hydrous iron oxide. Geochim. Cosmochim. Acta 41, 527-538.

HEMINGWAY, J.E. and TAMAR-AGHA (1975). The effects of diagenesis on some heavy minerals from the sandstones of the Middle Limestone Group in Northumberland. Proc. Yorks Geol. Soc. 40, 537-546.

HENSON, M.R. (1973). Clay minerals from the Lower New Red Sandstone of south Devon. Proc. Geol. Ass. 84, 429-445.

HIRST, D.M. (1962a). The geochemistry of modern sediments from the Gulf of Paria - I. The relationship between mineralogy and the distribution of major elements. Geochim. Cosmochim. Acta 26, 309-334.

HIRST, D.M. (1962b). The geochemistry of modern sediments from the Gulf of Paria - II. The location and distribution of trace elements. Geochim. Cosmochim. Acta 26, 1147-1187.

HIRST, D.M. and KAYE, M.J. (1971). Factors controlling the mineralogy and chemistry of an Upper Visean sedimentary sequence from Rockhope, County Durham. Chem, Geol. 8, 37-59.

HORN, D.R. WEING, M., HORN, B.M. and DELACH, M.N. (1971). Turbidites of the Hatteras and Sohm abyssal plains, Western North Atlantic. Mar. Geol. 11, 287-323.

HOWER, et al. (1976). Mechanism of burial metamorphism of argillaceous sediment: 1. Mineralogical and chemical evidence. Geol. Soc. Am. Bull. 87, 725-737.

HSU, E. and JENKYNS, H. (1974, Edit.). Pelagic sediments: On land and under the sea. Int. Assoc. Sedimentologists, 1.

HUBER, N.K. (1958). The environmental control of sedimentary iron minerals. Econ. Geol. 53, 123-140.

HUCKENHOLZ, H.G. (1963). Mineral composition and texture in greywackes from the Harz Mountains (Germany) and in arkoses from the Auvergne (France). Jour. Sed. Pet. 33, 914-918.

HUDSON, R.G. and COTTON, G. (1943). The Namurian of Alport Dale, Derbyshire. Proc. Yorks. Geol. Soc. 25, 142-173.

HUDSON, R.G. and COTTON, G. (1945). The Carboniferous rocks of the Edale Anticline, Derbyshire. Q. Jl. Geol. Soc. London 101, 1-35.

HUMPHRIS, S.E. and THOMPSON, G. (1978). Trace element mobility during hydrothermal alteration of oceanic basalts. Geochim. Cosmochim. Acta 42, 127-136.

IMBRIE, J. and POLDERVAART, A. (1959). Mineral composition calculated from chemical analysis of sedimentary rocks. Jour. Sed. Pet. 29, 588-595.

JACKA, A.D. (1974). Replacement of fossils by length-slow chalcedony and associated dolomitisation. Jour. Sed. Pet. 44, 421-427.

JACKSON, K.S., JONASSON, I.R. and SKIPPEN, G.B. (1978). The nature of metals-sediment-water interactions in freshwater bodies, with emphasis on the role of organic matter. Earth Science Reviews 14, 97-146.

JACKSON, M.L. (1956). Soil chemical analysis - advanced course. Dept. of Soils, University of Wisconsin.

JACKSON, T.A. (1977). A relationship between crystallographic properties of illite and chemical properties of extractable organic matter in Pre-Phanerozoic and Phanerozoic sediments. Clays and Clay Minerals 25, 187-195.

JACKSON, W. (1927). The succession below the Kinderscout Grit in North Derbyshire. Manch. Geol. Soc. Jour. 1, 15-32.

JOHNS, W.D., GRIM, R.E. and BRADLEY, W.F. (1954). Quantitative estimation of clay minerals by diffraction method. Jour. Sed.Pet. 24, 242-251.

KACHENKOV, S.M. (1967). Average contents of certain minor chemical elements in the principal types of sedimentary rocks. In: Chemistry of the Earth's Crust (Vinogradov, A.P., Ed.), 416-423.

KALLIOKOSKI, J. (1975). Chemistry and mineralogy of Precambrian paleosols in Northern Michigan. Geol. Soc. Am. Bull. 86, 371-376.

KAPPOR, B.S. (1976). Weathering of micaceous clays in some Norwegian podsols. Clay Minerals 9, 383-394.

KEITH, M.L. and DEGENS, E.T. (1959). Geochemical indicators of marine and fresh-water sediments. In: Research in Geochemistry. 38-61.

KELLER, W.D. (1963). Diagenesis in clay minerals - A review. Int. Conf. Clay Minerals Proc., Pergamon Press, 136-157.

KELLER, W.D. (1970). Environmental aspects of clay minerals. Jour. Sed. Pet. 40, 788-813.

KELLING, G., SHENG., H. and STANLEY, D.J. (1975). Mineralogical composition of sand-sized sediment on the outer margin off the Mid-Atlantic States: Assessment of the influence of the ancestral Hudson and other fluvial systems. Geol. Soc. Am. Bull. 86, 853-862.

KENT, P.E. (1966). The structure of the concealed Carboniferous rocks of north-eastern England. Proc. Yorks Geol. Soc. 35, 323-352.

KERR, P.F. (1959). Optical Mineralogy. McGraw Hill, Hew York.

KHAYLOV, K.M. (1968). Dissolved organic macromolecules in sea water. Geochim. Int. 5, 497-503.

KINTER, E.B. and DIAMOND, S. (1956). A new method for preparation and treatment of oriented-aggregate specimens of soil clays for X-ray diffraction. Soil Sci. 81, 111-120.

KNEBEL, H.J., CONOMOS, T.L. and COMMEAU, J.A. (1977). Clay-mineral variability in the suspended sediments of the San Francisco Bay System, California. Jour. Sed. Pet. 47, 210-229.

KNOWLES, B. (1961). The radioactive content of Coal Measures sediments in the Yorkshire-Derbyshire Coalfield. Ph.D. Thesis, University of Sheffield.

KOCH, G.S. and LINK. R.F. (1971). Statistical analysis of geological data. John Wiley and Sons, New York.

KOHN, B.P. (1970). Identification of New Zealand tephra-layers by emission spectrographic analysis of their titanomagnetites. Lithos 3, 361-368.

KOVALEV, V.A. and GENERALOVA, V.A. (1969). Geochemical aspects of the movement of iron in recent peat bogs of Byelorussia. Geochem. Int. 6, 144-153.

KRAUSKOPF, K.B. (1955). Sedimentary deposits of rare metals. Econ. Geol. 50th Anniversary Vol., 411-463.

KRAUSKOPF, K.B. (1956). Factors controlling the concentrations of thirteen rare metals in sea water. Geochim. Cosmochim. Acta 10, 1-26.

KROM, M.D. and SHOLKOVITZ (1978). On the association of iron and manganese with organic matter in anoxic pore waters. Geochim. Cosmochim. Acta 42, 607-611.

KRUMBEIN, W.C. and GRAYBILL, F.A. (1964). An introduction to statistical models in geology (1965). McGraw Hill Company.

KULBICKI, G. and MILLOT, G. (1963). Diagenesis of clays in sedimentary and petroliferous series. Proc. 10th Nat. Conf. Clays and Clay Minerals, 329-332.

KUNZE, G.W., KNOWLES, L.I. and KITANO, Y. (1968). The distribution and mineralogy of clay minerals in the Taku estuary of Southeastern Alaska. Mar. Geol. 6, 439-448.

LEBEDEV, B.A. (1967). Trace elements in marine and fresh water clays. Geochmist. Int. 4, 821-824.

LEONE, M. and ALAIMO, R. (1974). Magnesian calcite nucleation in ancient dolomitised limestones of western Sicily. Jour. Sed. Pet. 44, 54-59.

LERBEKMO, J.F. (1963). Petrology of the Belly River Formation, Southern Alberta foothills. Sedimentology 2, 54-86.

LE RICHE, H.H. (1959). The distribution of certain trace elements in the Lower Lias of Southern England. Geochim. Cosmochim. Acta 16, 101-122.

LE ROUX, J., RICH, G.I. and RIBBE, P.H. (1970). Ion selectivity by weathered micas as determined by electron microscope analysis. Clays and Clay Minerals 18, 333-337.

LI, Y., BISCHOFF, J. and MATHIEU, G. (1969). The migration of manganese in the Arctic Basin sediments. Earth Planet. Sci. Lett. 7, 265-270.

LOVE, L.G. (1971). Early diagenetic polyframboidal pyrite, primary and redeposited, from the Wenlockian Denbigh Grit Group, Conway, North Wales, U.K. Jour. Sed. Pet. 41, 1038-1044.

LOVELAND, P.J. and BULLOCK, P. (1975). Crystalline and amorphous components of the clay fractions in brown podzolic soils. Clay Minerals 10, 451-469.

MACFARLANE, R.B. (1978). Molecular weight distribution of humic and fulvic acids of sediments from a north Florida estuary. Geochim. Cosmochim. Acta 42, 1579-1582.

MACKAY, K.M. and MACKAY, R.A. (1972). Introduction to modern inorganic chemistry. Intertext Books - London.

MACPHERSON, H.G. (1958). A chemical and petrographic study of Precambrian Sediments. Geochim. Cosmochim. Acta 14, 73-92.

MAGRA, K. (1974). Compaction, ion filtration, and osmosis in shale and their significance in primary migration. Am. Assoc. Petrol. Geol. Bull. 58, 283-290.

MANKIN, C.J. (1970). Introduction to the symposium papers on environmental aspects of clay minerals. Jour. Sed. Pet. 40, 788-854.

MANSKAYA, S.M. and DROZDOVA, T.V. (1968). Geochemistry of organic substances. Translated and edited by Shapiro, L. and Breger, I.A. Pergamon Press.

MANSKAYA, S.M., KODINA, L.A. and GENERALOVA, V.N. (1968). Geochemical role of lignites. Geochem. Int. 4, 814-822.

MARSTON, S.A. (1967). The geochmeistry of certain seatearths. M.Sc. Thesis, University of Sheffield.

MASON, B. (1966). Principles of Geochemistry. John Wiley & Sons Inc.

MASON, M.H. (1961). The Mam Tor Sandstones: A turbidite facies of the Namurian of North Derbyshire. Ph.D. Thesis, University of Manchester.

MATTHEWS, D.H. (1971). Weathered and metamorphosed basalts. III: Altered basalts from Swallow Bank, an abyssal hill in the NE Atlantic and from a nearby seamount. Phil. Trans. Roy. Soc. Lond A, 268, 551-571.

MAXWELL, D.T. and HOWER, J. (1967). High grade diagenesis and low grade metamorphism of illite in the Pre-cambrian belt series. Am. Min. 52, 843-857.

MAYHEW, R.W. (1966). A sedimentological investigation of the Marsdenian Grits and associated measures in north-east Derbyshire. Ph.D. Thesis, University of Sheffield.

MAYNARD, J.B. (1976). The long-term buffering of the oceans. Geochim. Cosmochim. Acta 40, 1523-1532.

MCLAUGHLIN, R.J.W. (1958). Geochemical partition in two illitic clays. Geochim. Cosmochim. Acta, 15, 165-169.

MIDDLETON, G.V. (1972). Albite of secondary origin in Charny sandstone, Quebec. Jour. Sed. Pet. 42, 341-349.

MIESCH, A.T. (1962). Computing mineral compositions of sedimentary rocks from chemical analysis. Jour. Sed. Pet. 32, 217-225.

MIGDISOV, A.A. (1960). On the titanium/aluminium ratio in sedimentary rocks. Geochemistry USSR (Trans.) 2, 178-194.

MILLER, R.L. and KHAN, J.S. (1962). Statistical analysis in the geological sciences. John Wiley & Sons, New York.

MILLOT, G. (1952). The principal sedimentary facies and their characteristic clays. Clay Min. Bull. 7, 235-237.

MISHELL, D.R.F. (1966). Namurian and Westphalian miospores from the Bowland Fells and Ingleton Coalfield. Ph,D. Thesis. University of Sheffield.

MOHR, P.A. (1959). A geochemical study of the shales of the Lower Cambrian Manganese Shale Group of the Harlech Dome, North Wales. Geochim. Cosmochim. Acta 17, 186-200.

MOORE, C. and BOSTROM, K. (1978). The elemental compositions of lower marine organisms. Chem. Geol. 23, 1-9.

MOORE, J.G. (1965). Petrology of deep-sea basalt near Hawaii. Am. Jour. Sci. 263, 40-52.

MOORE, J.G. (1966). Rate of palagonitization of sumbarine basalt adjacent to Hawaii. U.S. Geol. Surv. Prof. Paper 550-D, D163-D171.

MOORE, J.G. (1970). Water content of basalt erupted on the ocean floor. Contr. Mineral. Petrol 28, 272-279.

MOORE, J.G. and CALK, L. (1971). Sulfide spherules in vesicles of dredged pillow basalt. Am. Min. 56, 476-488.

MOORE, J.G. and FABBI, B.P. (1971). An estimate of the juvenile sulfur content of basalt. Contr. Mineral. Petrol. 33, 118-127.

MORTON, R.A. (1972). Clay mineralogy of Holocene and Pleistocene sediments, Guadalupe delta of Texas. Jour. Sed. Pet. 42, 85-88.

MOSSLER, J.H. and HAYES, J.B. (1966). Ordovician potassium bentonites of Iowa. Jour. Sed. Pet. 36, 414-427.

MURAVYOV, V.I. (1970). Formation of carbonate cement in elastic rocks. Sedimentology 15, 139-145.

MURRAY, H.H. and HARRISON, J.L. (1956). Clay mineral composition of recent sediments from Sigsbee Deep. Jour. Sed. Pet. 26, 363-368.

NANCE, W.B. and TAYLOR, S.R. (1977). Rare earth element patterns and crustal evolution. II. Archean sedimentary rocks from Kalgoorlie, Australia. Geochim. Cosmochim. Acta 41, 225-231.

NAZARKIN, L.A. (1960). The role of the sedimentation rate in the accumulation of absolute masses of organic matter in a sediment. Dokl. Acad. Sci. USSR, Earth Sci. 130, 15-17 (Transl.).

NEWMAN, A.C.D. (1970). Cation exchange properties of micas. II. Hysteresis and irreversibility during potassium exchange. Clay Minerals 8, 267-273.

NEWMAN, A.C.D. and BROWN, G. (1966). Chemical changes during the alteration of mica. Clay Minerals 6, 297-309.

NICHOL, I. et al. (1970). Regional geochemical reconnaissance of the Derbyshire area. Rep. No. 70/2, Inst. Geol. Sci.

NICHOL, I. et al. (1971). Regional geochemical reconnaissance of part of Devon and Cornwall. Rep. No. 71/2, Inst. Geol. Sci.

NICHOLLS, G.D. (1962). A scheme for recalculating the chemical analysis of argillaceous rocks for comparative purposes. Am. Min. 47, 34-47.

NICHOLLS, G.D. and LORING, D.H. (1960). Some chemical data on British Carboniferous sediments and their relationship to the clay mineralogy of these rocks. Clay Min. Bull. 4, 196-207.

NICHOLLS, G.D. and LORING, D.H. (1962). The geochemistry of some British Carboniferous sediments. Geochim. Cosmochim. Acta 26, 181-223.

NISSENBAUM, A. (1977). Minor and trace elements in Dead Sea water. Chem. Geol. 19, 99-111.

NORRISH, K. and CHAPELL, B.W. (1967). XRF-spectrography in physical methods in determinative mineralogy. In: Zussman (Ed.).

NORRISH, K. and HUTTON, J.T. (1964). Preparation of samples for analysis by X-ray fluorescent spectrography. Div. Rep., Div. Soils CSIRO, 3/64.

NORRISH, K. and HUTTON, J.T. (1969). An accurate X-ray spectrographic method for the analysis of a wide range of geological samples. Geochim et Cosmochim Acta 33, 431-453.

NRIAGU, J.O. (1972). Stability of vivianite and ion-pair formation in the system $Fe_3(PO_4)_2$-H_3PO_4-H_2O. Geochim. Cosmochim. Acta 36, 459-470.

NRIAGU, J.O. and DELL, C.I. (1974). Diagenetic formation of iron phosphates in recent lake sediments. Am. Min. 59, 934-946.

OBERLIN, A. and COUTY, R. (1970). Conditions of kaolinite formation during alteration of some silicates by water at 200°C. Clays and Clay Minerals 18, 347-356.

OFTEDAHL, C. (1958). A theory of exhalative-sedimentary ores. Geol. For. Stockh. Forh. 80, 1-19.

ORME, G.R. (1974). Silica in the Visean limestones of Derbyshire, England. Proc. Yorks. Geol. Soc. 40, 63-104.

ORMOND, R.S. and TAYLOR, B.F. (1978). Sulfate reduction and methanogenesis in marine sediments. Geochim. Cosmochim. Acta 42, 209-214.

PARHAM, W.E. (1966). Lateral variations of clay mineral assemblages in modern and ancient sediments. Proc. Int. Clay Conf., Jerusalem 1, 135-145.

PARSONS, L.M. (1918). Dolomitisation and the Leicestershire dolomites. Geol. Mag. 55, 246-258.

PEDERSON, A.K., ENGELL, J. and RONSBO, J.G. (1975). Early Tertiary volcanism in the Skagerrak: New chemical evidence from ash layers in the Mo-clay of Northern Denmark. Lithos 8, 255-268.

PERRY, E., and HOWER, J. (1970). Burial diagenesis in Gulf Coast Pelitic sediments. Clays and Clay Minerals 18, 165-177.

PERRY, E. and HOWER, J. (1972). Late stage dehydration in deeply buried pelitic sediments. Am. Assoc. Pet. Geol. Bull., 56, No.10, 2013-2021.

PETERSON, M.N. (1962). The mineralogy and petrology of Upper Mississippian carbonate rocks of the Cumberland Plateau in Tennessee. Jour. Geol. 70, 1-31.

PETERSON, M.N.A. and VON DER BORCH, C.C. (1965). Chert: Modern inorganic deposition in a carbonate precipitating locality. Science 149, 1501-1503.

PETTIJOHN, F.J. (1957). Sedimentary Rocks. Harper and Row.

PHILIPPI, G.T. (1974). The influence of marine and terrestrial source material on the composition of petroleum. Geochim. Cosmochim. Acta 38, 947-966.

PICARD, G.L. and FELBECK, Jr. (1976). The complexation of iron by marine humic acid. Geochim. Cosmochim. Acta 40, 1347-1350.

PICARD, M.D. and HIGH, L.R. (1972). Criteria for recognising lacustrine rocks. In: Recognition of Ancient Sedimentary Environments. SEPM Special Publ. 16, 108-145.

PIERCE, J.W. (1970). Chemical changes during palagonitisation under marine and non-marine conditions. Science in Iceland 2, 31-36.

PIERCE, J.W. and SIEGEL, F.R. (1969). Quantification in clay mineral studies and sedimentary rocks. Jour. Sed. Pet. 39, 187-193.

PIPER, D.Z. (1973). Origin of metalliferous sediments from the East Pacific Rise. Earth Planet. Sci. Lett. 19, 75-82.

POLDERVAART, A. (1955). Chemistry of the Earth's Crust. Geol. Soc. Am. S.P. 62, 119-144.

POTTER, P.E., SHIMP, N.F. and WITTERS, J. (1963). Trace elements in marine and freshwater argillaceous sediments. Geochim. Cosmochim. Acta 27, 669-694.

POWELL, T.G., DOUGLAS, A.G. and ALLAN, J. (1976). Variations in the type and distribution of organic matter in some Carboniferous sediments from Northern England. Chem. Geol. 18, 137-148.

PRICE, N.B. and CALVERT, S.E. (1978). The geochemistry of phosphorites from the Namibian Shelf. Chem. Geol. 23, 151-170.

PRICE, N.B. and DUFF, P. MCL. D. (1969). Mineralogy and chemistry of tonsteins from Carboniferous sequences in Great Britain. Sedimentology 13, 45-69.

PRYOR, W.A. and GLASS, H.D. (1961). Cretaceous-Tertiary clay mineralogy of the Upper Mississippi embayment. Jour. Sed. Pet. 31, 38-51.

QUIGLEY, R.., ZAJIC, J.E., MCKYES, E. and YONG, R.N. (1973). Biochemical alteration and heave of black shale: Detailed observations and interpretations. Can. J. Earth Sci. 10, 1005-1015.

RAMSBOTTOM, W.H. et al. (1962). Boreholes in the Carboniferous rocks of the Ashover District, Derbyshire. Bull. Geol. Surv., No. 19, 75-168.

RANKAMAK and SAHAMA, T.G. (1950). Geochemistry. University of Chicago Press.

RASHID, M.A. (1972). Role of quinone groups in solubility and complexing of metals in sediments and soils. Chem. Geol. 9, 241-248.

RASHID, M.A. (1974). Absorption of metals on sedimentary and peat humic acids. Chem. Geol. 13, 115-123.

RASHID, M.A. and LEONARD, J.D. (1973). Modifications in the solubility and precipitation behaviour of various metals as a result of their interaction with sedimentary humic acid. Chem. Geol. 11, 89-97.

RAZDOROZHNYY, V.F. (1968). The natural acidity of coals and its role in the concentration of trace elements. Geochem. Int. 5, 79-85.

READING, H.G. (1964). A review of the factors affecting the sedimentation of the Millstone Grit (Namurian) in the Central Pennines. 340-346. In: Deltaic and Shallow Water Deposits (Ed. L.M.J.V. Van Staaten) xvi + 464 pp. Elsevier, Amsterdam.

REICHENBACH, H.G.V. and RICH, C.I. (1969). Potassium release from muscovite as influenced by particle size. Clays and Clay Minerals, 17, 23-29.

REIMER, T.O. (1972). Diagenetic reactions in Early Precambrian greywackes of the Barberton Mountain Land (South Africa). Sediment. Geol. 7, 263-282.

REINECK, H.E. and SINGH, I.B. (1975). Depositional sedimentary environments. Springer Verlag.

RICHARDSON, P.W. and HAWEKES, H.E. (1958). Adsorption of copper on quartz. Geochim. Cosmochim. Acta 15, 6-9.

RICKARD, D.T. (1975). Kinetics and mechanism of pyrite formation at low temperatures. Am. Jour. Sci. 275, 636-652.

RIMSAITTE, J. (1975). Natural alteration of mica and reactions between released ions in mineral deposits. Clays and Clay Minerals 23, 247-255.

ROBBINS, C. and KELLER, W.D. (1952). Clay and other other non-carbonate minerals in some limestones. Jour. Sed. Pet. 22, 146-152.

ROBBINS, J.A. and CALLENDER, L. (1975). Diagenesis of manganese in Lake Michigan sediments. Am. Jour. Sci. 275, 512-533.

ROSENQVIST, I. Th. (1970). Formation of vivianite in Holocene clay sediments. Lithos 3, 327-334.

ROSWELL, D.M. and DE SWARDT, A.M.J. (1976). Diagenesis in Cape and Karroo sediments, South Africa, and its bearing on the hydrocarbon potential. Trans. Geol. S. Afr. 79, 81-145.

RUPKE, N.A. and STANLEY, D.J. (1974). Distinctive properties of turbiditic and hemipelagic mud layers in the Algero-Balaeric Basin, Western Mediterranean Sea. Smithsonian Contributions to the Earth Sciences, No.13.

RUSSEL, K.L. (1970) Geochemistry and halmrolysis of clay minerals, Rio Ameca, Mexico. Geochim. Cosmochim. Acta 24, 893-907.

SAHU, B.K. (1964). Depositional mechanisms from the size analysis of clastic sediments. Jour. Sed. Pet. 34, 73-83.

SARGENT, H.C. (1918). On a spilitic facies of the Lower Carboniferous lava-flows in Derbyshire. Quar. Jour. Geol. Soc. 73, 11-23.

SAWHNEY, B.L. (1972). Selective sorption and fixation of cations by clay minerals: A review. Clay and Clay Minerals, 20, 93-100.

SAXBY, J.D. (1972). Organic matter in Red Sea sediments. Chem. Geol. 9, 233-240.

SAXBY, J.D. (1973). Diagenesis of metal-organic complexes in sediments: Formation of metal sulphides from cystine complexes. Chem. Geol. 12, 241-248.

SAYLES, F.L. and BISCHOFF, J.L. (1973). Ferromanganoan sediments in the equatorial East Pacific. Earth Planet. Sci. Lett. 19, 330-336.

SCHLANGER, S.O. (1957). Dolomite growth in colalline algae. Jour. Sed. Pet. 27, 181-186.

SCHNITZER, M. and KODAMA, H. (1974). Reactions betwen fulvic acid and Ca^{2+} montmorillonite. Clay and Clay Minerals 20, 359-367.

SCHOEN, R. (1962). Semi-quantitative analysis of chlorites by X-ray diffraction. Am. Min. 47, 1384-1392.

SCHOETTLE, M. and FRIEDMAN, G.M. (1973). Organic carbon in sediments of Lake George, New York: Relation to morphology of lake bottom, grain size of sediments and man's activities. Geol. Soc. Am. Bull. 84, 191-198.

SCLATER, F.R., BOYLE, E. and EDMOND, J.M. (1976). On the marine geochemistry of nickel. Earth Planet. Sci. Lett. 31, 119-128.

SELIM, A.A. and DUFF, P.D. (1974). Carbonate facies in the Lower Carboniferous (Visean) of St. Monance, East Fife, Scotland. Jour. Sed. Pet. 44, 806-815.

SELLY, R.C. (1976). An introduction to sedimentology. Academic Press.

SEYFRIED, W. and BISCHOFF, J.L. (1977). Hydrothermal transport of heavy metals by seawater: The role of seawater/basalt ratio. Earth Planet. Sci. Lett. 34, 71-77.

SHAPIRO, L. (1960). A spectrophotometric method for the determination of FeO in rocks. U.S. Geol. Surv. Prof. Paper, 400-B, 496.

SHAW, H.F. (1973). Clay mineralogy of Quaternary sediments in the Wash embayments, Eastern England. Mar. Geol. 14, 29-45.

SHISHKINA, O.V. (1964). Chemical composition of pore solutions in oceanic sediments. Geochem. Int., No.3, 522-528.

SHOLKOVITZ, E.R. (1976). Flocculation of dissolved organic and inorganic matter during the mixing of river water and seawater. Geochim. Cosmochim. Acta 40, 831-845.

SIEVER, R. (1962). Silica solubility 0^{o}-200^{o}C, and the diagenesis of siliceous sediments. Jour. Geol. 70, 127-150.

SINGER, A. and NAVROT, J. (1976). Extraction of metals from basalt by humic acids. Nature 262, 479-480.

SKRIPCHENKO, N.S. (1969). Stability of sulfides and oxides in low-temperature mineral formation. Geochim. Int. 6, 262-267.

SLAUGHTER, M. and EARLEY, J.W. (1965). Mineralogy and geological significance of the Mowry Bentonites, Wyoming. Geol. Soc. Am. Spec. Paper 83.

SMITH, E.G. et al. (1967). Geology of the country around Chesterfield, Matlock and Mansfield. Mem. Geol. Surv.

SMITH, J.V. and YODER, H.S. (1956). Experimental and theoretical studies of the mica polymorphs. Min. Mag. 31, 209-231.

SMITH, J.W. and ROBB, W. (1966). Ankerite in the Green River Formation's Mahogany Zone. Jour. Sed. Pet. 36, 486-490.

SORBY, H.C. (1859). On the structure and origin of the Millstone Grit in South Yorkshire. Proc. Yorks. Geol. and Polytechnic. Soc. 3, 669-675.

SPEARS, D.A. (1963). Geochemistry of the Mansfield Marine Band. Ph.D. Thesis, University of Sheffield.

SPEARS, D.A. (1964). The major element geochemistry of the Mansfield Marine Band in the Westphalian of Yorkshire. Geochim. Cosmochim. Acta 28, 1679-1696.

SPEARS, D.A. (1966). A Westphalian tonstein from South Staffordshire. Proc. Yorks Geol. Soc. 35, 523-548.

SPEARS, D.A. (1970). A kaolinitic mudstone (tonstein) in the British Coal Measures. Jour. Sed. Pet. 40, 386-394.

SPEARS, D.A. (1971). The mineralogy of the Stafford tonstein. Proc. Yorks. Geol. Soc. 38, 497-516.

SPEARS, D.A. and SOTIRIOU, R.K. (1976). Titanium in some Carboniferous sediments from Great Britain. Geochim. Cosmochim. Acta 40, 345-351.

SPENCER, D. (1966). Factors affecting element distribution in a Silurian graptolite band. Chem. Geol. 1, 221-249.

SPENCER, E. (1925). Albite and other authigenic minerals in limestones from Bengal. Min. Mg. 20, 365-381.

SRODON, J. (1978). The relation between coal ane clay diagenesis in the Carboniferous of the Silesian Coal Basin. Proc. 6th Int. Clay Conf. Development in Sedimentology, 27, 251-260.

STEELE, K.F. and WAGNER, G.H. (1975). Trace metal relationships in bottom sediments of a fresh water stream - the Buffalo River, Arkansas. Jour. Sed. Pet. 45, 310-319.

STEPHEN, J.V. et al. (1953). Geology of the country between Bradford and Skipton. Mem½ Geol. Surv.

STEPHENS, W.E., WATSON, S.W., PHILLIP, P.R. and WEIR, J.A. (1975). Element associations and distributions through a Lower Palaeozoic graptolitic shale sequence in the Southern Upland of Scotland. Chem. Geol. 16, 269-294.

STEVENSON, I.P. and GAUNT, G.D. (1971). Geology of the country around Chapel-en-le-Frith. Mem. Geol. Surv. U.K.

STRAKOV, N.M. (1976). Origin of increased amounts of elements in pelagic sediments of the oceans. Int. Geol. 18, 406-416.

SULAIMAN, A. (1972). The geochemistry of the Namurian argillites of Ireland. Ph,D. Thesis, University of Southampton.

SUMMERHAYES, C.P. (1972). Geochemistry of continental margin sediments from north-west Africa. Chem. Geol. 10, 137-156.

SWAIN, F.M. (1970). Non-marine organic geochemistry. Cambridge University Press.

SZALAY, A. and SZILAGYI, M. (1967). The association of vanadium with humic acids. Geochim. Cosmochim. Acta 31, 1-6.

SZILAGYI, M. (1971). The role of organic material in the distribution of Mo, V and Cr in Coal Fields. Econ. Geol. 66, 1075-1078.

TAGGART, M.S. and KAISER, A.D. (1960). Clay mineralogy of Mississippi river deltaic sediments. Geol. Soc. Am. Bull. 71, 521-530.

TANK, R.W. and McNEELY, L. (1970). Clay minerals associated with the Pre-Cambrian Gowganda Formation of Ontario. Clay Minerals 8, 471-477.

TARDY, Y. (1971). Characterisation of the principal weathering types by the geochemistry of waters from some European and African crystalline massifs. Chem. Geol. 7, 253-271.

TAYLOR, J.M. (1950). Pore space reduction in sandstones. Bull. Am. Assoc. Petrol. Geol. 34, 701-716.

TAYLOR, P.S. and STOIBER, R.E. (1973). Soluble material on ash from active central American volcanoes. Geol. Soc. Am. Bull. 84, 1031-1042.

THOMPSON, G. (1973). A geochemical study of the low temperature interaction of seawater and oceanic igneous rocks. Trans. Am. Geophysical Union 59, 1015-1019.

THOMSON, I. (1971). Regional geochemical study of the black shale facies with particular reference to trace elements disorders in animals. Ph.D. Thesis, Imperial College, London.

TIKHOMIROVA, Y.S. (1960). The problem of the geochemical mobility of elements during the formation of sulfide concretions in shale-bearing deposits of the Volga and Baltic Basins. Geochemistry 135, 1098-1100.

TILL, R. (1969). Correlation and regression. Computer Applications, No.3, Nottingham University.

TILL, R. (1974). Statistical methods for the earth scientist. M.S.E.

TILL, R. and Spears, D.A. (1969). The determination of quartz in sedimentary rocks using an X-ray diffraction method. Clays and Clay Minerals 17, 323-327.

TODD, W.T. (1968). Palaeoclimatology and the relative stabilities of feldspar minerals under atmospheric conditions. Jour. Sed. Pet. 38, 3, 832-844.

TOMKEIEFF, S.I. (1926). On some chloritic minerals associated with the basaltic Carboniferous rocks of Derbyshire. Min. Mag. 21, 73-82.

TOMKEIEFF, S.I. (1941). Metasomatism in the basalt of Haddenrig Quarry near Kelso and the veining of the rocks exposed there. Min. Mag. 26, 49-59.

TOURTELOT, H.A. (1964). Minor-element composition and organic matter content of marine and non-marine shales of Late Cretaceous age in the western interior of the United States. Geochim. Cosmochim. Acta 28, 1579-1604.

TOWNSEND, F.C. and REED, L.W. (1971). Effects of amorphous constituents on some mineralogical and chemical properties of a Panamanian Latosol. Clays and Clay Minerals 19, 303-310.

TREWIN, N.H. (1968). K-bentonites in the Namurian of Staffordshire and Derbyshire. Proc. Yorks. Geol. Soc. 37, 73-91.

TRIPLEHORN, D.M. (1970). Clay mineral diagenesis in Atoka (Pennsylvanian) sandstones, Crawford County, Arkansas. Jour. Sed. Pet. 40, 838-847.

TROSTEL, L.J. and WYNNE, D.J. (1940). Determination of quartz (free silica) in refractory clays. Jour. Am. Ceram. Soc. 23, 18-22.

TROUP, B.N., BRICKER, O.P. and BRAY, J.T. (1974). Oxidation effect on the analysis of iron in the interstitial water of recent anoxic sediments. Nature 249, 237-239.

TUREKIAN, K.K. (1968). Oceans. Prentice Hall, Inc.

TUREKIAN, K.K. (1977). The fate of metals in the oceans. Geochim. Cosmochim. Acta 41, 1139-1144.

TUREKIAN, K.K. and CARR, M.H. (1960). The geochemistry of chromium, cobalt and nickel. Int. Geol. Congress - Norden, 14-26.

TUREKIAN, K.K. and IMBRIE, J. (1966). The distribution of trace elements in deep sea sediments of the Atlantic Ocean. Earth Planet. Sci. Lett. 1, 161-168.

TUREKIAN, K.K. and WEDEPOHL, K.H. (1961). Distribution of elements in some major rock units of the Earth's crust. Geol. Soc. Am. Bull. 72, 175-192.

VAN TASSEL, R. (1971). A jarositic mineral on Permian coal from Ngwibi Mountains, Northern Natal. Trans. Geol. Soc. S. Afr. LXXIV, 237-239.

VELDE, B. (1965). Experimental determination of muscovite polymorph stabilities. Am. Min. 50, 436-449.

VELDE, B. and HOWER, J. (1963). Petrological significance of illite polymorphism in Palaeozoic sedimentary rocks. Am. Min. 48, 1239-1254.

VENKATARATHNAM, K., HENDERSON, L. and BISCAYE, P.E. (1976). Clay mineralogy and sedimentation in the western Indian Ocean. Deep Sea Research 23, 949-961.

VISTELLIUS, A.B. (1970). Statistical models of silicate analysis and results of investigation of G-1 and W-1 samples. Math. Geol. 2, 1-14.

WAGGER, L.R. (1944). A stage in the decomposition of biotite from the Shap Granite. Proc. Yorks Geol. Soc. 25, 366-372.

WAKATSUKI, T., FURUKAWA, H. and KYUMA, K. (1977). Geochemical study of the redistribution of elements in soil. I. Evaluation of degree of weathering of transported soil materials by distribution of major elements among the particle size fractions and soil extract. Geochim. Cosmochim. Acta 41, 891-902.

WALKER, R.G. (1966). Shale Grit and Grindslow Shales: Transition from turbidites to shallow water sediments in the Upper Carboniferous of Northern England. Jour. Sed. Pet. 36, 90-114.

WALKER, T.R. (1960). Carbonate replacement of detrital crystalline silicate minerals as a source of authigenic silica in sedimentary rocks. Geol. Soc. Am. Bull. 71, 145-152.

WALKER, T.R. (1962). Reversible nature of chert-carbonate replacement in sedimentary rocks. Geol. Soc. Am. Bull. 73, 237-242.

WEAVER, C.E. (1953). Mineralogy and petrology of some Ordovician K-bentonites and related limestones. Geol. Soc. Am. Bull. 64, 921-944.

WEAVER, C.E. (1956). The distribution and identification of mixed-layer clays in sedimentary rocks. 4th National Conf. Clays and Clay Minerals, 385-386.

WEAVER, C.E. (1963). Interpretative value of heavy from bentonites. Jour. Sed. Pet. 33, 343-349.

WEAVER, C.E. (1976). The nature of TiO_2 in kaolinite. Clays and Clay Minerals 24, 215-218.

WEAVER, C.E. and BECK, K.C. (1971). Clay water diagenesis during burial: How mud becomes gneiss. Geol. Soc. Am. s.p. 134.

WEBER, J.N. and MIDDLETON, G.V. (1961). Geochemistry of the turbidites of the Normanskill and Charny Formations. I. Effect of turbidity currents on the chemical differentiation of turbidites. Geochim. Cosmochim Acta 22, 200-243.

WEBER, J.N. and MIDDLETON, G.V. (1961). Geochemistry of the turbidites of the Normanskill and Charny Formations. II. Distribution of trace elements. Geochim. Cosmochim. Acta 22, 244-288.

WEDEPOHL, K.H. (1967). Geochemical and petrographic investigation of the 'Kuperschiefer' in N.W. Germany. In: Chemistry of the Earth's Crust (Vinogradov, Ed.), 424-440.

WEIR, A.H., ORMEROD, E.C. and EL MANSEY, I.M.I. (1975). Clay mineralogy of sediments of the western Nile delta. Clay Minerals 10, 369-386.

WENTWORTH, C.K. (1922). A scale of grade class terms for clastic sediments. Jour. Geol. 30, 377-392.

WHITTAKER, E.J.W. and MUNTUS, R. (1970). Ionic radii for use in geochemistry. Geochim. Cosmochim. Acta 34, 945-956.

WILLIAMS, H., TURNER, F.J. and GILBERT, C.M. (1954). Petrography: An introduction to the study of rocks in thin section. Freeman and Company, San Francisco.

WILSON, D.A. (1955). A new method for the determination of ferrous iron in rocks and minerals. Bull. Geol. Surv. Gt. Br. 9, 56-58.

WILSON, M.D. and PITTMAN, E.D. (1977). Authigenic clays in sandstones: Recognition and influence on reservoir properties and palaeo-environmental analysis. Jour. Sed. Pet. 47, 3-31.

WINLAND, H.D. (1968). The role of high Mg calcite in the preservation of micrite envelopes and textural features of aragonite sediments. Jour. Sed. Pet. 38, 1320-1325.

WOOD, G.V. (1961). Discriminating between refractory and non-refractory quartzite by quantitative petrography. Jour. Sed. Pet. 31, 530-533.

WRIGHT, M.D. (1964). Cementation and compaction of the Millstone Grit of the Central Pennines, England. Jour. Sed. Pet. 34, 756-760.

WRIGHT, P.L. (1974). The chemistry and mineralogy of the clay fraction of sediments from the Southern Barents Sea. Chem. Geol. 13, 197-216.

ZOBELL, C.E. (1963). Organic geochemistry of sulfur. In: Organic Geochemistry, Monograph 16 (Breger, I.A., Ed.). Int. Series of Monographs on Earth Sciences, 543-578.

ZEBELL, C.E. (1964). Geochemical aspects of the microbial modification of carbon compounds. In: Advances in Organic Geochemistry, Monograph 15, (Colobo, V. and Hobson, G.D., Eds.), Int. Series of Monographs on Earth Sciences, 339-356.

APPENDIX 1

Chemical and Mineralogical Data of the Mam Tor Rocks

Major Element Analysis of the Mam Tor Shales and Sandstones

Oxides	9a	$8b_2$	$8b_1$	$8a_2$	$8a_1$	7a
SiO_2	50.18	75.37	77.39	51.50	51.40	49.27
Al_2O_3	24.29	9.64	8.89	24.28	24.49	27.24
TiO_2	1.09	0.50	0.38	0.88	0.90	0.91
Fe_2O_3	1.69	2.15	1.80	3.83	3.83	2.70
FeO	3.70	3.32	3.54	1.22	1.41	2.10
MgO	1.89	0.87	0.92	1.64	1.62	1.85
CaO	0.31	0.33	0.28	0.39	0.33	0.36
Na_2O	0.46	1.06	1.00	0.38	0.39	0.37
K_2O	2.53	0.79	0.63	2.93	2.81	3.11
MnO	0.09	0.16	0.2	0.11	0.18	0.20
P_2O_5	0.14	0.10	0.09	0.20	0.16	0.14
SO_3	0.03	0.09	0.00	0.00	0.05	0.00
Ig. Loss	13.49	4.96	4.70	12.88	12.95	12.60
Total	99.89	99.34	99.82	100.24	99.71	100.85
Corg.	3.94	0.26	0.00	1.08	2.45	1.76
CO_2	0.00	1.52	2.28	3.12	0.00	0.00
H_2O+	7.84	2.86	2.43	6.25	7.12	8.43
H_2O-	1.66	0.51	0.33	2.38	3.36	2.39

(Whole rock sample)

Major Element Analysis of the Mam Tor Shales and Sandstones

Oxides	$6b_3$	$6b_2$	$6b_1$	6b	6a	5a
SiO_2	84.0I	82.79	79.91	73.89	51.42	53.23
Al_2O_3	8.06	7.56	10.44	24.32	23.76	
TiO_2	0.35	0.49	0.46	0.50	1.09	1.03
Fe_2O_3	1.83	2.68	2.38	1.42	4.16	3.31
FeO	0.59	0.69	1.11	4.00	1.89	1.66
MgO	0.48	0.51	0.53	0.91	1.85	1.80
CaO	0.13	0.12	0.12	0.31	0.26	0.08
Na_2O	1.20	1.13	1.09	0.90	0.46	0.58
K_2O	0.50	0.63	0.66	0.84	2.46	2.65
MnO	0.04	0.05	0.05	0.14	0.05	0.02
P_2O_5	0.08	0.09	0.09	0.14	0.16	0.13
SO_3	0.00	0.01	0.00	0.07	0.00	0.21
Ig. Loss	2.80	2.96	4.03	6.29	11.60	11.72
Total	100.07	99.64	100.30	99.85	99.72	99.97
Corg.	0.24	0.38	0.23	0.99	2.11	1.70
CO_2	0.00	0.00	0.00	1.40	0.19	0.00
H_2O+	2.18	2.07	3.12	3.21	7.55	4.05
H_2O-	0.36	0.51	0.70	0.48	1.74	5.52

(Whole rock sample)

Major Element Analysis of the Mam Tor Shales and Sandstones

Oxides	$4b_3$	$4b_2$	$4b_1$	$4a_2$	4c	4a
SiO_2	67.64	68.09	77.78	50.85	64.20	59.73
Al_2O_3	14.59	13.58	8.37	24.48	15.99	20.07
TiO_2	0.72	0.71	0.38	1.05	0.82	0.95
Fe_2O_3	3.68	3.76	0.85	3.33	4.15	2.76
FeO	2.08	1.75	1.13	1.73	2.18	1.83
MgO	1.42	1.31	0.80	1.89	1.24	1.72
CaO	0.24	0.85	3.77	0.10	0.22	0.17
Na_2O	1.00	1.03	1.17	0.58	1.12	0.82
K_2O	1.36	1.23	0.57	2.90	1.46	2.08
MnO	0.15	0.12	0.14	0.06	0.04	0.06
P_2O_5	0.18	0.13	0.09	0.11	0.19	0.14
SO_3	0.21	0.15	0.11	0.30	0.32	0.00
Ig. Loss	6.29	6.60	5.60	12.20	7.15	9.34
Total	99.56	99.31	100.76	99.58	99.08	99.67
Corg.	0.49	0.77	0.11	2.83	0.86	1.49
CO_2	0.00	0.38	3.12	0.00	0.00	0.25
H_2O+	4.62	4.40	2.03	6.53	5.05	3.05
H_2O-	1.20	1.04	0.33	3.12	1.42	3.65

(Whole rock sample)

Major Element Analysis of the Mam Tor Shales and Sandstones

Oxides	3b	3a	2c	2b	2a	1b	1a
SiO_2	80.09	51.50	70.66	78.51	50.20	56.33	49.18
Al_2O_3	9.36	23.17	12.61	9.79	23.49	12.94	23.04
TiO_2	0.44	1.04	0.64	0.45	1.00	0.60	0.99
Fe_2O_3	1.51	4.41	3.10	1.64	5.19	3.64	5.14
FeO	1.90	1.39	2.54	1.85	1.43	8.55	2.72
MgO	0.67	1.80	1.23	0.73	1.74	2.32	2.30
CaO	0.39	0.12	0.41	0.62	0.13	1.07	0.30
Na_2O	1.20	0.62	1.09	1.13	0.53	0.93	0.54
K_2O	0.58	2.64	1.12	0.68	2.96	1.02	2.65
MnO	0.18	0.05	0.12	0.09	0.03	0.29	0.19
P_2O_5	0.10	0.13	0.18	0.08	0.13	0.32	0.19
SO_3	0.15	0.00	0.20	0.07	0.00	0.26	0.29
Ig. Loss	4.18	12.31	5.63	4.37	12.24	10.86	11.82
Total	100.75	99.18	99.53	100.01	99.07	99.13	99.35
Corg.	0.00	2.94	0.73	0.23	2.04	0.46	1.69
CO_2	1.05	0.12	0.10	0.00	0.12	5.52	0.44
H_2O+	2.70	6.37	3.98	2.78	7.57	4.19	7.33
H_2O-	0.28	2.91	0.84	0.48	2.46	0.69	2.35

(Whole rock sample)

Mineralogy of the Mam Tor Shales and Sandstones

Minerals	1a	1b	2a	2b	2c	3a
Quartz	16.20	46.20	14.90	63.20	55.90	18.90
Chlorite	7.77	5.24	6.70	1.71	5.22	7.58
Illite+ MXL‡	21.80	6.96	25.32	4.32	7.41	21.27
Kaolinite	36.89	24.90	32.36	13.56	22.39	34.21
Na-feldspar	4.57	7.86	4.48	9.55	9.21	5.24
Siderite		13.62				0.28
Dolomite	0.96			1.84		
Calcite			0.26		0.22	
Pyrite	0.21	0.20	0.00	0.05		
TiO_2	0.99	0.60	1.00	0.45	0.64	1.04
Apatite	0.45	0.45	0.30	0.18	0.42	0.42
exc.H_2O^+	0.42	0.05	1.30	0.67	0.20	0.19
exc.SiO_2			3.77			0.38
exc.Fe_2O_3	4.99	3.52	5.20	1.57	3.11	4.41
Organic Carbon	1.69	0.46	2.04	0.23	0.73	2.94
Total	96.97	98.64	97.62	96.89	98.39	96.85
H_2O-	2.35	0.69	2.46	0.48	0.84	2.91
SiO_2- *	1.64	11.61			7.06	

* Considering combined silica determination, it is more accurate to calculate the clay minerals percentage on Al_2O_3 than on combined silica basis.
The minus sign indicates the amount of SiO_2 needed.

‡ Mixed layer.

Mineralogy of the Mam Tor Shales and Sandstones

Minerals	3b	4a	4c	$4a_2$	$4b_1$	$4b_2$
Quartz	68.70	31.3	49.62	21.70	63.50	53.50
Chlorite	2.04	7.25	6.48	8.15	1.59	4.55
Illite+ MXL‡	4.22	17.37	10.89	23.09	4.05	9.23
Kaolinite	15.43	30.16	25.37	35.67	13.38	22.77
Na-feldspar	10.15	6.94	9.47	4.90	9.89	8.71
Siderite	2.53					
Dolomite		0.85			0.96	
Calcite					6.04	0.86
Pyrite	0.10		0.23	0.22	0.08	0.10
TiO_2	0.44	0.95	0.82	1.05	0.38	0.71
Apatite	0.23	0.33	0.45	0.26	0.21	0.30
exc. H_2O^+	0.22		0.42			0.82
exc. SiO_2						
exc. Fe_2O_3	1.36	2.76	3.84	3.03	0.74	3.61
Organic Carbon	0.00	1.49	0.86	2.83	0.11	0.77
Total	100.09	99.42	99.87	96.19	99.95	98.22
H_2O-	0.28	3.65	1.42	3.12	0.33	1.04
SiO_{2-}*	5.32	1.00	10.00	4.70	0.97	7.73

* Considering combined silica determination, it is more accurate to calculate the clay minerals percentage on Al_2O_3 than on combined silica basis.
The minus sign indicates the amount of SiO_2 needed.

‡ Mixed layer.

Mineralogy of the Mam Tor Shales and Sandstones

Minerals	$4b_3$	5a	6a	6b	$6b_1$	$6b_2$
Quartz	51.6	22.60	22.24	57.00	66.40	68.30
Chlorite	5.25	6.81	6.20	3.79	2.43	2.30
Illite+ MXL‡	9.65	20.93	20.81	6.38	4.57	4.05
Kaolinite	25.23	37.08	40.45	18.33	16.79	10.67
Na-feldspar	8.45	4.90	3.89	7.61	9.21	9.56
Siderite			0.45	3.59		
Dolomite						
Calcite	0.35					
Pyrite						0.23
TiO_2	0.72	1.03	1.09	0.50	0.46	0.42
Apatite	0.42	0.30	0.38	0.33	0.21	0.21
exc.H_2O^+	0.28		0.26	1.08	0.42	0.26
exc.SiO_2						
exc.Fe_2O_3	3.68	3.31	4.17	0.72	2.38	2.36
Organic Carbon	0.49	1.70	2.11	0.99	0.23	0.38
Total	98.49	96.92	98.04	99.40	99.59	98.45
H_2O-	1.20	1.87	1.74	0.48	0.70	0.51
SiO_2- *	7.60	2.26	4.00	0.92	3.52	0.29

* Considering combined silica determination, it is more accurate to calculate the clay minerals percentage on Al_2O_3 than on combined silica basis.
The minus sign indicates the amount of SiO_2 needed.

‡ Mixed layer.

Mineralogy of the Mam Tor Shales and Sandstones

Minerals	$6b_3$	7a	$8a_1$	$8a_2$	$8b_1$	$8b_2$	9a
Quartz	73.10	11.70	13.60	18.6	67.7	56.10	13.90
Chlorite	1.86	8.69	6.05	5.13	1.90	3.05	7.40
Illite + MXL‡	3.83	26.19	26.03	25.87	4.41	6.07	20.18
Kaolinite	12.00	43.39	35.36	33.11	14.75	15.29	43.31
Na-feldspar	10.15	3.12	3.30	3.21	8.97	8.46	3.89
Siderite				2.57	5.87	3.82	0.00
Dolomite							
Calcite							
Pyrite							
TiO_2	0.35	0.91	0.90	0.88	0.38	0.50	1.09
Apatite	0.19	0.32	0.38	0.47	0.21	0.25	0.33
exc.H_2O+	0.35	0.46	0.09		0.04	0.20	0.26
exc.SiO_2			5.00	1.29		2.77	1.91
exc.Fe_2O_3	1.83	2.70	3.79	3.83	1.80	2.06	1.63
Organic Carbon	0.24	1.76	2.45	1.08	0.00	0.26	3.94
Total	99.83	97.28	96.95	96.00	99.84	99.34	97.84
H_2O-	0.36	2.39	3.36	3.38	0.33	0.51	1.66
SiO_2-*	4.06	0.86			5.68		

* Considering combined silica determination, it is more accurate to calculate the clay minerals percentage on Al_2O_3 than on combined silica basis.
The minus sign indicates the amount of SiO_2 needed.

‡ Mixed layer.

Some text bound close to the spine.

Major Element Analysis of Different Size Fractions (in μm) of Sample 2c

Oxides	0.5-1	1-2	2-3.9	3.9-7.8	7.8-15.6	15.6-22.1	22.1-31	31-53
SiO_2	46.14	46.62	49.66	50.23	53.33	58.61	59.29	67.14
Al_2O_3	27.67	25.91	24.80	22.67	21.32	18.71	17.97	14.83
TiO_2	1.03	1.18	1.07	1.12	1.40	1.30	1.08	0.97
Fe_2O_3	4.96	4.60	4.49	5.16	4.61	4.15	4.42	4.19
FeO	2.99	3.51	3.03	3.22	3.52	3.10	3.07	2.24
MgO	2.21	2.20	1.98	1.96	1.94	1.93	1.91	1.48
CaO	0.31	0.41	0.30	0.31	0.35	0.37	0.43	0.48
Na_2O	0.39	0.50	0.76	0.99	0.99	1.27	1.32	1.44
K_2O	3.16	2.57	2.27	2.08	2.06	1.90	1.74	1.27
MnO	0.11	0.14	0.13	0.17	0.19	0.18	0.17	0.17
P_2O_5	0.24	0.28	0.21	0.23	0.23	0.22	0.24	0.25
SO_3	0.29	0.34	0.34	0.44	0.67	0.64	0.42	0.44
Ig. Loss	11.35	11.23	11.20	11.36	10.01	7.80	7.79	5.64
[illegible]	[illegible]	[illegible]	[illegible]	[illegible]	[illegible]	[illegible]	[illegible]	[illegible]

Major Element Analysis of Different size Fractions (in μm) of Sample 4c

Oxides	< 2	2-3.9	3.9-7.8	7.8-15.6	15.6-22.1	22.1-31	31-53
SiO_2	43.82	44.32	45.46	49.14	56.05	60.40	72.01
Al_2O_3	23.85	23.34	22.35	20.78	18.21	16.36	12.25
TiO_2	1.03	1.09	1.08	1.10	1.07	1.00	0.80
Fe_2O_3	8.92	9.63	8.66	7.47	5.98	5.24	3.88
FeO	3.92	3.55	3.48	3.46	3.27	2.97	2.05
MgO	2.40	2.40	2.23	2.12	1.93	1.86	1.24
CaO	0.24	0.22	0.27	0.28	0.28	0.27	0.28
Na_2O	0.55	0.62	0.72	0.89	1.20	1.16	1.35
K_2O	2.22	2.13	2.05	2.03	1.90	1.72	1.28
MnO	0.12	0.14	0.14	0.18	0.12	0.09	0.06
P_2O_5	0.35	0.36	0.33	0.29	0.26	0.21	0.17
SO_3	0.00	0.21	0.00	0.00	0.00	0.26	0.19
Ig. Loss	12.61	12.49	13.39	12.80	10.11	8.13	4.87
Total	100.03	100.50	100.15	100.54	100.38	99.61	100.43

Major Element Analysis of Different Size Fractions (in μm) of Sample 2a

Oxides	< 0.5	0.5-1	1-2	2-3.9
SiO_2	47.57	47.74	47.80	49.19
Al_2O_3	29.62	28.74	28.66	27.60
TiO_2	0.63	0.76	0.79	0.89
Fe_2O_3	5.00	4.57	4.34	4.34
FeO	1.03	1.30	1.43	1.46
MgO	1.62	1.81	1.80	1.86
CaO	0.46	0.46	0.43	0.42
Na_2O	0.09	0.12	0.14	0.22
K_2O	3.71	3.57	3.52	3.36
MnO	0.07	0.08	0.06	0.06
P_2O_5	0.22	0.22	0.20	0.20
SO_3	0.14	0.00	0.15	0.05
Ig. Loss	10..27	11.18	10.75	10.95
Total	100.43	100.55	100.07	100.60

Major Element Analysis of Different Size Fractions (in μm) of the Sandstones

	3b			$4b_1$			6b			
Oxides	< 2	2-7.8	7.8-53	< 2	2-7.8	7.8-53	< 2	2-7.8	7.8-53	53
SiO_2	54.42	62.54	73.43	63.93	67.47	81.06	45.43	47.84	70.81	89.55
Al_2O_3	20.66	16.50	10.93	17.87	13.01	6.98	24.43	23.42	12.25	5.26
TiO_2	0.61	0.65	0.73	0.51	0.54	0.45	0.85	0.87	0.94	0.27
Fe_2O_3	3.74	3.38	2.64	2.24	1.93	0.98	7.36	6.25	3.38	1.12
FeO	4.32	3.56	2.89	1.48	1.32	0.96	4.12	4.75	2.65	0.30
MgO	1.47	1.15	0.88	1.06	1.00	0.71	1.84	1.65	1.01	0.22
CaO	0.48	0.49	0.48	2.67	4.33	2.70	0.36	0.37	0.38	0.12
Na_2O	1.05	1.35	1.61	1.15	1.47	1.58	0.74	1.03	1.82	1.44
K_2O	1.55	1.14	0.80	1.05	0.79	0.51	1.91	1.49	0.99	0.48
MnO	0.22	0.26	0.21	0.20	0.17	0.11	0.22	0.22	0.12	0.03
P_2O_5	0.21	0.17	0.18	0.10	0.14	0.12	0.27	0.24	0.20	0.04
SO_3	0.01	0.00	0.08	0.19	0.16	0.21	0.27	0.19	0.14	0.10
Ig.Loss	10.91	8.76	5.68	8.15	8.01	3.86	11.53	11.45	4.95	1.39
Total	99.65	99.95	100.54	99.60	100.34	100.23	99.60	99.77	99.64	100.50

Major Element Analysis of Different Size Fractions (in μm) of the Sandstones

Oxides	6b3				8b1			
	< 2	2-7.8	7.8-53	53	< 2	2-7.8	7.8-53	53
SiO_2	51.51	59.12	76.72	92.77	50.25	54.17	82.37	92.90
Al_2O_3	22.47	21.43	11.05	3.58	22.29	19.13	6.61	3.31
TiO_2	0.71	0.73	0.79	0.16	0.63	0.63	0.47	0.16
Fe_2O_3	9.43	4.81	2.84	0.43	7.08	6.28	2.12	0.68
FeO	1.55	1.62	0.92	0.19	4.40	5.29	1.30	0.41
MgO	1.24	0.92	0.63	0.11	1.58	1.41	0.38	0.17
CaO	0.26	0.20	0.24	0.14	0.29	0.36	0.32	0.21
Na_2O	0.87	1.45	2.20	1.23	0.77	1.07	1.47	1.14
K_2O	1.76	1.19	0.88	0.32	1.61	1.12	0.49	0.22
MnO	0.15	0.18	0.10	0.04	0.17	0.28	0.31	0.09
P_2O_5	0.22	0.14	0.13	0.05	0.16	0.14	0.11	0.05
SO_3	0.17	0.05	0.08	0.03	0.17	0.15	0.10	0.04
Ig. Loss	9.89	8.70	3.67	1.05	10.37	10.43	3.52	1.15
	100.22	100.60	100.07	100.10	99.77	100.46		

Major Element Analysis of Different Size Fractions (in μm) of the Shales

Oxides	1a			3a			5a		
	< 2	2-7.8	7.8-53	< 2	2-7.8	7.8-53	< 2	2-7.8	7.8-53
SiO_2	45.30	49.95	58.18	47.78	52.20	56.52	46.93	51.52	60.57
Al_2O_3	26.34	22.90	19.20	26.69	23.66	21.35	28.52	24.86	19.82
TiO_2	1.02	1.15	1.03	1.11	1.14	1.03	1.00	1.21	1.12
Fe_2O_3	5.72	6.80	6.59	4.25	3.49	4.43	4.40	3.60	3.22
FeO	2.54	2.30	2.05	1.58	1.70	1.35	1.30	1.38	1.22
MgO	2.13	1.92	1.57	1.80	1.68	1.46	1.93	1.91	1.50
CaO	0.14	0.19	0.22	0.09	0.12	0.15	0.10	0.12	0.17
Na_2O	1.33	0.79	1.16	1.26	1.08	1.18	1.26	0.91	1.23
K_2O	3.03	2.54	1.92	3.28	2.83	2.46	3.54	2.92	2.20
MnO	0.08	0.06	0.11	0.06	0.05	0.09	0.07	0.07	0.11
P_2O_5	0.15	0.14	0.12	0.12	0.07	0.07	0.11	0.09	0.07
SO_3	0.33	0.85	0.37	0.00	0.10	0.19	0.19	0.18	0.15
Ig.Loss	12.05	11.05	7.34	12.00	11.34	9.53	10.89	11.77	8.83
Total	100.16	100.64	100.26	100.02	99.56	99.81	100.24	[illegible]	100.27

Major Elements of Different Size Fractions (in μm) of the Shales

Oxides	6a			9a		
	< 2	2-7.8	7.8-53	< 2	2-7.8	78-53
SiO_2	45.84	48.13	55.17	45.45	46.70	54.29
Al_2O_3	29.15	27.53	22.78	29.25	27.16	22.33
TiO_2	0.94	1.17	1.15	1.02	1.18	1.16
Fe_2O_3	4.68	3.54	3.41	3.35	3.11	2.86
FeO	1.54	2.13	1.59	2.13	2.62	3.05
MgO	1.99	1.86	1.58	1.99	1.86	1.89
CaO	0.25	0.23	0.25	0.26	0.27	0.33
Na_2O	0.15	0.36	0.72	0.19	0.36	0.81
K_2O	3.45	2.81	2.34	3.27	2.84	2.35
MnO	0.14	0.09	0.11	0.13	0.12	0.09
P_2O_5	0.17	0.16	0.15	0.15	0.14	0.17
SO_3	0.10	0.17	0.18	0.20	0.37	0.50
Ig.Loss	11.51	12.20	10.64	12.17	12.57	10.21
[illegible]	99.51	100.39	100.32	99.56	99.30	[illegible]

Major Element Analysis of the Clay Fractions
of the remaining sandstones and shales

Oxides	2b	4a	$4a_2$	$4b_2$	$4b_3$	$6b_1$
SiO_2	50.47	46.38	47.76	44.35	48.26	47.02
Al_2O_3	24.14	28.18	26.25	26.31	24.19	24.59
TiO_2	0.76	1.04	1.10	1.07	1.11	0.75
Fe_2O_3	3.38	5.40	3.78	6.49	7.02	9.64
FeO	4.74	1.32	1.32	3.36	2.40	2.40
MgO	1.60	1.98	1.99	2.57	1.95	1.52
CaO	0.44	0.16	0.11	0.68	0.17	0.16
Na_2O	0.77	0.31	0.49	0.37	0.59	0.80
K_2O	1.95	3.50	3.23	2.74	2.54	2.07
MnO	0.29	0.10	0.06	0.22	0.23	0.08
P_2O_5	0.18	0.14	0.12	0.22	0.25	0.22
SO_3	0.24	0.00	0.00	0.20	0.05	0.24
Ig. Loss	10.56	12.32	13.25	11.87	11.48	10.73
Total	99.52	100.83	99.46	100.45	100.24	100.22

Major Element Analysis of the Clay Fractions
of the remaining sandstones and shales

Oxides	$6b_2$	7a	$8a_1$	$8a_2$	$8b_2$
SiO_2	51.82	47.16	48.78	48.18	47.38
Al_2O_3	22.03	30.32	28.32	27.86	25.06
TiO_2	1.04	0.84	0.88	0.85	0.89
Fe_2O_3	8.22	3.06	3.68	5.18	6.91
FeO	2.47	1.48	1.36	1.03	3.94
MgO	1.27	1.84	1.74	1.81	2.10
CaO	0.20	0.33	0.28	0.38	0.42
Na_2O	1.39	0.21	0.66	0.20	0.52
K_2O	1.29	3.62	3.38	3.41	2.49
MnO	0.09	0.07	0.12	0.10	0.32
P_2O_5	0.26	0.11	0.14	0.21	0.21
SO_3	0.24	0.15	0.07	0.07	0.19
Ig.Loss	9.73	10.70	10.20	10.91	10.28
Total	100.05	99.89	99.61	100.19	100.71

Trace Element Contents (ppm) of the Mam Tor Rocks

(a = shales; b,c = sandstones)

Sample No.	Ni	Co	Mn	V	Cr	Zn	Cu	Rb	Sr	Y	Zr	Pb	Ba
1a	100	26	1033	134	168	132	51	131	127	57	136	46	457
1b	43	19	2163	87	91	109	27	47	91	54	233	11	307
2a	59	2	175	142	171	77	50	137	98	34	141	47	460
2b	34	11	743	46	116	61	12	26	71	27	259	15	249
2c	66	30	828	76	98	93	20	50	87	39	254	22	273
3a	59	2	146	135	171	59	28	130	109	32	149	52	541
3b	38	20	1115	42	77	81	13	24	65	44	285	17	221
4a	56	1	148	113	153	60	34	106	104	35	254	37	422
4c	55	15	344	95	129	77	27	70	85	39	257	25	323
$4a_2$	75	24	471	139	181	73	41	144	120	43	151	56	553
$4b_1$	19	7	848	33	73	66	10	25	142	23	279	12	225
$4b_2$	39	7	670	86	100	62	22	57	100	27	261	28	275
$4b_3$	71	33	973	85	110	116	30	62	87	39	242	28	293
5a	76	8	147	141	166	68	46	128	122	35	155	48	469
6a	88	9	397	134	165	103	45	115	100	44	167	36	433
6b	41	24	932	55	76	86	18	34	59	32	237	14	174
$6b_1$	16	5	144	47	61	28	12	23	48	12	298	19	214
$6b_2$	16	17	116	43	74	31	11	22	47	15	257	20	139
$6b_3$	35	15	279	38	49	28	5	22	43	17	215	13	144
7a	113	31	951	143	166	76	51	145	110	30	101	45	425
$8a_1$	79	9	892	146	158	95	51	136	94	37	113	46	396
$8a_2$	76	4	984	153	158	80	57	145	99	38	118	49	387
$8b_1$	21	11	1497	44	57	52	12	27	57	18	258	19	154
$8b_2$	24	4	1351	54	70	46	14	34	64	21	208	16	182
9a	83	20	687	142	178	99	42	118	98	40	193	44	507

Trace Element Contents (ppm) of the Clay Fractions

(< 2μm), Mam Tor rocks

Sample No.	Ni	Co	Mn	V	Cr	Zn	Cu	Rb	Sr	Y	Zr	Pb	Ba
3a	66	0	113	152	202	91	49	163	133	30	103	63	521
3b	135	36	1962	96	107	279	48	72	97	77	77	51	329
$4a_2$	61	6	194	147	198	101	51	160	137	34	115	54	544
$4b_1$	58	4	1222	61	82	180	53	53	127	33	94	32	239
5a	88	3	104	164	222	162	83	173	146	46	105	53	526
6a	90	16	486	170	217	114	60	152	123	43	99	49	474
6b	99	37	1319	128	138	197	73	75	107	46	7I	39	322
$6b_2$	52	16	242	116	131	146	114	57	83	25	152	54	282
$6b_3$	67	29	891	116	136	180	44	72	104	29	74	42	267
7a	127	35	543	154	190	112	49	161	194	27	78	31	434
$8a_1$	96	15	703	165	188	121	63	163	113	32	80	45	394
$8a_2$	93	12	686	164	185	144	71	161	103	41	83	44	394
$8b_1$	61	17	1210	103	109	151	43	75	103	35	67	37	251
9a	118	41	826	177	225	119	64	149	135	39	102	53	447

Trace Element Contents (ppm) of Different Size Fractions, Mam Tor rocks

	Size in μm	Ni	Co	Mn	V	Cr	Zn	Cn	Rb	Sr	Y	Zr	Pb	Ba
3a	53-7.8	52	3	118	111	156	66	31	116	120	32	182	32	447
	7.8-2	56	0	127	117	168	71	28	141	131	28	133	33	484
	< 2	66	0	113	152	202	91	49	163	133	30	103	63	521
3b	53-7.8	54	16	1637	47	97	152	27	34	79	67	359	23	209
	7.8-2	84	20	1789	65	84	174	39	49	85	57	110	32	261
	2	135	36	1962	96	107	279	48	72	97	77	77	63	521
$4b_1$	53-7.8	22	3	690	21	56	87	28	15	129	27	356	11	161
	7.8-2	36	1	1503	40	60	207	66	31	175	33	131	16	200
	< 2	58	4	1222	61	82	180	53	53	127	33	94	32	239
6a	53-7.8	63	21	519	108	144	92	40	115	94	41	223	38	423
	7.8-2	82	21	462	135	169	116	57	139	115	44	113	46	458
	< 2	90	16	486	170	217	114	60	152	123	43	99	49	474
6b	53-7.8	44	9	668	61	95	113	34	42	80	50	602	22	225
	7.8-2	78	28	1509	103	123	184	56	67	82	44	101	30	296
	< 2	99	37	1319	128	138	197	73	75	107	46	71	39	322

APPENDIX 2

Chemical and Mineralogical Data of the Tansley Borehole Rocks

Major elements analysis of the Tansley Borehole Sediments

Oxides	1	2	3	4	5	6
SiO_2	47.73	49.36	50.29	82.34	52.59	82.00
Al_2O_3	23.57	24.87	20.90	7.91	6.04	7.64
TiO_2	0.82	0.93	0.89	0.53	0.16	0.28
Fe_2O_3	2.46	3.02	6.65	0.42	1.82	1.29
FeO	1.98	3.19	0.64	1.21	2.29	1.25
MgO	1.76	1.62	1.51	0.40	6.42	0.65
CaO	0.50	0.60	0.27	0.15	9.81	0.65
Na_2O	0.20	0.57	0.14	1.36	0.64	1.00
K_2O	2.38	2.31	3.61	2.14	2.09	2.18
MnO	0.07	0.09	0.04	0.01	0.23	0.05
P_2O_5	0.24	0.33	0.07	0.08	0.06	0.05
SO_3	0.52	0.25	3.96	0.30	0.80	0.42
Ig. Loss	17.78	12.02	10.55	2.33	16.88	1.75
Total	100.01	99.12	99.52	99.18	99.83	99.20
Corg.	9.05	2.74	4.24	0.75	0.63	0.18
CO_2	0.24	1.60	0.00	0.12	14.77	0.68
H_2O+	8.49	7.68	6.31	1.46	1.48	0.88
H_2O-	1.94	1.75	2.47	2.47	0.26	0.16

Major elements analysis of the Tansley Borehole Sediments

Oxides	7	8	9	10	11	12
SiO_2	72.73	64.00	61.29	68.41	54.30	78.46
Al_2O_3	11.26	16.20	18.38	13.35	23.25	6.50
TiO_2	0.66	0.89	0.98	0.55	1.09	0.36
Fe_2O_3	3.05	2.49	1.91	1.94	2.60	0.95
FeO	3.18	2.99	3.48	2.84	2.67	1.32
MgO	1.62	2.03	1.92	1.79	1.99	1.46
CaO	0.19	0.52	0.45	2.07	0.42	2.80
Na_2O	1.34	0.82	0.89	1.21	0.66	1.39
K_2O	2.32	2.79	2.84	1.51	3.24	0.75
MnO	0.05	0.11	0.56	0.22	0.05	0.11
P_2O_5	0.08	0.14	0.13	0.12	0.14	0.07
SO_3	0.40	0.52	0.19	0.48	0.34	0.34
Ig. Loss	3.81	6.44	7.31	6.31	9.25	5.57
Total	100.69	99.94	100.33	100.80	100.00	100.08
Corg.	0.53	1.55	1.74	0.99	2.34	0.80
CO_2	0.16	0.40	2.46	0.20	3.40	1.26
H_2O+	3.12	4.49	5.17	2.86	6.71	1.37
H_2O-	0.52	1.34	0.90	0.20	1.06	0.20

Major elements analysis of the Tansley Borehole Sediments

Oxides	13	14	15	16	17	18
SiO_2	64.25	55.85	56.94	60.33	60.76	56.01
Al_2O_3	16.13	23.14	21.54	20.23	18.75	21.32
TiO_2	0.65	1.01	0.99	0.94	0.94	0.94
Fe_2O_3	1.42	3.18	2.64	2.61	1.84	2.96
FeO	4.60	2.34	2.47	2.98	3.18	2.41
MgO	1.25	1.94	1.87	1.73	1.64	1.74
CaO	0.98	0.40	0.42	0.45	0.36	0.39
Na_2O	1.16	0.86	0.82	0.85	0.89	0.80
K_2O	1.78	2.98	2.80	2.76	2.54	2.66
MnO	0.32	0.06	0.10	0.12	0.08	0.09
P_2O_5	0.03	0.15	0.16	0.19	0.12	0.17
SO_3	0.22	0.30	0.25	0.70	0.38	0.41
Ig. Loss	8.02	8.59	9.31	6.11	7.56	9.97
Total	100.81	100.80	100.31	100.00	99.03	99.87
Corg.	2.71	1.75	2.65	0.19	1.78	2.95
CO_2	1.26	0.30	0.52	0.84	0.52	1.00
H_2O+	4.05	6.54	6.14	5.05	5.26	6.02
H_2O-	0.94	1.46	1.28	1.00	1.06	1.56

Major elements analysis of the Tansley Borehole Sediments

Oxides	19	20	21	22	23	24
SiO_2	52.38	51.64	52.08	52.86	54.00	52.13
Al_2O_3	24.18	25.54	24.79	23.06	21.79	24.41
TiO_2	0.91	0.90	0.87	0.90	0.92	0.91
Fe_2O_3	2.23	2.48	2.13	3.14	3.41	2.87
FeO	3.52	2.19	3.22	3.14	3.14	2.76
MgO	1.47	1.51	1.97	1.58	1.92	1.66
CaO	0.33	0.43	0.39	0.53	0.55	0.44
Na_2O	0.62	0.57	0.59	0.64	0.72	0.72
K_2O	2.44	2.41	2.48	2.42	2.36	2.37
MnO	0.06	0.05	0.13	0.09	0.11	0.04
P_2O_5	0.14	0.21	0.17	0.27	0.26	0.18
SO_3	0.00	0.30	0.41	0.27	0.63	0.60
Ig. Loss	11.25	11.29	10.71	10.86	10.69	11.44
Total	99.53	99.52	99.94	99.76	100.50	100.53
Corg.	2.67	2.22	1.59	2.48	2.67	2.50
CO_2	1.15	0.52	1.13	1.12	1.51	1.12
H_2O+	7.43	8.55	7.99	7.26	6.51	7.82
H_2O-	1.55	2.15	1.83	1.56	1.26	1.10

Major elements analysis of the Tansley Borehole Sediments

Oxides	25	26	27	28	29	30
SiO_2	51.19	40.28	50.26	56.35	48.84	49.29
Al_2O_3	22.41	17.13	24.29	21.95	20.92	20.55
TiO_2	0.95	0.70	0.92	0.94	0.79	0.80
Fe_2O_3	5.20	1.50	3.35	2.21	6.93	8.16
FeO	1.16	15.23	1.99	2.10	1.46	0.42
MgO	1.51	2.67	1.71	1.52	1.41	1.63
CaO	0.26	1.58	0.28	0.30	0.33	0.38
Na_2O	0.78	0.60	0.60	0.70	0.62	0.51
K_2O	2.03	1.57	2.29	2.23	2.69	2.87
MnO	0.06	0.35	0.02	0.09	0.01	0.14
P_2O_5	0.10	0.50	0.20	0.17	0.14	0.15
SO_3	3.20	0.00	1.47	0.68	4.48	3.65
Ig. Loss	11.00	17.71	12.53	11.65	12.06	11.03
Total	99.85	99.82	99.91	100.89	100.67	99.58
Corg.	2.90	0.84	4.78	4.59	4.33	3.44
CO_2	0.40	14.31	0.28	0.60	0.20	0.40
H_2O+	7.70	2.56	7.47	6.46	7.53	7.19
H_2O-	1.30	1.68	2.07	2.67	1.68	1.56

Major elements analysis of the Tansley Borehole Sediments

Oxides	31	32	33	34	35	36
SiO_2	42.51	46.51	44.70	49.76	44.82	41.77
Al_2O_3	17.15	19.21	18.17	22.65	19.43	18.21
TiO_2	0.70	0.73	0.72	0.77	0.66	0.63
Fe_2O_3	10.45	6.82	10.66	6.84	7.88	10.38
FeO	0.25	1.27	0.60	0.47	0.39	0.68
MgO	1.35	1.41	1.36	1.39	1.24	1.17
CaO	4.37	3.84	2.54	0.99	0.60	1.95
Na_2O	0.40	0.46	0.42	0.67	0.80	0.66
K_2O	2.53	3.01	2.81	2.57	2.36	2.25
MnO	0.11	0.04	0.06	0.10	0.06	0.08
P_2O_5	0.14	0.13	0.12	0.09	0.07	0.16
SO_3	6.98	4.18	7.28	3.05	1.50	3.80
Ig. Loss	12.52	12.19	11.01	9.86	19.79	17.66
Total	99.46	99.80	100.45	99.21	99.57	99.40
Corg.	3.33	2.98	3.41	1.45	11.90	10.86
CO_2	3.32	3.28	1.88	0.21	0.00	0.80
H_2O+	5.87	5.93	5.66	8.21	7.89	6.00
H_2O-	1.66	1.40	1.54	2.14	4.37	5.55

Major elements analysis of the Tansley Borehole Sediments

Oxides	37	38	39	40	41	42
SiO_2	39.07	46.53	63.21	66.68	57.45	53.72
Al_2O_3	13.24	12.92	15.69	15.59	20.45	20.84
TiO_2	0.61	0.61	0.74	0.75	0.86	0.84
Fe_2O_3	9.91	3.85	1.96	1.62	2.49	4.63
FeO	7.26	12.60	3.57	1.68	2.82	1.02
MgO	3.19	2.01	1.14	0.92	1.18	1.05
CaO	4.66	0.85	0.41	0.31	0.32	0.29
Na_2O	0.38	0.62	0.78	0.14	0.66	0.64
K_2O	1.75	1.65	1.87	1.77	2.23	2.33
MnO	0.41	0.21	0.10	0.08	0.10	0.05
P_2O_5	0.09	0.25	0.16	0.11	0.14	0.11
SO_3	2.73	1.84	0.00	0.51	0.70	2.13
Ig. Loss	16.65	15.10	9.78	8.20	10.11	12.14
Total	99.95	99.04	99.41	98.28	99.51	99.79
Corg.	1.55	1.65	3.67	2.98	3.70	3.40
CO_2	10.38	10.04	2.25	1.08	0.40	0.25
H_2O+	4.72	3.41	3.86	4.14	6.01	8.94
H_2O-	1.46	1.20	1.28	1.28	1.40	1.60

Major elements analysis of the Tansley Borehole Sediments

Oxides	43	44	45	46	47	48
SiO_2	54.17	28.74	50.93	47.78	44.76	38.68
Al_2O_3	23.15	11.74	23.16	18.12	17.69	14.65
TiO_2	0.87	0.47	0.75	0.67	0.65	0.58
Fe_2O_3	2.87	5.86	5.43	9.18	10.29	8.37
FeO	1.47	21.14	0.74	0.27	0.24	1.77
MgO	1.23	3.17	1.28	1.43	1.34	2.46
CaO	0.27	1.46	0.24	2.17	3.89	9.84
Na_2O	0.74	0.43	0.66	0.59	0.47	0.41
K_2O	2.23	1.22	2.46	2.87	2.57	2.23
MnO	0.07	0.62	0.02	0.06	0.08	0.17
P_2O_5	0.13	0.69	0.87	0.11	0.11	0.16
SO_3	0.22	2.73	2.33	3.43	6.38	3.00
Ig. Loss	13.06	21.17	11.64	12.47	11.96	18.86
Total	100.48	99.98	99.72	99.24	100.43	100.68
Corg.	5.55	0.33	3.51	4.68	3.35	3.88
CO_2	0.30	18.43	0.40	0.76	2.32	10.40
H_2O+	7.21	2.96	7.73	7.03	6.29	4.58
H_2O-	1.97	0.85	1.88	2.13	2.32	1.40

Major elements analysis of the Tansley Borehole Sediments

Oxides	49	50	51	52	53	54
SiO_2	34.44	46.92	51.33	49.52	48.06	45.44
Al_2O_3	12.80	19.50	24.62	21.66	17.97	16.80
TiO_2	0.48	0.73	0.82	0.81	0.74	0.75
Fe_2O_3	9.00	7.56	4.55	7.77	8.43	5.96
FeO	0.52	0.34	1.46	0.75	0.40	0.04
MgO	2.33	1.40	1.65	1.79	1.54	1.92
CaO	12.57	2.11	0.35	0.44	3.01	7.67
Na_2O	0.36	0.64	0.57	0.84	0.51	0.39
K_2O	2.08	2.40	2.59	2.35	2.50	2.00
MnO	0.16	0.06	0.03	0.13	0.04	0.10
P_2O_5	0.27	0.11	0.15	0.14	0.13	0.15
SO_3	5.54	5.30	2.38	4.28	5.18	2.85
Ig. Loss	20.14	11.04	9.18	10.39	11.97	15.37
Total	100.54	98.09	99.68	100.87	100.48	100.44
Corg.	5.32	3.89	1.19	1.57	4.18	3.13
CO_2	10.46	0.57	0.24	0.50	2.04	6.97
H_2O+	4.18	6.49	7.75	8.32	5.75	5.27
H_2O-	1.18	1.90	1.51	1.70	1.77	1.48

Major elements analysis of the Tansley Borehole Sediments

Oxides	55	56	57	58	59	60
SiO_2	54.43	48.55	47.87	31.75	39.59	47.97
Al_2O_3	20.70	19.76	18.65	12.35	15.20	17.31
TiO_2	0.89	0.81	0.82	0.47	0.62	0.76
Fe_2O_3	5.62	7.39	8.00	8.93	7.64	6.80
FeO	0.59	0.42	0.72	0.89	0.71	0.71
MgO	1.37	1.31	1.32	2.16	1.45	1.87
CaO	2.05	2.29	1.65	14.26	8.73	4.58
Na_2O	0.42	0.41	0.49	0.41	0.44	0.56
K_2O	3.01	2.83	2.63	1.74	2.33	2.74
MnO	0.10	0.48	0.05	0.09	0.09	0.08
P_2O_5	0.15	0.13	0.13	0.27	0.23	0.17
SO_3	1.78	3.23	4.40	3.60	4.40	2.53
Ig. Loss	9.95	11.90	12.90	24.01	17.83	12.94
Total	101.06	99.11	99.63	100.91	99.25	99.02
Corg.	2.37	4.88	4.58	6.44	5.15	3.99
CO_2	1.60	1.36	0.92	12.75	7.20	3.36
H_2O+	5.98	6.66	7.40	4.77	5.48	5.58
H_2O-	1.23	1.90	1.90	1.05	1.39	1.85

Major elements analysis of the Tansley Borehole Sediments

Oxides	61	62	63	64	65	66
SiO_2	39.04	44.98	47.62	48.71	32.09	21.66
Al_2O_3	13.29	16.50	19.21	18.27	10.74	5.66
TiO_2	0.55	0.80	0.83	0.82	0.54	0.25
Fe_2O_3	8.95	6.93	8.09	8.14	6.89	3.27
FeO	0.52	0.77	0.61	0.70	0.83	0.51
MgO	1.73	1.76	1.67	1.76	5.26	10.76
CaO	10.04	6.69	1.26	2.83	13.60	20.22
Na_2O	0.47	0.57	0.58	0.66	0.42	0.03
K_2O	2.30	2.59	2.89	3.41	2.06	1.16
MnO	0.06	0.16	0.18	0.16	0.27	0.49
P_2O_5	0.17	0.16	0.15	0.20	0.25	0.20
SO_3	6.90	4.00	4.75	5.25	3.85	1.60
Ig. Loss	16.72	14.57	12.19	8.47	24.03	34.68
Total	100.76	100.48	100.03	99.38	100.83	100.49
Corg.	4.85	3.42	4.85	0.95	4.18	5.25
CO_2	7.84	5.43	0.38	2.04	15.05	27.08
H_2O+	4.03	5.72	6.96	5.48	4.80	2.35
H_2O-	1.50	1.45	1.80	1.57	1.24	0.60

Major elements analysis of the Tansley Borehole Sediments

Oxides	67	68	69	70	71	72	73
SiO_2	56.80	63.16	41.32	34.07	43.33	43.96	52.85
Al_2O_3	8.86	11.21	8.50	9.73	9.65	9.20	18.16
TiO_2	0.37	0.44	0.34	0.36	1.29	1.30	2.45
Fe_2O_3	3.90	4.58	2.47	2.05	22.88	23.41	6.11
FeO	0.22	0.14	2.36	1.78	0.20	0.38	0.50
MgO	1.10	1.40	1.03	2.11	1.79	1.89	3.02
CaO	8.46	4.02	18.30	22.70	0.57	0.66	0.68
Na_2O	0.37	0.54	0.31	0.10	0.15	0.14	0.11
K_2O	1.80	2.21	1.69	2.29	2.61	2.70	5.13
MnO	0.10	0.06	0.05	0.25	0.06	0.02	0.01
P_2O_5	0.08	0.05	0.25	0.34	0.02	0.01	0.01
SO_3	2.10	1.78	0.80	1.90	10.75	13.28	4.88
Ig. Loss	16.31	11.12	22.60	23.09	6.19	3.73	5.65
Total	100.47	100.71	100.02	100.91	99.49	100.84	99.56
Corg.	2.67	5.33	2.35	1.06	0.58	0.00	0.01
CO_2	10.56	2.91	17.27	19.30	0.00	0.00	0.00
H_2O+	3.08	2.88	2.98	2.81	5.61	3.73	5.64
H_2O-	1.07	1.25	1.09	1.30	1.44	1.67	2.02

Mineralogy of the Tansley Borehole Sediments

Minerals	1	2	3	4	5	6	7
Quartz	17.15	16.02	20.84	50.12	32.76	63.45	47.79
Chlorite	7.21	6.54	5.38	2.99	2.94	2.11	7.15
Illite	19.49	21.59	29.22	12.94	7.05	3.30	10.67
Kaolinite	40.76	40.10	22.54	4.59	7.11	8.91	12.66
Na-feldspar	0.18			4.56	2.54	8.46	7.27
K-feldspar		0.95	0.65	7.38	7.54	9.39	7.97
Siderite		4.08					
Dolomite	0.63			0.24	27.07	0.62	0.29
Calcite			0.32		3.99	0.84	
Pyrite	0.39	0.18	2.96	0.15	0.48	0.31	0.30
TiO_2	0.82	0.93	0.89	0.53	0.26	0.28	0.66
Apatite	0.56	0.78	0.17	0.17	0.14	0.16	0.18
exc. H_2O+	1.15	0.63			0.59		0.46
exc. SiO_2		0.15	2.67	15.12	5.90	0.40	1.55
exc. Fe_2O_3	2.28	2.89	4.78	0.34	1.51	1.08	2.85
Organic Carbon	9.05	2.74	4.24	0.75	0.63	0.18	0.53
Total	99.67	99.93	94.55	99.88	100.36	99.48	100.33

Mineralogy of the Tansley Borehole Sediments

Minerals	8	9	10	11	12	13	14
Quartz	32.18	31.45	39.56	19.82	60.79	37.62	24.33
Chlorite	6.69	8.02	5.42	6.69	1.99	6.67	6.64
Illite	17.87	22.54	11.38	27.10	6.80	16.54	28.96
Kaolinite	20.90	23.92	19.86	32.19	6.82	23.31	29.38
Na-feldspar	6.94	7.53	7.27		8.37	4.91	
K-feldspar	4.84	2.30	2.35	5.43		4.37	4.72
Siderite							
Dolomite	0.84	0.92	3.66		4.86	1.86	0.63
Calcite			1.59	0.43	2.40	0.82	
Pyrite	0.40	0.15	0.37	0.25	0.25	0.16	0.24
TiO_2	0.89	0.98	0.55	0.09	0.34	0.65	1.01
Apatite	0.32	0.30	0.27	0.31	0.17	0.06	0.34
exc.H_2O+		0.21	0.30	0.35	0.36		0.40
exc.SiO_2	3.85	0.99	6.16	1.23	5.07		
exc.Fe_2O_3	2.25	1.81	1.68	2.44	0.79	1.30	3.02
Organic Carbon	1.55	1.74	0.99	2.34	0.80	1.71	1.75
Total	99.48	102.82	101.41	99.67	99.81	99.98	100.57

Mineralogy of the Tansley Borehole Sediments

Minerals	15	16	17	18	19	20	21
Quartz	19.55	25.78	29.97	28.33	18.27	16.68	14.39
Chlorite	5.88	6.33	6.42	3.16	5.44	6.11	6.42
Illite	28.49	26.71	25.65	27.17	26.64	27.99	28.25
Kaolinite	26.57	23.86	21.94	26.93	40.70	37.21	36.20
Na-feldspar	1.10	1.44	1.52				
K-feldspar	2.65	4.31	2.95	3.60	1.54		
Siderite	1.20	1.49	1.19	2.48	2.83	1.25	2.72
Dolomite							
Calcite							
Pyrite	0.18	0.52	0.28	0.31		0.32	0.31
TiO_2	0.99	0.94	0.94	0.94	0.91	0.90	0.87
Apatite	0.38	0.43	0.28	0.40	0.32	0.50	0.40
exc.H_2O+	0.48	0.56	0.38	0.52		1.32	0.93
exc.SiO_2	7.39	5.22	3.65			2.49	5.52
exc.Fe_2O_3	2.52	2.26	0.85	2.76	2.22	2.33	1.91
Organic Carbon	2.65	0.19	1.78	2.95	2.67	2.22	1.59
Total	100.00	100.04	97.79	99.55	101.54	99.33	99.51

Mineralogy of the Tansley Borehole Sediments

Minerals	22	23	24	25	26	27	28
Quartz	18.07	23.84	15.76	19.54	20.17	17.19	25.55
Chlorite	4.96	5.49	4.00	4.65	5.20	5.89	5.11
Illite	26.43	21.44	24.87	20.03	16.52	23.29	23.66
Kaolinite	32.14	32.98	38.02	35.74	26.46	39.44	37.64
Na-feldspar		6.09		3.72			
K-feldspar	1.59		1.29			1.30	1.60
Siderite	3.80	3.51	2.79	0.84	28.17		1.51
Dolomite							
Calcite						0.45	
Pyrite	0.18	0.47	0.46	2.39		1.09	0.53
TiO_2	0.90	0.92	0.91	0.95	0.70	0.92	0.94
Apatite	0.62	0.62	0.42	0.23	1.18	0.50	0.38
exc.H_2O+	0.96	0.22	1.06	1.40			0.80
exc.SiO_2	4.77		4.71	1.55		1.06	
exc.Fe_2O_3	3.01	2.78	2.27	2.01	1.50	2.61	1.86
Organic Carbon	2.48	2.67	2.50	2.90	0.84	4.78	4.59
Total	99.10	100.01	99.06	95.95	100.74	98.52	98.18

Mineralogy of the Tansley Borehole Sediments

Minerals	29	30	31	32	33	34	35
Quartz	19.18	17.68	17.81	20.52	16.86	17.14	16.36
Chlorite	5.41	4.61	3.02	4.03	3.56	4.23	2.47
Illite	29.65	30.72	24.86	29.06	27.74	30.25	30.26
Kaolinite	23.93	21.32	18.48	19.70	18.92	27.58	20.49
Na-feldspar			2.62	2.28	1.17		
K-feldspar							
Siderite							
Dolomite	0.46	0.93		1.54			
Calcite			7.54	5.77	4.26	0.45	
Pyrite	3.35	2.72	5.23	3.13	5.45	2.29	1.14
TiO_2	0.80	0.80	0.70	0.73	0.72	0.77	0.66
Apatite	0.32	0.36	0.33	0.31	0.27	0.22	0.17
exc. H_2O+	2.28	2.21	1.49	1.30	1.28	1.45	2.93
exc. SiO_2	2.90	5.70	1.75	0.55	4.18	4.23	4.08
exc. Fe_2O_3	2.46	4.52	3.51	2.65	3.39	3.79	6.36
Organic Carbon	4.33	3.44	3.33	2.98	3.41	6.95	11.90
Total	95.07	95.01	91.09	94.55	91.21	100.48	98.67
Gypsum			0.42			2.24	1.85

Mineralogy of the Tansley Borehole Sediments

Minerals	36	37	38	39	40	41	42
Quartz	11.77	22.54	24.77	34.91	34.65	22.74	24.87
Chlorite	2.59	1.93	1.40	3.47	2.01	2.44	3.82
Illite	28.54	20.34	19.06	23.50	17.60	25.38	25.89
Kaolinite	19.35	17.12	13.42	16.12	21.23	26.38	27.88
Na-feldspar							
K-feldspar			0.94			0.88	
Siderite		17.54	25.10	5.75	3.28	1.04	
Dolomite		5.99					
Calcite	1.80						0.25
Pyrite	2.85	2.04	0.63		0.04	0.52	1.59
TiO_2	0.63	0.61	0.61	0.74	0.75	0.86	0.84
Apatite	0.38	0.21	0.59	0.38	0.25	0.34	0.26
exc.H_2O+	0.34	0.24	0.65	0.27		0.87	3.16
exc.SiO_2	6.97		5.53	8.54	12.18	9.45	2.65
exc.Fe_2O_3	6.59	7.19	3.41	1.96	1.56	2.23	2.50
Organic Carbon	10.86	1.55	1.65	3.67	2.98	3.70	3.40
Total	95.90	97.30	97.76	99.31	96.53	96.73	97.11
Gypsum	2.85						

Mineralogy of the Tansley Borehole Sediments

Minerals	43	44	45	46	47	48	49
Quartz	23.96	12.42	18.37	19.14	21.36	19.30	15.70
Chlorite	4.12	0.00	3.40	3.47	2.99	2.63	2.95
Illite	28.05	13.42	27.67	30.22	20.14	23.46	23.73
Kaolinite	32.27	16.77	31.64	16.78	17.63	14.79	12.60
Na-feldspar							
K-feldspar				1.58			
Siderite		42.72					
Dolomite			0.79			10.24	2.96
Calcite	0.20			1.60	5.27	12.08	20.93
Pyrite	1.61	2.04	1.74	2.57	4.78	2.63	4.23
TiO_2	0.87	0.47	0.75	0.67	0.65	0.58	0.48
Apatite	0.29	1.63	0.17	0.26	0.26	0.36	0.61
exc.H_2O+	0.96	0.25	1.79	2.15	1.58	1.27	0.92
exc.SiO_2	0.81	2.49	3.76	4.99		1.00	0.52
exc.Fe_2O_3	1.80	3.14	3.11	5.72	3.92	4.86	3.50
Organic Carbon	5.55	0.33	3.51	4.68	2.55	3.88	5.32
Total	100.49	95.68	96.70	94.55	93.00	97.08	94.38
Gypsum				3.69	2.87		

Mineralogy of the Tansley Borehole Sediments

Minerals	50	51	52	53	54	55	56
Quartz.	18.94	15.39	18.19	18.79	20.46	24.71	17.44
Chlorite	3.13	5.94	5.60	3.60	2.70	3.47	3.28
Illite	27.50	28.29	28.65	25.28	22.02	28.95	28.73
Kaolinite	23.06	34.92	28.05	20.81	21.86	24.94	23.48
Na-feldspar							
K-feldspar							
Siderite							
Dolomite					4.02		
Calcite	1.27	0.63		4.64	11.22		3.09
Pyrite	3.98	1.77	3.21	3.88	2.12	1.33	2.24
TiO_2	0.73	0.82	0.81	0.74	0.75	0.89	0.81
Apatite	0.24	0.34	0.33	0.31	0.35	0.34	0.29
exc.H_2O+	0.92	0.01	1.92	0.85	0.63	0.93	1.79
exc.SiO_2	3.39	4.18	2.86	5.78	2.15	3.58	5.83
exc.Fe_2O_3	3.27	2.18	3.49	3.70	4.28	4.50	4.16
Organic Carbon	3.89	1.19	1.57	4.18	3.13	2.37	4.88
Total	94.60	95.66	96.02	94.70	98.01	96.01	97.90
Gypsum	4.28		1.34	2.14			1.70

Mineralogy of the Tansley Borehole Sediments

Minerals	57	58	59	60	61	62	63
Quartz	21.31	10.20	15.88	20.64	19.84	20.85	18.84
Chlorite	3.49	2.66	3.42	3.31	2.32	4.05	3.85
Illite	29.99	18.49	22.47	26.72	21.63	33.28	25.82
Kaolinite	23.55	15.01	15.32	16.57	13.04	16.52	14.98
Na-feldspar			3.72	4.74	3.93	1.10	4.82
K-feldspar							
Siderite							
Dolomite		7.00	1.22	2.60			1.30
Calcite	2.10	21.31	14.91	6.87	17.77	0.86	10.92
Pyrite	3.30	2.71	3.31	1.89	4.94	3.56	3.00
TiO_2	0.82	0.47	0.62	0.76	0.55	0.83	0.80
Apatite	0.30	0.63	0.50	0.40	0.40	0.35	0.37
exc.H_2O+	2.58	1.66	1.68	1.39	0.79	1.93	0.27
exc.SiO_2	2.86	4.40	2.52	3.09		0.98	2.54
exc.Fe_2O_3	3.60	5.32	3.23	4.28	2.38	3.35	2.93
Organic Carbon	4.58	6.44	5.15	3.99	4.85	4.85	3.42
Total	99.93	96.30	94.57	97.25	92.44	94.31	93.86
Gypsum	1.45					1.80	

Mineralogy of the Tansely Borehole Sediments

Minerals	64	65	66	67	68	69	70
Quartz	23.82	16.42	11.17	31.84	31.43	12.44	10.24
Chlorite	4.68	3.06	1.21	0.00	1.77	1.00	2.31
Illite	32.86	20.26	11.14	24.36	24.36	15.93	24.22
Kaolinite	12.18	6.96	2.35	3.05	4.01	4.75	2.56
Na-feldspar	2.69	3.52	2.45	3.12	4.57	2.62	1.35
K-feldspar						2.19	
Siderite							
Dolomite		17.50	43.58	4.60		6.45	6.72
Calcite	4.63	15.03	13.80	12.60	7.06	30.30	36.31
Pyrite	3.95	2.88	1.19	1.57	1.33	0.60	1.42
TiO_2	0.82	0.54	0.25	0.37	0.44	0.31	0.36
Apatite	0.47	0.58	0.46	0.17	0.12	0.58	0.81
exc.H_2O+	0.56	2.22	0.80	1.54	0.48	1.14	0.53
exc.SiO_2			2.84	13.09	14.95	17.79	9.49
exc.Fe_2O_3	3.67	3.05	1.68	1.81	0.81		0.16
Organic Carbon	0.95	4.18	5.25	2.67	5.33	2.35	1.06
Total	91.28	96.18	98.17	100.81	96.66	100.55	97.54

Mineralogy of the Tansely Borehole Sediments
(K - Bentonites)

Minerals	71	72	73
Quartz	23.26	24.75	15.99
Chlorite	4.52	5.01	7.77
Illite	22.07	22.85	43.36
Kaolinite	2.35	0.47	3.33
Na-feldspar	1.27	1.18	0.93
K-feldspar			
Siderite			
Dolomite			
Calcite			
Pyrite	9.45	9.91	3.66
TiO_2	1.29	1.30	2.45
Apatite	0.04	0.13	0.03
exc.H_2O+	3.39	2.73	2.83
exc.SiO_2	6.19	5.72	5.75
exc.Fe_2O_3	10.21	10.15	3.17
Organic Carbon	0.58	0.00	0.00
Total	86.35	86.23	91.28
Gypsum	1.74	2.04	2.02

Trace Element Contents (ppm) of the Tansley Borehole Sediments

Element	1	2	3	4	5	6	7	8	9	10	11	12	13	14	15	16	17	18	19	20
Ni	142	81	54	11	13	1	33	48	49	27	78	202	47	67	66	76	58	65	122	97
Co	49	24	17	40	36	29	58	40	27	43	34	59	22	24	30	34	26	16	47	27
Mn	390	087	156	106	1980	143	224	415	368	944	275	858	561	302	371	684	420	485	696	314
V	138	142	117	44	32	20	72	104	105	63	125	23	93	121	108	117	111	117	128	144
Cr	159	158	148	70	62	36	135	133	155	88	169	40	147	179	153	155	151	169	154	165
Zn	71	93	53	15	18	6	46	70	83	195	81	20	84	80	79	105	93	91	77	95
Cu	58	66	13	3	5	8	6	27	34	5	44	5	25	44	40	40	34	41	45	62
Rb	111	133	149	45	46	49	76	126	134	61	152	22	95	141	130	124	118	125	116	124
Sr	153	141	105	92	106	119	94	115	121	80	141	58	117	137	130	134	124	133	130	145
Y	40	43	26	20	5	7	14	28	28	12	31	13	30	35	34	40	33	40	33	31
Zr	93	97	129	407	55	164	293	281	299	234	238	240	267	210	210	257	322	214	130	96
Pb	38	40	34	17	8	11	16	30	31	21	30	13	42	26	31	48	27	29	43	42
Ba	403	492	485	548	438	488	471	780	495	353	497	193	496	524	509	482	448	452	498	507

Trace Element Contents (ppm) of the Tansley Borehole Sediments

Element	21	22	23	25	26	27	28	29	30	32	38	39	40	41	42	44	45	46	47	48
Ni	78	77	59	76	60	82	59	133	128	110	46	48	62	96	94	87	87	95	105	103
Co	17	21	12	16	64	64	11	32	46	35	55	34	18	39	28	107	13	35	40	31
Mn	605	989	845	402	4053	4284	440	313	529	594	1692	705	338	800	152	4330	99	455	417	1041
V	131	129	122	108	100	106	109	249	228	510	114	114	112	156	168	93	153	156	199	204
Cr	159	153	148	139	109	117	153	163	144	250	116	140	129	149	149	92	138	137	145	121
Zn	63	91	93	70	47	30	86	109	116	103	75	72	71	102	79	73	90	89	92	82
Cu	45	43	42	45	25	11	37	248	163	143	42	43	38	68	89	47	86	103	135	108
Rb	129	114	114	103	45	35	107	126	138	134	79	88	86	111	119	55	128	123	111	91
Sr	125	128	115	120	116	75	216	127	112	178	83	96	97	108	103	88	105	128	161	304
Y	32	37	49	31	62	41	29	40	43	36	39	33	26	31	38	47	35	32	31	35
Zr	102	130	173	180	115	75	224	109	106	106	131	197	232	150	130	75	82	93	85	81
Pb	40	36	24	46	13	8	17	165	220	184	32	27	36	52	75	46	78	195	232	134
Ba	505	501	456	406	357	351	432	377	409	482	287	290	290	328	325	321	313	351	381	458

Trace Element Contents (ppm) of the Tansley Borehole Sediments

Element	49	50	51	52	53	54	55	56	57	61	62	64	66	67	69	70	71	72	73
Ni	225	107	81	96	114	89	72	106	116	215	151	189	69	113	253	155	286	298	322
Co	51	21	16	25	24	17	15	26	34	45	60	71	12	18	7	22	86	61	30
Mn	728	380	176	348	332	719	332	595	423	414	1269	844	4198	321	426	2112	101	70	60
V	628	180	159	140	233	175	347	226	184	466	216	287	114	455	175	80	146	168	238
Cr	241	171	167	140	141	142	142	150	156	121	144	134	57	105	141	63	166	238	482
Zn	124	87	103	95	112	68	94	114	97	119	105	126	59	113	365	198	30	40	44
Cu	194	90	64	112	136	94	119	125	145	155	206	1039	79	112	112	46	78	67	56
Rb	83	107	131	111	111	89	128	124	118	94	131	151	40	68	67	84	66	80	154
Sr	350	121	106	115	147	216	128	141	139	316	170	195	283	272	695	543	52	70	116
Y	24	19	50	38	41	33	51	37	46	44	57	35	18	14	22	50	10	6	9
Zr	66	99	92	92	101	102	141	119	119	90	128	117	35	64	65	62	88	117	205
Pb	175	174	51	122	184	99	95	119	142	128	137	209	29	82	55	51	65	70	24
Ba	777	348	351	322	366	296	423	412	388	521	420	430	160	189	265	170	101	124	91

PLATE 1

A. Poorly sorted sandstone (x 100)

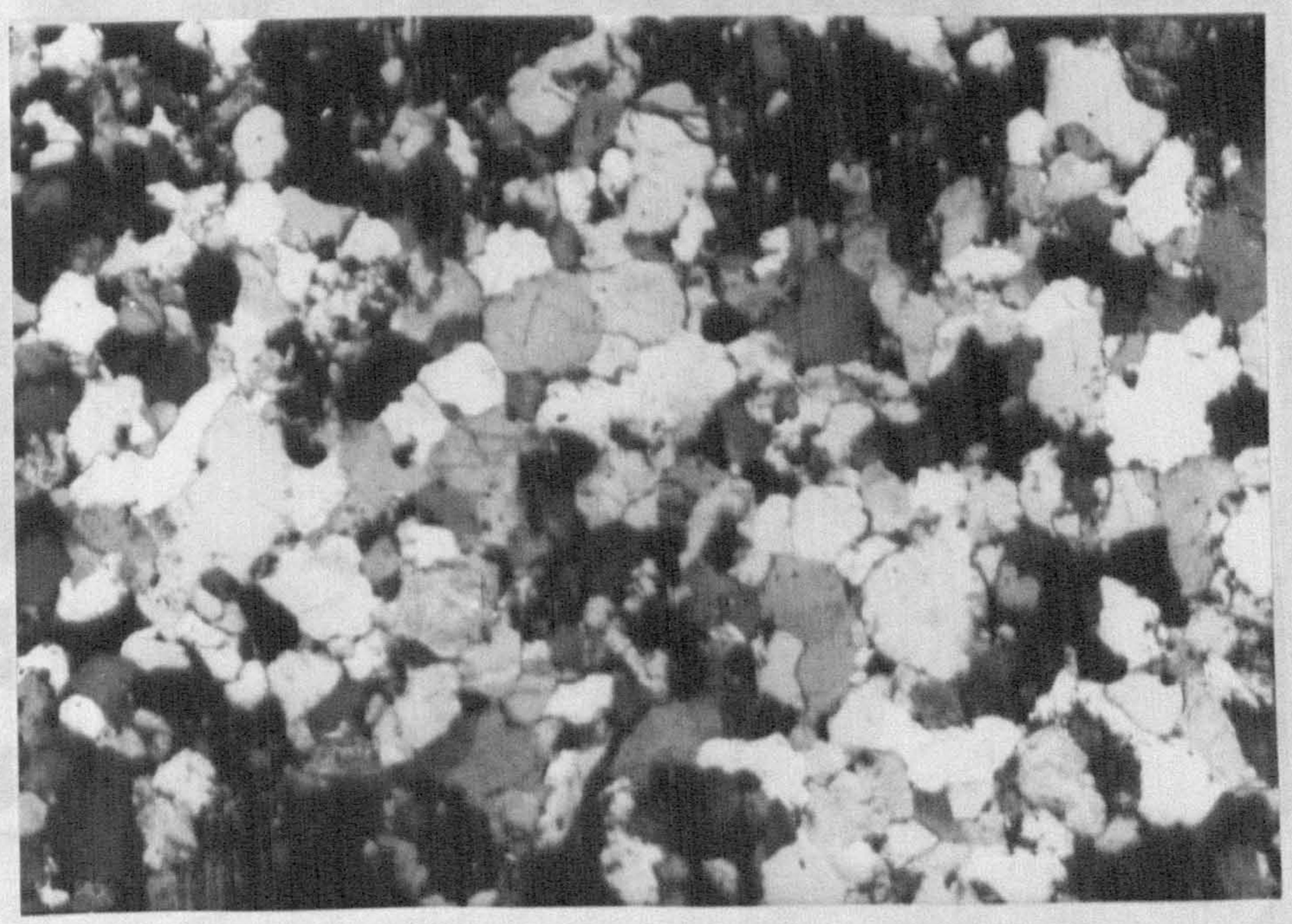

B. Quartz cemented sandstone with good sorting (x 100)

PLATE 2

A. Sandstone with patchy calcite cement replacing the detrital grains (x 100)

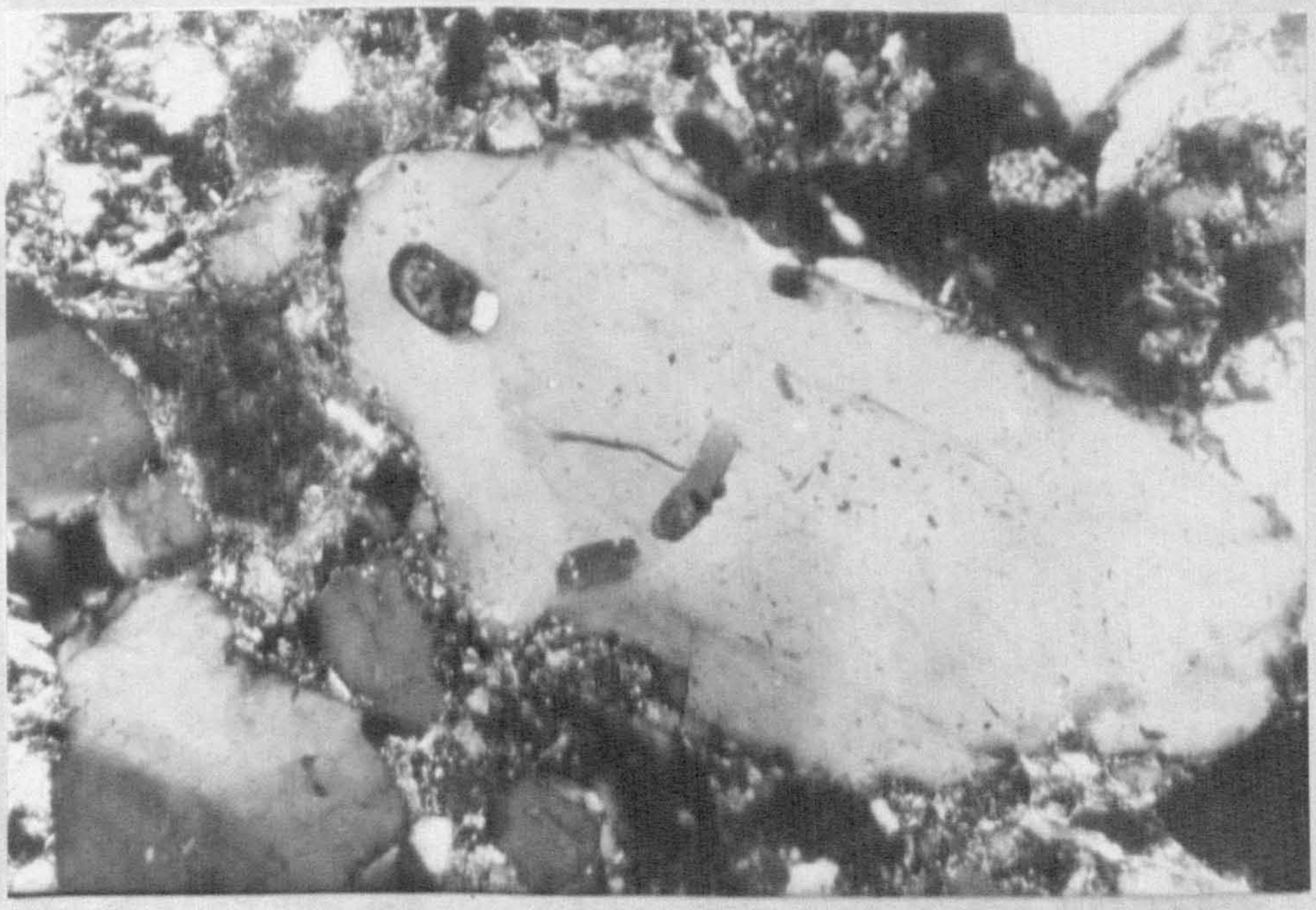

B. Inclusion of tourmaline inside quartz (x 100)

PLATE 3

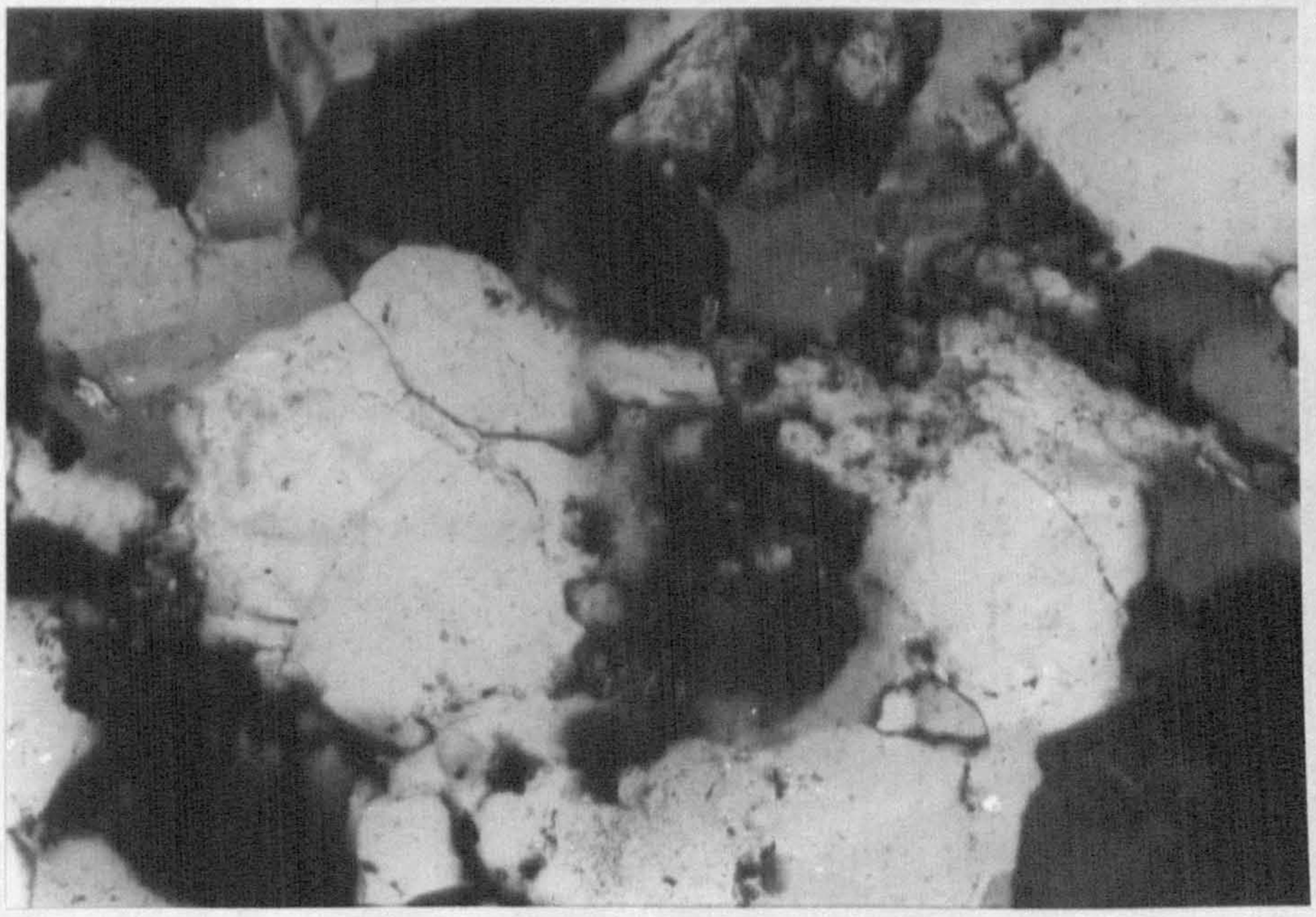

A. Quartz overgrowth separated by a dusty outline from the original clastic quartz grain (x 100)

B. Albite with polysynthetic twinning (x 100)

PLATE 4

A. Replacement of feldspar by calcite (x 100)

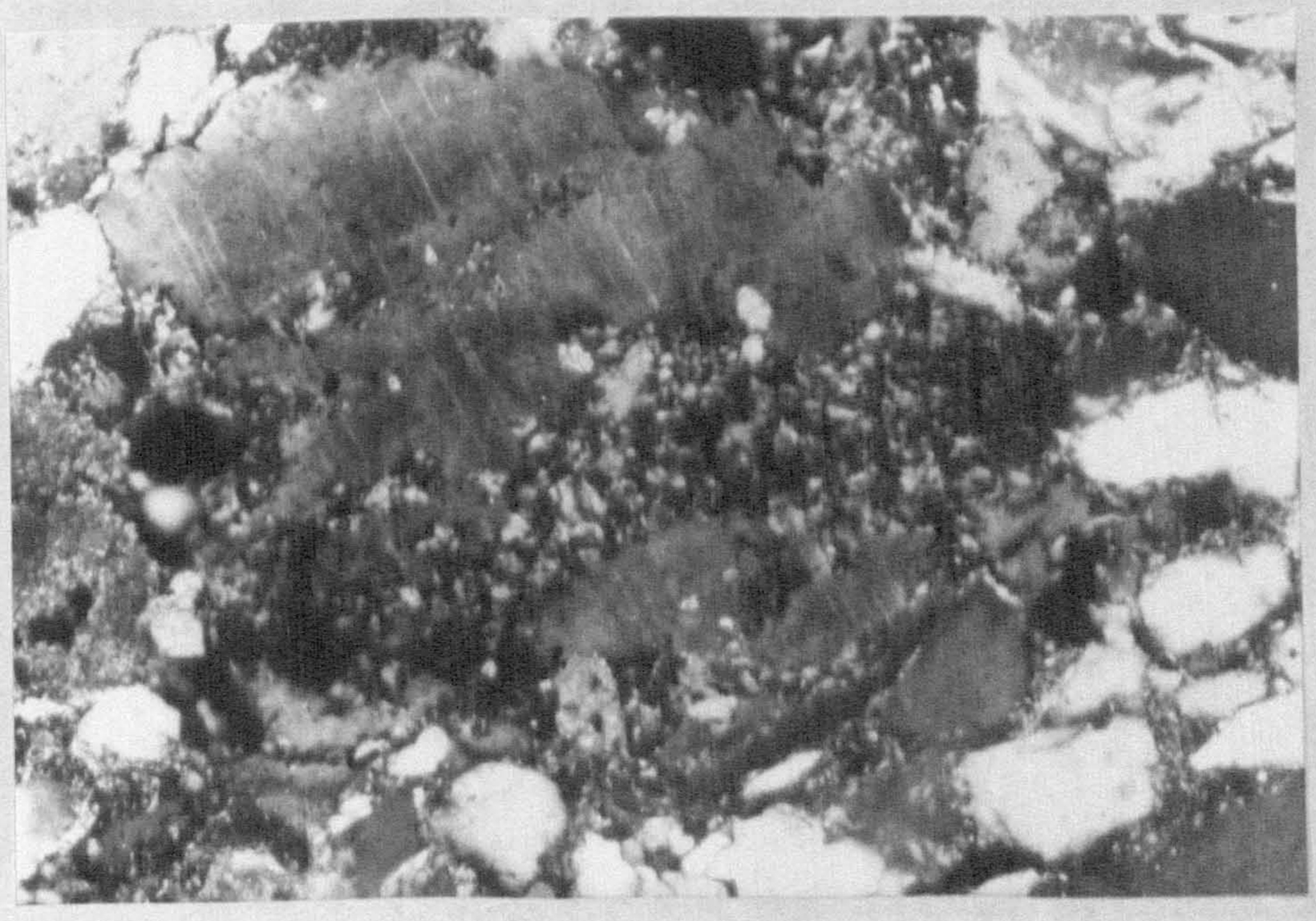

B. Partial alteration of K-feldspar to microcrystalline aggregates of kaolinite (x 100)

PLATE 5

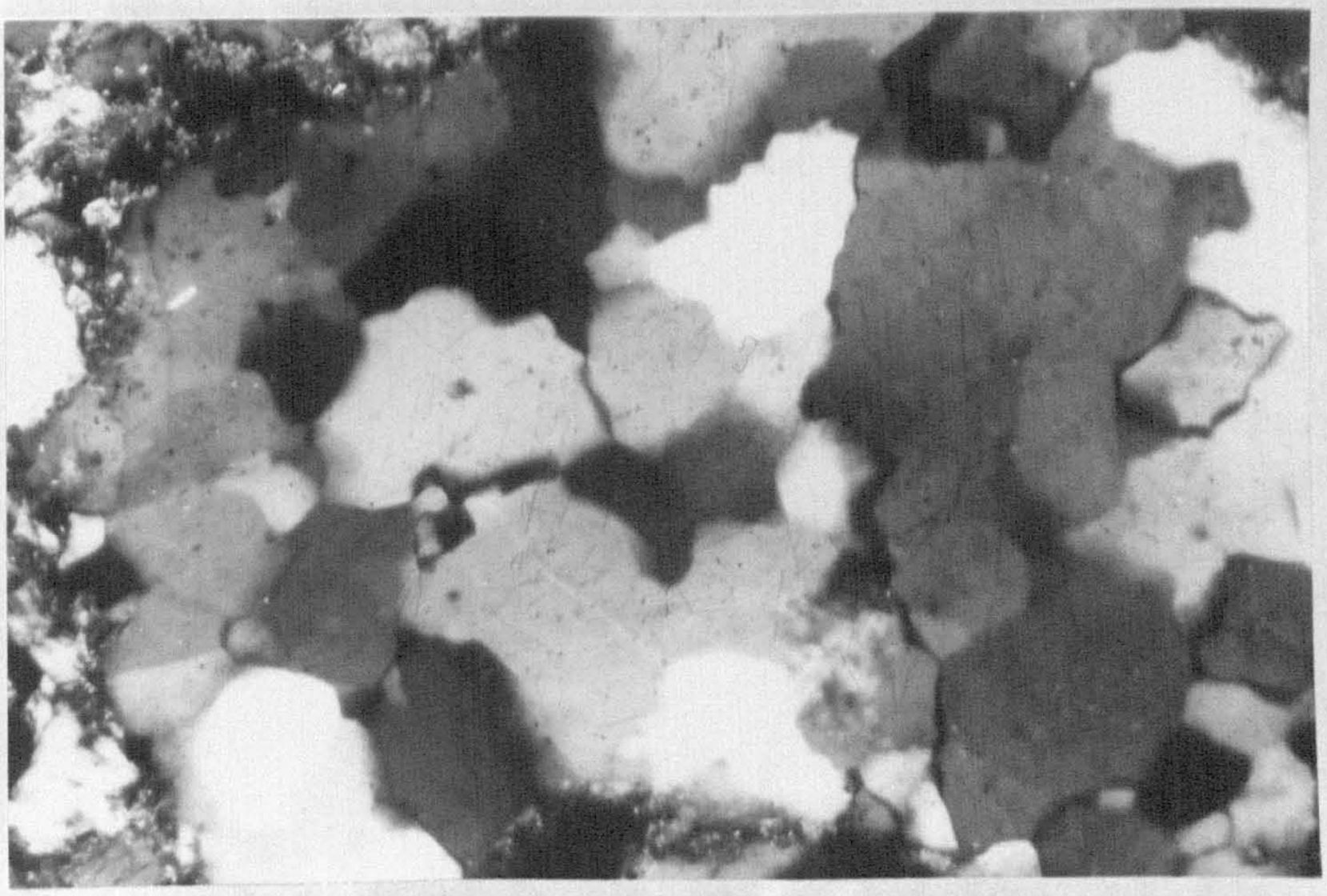

A. Igneous rock fragment consisting of many quartz grains (x 100)

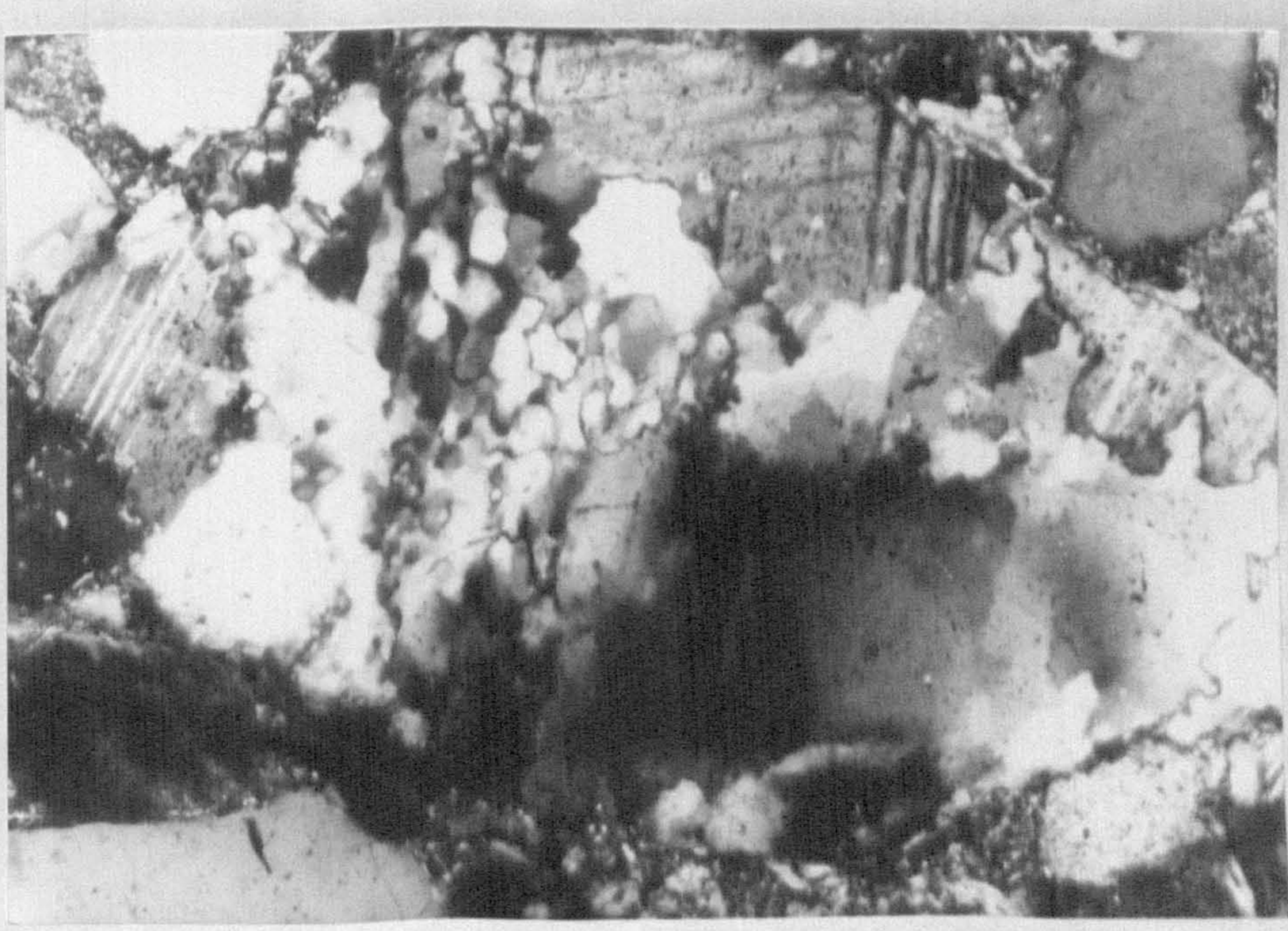

B. Igneous rock fragment consisting of quartz and feldspar (x 100)

PLATE 6

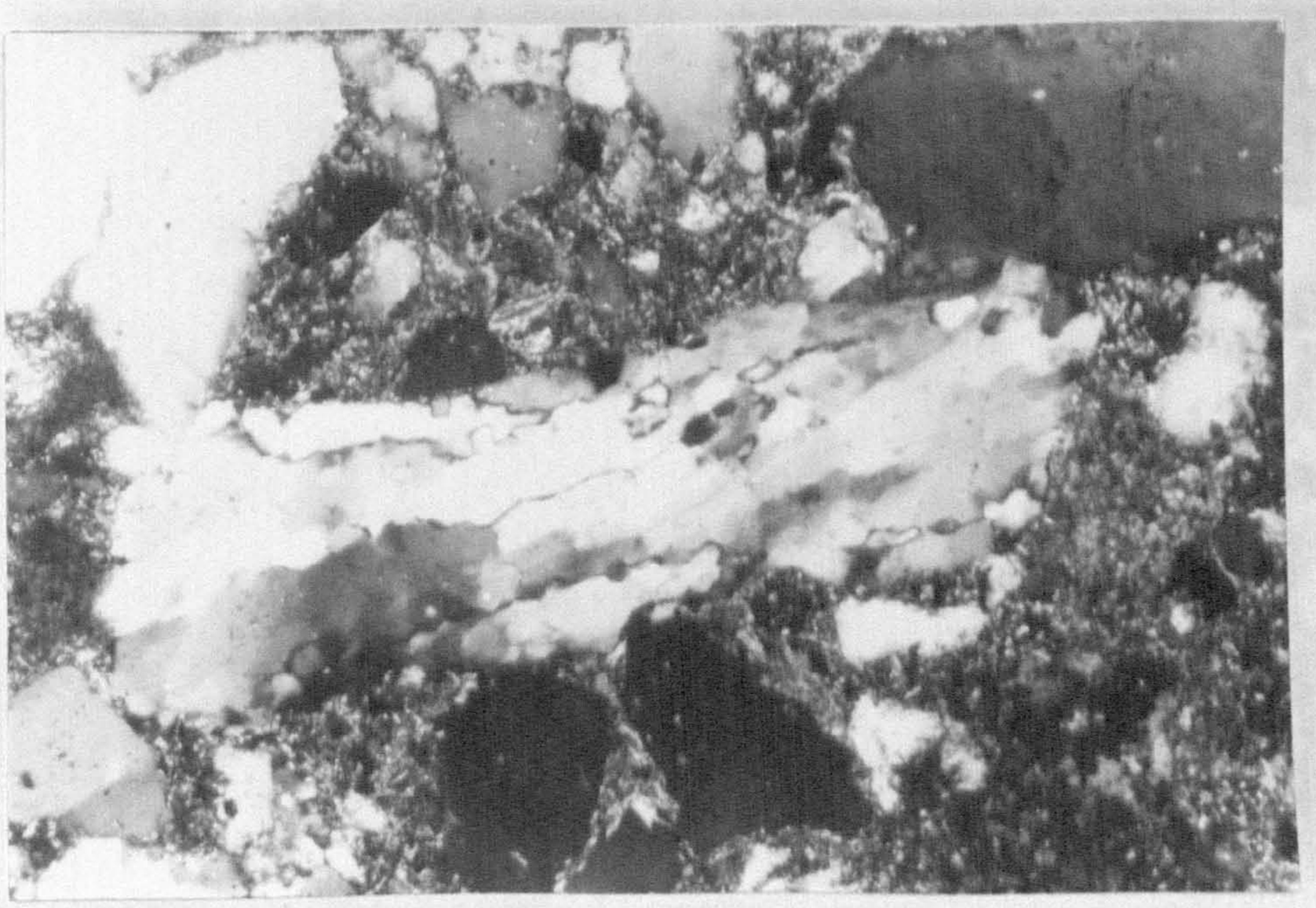

A. Metamorphic rock fragment consisting of several elongated quartz grains (x 100)

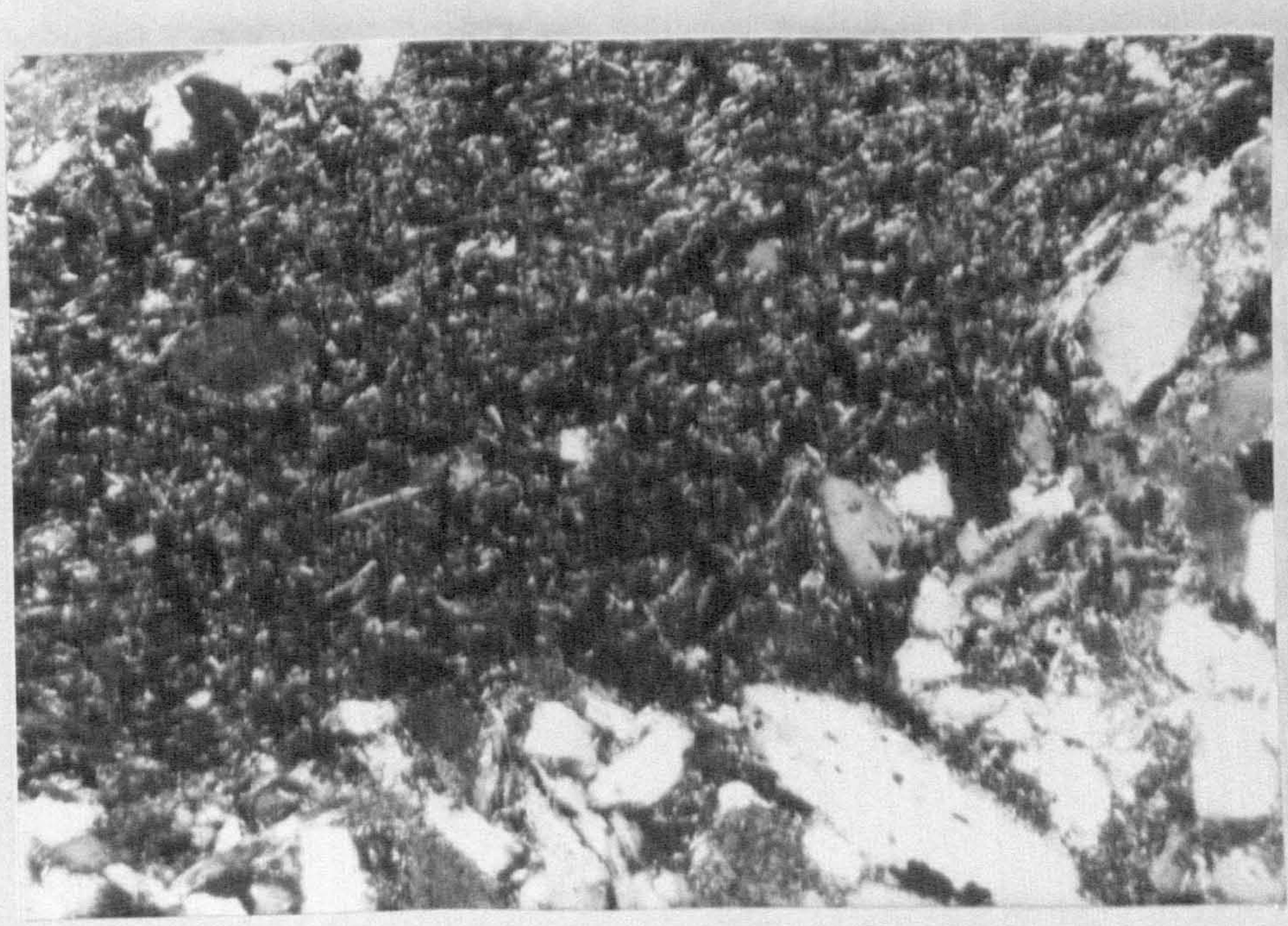

B. Shale rock fragment (x 100)

PLATE 7

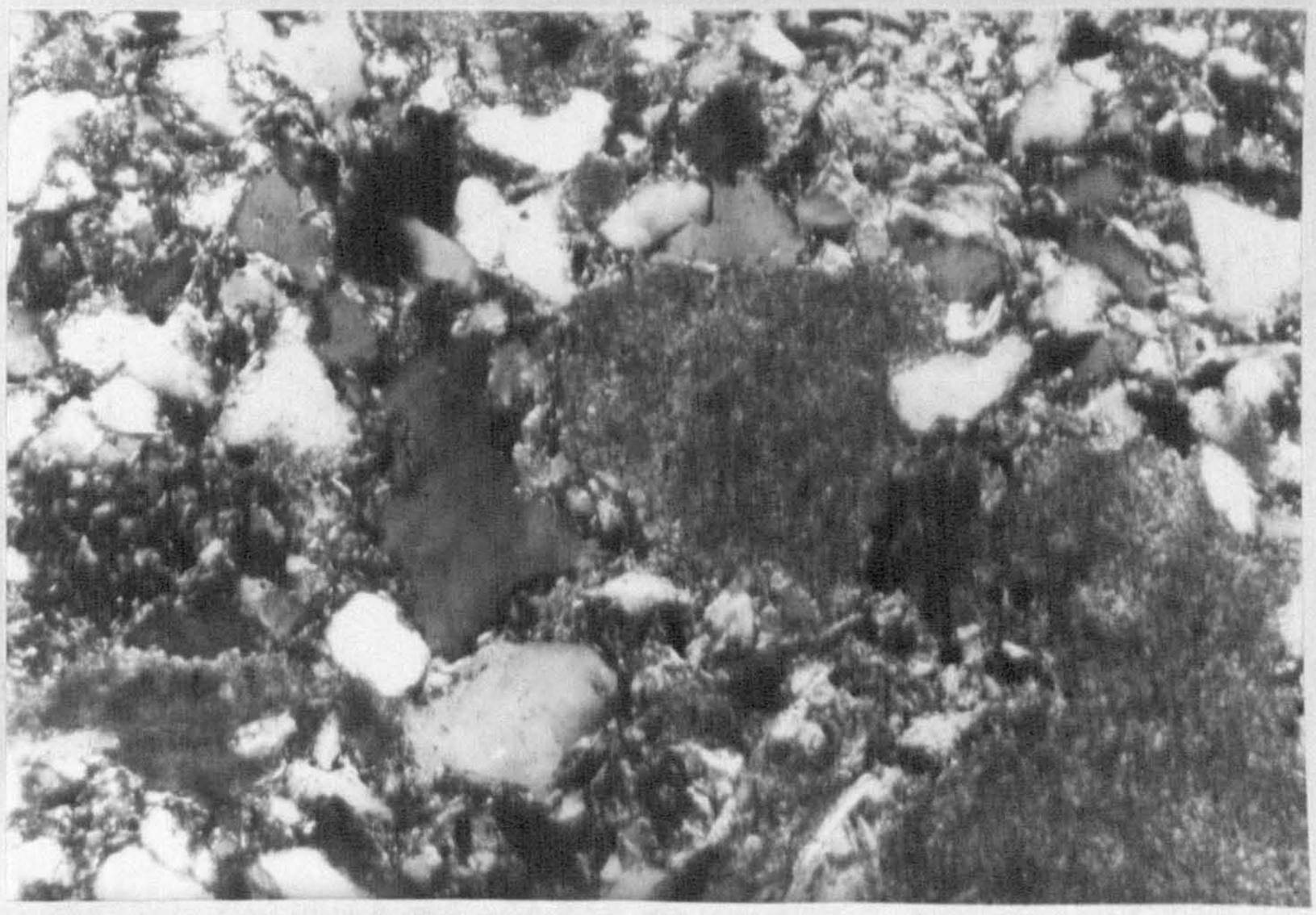

A. Dark brown sideritic mudstone grains, probably detrital (x 100)

B. Flakes of muscovite (light) and biotite (dark brown) (x 100)

PLATE 8

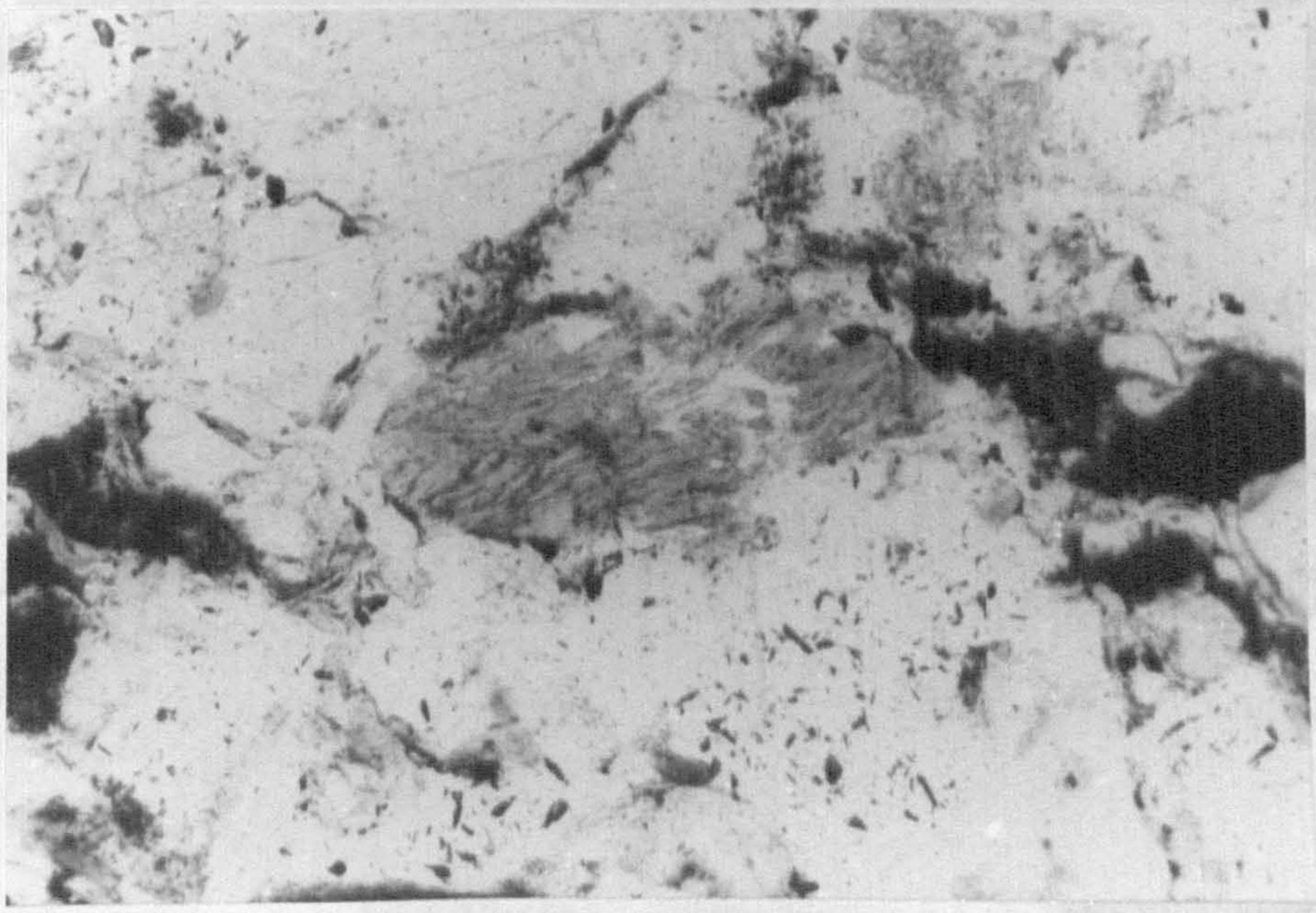

A. Authigenic chlorite with iron oxide after biotite (x 100)

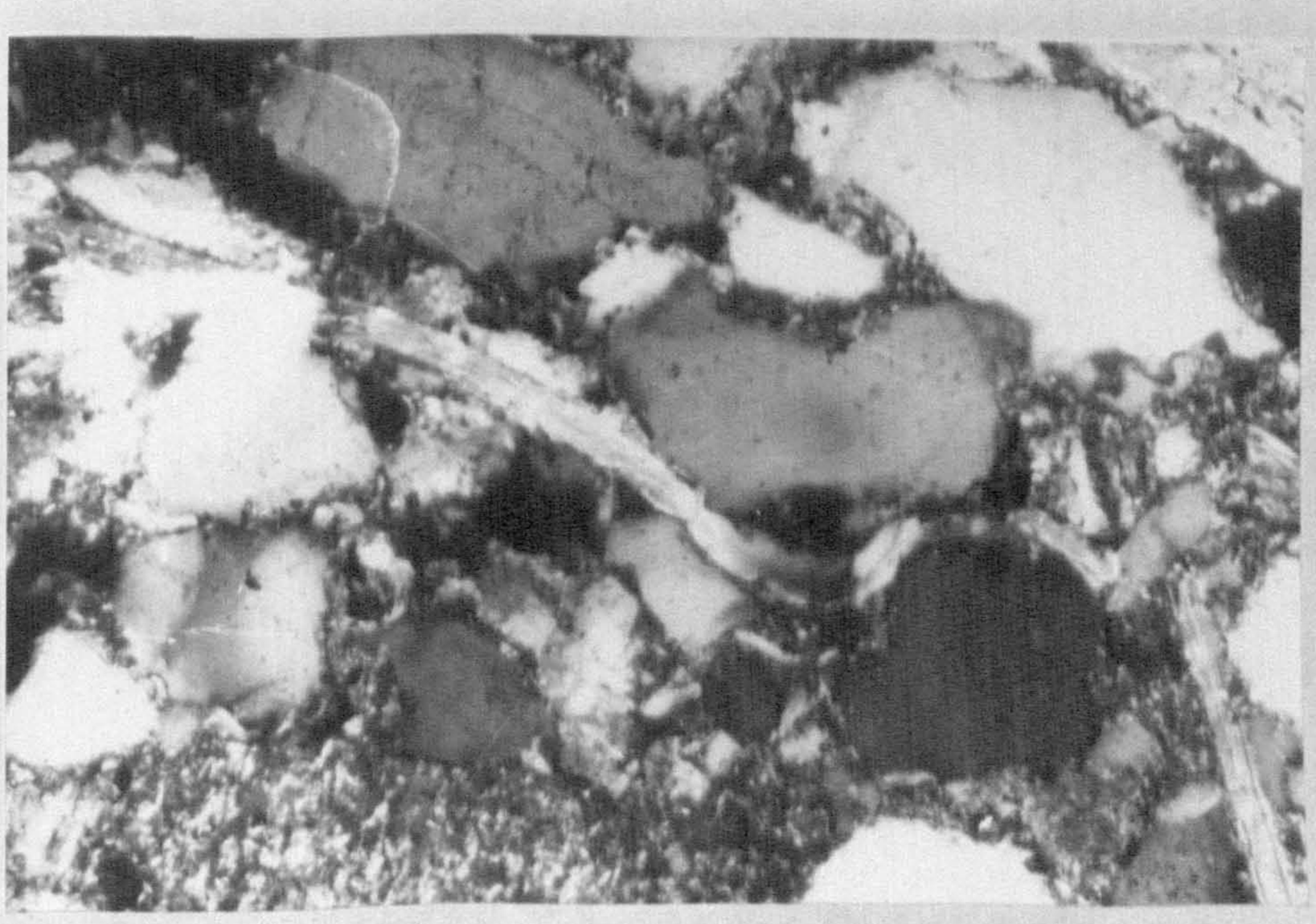

B. Bending of mica between quartz grains, due to compaction (x 100)

PLATE 9

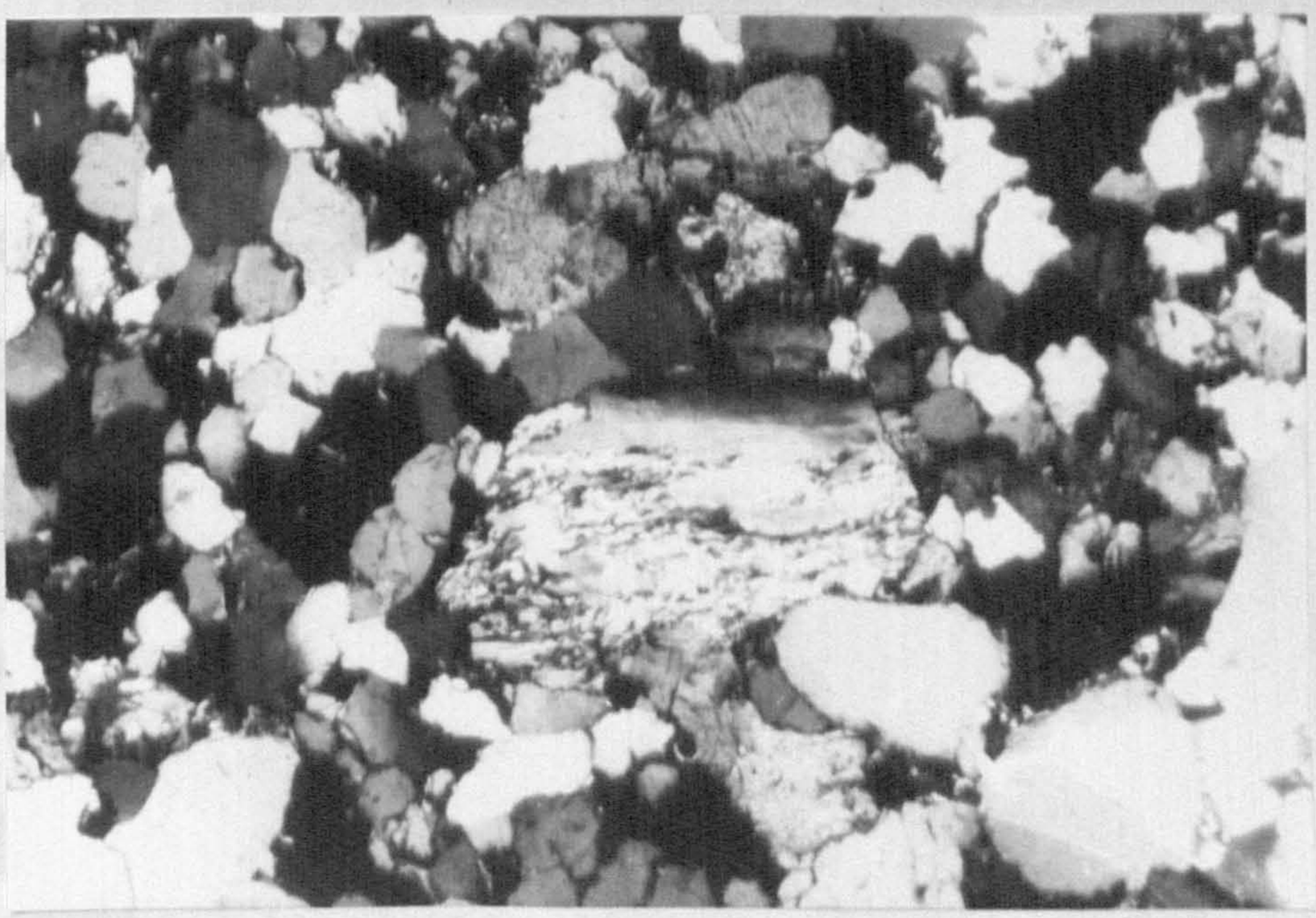

A. Tightly packed sandstone. Note the metamorphic rock fragment in the middle (x 30)

B. Carbonate cemented sandstone (x 100)

PLATE 10

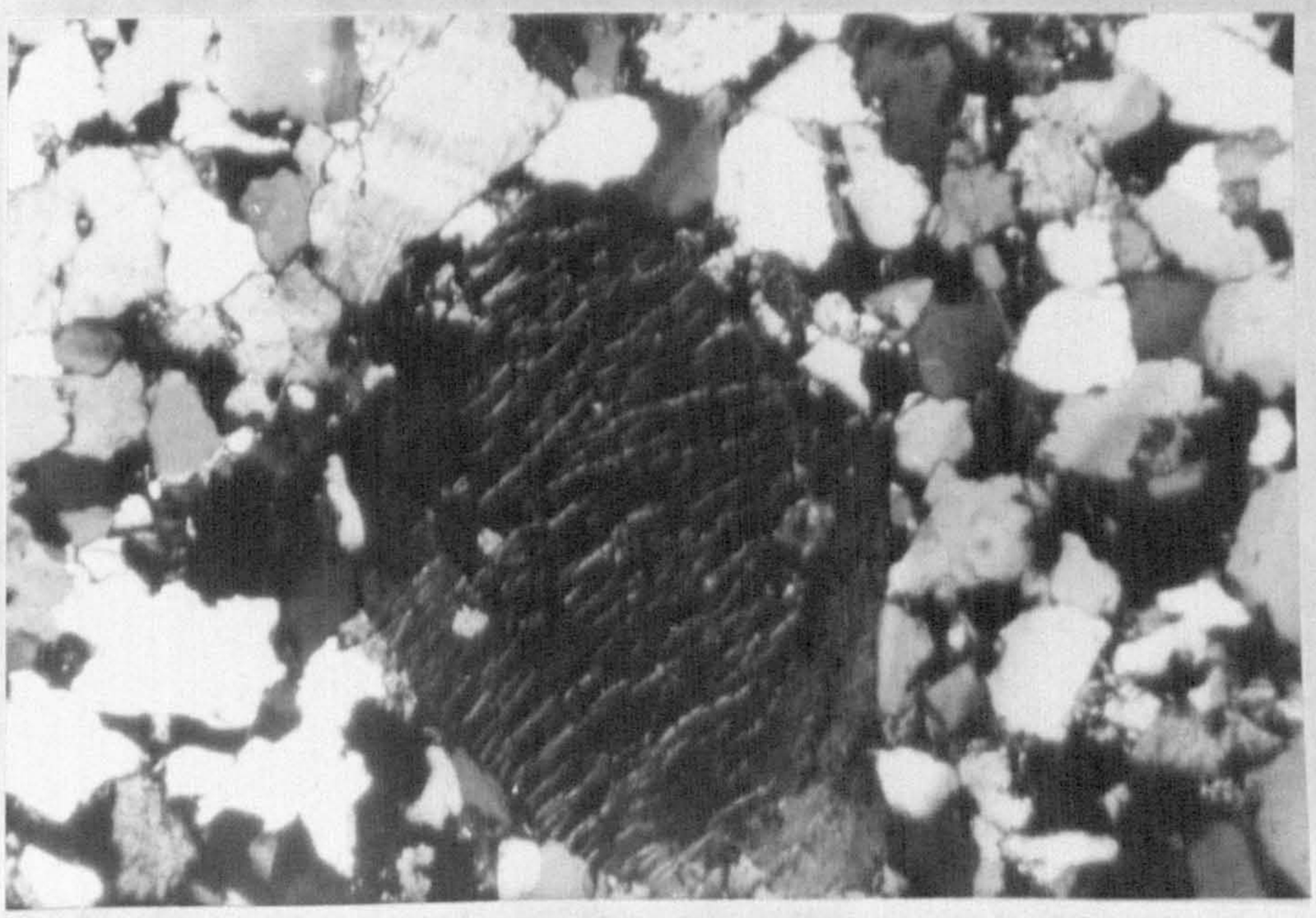

A. Perthitic orthoclase, crossed nicols (x 30)

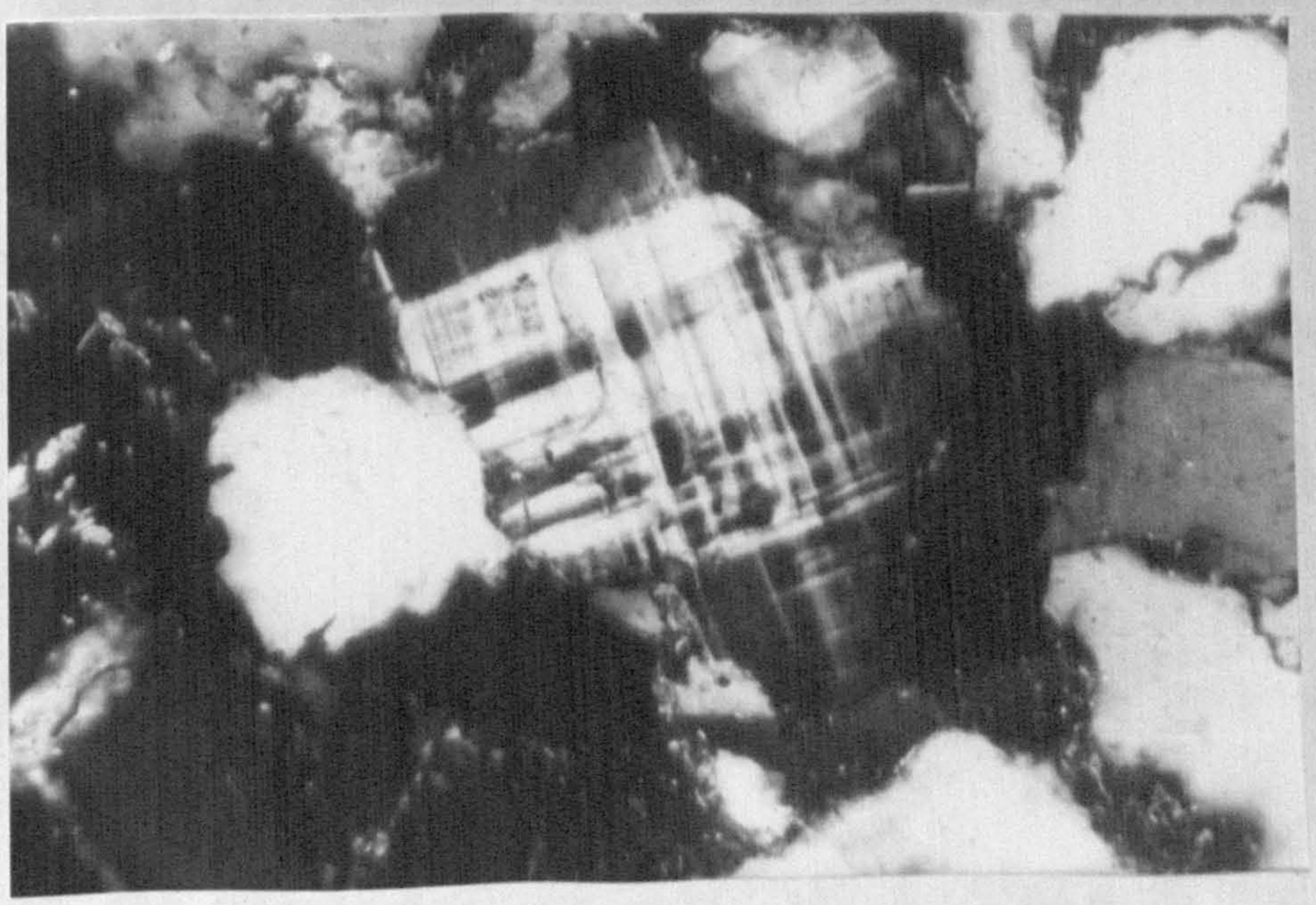

B. Microcline (x 100)

PLATE 11

A. Long and short prismatic, euhedral crystals of zircon (x 150)

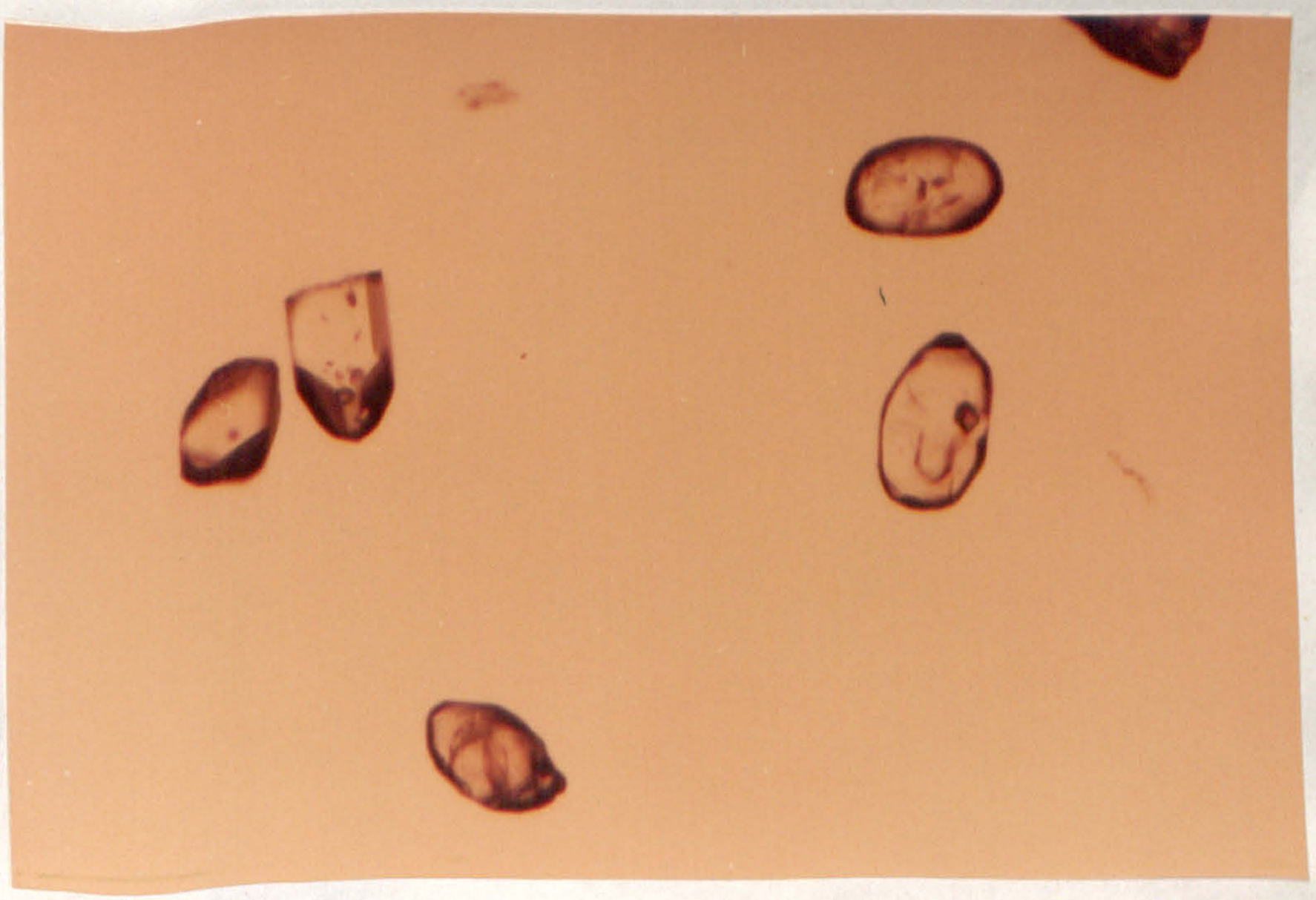

B. Very well rounded grains of zircon (x 100)

PLATE 12

A. Yellowish brown, prismatic crystals of rutile (anatase?) (x 170)

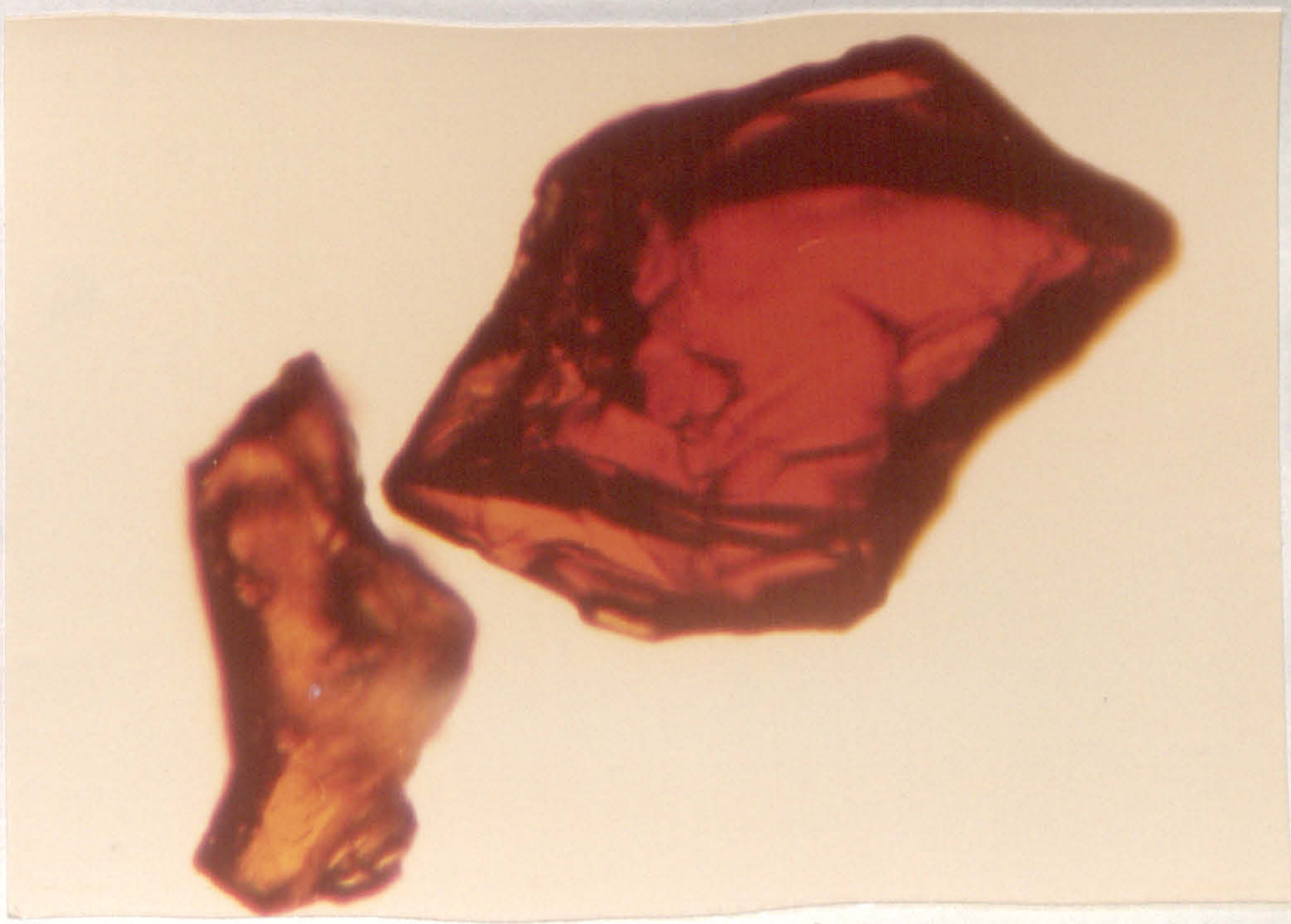

B. Reddish brown and red grains of rutile (x 200)

PLATE 13

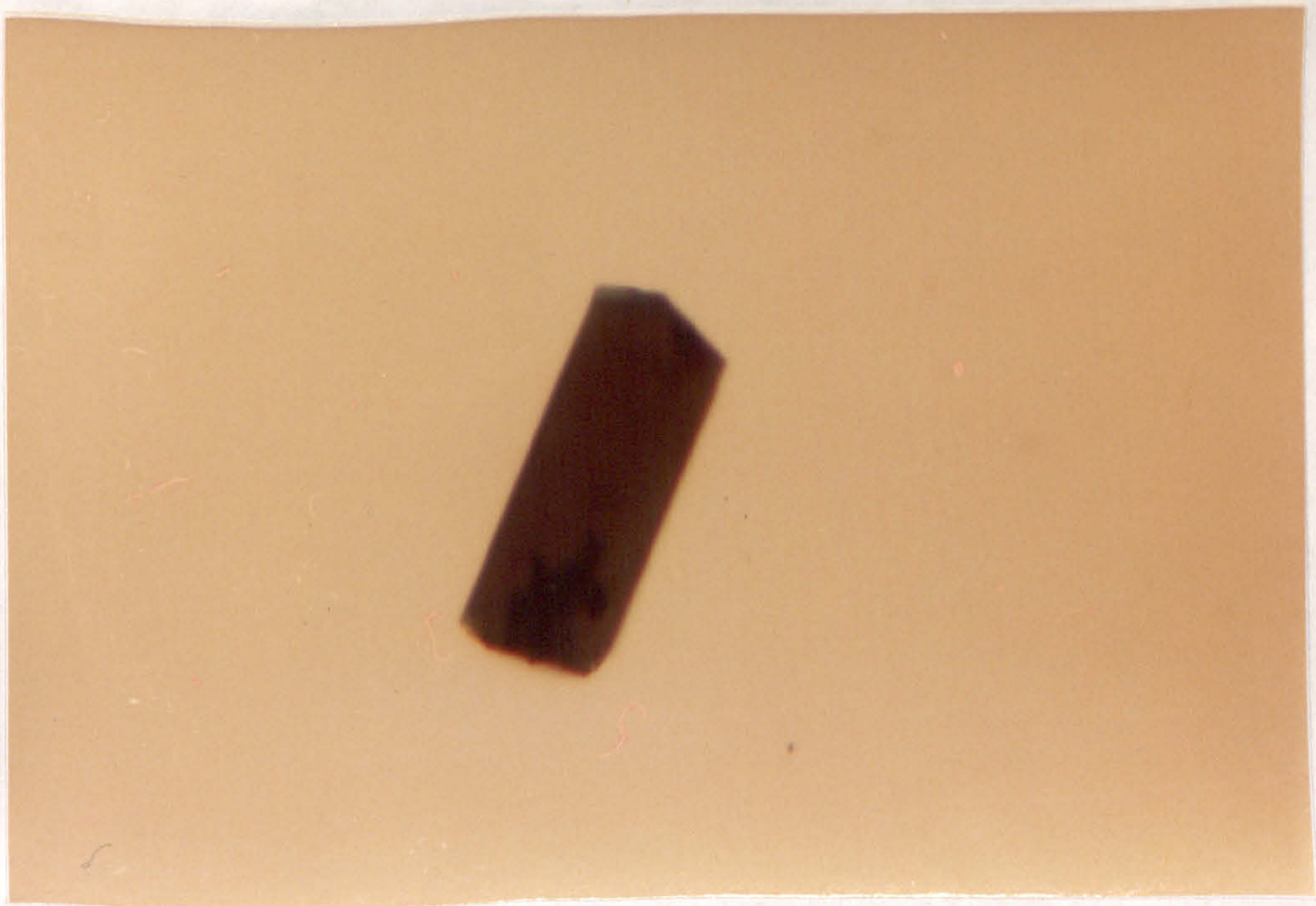

A. Euhedral crystal of green tourmaline with black inclusion (x 100)

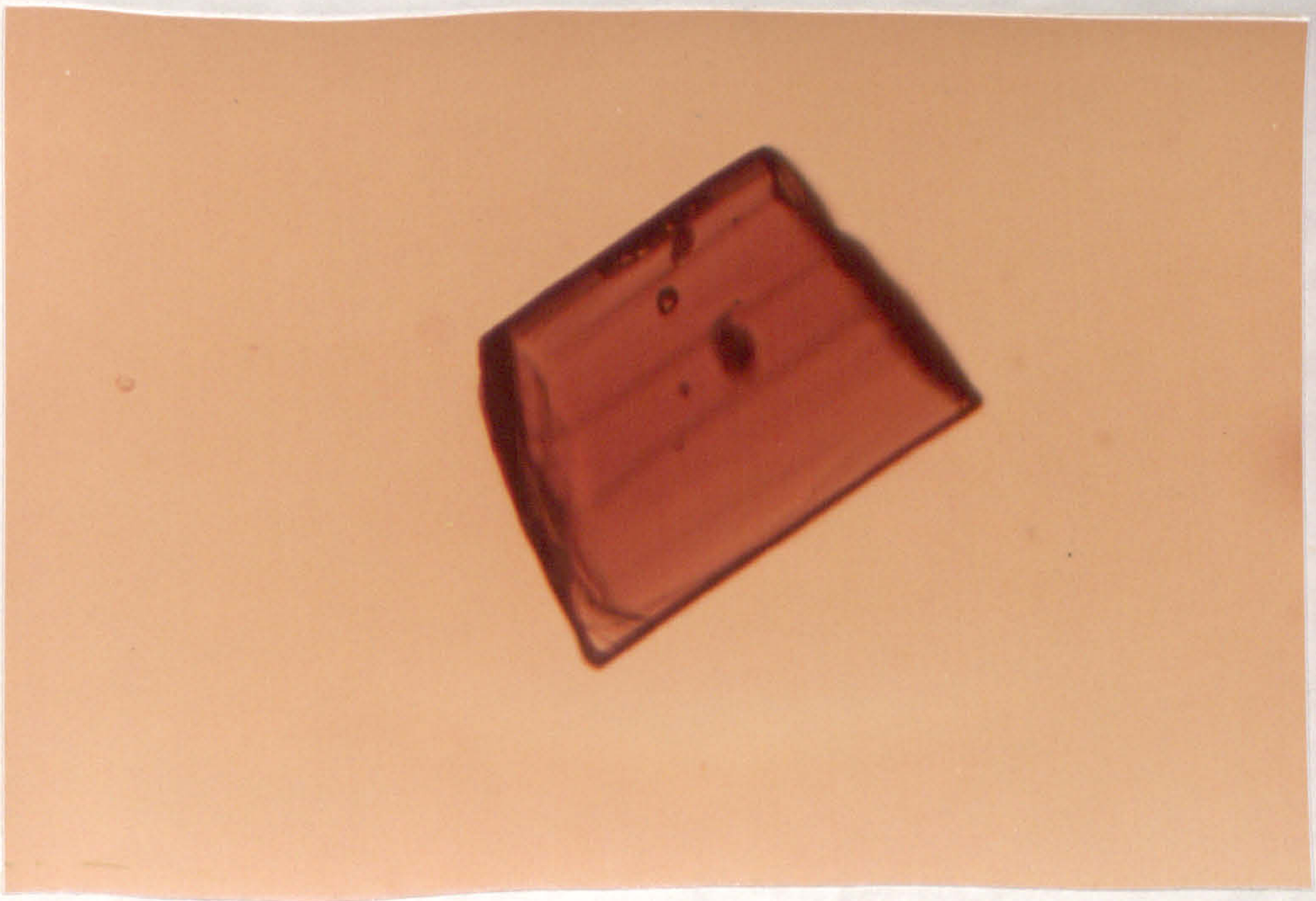

B. Euhedral crystal of brown tourmaline (x 200)

PLATE 14

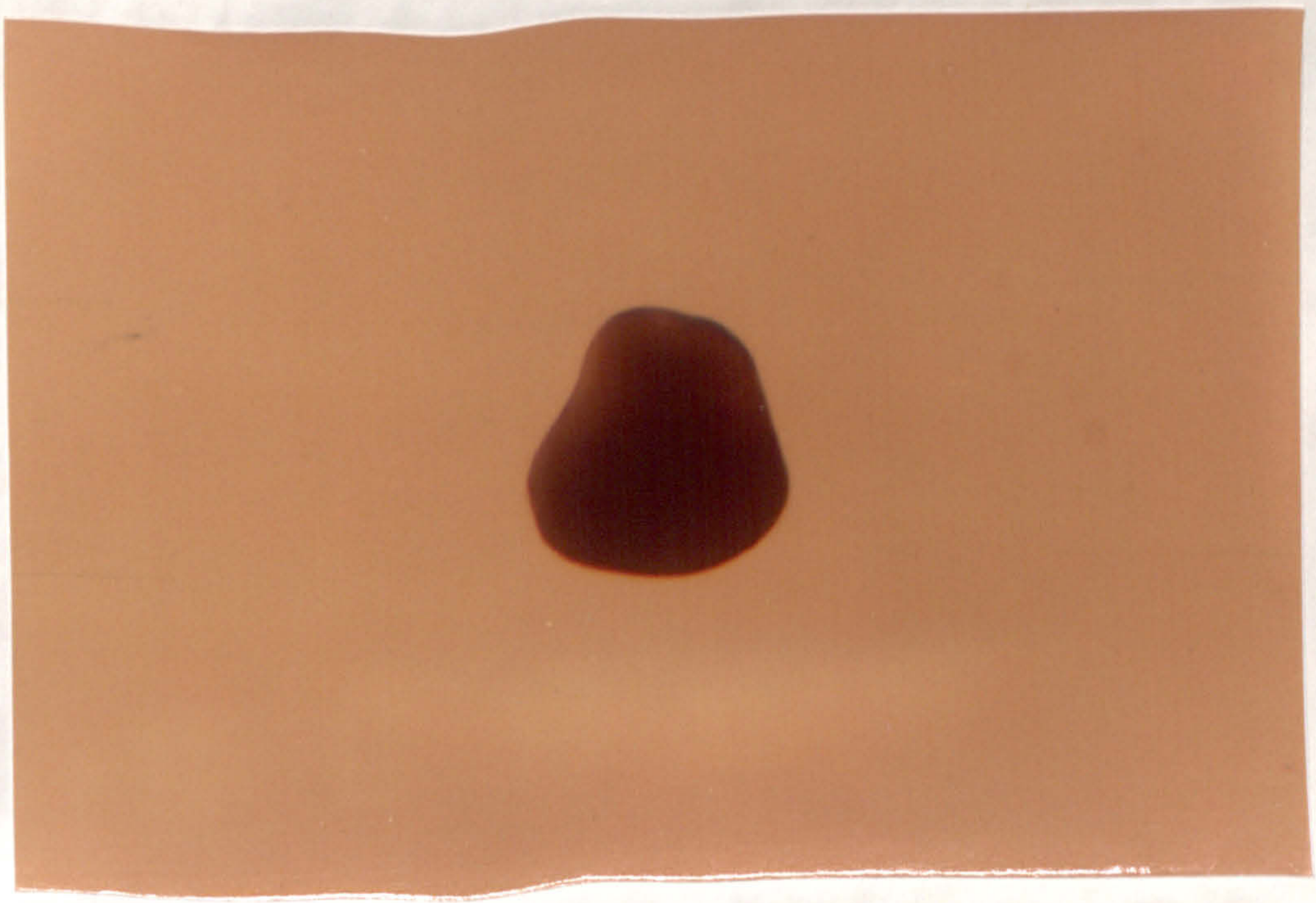

A. Rounded grain of dark green tourmaline (x 200)

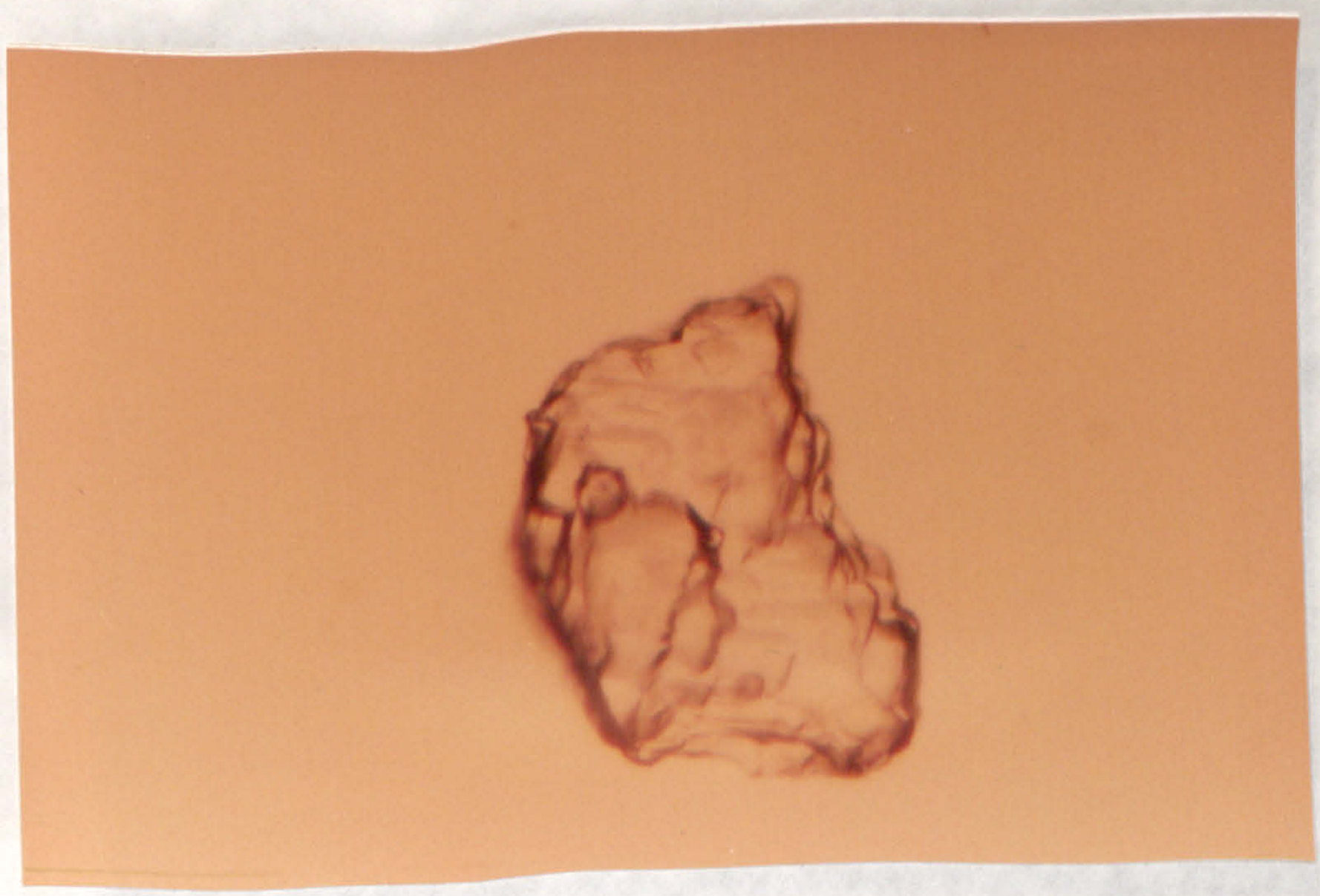

B. Pink garnet, with rhombic pattern of etching (x 170)

PLATE 15

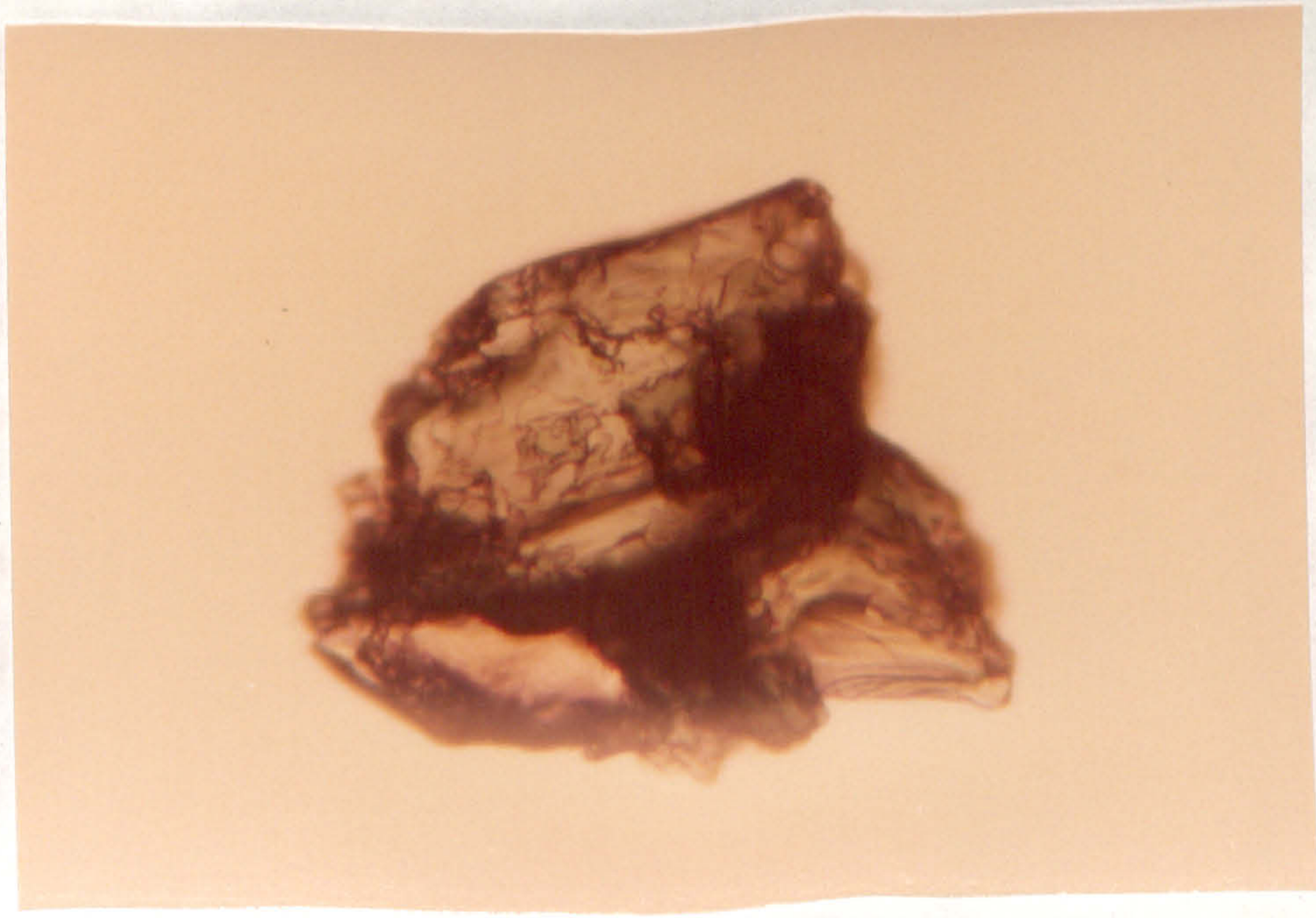

A. Composite grain of green epidote and pink garnet in the lower left corner (x 125)

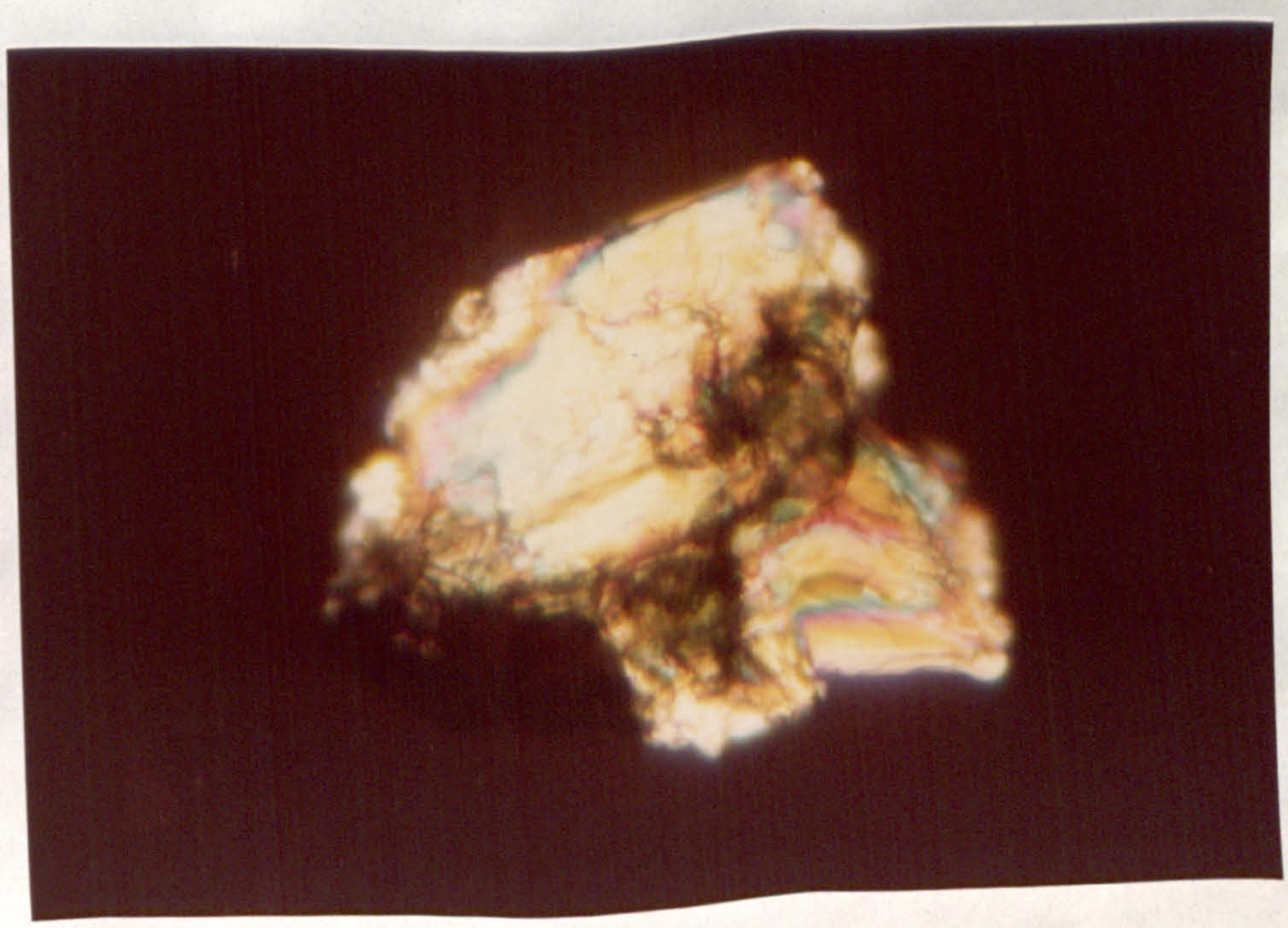

B. The same composite grain under crossed nicols, note the garnet is isotropic (x 125)

PLATE 16

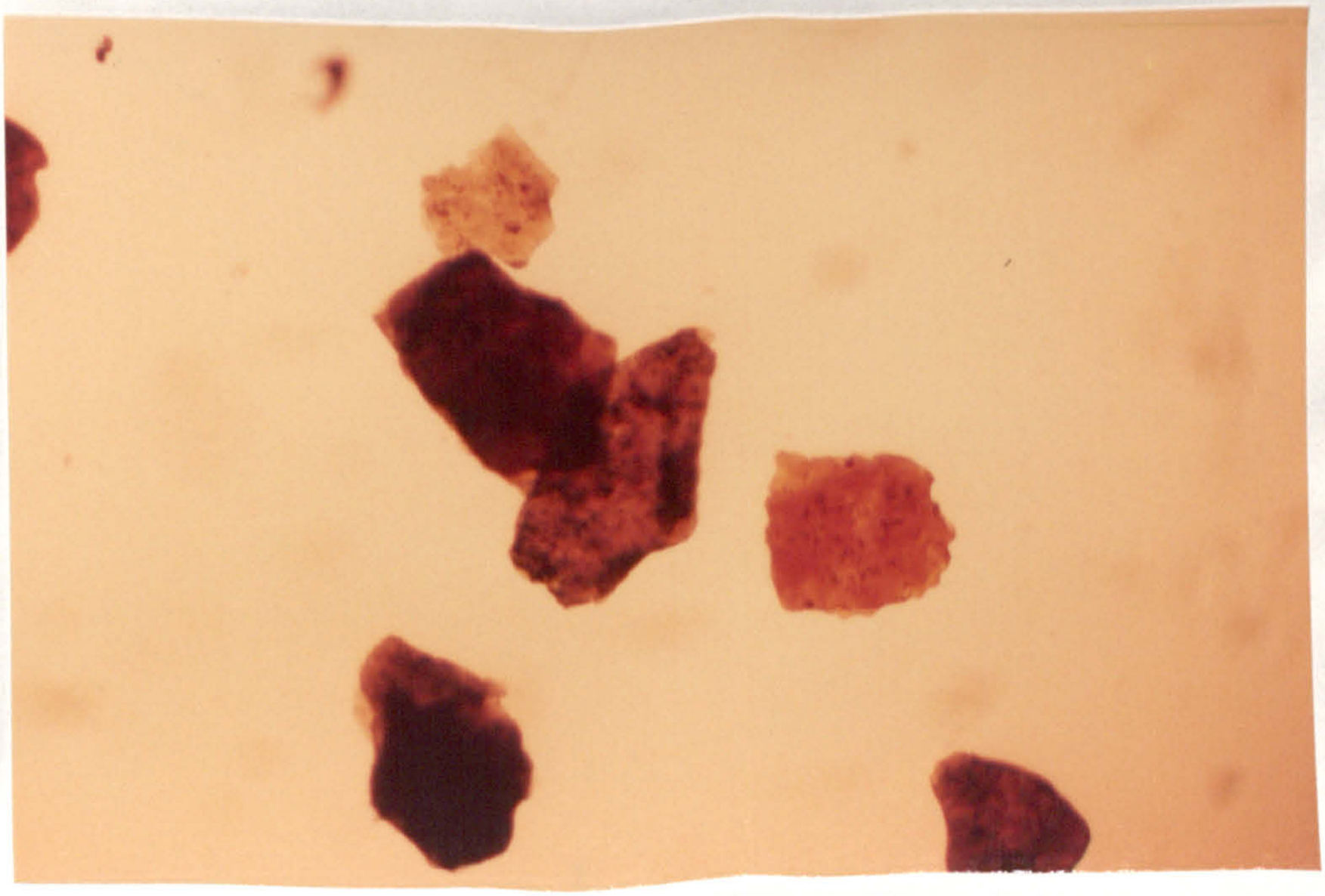

A. Flakes of brown and reddish brown biotite (x 30)

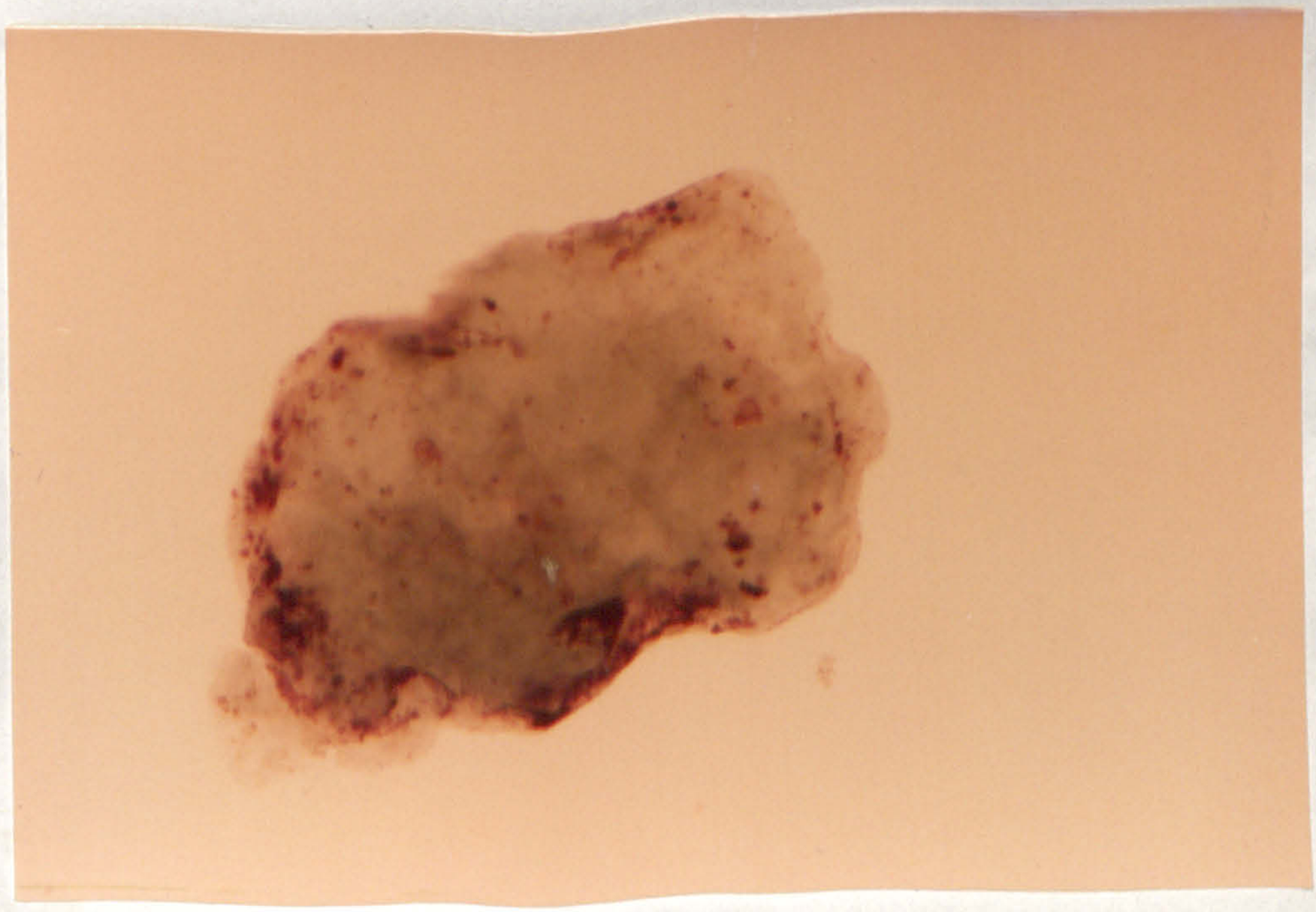

B. Alteration of biotite to chlorite (x 100)